## The origin of massive sandstone facies in an ancient braided river deposits

Charlotte Ann Lesley Martin

# The Origin Of Massive Sandstone Facies in Ancient Braided River Deposits.

A thesis presented for the degree of
Doctor of Philosophy

by

## Charlotte Ann Lesley Martin

8 MAY 1995

# Abstract

# The Origin Of Massive Sandstone Facies in Ancient Braided River Deposits.

Lateral profiling techniques have been utilised to define the three-dimensional fluvial architecture of the Fell Sandstone Group (Arundian-Holkerian) of the Northumberland Basin, UK; the Lee-type sandstones (Morrowan-Atokan) of the central Appalachian Basin, USA; the Mansfield and Brazil Formations (Morrowan-Atokan) of the Illinois Basin, USA; and the Anisian Hawkesbury Sandstone of the Sydney Basin, Australia. These strata are characterised by sandstones of braided fluvial origin.

Individual fluvial channels are dominated by downstream accreting mesoforms and macroforms, interpreted to represent mid-channel and bank attached bars and dunes. Palaeocurrents are unimodal and of low variance. Evidence of low stage reworking is rare, indicating that the fluvial systems were perennial.

Cross-stratified sandstones are interbedded with structureless sandbodies, which display three distinct geometric forms: Sms, Smc and Sme. The texture and composition of facies Sms, Smc and Sme are distinct from associated structured facies.

Facies Sms forms erosively based sandsheets <8 m thick and >250 m parallel and transverse to the flow. The upper surface is planar. Facies Smc forms elongate channels trending at high angles to the palaeoflow of fluvial channels. The sandbodies preserve a symmetrical cross-section with margins dipping <50°. Concentric laminae are preserved parallel to these margins, and grade into a structureless sandstone fill. Individual units of facies Sme are >6 m thick, and may be traced >200 m parallel and transverse to flow direction. Amalgamation of the facies results in sandsheets >20m thick. Scours, elongate both parallel and oblique to fluvial flow are preserved along the basal surface.

A classification scheme of massive sandstone facies has been developed. The facies are interpreted in terms of deposition from highly concentrated, laminar sediment/water flows. Sediment-laden currents were generated through primary and secondary mechanisms related to flooding and mass flow.

# Acknowledgments.

# Declaration.

I declare that the work contained in this thesis has not been submitted elsewhere for any other degree or qualification, and is my own work, unless otherwise referenced.

# Statement of Copyright.

The copyright of this thesis rests with the author. No quotation from it should be published without prior written consent and information derived from it should be acknowledged.

Frontispiece. Massive sandstone facies (Smc), Natural Bridge State Park, Kentucky, USA.

# List Of Contents.

# Appendices

# List Of Figures.

# List Of Tables

# List Of Plates

# Chapter 1

# Introduction

## 1.1. Aims And Objectives Of This Study.

A massive sandstone facies has been documented by many workers from the deposits of deep marine turbidites (Pickering *et al* 1989) and a locally developed, largely structureless, 'massive' sandstone has also been noted in the deposits of ancient braided streams. However, no satisfactory mechanism has been suggested for the deposition of these massive fluvial sandstone units, which are more common than previously thought. This is reflected by the fact that this facies has been largely ignored, or explained simply in terms of deposition from upper flow regime or dense sediment laden currents. No systematic study of these unusual sandstones has been undertaken, and their origin remains enigmatic. Indeed, some sedimentologists are reluctant to acknowledge the existence of a separate massive sandstone facies, and Miall (1977) has no massive sandstone facies included within his proposed lithofacies scheme, although he does recognise a massive gravel (Miall 1985).

The objective of this research was to assess the existence of the massive sandstone facies, and to document and describe the facies in detail. The aims of this thesis may be summarised as the following:

- To identify the types of river systems within which the massive sandstone facies will tend to be preserved, and to document the three dimensional architecture of the fluvial sediments.

- To define the three-dimensional architectural geometry of the massive sandstone facies.

- To identify textural and compositional characteristics of the massive sandstone facies, as compared with those of the structured facies.

- To establish a classification scheme for the massive sandbodies.

- To establish the mode of deposition of the massive sandstone facies.

- To assess the importance of the massive sandstone facies in the rock record.

## 1.2. Sites Chosen For Study.

Laterally extensive outcrops offering three-dimensional exposure of braided fluvial sandbodies were a pre-requisite for this study. These were identified from the literature. A number of studies have documented a massive sandstone facies from braided alluvium. These include the work of Turner & Monro (1987) in the Fell Sandstone Group of northeastern England and that of Wizevich (1991, 1992) concerning the Lee sandstones of Kentucky, USA. Fishbaugh *et al* (1989) documented a massive sandstone facies from the Mansfield Formation of Indiana, USA, and laterally extensive massive sandbodies have been described from the Hawkesbury Sandstone of Sydney, Australia (Conaghan & Jones 1975; Conaghan 1980; Jones & Rust 1983; Rust & Jones 1987).

These studies were used to identify the field areas used within this study. These areas are the Carboniferous Fell Sandstone Group (Arundian-Holkerian) of the Northumberland basin, England; Lower Pennsylvanian Lee-type sands of the Breathitt Group (Morrowan-Atokan), central Appalachian basin, USA; Lower Pennsylvanian Mansfield Formation (Morrowan-Atokan) of the Illinois basin, USA, and the Triassic Hawkesbury Sandstone (Anisian) of the Sydney basin, Australia. These sandstone units were chosen for this study due to good exposure and ease of access.

## 1.3. Methodology.

General reconnaissance of each of the above formations resulted in the identification of a number of laterally extensive sandbodies exposing representative facies. Photomosaics were constructed for each of the outcrops using a 50 mm lens, to minimise distortion. Architectural analysis of each outcrop consisted of recording decimetre scale features on transparent overlays of the field photographs. Smaller scale features were recorded in field note books, and the sections were logged in detail to allow for the assessment of vertical and lateral relationships between the sedimentary facies and structures. Detailed palaeocurrent measurements were made to allow for reconstruction of bedforms and fluvial flow characteristics.

A representative suite of hand specimens was collected from outcrops of each formation studied. Thin sections cut from these have been used to assess the texture and composition of rock units, and the existence, if any, of variations between facies. Petrographic methods and tabulated results are outlined in Appendix III. A study of grain size was also undertaken from thin sections, and a detailed description of the techniques used is given in Appendix III. A permeability study of a small number of

hand specimens was made possible through the use of a mini-permeameter. XRD analysis was used to identify clay fraction composition and heavy mineral suites. The techniques used, and results are outlined in Appendix IV.

## 1.4. Thesis Outline.

This thesis is composed of eight chapters. This first chapter introduces the aims of this study. The contents of the proceeding chapters are outline below.

*Chapter 2:*

Within this chapter the concept of a braided river, and some modern and ancient examples of such systems are introduced. The techniques of architectural element, bounding surface and facies analysis, to be used within this study are reviewed and described. Methods of palaeohydrological estimation, using the deposits of ancient sandstones are introduced and discussed.

*Chapters 3 to 6:*

Each of these chapters details the fieldwork undertaken for this study. The sediments are described in order of decreasing age: the Lower Carboniferous (Arundian-Holkerian) of the Northumberland basin (Chapter 3), the Upper Carboniferous (Morrowan-Atokan) of the central Appalachian basin (Chapter 4), the Upper Carboniferous (Morrowan-Atokan) of the Illinois basin (Chapter 5) and Triassic (Anisian) of the Sydney basin (Chapter 6).

Within each of these field related chapters the sedimentary facies encountered are described in detail, with the exception of the massive sandstone facies. Representative sedimentary logs and lateral profiling techniques have been utilised to illustrate fluvial sandbody architecture. Architectural element analysis has been used to identify the geometry of macroforms preserved within the fluvial systems, including that of the massive sandstone facies. Textural and compositional parameters of the separate facies are discussed for each basin.

To conclude each of these chapters an overall interpretation of the fluvial environment is suggested and discussed. Factors such as planform geometry, macroform types, climate and tectonic influences are drawn together to create a unifying model of the fluvial system.

*Chapter 7:*

This chapter details the geometry, textural and compositional characteristics of the massive sandstone facies. The three separate facies types identified through

fieldwork are described and interpreted in terms of likely depositional mechanisms. The possible implications of preservation of the massive sandstone facies are discussed.

*Chapter 8:*

This chapter lists the conclusions of this study, and suggests possible directions of future research in this area of fluvial sedimentology.

# Chapter 2

# An Introduction To Braided Alluvial Systems

## 2.1. Classification Of Alluvial Systems.

A vast range of channel morphologies or planform types exist for alluvial systems, and hence for reasons of convenience geologists tend to recognise five major river types: meandering, wandering, braided, anastomosing and straight. Fluvial channels may be classified in terms of the channel pattern (Leopold & Wolman 1957; Rust 1978a) or by the transported sediment load (Schumm 1968a & b). The former method is most widely used.

River style or channel pattern is generally characterised on the basis of three criteria: 1) sinuosity, 2) braiding index, and 3) lateral channel stability. Meandering and straight systems have only one channel, whilst braided and anastomosing rivers are multi-channelled. Wandering gravel bed rivers are intermediate, and typically have 2 or 3 channels. It has been demonstrated, both empirically and theoretically, that a continuum exists between these planforms types (Bridge 1985), and it is therefore likely that different river morphologies share similarities in flow and sediment characteristics.

Individual channel planform types do not reflect a specific geomorphic process occurring under unique sets of circumstances, but instead reflect fluvial adjustment to combinations of inter-related variables which vary between channel patterns. Fluvial channel pattern is dominantly controlled by the supply of water and sediment, and the valley gradient (Bridge 1985, 1993a). Discharge variability is not expected to have a major influence on channel pattern as most channel morphologies have been formed in laboratory flumes at a constant discharge (Bridge 1985). The presence or absence of riparian vegeatation is also a controlling factor on channel planform. A lack of vegetation reduces channel bank stability, and hence may lead to lateral channel migration.

One of the fundamental properties used to characterise channel pattern is sinuosity, $P$, which is defined as the thalweg length/valley length (Rust 1978a). River systems are subdivided into 'low sinuosity' systems represented by straight and braided channels, and 'high sinuosity' represented by meandering and anastomosing systems, using an arbitrary value of 1.5 (Rust 1978a).

Functions used to differentiate among modern day braided and meandering planform types have been based on relationships between channel slope, $S$,

discharge, $Q$, and particle size, $D$ (see Bridge 1993a). Meandering rivers are favoured by a predominance of suspended load, cohesive banks and gentle slopes. Braided rivers generally have a width/depth ratio greater than 40, and sinuosity <1.5. Modern braided rivers tend to occur in high energy environments, associated with coarse bedload and unstable banks. It has been shown empirically that the channel width/depth ratio increases as discharge increases for a given slope, as slope is increased at a given discharge (Leopold & Wolman 1957), or as grain size of bed material increases (Bridge 1985). The hydraulic controls of the meandering to braided transition are discussed by Bridge (1993a). Despite many efforts to differentiate the factors controlling the meandering to braided transition Murray & Paola (1994) have recently stated that the 'fundamental factors that distinguish braided from meandering rivers are still unclear'.

Leopold and Wolman (1957) described a braided river as 'one which flows in two or more anastomosing channels around alluvial islands'. Schumm (1977) defined braided channels as single channel bedload rivers which contain emergent islands of sediment at low water levels.

There is clearly a conflict of opinion as to what constitutes a braided river, particularly as the appearance of a braided river may change with flow stage. Confusion also exists as to the definition of bars and islands. The simplest way of identifying a braided river is as one which contains mid-channel bars (Bristow 1987a). A mid-channel bar may be classified as an in-channel element, which splits the thalweg of the river. Bars are generally accepted to be emergent, scaled to the width of the fluvial channel, and have long response times relative to flow changes. Islands are vegetated bars, and hence bars and islands share a common geometry and genesis.

## 2.2. Bedform Terminology.

The plethora of nomenclature currently used for fluvial systems is highly confusing, and hence the terms to be used within this study are defined here. Ideally, bedforms represent deposition from steady and uniform flows, and hence represent equilibrium conditions between the fluid and the sediment in transport. Steady flow defines a flow which does not vary in time, uniform flow remains the same at all cross sections of the flow (Middleton & Southard 1978). Periodic bedforms form within the channel in response to the movement of water, and will be in equilibrium with formative flow conditions. Rivers generally have unsteady or non-uniform flow, resulting in disequilibrium between fluid and bedforms, and sediment lag. Sediment is stored in bedforms, the size and shape of which change as a consequence of erosion or non-

deposition, as flow conditions vary through time. Sediment lag or storage time increases with both bedform and river size (Allen 1983a).

In the past bedforms within braided rivers have been termed 'bars' (section 2.1), which is a highly misused term. Smith (1978) suggested that modified, non-periodic bedforms should be termed 'bars' and regarded as separate from unmodified periodic, 'unit bars'.

A unifying model of bedform types was invoked by Jackson (1975) which recognised three groups of bedforms. Each of these groups was defined by the bedform size and the time span of existence, with the groups termed microforms, mesoforms and macroforms (Table 2.1). Unfortunately this classification muddled the periodic and non-periodic bedforms observed within a river system.

| SEDIMENT STORAGE BODY | | COMMONLY USED TERMS | JACKSON (1975) | ASHLEY (1990) |
|---|---|---|---|---|
| Ripples *Periodic* | | | Microform | |
| Dunes *Periodic* | 2-D/ 3-D | Transverse bar, Linguoid bar | Mesoform | Relatively dynamic units. Relatively short response time to changes in flow characteristics. Morphology varies with relation to flow strength |
| Channel Form *Periodic* | | Point bar, diagonal bar, side bar, alternate bar, mid-channel bar | Macroform | An order of magnitude greater than dunes occurring in the same channel. Response times are relatively long. Scaled to bankfull width. |
| Unit Bars *Solitary* | | Longitudinal bar, chute bar, scroll bar, tributary bar | Mesoform | Scales to channel depth. Simple depositional history controlled by local hydraulic conditions such as changes in water depth. |
| Braid Bar Complexes *Solitary* | | Longitudinal bar, mid-channel bar | Macroform | Amalgamation of above forms. Product of a history of erosion and deposition. |

*Table 2.1. Definition of terms used for sediment storage units.*

A simplified nomenclature has been established by Ashley (1990) illustrated in Table 2.1. An obvious distinction exists between small scale bedforms (ripples) and larger scale bedforms formed under uni-directional flow conditions. Theoretical

investigations suggest that under steady state conditions ripples and dunes are distinguished at a wavelength of 0.6 m (Allen 1968; Allen & Collinson 1974). However, field studies indicate that bedforms occur over a wide range of linear scales in nature. For instance Coleman (1969) distinguished four categories of large scale transverse bedforms from the Brahmaputra which were termed ripples, megaripples, dunes and sandwaves.

Using the terminology of Ashley (1990) all large scale flow transverse bedforms, with the exception of antidunes, are termed dunes (Table 2.1). These combine to form larger scale sediment storage bodies. Dunes are described by size, but variations in scale are not used to sub-divide the class.

Dunes form as a function of resistance to flow, and migrate under shear stress imparted on the channel bed by the moving fluid. Dunes are short lived relative to major changes in flow, are periodic, and scaled to boundary layer thickness i.e. water depth, $d$. Dunes occur as both straight crested or planar 2-D forms and 3-D, curved crested or trough forms. 2-D dunes tend to form under slower flow conditions than do 3-D forms, for given depth and grain size (Figure 2.1). This change in morphology reflects a change in the fluid flow structure at higher velocities. Ashley (1990) recognises a complete continuum between the 2-D and 3-D dunes, indicating that a genetic relationship exists between the two populations.
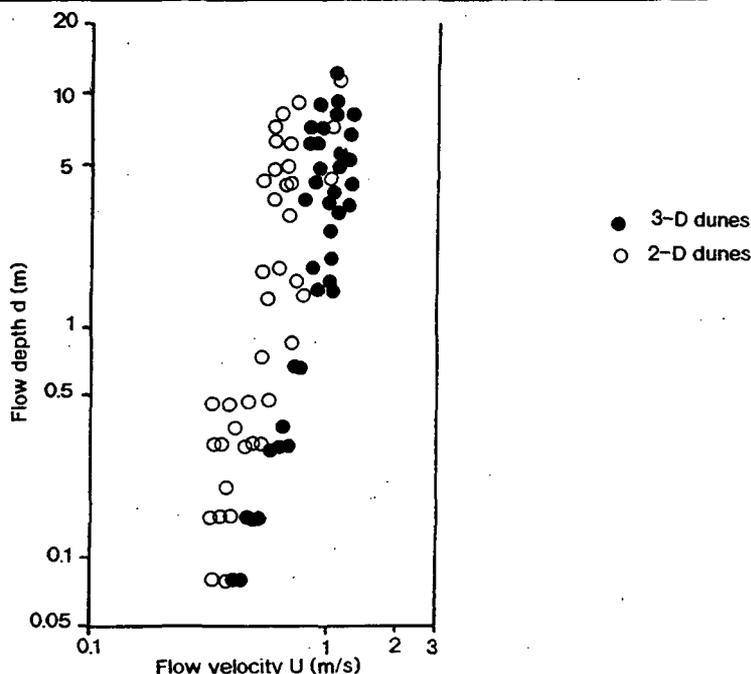


Figure 2.1. A depth-velocity diagram, showing the relationship between velocity and dune types in medium to coarse sands. Modified from Harms et al (1982).

Superimposition of dunes is common. Field based fluvial studies have documented the simultaneous migration of smaller bedforms, and the larger ones upon which they are superimposed (Collinson 1970; Bridge 1985). Allen & Collinson (1974) interpreted the superimposition of dunes to be a result of large and rapid hydrological changes. However, superimposed dunes have been formed in the laboratory flumes under steady equilibrium conditions (Jopling 1966). In steady flow conditions it is believed that the larger bedforms may generate a boundary layer within which the smaller forms are stable (Ashley 1990). Where a smaller bedform migrates down the lee face of a larger form superimposition results in compound bedforms (Allen 1982). These compound dunes are recognised as a variation of basic dune types.

*Channel forms* (Table 2.1) are periodic, but are an order of magnitude greater in size than the dunes of the same channel. Periodicity is related to the planform geometry of the thalweg, which in turn is scaled to the bankfull or channel forming width. The response time of channel forms is long, relative to major changes in flow characteristics (Ashley 1990). Channel forms commonly serve as the substrate for migrating superimposed bedforms (Bridge 1985; Ashley 1990).

*Unit bars* (Table 2.1) are quasi-periodic or solitary storage bodies which occur scaled to depth within the channel. These forms have simple depositional histories controlled by the local hydraulic conditions (Ashley 1990). *Braid bar complexes* (Table 2.1) are large storage bodies which may exist for many years. They consist of an amalgamation of the other three types of bedform and are the product of a history of deposition and erosion. These depositional units are commonly vegetated.

In this study the suggested terminology of Smith (1978) is used for convenience. All non-periodic bedforms (i.e. unit bars and braid bar complexes of Table 2.1) are termed bars.

## 2.3. Modern Braided Rivers.

### 2.3.1. Processes.

The processes involved in the initiation and growth of braid bar complexes are described by Schumm *et al* (1987) and Bridge (1985, 1993a). Braiding occurs at points in river channels where either local flow competence is exceeded or the channel becomes overloaded with sediment, following which sediment deposition occurs in regions of flow divergence. Initially sediment is trapped in 'alternate bars' (Table 2.1). With increased thalweg amplitude, erosion of cut banks occurs and scours develop on either side of the alternate bar. The channel widens (Schumm *et al* 1987), resulting in a drop of water level and emergence of a 'mid-channel bar'. Erosion and subsequent

deposition around the bar margins results in the development of bar head and bar tail regions. The development of braiding therefore requires that flow is not constrained laterally (Murray & Paola 1994).

It is possible for braid bar complexes to develop within a channel under constant discharge (Bridge 1993a). In such perennial systems the bedforms will be submerged for large portions of time, and hence low stage modification will be limited. The river will effectively act as a single channel system (Bristow & Best 1993), with submerged sediments capable of splitting the channel thalweg. Fluctuations in discharge are, however, common features of modern braided streams. A fall in discharge will result in the emergence and dissection of bedforms (Collinson 1970; Rust 1972; Cant & Walker 1978). The majority of braided rivers maintain bars at all flow stages with braiding most evident at lower stages (Bristow & Best 1993).

Flow in braided reaches may be envisaged as a series of channel segments which divide and rejoin around bedforms. Where the bedform or 'bar' is emergent, channels on either side have flow characteristics broadly equivalent to those of single channel sinuous rivers. Curved flow around the bar results in the development of spiral flow and deposition along lateral accretion surfaces, similar to point bars of meandering systems. Within all curved channel segments it can be predicted that the maximum grain size of bed material will follow the zone of maximum fluid velocity. Thus grain size fines over the top of modern braid bars and remains relatively coarse within the thalweg.

In braided rivers, flow may expand vertically and laterally as one channel segment joins another of a different hydraulic geometry. River channel confluences form important morphological elements of every river system, and the flow in confluence regions has been studied by Best (1987, 1988) and Bristow et al (1993). Flow patterns will change with flow stage, and flow through curved channel segments will converge and diverge in different ways depending on whether bars are emerging or being submerged (Bridge 1985).

Within braided rivers the degree of channel splitting or braiding is defined by a braiding parameter. The most useful measure of braiding considers the mean number of active channels or braid bars per transect across the channel belt (Bridge 1993a). Care must be taken when determining the braiding parameter, so as to only consider those features which scale to width (Table 2.1).

## 2.3.2. Deposits of modern braided rivers.

Within the geological and geomorphological literature there has been a long held distinction between gravel-bed and sand-bed braided rivers. However, it is rare for rivers to have only one type of bed material. Rivers will be sand, gravel and rarely silt or mud dominated (Rust 1978b). A representative range of braided river types are listed in Table 2.2. Sandy braided streams tend to be gradational with coarser grained systems, and also with meandering streams. Modern braided rivers are widely described from areas with highly variable discharge and reduced plant activity, which include semi-arid regions of low relief receiving discharge from mountain areas, and pro-glacial environments (Table 2.2).

Studies of modern braided stream deposits are limited by their dependency on trenching. The 'outcrops' are of limited lateral extent, and will be biased in favour of the higher and hence drier portions of the river tract. It is possible to conjecture that bar top sequences should be preserved after avulsion or migration, but it is likely that the sandbody may be dominated by the deeper channel deposits, as upper bar deposits are removed by erosion. Low rates of aggradation cause the preferential preservation of the deeper portions of a fluvial channel (Bristow & Best 1993).

In the past there has been a clear distinction between channel deposits and 'bars' (Miall 1976, 1977). Observations of the morphology of modern braid channel sediments are limited, as the most active channels are constantly filled with water. It is however, probable that the deposits within the active channels are dunes or unit bars. In an aggradational system dunes will amalgamate and vertically accrete with time to become 'bars'. Studies such as that of Bristow (1987a) indicate that alluvial channel fill is a relatively minor component of preserved braided river deposits, and that the dominant sediment component is the product of accretion to bars.

A range of braided fluvial systems have been studied, and these cover a wide range of modern environments. Some important studies are detailed in Table 2.2. Ephemeral braided rivers, such as Bijou Creek (Table 2.2), tend to contain sediments which are dominated by scours and upper plane bed deposits. The deposits of more perennial braided rivers such as the Platte and Brahmaputra (Table 2.2) generally exhibit interbedding of trough and planar cross-stratification.

At high flow stages the most common type of bed configuration in braided rivers is that of 3-D dunes. Straight crested 2-D bedforms are common on the higher parts of bars where flow velocity and depth are relatively low, and upper stage plane beds occur locally in areas of high velocity. Downstream accretion to dunes results in the interbedding of planar and trough cross-stratification. Recent studies have

described large scale lateral accretion surfaces from the Brahmaputra (Bristow 1987a & b) and Calmus (Bridge *et al* 1986) braided rivers (Table 2.2).

| RIVER | LOCALITY | WORKERS | DOMINANT BEDLOAD | CLIMATE (Rudloff 1981) |
|---|---|---|---|---|
| **North America** | | | | |
| Scott Fan | Alaska | Boothroyd & Ashley (1975) | Gravel | Sub-arctic oceanic |
| Platte | Nebraska | Smith (1970 1971) | Sand | Temperate continental |
| Bijou Creek | Colorado | McKee *et al* (1967) | Sand | Steppe |
| South Saskatchewan | Alberta | Cant (1978) Cant & Walker (1978) | Sand | Temperate Continental |
| Donjek | Yukon | Williams & Rust (1969) Rust (1972) | Gravel | Sub-arctic continental |
| **South America** | | | | |
| Orinoco | Venezuela | McKee (1989) | Sand | Tropical rain |
| **Europe** | | | | |
| Tana | Norway | Collinson (1970) | Sand | Sub-arctic oceanic |
| Klifandi & Svinufellsa | Iceland | Maizels (1993) | Gravel | Sub-arctic oceanic |
| **Asia** | | | | |
| Ganges | India | Singh & Kumar (1974) | Sand | Sub-tropical summer rain |
| Brahmaputra | Bangladesh | Coleman (1969) Bristow (1987a) | Sand | Tropical monsoonal rain |
| **Australasia** | | | | |
| Ashley | New Zealand | Warburton *et al* (1993) | Gravel | Temperate oceanic |
| Cooper Creek | Australia | Nanson *et al* (1986) | Mud | Desert |
| Finke | Australia | Williams (1971) | Sand | Desert |

*Table 2.2. A general list of major studies of modern braided river systems and the climates in which they occur.*

Within braided systems re-activation surfaces and ripple cross-lamination record fluctuations in water level and low stage re-working of sediments. These surfaces of discontinuity have been described from an large number of modern braided rivers including the Tana River, Norway (Table 2.2) by Collinson (1970).

## 2.4. Braided Systems In The Rock Record.

Preservation of braided river channels may be viewed as a function of frequency of channel avulsion, rate of lateral migration, rate of change of discharge and aggradation rate (Cant & Walker 1978; Bridge & Leeder 1979; Bristow & Best 1993). The deposits of braided rivers are generally identified in the rock record using a number of criteria including the ratio of coarse member thickness to fine member thickness, internal geometry of coarse channel belt deposits, and palaeocurrent patterns (Collinson 1978). Some workers have attempted to use simplified models of modern systems as direct analogues for ancient sediments, such as the comparison of the Platte River and Silurian sediments of the Appalachian Basin (Smith 1970), and the comparison of the South Saskatchewan River and the Devonian Battery Point Formation (Cant 1978).

In the past, the majority of sediments from the rock record have been described in terms of vertical profiles (Miall 1977, 1978) or pseudo three-dimensional models (Cant & Walker 1978). However, channel type and behaviour can never be unambiguously predicted from vertical sequences. The geometry and connectivity of fluvial channels have been recognised as an important indicator of channel type. Friend (1983) developed a classification scheme of fluvial channel geometry which used descriptions of channel margins and the lateral or vertical stacking of channel sediments to describe channels as either fixed, mobile or sheet-like. Fixed channels are narrow with a width/depth ratio less than 15. Mobile channels have a width/depth ratio of greater than 15, and are filled by a process of channel migration and switching. Where width/depth ratio is greater than 100 the channel is termed sheet-like.

Studies including that of Friend (1983) and Allen (1983b) have shifted attention from the simple vertical models towards the internal geometry of fluvial sandstone bodies. Planar to gently concave-up intersecting erosional surfaces are now recognised as indicative of low sinuosity streams (Allen 1983b). Friend (1983) classified the sediment packages deposited between these scour surfaces as storeys. Fluvial channels are commonly multi-storey, with stacked storeys (Friend 1983) or complexes (Allen 1983b) developed within larger channel elements.

Allen (1983b) first introduced the concept of architectural elements to fluvial sediments, which can be considered as a form of facies association analysis (Walker 1990). Architectural elements are associations of facies, or individual facies which are separated by a hierarchy of bedding contacts (Table 2.3). Allen (1983b) recognised eight architectural elements in the Devonian Brownstones of the Welsh Borders, which are defined by grain size, bedform composition, internal sequence and bedform morphology. The eight elements vary in scale and complexity.

| ALLEN (1983b) | HASZELDINE (1983 a&b) | MIALL (1988) | THIS STUDY |
|---|---|---|---|
| 0. Non-erosional, concordant bedding contacts | 4. Surfaces occur within sets & mark discontinuance's between bundles of foresets | | 0. Surfaces occur within sets & mark discontinuance's between bundles of foresets |
| 1. Bound individual sets. Surface contact may be erosional & planar or concave up. | 3. Surfaces separate sets. Contacts may be planar to concave up.<br><br>2. Separate sets & cross-cut 3rd. order surfaces. | 1. Represent cross-bed set boundaries which were deposited with little or no erosion. Subtle modifications in foresets due to reactivation. | 1. Bound sets. |
| 2. Bound clusters of sedimentary units (complexes) defined by 1 st. order surfaces. Contacts may be planar to concave up. | 1. Bound cosets. Surfaces are of low angle, & lateral importance. | 2. Represent simple coset boundaries (McKee & Weir 1953). Define changes in flow direction without significant time break.<br><br>3. Define cross-cutting erosional surfaces within macroforms. Commonly draped with intraclast breccia. Surfaces dip <15°. | 2A. Basal surface of cosets of McKee & Weir (1953).<br><br>2B. Basal surface of cosets formed by the migration of dunes down the slip-face of a larger bedform. Surfaces dip <15°.<br><br>2C. Lower bounding surface of facies Smc. |
| | | 4. Represent upper bounding surfaces of macroforms. Surface flat to convex up. Underlying surfaces truncated at a low angle. | 3. Bound genetically related cosets into macroforms. Surfaces undulose to concave up with <10° dip. |
| 3. Divide groups of complexes. Surfaces often overlain by gravels. Surface planar to concave up. | | 5. Surfaces bound major sand sheets e.g. channel fill complexes. Surfaces flat to concave up. | 4. Define channel fills. Surfaces commonly covered in gravel & concave up. |
| | | 6. Surface defines groups of channels or palaeovalleys. Represent mappable stratigraphic units e.g. members. | 5. Define groups of channels. Commonly covered by a conglomerate. Represent mappable stratigraphic units. |

*Table 2.3. Bounding surface classifications of selected workers, as compared with that of this study.*

The concept of architectural element analysis was expanded by Miall (1985) and the method of architectural analysis has been modified and used by workers such as Wizevich (1991) to aid the study of fluvial deposits. However, the method has been criticised by Walker (1990) and Bridge (1993b) due to the fact that the architectural elements are defined by different parameters.

The hierarchy of sedimentary storage units, or architectural elements, within braided streams reflect the physical scales of the deposit and the time scale during which they formed. Three-dimensional division of sedimentary units may be attempted using internal bounding surfaces. The concept of bounding surfaces within braided alluvium has been tackled by several workers including Allen (1983b) and Miall (1985, 1988) as detailed in Table 2.3. Such a system is logical, but difficult to use. The complex descriptions of surfaces by Miall (1988) means that the second to fifth order bounding surfaces are difficult to distinguish, even in well exposed sediments, and the minor surfaces change rank laterally. Schemes of hierarchical bedding contacts have been developed by a number of workers which are specific to certain fluvial environments. The study of Haszeldine (1983a & b) is such a study (Table 2.3).

## 2.5. Concepts Used Within This Study

### 2.5.1. Facies Analysis

As described in Chapter 1 this study is concerned with sediments from a number of different formations, deposited within four separate sedimentary basins. It has, therefore, been necessary, to establish a generalised framework for facies descriptions which may be used for all sediments, in order to facilitate comparisons between different formations and basin fill successions. The facies scheme developed for this study is outlined in Table 2.4, with more detailed descriptions of facies included within Chapters 3-6.

As is clear from Table 2.4, the coarsest sediments studied are sandy conglomerates and breccias. Thus, this study concentrates on the deposits of sand dominated fluvial systems. A summary of the hydrological parameters of modern-day sand dominated braided rivers is given in Table 2.5.

The bounding surface system developed for this study is detailed in Table 2.3. and Figure 2.2. This classification has been simplified from that of Miall (1988). Such a system is particularly useful for tracing out erosional surfaces in the field, thus allowing for correlation between closely spaced outcrops. The use of bounding surfaces enables sediments to be divided into genetically related packages or macroforms.

| | FACIES | SUB-FACIES | GEOMETRY | DESCRIPTION |
|---|---|---|---|---|
| SANDSTONE | Conglomeratic Sandstone *Scg* | | 0.05-5 m thick, with thickness varying laterally, Extend >100 m parallel to flow | Poor-moderate sorted matrix supported conglomerate. Clasts (quartz, mudstone, plant fragments ) sub-angular-sub-rounded <5-120 cm diameter. |
| | Mudstone Breccia *Sb* | | 0.50-3 m thick & <20m in lateral extent. | Matrix supported breccia containing mudclasts <0.80 m diameter & graphite flakes & quartz granules. Normal & inverse grading. |
| | Trough cross-stratified *St* | | Lenticular shaped sets. Stl (0.75-2 m thick) Stm (0.4-0.75 m thick) Sts (0.5-0.4 m thick) | Fine-very coarse sand. Foresets dip 15-22°, commonly overturned. Symmetric & asymmetric set fill. |
| | Planar cross-stratified *Sp* | Angular foresets *Spa* | Set bases planar to undulose. Occur on 3 scales (large, medium, small) | Fine-very coarse sand. Foresets dip 20-26°. Quartz granules commonly preserved in base of sets. |
| | | Tangential foresets *Spt* | Stl (0.75-2 m thick) Stm (0.4-0.75 m thick) Sts (0.5-0.4 m thick) | Reactivation surfaces occur on limited scale. No mud drapes or low stage reworking of foresets observed. |
| | Giant cross-stratified *Sg* | | 2-6 m thick & > 40 m parallel to flow. Upper & lower surfaces approximately parallel. | Medium grained sand-granulestone. Normal grading upward through the set common. Foresets dip 15-28°, display normal & inverse grading internally. Reactivation surfaces locally preserved, not associated with significant reworking. Bottomsets locally preserved. |
| | Compound cross-stratification *Sc* | | 1-5 m thick, 10-100 m wide & < 20 m wide. | Fine-coarse sand. Foresets dip <15°, & contain intrasets of Sp & St which dip 25-30°. Reactivation surfaces locally preserved, but not associated major reworking. |
| | Low angle cross-stratification *Sl* | | <3 m thick & 50-100 m lateral extent. Lenticular shape. | Fine-coarse grained sand. Forests dip <15° perpendicular to flow. Normally graded. Contain abundant mica & organic matter along foresets. |

*Table 2.4. An outline of the facies scheme developed for this study. More detailed descriptions of the facies are given in Chapters 3-6.*

| | | | | |
|---|---|---|---|---|
| **SANDSTONE** | | Diffuse cross-stratification *Sd* | | <1 m thick & <5 m lateral extent. Poorly defined lower surface. Sharp upper surface. | Medium-coarse grained sand. Sets of St & Sp 0.1-0.4 m thick. Foresets poorly defined. Tangential, dip 10-20°. |
| | Horizontal stratification *Sh* | | 0.05-0.5 m thick & <3 m lateral extent. Planar upper & lower boundaries. | Fine-medium grained sand with abundant mica. Laminae 5-10 mm apart. |
| | Massive sandstone *Sm* | Sheet-like *Sms* | 3-10 m thick & >200 m lateral extent. Undulose lower boundary & planar upper boundary. | Fine-medium grained sand. Internally contains sweeping laminae, solitary 2-D & 3-D dunes & water escape structures. |
| | | Channel-like *Smc* | Lenticular cross-section. Variable width depth ratios <12 & >20. Elongate in flow direction >30 m. | Fine-medium grained sand. Displays concentric marginal laminae (<45° dip) which grade into a massive sandstone fill. Undulose laminae & water escape structures in upper fill. |
| | | Erosively based sheets *Sme* | Scoured base <7 m relief. Overlying sheets <6 m thick & >250 m lateral extent. Amalgamate to form units >20 m thick & 1000 m lateral extent. | Medium grained sand-granulestone. Faces Sb commonly preserved in scours. Sand contains large volume of mica, graphite & clay minerals. Largely structureless, with sweeping laminae. |
| **FINES** | | Cross-laminated *Fx* | | <0.5 m thick & >20 m lateral extent. | Fine grained sand-silt. Flasar bedded. Ripples asymmetric and symmetric. Abundant disseminated organic matter and mica. Bioturbation rare. |
| | Rhythmites *Fr* | | <2 m thick & <50 m lateral extent. | Flasar-wavy bedded sand draped with mud, climbing ripples common. Ripples increase & decrease in size rhymically in vertical scale. Commonly bioturbated with low diversity traces. |
| | Mudstone *Fm* | | <0.3 m thick & <5 m lateral extent. | Silty, dark mud with weak horizontal lamination. Organic-rich, with siderite nodules. Trace & body fossils locally preserved. |
| **ORGANIC** | | Palaeosol *P* | | <2 m thick, <10 m lateral extent. | Root traces, locally replaced by siderite. Extend <2 m into facies Fx & Fr. May or may not be overlain by coal. |
| | Coal *C* | | Occur on 2 scales: Pods <0.3-0.5 m thick & <10 m wide. Beds <1 m thick & > 5,000 m lateral extent. | Black, dull, friable. Low sulphur and ash content. |

*Table 2.4. continued.*

| RIVER | WORKERS | Qm (m³/s) | Qma (m³/s) | Qmax (m³/s) | Width (m) | Depth (m) | W/D | Mean Slope (m/m) | Mean Velocity (m/s) | Drainage Area (km²) | S/ment Load tonnes/y |
|---|---|---|---|---|---|---|---|---|---|---|---|
| Platte, USA | Smith (1971) | 109 | | 3,200 | 400-600 | | 98 | $0.1 \times 10^{-5}$ | | 235,000 | |
| Platte, USA | Blodgett & Stanley (1980) | | 271 | | | 1.13-1.25 | | | | 0.76-1.04 | | |
| South Saskatchewan, Canada | Cant(1978) | | | | 150 | | | $0.3 \times 10^{-3}$ | | | |
| South Saskatchewan, Canada | Cant & Walker (1978) | 275 | 1,200 | 3,800 | 70-200 | 5 | | | | 0.75-1.75 | | |
| Tana, Norway | Collinson (1970) | 158 | 1,767 | 3,544 | 600-1500 | | | $0.2 \times 10^{-3}$ | | 114,000 | |
| Brahmaputra, Bangladesh | Coleman (1969) | 19,000 | 40,000 | 71,000 | 13,000 | 15 | | $0.7 \times 10^{-4}$ | 2.4 | 580,000 | |
| Brahmaputra, Bangladesh | Bristow (1987a) | | | 76,500 | 1,000 | | 50-500 | $0.6 \times 10^{-4}$ | 3 | 380,000 | |
| Brahmaputra, Bangladesh | Thorne et al (1993) | 12,200 | 65,500 | | | | | | | 666,000 | $500 \times 10^{6}$ |
| Kosi, India | Singh et al (1993) | 1,648 | | | | 8-10 | | | | 59,000 | |
| Kosi, India | Sinha & Friend (1994) | 2,036 | 7,200 | | 631 | 4.75 | 78 | | | 88,480 | $43 \times 10^{9}$ |
| Orinoco, Venezuela | Nordin & Perez-Hernandez (1989) | 36,000 | 64,600 | 75,800 | 2,500 | 28 | | $0.5 \times 10^{-4}$ | 0.48-1.64 | 830,000 | $190 \times 10^{6}$ |
| Yellow, China | Shu & Findlayson (1993) | 1,332 | 8650 | | | | | | | 770,000 | $1.6 \times 10^{9}$ |

*Table 2.5. A summary of the hydrological parameters of some modern braided river systems.*
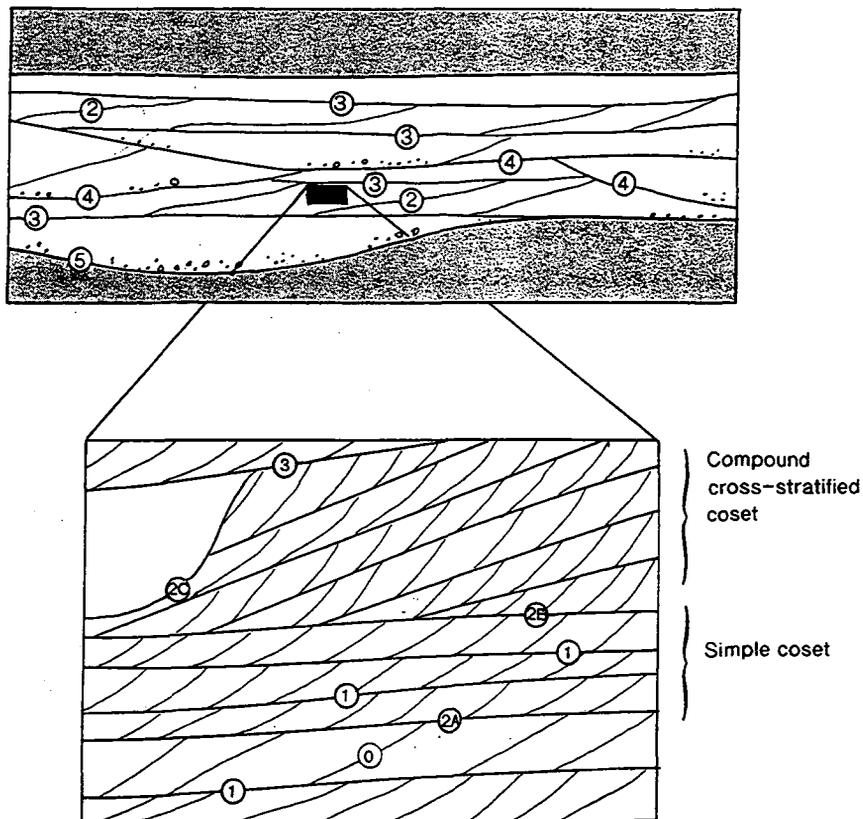
*Figure 2.2. Explanation of the bounding surface hierarchy developed for this study.*

The hierarchy of bedding contacts identified defines a number of depositional units, or architectural elements within fluvial deposits. Architectural elements identified from this study have been divided into intra-channel, channel-margin and inter-channel types. Intra-channel elements combine to form major channel elements (CH of Miall 1985). The terminology used here has been developed for this study and therefore cannot be directly related to previous work.

*Intra-channel Architectural Elements.*

Within the fluvial channel a number of architectural elements have been identified, which are detailed in Table 2.6. The intra-channel elements may be divided into gravelly and sandy forms, which are outlined below, and described more fully within the fieldwork chapters of this study (Chapters 3-6).

The gravelly bedform element, GB (Table 2.6) takes the form of sheets <5 m thick and 10-100 m long. These sheets may be traced >25 m transverse to flow. The base of element GB is defined by a flat or irregular fourth order bounding surface Figure 2.2). The sediments are conglomerates to sandy conglomerates (Table 2.4), with clasts normally graded, from cobbles to coarse sands, indicating a waning of flow.

| MAJOR CHANNEL ELEMENT (CH) | INTRA-CHANNEL ELEMENTS | GRAVEL BEDFORM GB | Sheets <5 m thick & 25-100m lateral extent. Base represented by 3 rd. order bounding surface or higher. Internally crudely cross-stratified, indicating downstream accretion. |
|---|---|---|---|
| | | LATERAL ACCRETION LA | Planar lower 2 nd. order bounding surface dipping <15° oblique to transport direction. Overall fining upwards. Lower terminations downlap channel floor.<3 m extent in all directions. |
| | | DOWNSTREAM ACCRETION DA | TYPE 1. Bounded by 3 rd. order surface. 1-5 m thick & 20 m lateral extent. Unit comprises basal conglomerate, passing upward into large scale Sp/St and Sc. An upwards decrease in set size common. <br> TYPE 2. Solitary, simple Spg or Stg sets bounded by 3 rd. order surfaces. 1-5 m thick & 20 m lateral extent. Foresets may show some modification by intrasets. |
| | | SANDY BEDFORM SB | TYPE 1. Sp or St or combination of the two arranged in units of upwardly decreasing set size. Bounded by 2 nd. order surfaces. 1-2 m thick & <10 m lateral extent. <br> Type 2. Vertically stacked 2-D & 3-D dunes bounded by planar to concave up 2 nd. order bounding surfaces. 0.50-2 m thick & <10 m lateral extent. No clear variation in set size. High palaeocurrent variance. |
| | | MASSIVE SM | TYPE 1. Laterally extensive sheets bounded by 3 rd. order surfaces.<8 m thick & >250 m lateral extent. Basal scour overlain by massive sandstone containing diffuse laminae and solitary 2-D or 3-D dunes. <br> TYPE 2. Channelised sediments bounded by 2C bounding surfaces. <120 m wide & 4.5 m deep. Elongate parallel to flow >30 m. Erosional/non-erosional base passes upwards into massive sandstone fill with/without concentric marginal laminae and water escape structures. <br> TYPE 3. Erosively based, laterally extensive sheets bounded by 3 rd order surfaces or higher. >250 m lateral extent & <6 m thick. Basal scours <8 m deep. Internally massive sandstone contains angular mudclasts <10 m diameter. |
| | | HETEROLITHIC H | Interbedded sandstone/mudstone <5 m thick & 20 m lateral extent. Bounded by 3 rd. order bounding surfaces. Uni-directional palaeocurrents with high variance. Set size and grain size fine upwards with increased organic content. |
| | CHANNEL MARGIN ELEMENTS | CHANNEL MARGIN CM | Upward coarsening mudstone to sandstone with upward increase in set size. High organic content and localised rooting. Bounded by 3 rd order bounding surfaces. <1 m thick & <5 m lateral extent. Palaeoflow perpendicular to main fluvial channel. |
| | INTER-CHANNEL ELEMENTS | INTER-CHANNEL IC | TYPE 1. <0.50 m thick > 20 m lateral extent. Consists of alternations of mudstone/siltstone & palaeosol. <br> TYPE 2. < 2 m thick & < 50 m lateral extent. Consists of alternations of rhythmically bedded mudstone/siltstone, palaeosol, coal & marine shale. |

Table 2.6. A summary of the architectural elements identified within this study.

This element is generally structured by diffuse cross-stratification, indicating downstream accretion. The element is therefore interpreted as a downstream migrating bedform, deposited during periods of high flow competence.

Sand dominated architectural elements take a number of forms which are both downstream and laterally accreting (Table 2.6). Downstream accreting macroform scale elements (DA) are divided into two types (Table 2.6). The identification of a macroform is made on the evidence of long term accretion along an inclined plane (Friend 1983, Miall 1988).

DA Type 1 (Figure 2.3a) is characterised by a fining upwards assemblage of facies, deposited over an undulose third order bounding surface. An idealised sequence consists of 1) thin conglomerate, 2) large scale or giant planar or trough cross-stratification (Table 2.4), and 3) compound cross-stratification (Figure 2.2). The compound cross-stratification may grade downstream into small scale trough or planar cross-stratification (Table 2.4). Palaeocurrent variance within the larger scale bedforms of the element is low, and increases in the small scale dunes. An upward decrease in set size is common, indicating waning flow conditions (Figure 2.3a).

Architectural element DA Type 1 is interpreted in terms of a macroform (Table 2.1) deposited within a major channel. This type of element is similar to the mid-channel bars of Haszeldine (1983a & b). The basal third order bounding surface is interpreted as the scour surface of a migrating macroform. The thin conglomerate represents deposition on the channel floor, and the large scale cross-stratification represents the deposits of 2-D and 3-D migrating dunes. Compound cross-stratification developed due to the migration of medium and small scale bedforms down the lee face of a larger bedform. The downstream evolution of compound cross-stratification into small scale dunes indicates deposition across the bar platform and tail (Haszeldine 1983a). Splitting of the flow by the bar resulted in oblique dune migration and hence an increase in palaeoflow variance (Figure 2.3a).

The DA Type 2 element (Table 2.6, Figure 2.3b) consists of isolated planar or trough cross-stratified sets of a large or giant scale (Table 2.4). The base and upper surfaces of these units are marked by third order bounding surfaces (Figure 2.2, Table 2.3). Sets may be traced in excess of 50 m downstream, and have a width, transverse to flow of >20 m. Internally these bedforms are of simple structure, with steep foresets, which may include locally developed intrasets (Figure 2.3b). Small scale reactivation surfaces within the element reflect either minor changes in sediment accretion due to local flow fluctuations, or minor discharge variations in the channel (McCabe & Jones 1977).

5 m

Plan View

Tail

Head

Palaeoflow direction
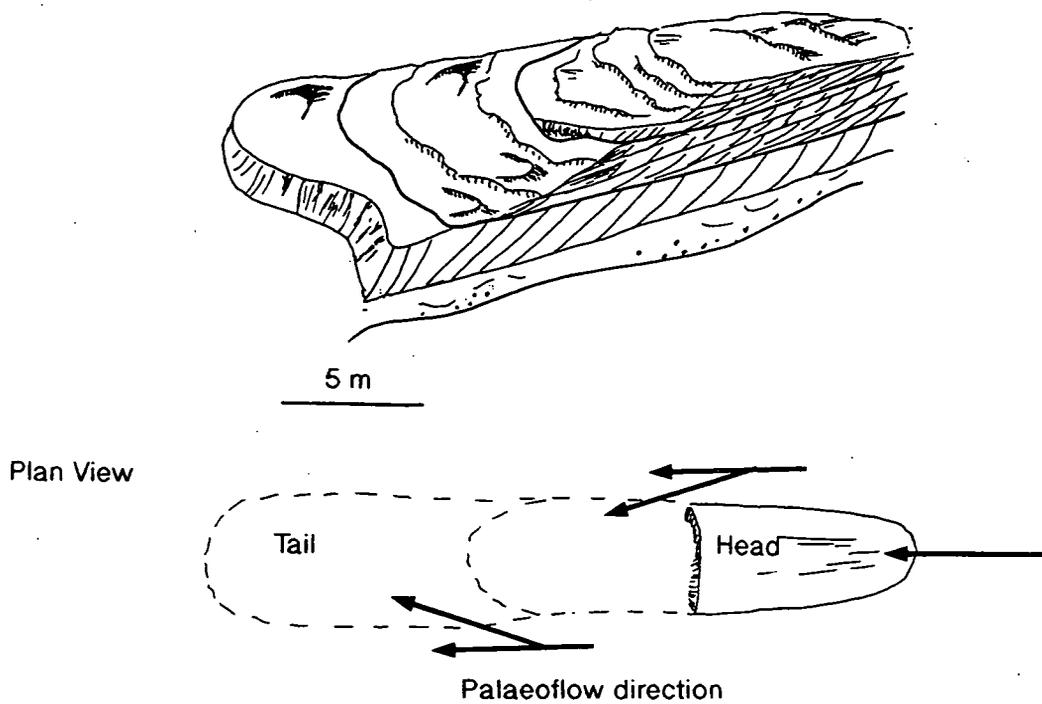
*2.3a. Reconstruction of a DA Type 1 macroform architectural element, and palaeoflow patterns associated with such a mid-channel bar.*



5 m

Plan View

Bank

Head

Tail
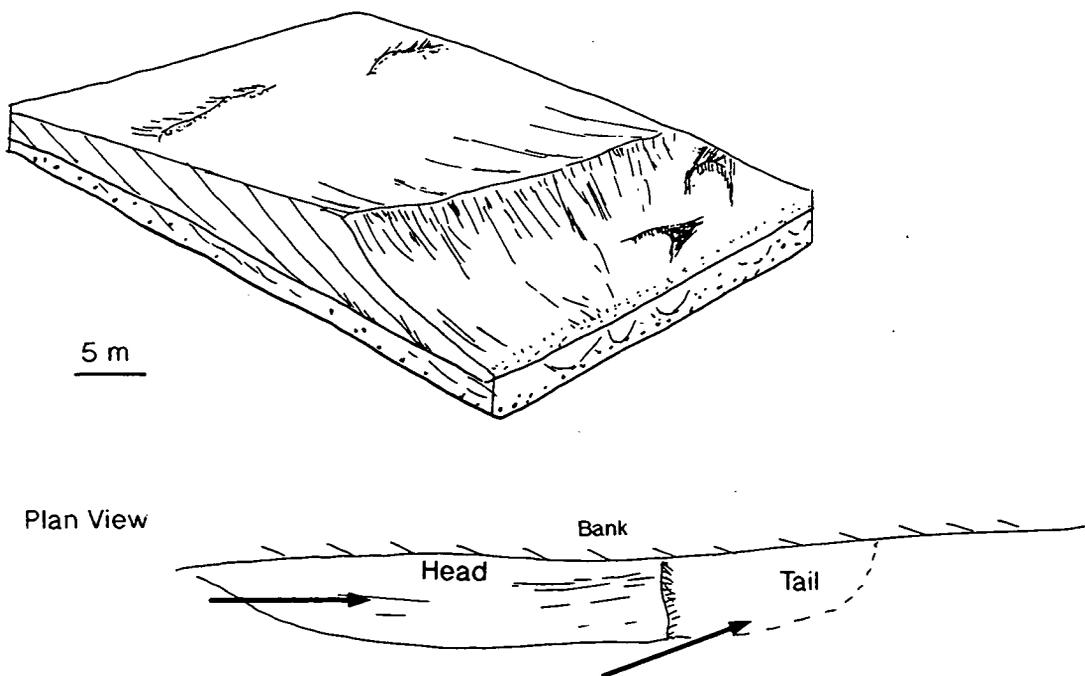
*2.3b. Reconstruction of a DA Type 2 macroform architectural element, and palaeoflow patterns associated with such bank attached bars.*

*Figure 2.3. Diagrammatic representations of the DA architectural elements described within the text and in Table 2.6.*

Miall (1985) interpreted such giant cross-bedded deposits as mesoforms, deposited by migrating 3-D dunes. McCabe (1977) interpreted giant cross-beds to be downstream accreting slip-face deposits of alternate, bank attached bars (Table 2.1), deposited in a low sinuosity channel. The evidence of small scale reactivation within the bedforms, and the localised development of intrasets, indicates that DA Type 2 elements existed for considerable lengths of time (in excess of one flood cycle), and hence may be described as macroforms. The DA Type 2 element is therefore interpreted as a simple macroform deposit, of either bank attached or mid-channel affinity.

Many cross-bedded sandstone facies deposited by downstream accreting bedforms do not relate to the deposition of macroforms, and occur on the scale of mesoforms. Such deposits include isolated sets or cosets of planar and trough cross-stratification which are the deposits of trains of straight crested or curved crested dunes. Two mesoform scale architectural elements have been identified. These are termed SB Types 1 and 2 (Table 2.6).

The SB Type 1 architectural element consists of planar or trough cross-stratified cosets showing an upward decrease in set size from medium to small scale (Table 2.4). Palaeocurrent variance increases upwards through the element. The SB Type 1 element is bounded by planar to concave up second order bounding surfaces. Sediments similar in character to SB Type 1 architectural elements have been described from the modern Platte River as linguoid (Blodgett & Stanley 1980) or transverse (Smith 1970) bars. These bars consist of well developed sets of planar cross-stratification which grade upstream and vertically into trough cross-stratification. Transverse and linguoid bars have been interpreted as the deposits of waning flow conditions (Smith 1970, Blodgett & Stanley 1980). The SB Type 1 architectural element is therefore interpreted as the deposit of a single flood cycle, with deposition occurring under waning flow conditions. An increase in palaeoflow variance upwards through the architectural element is due to shallowing of flow conditions over the dune.

The SB Type 2 architectural element of Table 2.6. consists of cosets of cross-stratification divided by second order bounding surfaces (2A of Table 2.3). There is no recognisable vertical variation in set size within this element. Palaeocurrent variance is high. The SB architectural element is interpreted in terms of vertical aggradation during long or short term changes in flow regime. The elements may occur in the channel or over bars (Miall 1985).

Lateral accretion elements (LA) are recognised by the presence of low angle bedding surfaces (<15-20°) which dip in a direction normal to the palaeoflow as measured from cross-stratification (Table 2.6). The base of the LA element is erosional and marked by a third order bounding surface. The upper surface is gradational, where

it has not been removed through migration of an overlying bedform. The internal geometry of this element is highly variable. Planar and trough cross-stratification are developed, and display variable palaeocurrent directions. A conglomerate may be deposited at the base of the element. The thickness of element LA is directly related to the bankfull depth of the channel.

Three gross geometries of massive sandstone (SM) architectural elements have been identified, and these are illustrated in Table 2.6. The variation in geometry of the architectural element types reflects differences in depositional processes which are discussed in detail in Chapter 7.

An upward-fining heterolithic element, H (Table 2.6), consists of thin beds of fine sand and mudstone, with the bed thickness of sandstone decreasing upwards. The sediments contain large amounts of organic matter and thin coal horizons. Sandstones are structured by ripple cross-lamination indicating deposition from a uni-directional current. This element is interpreted as a channel abandonment facies. Waning of flow is indicated by the decrease in bed thickness and the reduction in grain size.

Intra-channel architectural elements combine to form major channel elements (CH) of 10-30 m in thickness. Major channel elements comprise a complete fluvial channel belt, and as such are defined by fourth order bounding surfaces (Table 2.3) which have concave-up erosional bases, and sloping margins. The fourth order bounding surfaces represent scour surfaces generated during initiation of channels b y avulsion, or lowering of local base level. Fining-upward trends define channel fills, with a basal conglomerate or conglomeratic sandstone (GB) passing into cross-bedded sandstone and fine grained sands and silts (H). The fining-upwards of sediments indicates a waning of the depositional current. Complete channel fills of this type are rare, as the deposition of an overlying channel commonly erodes the upper portion of the preserved section beneath. Amalgamation of partially preserved CH elements results in the preservation of a multistorey sheet sandbody.

*Channel-margin Architectural Elements.*

The channel-margin element (CM) preserves sediments deposited in overbank areas under the influence of the fluvial channel. The element is preserved adjacent to the channel. CM (Table 2.6) is <1 m thick and may be traced laterally for up to 5 m. Element CM consists of alternations of carbonaceous claystone and fine grained sandstone, with bed thickness and grain size both upward-coarsening and upward-fining. Sandstones display ripple cross-lamination, with disseminated organic matter concentrated in the base of the beds. Sandstone beds thin away from the channel.

Element CM is interpreted as the deposit of levees and/or crevasse splays. The lack of three-dimensional exposure results in the lack of differentiation between levee and crevasse splay deposits. The upward increase in grain size and bed thickness indicates an increase in bed shear stress, related to flood events, and vertical aggradation. Fining-upwards units represent deposition under conditions of waning flow and abandonment.

*Inter-channel Architectural Elements.*

Inter-channel elements are defined as those deposited in regions removed from the influence of the channel sandbody. Inter-channel architectural elements are divided into two types (IC Type 1 and IC Type 2) as illustrated in Table 2.6. Both types of inter-channel element contain alternations of fine grained sandstone and mud, with coal and palaeosol horizons. IC Type 1 elements are interpreted as the deposits of a fluvial floodplain which was periodically vegetated.

The IC Type 2 architectural element is more complex than the IC Type 1. The element is flasar to wavy bedded, with each sandstone ripple draped by a laterally persistent mud layer. In the vertical scale the height of the sandstone ripples systematically increases and decreases. Such cycles have been interpreted as the deposits of neap-spring cycles (Fishbaugh *et al* 1989), in estuarine environments. IC Type 2 also contains thin shale bands of marine affinity. This architectural element is therefore interpreted as the preserved remains of a tidal flat or tidally influenced floodplain.

## 2.5.2. Palaeohydrology.

The term palaeohydrology is used to describe the reconstruction of fluvial channel pattern and hydrology from sediments preserved in the rock record. All methods of palaeoflow reconstruction are based on direct analogues. The micro approach concentrates on the geomorphic relationships between sediment and flow parameters in modern rivers or flumes. This approach therefore estimates short term velocity and discharge conditions. Alternatively the macro approach assesses the geomorphological relationships between channel morphology, channel sediments and channel discharge in modern rivers, thus estimating the longer term development of equilibrium conditions between the channel and flow (Maizels 1983).

Many studies have concentrated on reconstructing channel depth using point bar deposits, as defined by lateral accretion surfaces (Cotter 1971; Leeder 1973). Maximum channel depth is equivalent to the thickness of the channel sand, if only one

fining-upward cycle is preserved. However, large scale lateral accretion surfaces are rare or absent within ancient braided stream deposits

As discussed in section 2.1. channel pattern is controlled by variations of discharge and sediment load which have been quantified in studies of modern rivers including those of Leopold & Wolman (1957), Allen (1968) and Schumm (1960,1968a,1972). These studies have identified the empirical relationships existing between sedimentary and hydrological variables.

The family of empirical relationships developed by Schumm (1960, 1968a) were based on data gathered from rivers transporting only sand and finer grade of sediment in sub-humid and sub-arid climates of the central USA and Australia. As such these relationships may be applied to the sand grade sediments studied herein. The rivers studied by Schumm (1960, 1968a) had a bankfull depth of less then 2 m. Care must be taken with use of these equations, due to the limited data set used to establish them. Another important factor to consider is that Schumm (1968a) defined the width/depth ratio of a river as a parameter which could be used to differentiate between modern channel planforms. The width/depth ratio was then related directly to the sediment load parameter $M$. However, the width/depth ratio of large sinuous rivers overlaps with that of smaller low sinuosity rivers (Leeder 1973), thus width/depth ratio alone is not a reliable measure of river planform. It is therefore important to avoid the use of $M$ where it is directly correlated with the width/depth ratio. In this study this problem has been circumvented by avoiding the use of $M$ as a parameter.

Several workers have attempted to construct flow parameters of braided systems from the rock record using the empirical relationships established by Schumm (1968a). Miall (1976) reconstructed the sinuosity, flow velocity and discharge of the Isachen Formation, a Cretaceous braided stream deposit from Banks Island, Canada. Turner (1980) reconstructed palaeohydraulic parameters including discharge and drainage area of the Upper Triassic of the Karoo Basin, South Africa. This method of palaeohydraulic reconstruction has passed out of fashion. Palaeohydrological reconstruction is used here to establish the order of magnitude of flow rather than any precise parameters.

In order to estimate palaeoflow parameters major assumptions must be made. Steady, uniform flow must be assumed, and one must also assume that the channel cross section remains rigid with no sediment movement (Maizels 1983). Where flow is steady and uniform it is assumed that the bed configuration is in equilibrium with the flow (Middleton & Southard 1978).

Sinuosity is characteristic of channel pattern, and palaeocurrent variance has long been used to infer relative sinuosity of ancient rivers e.g. Kelling (1968). The

palaeocurrents of ancient fluvial deposits are linked to the directional range and sinuosity of a river channel. However, a relationship between directional variance and channel sinuosity can only be expected where the direction of bedform migration is generally parallel to the channel banks. Miall (1976) identified that the sedimentary structures preserved within braided rivers have greatest preservation potential where they are oriented parallel to the persistent current. It is therefore logical to assume that the majority of larger scale preserved bedforms migrated parallel to the channel banks. Such migration is illustrated in Figures 2.3 a and 2.3b.

To estimate the palaeocurrent of a channel from preserved bedforms one must assume that the bedforms within the braided river were non-emergent and migrating downstream (i.e. with no lateral accretion component). A circular normal distribution must also be assumed (Olsen 1993). A large number of palaeocurrent measurements from all hierarchies within the fluvial system must be taken so as to avoid any bias towards smaller scale structures with a higher directional variance.

If the system is envisaged as a part of a circle, then the arc of the circle represents the shape of the channel, and the chord of the circle represents the sinuosity (Le Roux 1992). The length of the arc is defined by the angular range of palaeocurrent measurements ($\theta$). Although based on a single meander, this theory may be applied to successive meanders (Le Roux 1992). Problems arise when the full range of palaeocurrent data is used as this may result in over-estimation of the sinuosity. Le Roux (1992, 1993, 1994) offers a method whereby an operational range of palaeocurrent values are used to establish sinuosity, with the operational range derived from the standard deviation of the original palaeoflow readings. However, it is useful to know the maximum sinuosity, and therefore only measurements from the original data set have been used within this study.

Sinuosity ($P$) of fluvial channel has been estimated using $\theta$ to represent the angular range of the palaeocurrent measurements.

$$P = \pi \ (\theta/360)/\{\sin \ (\theta/2)\}$$

where the operational range is less than 180°, and

$$P = \pi \ (\theta/360)/\{\sin \ [(360-\theta)/2]\}$$

where the operational range is greater than 180°.

The width/depth ratio ($F$) of modern streams is related to the sinuosity (Schumm 1968a, 1972) by:

$$P = 3.5 \ F^{-0.27}$$

By rearranging this equation:

$$F = (P \ / \ 3.5)^{-1/0.27}$$

it is possible to estimate the width/depth ratio of a palaeochannel using values of the sinuosity.

Water depth $(d)$ may be estimated from the height, $h$, of preserved bedforms. The height of dunes is related to the boundary layer thickness (Allen 1968 1982) i.e. the depth of the formative flow. A relationship exists between the mean dune height, $h$, and mean water depth, $d$, which is illustrated in Figure 2.4. It is clear that a wide spread of values exists, and this is a possible reflection of unsteadiness and non-uniformity of flow, and differences in the water temperature of the different rivers measured.
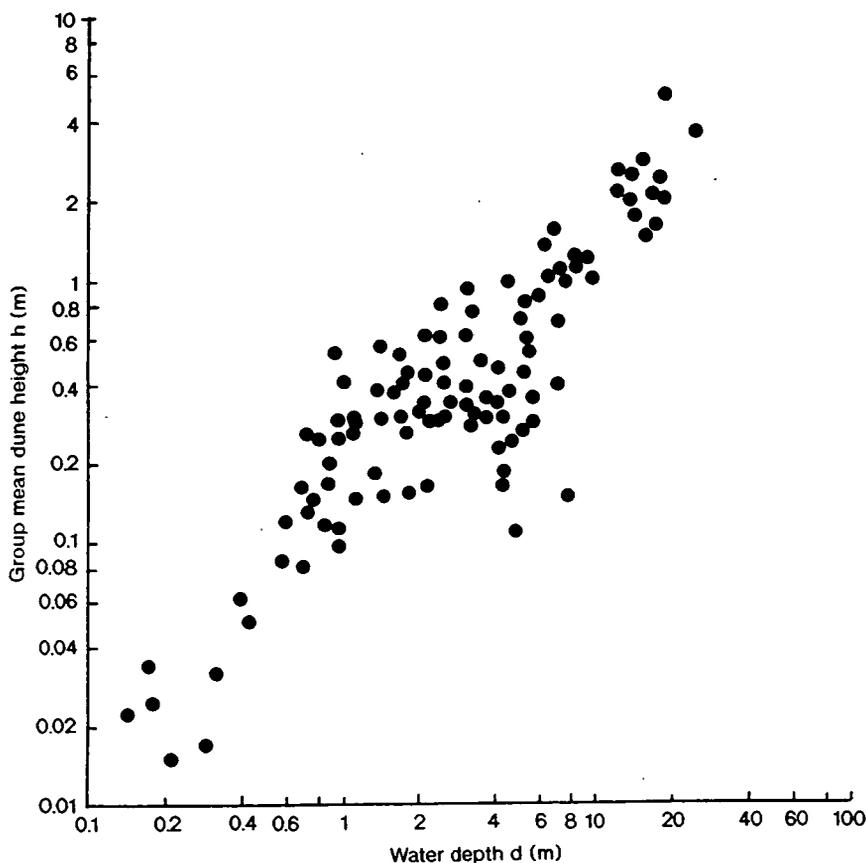


Figure 2.4. Correlation between group mean height (h) and mean water depth (d) for dunes in modern rivers (modified from Allen 1982).

In order to estimate the depth of flow from the height of preserved bedforms it is necessary to measure a large number of bedforms which were deposited by migrating dunes (i.e. scaled to depth). The erosion of the foreset tops of a bedform means that the preserved cross-strata represent the minimum thickness of a dune. Compaction of sand also results in the under-estimation of the original dune height. Correction may be made for compaction using:

$$h_o = h_c \left[ (1 - \phi_c) / (1 - \phi_o) \right]$$

Where $h_o$ represents the original thickness of the bedform and $h_c$ represents the compacted thickness of the bedform. $\phi_o$ represents the original porosity. The primary porosity of fluvial sands was addressed by Pryor (1973) who established that fluvial sands as represented by point bar deposits have depositional porosities ranging from 17-52%, with a mean of 40%. This value has been used as the primary depositional value within this study. The compacted porosity ($\phi_c$) is estimated through measurements from thin sections of sandstone samples. The value calculated for $h_o$ may then be used to estimate the water depth at the time of deposition using Figure 2.4. The mean width ($W$) of the fluvial channel may be established using values established for the flow depth and width/depth ratio.

The reconstruction of flow velocity may be attempted in many ways, both through the macro and micro approaches. Flow competence may only be directly related to particle size where median or mean grain size is > 5 mm (Maizels 1983). Bedform existence fields such as those developed by Jopling (1966) define the hydrological parameters for the existence of bedforms within uni-directional flow. However, studies such as those of Southard & Boguchwal (1990) do not generally analyse flows of greater than 1 m in depth.

An estimate of the flow velocity within a fluvial channel assumes that the sediments carried by the flow represent the maximum competence of that flow. Within a braided river system the sediment is known to have been transported as bedload. It is well established experimentally that for steady uniform flow over an erodable sediment bed in a channel of given geometry, $d$ and $v$ will specify the flow (Middleton & Southard 1978). By relating the sedimentary structures preserved, to the bed configuration, the velocity profile or $d$ is taken into account (Turner 1980). The velocity of flow may be established by relating the bedforms present, and their grain size, to velocity using the diagrams of Harms et al (1982) as illustrated in Figure 2.1. A range of velocity values will be measured from the graph, and for the purposes of the study the mean of this range of values is taken as the velocity of the flow.

In assuming no change in the vertical velocity profile through the river channel, and assuming that the channel boundary is rigid, it is possible to assume constancy of the equation:

$$Q_m = W.\ d.\ v$$

Where $Q_m$ represents the mean average discharge of the fluvial system (m³/s).

Although empirical relationships exist to calculate the flood discharge, length and area of the drainage net, it is felt that these equations are too generalised, and will offer no useful information to this study.

# Chapter 3
# The Northumberland Basin

## 3.1. Regional Geological History Of The Northumberland Basin.

In late Devonian to early Carboniferous times the structure of northern England was dominated by a number of basins and blocks. Differential subsidence allowed for the accumulation of thick sedimentary successions in the rapidly subsiding basins, with thinner incomplete successions deposited over the blocks. The relative positions of the positive blocks and basinal areas during the Dinantian are illustrated in Figure 3.1.
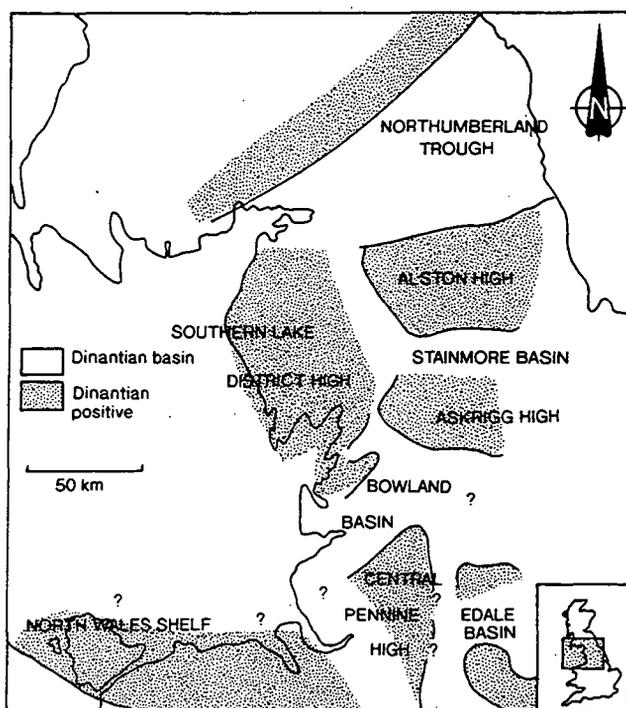


*Figure 3.1. The Dinantian palaeogeography of northern England (modified from Gawthorpe et al 1989).*

The largest of the Carboniferous basins was the Northumberland Trough (Figure 3.1), a northeast-southwest oriented half graben structure, bounded to the north by the Southern Uplands, and to the south by the Alston Block along the line of the Stublick-Ninety Fathom Fault system (Figure 3.2a & b).
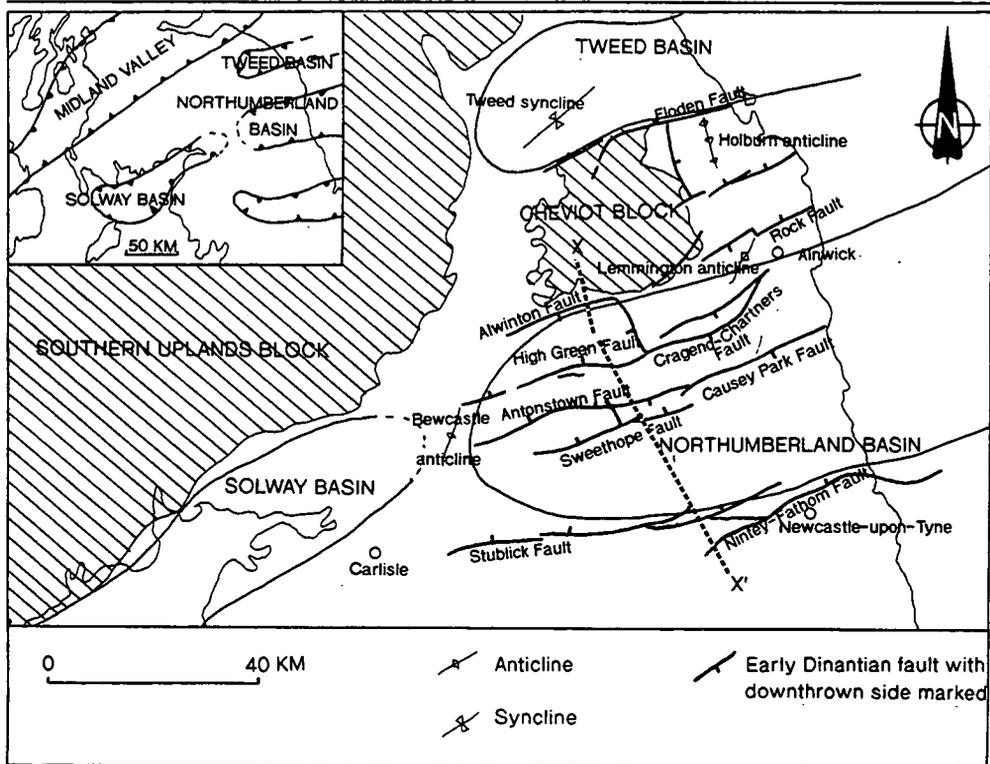
*Figure 3.2a. The structure of the Northumberland Trough (modified from Johnson 1984; Leeder et al 1989 & Turner et al 1993).*
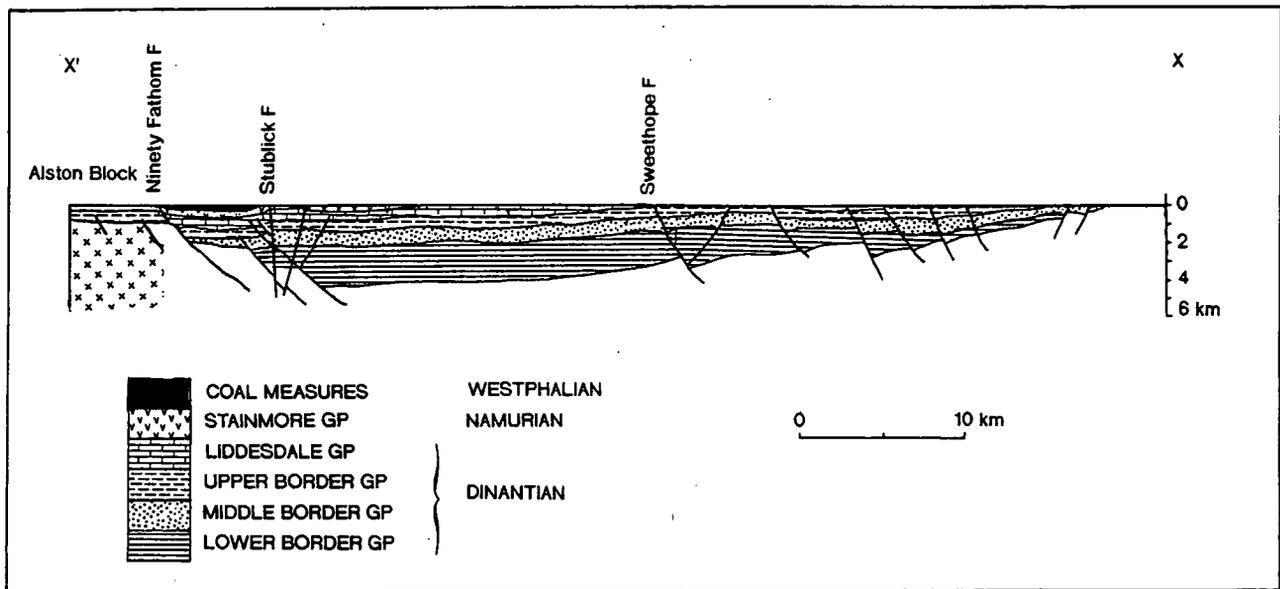


*Figure 3.2b. A present day geological cross-section of the Northumberland Basin (modified from Kimbell et al 1989).*

The Northumberland Trough contains two basins: the Solway Basin to the west and the Northumberland Basin to the east (Figure 3.2a). The basins are separated by a shallow shelf formed by an uplifted basement block underlying the Bewcastle Anticline (Figure 3.2a). The Northumberland Basin includes the smaller Tweed Basin to the northeast which is separated from the main Northumberland Basin by the east/west oriented Cheviot axis (Figure 3.2a). The stratigraphical nomenclature of the Northumberland Basin is detailed in Figure 3.3, and a generalised history of the basin is illustrated in Table 3.1.

| SYSTEM | | SERIES | STAGE | AGE Ma | ALSTON BLOCK | NORTHUMBERLAND BASIN WEST | NORTHUMBERLAND BASIN EAST |
|---|---|---|---|---|---|---|---|
| UPPER CARBONIFEROUS | SILESIAN | WESTPHALIAN ST | | 300 / 305 | | Upper Coal Measures | |
| | | WESTPHALIAN | D | 308 | | Upper Coal Measures | Middle Coal Measures |
| | | WESTPHALIAN | C | 311 | | Middle Coal Measures | Middle Coal Measures |
| | | WESTPHALIAN | B | | | Middle Coal Measures | Middle Coal Measures |
| | | WESTPHALIAN | A | 315 | | Lower Coal Measures | Lower Coal Measures |
| | | NAMURIAN | Yeadonian Marsdenian Kinderscoutian Alportian Chokierian Arnsbergian Pendleian | | Stainmore Group | Millstone Grit Series | Millstone Grit |
| | | | | 326 | Stainmore Group | Millstone Grit Series | Upper Limestone Group |
| LOWER CARBONIFEROUS | DINANTIAN | VISEAN | BRIGANTIAN | | Upper Alston Group | Upper Liddesdale Group | Middle Limestone Group |
| | | | | | Upper Alston Group | Lwr Liddesdale Group | Lwr Limestone Group |
| | | | ASBIAN | | Lwr Alston Group | Upper Border Group | Scremerston Coal Group |
| | | | HOLKERIAN | 335 | Orton Group | Middle Border Group ?– | Fell Sandstone Group |
| | | | ARUNDIAN | | Orton Group / Cambeck Beds | Cambeck Beds / Lower Border Group | Fell Sandstone Group |
| | | | CHADIAN | | Weardale Granite | Lower Border Group | Cementstone Group |
| | | TO | COURCEYAN | 350 / 360 | | —?— ?— | not exposed |
| DEVONIAN | | | | | | | |

Figure 3.3. Stratigraphy of the Northumberland Basin succession (after Kimbell et al 1989; Fordham 1989 & Turner et al 1993). Radiometric ages after Leeder (1988a).

| SYSTEM | SERIES | STAGE | AGE (MA) | CLIMATE | PALAEO LAT | EXTENSION | COMPRESSION | SEDIMENTATION | TECTONICS |
|---|---|---|---|---|---|---|---|---|---|
| PERMIAN | | | 250 | | | | | | |
| PERMIAN | Tartarian | | | | | | | | |
| PERMIAN | Kazanian | | 260 | Arid | | | | | Tectonic instability leading to local erosion. |
| PERMIAN | Kungurian | | 270 | Arid | | | | | |
| PERMIAN | Samarian | | 280 | | | | | Mid-Permian yellow sands. | Permo-Mesozoic dextral transtension related to early rifting in the northern North Sea. |
| PERMIAN | Asselian | | 290 | | | | | | |
| PERMIAN | | | 300 | | | | | | Renewed extension associated with the emplacement of the Whin Sill. Inversion Event. |
| CARBONIFEROUS | STEPHANIAN | | | | | | | | |
| CARBONIFEROUS | WESTPHALIAN | D | | Uniform wet | | | | Latest preserved sediments of Westphalian C age. | |
| CARBONIFEROUS | WESTPHALIAN | C | 310 | | | | | Coal Measures: fluvio-deltaic sedimentation with short-lived marine incursions. Cyclic sedimentation. Some small fault control. | |
| CARBONIFEROUS | WESTPHALIAN | B | | | | | | | |
| CARBONIFEROUS | WESTPHALIAN | A | | | | | | | Thermal relaxation. |
| CARBONIFEROUS | NAMURIAN | | 320 | Humid | | | | Namurian Yoredale cycles associated with delta progradation and drowning. | Active faulting ceases in the early Namurian. |
| CARBONIFEROUS | NAMURIAN | | | | | | | Deltaic sedimentation with periodic marine drowning. Limestone horizons regionally extensive. | |
| CARBONIFEROUS | VISEAN | Brigantian | 330 | | | | | | |
| CARBONIFEROUS | VISEAN | Asbian | | | | | | Fluvio-deltaic environment of sedimentation with coal horizons common. Braided rivers drained into deltas in the west of the basin. | |
| CARBONIFEROUS | VISEAN | Holkerian | | | | | | | |
| CARBONIFEROUS | VISEAN | Arundian | 340 | Sub-humid | | | | | Pulsed syn-depositional faulting, normal and antithetic faulting. Most deformation within the Lower Border Group & equivalents (early-middle Dinantian). |
| CARBONIFEROUS | VISEAN | Chadian | | | | | | Lower Border Group: fluvio-deltaic sedimentation with localised hypersaline lakes. | |
| CARBONIFEROUS | TOURNASIAN | Courceyan | 350 | Arid | | | | | |
| CARBONIFEROUS | TOURNASIAN | Courceyan | 360 | | | | | | Time scale from Leeder (1988a). Information derived from: Collier (1989); Leeder et al (1989); Kimbell et al (1989); Chadwick et al (1993). |
| DEV | Famennian | | | | | | | | |

34

*Table 3.1. A generalised history of the Northumberland Basin.*

The basement of the Northumberland Trough is composed of Lower Palaeozoic and early Devonian sedimentary, volcanic and intrusive rocks (Chadwick *et al* 1993). During the Upper Devonian, reddened conglomerates, sands and silts were deposited in northeast flowing alluvial systems (Leeder 1974), as illustrated in Figure 3.4a. In the west of the Northumberland Basin, the Upper ORS sediments are overlain by basaltic lavas (Table 3.1), which mark the onset of the Northumberland Trough as a structural entity (Kimbell *et al* 1989). A number of workers have invoked models to explain the extensional initiation of the Northumberland Trough, and these are discussed by Leeder (1988a), Turner (1989) and Chadwick & Holliday (1991).
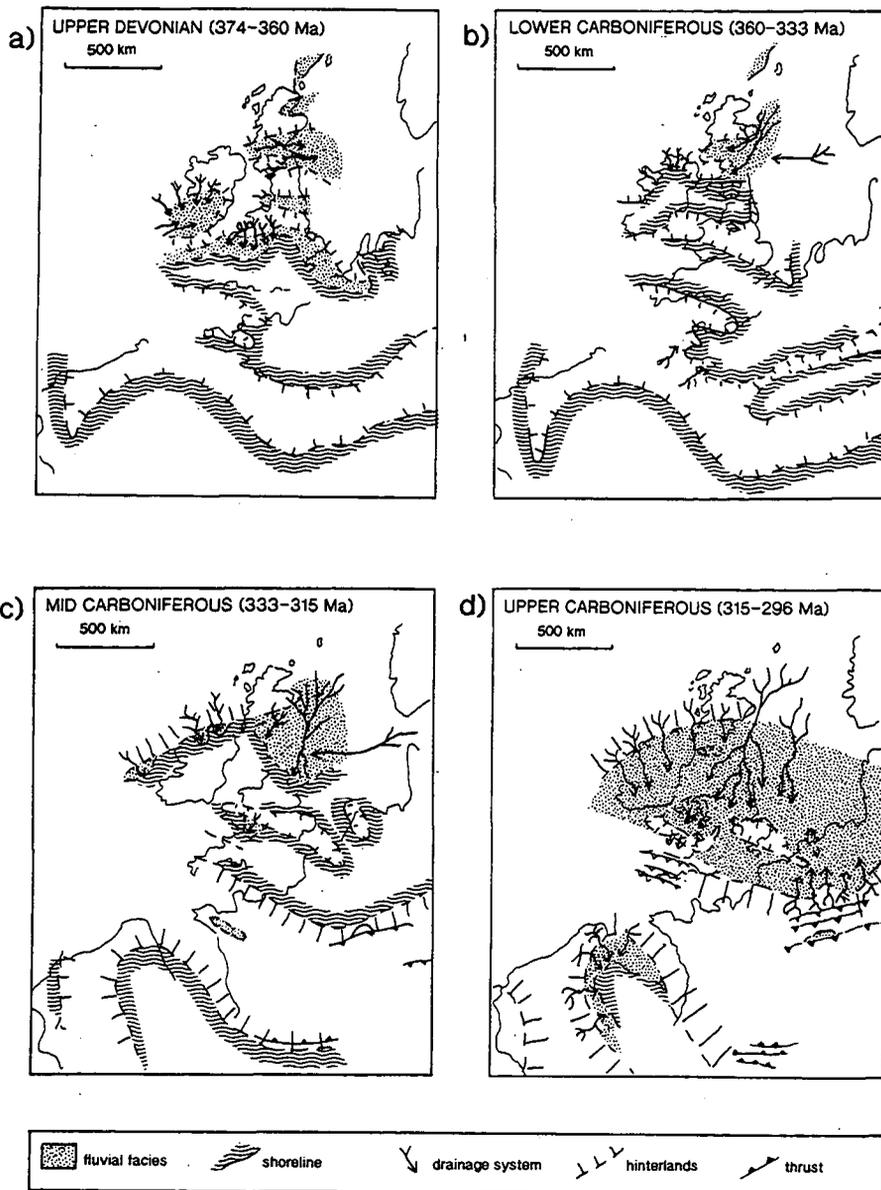


Figure 3.4. Palaeogeographic reconstructions of northwest Europe (modified from Leeder 1988b & Leeder et al 1989).

Carboniferous syn-sedimentary subsidence occurred across the entire Northumberland Trough, but was greatest on the southern boundary, along the Stublick-Ninety Fathom Fault System (Figure 3.2a), resulting in an asymmetric basin profile (Figure 3.2b). Extension has been inferred to have take place during one episode with greatest subsidence in the Dinantian (Kimbell *et al* 1989), or as a number of tectonically active phases separated by intervals of quiescence (Gawthorpe *et al* 1989; Fraser & Gawthorpe 1990). Chadwick *et al* (1993) concluded that basin subsidence was pulsed, with the timing and magnitude of extension varying across the basin.

Syn-depositional faults inferred to have been active during the Dinantian are illustrated in Figure 3.5. Faults were dominantly oriented east-west, with dip directions to the north, such as the Stublick-Ninety Fathom Fault System (Kimbell *et al* 1989). Other faults, especially those to the south of the Cheviot Block, dip south and are interpreted as antithetic faults (Kimbell *et al* 1989). Some syn-depositional faults are oriented northwest or north-northwest, oblique to the dominant plane, and these are interpreted as transfer faults (Kimbell *et al* 1989).

The Carboniferous is represented by approximately 4,500 m of sediment within the Northumberland Basin, thinning to 1,500 m across the Tweed Basin. During the Courceyan and Chadian extensional subsidence was rapid, resulting in the destruction of the Old Red Sandstone internal drainage system (Chadwick *et al* 1993).

The Lower Border Group, and its lateral equivalents (Figure 3.3) reach a maximum thickness of 900 m in the Northumberland Trough (Leeder *et al* 1989). The Cementstones (Figure 3.3) comprise a thick succession of shales, impure limestones and sandstone (Johnson 1984), and represent deposition within fluvial, deltaic and coastal plain environments (Leeder 1974). Fluvial systems of the Fell Sandstone Group, and equivalents in the Lower Border Group, drained south and west across the basin into a shallow gulf in the west (Figure 3.4b). A thick succession of Chadian to Holkerian sediments in the area of the Bewcastle anticline (Figure 3.2a) comprises fluvio-deltaic facies, which alternate with marine carbonates of the Cambeck Beds.

The Middle Border Group exhibits marked lateral changes in facies, reflecting an increase in clastic supply from the northeast. The Group is dominated by sandbodies of low sinuosity, braidplain origin which are separated by thin red mudstones. Palaeoflow was to the south and west, and thickening trends indicate significant syn-sedimentary fault movements. The fluvial sediments of the Fell Sandstone were deposited across a tectonically active floodplain (Turner *et al* 1993), which was open to marine influences to the southwest via the Bewcastle delta system (Armstrong & Purnell 1987). To the south, marine conditions are represented by limestones of the Orton Group (Figure 3.3).
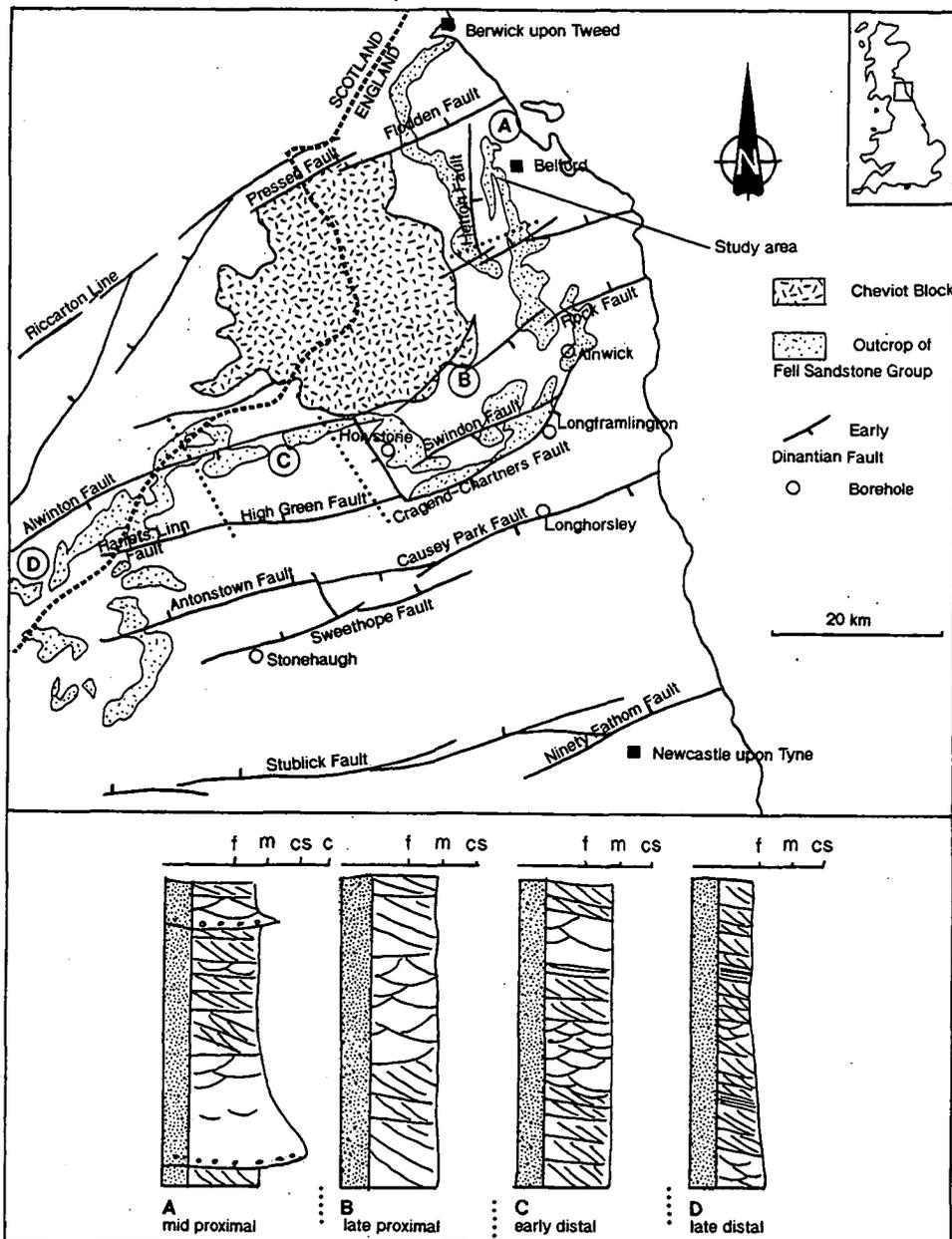
*Figure 3.5. Dinantian fault systems of the Northumberland Basin, together with the outcrop pattern of the Fell Sandstone Group and the facies associations identified b y Monro (1986).*

The Upper Border Group and the equivalent Scremerston Coal Group (Figure 3.3) were deposited in deltaic environments, with sedimentary cycles consisting of argillaceous limestone, shale, quartzitic sandstone, seatearth and coal (Johnson 1984). Palaeoflow was to the south and west (Leeder *et al* 1989).

The Lower and Middle Limestone Groups and the Liddesdale Group (Figure 3.3) were more uniformly deposited across the Northumberland Trough than the underlying sediments, although there is evidence to suggest continued differential subsidence (Leeder *et al* 1989). At this time the Cheviot axis was subdued and the Northumberland and Tweed Basins were connected. The Liddesdale Group and equivalents were deposited in fluvio-deltaic systems, flowing towards the southeast and southwest (Leeder *et al* 1989), with coal swamps developed in inter-distributary channel areas. Sedimentation was cyclical, with deltas periodically drowned by marine inundations. Thick limestones extended northwards and eastwards over the Northumberland Trough and Cheviot axis.

Active extension within the Northumberland Trough ceased in the early Namurian, although thermal subsidence continued into the Westphalian (Table 3.1). Sedimentation continued to occur in fluvio-deltaic environments, and the Upper Limestone and equivalents (Figure 3.3) are similar in lithology to the underlying Dinantian sediments. The Millstone Grit (Figure 3.3) was deposited by southerly flowing braided fluvial systems, as the Namurian deltas expanded (Figure 3.4c).

Sediments of the Coal Measures, represented by strata of Westphalian A, B and C age, were deposited across the lower and upper delta plain within lacustrine, levee, back swamp and distributary channel environments (Figure 3.4d). Fluvial channel sands were deposited by predominantly low sinuosity fluvial systems (Haszeldine 1983a & b) draining a tectonically controlled southerly palaeoslope (Leeder *et al* 1989; Turner & O'Mara in press).

During the late Westphalian and early Permian the Northumberland Trough was subjected to an inversion event, resulting in widespread erosion and deformation. A series of reverse faults (Kimbell *et al* 1989) and folds such as the Bewcastle anticline (Figure 3.2a) provide evidence for basin inversion.

The provenance of Carboniferous sandstones has been studied by a number of workers, and is discussed in detail by Cliff *et al* (1991). Using U-Pb dating techniques Cliff *et al* (1991) interpreted the Carboniferous sediments to have been sourced from hinterlands containing Caledonian granitiods, Proterozoic meta-sediments, and relatively minor outcrops of Archaean basement. These source rocks are interpreted to have been located in Scotland and Scandinavia (Figures 3.4a-d).

## 3.2. The Fell Sandstone Group.

The Fell Sandstone Group forms part of the Viséan fluvio-deltaic succession of the Northumberland and Tweed Basins. The Fell Sandstone overlies the

Cementstone Group with a diachronous base, and ranges in age from Arundian to Holkerian in the eastern Northumberland Basin, and is of Holkerian age in the west (Figure 3.3). The Group reaches a maximum thickness of 350 m in the central parts of the Northumberland Basin, and its outcrop extends in an arc from Burnmouth in southeast Scotland to the Bewcastle area of Cumbria (Figure 3.5).

The Fell Sandstone Group represents a period of source area uplift when fluvial systems prograded across the Northumberland and Tweed Basins (Monro 1986). Sediments were deposited in tropical latitudes, with a warm and temperate climate (Raymond 1985).

The Fell Sandstone Group is dominated by sandstone, with mudstones, limestones and thin coals locally developed. The base of the Group is represented by a poorly exposed conglomerate (Turner *et al* 1993). Sandstones at the base of the Group tend to be more arkosic and lithic than those higher in the succession, particularly in the Tweed Basin (Turner 1989). Monro (1986) recognised four regional facies associations within the Fell sandstone, which are related to a decrease in grain size towards the southwest (Figure 3.5).

In the eastern portions of the Northumberland Trough the Fell Sandstone has relatively clear boundaries. The upper boundary is taken as the top of the first sandstone encountered below the lowest coal seam in the Scremerston Coal Group, and the lower boundary is taken at the base of the lowest sandstone before the Cementstones (see Turner *et al* 1993 for discussion). In the western Northumberland basin the equivalent of the Fell Sandstone is believed to form part of the Lower and Middle Border Groups (Figure 3.3). However, correlation across the basin is difficult due to a lack of lithological markers and poor biostratigraphic control.

Early workers considered the Fell Sandstone to have been deposited in a wholly or partly marine environment (Robson 1956). However, more recent studies (Hodgson 1978; Monro 1986; Turner & Monro 1987) suggest that the Fell Sandstone was deposited by a braided river system which drained southwestward and westward into a shallow marine area.

The Fell Sandstone river delta was located in the Bewcastle area (Figure 3.2a) where the Fell Sandstone splits into at least two major sandstone units, separated b y fine grained marine clastics and carbonates of the Cambeck Beds (Figure 3.3). The sandstone progradation reflects phases of tectonic or autocyclic gradient induced delta shifting and abandonment within the basin, and not, as previously thought, eustatic sea level changes (Turner *et al* 1993). A marine fauna has been recorded by Fordham (1989) from 70.50 m depth in the Alnwick borehole (Figure 3.5) indicating that marine influences extended far into the Northumberland Basin.

The Fell Sandstone Group has been described as a laterally extensive, tabular sheet sandbody (Robson 1980; Heward 1981; Turner & Monro 1987), and Monro (1986) interpreted the deposition of the Fell Sandstone river to have taken place within a non-cyclic braided river system, comparable in size to the Brahmaputra River. However, recent studies of outcrop and cored sections have revealed that the sandstone/shale ratio of the Fell Sandstone varies considerably over the Northumberland and Tweed Basins. The Middle Border Group (Figure 3.3) typically contains 25% sandstone (Fordham 1989). At Burnmouth the Fell Sandstone interval consists of 95% sandstone (Monro 1986), whereas in the Berwick-upon-Tweed area sandstone accounts for only 18% of the section (Turner et al 1993). Such lateral facies variations suggest a tectonic control on deposition.

In the central portion of the Northumberland Basin Fordham (1989) noted preferential stacking of sandbodies near the footwalls of major faults. The Stonehaugh and Longhorsley boreholes (Figure 3.5) are positioned in the hangingwalls of faults, and preserve significant thicknesses of shale (Fordham 1989). Similar sediment distribution patterns have been noted by Turner et al (1993) from the Tweed Basin, where the footwall of the Pressen-Flodden Fault (Figure 3.5) concentrated sand deposition.

Crustal extension and active normal faulting in the Northumberland Trough were particularly active prior to the onset of Fell Sandstone deposition (Turner et al 1993), and the sediment distribution of the Fell Sandstone Group was therefore influenced by syn-sedimentary faulting. The area of maximum basin subsidence during the Dinantian was adjacent to the Stublick-Ninety Fathom Fault system (Leeder 1987, Kimbell et al 1989). Models for sedimentation in continental half grabens show axial drainage systems which migrate downslope towards the area of maximum subsidence along the base of the uplifted footwall block (Leeder & Gawthorpe 1987). Preferential stacking of Fell Sandstone Group sandbodies would therefore be expected to occur in the footwall of the Stublick-Ninety Fathom Fault system, with the deposition of fine grained overbank deposits to the north.

The outcrop pattern of the Fell Sandstone lies close to the northern margin of the Northumberland basin (Figure 3.5), rather than the south, and palaeocurrent measurements indicate that the Fell Sandstone river flowed across, rather than down the regional palaeoslope (Figure 3.6). Fordham (1989) and Turner et al (1993) have interpreted this flow pattern as the result of syn-sedimentary fault control, with tectonic highs, acting as local barriers to the drainage system (Figure 3.6). Thus the Fell Sandstone was not a basinwide river system as depicted in the model of Monro (1986), but instead consisted of a number of active braided plains locally confined b y intrabasinal syn-depositional normal faults (Turner et al 1993) such as that illustrated in Figure 3.6.
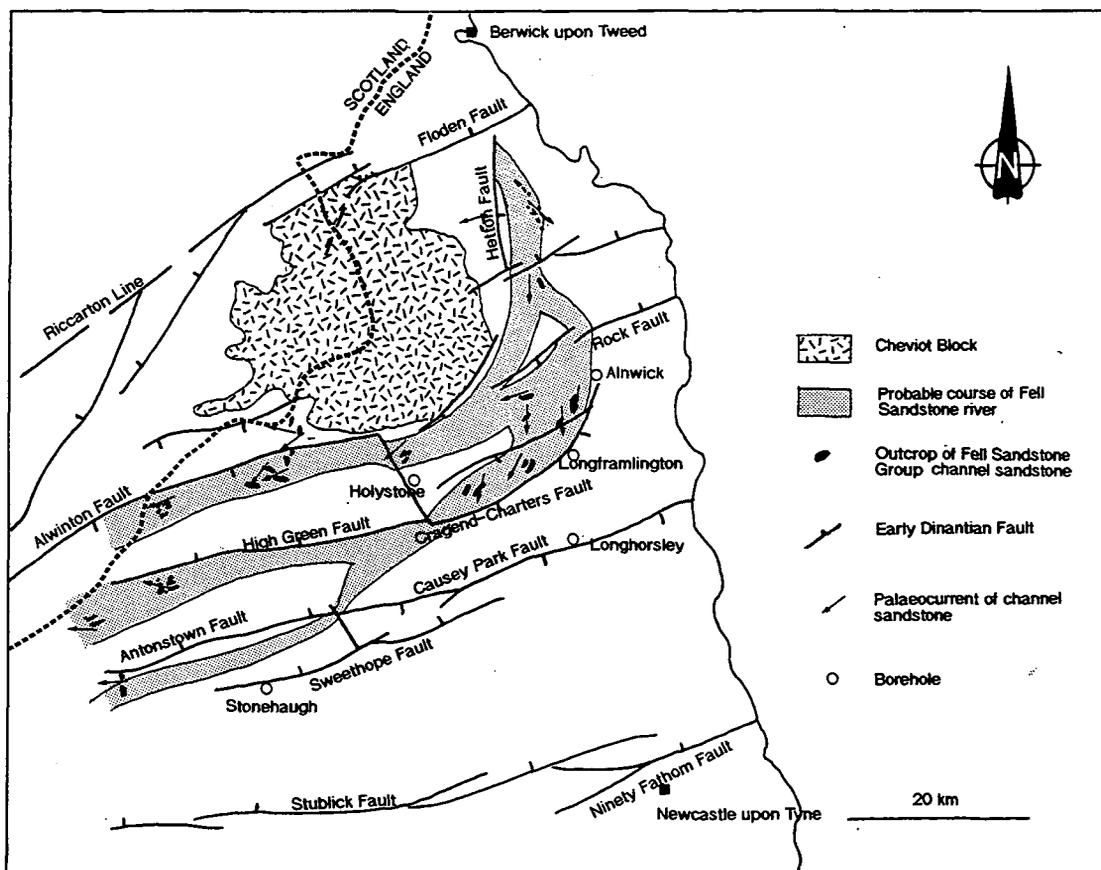
Figure 3.6. Syn-sedimentary faults of the Northumberland Basin and the likely flow pattern of the Fell Sandstone river (modified from Turner et al 1993).

## (i) Sedimentology Of The Study Area.

Sites within the Fell Sandstone Group were identified from the work of Monro (1986). The area chosen for study lies to the west of Belford (Figure 3.5) on the Cheviot axis. During deposition of the Fell Sandstone Group the Cheviot Massif was topographically subdued, although the river system was deflected around the flanks of the area (Monro 1986), as depicted in Figure 3.6. Figure 3.7 illustrates a geological map and stratigraphic column of the study area, which is highly simplified due to the presence of large quantities of drift obscuring bedrock.

The outcrop of the Fell Sandstone Group in the study area is dominated by a series of named sandstone crags, which are located stratigraphically immediately below the Scremerston Coal Group, on the northeastern limb of the Holburn Anticline. The escarpments form a succession of sandstone cuestas separated by a softer, unexposed rock, which is inferred to be a siltstone or mudstone (Figure 3.7). Outcrop

occurs dominantly in an orientation parallel to the local palaeocurrent direction, with smaller outcrops affording sections transverse to the flow direction.
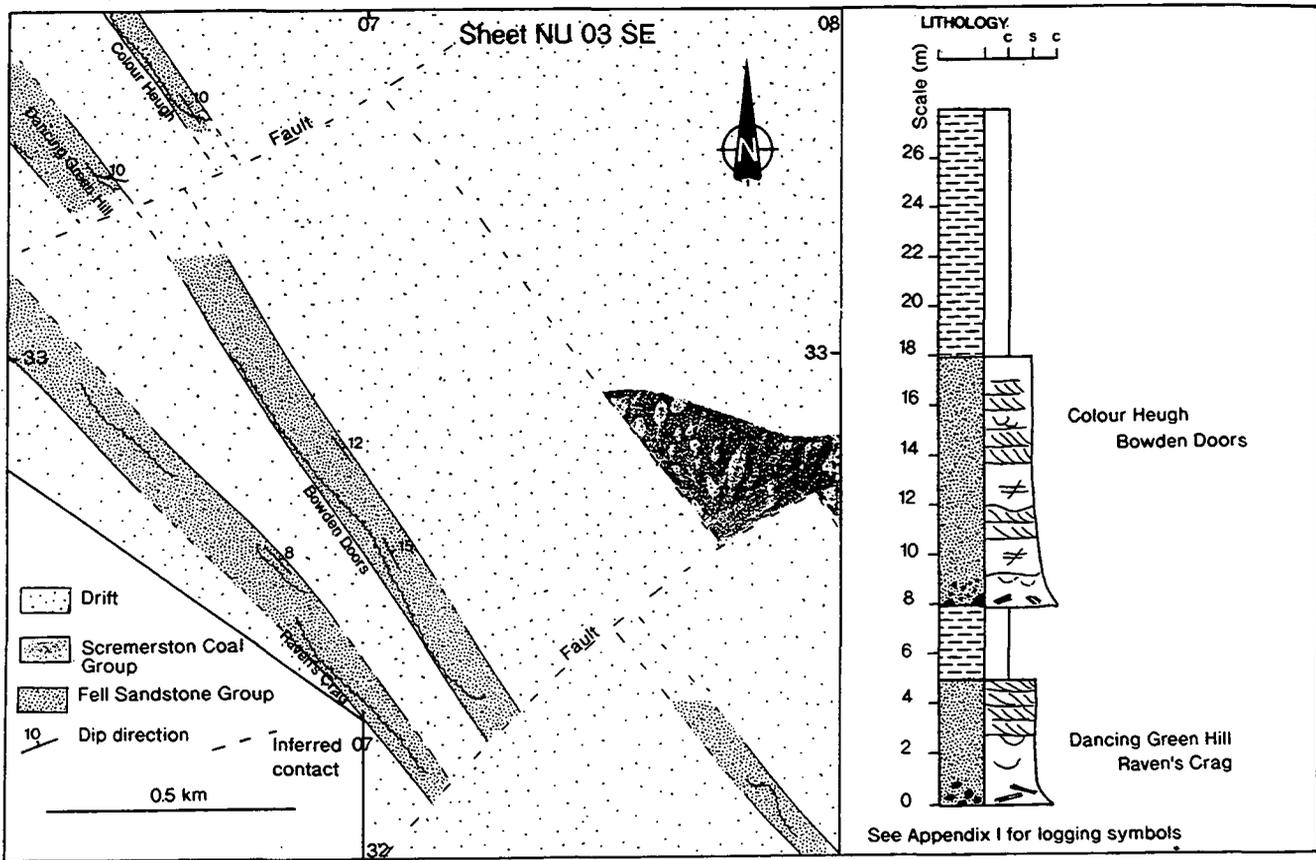


*Figure 3.7. A simplified geological map of the study area and an interpolated cross-section.*

The presence of stacked sandbodies in the Belford area indicates that fluvial sedimentation may have been affected by syn-sedimentary fault movements. Leeder (1987) inferred syn-depositional movement on an east/west oriented extensional fault located near Bowden Doors. However, Turner *et al* (1993) identified a north/south oriented syn-sedimentary fault, the Hetton Fault (Figure 3.5). Subsidence across the Hetton Fault during the Dinantian would have caused westward migration of the Fell Sandstone river system into the footwall, hence concentrating channel sands.

The sandstone units of the Belford area are 5 to 10 m thick (Figure 3.7), and offset by normal faults (Figure 3.7). The most laterally extensive, and best exposed sandstones are those termed Colour Heugh (NU 062 347) and Bowden Doors (NU 070 327) which are stratigraphically equivalent (Hodgson 1978). Dancing Green Hill (NU 065 336) and Raven's Crag (NU 070 323) are also directly correlatable. These

smaller outcrops are located stratigraphically beneath Colour Heugh and Bowden Doors respectively, and are believed to be separated from the overlying thicker sandstones by a mudstone unit (Figure 3.7).

The sands of the Belford area lie within the mid-proximal facies association of Monro (1986) as illustrated in Figure 3.5. The stratigraphically lower scarps (Dancing Green Hill and Raven's Crag) consist of a fining-upwards succession of conglomerate to sandstone (Figure 3.7). The upper scarps (Colour Heugh and Bowden Doors) expose medium and fine grained sandstone structured by uni-modal planar and trough cross-stratification. Within the sandstone units a number of facies have been identified, and these are described below. The notation used is that of Table 2.4.

*Conglomerate (Scg).*

A reddened, matrix supported, conglomerate is preserved as erosively based units 0.75-1.50 m thick. The conglomerate matrix consists of a very coarse, quartzose sandstone to granulestone, which contains rounded red sandstone, and black and green mudstone pebbles <30 mm in diameter. Basal scours are oriented northwest/southeast and are commonly lined by wood fragments <30 cm wide and >2 m long, aligned parallel to the scour axis. Smaller pieces of wood (<10 cm across) are also present, but the orientation of these tends to be more random.

The base of the conglomerate is massive or normally graded, and passes upwards into coarse and medium quartzose sands structured by diffuse trough cross-stratification. Sets are 60-80 cm thick, with poorly defined foresets 15-20 mm apart. The troughs reach 8 m across, and are commonly floored with a granulestone lag.

*Giant cross-stratification (Sg).*

At Colour Heugh (NU 062 347) giant scale planar cross-stratification is developed in a single set 2.10-2.65 m thick, bounded by third order surfaces. The set may be traced up to 50 m downstream, where the simple bedform evolves into a compound form.

The giant cross-stratified set is composed of quartzose sandstone containing disseminated organic matter and mica flakes. Tangential foresets dip at a low angle (10-15°) and are 5-50 mm apart. The foresets are undeformed and display internal normal grading from coarse to medium sandstone. In the base of sets, mudstone and sandstone granules <5 mm in diameter are held within the matrix of coarse sand. Randomly spaced minor reactivation surfaces cut across the set, and are marked b y concentrations of granules of iron cemented sandstone and mudstone. There is no evidence of low stage re-working along the reactivation surfaces, and hence these

discontinuities are interpreted in terms of changes in flow strength and/or depth without large scale emergence of the bedform.

*Large scale planar cross-stratification (Sp₁).*

Large scale planar cross-stratified sets are composed of a medium to fine grained, moderately well sorted quartzose sandstone with variable amounts of disseminated mica. Sets are 0.80 to 1.10 m thick and form simple units bounded by sub-horizontal first order surfaces. Foresets are generally tangential and dip 22-28° with overturning of foresets common. Along the foresets, grain size tends to fine upwards, from medium grained to fine grained sand. Mica is generally concentrated in the lower portion of the sets along the foreset surface. The sets are cut by minor reactivation surfaces, which show no evidence of low stage re-working.

*Medium scale planar cross-stratification (Spₘ).*

This facies is composed of a moderately well sorted, quartzose sandstone. Sets occur as isolated simple bedforms 40-65 cm thick, which may be traced in the direction of flow for up to 10 m. Foresets are generally tangential and dip 18-25°. Textural changes occur between the foresets, with some laminae having a higher mica content and hence a flaggy appearance. Small scale reactivation surfaces occur within sets but there is no evidence of low stage re-working.

*Medium scale trough cross-stratification (Stₘ).*

This facies is composed of medium to fine grained and moderately well sorted, quartzose sandstone. Cosets reach 2 m in thickness, with individual sets ranging from 40-80 cm thick. The troughs are 1-3 m in diameter and symmetrically filled. Foresets dip 22-26° and are tangential. The trough cross-stratification may also be interbedded with planar cross-stratification of a similar scale.

*Compound cross-stratification (Sc).*

Compound bedforms are composed of a moderately well sorted medium to fine grained quartzose sandstone. The bedforms range in thickness from 0.50 to 0.85 m, with 2B order bounding surfaces (Table 2.3) dipping from horizontal to 8°. Compound bedforms may be traced in excess of 30 m in the direction of palaeoflow.

The foresets of the compound bedforms dip 10-15° and are commonly convex-upwards in shape. Such foresets have been interpreted by Allen (1968) to be due to scour and flow separation in the lee of a bedform with a crest oriented perpendicular to flow. Reactivation planes are common. However, these are not planes of reworking but rather truncation planes related to small changes in flow conditions. Intrasets are

generally a combination of planar and trough cross-stratified forms, 5-15 cm thick, which display angular to tangential foresets dipping 25-35°. Overturning of intrasets is common. Small scale internal reactivation surfaces are evident with the intrasets.

*Small scale trough and planar cross-stratification (St$_s$ & Sp$_s$).*

Small scale planar and trough cross-stratification sets are developed in fine to medium grained quartzose sandstone. Cosets range in thickness from 0.75-5 m, and are separated by sub-horizontal second order (2A) bounding surfaces.

Small scale planar sets are 20-40 cm thick. Foresets are tangential and dip 25-30°. The foresets may be locally overturned. Debris is concentrated at the base of some foresets and consists of quartz granules <5 mm in diameter, and disseminated organic matter which appears as dark friable layers.

Small scale planar cross-stratification may be preserved as rare form sets. At Colour Heugh (NU 062 347) a train of dune form sets are developed over a third order bounding surface. The form sets are 35 cm high and have a wavelength of 5.50 m (crest to crest).

Trough cross-stratification is preserved in sets 20-45 cm thick and troughs 2 to 5 m across. The set fill is generally symmetrical. Foresets dip 20-25°, although locally foresets are highly deformed with almost total loss of structure.

*Horizontal stratification (Sh).*

Horizontal stratification, related to deposition under upper flow regime conditions, is locally developed in the fine grained sandstones of Bowden Doors and Colour Heugh. Deposits may be traced for a maximum of 3 m parallel to palaeoflow and are approximately 5 cm thick. Laminae are 2-10 mm apart and may display concentrations of mica.

*Massive sandstone (Sm).*

Massive sandstone facies take two geometric forms which are sheet-like and channel-like in geometry (Sms and Smc of Table 2.4). The lithology of these facies are identical to that of the structured sediments, i.e. a medium to fine grained quartzose sandstone.

The sheet-like massive sandstone facies (Sms) is well exposed at Bowden Doors and Colour Heugh. Largely structureless sands up to 3.50 m thick may be traced along the outcrops in excess of 300 m parallel to the palaeoflow. The lateral extent of the facies perpendicular to flow could not be established. The base of facies Sms is undulose and may attain a local relief of 0.75 m. Scour-like structures are

developed along the basal surface which are oriented parallel and oblique to the regional palaeoflow direction (Plate 3.1). The margins of the scours dip <45°. The base of facies Sms is locally related to overturning of foresets in the underlying cross-stratified sediments (Plate 3.2).



*Plate 3.1. DA Type 1 architectural element overlain by facies Sms, Bowden Doors. The base of the section is composed of the preserved portion of a DA Type 1 architectural element consisting $Sp_m$-Sc. The bedform is cut out by the scoured base of facies Sms. No deformation of the foresets is apparent. Facies Sms is without internal structure.*



*Plate 3.2. Overturned forests of facies $Sp_m$, Bowden Doors. The deformation is of Type 1 of Allen & Banks (1972), with the axial plane of the fold approximately parallel to the base of the deformed unit. The hinge is a smooth curve. The deformed set is overlain by facies Sms. The third order bounding surface developed between the two facies is indistinct.*

Isolated sets of cross-stratification related to 2-D and 3-D dunes are locally preserved within the massive sheets (Plate 3.3). The massive sandstone sheets also preserve diffuse laminae which have a trough-like appearance (Plate 3.3). Laminae occur 5-50 mm apart and are recognisable due to slight changes in texture of the sandstone. In the upper portion of the sheet-like massive sandstones water escape structures are developed which reach up to 1.20 m in height (Plate 3.4).



*Plate 3.3. Facies Sms and Smc, Bowden Doors. The section is 6.50 m high. Facies Sms is preserved in the lower portion of the outcrop and contains diffuse laminae and isolated sets of cross-stratification. Facies Sms is cut by a channel-like form of facies Smc, Channel 3 of Figure 3.10. The channel is lenticular with near symmetrical margins dipping 41° upstream and 22° downstream. Concentric laminae are preserved at the margin of the unit, and diffuse undulose laminae are preserved in the upper part. The remaining fill is massive. Facies Smc is overlain by a third order bounding surface. A DA Type 1 architectural element is preserved overlying this surface Macroform III of Figure 3.10).*

Channel-like massive sands of facies Smc are preserved within both the Colour Heugh and Bowden Doors outcrops. The channel features are lenticular in geometry when viewed in cross-section (Plate 3.3). The channels are oriented oblique or perpendicular to the fluvial palaeoflow, and hence the lateral extent of the channels cannot be determined.

The majority of the channel-like features have only the southern (downstream) margin preserved, with a small number of channels having both margins preserved. The channel margins of facies Smc are sharp and show no evidence of slumping. The margins slope between 15° and 55°. The angle of the surface tends to be shallower where cutting through sheet-like massive sands and steeper where cutting through cross-stratified sands.

*Plate 3.4. Water escape structures, Bowden Doors. The base of the outcrop exposes facies Sp$_m$ of Macroform I (Figure 3.10). The foresets are overlain by facies Sms, which is internally featureless. In the upper portion of facies Sms large water escape structures are preserved. Fluid expulsion prior to deposition of the overlying cross-stratified sediments is clear due to the lack of deformation in the overlying facies. Facies Sms is overlain by a third order bounding surface, which is in turn overlain by a DA Type 1 architectural element (Macroform VI of Figure 3.10).*

The channel-like features are filled by medium to fine grained sandstone. The channel fill is structureless, except towards the channel margins, where a series of concordant concentric laminae, 15-35 mm apart are preserved (Plates 3.3 & 3.5). The marginal laminae reach 20 cm in thickness before grading into structureless sandstone fill. Individual laminae are faint and are defined due to textural changes within the channel fill. Faint laminae are also developed at the top of the channel fill which may be cross-cutting in nature (Plate 3.3).



*Plate 3.5. Channel 4 of Bowden Doors. The section is oriented transverse to fluvial flow direction, as established through cross-stratification. Facies Smc clearly cuts through the structured sediments of Macroform II (Figure 3.10). The direction of movement was to N290°. Emplacement of the channel has caused little deformation of the cross-stratified sediments. The fill of facies Smc is largely structureless. Note the concentric marginal laminae of facies Smc.*

## (ii) Lateral Profile Analysis.

Two sections are described here: Colour Heugh and Bowden Doors (Figure 3.7). The sediments of these sections have been sub-divided into a series of macroforms defined by third order bounding surfaces. A number of architectural elements of macroform and mesoform scale have also been identified.

*Section 1: Colour Heugh.*

Colour Heugh forms the upstream extension of a continuous exposure (Figure 3.7). The outcrop is approximately 200 m long and 10 m high. The section is oriented southeast/northwest approximately parallel to the palaeoflow direction. A simple line drawing of the lateral profile is given as Figure 3.8. The sediments exposed at Colour Heugh are laterally variable and are summarised by two vertical sedimentary logs (Figure 3.9a & b).

The stratigraphically lowest sediments exposed within the Colour Heugh section are medium grained sandstones structured by medium scale trough and planar cross-stratification with high palaeocurrent variance (Macroforms I and II of Figure 3.8). In parts these sediments are highly deformed, resulting in the total loss of structure. Water escape structures are locally developed within these sands (Figure 3.9b).

Macroform III of Figure 3.8 is preserved over a fourth order bounding surface which may be traced across the majority of the outcrop (Figure 3.8). Macroform III is composed of an overall fining-upwards unit of conglomerate to medium grained sandstone. Facies Scg forms a crudely bedded GB element (Table 2.6) which fines upwards into sets of randomly interbedded St$_t$ and St$_m$ combined to form a SB Type 2 architectural element. The palaeocurrent measurements taken from these beds are variable (Figure 3.8).

Macroform III is truncated by an overlying third order bounding surface (Figure 3.8). Overlying Macroform III, the sandstone succession of Colour Heugh becomes laterally variable. The upstream portion of Colour Heugh is composed of a series of macroforms (IV, V and VI), which are structured by a combination of trough and planar cross-stratification on all scales (Figure 3.9a). The simple giant cross-stratified set of Macroform IV is a DA Type 2 architectural element. Small scale reworking of the toesets of the element indicate fluvial currents which flowed oblique to the main fluvial current as illustrated in Figure 2.3b. In the downstream direction Macroform IV evolves into a compound cross-stratified unit with intrasets formed of small scale Sp and St.

Macroforms V and VI are complex forms (Figure 3.8). Both macroforms are composed of stacked sets of Sp$_s$ and St$_s$ which form SB Type 2 architectural elements bounded by second order surfaces. Overlying the basal third order bounding surface

NNW

Figure 3.9a    ORIENTATION N140/320

③ ············ Macroform VI

Macroform VII

Macroform V

④ ④ ·············

N

Macroform IV

n=7

10    20    40    50    60    70    80    90    100    110

ORIENTATION N 145/335    SSE

Figure 3.9b

N

Macroform VIII

③ ·········

④ ·········· Macroform I

Macroform III

n=15

N    N

Macroform II    Macroform IX

n=7

120    130    140    150    160    170 m

n=18

**Fourth Order Bounding Surface**

④

**Third Order Bounding Surface**

③

**Interpolated Bounding Surface**

· · · · ·

10 m

Scale
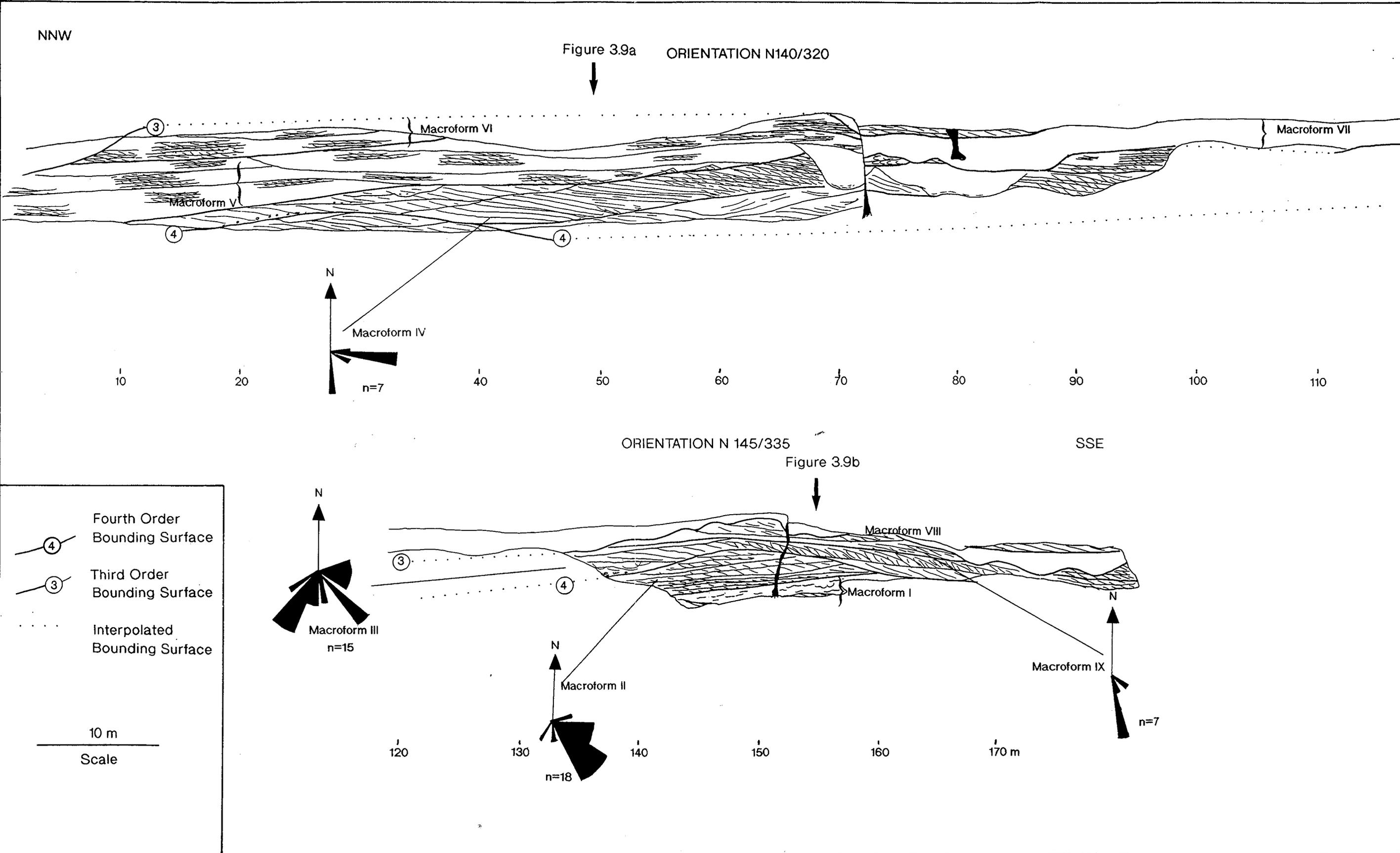
Figure 3.8. A simplified line drawing of the Fell Sandstone Group section exposed at Colour Heugh (NU 062 347) produced from distortion free photographs.

**3.9a)**

**3.9b)**

MAJOR CHANNEL ARCHITECTURAL ELEMENT (CH)

4 th. Order Bounding Surface

Base not seen
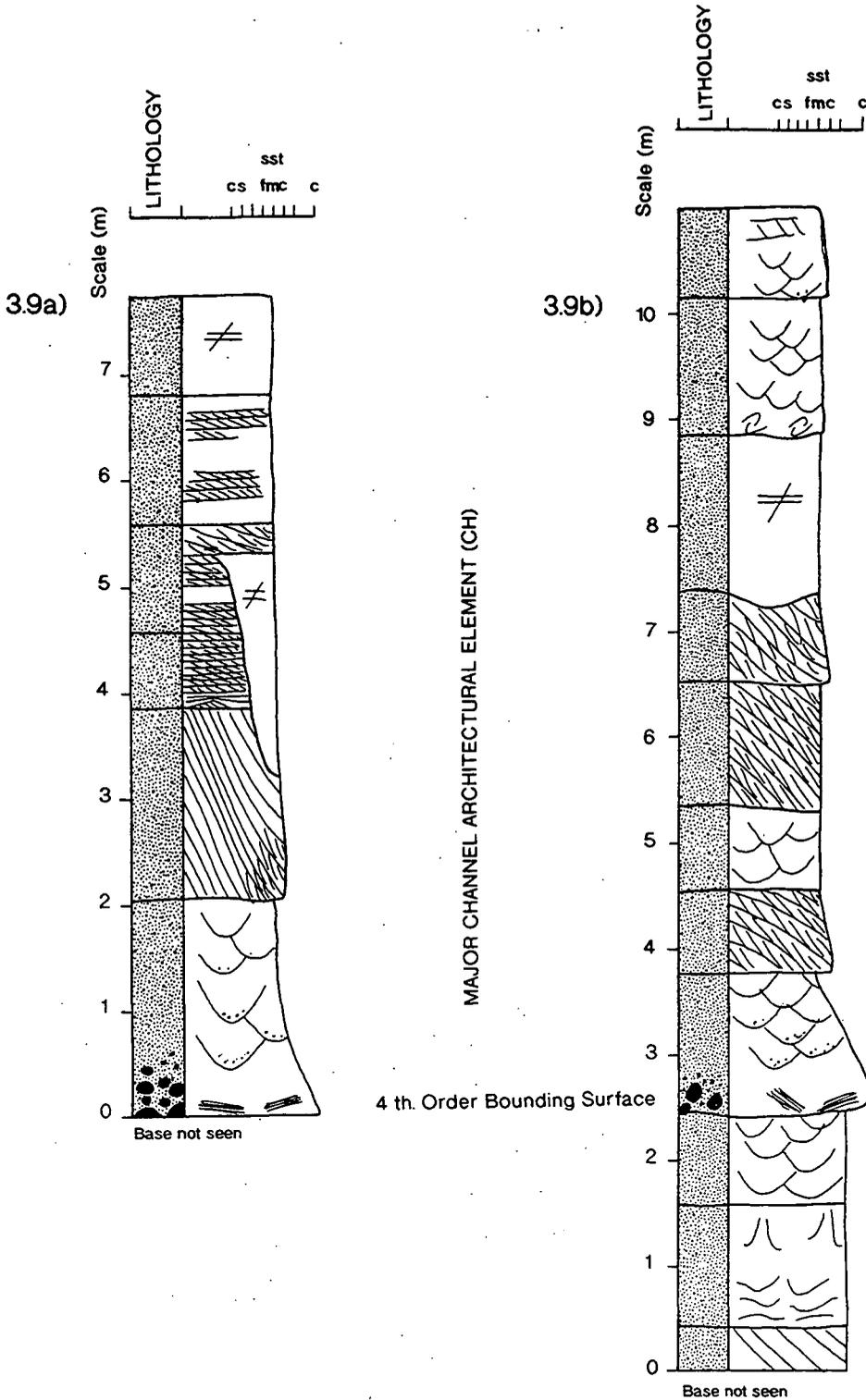
See Appendix I for logging symbols

*Figure 3.9. Sedimentary sections through the Fell Sandstone Group exposed at Colour Heugh.*

of the Macroform V, form sets are locally developed, as described above. The form sets are overlain by horizontally stratified sediments, which in turn are blanketed b y the SB element (Figure 3.8). These sedimentary structures indicate rapid aggradation rates.

The stratigraphically equivalent strata in the downstream portion of Colour Heugh (Macroforms VIII & IX) are similarly medium and fine grained sandstones. The sediments are arranged in DA Type 1 architectural elements (Table 2.6) structured b y simple medium scale trough and planar cross-stratification, overlain by compound cross-stratification (Figure 3.9b).

A sheet-like massive sandstone is preserved across a large portion of the Colour Heugh section, and defines Macroform VII of Figure 3.8. The sheet has an undulose base with a relief of 0.45 m, which is classified as a third order bounding surface (Figure 3.8). The basal surface of the massive sandstone sheet is locally erosive, and has caused the deformation of underlying structured sediments. Some laminae occur parallel to the base of the sheet, although these are generally restricted to regions of scouring. Internally the massive sheet is largely structureless. However, diffuse laminae 5-50 mm apart are developed locally within the sheet (Figure 3.8). The laminae are defined due to slight variations in sandstone texture.

The upper surface of Macroform VII is an undulose third order bounding surface (Figure 3.8). The sediments overlying this surface are medium grained sandstones structured by a combination of medium scale trough, planar and compound cross-stratification arranged in DA Type 1 architectural elements (Figure 3.8).

Two channel-like units of facies Smc are preserved within the Colour Heugh section between 60-80 m of Figure 3.8. These are laterally restricted to Macroforms IV and V. The channel-like features are 1.80 and 3.10 m thick, and cut through structured sediments, with preservation of both marginal surfaces. The channel margins dip 35-50°, and there is no evidence of slumping. No sense of sediment movement may be discerned. Internally the channel-like features are structureless.

*Section 2: Bowden Doors.*

The Fell Sandstone Group is continuously exposed for approximately 450 m along the Bowden Doors escarpment (Figure 3.7), which forms the downstream extension of Colour Heugh. The outcrop is oriented southeast to northwest and lies approximately parallel to the local palaeoflow direction. The majority of the outcrop is less than 4 m high, but to the south (downstream) it attains a height of 8 m. A simplified line drawing of the outcrop is illustrated in Figure 3.10, and a simplified vertical log of the section is shown in Figure 3.11.

NNW

ORIENTATION N 150/330

Figure 3.11

1

2

3

Macroform II

10    20    N 30    40    N    50    60    70    80    90    100    110    120    130

Macroform VIII    Macroform IX    N

Macroform IIb

n=24    n=10    n=8    Macroform III    n=15

ORIENTATION N 150/330    SSE

Macroform IV    Macroform VII

Macroform V

4

140    150    160    170    180    190    200    210    220    N    230    240    N 250    260 m

Third Order
Bounding Surface    10 m

Interpolated    Scale
Bounding Surface

Macroform I    Macroform VI

n=12    n=7

Figure 3.10. A simplified line drawing of the Fell Sandstone Group section exposed at Bowden Doors(NU 070 327) produced from distortion free photographs.

*Figure 3.11. A representative sedimentary section through the Fell Sandstone exposed at Bowden Doors.*

At the base of this section Macroform I is preserved (Figure 3.10). The lower portion of Macroform I is composed of a GB architectural element consisting of a reddened granulestone to conglomerate. Clasts within the matrix supported conglomerate include rounded sandstone, vein quartz and mudstone pebbles which are <15 mm in diameter. The GB element is believed to be the lateral equivalent of the GB element exposed within the Colour Heugh section (Figures 3.9a & b). The conglomeratic sandstone fines upwards into a medium grained cross-stratified

sandstone structured by a combination of medium scale planar and trough cross-stratification. The facies combine to form a DA Type 1A architectural element (Figure 3.11 & Plate 3.1). Deformation of these sediments is common, and takes the form of overturned foresets (Plate 3.2).

The upper surface of some bedforms preserved within Macroform I have been dissected by cross-cutting channels which are filled with a structureless sandstone. These channel-like features are 20 cm deep and <55 cm across.

Macroform I is overlain by a third order bounding surface which may be traced over much of the outcrop (Figure 3.10), although it is sporadically lost in drift. The bounding surface has an undulose base with a relief of up to 0.75 m (Plate 3.1). Macroform II (Figure 3.10) varies between 1.50 to 3.50 m thick and is dominated by a sheet-like massive sandstone (facies Sms) containing locally developed diffuse laminae which take the form of giant scale, poorly defined, trough-like structures (Plate 3.3). Isolated sets of cross-stratification (Figure 3.10) are also locally preserved as illustrated in Plate 3.3. Between 50 m and 100 m of the section within Macroform II (Figure 3.10), a series of stratified sediments are preserved, which are here termed Macroform IIb (Figure 3.10 & 3.11). This sedimentary unit appears to be developed within the massive sandstone sheet, but displays a bounding surface hierarchy typical of a DA Type 1 macroform.

Both the structured sediments of Macroform IIb, and the largely structureless sediments of Macroform II, are cut by a series of steep sided channel-like forms of facies Smc (Plates 3.3 & 3.5). The channels are generally poorly preserved, with only the downstream margin clear. However, some channel-like features are completely preserved (Channels 1, 2, 3 & 4 of Figure 3.10). These complete features have a lenticular appearance, with sharp margins which dip from 30-50°. The channel forms vary in depth from 0.75-1.95 m and where width can be established, reach 9.5 m across. Channel 4 (Figure 3.10) is exposed in three-dimensions and the basal surface of the channel form can be seen to be erosive and undulose (Plate 3.5). A sense of movement of the sediment may be established, which indicates flow towards N290°. The upper margins of facies Smc are flat or undulose, and are co-incident with second order or, more commonly, third order bounding surfaces (Figure 3.10). Internally units of facies Smc are largely structureless. However, concentric marginal laminae are preserved (Plates 3.3 & 3.5).

The third order bounding surface overlying Macroform II may be traced from 20 m to 210 m along the outcrop (Figure 3.10). The surface is overlain by a series of macroforms (III-IX) which contain well developed DA Type 1 architectural elements of 1.75-2.50 m thick and SB Type 1 elements (0.85-1.20 m thick). Macroform III (traced from 80-100m along section) is composed of a DA Type 1 element (Plate 3.6), as is

Macroform IV. Macroforms VIII and IX are composed of SB Type 1 architectural elements (Figure 3.11).

Macroform V is dominated by a sheet-like massive sandstone unit which has an undulose base associated with deformation of the underlying sediments of Macroform I. Facies Sms cuts downstream through sediments of Macroform V (Figure 3.10 & Plate 3.6). The massive sandstone sheet is largely internally structureless, although isolated sets of small scale cross-stratification are preserved (Figure 3.10). At the downstream margin of the outcrop large scale water escape structuresup to 1.75 m in height are preserved (Figure 3.10 & Plate 3.4).



*Plate 3.6. Margins of facies Sms, Bowden Doors. At the base of the outcrop a DA Type 1 architectural element of Macroform III (Figure 3.10) is exposed. Note the upward change in facies from $Sp_m$-Sc. Foresets of facies $Sp_m$ are locally overturned. Facies Sms cuts downstream through facies Sc, with minimal deformation. Internally facies Sms is featureless.*

Macroform V is overlain by a third order bounding surface, which is in turn overlain by Macroform VI, composed of a DA Type 1 architectural element. The sediments display local overturning of foresets, particularly within the intrasets of compound bedforms. There is a small amount of bedding deformation at the base of Macroform VI associated with the water escape structures preserved in Macroform V. It would, however, appear that the majority of the water from the massive sandstone was ejected prior to the deposition of the overlying macroform.

## (iii) Petrology And Textural Characteristics.

*Textural information and grain size analysis.*

Eighteen thin sections were made from samples taken from Colour Heugh and Bowden Doors. These samples included representatives of all the facies described above.

The results of grain size analyses are shown in Figure 3.12a, b and c, and the techniques used to assess the grain size are detailed in Appendix III. The median grain size of samples varies between $2.3\phi$ and $3.1\phi$ and hence the sands are fine to medium grained. Facies Smc has a median grain size of $2.98\phi$, facies Sms has a median grain size of $3\phi$ and the structured sandstones have a median grain size of $2.8\phi$.
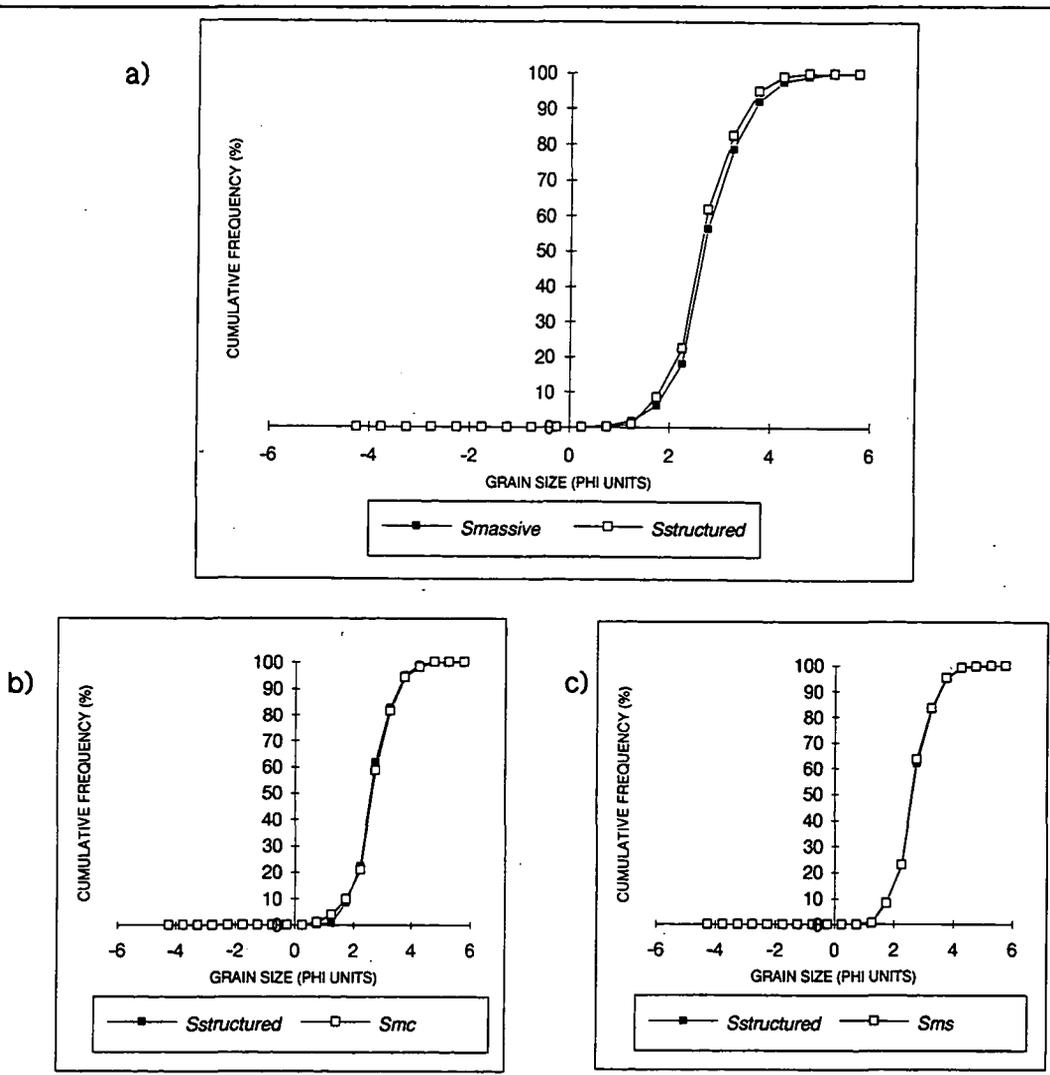
*Figure 3.12. Cumulative frequency graphs of the grain size distribution of the Fell Sandstone Group exposed at Belford.*

Figure 3.12a illustrates that overall the massive sandstone facies contains sediments which are marginally finer grained than the structured sediments. However, when the massive sandstone facies is sub-divided into sheet-like (Sms) and channel-like (Smc) types it appears that a definite division of grain size characteristics exists between the units. Facies Smc (Figure 3.12b) appears to have a coarser grain size distribution than the structured sediments, whereas facies Sms (Figure 3.12c) appears to have a similar grain size distribution to that of the structured sediments.

Sorting of the sandstone facies varies between moderately well and well sorted (Appendix III). Facies Sms tend to be less well sorted than the structured sandstones and facies Smc (see Appendix III for detail).

The primary porosity of the sandstone samples, assessed from point counting, varies between 11.3% and 20.6% (Appendix III), with an average of 16%. Facies Sms has a primary porosity averaging 18.6%, with facies Smc a porosity of 15.5%, and the structured facies averaging 14%. The development of secondary porosity is limited and averages 1.1% across the sample suite. No study of the permeability from outcrops has been attempted. The sandstones exposed at Bowden Doors and Colour Heugh are highly weathered, and hence measurements would be prone to error.

Fordham (1989) carried out a detailed study of the porosity and permeability characteristics of the Fell Sandstone, concentrating on borehole samples. The Alnwick borehole (Figure 3.5) has been used here to quantify the permeability of the Fell Sandstone. The borehole lies in the late proximal facies association of Monro (1986), and lies down the depositional slope from the outcrops at Belford. Stratigraphically the sediments of the Alnwick borehole lie near the top of the Fell Sandstone Group.

The Alnwick borehole contains sediments of structured and massive sandstone facies. A generalised sedimentary log of the cored section is illustrated in Figure 3.13. Porosity and permeability measurements were made by Fordham (1989) from core plugs, and these measurements have been used to create the graphs shown in Figures 3.14a & b. Measurements from the upper 20 m of the borehole have not been used, as Fordham (1989) recognised this as a zone of leaching.

The sandstones of the Alnwick borehole have an effective porosity of between 9.3% and 24.7%, with an average of 18.7% (Fordham 1989). These values are similar to those established from the outcrop studies made here. The Alnwick borehole sediments display horizontal permeability (Kh) values of 29 mD to 6 D with a geometric mean of 753.8 mD. Vertical permeability (Kv) of the samples varies between 0.1 mD and 4575 mD with a geometric mean of 373.31 mD. The massive

sandstone facies (Figure 3.14b) show a more grouped porosity and permeability field than the structured sediments (Figure 3.14a), but towards higher values.
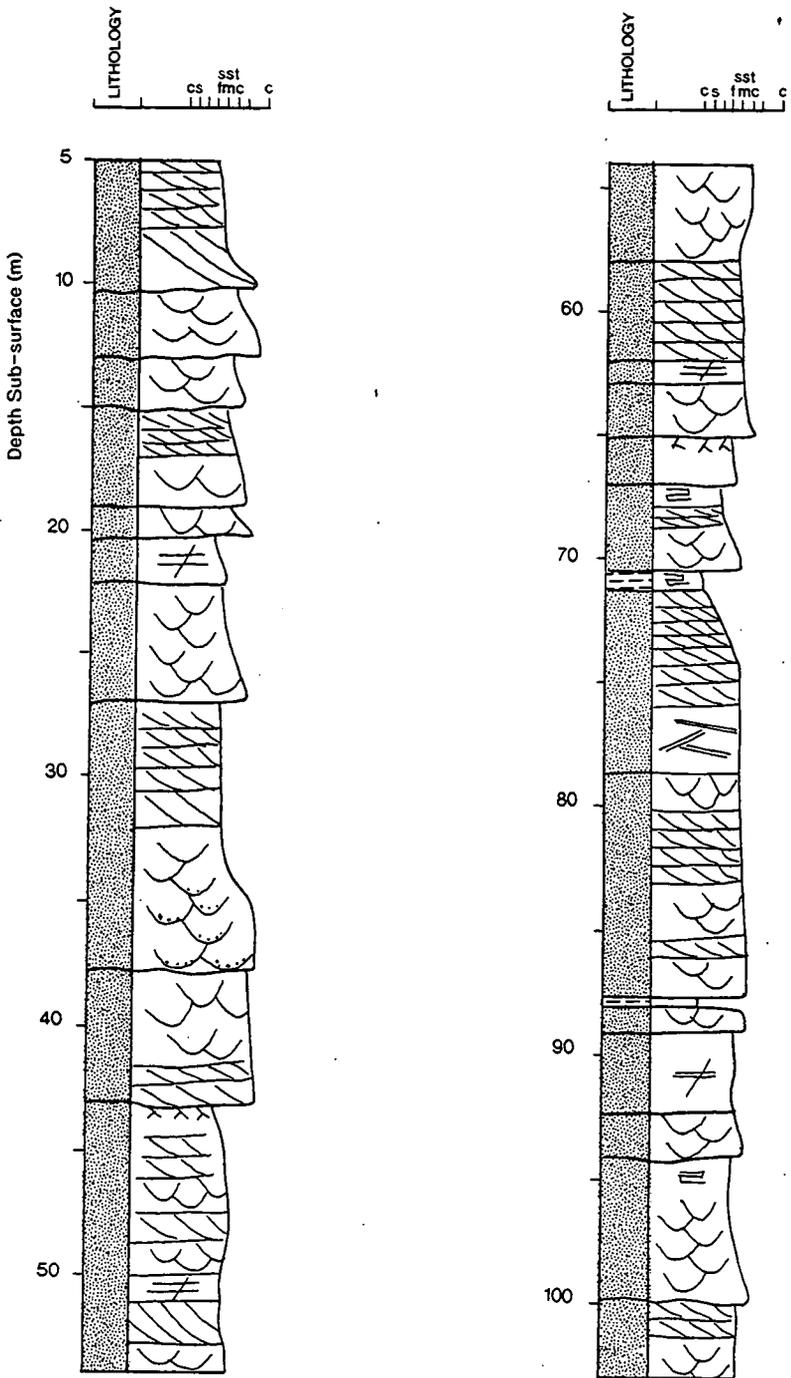


See Appendix I for logging symbols

Figure 3.13. A sedimentary log of the Alnwick borehole sediments, as described by Fordham (1989).
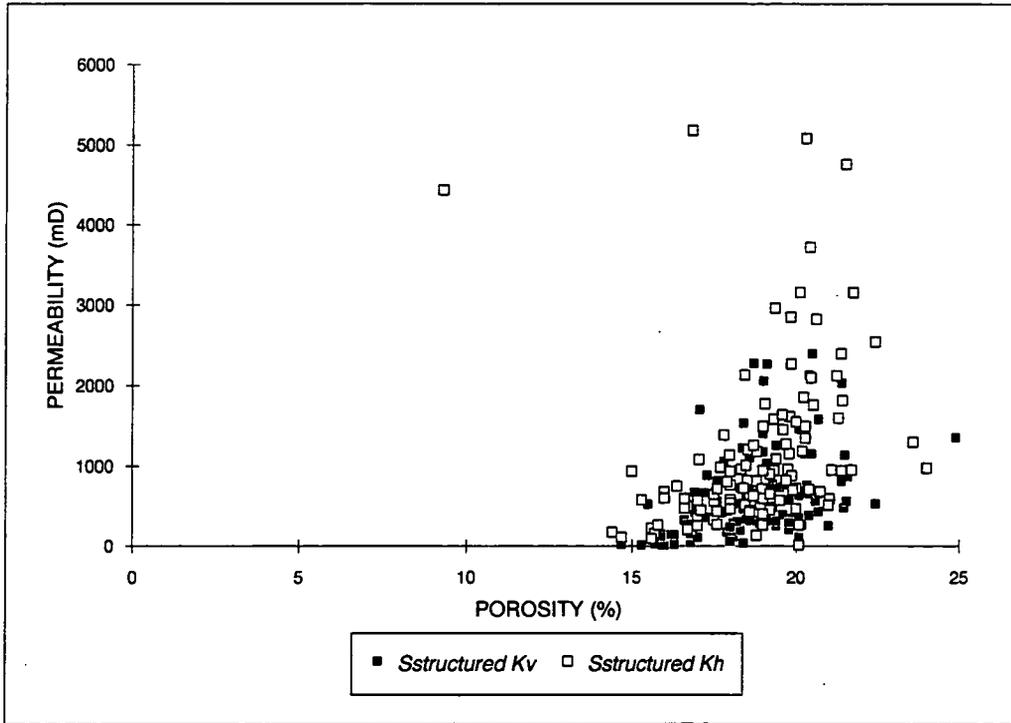
*Figure 3.14a. Permeability vs. porosity for the structured sandstones of the Alnwick borehole (data from Fordham 1989).*
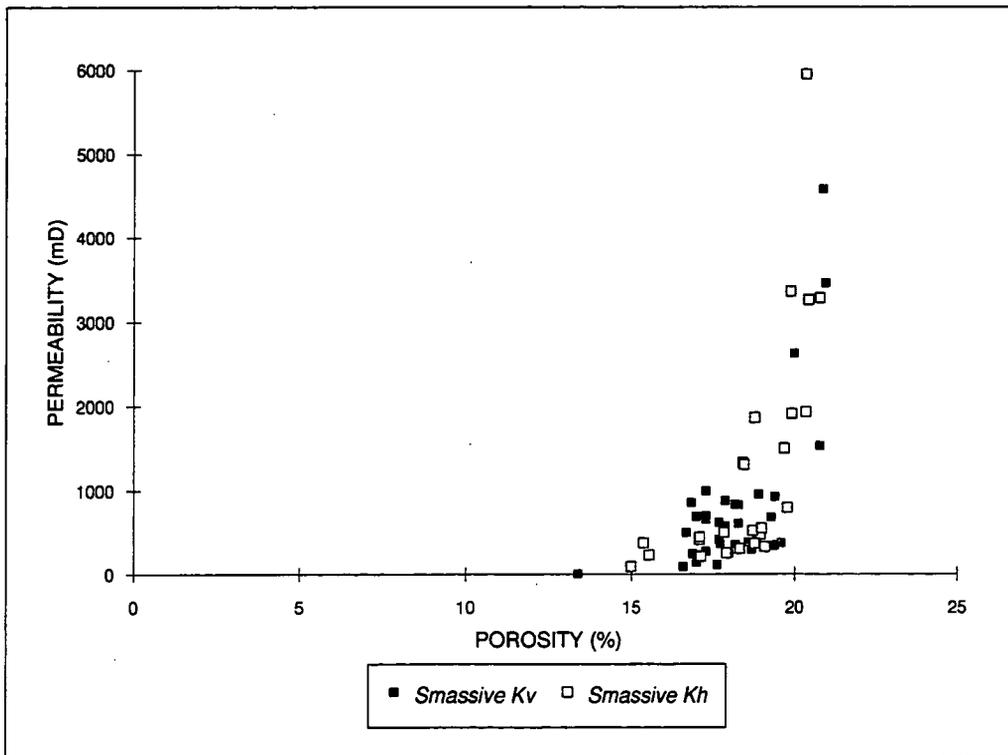


*Figure 3.14b. Permeability vs. porosity for the massive sandstones of the Alnwick borehole (data from Fordham 1989).*

The compaction index (CI) or average number of grain contacts, of sandstone samples has been assessed for this study, and the methodology is described in Appendix III. The different sandstone facies display slight variations in CI, with structured sandstones having a CI of 3, facies Smc having an average CI value of 2.8, and facies Sms a value of 3.1.

*Composition.*

Point counting has been used to assess the modal composition of the Fell Sandstone as exposed at Bowden Doors and Colour Heugh. The compositional information discussed here is detailed in Appendix III. The outcrops are highly weathered with a leached zone extending at least 30 cm into the outcrop. The modal estimate of feldspars and lithic fragments is consequently expected to be lower than the true composition.

Figure 3.15a indicates that the sandstones of the Belford outcrops are quartz arenites, sub-arkoses and sub-litharenites (Folk 1980). The sands sit in the recycled orogen province of the Qm-Lt-F diagram of Dickinson (1985), as illustrated in Figure 3.15b. The is no pattern of compositional variation between facies types.
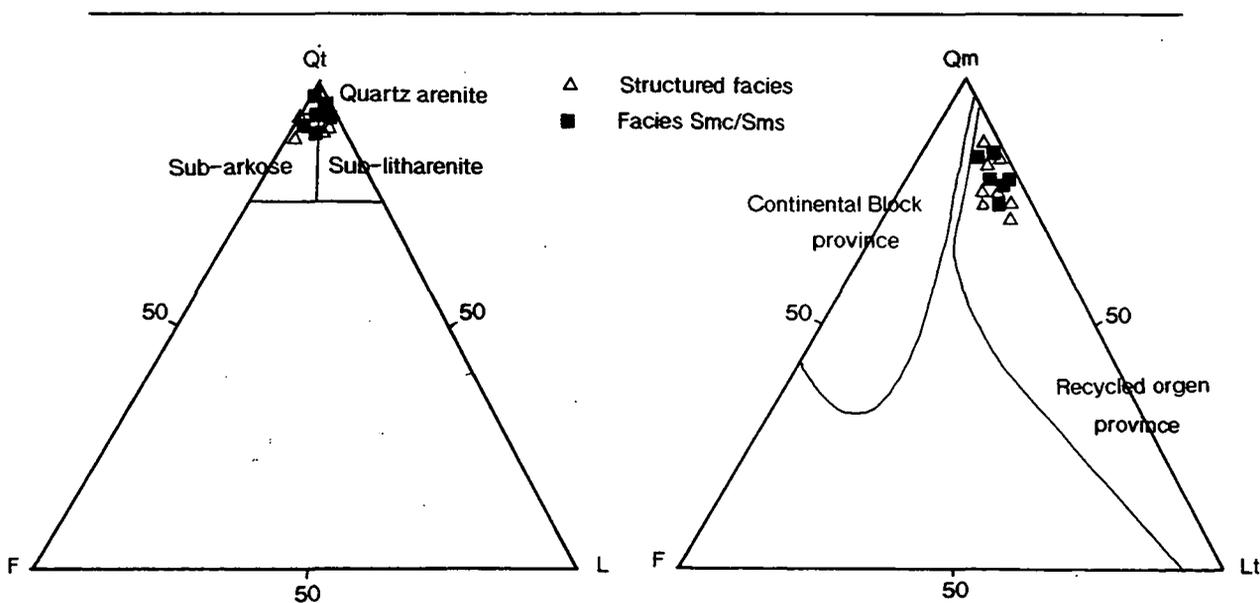


*Figure 3.15a. Modal compositional data from the Fell Sandstone Group (after Folk 1980).*

*Figure 3.15b. Provenance data from the Fell Sandstone Group (after Dickinson 1985).*

The Fell Sandstone samples are dominated by quartz, which accounts for over 90% of the detrital component of all samples. The detrital grains are sub-rounded and equant. Monocrystalline quartz is the dominant type, and grains generally exhibit

undulose extinction (Plate 3.7). Polycrystalline quartz grains are present in small amounts and display metamorphic textures. Rare chert grains are also preserved.
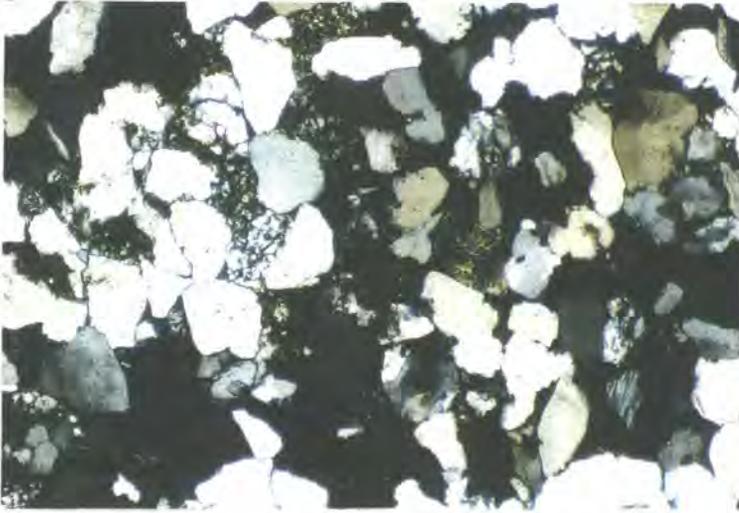


Plate 3.7. Fell Sandstone, facies $Sp_m$. Field of view 3.5 mm. Detrital quartz takes both monocrystalline and polycrystalline forms. Polycrystalline quartz grains have metamorphic textures. Contacts between authigenic quartz overgrowths are tangential to planar. Microcline and plagioclase feldspars both present. Plagioclase tends to be more highly weathered. A fine grained lithic fragment displays alteration to clay minerals. Pore filling kaolinite also developed.

The lithic component of the Fell Sandstone is dominated by sedimentary rock fragments of intraformational mudstone, siltstone and fine grained sandstone. Fine grained volcanic clasts of extraformational origin are also present, although these are highly altered (Plate 3.7). Lithic clasts are sub-round to rounded and equant in shape.

Feldspars are present in all sections, although the volume of these grains is assumed to have been underestimated, due to the extensive weathering of outcrops. Both plagioclase and potassium feldspars are represented (Plate 3.7). The plagioclase grains are commonly altered, and may be completely removed or replaced. Alteration is most pronounced along cleavage planes. Microcline and orthoclase grains are generally fresh, or slightly cloudy. Mica is present in small quantities and takes the form of both fresh and altered muscovite, and rare biotite. Grains commonly show the effects of compaction.

*Diagenesis.*

The major diagenetic phases of the Fell Sandstone are authigenic quartz, pyrite and clay minerals in the form of kaolinite and illite. The relative growth of these phases is illustrated in Figure 3.16. The diagenetic sequence of events does not vary between sandstone facies.

| Diagenetic phase | Early | | Late |
|---|---|---|---|
| Authigenic Quartz growth | _____ | | _____ |
| Quartz dissolution | | _____ | |
| Feldspar & lithic dissolution | | _____ _ _ _ _ | |
| Pyrite precipitation | | _____ | |
| Pyrite dissolution | | | ____ |
| Kaolinite precipitation | | | _____ |
| Illite precipitation | — | | __ |

Figure 3.16. Relative timing of diagenetic sequence within the Fell Sandstone Group.

Authigenic silica is volumetrically the most important diagenetic phase. The growth of quartz cements started early during burial and continued sporadically (Figure 3.16). Where clay rims are visible on detrital quartz grains the detrital grains clearly have tangential contacts, or are not in contact at all. Thus compaction of the sediments prior to cementation was limited. Authigenic overgrowths have tangential to planar contacts, thus indicating that large amounts of secondary quartz were deposited around detrital grains (Plate 3.7).

Pyrite was an early diagenetic phase which postdates early quartz (Figure 3.16), and in many sections replaces the quartz overgrowth cements. Pyrite takes cubic and massive forms, and is commonly associated with lithic grains, and along the cleavage planes of degrading feldspars. Pyrite has been partially replaced in some sections and pores have been infilled with later kaolinite.

Clays are represented by kaolinite and illite (see Appendix IV for detail). Kaolinite is the most abundant phase and fills pores, post dating pyrite and early quartz (Plates 3.7 & 3.8). Kaolinite also replaces plagioclase feldspar grains. Illite is a late diagenetic phase which takes a grain coating form. Feldspar and lithic grain dissolution continued after the growth of pore filling kaolinite, causing the development of oversized pores (Plate 3.8).
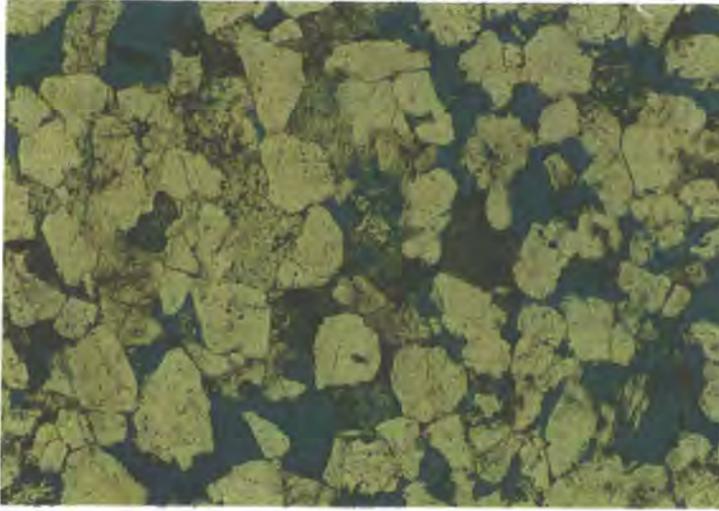
*Plate 3.8. Fell Sandstone, facies Sp$_m$. Field of view 3.5 mm. Authigenic quartz overgrowths well developed. Lithic fragments have dissolved to fine grained clay minerals (illite) and pore filling kaolinite is extensively developed. Late diagenetic dissolution of plagioclase feldspar has resulted in the development of oversized pores.*

The red colour of the Fell Sandstone Group is attributed to the oxidation of the pyrite to goethite. This phase of diagenesis is related to recent uplift and Fordham (1989) suggested that water table movements may control the oxidation process.

*Discussion.*

The Fell Sandstone, as exposed in the Belford outcrops, is moderately mature to mature. The grain size data illustrate some minor textural differences between the sedimentary facies. The structured sediments and the sheet-like massive sands (Sms) are finer grained overall than the channel-like facies Smc. The sorting of facies Smc sandstones and the structured sandstones are better than those of facies Sms. Primary porosity is greatest in facies Sms and approximately equal in facies Smc and cross-stratified sandstones.

The composition of all the Fell Sandstone samples examined falls within the recycled orogen province of Dickinson (1985). There is no recognisable compositional variation between sedimentary facies, indicating that all the sandstones were derived from the same sedimentary source.

The rounding and sorting of detrital grains indicates considerable transport prior to deposition within the Fell Sandstone river system. The sands were probably sourced from an area containing volcanic and plutonic rocks, due to the high volume of monocrystalline quartz grains, and volcanic lithic fragments. A granitic source is

suggested due to the presence of plagioclase and potassium feldspars, and biotite within the sediment. Muscovite is generally supplied by metamorphic rocks, and metamorphic fabrics have been noted from polycrystalline quartz grains.

The diagenetic sequence of events is identical in all sandstone facies studied, indicating that the massive appearance of the sandstones is not due to diagenetic overprinting of originally structured sediments.

The high quantity of secondary quartz cement within the Fell Sandstone indicates a large source of silica. However, the lack of contact between detrital grains indicates that pressure solution was not an important process. The source of silica is believed to have been nearby shales, possibly those interbedded with the sandstones (Figure 3.7). De-watering of the shales would provide silica to the porous sandstones.

Pyrite was an early diagenetic phase, with iron derived from the breakdown of unstable detrital grains. Pyrite in the Fell Sandstone is commonly associated with unstable lithic grains and plagioclase feldspars, which could supply the necessary iron. The close association of the pyrite with the source of iron suggests that during formation circulation of formation waters was limited. A fall in circulation would also have prevented the further deposition of authigenic quartz, enabling overgrowths to be replaced by pyrite. Later formation fluid circulation is indicated by the continued growth of quartz (Figure 3.16)

## 3.3. Fluvial Interpretation.

Previous studies of the Fell Sandstone Group including those of Hodgson (1978), Monro (1986) and Fordham (1989) have interpreted the sediments to have been deposited by braided streams. The Fell Sandstone river has been interpreted in terms of a single, laterally extensive system (Monro 1986), or as a smaller braided river system laterally confined by intrabasinal syn-depositional faults (Fordham 1989; Turner et al 1993).

The coarse grained sediments preserved in the Belford area of the Northumberland basin take the form of fining upwards cycles 5-10 m in thickness bounded by fourth order surfaces. These sand dominated units are separated by thin mudstone units, interpolated to vary between 5 and 15 m thick (Figure 3.7). The lateral extent of the sandbodies is unknown, due to large amounts of drift. The preferential stacking of fluvial channel sandstones in the Belford area is interpreted in terms of a syn-depositional control on sedimentation, with syn-depositional movements across

the north/south oriented Hetton Fault causing westward migration of the fluvial system into the footwall.

The sedimentary units of the Fell Sandstone deposited between fourth order bounding surfaces are interpreted in terms of deposition from a major channel element (CH). The CH architectural element of Bowden Doors and Colour Heugh consists of an overall fining-upwards cycle of conglomerate and sandstone (Figure 3.9a & b). However, the fine grained facies associated with channel abandonment are absent. Fourth order bounding surfaces are formed by avulsion of a fluvial system which is in turn controlled by allocyclic controls such as base level change, tectonics and climate change, or a combination of these. Due to the limited study of the Fell Sandstone it has been impossible to determine the nature of the allocyclic controls on sedimentation. The fact that the Fell Sandstone river was controlled by syn-sedimentary faults (Turner *et al* 1993) suggests however, that tectonic movements may have been the major control on the development of the exposed fourth order bounding surface.

The fourth order bounding surface exposed at the base of Colour Heugh, and inferred to lie below the base of Bowden Doors, represents a period of channel shifting and downcutting associated with avulsion. The scours in the base of the GB architectural element display an orientation parallel to the regional palaeoflow. The presence of large quantities of wood within the conglomeratic channel lag suggests deposition during a flood event. The presence of locally derived mudstone and sandstone clasts also indicates a flood event, perhaps associated with re-working of an older channel or floodplain sediments.

Deposition of the GB architectural element under decelerating conditions is indicated by the upward decrease in grain size. Overlying the GB element DA Type 1 and SB Type 2 elements are preserved. In the upper portion of the DA Type 1 element of Bowden Doors, dissection of bedforms occurred, with cross-channel oriented features preserved. The presence of these cross-channel oriented units suggests that flow dropped sufficiently to allow emergence of bedforms.

Overlying the basal macroform of the CH architectural element (Macroform III of Colour Heugh and Macroform I of Bowden Doors) a third order bounding surface is preserved. The sediments overlying this surface are sand dominated, and represent a prolonged period of fluvial deposition. The sandstones of Colour Heugh and Bowden Doors are composed of a number of macroforms divided by third order bounding surfaces.

The development of third order bounding surfaces is controlled by dominantly autocyclic mechanisms. To produce a channel fill containing more than one macroform separated by third order bounding surfaces two possible mechanisms exist: 1) A

river containing multiple channels which migrate laterally to produce a hierarchy of bedforms and bounding surfaces or 2) a single channel river containing mid-channel bars, which with vertical aggradation are superimposed to produce a multistorey sandbody. There is no evidence of lateral accretion deposits within the Fell Sandstone Group in the Belford area and hence the river is interpreted as a single channel system as in the second model above. An example of such a single channel river is the Orinoco.

DA Type 1 architectural elements are interpreted in terms of a mid-channel bar of a major fluvial channel (Table 2.6). The basal third order bounding surface represents the erosional base of a migrating bedform. A thin conglomerate, where present, represents deposition along the channel floor, and medium scale trough and planar cross-stratification represent the deposits of downstream migrating 3-D and 2-D dunes. The compound bedforms represent migration of medium scale bedforms over a larger scale unit. Local flow fluctuations are indicated by the presence of small scale reactivation surfaces within bedforms. However, mud drapes, and evidence of low stage re-working are absent, and it is therefore assumed that these elements were deposited within a river which was a perennial system with a relatively constant discharge.

The DA Type 2, giant planar cross-stratified bedform preserved within Macroform IV of Colour Heugh is interpreted to be the deposit of 2-D dune greater than 2 m high. The local development of intrasets within the giant form suggests some component of oblique flow and sediment deposition. Such flow is indicative of a bank attached bar, such as that illustrated in Figure 2.3b. Minor reactivation surfaces which cross-cut the giant scale bedform reflect either minor changes in the direction of sediment accretion, or small scale discharge variations in the channel. There is no evidence to suggest dissection and emergence of the bedform. This again suggests perennial flow within the fluvial channel.

Sandy bedform (SB) architectural elements represent mesoform scale bedforms developed within the fluvial channel or superimposed on macroforms. SB Type 1 elements are preserved within Bowden Doors and Colour Heugh. These units display an upward decrease in set size indicative of deposition during waning flow conditions.

Sediments of SB Type 2 elements are exposed in Colour Heugh (Macroforms V & VI). These units indicate rapid sedimentation under conditions of changing flow (Miall 1985). The presence of form sets and horizontal stratification at the base of Macroform V at Colour Heugh indicates unusual conditions of sandstone deposition. The form sets display angular foresets which evolve downstream into tangential and then asymptotically-based foresets. These changes indicate an increase in current

strength with time (Jopling 1965). With increasing velocity of streamflow a greater proportion of sediment is taken into suspension, and carried beyond the crest of the bedform. If the bedforms are out of harmony with the flow conditions, because of insufficient time for adjustments to take place, form sets may be preserved, due to a rapid rate of suspended-load deposition (Jopling 1966). The form sets are draped with horizontally stratified sediments deposited under upper flow regime conditions. It is therefore possible that the form sets and horizontal stratification represent a period of rapid increase in flow.

The deposits of normal fluvial flow i.e. the cross-stratified sediments described above are interbedded with massive sandstones. The massive sandstone units take two geometric forms: Sms and Smc. These facies form SM Type 1 and Type 2 architectural elements (Table 2.6). Facies Sms (SM Type 1 element) takes the form of a laterally extensive body with an undulose to erosional base. Scours developed along the basal surface are locally associated with deformation of underlying sediments, indicating a dynamic sedimentation process. Within the element structured sediments are locally preserved, as are sweeping undulose laminae. The presence of water escape structures within the massive sandstone sheets indicates liquefaction or deformation of the sediments on pore fluid expulsion.

Facies Smc forms the SM Type 2 architectural element of Table 2.6. The units are lenticular in section and erosionally based, and contain a fill of massive sand. Concentric laminae are developed at the channel margins, and these grade into a structureless sandstone channel fill. The upper portion of the channel fill may display mutually interfering cross-laminae (Plate 3.3).

The lack of large scale reactivation surfaces within the Fell Sandstone suggests that the Fell Sandstone river system was a perennial one which flowed constantly, and hence the climate must have been relatively wet. Raymond (1985) interprets the climate during the Dinantian to have been warm, tropical and humid. Periodic flooding occurred within the river to produce the large scale bedforms of DA Type 2 and the mesoform scale bedforms of SB Type 1.

As mentioned above, the lateral extent of the fluvial channel sandstones exposed in the Belford region could not be ascertained. Using the methods outlined in section 2.4.2 it has been possible to reconstruct some aspects of the palaeohydrology of the sandstones exposed. These parameters are detailed in Table 3.2. It has been established that the sinuosity of the channel represented by Bowden Doors and Colour Heugh, was approximately 1.2, and hence the sediments were deposited by a low sinuosity system. Using the empirical relationships of Schumm (1968b) it may be established that the width/depth ratio of the Fell Sandstone river at Belford was approximately 50.

The height of thirty periodic bedforms were measured to establish the depth of the fluvial channel (see section 2.2.4). It is clear that there are two scales of bedform developed within the outcrops at Colour Heugh and Bowden Doors. The larger scale bedforms are only preserved within the Colour Heugh section as macroform IV. Smaller scale periodic bedforms are ubiquitous throughout both sections. It is likely that the larger scale bedforms are related to periods of greater flow depth, and/or higher flow stage. The presence of dune form sets and horizontal stratification within Macroform V at Colour Heugh also suggests a higher flow rate. A flow depth of between 6 and 8 m has been estimated for the normal flow depth, and a depth of 12-18 m has been estimated for the formation of the larger scale bedforms (Table 3.2).

| Average dune height (m) | Height after decompac tion (m) | Estimated water depth (m) | Channel w/d ratio | Width (m) | Average velocity (m/s) | Average discharge (m³/sec) |
|---|---|---|---|---|---|---|
| Average of 5 (Colour Heugh) 2.12 | 2.96 | 12-18 | 50 | 600-900 | 0.8 | 9,000 |
| Average of 25 (Bowden Doors) 0.89 | 1.24 | 6-8 | 50 | 300-400 | 0.8 | 1,960 |
| | $\phi_c = 0.16$ $\phi_o = 0.4$ | | | | | |

Table 3.2. Reconstructed palaeohydrological parameters of the Fell Sandstone river, as established from the outcrops at Belford.

Using the estimates of flow depth and a width/depth value of 50, the width of the Fell Sandstone river was approximately 350-750 m. Hence the Fell Sandstone river was not the basinwide system envisaged by Monro (1986) but rather the smaller, fault controlled system of Fordham (1989) and Turner et al (1993). Modern

rivers of a similar scale include the Platte River of the USA and the Tana River of Norway (Table 2.5).

The sediments which are preserved within the Fell Sandstone Group of the Belford region are quartz arenites, sub-litharenites and subarkoses (Figure 3.15a), which lie in the recycled orogen province (Figure 3.15b) of Dickinson (1985). The sediments are inferred to have been provided from the Fenno-Scandanavian high to the north (Monro 1986, Cliff *et al* 1991). However, quartz arenites are unusual in fluvial environments. First cycle quartz arenites have been documented from the modern day Orinoco river of Venezuela by Johnsson *et al* (1988) where tropical weathering produced mature sandstones rapidly from granitic basement. Such a climate has been inferred during deposition of the Fell Sandstone Group.

## 3.4. Summary.

The Fell Sandstone river was a laterally restricted perennial system, which flowed across a flood plain controlled by intrabasinal faults. Channel sandbodies were funnelled into areas of rapid subsidence, located in the footwalls of the major syn-sedimentary faults such as the Hetton Fault.

Sediment was provided from the northeast, from a source containing meta-sedimentary, volcanic and plutonic bodies. Sediment was transported significant distances before being deposited within the Fell Sandstone river. Humid, tropical weathering resulted in the rapid degradation of unstable framework grains and the deposition of a first cycle quartz arenite.

The sinuosity of the Fell Sandstone river channel was approximately 1.2. The river channel contained mid-channel bars (DA Type 1 elements) and bank attached bars (DA Type 2 elements). Mesoform elements were composed of 2-D and 3-D dunes (SB elements). These bedforms were rarely emergent and hence the braiding index of the river is assumed to have been low.

The massive sandstone facies (architectural elements SM Types 1 and 2) were deposited by flow unrelated to normal fluvial currents. Cross-stratification is largely absent, and hence the flow responsible for the deposition of the massive facies did not maintain traction currents. The massive sandstone facies will be discussed in more detail in Chapter 7.

# Chapter 4
# The Central Appalachian Basin

## 4.1. Regional Geological History Of The Central Appalachian Basin.

The Appalachian Basin (Figure 4.1) is classified as a multistage foreland basin, which developed in response to loading by successive thrust sheets of the Taconian (mid to late Ordovician), Acadian (early to late Devonian) and Alleghanian (Pennsylvanian to Permian) orogens. The Appalachian orogenic belts were obducted across an earlier extensional margin (Tankard 1986a). The Appalachian Basin is separated from the Illinois and Michigan Basins by a system of arches and domes, as illustrated in Figures 4.1 and 4.2a.
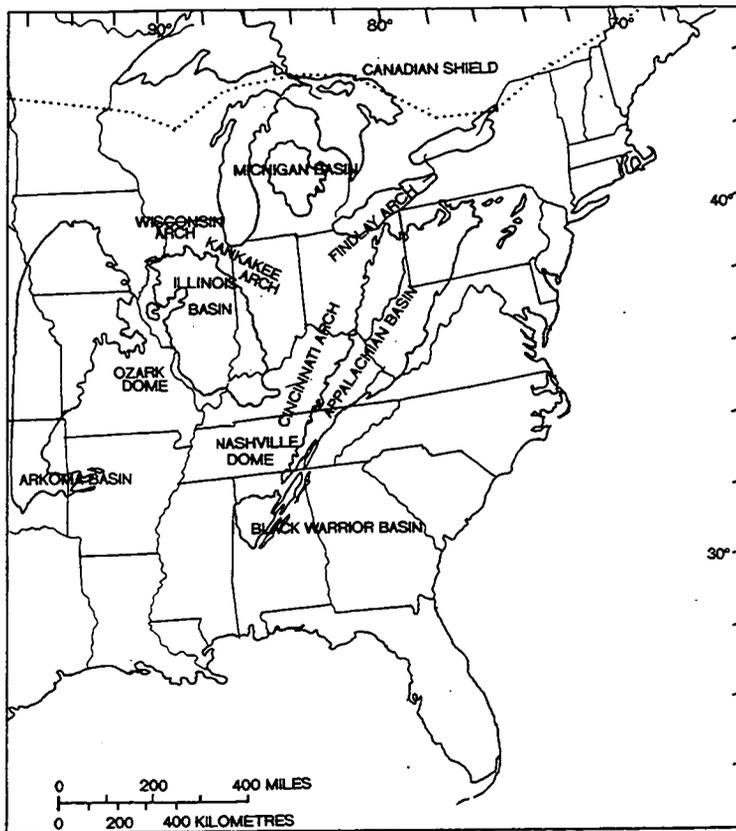


Figure 4.1. The regional setting of the Appalachian Basin.

The Appalachian Basin contains one of the most complete Palaeozoic stratigraphic sections in North America, with the basin-fill ranging in age from late
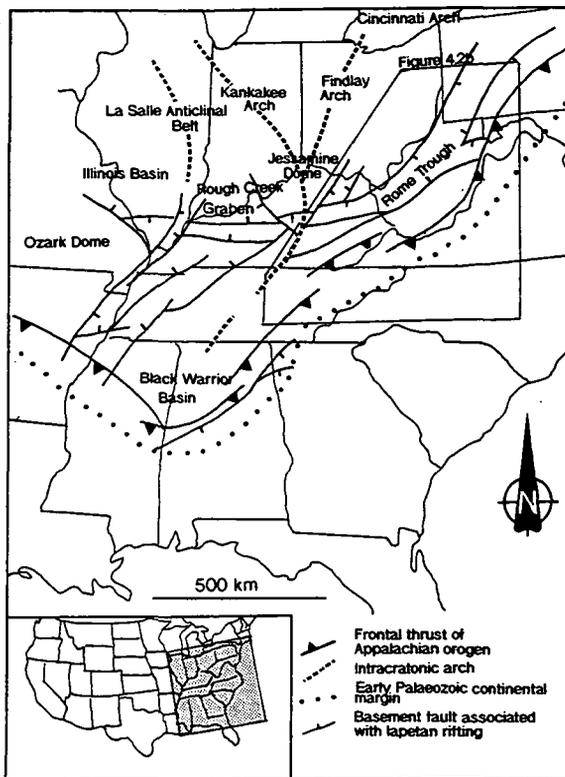
Figure 4.2a. Structural elements of the central United States (modified from Ettensohn 1992).
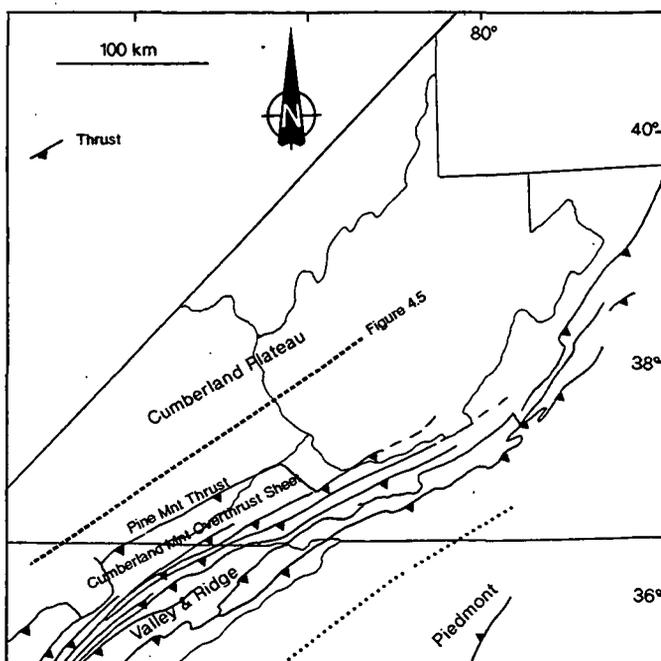


Figure 4.2b. Structural framework of the Appalachian fold belt adjacent to the central Appalachian Basin.

Precambrian to lowest Permian. Appalachian stratigraphy records four major unconformity bounded sequences, which are attributed to pre-convergence deposition, and sedimentation associated with the successive, although diachronous, deformation episodes (Tankard 1986b). A simplified basin history is given in Table 4.1.

This study concentrates on the central Appalachian Basin, which is defined as eastern Kentucky, Virginia and Tennessee, together with the area of West Virginia south of 38° (Wanless 1975). The adjacent Appalachian fold belt is a composite unit, recording peaks of deformation and metamorphism related to the Taconian, Acadian and Alleghanian orogenies (Rast & Skehan 1993). The central Appalachian orogen and foreland basin consist of a number of structural provinces which are illustrated in Figure 4.2b. The Valley and Ridge and Cumberland Plateau provinces (Figure 4.2b), where this study was undertaken, expose strata of predominantly Carboniferous age, which were deformed in the late Palaeozoic.

The Rome trough and Rough Creek graben (Figure 4.2a) are part of a late Precambrian to Cambrian cratonic rift system, which formed contemporaneously with rifting of the early Palaeozoic Iapetus margin (Ettensohn 1992). Syn-sedimentary basement fault movement in the Appalachian Basin was due mainly to thermal subsidence (Kolata & Nelson 1990), and resulted in a thick (3,000 m) graben fill succession of marine sedimentary and volcanic rocks (Slingerland et al 1989).

The passive margin of the North American Craton was disrupted in the upper Ordovician by the Taconian orogeny, caused by the collision of eastern Laurentia (North America, Greenland, Scotland and northern Ireland) with an island arc, and a set of micro-continents. The Blue Ridge province, and Piedmont of the central Appalachian fold belt (Figure 4.2b) represent exotic terranes, accreted to the North American Craton at this time (Table 4.1). Juxtaposition of tectonic belts occurred along major fault zones, with emplacement occurring along near horizontal thrust sheets (Higgins et al 1988).

The Appalachian foreland Basin developed with the inception of the Taconian orogeny. The forebulge of the Appalachian thrust fault, represented by the Cincinnati Arch and Jessamine Dome (Figure 4.2a), developed due to lithospheric flexural interaction between the Appalachian Basin and the contemporaneous intracratonic Michigan and Illinois Basins (Quinlan & Beaumont 1984). Over 1,800 m of sediments were deposited in the foreland between the middle Ordovician and early Silurian (Slingerland et al 1989), and these record passage from marine carbonates to clastic tidal and deltaic facies. The middle Silurian to early Devonian is represented by carbonates, evaporites and fine grained clastics (Slingerland et al 1989).

| SYSTEM | SERIES | STAGE | AGE (MA) | CLIMATE | PALAEO LAT | EXTENSION | COMPRESSION | TECTONICS | SEDIMENTATION |
|---|---|---|---|---|---|---|---|---|---|
| PERMIAN | | | 250 | Dry | 7°N | | Alleghanian | Pine Mountain thrust represents the most westward extension of thrusting. Alleghanian Orogeny developed through thin skinned thrusting with major detachment in the Cambrian strata. Valley & Ridge & Plateau province created. | |
| CARBONIFEROUS — PENNSYLVANIAN | Virgilian | | 300 | | | | | | Conemaugh & Monongehela Formations. Floodplain/marginal marine environments. |
| | Missourian | | | Seasonal Humid | | | | | Mid-Pennsylvanian cyclic sedimentation in low lying coastal environments. |
| | Desmoinesian | | | | | | | | Lower Pennsylvanian Lee-Breathitt Basin. Lee-type sands represent axial fluvial drainage system, carrying quartzose sand. Breathitt-type lithologies represent transverse fluvial/estuarine systems sourced from Appalachian front. |
| | Atokan | | | Tropical Humid | 7°S | | | Mid-Carboniferous unconformity represents onset of Alleghanian uplift & migration of forebulge. | Unconformity surface records major erosion by streams flowing southwest. |
| | Morrowan | | | | | | | | Upper Mississippian: westward migration of Paragon/Pocohontas clastic wedge sourced from Alleghanian highlands. |
| CARBONIFEROUS — MISSISSIPPIAN | Chesterian | | | Dry | | | | | Lower Mississippian: Bordern & Fort Payne Formations: Marginal/shallow marine environments. |
| | Valmeyran | Meramecian | 350 | | 15°S | | Acadian | Thrusting in Blue Ridge & Piedmont terrains. | |
| | | Osagean | | | | | | | |
| | Kinderhookian | | | | | | | | |
| DEVONIAN | Chautauquan | | | | | | | | Ohio Shale represents highstand of sea level, followed by regression & progradation of Catskill delta. |
| | Senecan | | | | | | | | |
| | Erian | | | | | | | | |
| | Ulsterian | | 400 | | | | | | Deep marine, distal deposits of Catskill delta. |
| SILURIAN | Cayugan | | | | | | | Avalon micro-plate thrust against North American Craton. | |
| | Niagaran | | | | | | | | |
| | Alexandrian | | | | | | | | Thick carbonate development & fine grained siliciclatics. |
| ORDOVICIAN | Cincinnatian | | | | 20–25°S | | Taconian | Basin & arch system established. Cincinnati Arch represents the forebulge of the thrust front. | |
| | Champlaninian | | 450 | | | | Blountian | Orogeny centred in New England. Thrusting within Blue Ridge & Piedmont provinces. Initiation of Appalachian Basin. | |
| | Canadian | | | | | | | | |
| CAMBRIAN | St.Croixan | | 500 / 550 | | | | | Development of a series of grabens including Rome Trough | Timescale from Shaver et al 1985. Information derived from: Hatcher & Odom (1980); Fiall (1985); Secor et al (1986); Higgins et al (1988); Cecil et al (1985); Sinha et al (1989); Ettensohn (1992); Rast & Skehan (1993); Hamilton-Smith (1993). |

Table 4.1. A generalised history of the central Appalachian Basin.

Commencing in the early Devonian, convergence between Laurentia and an unspecified plate produced the Acadian orogeny, which was centred in New England (Slingerland *et al* 1989). The Acadian period of the central Appalachian Basin was characterised by long periods of relative quiescence. The Cincinnati-Findlay arch system (Figure 4.2a) periodically subsided and uplifted, alternately yoking together and decoupling the Appalachian and Illinois Basins (Tankard 1986b). The Appalachian highlands to the east shed vast quantities of clastic debris into the subsiding foreland basin, which were deposited in the progradational Catskill deltaic wedge. The black shales of the Ohio and New Albany Shales (Figure 4.3) were deposited in anaerobic conditions as the seaward extension of the Catskill Delta (Chesnut 1988). The Bedford-Berea shale/sandstone (Figure 4.3) unit represents lowstand deposition between the Catskill and Pocono clastic wedges (Ettensohn 1992).
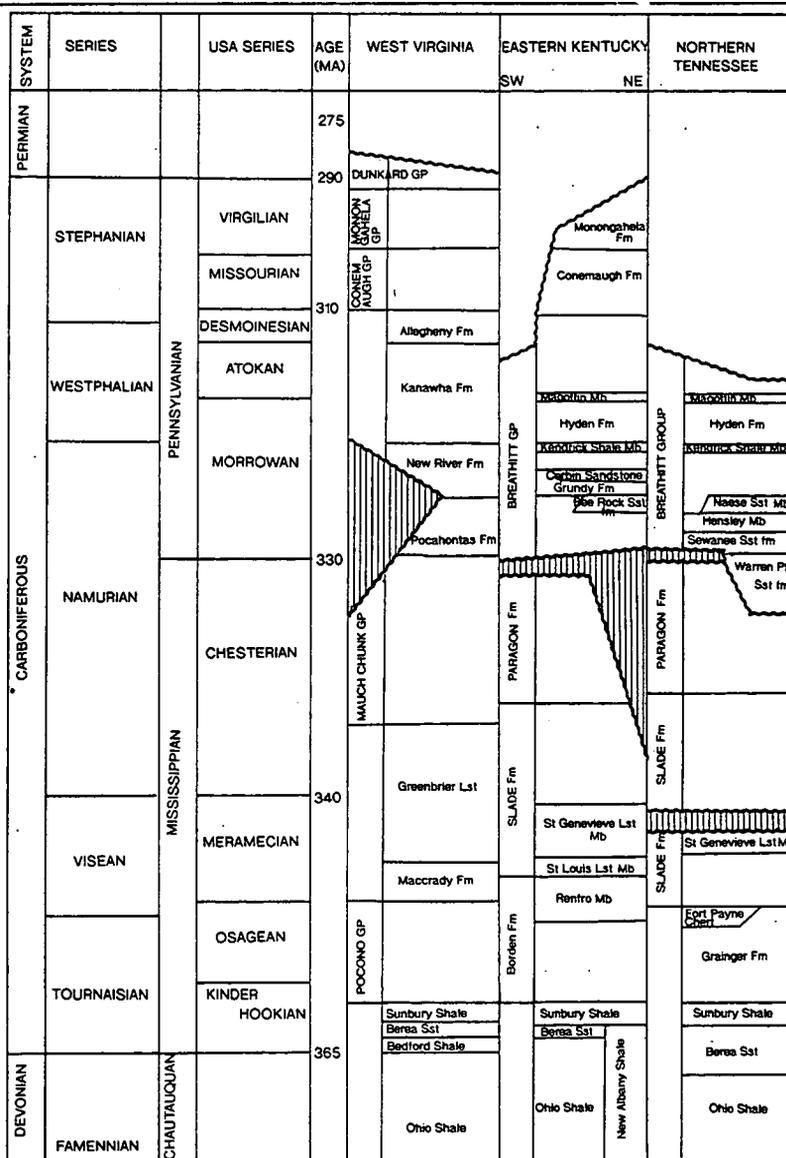


*Figure 4.3. A generalised stratigraphy of the central Appalachian Basin.*

The Sunbury Shale (Figure 4.3) represents a period of black shale deposition related to basin deepening. Progradation of the Borden and Fort Payne (Figure 4.3) deltaic sediments (Pocono wedge) from the northeast marked the final stages of the Acadian Orogeny. In late Mississippian times a widespread carbonate unit, the Slade Formation (Figure 4.3), was deposited across a stable platform during a period of quiescence (Chesnut 1988).

The overlying Chesterian clastic wedge of the Paragon/Mauch Chunk Groups (Figure 4.3) represents deposition in a wide range of shallow deltaic, marine and inter-tidal clastic environments (Chesnut 1988). The Appalachian Basin apparently experienced minimal subsidence during the deposition of this wedge (Chesnut 1988). The palaeogeography of the Chesterian is illustrated in Figure 4.4a.
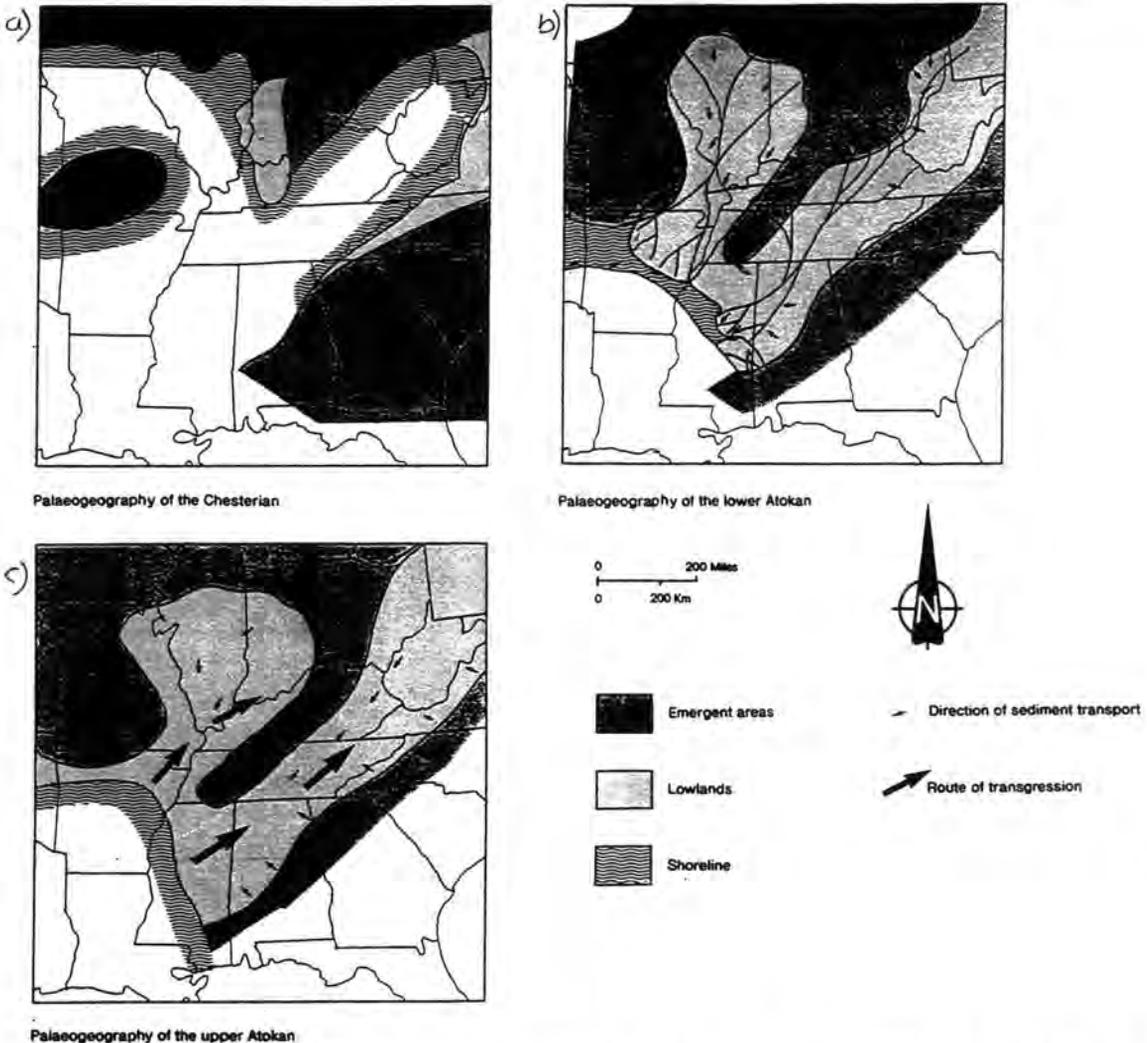


*Figure 4.4. Palaeogeography of the central United States (reconstructions after Potter & Siever 1956; Graham et al 1976; Rice 1984; Donaldson et al 1985; Ettensohn 1992 & this study)*

Closing of the proto-Atlantic continued through late Mississippian to Permian time, culminating in the collision of Gondwana with Laurussia, and the Alleghanian orogeny. The nature of Alleghanian tectonism is poorly constrained chronologically and tectonically (Chesnut 1988), and the timing of collision is controversial. Some models place the collision in the Late Pennsylvanian to Permian (Rast 1988), with other models supporting collision during earliest Pennsylvanian (Hatcher *et al* 1989). The direction of subduction between Laurussia and Gondwana is also controversial (Secor *et al* 1986).

A conformable contact exists between the upper Mississippian and lower Pennsylvanian in the deepest parts of the central Appalachian Basin. However, in most of the basin a major unconformity is developed (Figure 4.3). The unconformity truncates the Pennsylvanian Pocahontas Formation (Figure 4.3), and hence is correctly termed the early Pennsylvanian unconformity (Chesnut 1988).

The early Pennsylvanian unconformity may be traced over much of the eastern United States, and has been attributed to a worldwide eustatic sea level change (Saunders & Ramsbottom 1986), tectonic uplift created by relaxation of stress (Chesnut 1988), or tectonic uplift created by continent-continent collision (Tankard 1986b). The unconformity in the Appalachian Basin probably reflects the inception of the Alleghanian orogeny (Ettensohn 1992). During the early Alleghanian orogeny the sea retreated to the southwest, resulting in emergence of much of the North American Craton (Rice & Schwietering 1988). A well defined southerly palaeoslope existed over much of the eastern United States, which was inherited from a similar drainage system of late Mississippian age or older (Donaldson & Schumaker 1981).

Emplacement of the Alleghanian thrusts depressed the lithosphere and resulted in the location of the Lee-Breathitt foreland basin to the northwest of the Paragon/Mauch Chunk foreland basin. During the Alleghanian orogeny 200 km of crustal shortening occurred (Tankard 1986b). The transport of thrust sheets for such considerable distances resulted in the loading of thick and thermally mature continental crust. This continental crust had great rigidity, and was therefore sluggish in its initial response to loading (Tankard 1986b). However, isostatic flexure maintained the Cincinnati Arch along the landward margin of the basin. Uplift of the Cincinnati Arch resulted in the development of a low, north facing cuesta (Wanless 1975), which defined the northwest margin of the central Appalachian Basin (Rice & Schwiering 1988). With time the forebulge slowly migrated away from the area of tectonism (Chesnut 1988).

Widespread sub-aerial erosion and intensive weathering of the Mississippian and early Pennsylvanian surface is manifested by karst topography and high aluminium soils (Donaldson *et al* 1985). Extensive palaeovalley drainage systems,

incised up to 135 m, have been documented at the mid-Carboniferous unconformity in the central Appalachian Basin, particularly along the western margin (Rice 1984). These palaeovalleys are related to similar features in the Illinois Basin (Chapter 5). The flow direction inferred from the incised valleys is towards the south and south west, sub-parallel to the regional palaeoslope.

With a rise in base level, sediment accumulated across the North American Craton (Donaldson et al 1985). Sediments of Morrowan age overlie the mid-Carboniferous unconformity in the central Appalachian Basin (Chesnut 1988) and progressively onlap older Mississippian sediments to the northwest. The fact that younger units onlap the unconformity northwestwards, indicates that some migration of the peripheral bulge occurred (Chesnut 1988). Morrowan and Atokan sediments of the central Appalachian Basin are represented by the Breathitt Group and Lee-type sands (Figure 4.3). These sediments are similar in composition to those of the same age deposited in the Illinois, Michigan and Black Warrior Basins (Figure 4.1).

The Breathitt Group (Figure 4.3) is composed of shales, siltstones, immature sandstones and numerous economically important bituminous coal beds. The sediments were deposited in fluvio-deltaic and marginal marine environments with clastic material derived from the Appalachian mountains to the east. The lower part of the Breathitt Group contains Lee-type sandbodies (Figure 4.3). The Lee-type sandstones are sub-litharenites to quartz arenites, which were deposited within braided fluvial systems. The rivers flowed axially down the Appalachian Basin and carried sediment derived from a cratonic source to the north (Chesnut 1988). The Lee sandbelts are interpreted to represent fluvial trunk streams situated between the mid-Carboniferous forebulge to the northwest and the Breathitt clastic wedge to the southeast (Chesnut 1988).

Morrowan and Atokan sediments did not crest the emergent forebulge to the west, and hence the only outlet available for sediment was southwest, towards the Ouachita trough of the Arkoma Basin, along the Black Warrior-Appalachian foreland Basins (Graham et al 1976). Figure 4.4b illustrates the palaeogeography and sediment transport paths of the early Pennsylvanian. Deposition of Morrowan sediments in the Michigan and Illinois Basins occurred in fluvial systems (Potter & Siever 1956), similar to those depositing the Lee-type sands in the Appalachian Basin. Deposition in the Black Warrior Basin occurred primarily in deltaic and shallow marine environments (Graham et al 1976), and turbidites represent the same time interval in the Ouachita trough of the Arkoma Basin (Morris 1974).

The palaeogeography of the mid Pennsylvanian (Atokan) is illustrated in Figure 4.4c. The sediments of the Breathitt Group were deposited in a marginal marine environment, and contain well developed sedimentary cycles comprising sandstone,

seatearth, coal and marine mudstone (Klein & Willard 1989). Each cyclothem represents 430 Ka, and corresponds to the 430 Ka glacio-eustatic cycle, modulated by secondary earth orbital eccentricity (Ettensohn 1992). Thus the cycles are interpreted in terms of glacially driven eustatic processes by Ettensohn (1992). This interpretation contrasts with that of Klein & Willard (1989) and Tankard (1986b), where the Breathitt cyclothems are believed to be the result of flexural tectonics at the collision margin of North America.

The mid Pennsylvanian marked a period of intermittent cresting of the foreland bulge by the westward prograding Breathitt Group. Marine transgressions entered the foreland basin from the west through saddles in the forebulge (Ettensohn 1992), and are preserved as marine shales such as the Kendrick and Magoffin Shale Members (Figure 4.3).

The emplacement of a further thrust sheet during the Desmoinesian resulted in the formation of the Allegheny basin (Chesnut 1988), another foreland basin located to the northeast of the Lee-Breathitt foreland basin in Virginia and southern Pennsylvanian (Chesnut 1988). Deposition of the late Pennsylvanian is represented by the Conemaugh and Monongahela Formations (Figure 4.3) which contain abundant red beds and pedogenic flint clays. The sediments were deposited in westward prograding deltas. During late Pennsylvanian time marine waters entered the Appalachian basin only across the diminished forebulge north of the Jessamine Dome (Englund & Thomas 1990). By this time the Ouachita trough had apparently been closed by collision with Gondwana and access of marine waters to the basin was blocked (Ettensohn 1992). Limestones were deposited during marine incursions.

## 4.2. The Lower Pennsylvanian: Breathitt Group And Lee-Type Sands.

The Pennsylvanian rocks of the central Appalachian Basin take the form of a coal bearing wedge of sandstone, siltstone and shale which thickens towards the basin axis in the southeast. Sediments were deposited at near equatorial latitudes (Scotese 1990, Table 4.1) in a tropical ever-wet climate (Winston 1990; Cecil 1990).

Pennsylvanian sediments are decoupled from the Mississippian by the early Pennsylvanian unconformity. Entrenched into the unconformity surface, along the northwest margin of the Appalachian Basin, are a series of sub-Pennsylvanian valleys which reach 6 km in width (Rice 1984; Rice & Schwietering 1988). The sub-Pennsylvanian channels are filled with Lee-type conglomeratic sandstones and quartz arenites such as the Livingstone Conglomerate (Figure 4.6b) which were deposited by southerly flowing streams. The streams radiated away from the Jessamine Dome

of the Cincinnati Arch, and connected with an axial river which flowed from a northerly source (Rice 1984).

With relative sea level rise, and an increase in sediment supply due to the advance of the Alleghanian front (Rice 1984), sediments aggraded in the central Appalachian Basin. The coarse grained Lee-type sediments filled the palaeovalleys, and spread across the basin floor.

The lower part of the Breathitt is divided into formations (informal terminology of Chesnut 1988) by the Lee-type sandstones and by coal horizons where the Lee is absent (Figure 4.5). Lateral and vertical variations of lithology in the Pennsylvanian strata make correlation and stratigraphic analysis difficult. Diagnostic marine and plant fossils are uncommon (Rice 1984).

| N TENNESSEE | E KENTUCKY | SW VIRGINIA |
|---|---|---|
| Conemaugh & Monongahela Formations | | |
| Princess formation | | |
| Stoney Fork member | | |
| Four Corners formation | | |
| Magoffin member | | |
| Hyden formation | | |
| Kendrick Shale member | | - |
| Pikeville formation | | |
| Betsie Shale member | | |
| Corbin Sandstone formation | Manchester Coal / Grundy formation | |
| Rex Coal / Naese Sst | Pine Creek Sst / Rockcastle Sst — Bee Rock Sandstone formation | Alvy Creek formation |
| Dave Branch Shale member | | Coal Upper Seaboard |
| Sewanee formation | | Bottom Creek formation |
| Dark Ridge Member | | Pocahontas No 8 |
| Warren Point Sandstone formation | | Pocahontas Formation |
| SLADE FORMATION & OLDER | | |

Figure 4.5. A detailed stratigraphy of the Breathitt Group using the informal nomenclature of Chesnut (1988).

The Lee-type units consist of several thick sandstone formations which contain a minor amount of mudstone. Chesnut (1988) recognised four informal formations within the Lee: Warren Point, Sewanee, Bee Rock Sandstone and Corbin

(Figure 4.5). Individual units are defined by lithology, and any significant fine grained units are assigned to the interfingering Breathitt Group. The Lee-type sandstone units have scoured bases and fine upward to mudstones which are typically truncated by subsequent sandstone units (Wizevich 1991). The sandstones are relatively coarse grained, commonly pebbly, and in places conglomeratic, and are characteristically composed of 90-99% quartz. The quartz pebbles are well rounded (Siever & Potter 1956). The sandstone belts are typically overlain by coal beds and rooted seatearths. In places brackish or marine shales may directly overlie the sandstones. Where coal horizons are absent, the uppermost part of the sandbodies may be bioturbated and show evidence of marine reworking (Chesnut 1989).

Lee-type sandstones take the form of linear, or broadly lobate bodies (Rice 1984). The outcrop of Lee-type sandstones is illustrated in Figure 4.6a, and a cross-section in Figure 4.6b. Individual formations of the Lee are 17-100 km wide, and occupy southwest-northeast trending belts up to 200 m thick (Chesnut 1988). The sandstone belts were deposited adjacent to the forebulge of the central Appalachian Basin (Figure 4.4b), and are arranged so that the westernmost formation, the Corbin, is the youngest (Figures 4.5 & 4.6b). Internally the Lee sandstone belts are composed of multilateral and multistorey sandbodies, structured by uni-directional cross-bedding.
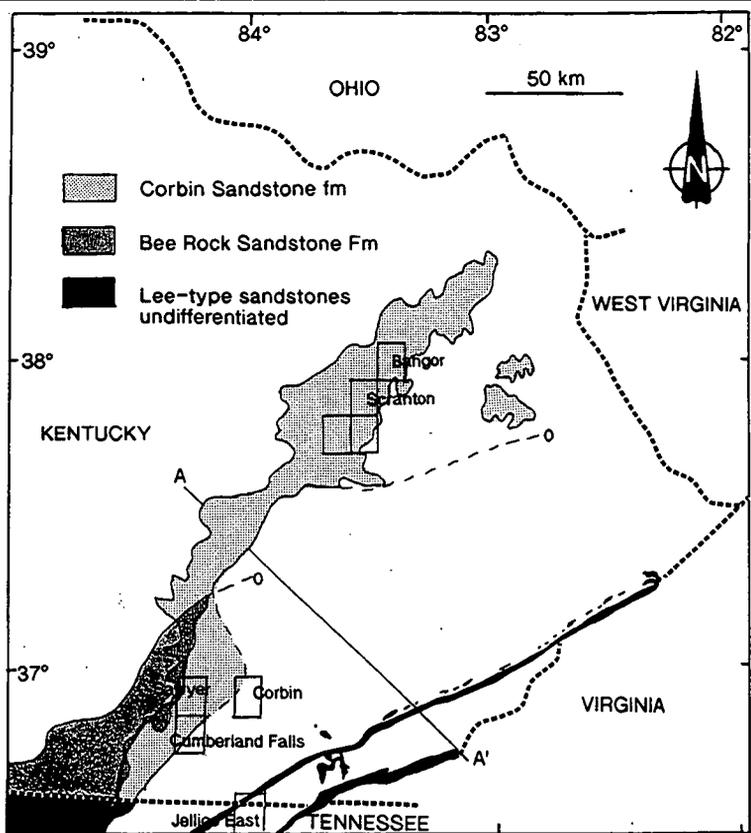


Figure 4.6a. Outcrop patterns of the Lee-type sandstones of the central Appalachian Basin. Terminology is that of Chesnut (1988).

A
Corbin Sst fm

Breathitt Gp

Bee Rock Sst fm

Livingston Conglomerate

Slade Fm

300 m

Paragon Fm

Sewanee Sst Fm

50 km

Warren Point Sst fm

Datum: Manchester Coal Bed (Figure 4.5).

Section restored through
Pine Mountain overthrust zone

A'
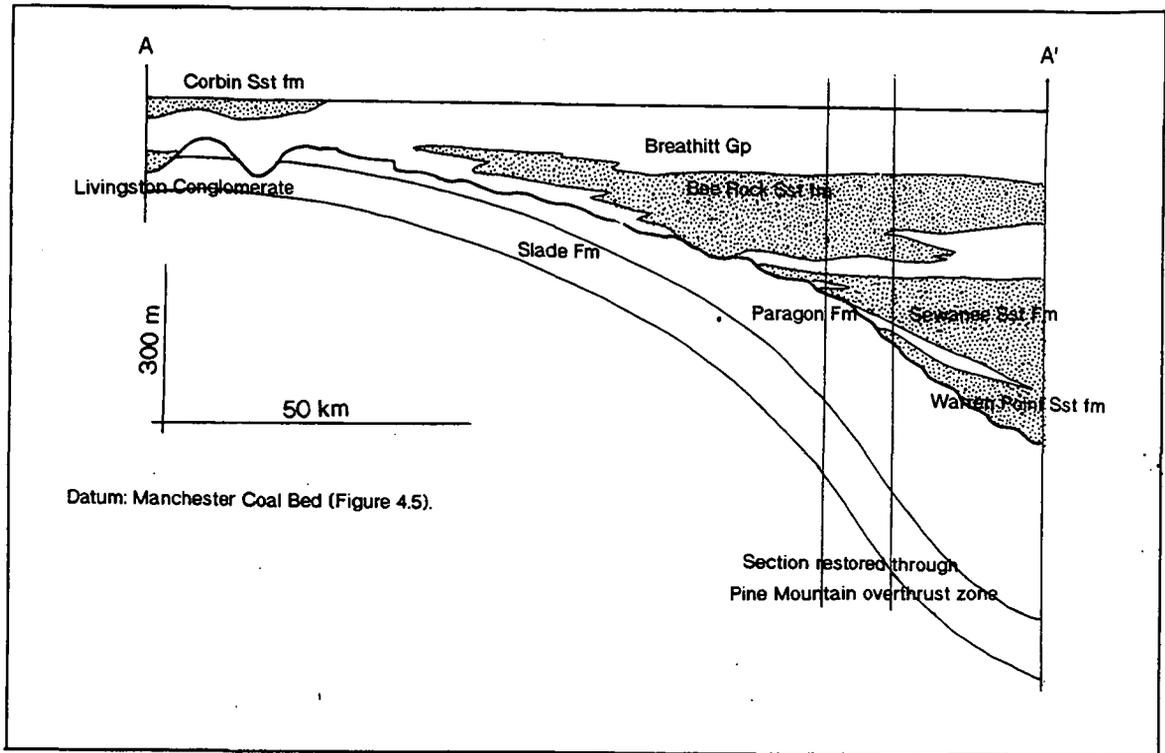
*Figure 4.6b. A cross-section through the central Appalachian Basin (modified after Rice 1984).*

The Breathitt Group includes shales, siltstone, 'dirty' sandstones, coal and some thin limestones. The sandstones are fine grained sub-litharenites and litharenites, which contain angular to sub-rounded grains of feldspar and quartz, conspicuous mica and small fragments of schist and igneous rocks (Rice 1984). Sandbody orientation and cross-stratification indicate that the Breathitt Group represents many cycles of west or northwesterly clastic progradation (Chesnut 1988), thus indicating that these sandstones were derived from the rising Appalachian highlands.

Several scales of depositional unit are recognised in the Breathitt Group. The smallest of these is the cyclothem consisting of sandstone, seatearth, coal and marine mudstone (section 4.1). Intermediate scale features are represented by eight coal bearing units (Figure 4.5) which are separated by major marine horizons. Each of these informal formations comprises on average 6 cyclothems, and each formation represents approximately 2.5 Ma. An overall coarsening-upward in the Breathitt Group relates to multiple progradation events controlled by the intensity of the Alleghanian orogeny (Ettensohn 1992).

In the past the Breathitt Group was interpreted to have been deposited in restricted coastal marine and coastal lowland environments. Detailed mapping by Chesnut (1988) has demonstrated that tonsteins, coals and marine horizons are regional in extent, and may occur across the entire central Appalachian Basin with only local interruptions. Alternations of extensive coal beds and marine strata with fluvial sandstones suggest deposition on a broad coastal plain, traversed by small shallow streams, which was subjected to repeated transgressions during rising relative sea level (Ettensohn 1992). Rhythmically bedded facies within the Breathitt Group are indicative of deposition within tidally influenced environments (Martino & Sanderson 1993; Greb & Chesnut 1992a).

A number of models have been invoked to explain the relationship between the clean quartzose Lee-type sandstones and the lithic-rich Breathitt Group, which are reviewed by Chesnut (1988). Horne et al (1974) inferred that the Lee sandstone units were deposited in a beach or barrier bar environment, with land to the southeast and sea to the northwest. In this model the Lee-type sands were transported into nearshore environments by westward, or northwestward flowing streams, draining the emerging land areas of the central Appalachian fold belt. In the high energy nearshore environment, wave action eliminated the less stable minerals and finer grained clastics. The general southwestward current direction, implied by cross-bedding, was attributed to longshore drift, and the southwestward migration of tidal channels.

Many geologists (Rice 1984; Chesnut 1988; Wizevich 1991) now postulate a fluvial origin for the Lee-type sands. Among the definitive characteristics are the disconformable bases and multistorey nature of the sandstones, the fining-upwards of grain size, the dominance of planar and trough cross-stratification, and the common occurrence of coalified plant remains.

The orientation of the sandbelts of the Breathitt and Lee were controlled by the position of the forebulge. The Breathitt Group represents short alluvial wedges prograding to the Lee sandbelts where the Breathitt rivers became tributaries to the Lee. The Lee rivers flowed to the southwest where they encountered Breathitt-type alluvial wedges and deltas prograding to the north from the Ouachita highlands. The Lee rivers were deflected by the clastic wedge and flowed south (Figure 4.4b).

If the Lee Formation is accepted as fluvial, as it is in this study, then the thin Breathitt lithologies within the Lee formation represent local overbank deposits and peat swamps. The extensive Breathitt lithologies occurring between the Lee sandstone belts represent either westward progradation of Breathitt deltas over Lee sandbodies or marine transgressions (Chesnut 1988).

## 4.3. The Bee Rock Sandstone formation.

The Bee Rock Sandstone formation (informal nomenclature of Chesnut 1988) forms a northeast-southwest trending belt (Figure 4.6a & b) of approximately 91 km wide (Chesnut 1988), separated from the Sewanee by the Alvy Creek formation (Figure 4.5). The upper part of the Bee Rock Sandstone interbeds with the Dave Branch shale member of the Grundy formation, and the sandstone belt thins to the northwest and southeast. Chesnut (1988) calculated the gradient of depositional slope during Bee Rock Sandstone times as approximately 0.0004 (0.4 m/km).

The Bee Rock Sandstone formation includes sandstone units originally mapped as the Rockcastle, Naese, 'K' and 'G' Sandstones (Chesnut 1988), together with other small, unnamed units. Quartzose Lee-type sandstones are separated by thin coals and mudstones of brackish, and marginal marine affinity.

The Bee Rock Sandstone formation was examined in Sawyer quadrangle (Figure 4.6a), where the Rockcastle and Pine Creek (formerly 'K') Sandstone members are exposed (terminology of Chesnut 1988). Overall the sediments of the formation fine upwards (Figure 4.7) and display variations in fluvial style. The lateral equivalent of the Rockcastle in Tennessee is the Naese Sandstone. This unit was examined in the Jellico East quadrangle of northern Tennessee (Figure 4.6a).

## 4.3.1. Sedimentology.

### 4.3.1.1. The Rockcastle & Naese Sandstone members.

The Rockcastle member is erosively based, and reaches a maximum thickness of 70 m, although it is generally 30 m thick (Rice 1984). The unit occupies a belt oriented approximately northeast to southwest, and displays dominantly southwesterly palaeocurrents (Rice 1984). The Rockcastle splits into siltstone tongues to the northwest (Rice 1984).

The Rockcastle is stratigraphically located between the Coal Cliff Shale and Barren Fork Coal (Greb & Chesnut 1989) in the Sawyer quadrangle (Figure 4.6a). The Rockcastle is composed of a lower pebbly unit, which grades upwards into an upper sandstone dominated unit. The uppermost beds grade upward from coarse to fine grained sandstone and siltstone (Figure 4.7).

The Rockcastle has been traced southwards into Tennessee where the lower portion is correlated by Englund (1968) with the Naese Sandstone member, the uppermost Lee-type sandstone in the Cumberland overthrust sheet (Figure 4.2b).
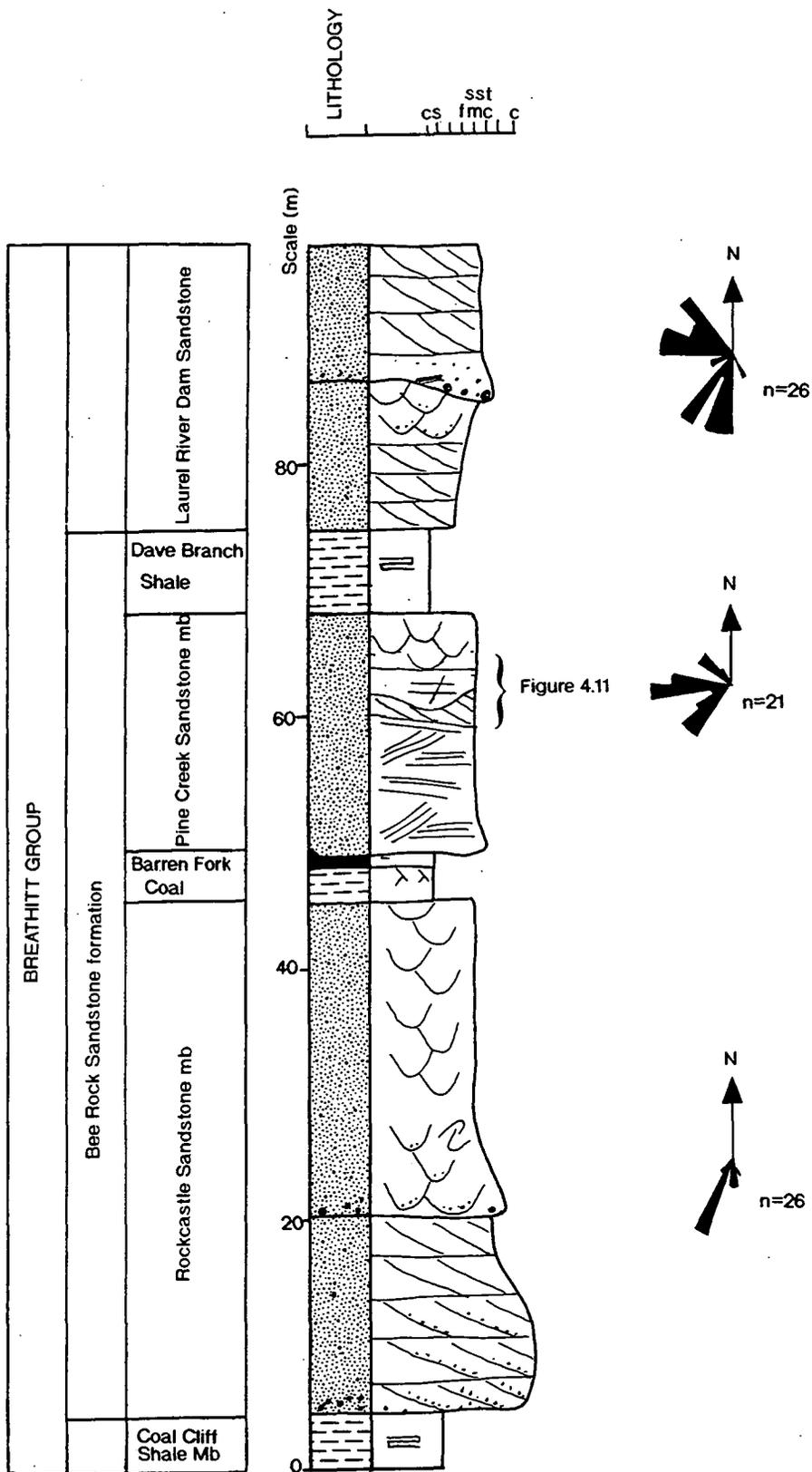
See Appendix I for logging symbols

*Figure 4.7. A generalised sedimentary log through the Bee Rock Sandstone formation exposed in the Sawyer qudrangle (Lat. 36° 57' 30" Long. 84° 16').*

The Naese Sandstone decreases in grain size upwards, and grades laterally into the Breathitt Group. The top of the Naese Sandstone is gradational and hence the upper contact is placed at the base of the overlying Naese Coal Bed (Englund 1968; Rice & Newell 1990). A sandstone of Breathitt-type lithology is placed between the Naese Sandstone and the Rex Coal Bed (Figure 4.5), which marks the top of the Bee Rock Sandstone formation in Kentucky (Chesnut 1988).

Facies of the Rockcastle and Naese Sandstones are outlined below. The sandstones are generally coarse grained and quartzose. Rounded quartz pebbles up to 2 cm in diameter are present within the sediments. The size and volume of these pebbles decreases upwards through the section, and in the downstream direction.

## (i) Facies Descriptions.

*Conglomeratic sandstone (Scg).*

A matrix supported conglomerate takes the form of erosively based sheets 20-120 cm thick and <5 m in lateral extent. The matrix of the conglomerate is a coarse, to very coarse quartzose sandstone. Clasts include abundant rounded to sub-rounded quartz pebbles (<30 mm), mudstone pebbles (<50 mm) and plant fragments. The beds are normally graded with diffuse troughs locally developed.

*Large scale planar cross-stratification (Sp$_l$).*

Sets of 85 to 125 cm thick are developed in medium to very coarse grained sandstone. Foresets are angular to tangential, and dip 25-30°. Normal grading commonly occurs upwards through the foreset with sub-rounded quartz granules (<5 mm) preserved at the base of bedforms. Minor changes in foreset angle indicate small changes in depositional flow characteristics. There is, however, no evidence of large scale reactivation or reworking of foresets such as would be associated with low stage flow. Counter-current ripples are commonly developed in the lower 10 cm of sets.

*Medium scale planar cross-stratification (Sp$_m$).*

Sets of medium scale planar cross-stratification are developed in coarse and medium grained sandstones. Foresets are tangential to angular and dip 15-22°. Normal grading along foresets is common, with rounded quartz granules and small pebbles (2-20 mm diameter) concentrated along the base of foresets. Locally overturning of foresets is a pervasive phenomena, and stacked sets of deformed cross-strata are

locally preserved. Extreme deformation results in the total loss of structure and homogenisation of sediment into thin (<50 cm thick) layers of structureless sandstone.

*Compound cross-stratification (Sc).*

Compound bedforms are developed in medium and coarse grained sandstone. Cosets are 0.75-1.50 m thick and display an overall fining upwards trend. Foresets are tangential to convex-up and dip 5-15°; intrasets dip 25-38°. Within both intrasets and foresets small scale reactivation surfaces indicate changes in flow strength and/or direction. There is, however, no evidence of significant reworking and mud drapes are absent.

*Sheet-like massive sandstone (Sms).*

The lithology of facies Sms does not vary from the structured sediments and remains a medium or coarse grained sandstone with rare, floating, rounded quartz granules <5 mm in diameter. The sheet-like units reach a maximum of 8 m in thickness and generally display a sharp lower bounding surface, although locally the boundary may be poorly defined. The basal surface is undulose with a relief of up to 1.85 m; scours along the basal surface indicate downstream directed erosion. Mudstone pebbles <25 mm in diameter are located within the scours. Weathered pockets 10-50 cm wide may also represent the remanents of mudstone pebbles floating within the massive sandstone.

Internally facies Sms is largely without structure. However, diffuse laminae (5-10 mm apart) are preserved which take the form of mutually interfering trough-like, and sub-horizontal structures. The laminae are picked out by slight changes in texture.

*Channel-like massive sandstone (Smc).*

Facies Smc forms lenticular bodies which range from 1.10-3.30 m in thickness, and 10-105 m in width. The lithology of facies Smc is similar to the surrounding cross-stratified sediments, a medium to coarse grained sandstone. The units display shallow, to steeply dipping margins (<10°-55°), and are slightly asymmetric to symmetric in shape. The near symmetric shape of channels indicates that the channels trend at a high angle to the regional palaeoflow, and hence the structures have a cross-cutting relationship with surrounding structured sediments, within which they are preserved.

The basal contact of channel-like sandstones is sharp and erosive. Clasts are generally concentrated along the scoured bases and include mudstone pebbles (<25 mm), quartz pebbles (<10 mm) and organic debris. Floating sub-rounded to rounded quartz granules (<5 mm) are also preserved within the sediment body. Diffuse and

discontinuous concentric laminae occur parallel to the margins of the channel forms. These grade into the structureless fill. Sub-horizontal laminae also occur in the upper portion of facies Smc.


## (ii) Lateral Profile Analysis.

The upper portion of the Naese Sandstone has been studied in the Jellico East quadrangle of Tennessee (Figure 4.6a). Three representative lateral profiles are described below. The sections are all composed of a medium to fine grained sandstone which contain a small number of quartz pebbles <10 mm in diameter.


*Naese Sandstone, Section 1.*

This outcrop exposes 10 m of vertical section and is approximately 170 m long. The lateral profile is illustrated in Figure 4.8. The outcrop is oriented parallel to the flow direction, as established from cross-bedding.

Within the profile seven macroforms have been identified, which are separated by third order bounding surfaces (Figure 4.8). At the base of the outcrop a fourth order bounding surface is exposed. Below this erosional surface palaeoflow, established from cross-stratification, was to the southeast. Above this surface palaeocurrents are towards the southwest.

Macroform I overlies the fourth order bounding surface and consists of a gravelly bedform (GB) architectural element composed of facies Scg, SB Type 2 elements composed of $St_m$ and $Sp_m$ and an SM Type 1 element (Table 2.6). Palaeocurrents within this macroform indicate palaeoflow to the southwest with low variance (Figure 4.8).

Macroforms II, III, IV, and V (Figure 4.8) are composed of stacked sets of $Sp_m$, $Sp_s$ and $St_m$, combined to form SB Type 2 architectural elements divided by 2A bounding surfaces. Palaeoflow was to the southwest (Figure 4.8). These macroforms are particularly interesting due to the preservation of stacked sets containing almost completely overturned cross-bed foresets (Figure 4.8) as illustrated in Plates 4.1 and 4.2. Erosional truncation by overlying beds has limited the sets to 2-8 m in length. Most recumbent folds are simple, nested recumbent V's or U's classified within the Type 1 folds of Allen & Banks (1972). The axial plane of deformation is generally near the horizontal, although it ranges from 10° upstream to 15° downstream. In some sets
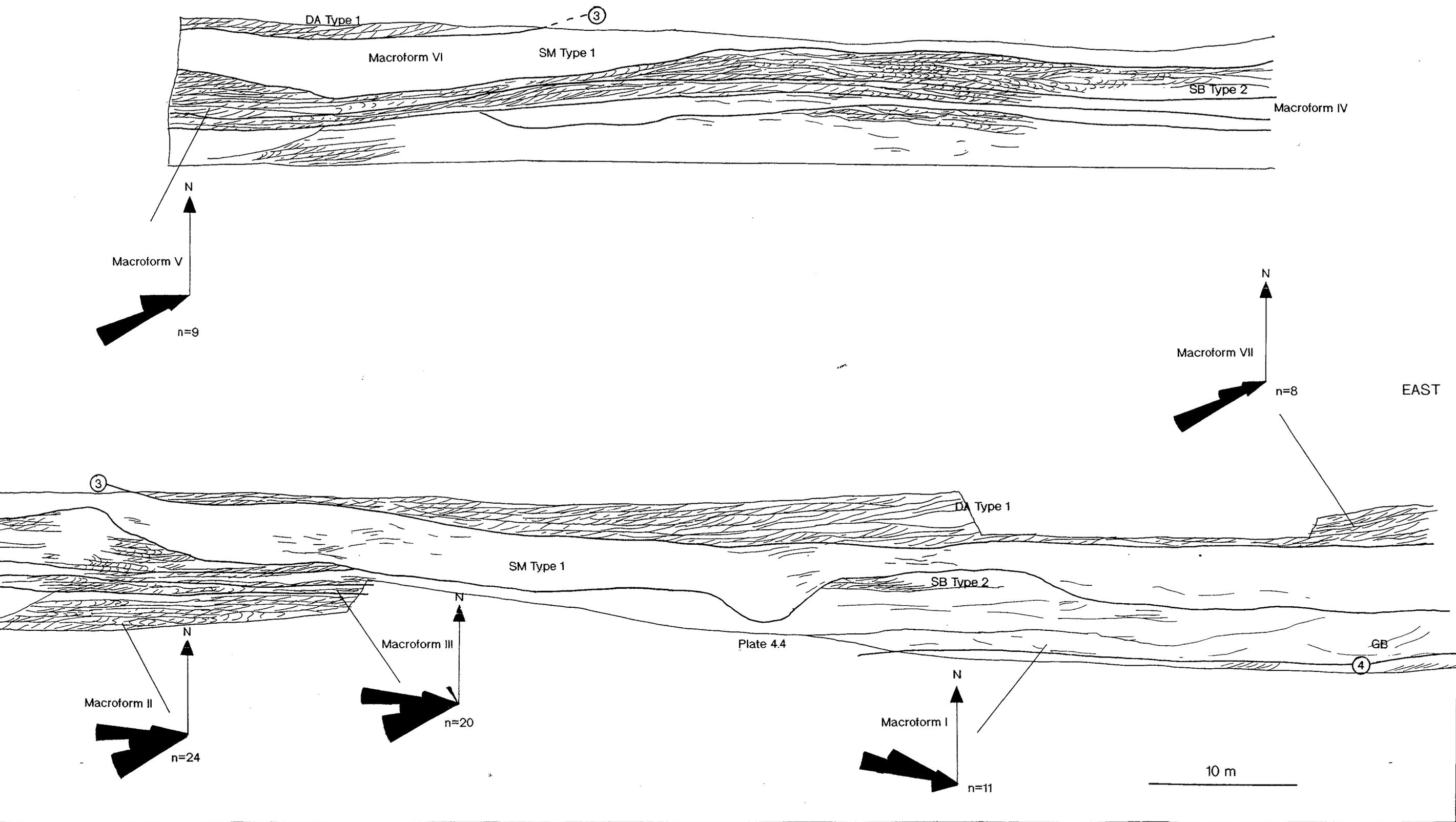
Figure 4.8. A line drawing of Naese Sandstone member, Section 1 (Lat. 36° 31' 1",
Long. 84° 4' 10").

Plate 4.1. Macroform II, Naese Sandstone member, Section 1.
Stacked sets of Spm and Stm are combined to form SB Type 2 architectural elements separated by 2A bounding surfaces. The sets display pervasive overturning of Types 1 & 2 of Allen & Banks (1972), with the hinge line lying from approximately horizontal to 10° upstream.



Plate 4.2. Macroform II, Naese Sandstone member, Section 1.
Stacked sets of Spm and Stm are combined to form SB Type 2 architectural elements. Deformation takes the form of the Type 1 recumbent folds of Allen & Banks (1972). Nested V's and U's occur with the hinge line varying between horizontal and 10° upstream. Intense deformation has resulted in the total loss of structure within sediment layers of <50 cm thick.

complete loss of structure has occurred, and sandstones are preserved as thin, homogenous layers (Plate 4.2). Within Macroform V stoss side climbing sets of highly

deformed strata are preserved (Figure 4.8). However, the overturned foresets are generally near horizontal.

In the upper portion of Macroform II two channel-like massive sandstone units (facies Smc) are developed. One of these is illustrated in Plate 4.3, and forms a unit 1.75 m thick and 10 m wide. The preserved upstream margin of the channel form dips 22°, the downstream margin is less well defined. Facies Smc is internally structureless with concentric laminae 5-10 mm apart preserved parallel to the lower bounding surface (Plate 4.3). The upper surfaces of facies Smc are coincident with overlying third order bounding surfaces (Figure 4.8). The near symmetrical appearance of facies Smc sandbodies indicates that they trend at a high angle to the fluvial flow and were emplaced along a plane near perpendicular to that of the flow direction.



*Plate 4.3. Macroform II, Naese Sandstone member, Section 1.*
*Stacked sets of deformed cross-strata are cut by a unit of facies Smc. Note lens cap for scale. Facies Smc displays sharp margins dipping 22° which truncate sets of deformed cross-stratification. Facies Smc displays concentric laminae developed at the channel margins. These grade into a structureless sandstone.*

Macroform VI is composed of a sheet-like massive sandstone (facies Sms) which may be traced laterally in excess of 200 m parallel to flow, and is inferred to be equivalent to a unit of facies Sms situated approximately 250 m laterally. The undulose base of the sheet appears to be erosional (Figure 4.8) due to truncation of cross-bedding (Plate 4.4). Internally facies Sms is largely without structure (Plate 4.4) but locally preserves diffuse trough-like laminae (Figure 4.8) and mudstone clasts as described above.

Macroform VI is overlain by an undulose third order bounding surface which is in turn overlain by Macroform VII. Macroform VII is composed of simple sets of $Sp_l$ and Sc which are arranged in DA Type 1 architectural elements (Plate 4.4). Palaeoflow within the macroform was to the southwest (Figure 4.8).
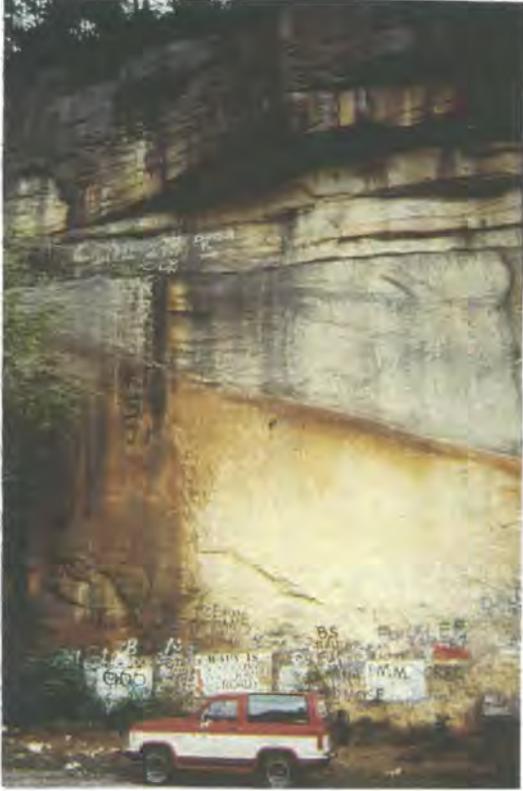


*Plate 4.4. Facies Sms of Macroform IV, Naese Sandstone member, Section 1. A unit of facies Sms ≤10 m thick, is preserved through the section. The unit cuts out cross-stratification, thus indicating scours developed across the lower boundingsurface. Facies Sms is internally structureless. Macroform IV is overlain by a third order bounding surface, which is in turn overlain by a DA Type 1 architectural element consisting of facies Stm and Sc.*

*Naese Sandstone, Section 2.*

Section 2 is approximately 30 m in length and exposes 6 m of vertical section. The lateral profile, illustrated in Figure 4.9, is oriented approximately parallel to the flow direction.

Three macroforms have been identified from this section. Macroform I is composed of structured sediments arranged in a DA Type 2 architectural element (Table 2.6). The cross-bed sets display angular to concave-up foresets which dip <25° and show no evidence of low stage reworking. Palaeoflow was to the southwest. The DA Type 2 element is cut by a unit of facies Smc (SM Type 2 architectural element). The SM Type 2 architectural element is 1.10 m thick and >25 m in lateral extent. The downstream margin dips <28° with the upstream margin poorly defined. The top of the massive sandstone unit is coincident with a third order
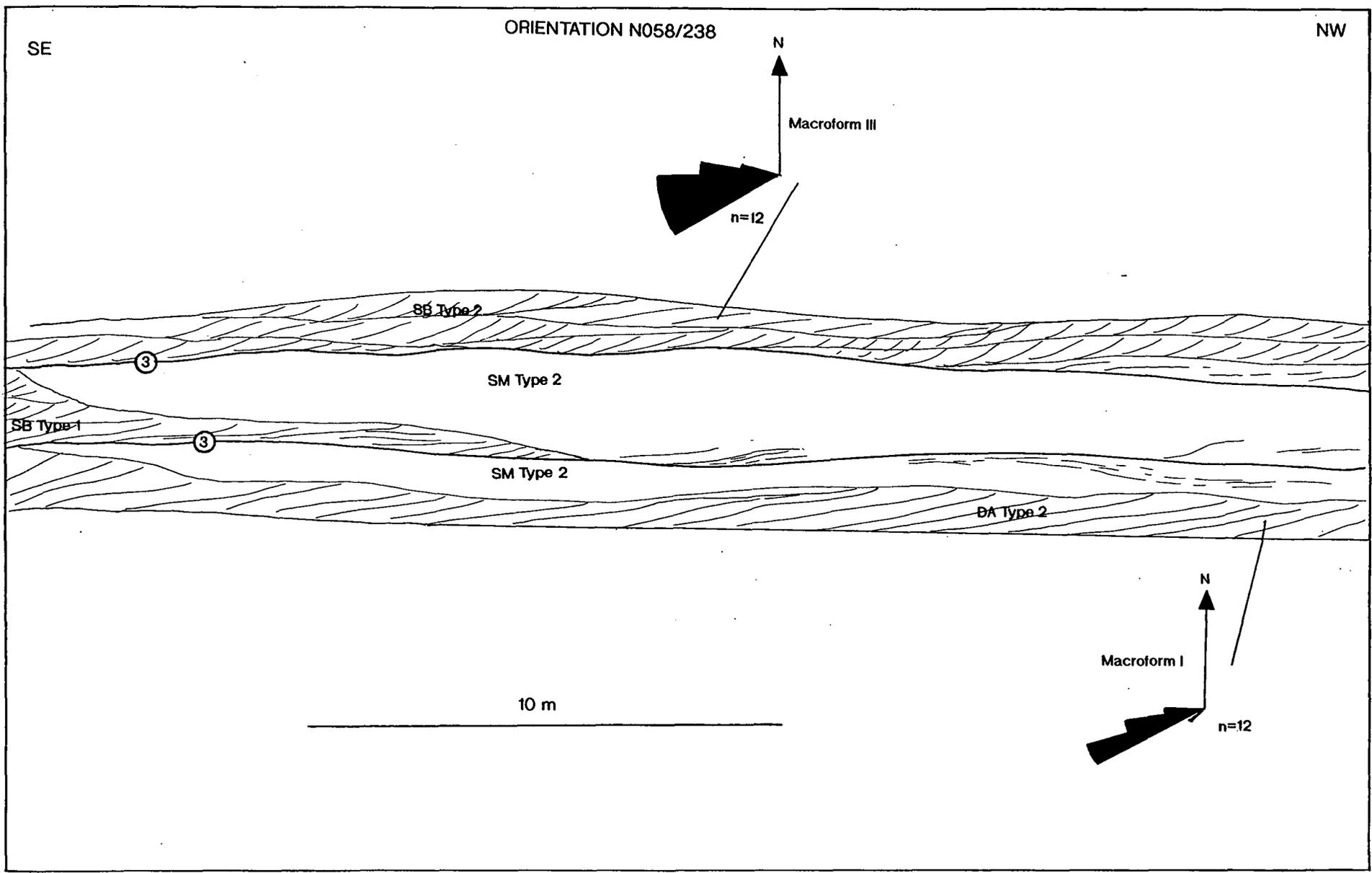
Figure 4.9. A line drawing of Naese Sandstone member, Section 2 (Lat. 36° 33' 15",
Long. 84° 3' 40").

bounding surface (Figure 4.9). Internally the unit is largely structureless. However, laminae 2-10 mm apart are preserved parallel to the margin of the sandstone body (Plate 4.5). These grade into the structureless sandstone fill.



*Plate 4.5. Facies Smc, Naese Sandstone member, Section 2. Facies Smc preserves concentric laminae parallel to the erosive base of the unit. Facies Smc is otherwise internally homogenous. Overlying facies Smc a third order bounding surface is developed which is in turn overlain by SB Type 2 architectural elements.*

Macroform II is composed of SB Type 1 and 2 elements, separated by second order bounding surfaces. These structured facies are cut by a unit of facies Smc which is in excess of 25 m wide and <3.30 m thick. The downstream margin of the unit dips 10°. Internally facies Smc displays little structure. Disseminated organic debris and mudclasts (<5 mm) are located in the lower 10 cm, but are lost upwards.

Macroform III is poorly exposed and consists of facies $Sp_m$ and $St_m$ arranged in SB Type 2 architectural elements separated by second order bounding surfaces. The macroform is lost in the overlying vegetation.

Palaeocurrents for Macroforms II and III indicate flow was to the southwest. The symmetrical appearance of facies Smc indicates that the sediment bodies are cross-sections of channels which trend at a high angle to the fluvial flow direction as established through cross-bedding measurements.

*Naese Sandstone, Section 3.*

Section 3, illustrated in Figure 4.10, covers approximately 40 m of outcrop and is oriented parallel to the flow direction. Three macroforms have been identified within the section (Figure 4.10). Macroform I consists of $Sp_m$ and $St_m$ arranged in SB Type 2 architectural elements separated by second order bounding surfaces (Table 2.6). A

lag of organic debris is often preserved in the base of cosets. Palaeocurrents are to the southwest and display low variance (Figure 4.10).

Macroform II is composed of a large scale planar cross-stratified set 1.85-1.95 m thick forming a DA Type 2 architectural element. A lenticular unit of facies Smc (SM Type 2) is preserved within the upper portion of Macroform II, with the upper surface coincident with the overlying third order bounding surface. The channel-like unit of facies Smc is 12 m in length, and 1.35 m thick (Plate 4.6). The margins of the structure dip 15-18°, with the upstream margin parallel to the foresets of the $Sp_l$ set. The near symmetrical appearance of the channel indicates a flow direction perpendicular to that of the currents depositing the cross-stratified sediments.



*Plate 4.6. Facies Smc, Naese Sandstone member, Section 3.*
*A unit of facies Smc is preserved within Macroform II of Figure 4.20. The upper surface of the facies is coincident with a third order bounding surface. Both upstream and downstream margins of facies Smc are preserved. The upstream margin dips 10°, and the downstream margin 18°. The channel-like unit is 12 m wide and 1.35 m deep. The upstream margin of facies Smc lies parallel to the foresets of the adjacent DA Type 2 architectural element.*

Macroform III is composed of $Sp_m$ sets arranged in a SB Type 2 architectural element. All three macroforms display palaeocurrents to the southwest (Figure 4.10).
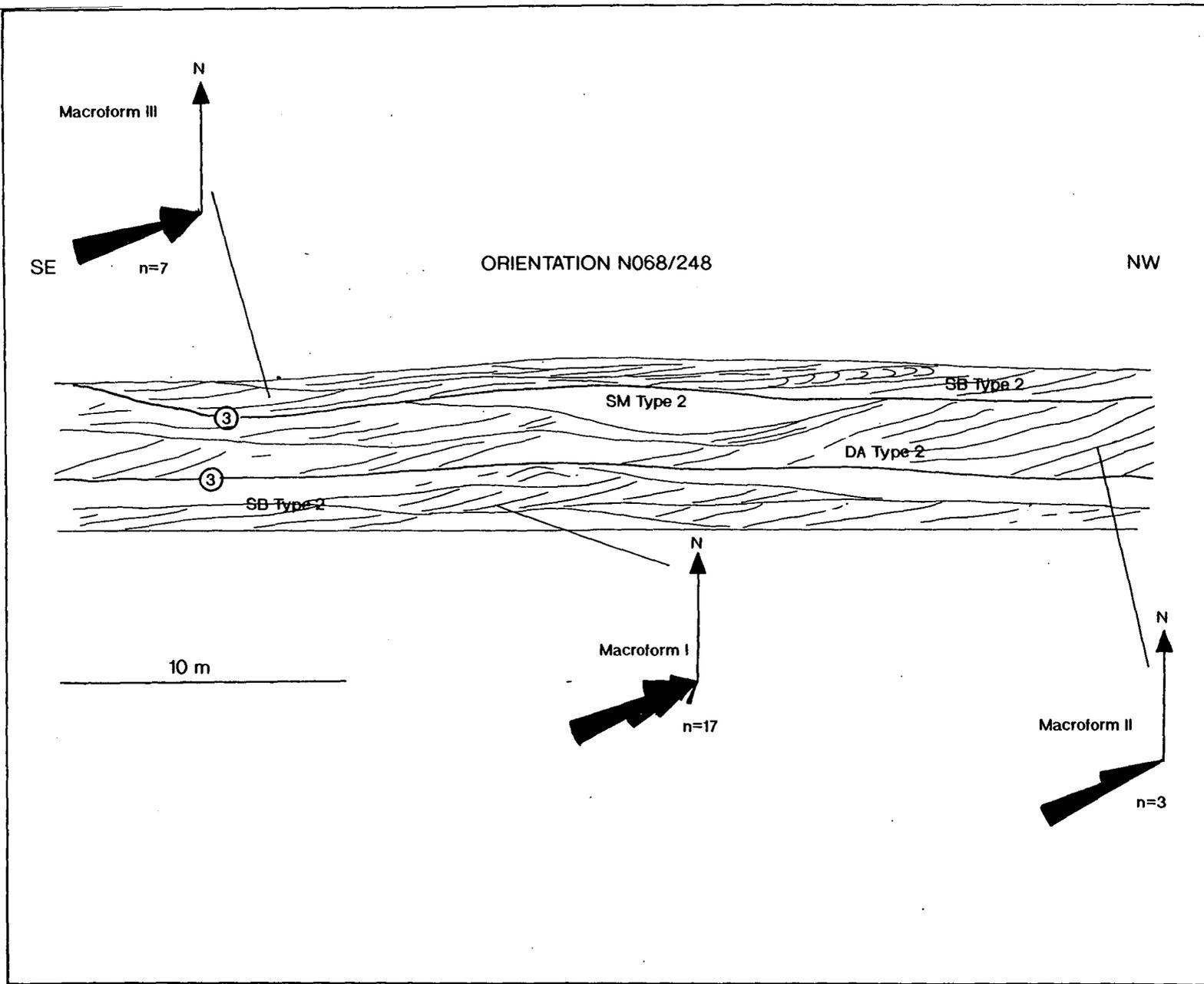
Figure 4.10. A line drawing of Naese Sandstone member, Section 3 (Lat. 36° 33' 5",
Long. 84° 3' 10").

## 4.3.1.2. The Pine Creek Sandstone member.

The Pine Creek Sandstone is located stratigraphically between the Barren Fork Coal and the Dave Branch Shale in the Sawyer quadrangle (Figure 4.7) and is classified as the first sandstone to overlie the Rockcastle in eastern Kentucky (Chesnut 1988). The facies preserved within the Pine Creek Sandstone are outlined below.

### (i) Facies Descriptions.

*Low angle cross-stratification (Sl).*

The depositional surfaces of this facies dip < 5° in a direction which is perpendicular to the fluvial current directions. Individual sets are 30-60 cm thick and display normal grading. The base of the sets may contain sub-angular to sub-rounded quartz pebbles < 15 mm in diameter. Mica is often concentrated along the foreset surfaces, imparting a flaggy appearance. These sets are interpreted as lateral accretion deposits.

*Medium scale planar cross-stratification ($Sp_m$).*

Sets of this facies are 60-80 cm thick, and composed of medium grained sandstone, with minor mica and disseminated organic matter. Foresets are dominantly tangential and dip 18-25°. At the base of some sets sub-rounded quartz granules (<5 mm) are preserved which grade upwards into medium and fine grained sandstone. Locally the foresets are overturned and take the form of the Type 1 deformation of Allen & Banks (1972). The hinge of deformation is generally parallel to the basal surface. Small scale changes in the angle of foresets indicate changes in depositional conditions. However, there is no evidence of large scale reduction in water depth, associated with reworking.

*Medium scale trough cross-stratification ($St_m$).*

Trough cross-stratified sets 40-65 cm thick are developed in medium and fine grained sandstone. The fill of trough cross-stratified sets may be either symmetrical or asymmetric. Lags of sub-rounded quartz pebbles <15 mm long are commonly preserved in the trough axes, and above this lag sets are normally graded.

*Small scale trough (St$_s$) & planar (Sp$_s$) cross-stratification.*

Small scale sets of trough and planar cross-stratification are developed in fine and medium grained sandstone. Foresets are generally tangential and dip 18-25°. Deformation of the foresets is common and takes the form of simple recumbent folds (Type 1 of Allen & Banks 1972). Sets of trough and planar cross-stratification are arranged in cosets 30-50 cm thick, which are bounded by essentially horizontal second order surfaces.

*Channel-like massive sandstone (Smc).*

Lenticular units of facies Smc are preserved in medium grained sandstone. The units display erosive basal surfaces which are associated with deformation of the underlying cross-stratification. The basal surface commonly has relief of up to 1.40 m and scours tend to be lined with mudstone pebbles (<15 mm in diameter) and rounded quartz pebbles (<10 mm). Quartz granules (<5 mm in diameter) are also preserved floating in the sandstone.

*Rippled sandstone/siltstone (Fx).*

Rippled fine grained cosets are 5-25 cm thick, and are often lenticular in geometry. The rippled sandstones are generally fine grained and contain large quantities of disseminated organic matter and mica, together with rounded mudstone pebbles (<15 mm). Ripples are asymmetric with rounded crests and wavelength from 30-35 mm.

*Mudstone (Fm).*

The mudstone facies forms units <12 m thick, of unknown lateral extent, such as the Dave Branch Shale (Figure 4.7). The facies is carbonaceous and contains a high percentage of mica. Siderite nodules are locally preserved and are commonly associated with intense bioturbation of low diversity traces. Thin lenses of mudstone (<5 cm thick) are found within sandstone units and represent the top of fining-upwards units.

**(ii) Lateral Profile Analysis.**

*Pine Creek Sandstone, Section 1.*

The Pine Creek Sandstone is 25 m thick in this area (Figure 4.7). Section 1 forms the upper part of the Pine Creek Sandstone as exposed in the Laurel River Dam spillway section of Sawyer quadrangle (Figure 4.6a). Section 1, illustrated in

Figure 4.11, covers 11 m of vertical section and extends approximately 100 m laterally parallel to the palaeoflow.

Three macroforms have been identified within this section. Macroform I is composed of sets of facies Sl which form a part of a LA architectural element (Table 2.6). Palaeocurrent indicators preserved within the macroform are to the southeast with a considerable spread (Figures 4.7 & 4.11). This flow orientation is oblique to the palaeoflow established from cross-bedding within the remainder of the section.

Macroform II is composed of facies $Sp_m$ and $Sp_s$ which are combined to form three SB Type 2 architectural elements. Palaeoflow within these macroforms is to the west and southwest. The SB elements are cut by a unit of facies Smc which forms a SM Type 2 architectural element. The channel-like sandstone is 105 m wide and reaches a maximum thickness of 4.40 m (Figure 4.11). The upstream margin dips at 55° and the downstream margin at 20°. The unit displays internal scour surfaces lined by rounded quartz granules <5 mm in diameter. Disseminated organic matter is also concentrated along the basal surface and the internal scours. Concentric laminae are developed in the base of the unit (Figure 4.11, Plate 4.7) but are lost upwards. Dynamic emplacement of this feature is indicated by the deformation of the underlying cross-bedding (Plate 4.8). The direction of facies Smc emplacement is believed to be perpendicular to the palaeoflow, as established from cross-bedding.



Plate 4.7. Pine Creek Sandstone member, Section 1.
A unit of facies Smc is preserved overlying SB Type 2 architectural elements. Scale represents 1 m. Facies Smc has sharp, erosive boundaries, of which the downstream margin is steeper and reaches a dip of 55°. Concentric laminae are preserved parallel to the margins of the channel form. These grade into a structureless sandstone fill.

WEST

EAST

N

Macroform III

n=26

SB Type 1

SB Type 1

KYC3

KYC2

SM Type 2

KYC1

SM Type 2

③

KYC

KYC4

③

LA

N

Macroform I

n=24

N

Macroform II

n=17

10 m
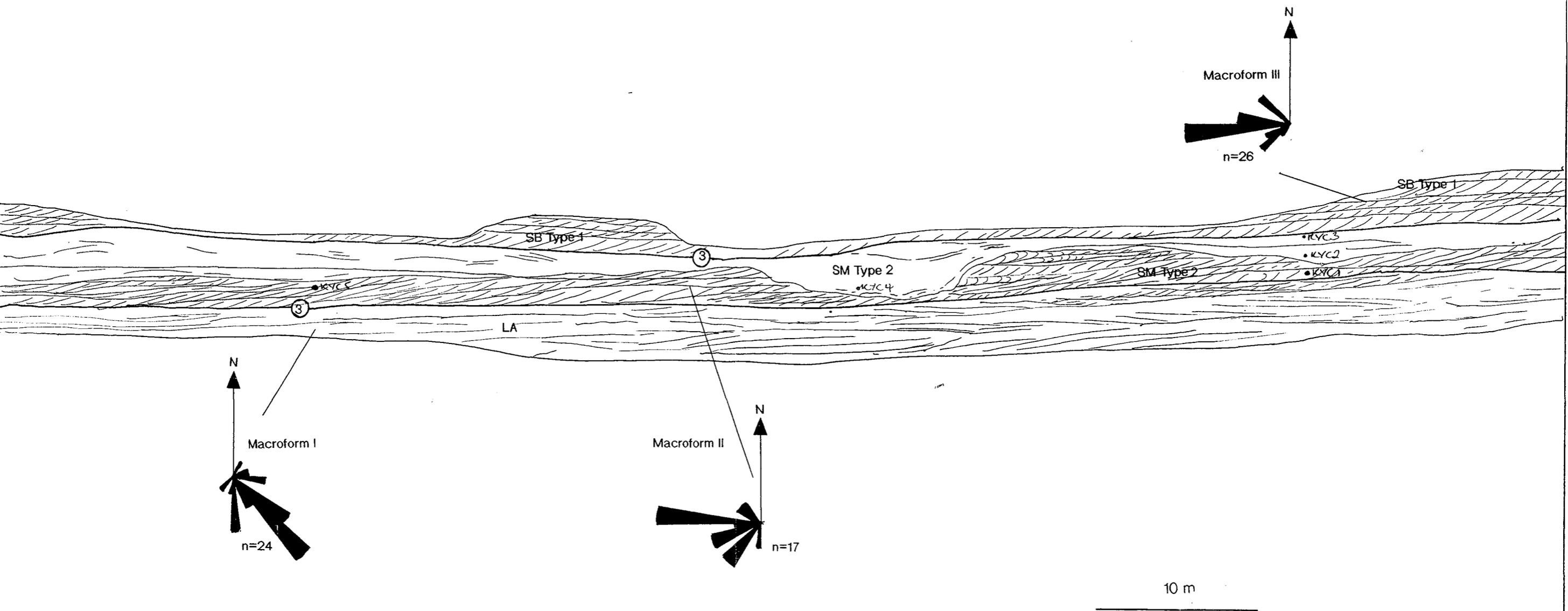
Figure 4.11. A line drawing of Pine Creek Sandstone member, Section 1 (Lat. 36° 57' 30", Long 84° 16').

The upper surface of the SM Type 2 architectural element is coincident with a third order bounding surface. In part of the section this upper surface is exposed, and small asymmetric ripples with rounded crests are preserved across the top of the unit. The ripples are oriented along a plane N060/240° and indicate a palaeoflow to the southeast. Thus the current flowing over the channel-like massive sandstone was oriented oblique to fluvial palaeoflow established from the cross-stratification.



*Plate 4.8. Base of facies Smc, Pine Creek Sandstone member, Section 1.*
*The emplacement of facies Smc has caused deformation of underlying cross-stratified sediments which are composed of a SB Type 2 architectural element.*

Macroform III is composed of $St_m$ and $St_s$ arranged in a number of SB Type 1 architectural elements of 0.70-0.90 m thick separated by second order bounding surfaces (Table 2.6). Palaeocurrent directions indicate that flow was to the west.

*Pine Creek Sandstone, Section 2.*

Section 2 of the Pine Creek Sandstone is 65 m long and 4.50 m high and is illustrated in Figure 4.12. The section contains no major bounding surfaces. However, the section contains two CM architectural elements. Fine grained sandstones, siltstones and mudstones of facies Fx and Fm are arranged in units which display upward-coarsening and upward increase in set size, interpreted to be of levee origin. Palaeoflow was to the southeast away from the fluvial channel to which the channel

SOUTH

ORIENTATION N172/352

NORTH

SM Type 2

CM

CM

N

n=17

10 m
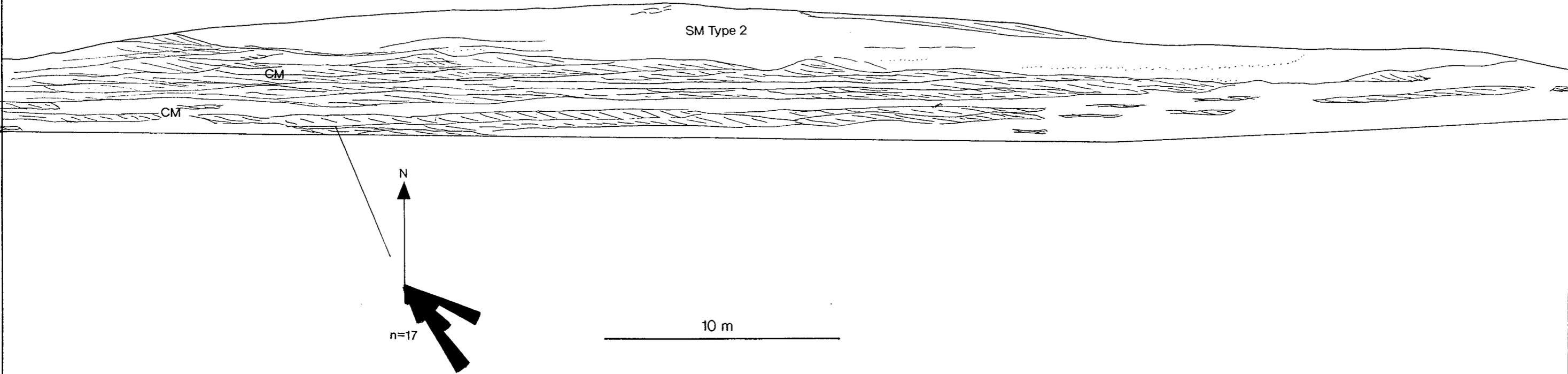
Figure 4.12. A line drawing of Pine Creek Sandstone member, Section 2 (Lat. 36° 57' 15", Long 84° 16' 40").

margin deposits are related. Thus the river channel is inferred to have flowed towards the southwest.

The CM elements are overlain by a channel-like massive sandstone of facies Smc (SM Type 2 element). The lenticular channel-like massive sandstone is 56.60 m wide and reaches a maximum depth of 2.08 m (Plate 4.9). The channel margins dip at a low angle (<15°). Internal erosion surfaces are marked by concentrations of quartz granules (<5 mm) and mudclasts (<10 mm). Disseminated organic matter is common throughout the unit. The symmetric appearance of the channel-like unit indicates that it was emplaced along a plane oriented east/west, and hence perpendicular to the flow of the fluvial channel.



*Plate 4.9. Facies Smc, Pine Creek Sandstone member, Section 2.*
*Facies Smc (SM Type 2 architectural element) is preserved overlying fine grained sediments of CM architectural elements. The CM elements display coarsening and increasing bed thickness upwards. Facies Smc has sharp margins with the basal scour and internal erosional surfaces picked out by concentrations of quartz granules. Concentric laminae are preserved parallel to the margins of the facies.*

### 4.3.2. Petrology & Textural Characteristics Of The Bee Rock Sandstone formation.

### (i) The Rockcastle & Naese Sandstone members.

*Textural information and grain size analysis.*

Overall the grain size of the Rockcastle Sandstone member decreases to the southwest, i.e. in the downstream direction. When the Rockcastle is traced

southwards into Tennessee the equivalent Naese Sandstone is a finer grained sandstone.

Only sandstone facies have been included within this study of grain size. Grain size distribution of sandstones within the Rockcastle Sandstone member is illustrated in Figure 4.13a, with Figure 4.13b illustrating the grain size distribution of the Naese Sandstone member. Figure 4.14 illustrates a more detailed grain size analysis of the Naese Sandstone, as exposed in the Jellico East quadrangle (Figure 4.6a).
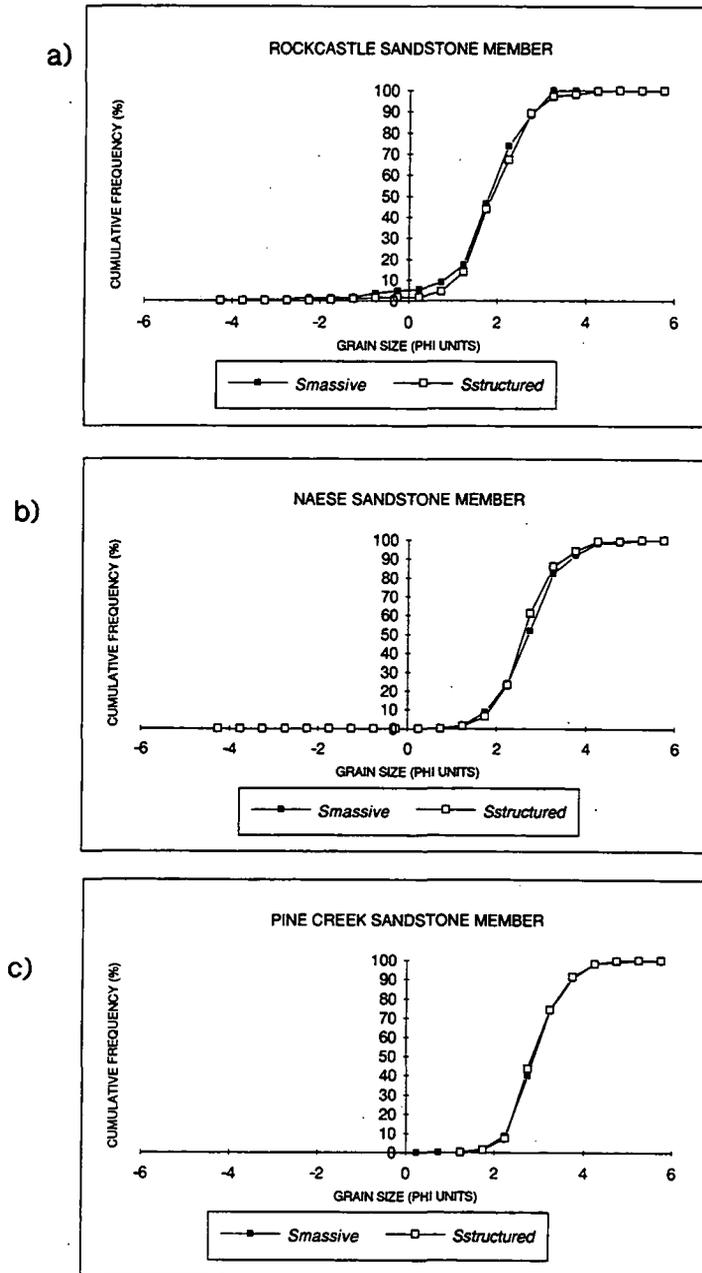


Figure 4.13. Grain size cumulative frequency graphs for the Bee Rock Sandstone formation.

*Figure 4.14. Cumulative frequency graphs of grain size distribution comparing structured and massive sandstone facies of the Naese Sandstone member.*

The mean grain size of the Rockcastle Sandstone member samples varies between 2-2.4φ (medium grained sandstone), and the mean grain size of the Naese Sandstone member varies between 2.6-3.4φ classifying it as a fine to medium grained sandstone (see Appendix III for detail). From Figures 4.13a & b it is clear that the massive sandstone facies are marginally coarser grained than the structured facies. The massive sandstone facies (Sms and Smc) also tend to be better sorted (moderately well to moderately sorted) with the structured facies moderately sorted (Appendix III).

Figure 4.14. Cumulative frequency graphs of grain size distribution comparing structured and massive sandstone facies of the Naese Sandstone member.

The mean grain size of the Rockcastle Sandstone member samples varies between 2-2.4φ (medium grained sandstone), and the mean grain size of the Naese Sandstone member varies between 2.6-3.4φ classifying it as a fine to medium grained sandstone (see Appendix III for detail). From Figures 4.13a & b it is clear that the massive sandstone facies are marginally coarser grained than the structured facies. The massive sandstone facies (Sms and Smc) also tend to be better sorted (moderately well to moderately sorted) with the structured facies moderately sorted (Appendix III).

Rockcastle & Naese Sandstone members (after Folk 1980).

Rockcastle & Naese Sandstone members (after Dickinson 1985).

The sandstones are dominated by monocrystalline quartz (Plate 4.10) which generally exhibits undulose extinction. Inclusion trails are common within the quartz grains (Plate 4.11). Polycrystalline quartz is present within the sections and generally represents the majority of quartz clasts within the sandstone, particularly in the Rockcastle Sandstone member. The polycrystalline quartz grains commonly display a schistose fabric (Plate 4.12).
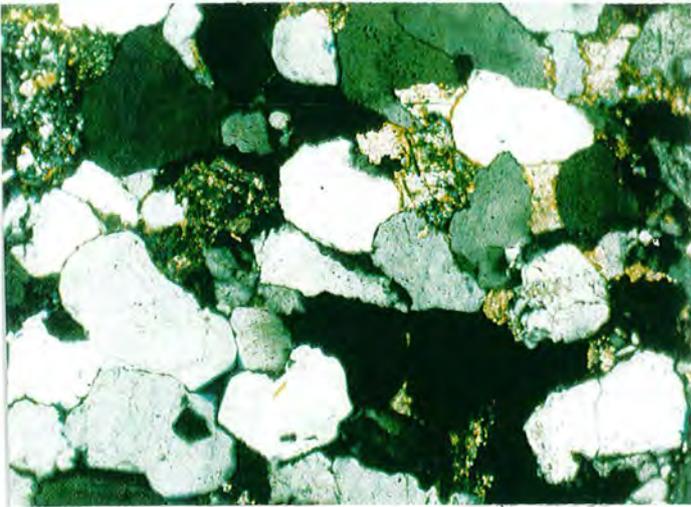


Plate 4.10. Naese Sandstone member. Facies Sms. Field of view 1.5 mm. Section is dominated by monocrystalline quartz. Detrital grains are sub-rounded in shape. Contacts between detrital grains are point. Authigenic quartz overgrowths are extensive, resulting in planar to concavo-convex contacts. Pore spaces are filled with early diagenetic dolomite.
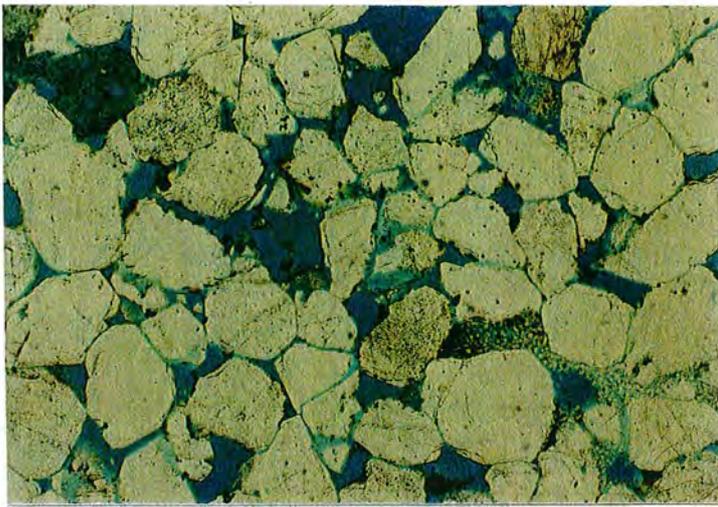


Plate 4.11. Rockcastle Sandstone member. Facies Sg. Field of view 3.25 mm.
Clean, moderately poorly sorted sandstone. Detrital quartz grains are sub-angular to sub-rounded, and may be distinguished by dust rimes. Authigenic quartz overgrowths have resulted in point to planar contacts. Lithic grains display dissolution with secondary porosity development. Complete dissolution of framework grains has resulted in the development of oversized pores. Diagenetic kaolinite is a pore filling phase.
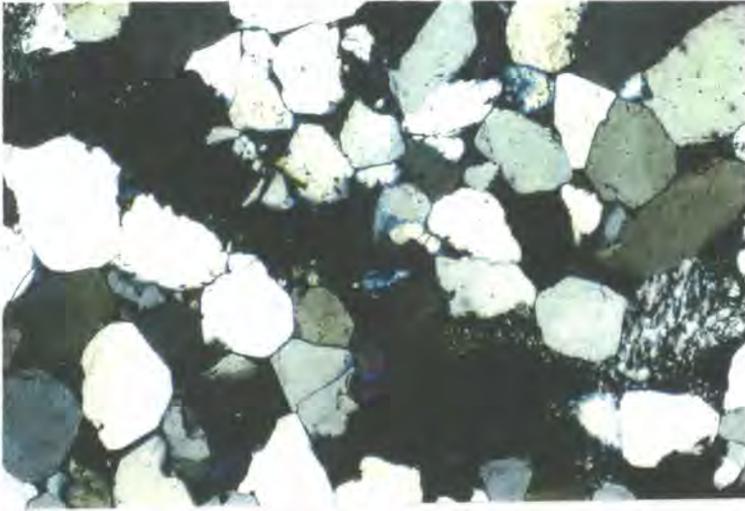
*Plate 4.12. Rockcastle Sandstone member. Facies Sg. Field of view 3.25 mm. Monocrystalline quartz grains dominate the section and show undulose extinction and fluid inclusions. A polycrystalline quartz grain displays a schistose fabric.*

The rock fragment component of the sandstone is dominated by low grade metamorphic clasts (quartz mica schist and phyllite) together with a smaller proportion of partially lithified sandstone and mudstone clasts. The feldspar content of the sandstones is variable (Appendix III). The finer grained Naese Sandstone tends to have a higher percentage of feldspar. In both sets of samples potassium feldspar, represented by microcline, is the dominant clast type. Plagioclase grains tend to be highly altered to pyrite and clay mineral complexes. Mica is dominated by muscovite, although biotite is present in small amounts.

The heavy mineral component of the Naese and Rockcastle Sandstones is identical, and consists of rounded grains of zircon and tourmaline, pyroxene, rutile and intergrowths of magnetite and ilmenite.

*Diagenesis.*

Petrographic and SEM studies indicate no difference in the diagenetic sequence of events between the massive and structured facies in the Naese or Rockcastle Sandstone members. The diagenetic sequence of events in the Rockcastle is simple, due to a dominance of quartz (Appendix III), and generally consists of only quartz cementation, with minor developments of pore filling kaolinite (Plates 4.11 & 4.13). The diagenetic phases of the Naese Sandstone member are more complex and are illustrated in Figure 4.16.

*Plate 4.13. Rockcastle Sandstone member. Facies Sg.*
*Open sandstone texture with well developed authigenic quartz overgrowths. Early diagenetic kaolinite coats pore spaces.*

| Diagenetic phase | Early | Late |
|---|---|---|
| Quartz precipitation | —— ———— | |
| Dolomite precipitation | — | |
| Pyrite precipitation | — | |
| Labile grain dissolution | ——————— - - - - - | |
| Siderite precipitation | — | |
| Kaolinite precipitation | —— | |
| Illite precipitation | —— | |
| Carbonate dissolution | — | |

*Figure 4.16. The diagenetic sequence within the Bee Rock Sandstone formation.*

Within the Bee Rock Sandstone formation the dominant diagenetic phase is quartz. However, where primary grains of quartz are clear it appears that the detrital grains have either floating or point contacts (Plates 4.10 & 4.14). Quartz cementation is variable. In the coarser grained sediments of the Rockcastle Sandstone cementation has resulted in point contacts (Plate 4.11). The finer grained Naese Sandstone displays largely planar contacts (Plate 4.14).
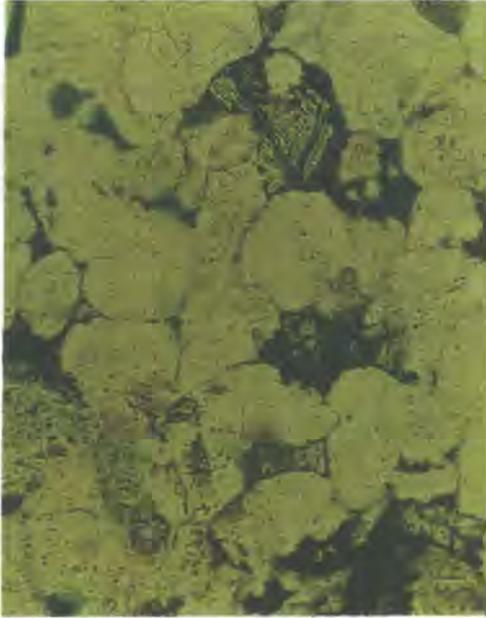


*Plate 4.14. Naese Sandstone member. Facies Sms. Field of view 1.5 mm. Early diagenetic dolomite fills pore spaces. Later dissolution of dolomite has resulted in a skeletal appearance.*

Within the Naese Sandstone member carbonate cements in the form of siderite and dolomite are locally developed (Figure 4.16). Pyrite is also a diagenetic phase. The siderite and pyrite tend to form within lithic fragments and plagioclase feldspar, which acted as the local source of iron. The carbonate cements within the Naese Sandstone are the result of reducing conditions. Iron-rich dolomite would have formed in pore spaces early, under reducing conditions, established due to bacterial decomposition of organic matter (Plate 4.10 & Plate 4.14). Further reduction resulted in the production of pyrite followed by siderite.

Clay mineral phases are dominated by kaolinite and illite with a minor development of mixed layer clays in the form of vermiculite (Appendix IV). The proportion of kaolinite:illite varies between samples (Appendix IV). Kaolinite takes a pore filling character (Plates 4.11 & 4.15). Later removal of carbonate cements is indicated by the presence of rhomb-like oversized pores.
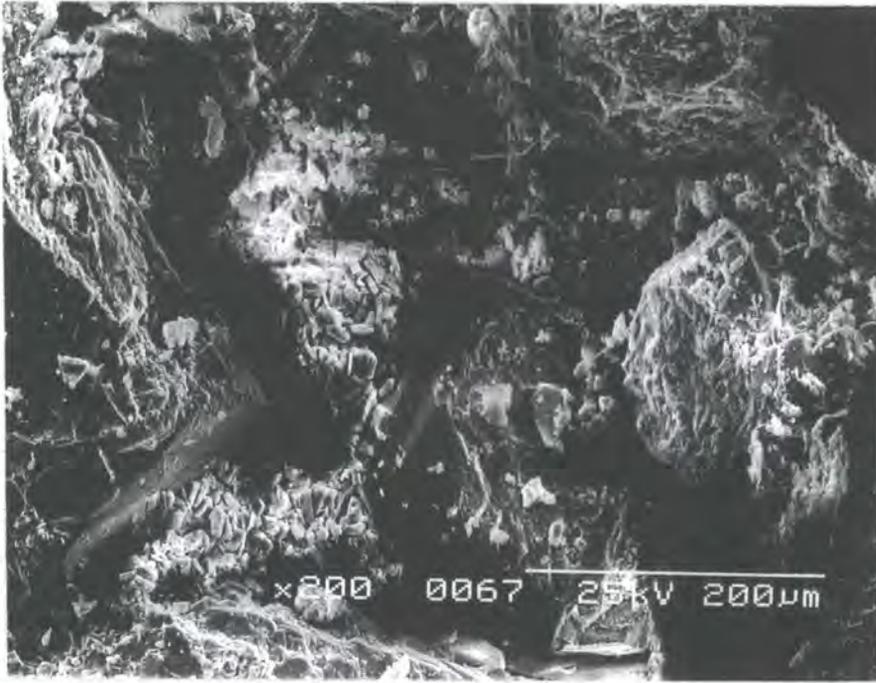
*Plate 4.15. Naese Sandstone member. Facies Sp$_m$.*
*Well cemented sandstone with extensive authigenic quartz overgrowths coated b y*
*kaolinite. The dissolution of framework grains has resulted in limited intergranular*
*secondary porosity.*

### (ii) The Pine Creek Sandstone member.

*Textural information and grain size analysis.*

The grain size distribution of the Pine Creek Sandstone member is illustrated in Figure 4.13c. The mean grain size of the samples varies from 2.89-3.1$\phi$ (Appendix III), and hence the sands are fine grained. The sediments are moderately to well sorted (Appendix III). The massive and structured facies have similar grain size distributions (Figure 4.13c). However, the massive facies (Smc) appears to have a slightly coarser grained tail. The cross-stratified sandstones have a mean grain size of 3$\phi$ and facies Smc has a mean grain size of 3.14$\phi$.

The primary porosity of the Pine Creek Sandstone member samples varies between 4-12% (Appendix III) with a mean of 8%. Porosity appears to vary between facies with the cross-stratified sandstones having a mean porosity of 6.8% and facies Smc a mean porosity of 9.3%. A limited study on the permeability of the Pine Creek Sandstone offers some indicators that the massive sandstone facies tends to have a greater spread of permeability values than the structured sediments when plotted against porosity (Figure 4.17a) and sorting (Figure 4.17b). However, such a study is far from conclusive.
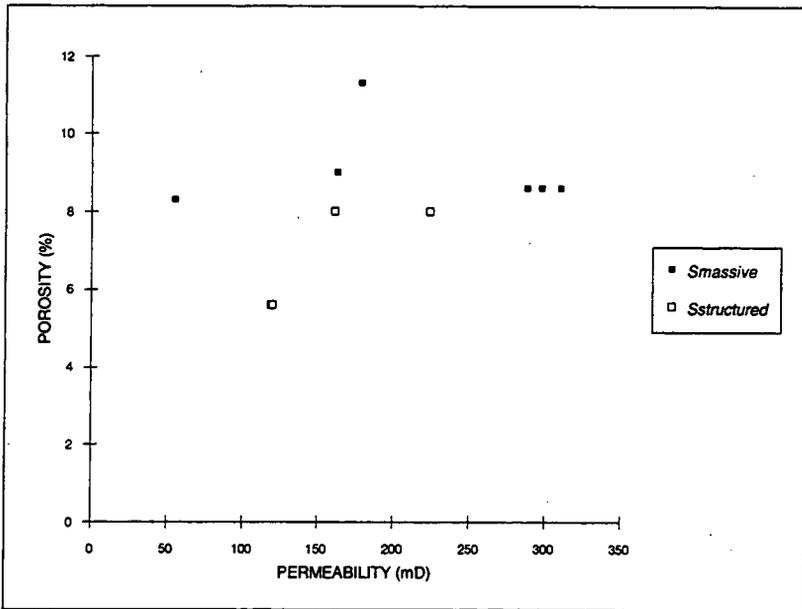
Figure 4.17a) Porosity versus permeability of sandstone facies within the Pine Creek Sandstone member.
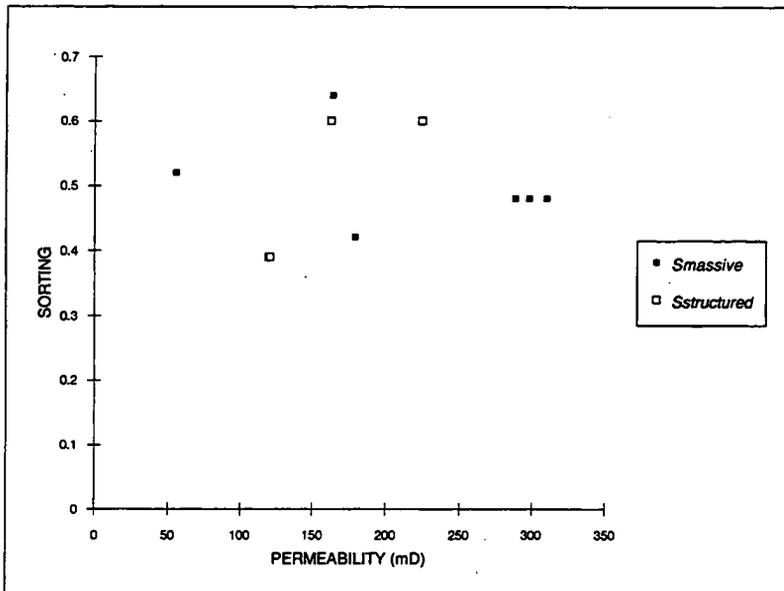


Figure 4.17b) Sorting versus permeability of sandstone facies within the Pine Creek Sandstone member.

The packing of samples of the Pine Creek Sandstone member has been assessed through use of the Compaction Index (CI) as outlined in Appendix III. Facies Smc has an average CI of 4 and the cross-stratified sandstones have an average CI of 3.6.

*Composition.*

The sediments of the Pine Creek Sandstone member are quartz arenites and sub-litharenites (Figure 4.18a), and plot within the recycled orogen province of Dickinson (1985) as illustrated in Figure 4.18b.

112
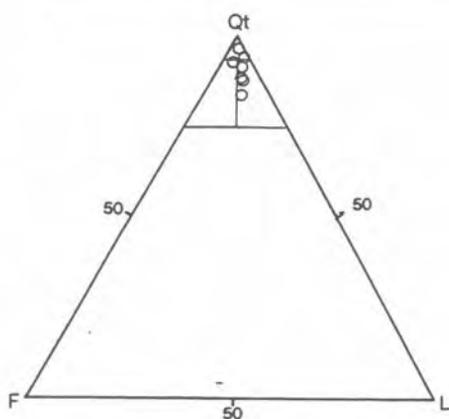
Figure 4.18a. Composition of the Pine Creek Sandstone member (after Folk 1980).
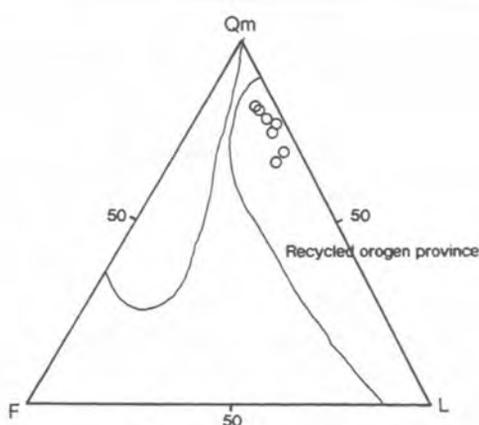
Figure 4.18b. Provenance of the Pine Creek Sandstone member (after Dickinson 1985).

The samples are dominated by monocrystalline quartz (Plate 4.16) with the majority of grains displaying undulose extinction. Many grains also contain well developed fluid inclusion trails. Feldspar grains are rare (Appendix III) and where present are dominantly microcline. Rock fragments take the form of low grade metamorphics including slate, phyllite and quartz mica schist. Some chert is also present. The rock fragments show varying degrees of alteration to clay/pyrite complexes. Mica is represented by muscovite (Plates 4.16 & 4.17). The heavy mineral fraction is composed of magnetite/ilmenite intergrowths and pyroxene. The finer grained levee deposits of section 2 display concentrations of organic material and mica.
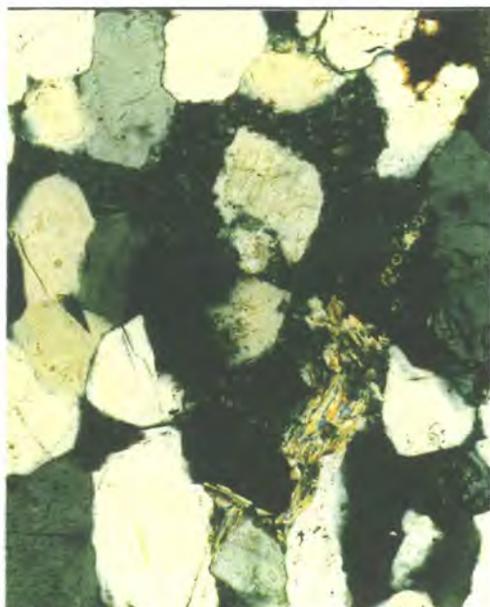


Plate 4.16.

Plate 4.17.

Pine Creek Sandstone member. Facies $Sp_m$. Field of view 1.5 mm.

Section is dominated by monocrystalline quartz. Detrital grains are sub-angular to sub-rounded and display point contacts. Authigenic quartz overgrowths have resulted in planar contacts. Muscovite flakes show evidence of extensive compaction. Diagenetic kaolinite fills pores, resulting in a loss of porosity and permeability. Muscovite shows evidence of alteration with pyrite preserved along cleavage planes.

113

*Diagenesis.*

The sequence of diagenetic events of the Pine Creek Sandstones is illustrated in Figure 4.19. The dominant diagenetic phase is quartz with authigenic overgrowths resulting in planar contacts and near complete cementation (Plate 4.16). However, where the detrital quartz grains are highlighted by a 'dust rim', the grains have only point contacts, or are not in contact (Plates 4.16 & 4.17).

| Diagenetic phase | Early                                    Late |
|---|---|
| Quartz precipitation | ⊢— ———————— |
| Pyrite precipitation | —— |
| Labile grain dissolution | — — — — — — ———————— — — — — — |
| Kaolinite precipitation | ——— |
| Illite precipitation | /                                  —— |

*Figure 4.19. The diagenetic sequence within the sandstone facies of the Pine Creek Sandstone member.*

Clay minerals within the Pine Creek Sandstone member are represented by kaolinite and illite. Vermicular kaolinite is a largely pore filling phase (Plate 4.17) whereas illite is replacive and is found in association with degrading rock fragments (Plate 4.18). Pyrite is commonly located within degraded detrital labile grains closely assocaited with illite (Plate 4.17).
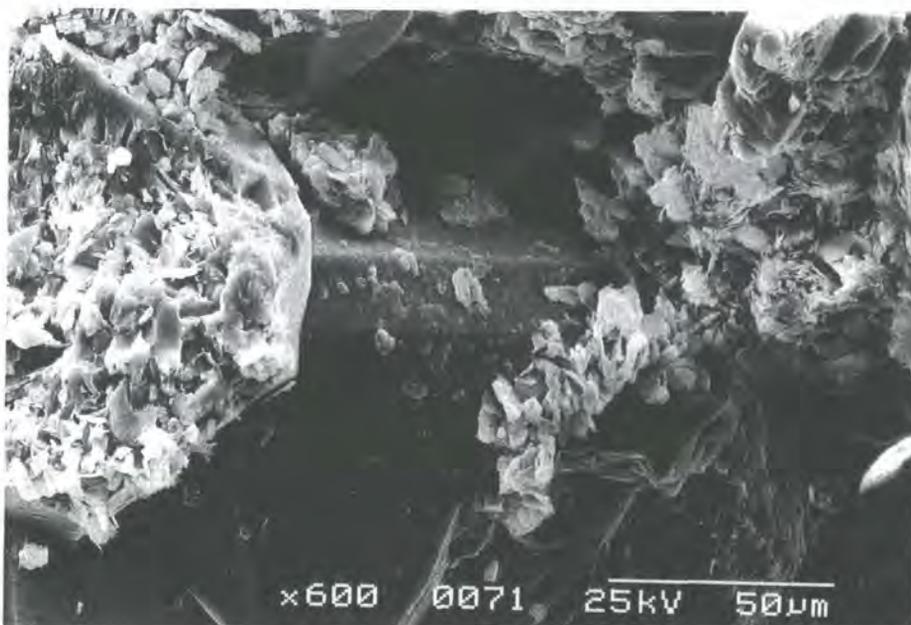
*Plate 4.18. Pine Creek Sandstone member. Facies Smc.*
*Well developed authigenic quartz has been coated with kaolinite. Unstable framework*
*grains show alteration to illite.*

## (iii) Discussion.

The overall southwards fining of the Rockcastle-Naese Sandstone members indicates a northern source for the quartz pebbles within the sands. The rounded quartz pebbles have a schistose fabric indicating source from a far removed metamorphic area. The rounding of tourmaline and zircon grains indicates a considerable distance of transport, or a second cycle origin for the clasts. The Pine Creek Sandstone member is also a quartz arenite, but finer grained than the underlying Rockcastle-Naese Sandstone members.

The presence of low grade metamorphic rock fragments in the Naese and Pine Creek Sandstone members suggests a more local source for these clasts. Cameron & Blatt (1971) have indicated that such clasts are mechanically unstable and would be destroyed by 16 km of transport. It would therefore appear that a more local source was providing lithic rich material to the Naese and Pine Creek Sandstone river systems.

Thus the Bee Rock Sandstone formation may be interpreted as a hybrid sandstone which contains sediment provided from two distinct sources: a high grade metamorphic source to the north, providing quartzose sediment, and a more local low grade metamorphic source.

The changes in diagenesis of the different members of the Bee Rock Sandstone formation indicates differences in primary composition and groundwater conditions. The clean Rockcastle Sandstone member shows quartz cementation with minor amounts of pore filling kaolinite (Plates 4.11 & 4.12). The finer grained, more lithic rich, Naese and Pine Creek Sandstone members have more complex diagenetic histories, including the development of pyrite and iron-rich carbonates (Plates 4.15-4.18).

The lack of contact between detrital quartz grains and the large volume of authigenic quartz cement indicates that the source of quartz was not through pressure solution of detrital quartz grains. It is most likely that the quartz was provided from outside the sandstone beds through de-watering of nearby shales during burial.

## 4.4. The Corbin Sandstone formation.

### 4.4.1. Sedimentology.

The Corbin Sandstone formation forms a belt of approximately 64 km wide, oriented northeast-southwest (Figure 4.6a & b). The Corbin Sandstone is generally less than 60 m thick (Rice 1984) and consists of a series of local sandstone bodies interfingering with the Grundy formation (Figure 4.5). The Corbin Sandstone pinches out to the northwest and southeast (Figures 4.6a), and extends eastward into the subsurface. The belt has been traced southwards into Tennessee (Rice 1984).

The basal contact of the Corbin Sandstone formation is sharp and irregular, and has a relief of up to 30 m over a distance of 305 m (Rice 1984). Deep scours, which underlie the Corbin, trend sub-parallel to westerly or southwesterly current directions indicated by cross-stratification (Rice 1984). In the northern part of the outcrop belt the Corbin Sandstone formation is at or near the base of the Pennsylvanian, and commonly fills channels eroded into the Slade Formation (Figure 4.3). To the south the Pennsylvanian strata thicken so that at the Tennessee border the Corbin Sandstone is as much a 215 m above the base of the Pennsylvanian (Rice 1984).

The Corbin Sandstone formation has a coarse grained, conglomeratic base with locally developed lenses of quartz pebbles. Rounded quartz pebbles up to 5 cm in diameter are present throughout the unit (Rice 1984). However, both the number and diameter of the pebbles decreases southward along the sandstone belt. The Corbin grades laterally in many places into lenses of light brown rooted sandstone as much as 7 m thick (Rice 1984).

During this study the Corbin Sandstone formation was studied in a number of quadrangles along the outcrop belt, as illustrated in Figure 4.6a. The facies of the Corbin Sandstone as determined from fieldwork are described below.


## (i) Facies Descriptions.

*Conglomeratic sandstone (Scg).*

Erosively based, matrix supported, normally graded conglomeratic sheets are preserved in units 10 cm to 1.20 m thick and <100 m lateral extent. The conglomerate fines upwards into coarse sandstone. The conglomeratic sandstones are composed of a coarse grained quartzose sandstone matrix which contains sub-round to sub-angular pebbles and cobbles of quartz (<50 mm diameter), mudstone (<1.20 m diameter) and wood fragments (<50 cm diameter). The units may be structured by diffuse trough cross-stratification.

*Large scale planar cross-stratification ($Sp_l$).*

Large scale planar cross-stratified units are developed in sets of 1.50 to 1.95 m thick composed of coarse to medium grained sandstone. Foresets are angular to tangential and dip 16-25°. Quartz granules and pebbles <10 mm in diameter, or more commonly <5 mm, are preserved in the base of normally graded foresets. The foresets are also cut by minor reactivation surfaces which reflect minor changes in flow direction and/or velocity. There is no evidence of large scale reworking or development of mud drapes. Counter-current reworking of toesets is locally preserved in the form of small ripples.

*Medium scale planar cross-stratification ($Sp_m$).*

Sets of 40-65 cm thick are developed in medium and coarse grained sandstone. Foresets are planar to tangential, and dip 18-22°. Quartz granules (<5 mm) are locally preserved in the lower portion of normally graded foresets. Some small scale changes in foreset angle indicate minor changes in flow strength and/or direction. Overturning of foresets is common, although this tends to be concentrated in certain horizons. The deformation takes the form of the Type 1 recumbent folds of Allen & Banks (1972).

*Medium scale trough cross-stratification ($St_m$).*

Sets are developed in medium and coarse grained sandstone with quartz granules (< 5 mm diameter) locally preserved in the base of the troughs Troughs are

2-5 m across and trough fills are both symmetrical and asymmetrical. Foresets display normally grading.

*Compound cross-stratification (Sc).*

Compound bedforms are developed in coarse and medium grained sandstone with cosets reaching 2.20 m thick. Compound cosets may be traced in excess of 50 m parallel to flow and 20 m transverse to the flow direction, and are bounded by 2B bounding surfaces. Foresets are convex-up to angular and dip 10-15°. Normal grading of sediment is apparent along the foresets. Intrasets are dominantly tangential and dip 20-28°. Internal reactivation surfaces are locally developed and cross-cut intrasets, indicating small scale changes in flow conditions. However, there is no evidence of mud drapes of low stage reworking across these surfaces.

*Small scale planar (Sp$_s$) & trough (St$_s$) cross-stratification.*

Small scale sets are arranged in cosets of 30-50 cm bounded by essentially horizontal second order surfaces (2A of Table 2.3). Quartz granules are locally preserved and are concentrated along the base of cosets. Sets of small scale cross-stratification are composed of medium and fine grained sandstone. Planar cross-stratified sets display angular and tangential foresets which dip 18-24°. Troughs are 1-3 m across and set fill may be both symmetrical and asymmetrical. The sets display highly variable palaeocurrent directions.

*Low angle cross-stratification (Sl).*

Sets are 40-80 cm thick and composed of medium and coarse grained sandstone. Depositional surfaces dip <15° in a direction which is oblique to the palaeocurrent. Grain size decreases upwards along the foreset surface.

*Sheet-like massive sandstone (Sms).*

The sheet-like massive sandstone facies is composed of medium and fine grained sandstones which reach a maximum thickness of 5 m. The base of units are undulose to erosive and associated with minor deformation of underlying stratified sediments. A lag of quartz granules and small pebbles (<10 mm in diameter) may be developed in the basal 10-30 cm of these units. Floating quartz granules tend to be distributed throughout the sheet, as well as disseminated organic matter. Internally facies Sms sandbodies are largely without structure. Small changes in texture define locally developed diffuse laminae 5-50 mm apart, which are trough-like and sub-horizontal.

*Channel-like massive sandstone (Smc).*

Channel-like massive sandstones are composed of fine to medium grained sandstone. The units have erosive bases and display scours of up to 1.70 m in relief, which are associated with localised deformation within underlying cross-stratified sediments. Quartz granules (<5 mm diameter) are concentrated in the base of scours and granules are also distributed evenly throughout the sediment. Internally facies Smc preserves concentric laminae along the margins of units with a maximum thickness of 15 cm. These laminae are lost upwards in a structureless sandstone fill. Undulose laminae 20-50 mm apart are also developed within facies Smc sandbodies. These are poorly defined and are sub-horizontal and mutually interfering in character.

*Rippled fine sandstone (Fx).*

Ripples are developed in cosets <50 cm thick with individual ripples 20-25 mm high. The ripples are asymmetric with rounded crests, and locally preserved climbing forms. Organic material and mica are common in the base of ripples. Locally the sediments are rooted and overlain by thin coals.

*Mudstone (Fm).*

Mudstone is developed in thin units generally <15 cm thick. The sediment is dark, commonly carbonaceous, and locally rooted and bioturbated. Siderite in the form of layers (<5 cm thick) and nodules is locally preserved and is associated with intensely bioturbated horizons.

## (ii) Lateral Profile Analysis.

Sections through the Corbin Sandstone formation are presented from the Bangor and Scranton quadrangles (Figure 4.6a). Lateral profiles of the Corbin Sandstone are described from the Cumberland Falls and Corbin quadrangles (Figure 4.6a).

*Corbin Sandstone formation, Section 1.*

The most northerly i.e. upstream exposure of the Corbin Sandstone examined in this study was in the Bangor quadrangle (Figure 4.6a). Figure 4.20 illustrates a vertical profile of the section, located near Cave Run Lake , within which 27 m of the lower Corbin Sandstone formation is exposed. The Corbin Sandstone directly
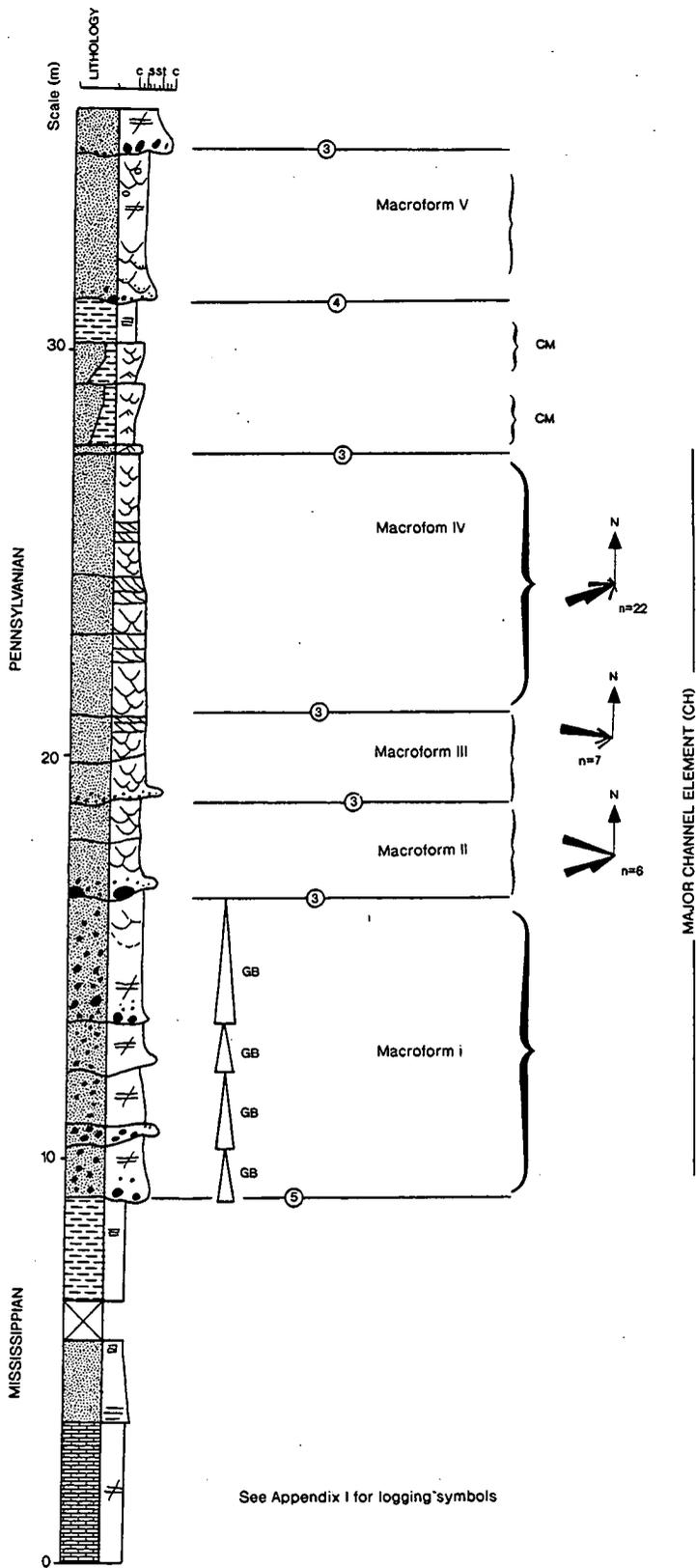
Figure 4.20. A sedimentary log of Corbin Sandstone formation, section 1 (Lat. 38° 1' 10", Long 83° 26' 30").

overlies the early Pennsylvanian unconformity at this locality, with the contact marked by a fifth order bounding surface (Figure 4.20).

A complete CH architectural element is defined in the Corbin Sandstone formation of section 1 (Figure 4.20). The CH element contains a number of intra-channel macroforms which are defined by third order bounding surfaces as illustrated in Figure 4.20. Within the CH element an overall fining-upwards trend in grain size is present, with rippled sandstones and silts marking the upper portion of the element. Palaeocurrents were to the west and southwest during deposition of the unit but with the basal elements showing more variability in the flow direction.

The basal 7.50 m of the CH element is composed of Macroform I which contains a conglomeratic sandstone (Scg) defining GB architectural elements. These conglomeratic sheets which are largely without internal structure, show limited normal grading, and poor development of foresets indicating downstream accretion.

Facies Scg grades upwards into coarse and medium grained sandstones of Macroform II which are structured by facies $Sp_m$, $Sp_s$ and $St_m$ combined to form SB Type 2 architectural elements separated by second order bounding surfaces. Macroforms III and IV are composed of similar facies which are combined in SB Type 1 and 2 architectural elements. Trough cross-set fill is dominantly symmetrical and palaeoflow variance is low (Figure 4.20).

Channel margin architectural elements are preserved overlying the upper portion of the CH element. These are composed of facies Fx and $Sp_s$ which are combined in upward-coarsening cycles interpreted as levee deposits. The sediments have a high organic content and contain large volumes of mica. CM elements are capped by a unit of facies Fm <10 cm thick.

*Corbin Sandstone formation, Section 2.*

Approximately 15 km downstream of section 1, a complete section through the Corbin Sandstone formation is exposed in Scranton quadrangle (Figure 4.6a). This section is illustrated in Figure 4.21. At this locality the Corbin Sandstone formation is underlain by a thick succession of Breathitt lithologies including sandstone, siltstone and coal which are arranged in two regressive units capped by coals. Rhythmically laminated silts and sands in the Breathitt contain *Planolites* traces and *Lingula* brachiopods (Figure 4.21). These indicate deposition in restricted marine or brackish waters, possibly a tidal creek (Greb & Chesnut 1992b). The coal horizons represent emergence and vegetation growth in a coastal freshwater swamp.
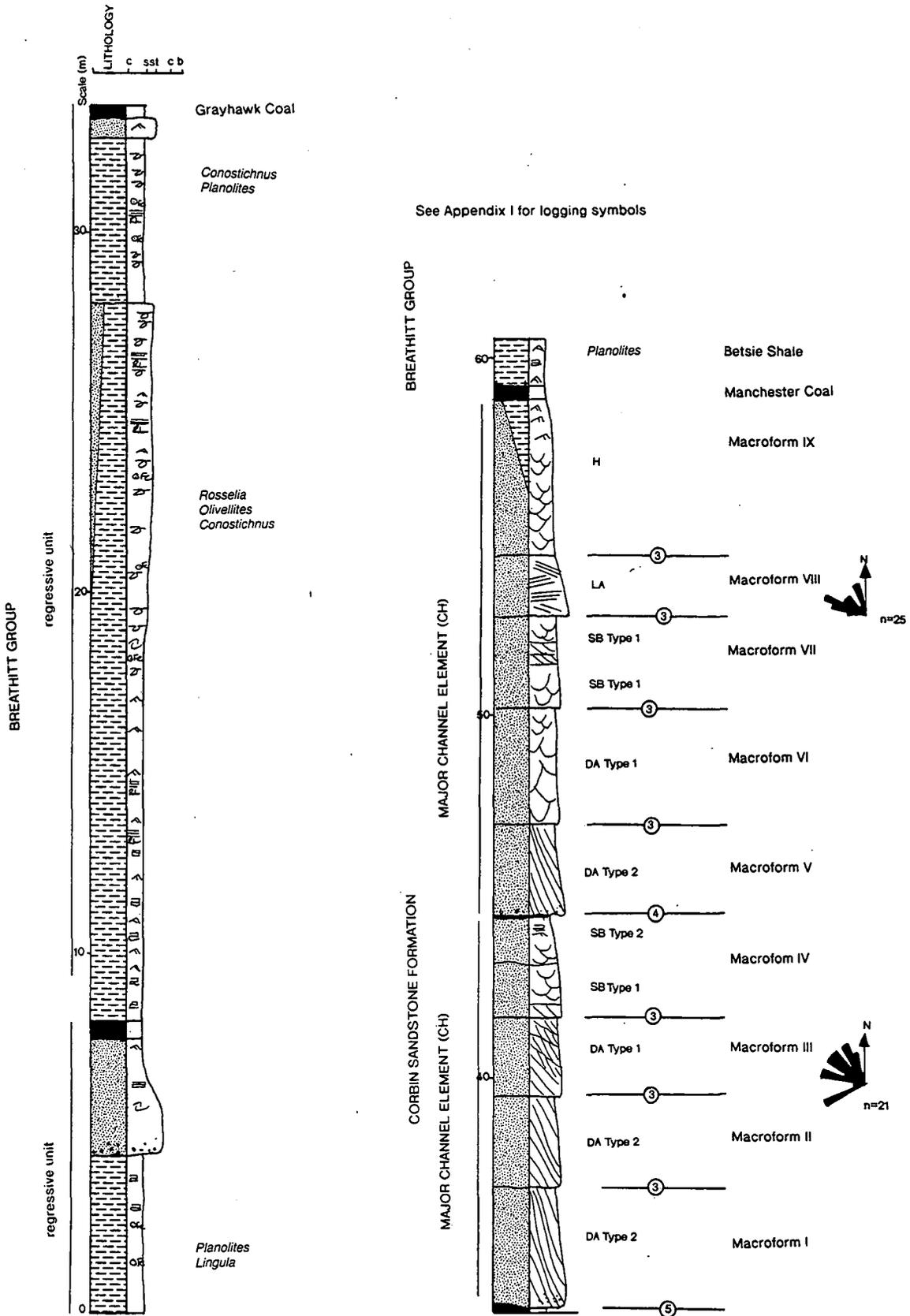
*Figure 4.21. A sedimentary log of Corbin Sandstone formation, section 2 (Lat. 37° 56'
15", Long 83° 37' 15").*

The Corbin Sandstone formation is represented by two major upward fining channel elements (architectural element CH) of 10.50 m and 14.50 m thick (Figure 4.21). The CH elements are defined by basal fourth order bounding surfaces which are overlain by facies Scg, fining upwards to medium grained sand. The CH elements are capped by coal.

Internally the CH elements of the Corbin Sandstone formation are composed of a number of macroforms separated by third order bounding surfaces (Figure 4.21). The macroforms are in turn structured by a combination of $Sp_l$, $Sp_m$ and $St_m$ which are arranged in LA, DA Type 1 and 2 and SB Type 1 and 2 architectural elements as illustrated in Figure 4.21. Palaeocurrents within the section remain to the west and northwest throughout. The CH elements are capped by fining upwards units of H architectural elements (Table 2.6) which are indicative of channel abandonment.

Overlying the Corbin Sandstone Formation is the regionally important Manchester Coal, which is in turn overlain by the Betsie Shale horizon (Figures 4.21 & 4.5). The Betsie Shale contains traces of *Chondrites* and *Planolites* indicating marine influence during deposition (Greb & Chesnut 1992b).

Section 2 therefore preserves a period of fluvial sedimentation represented by the Corbin Sandstone formation, which is both underlain and overlain by finer grained Breathitt-type lithologies displaying evidence of marine influence. The channel elements of the Corbin Sandstone formation are multistorey in nature, and are separated by fourth order bounding surfaces indicative of avulsion.

*Corbin Sandstone formation, Section 3.*

This section, located near the town of Corbin, exposes sediments of the uppermost Corbin Sandstone formation in the Corbin quadrangle (Figure 4.6a). A vertical log through the Corbin Sandstone section, and the passage into the overlying Breathitt Group sediments is illustrated in Figure 4.22. The exposure preserves a section through a complete CH architectural element (Figure 4.22), the base of which is marked by a fourth order bounding surface. The CH architectural element contains intra-channel architectural elements of macroform and mesoform scale, and is capped by channel margin elements (Table 2.6).

Figure 4.23 illustrates a lateral profile of section 3. The profile encompasses approximately 20 m of vertical section and extends parallel to the palaeoflow direction for 140 m. The base of section 3 is marked by a fourth order bounding surface. Below this surface palaeocurrents are to the southwest (Figure 4.23) and above the surface
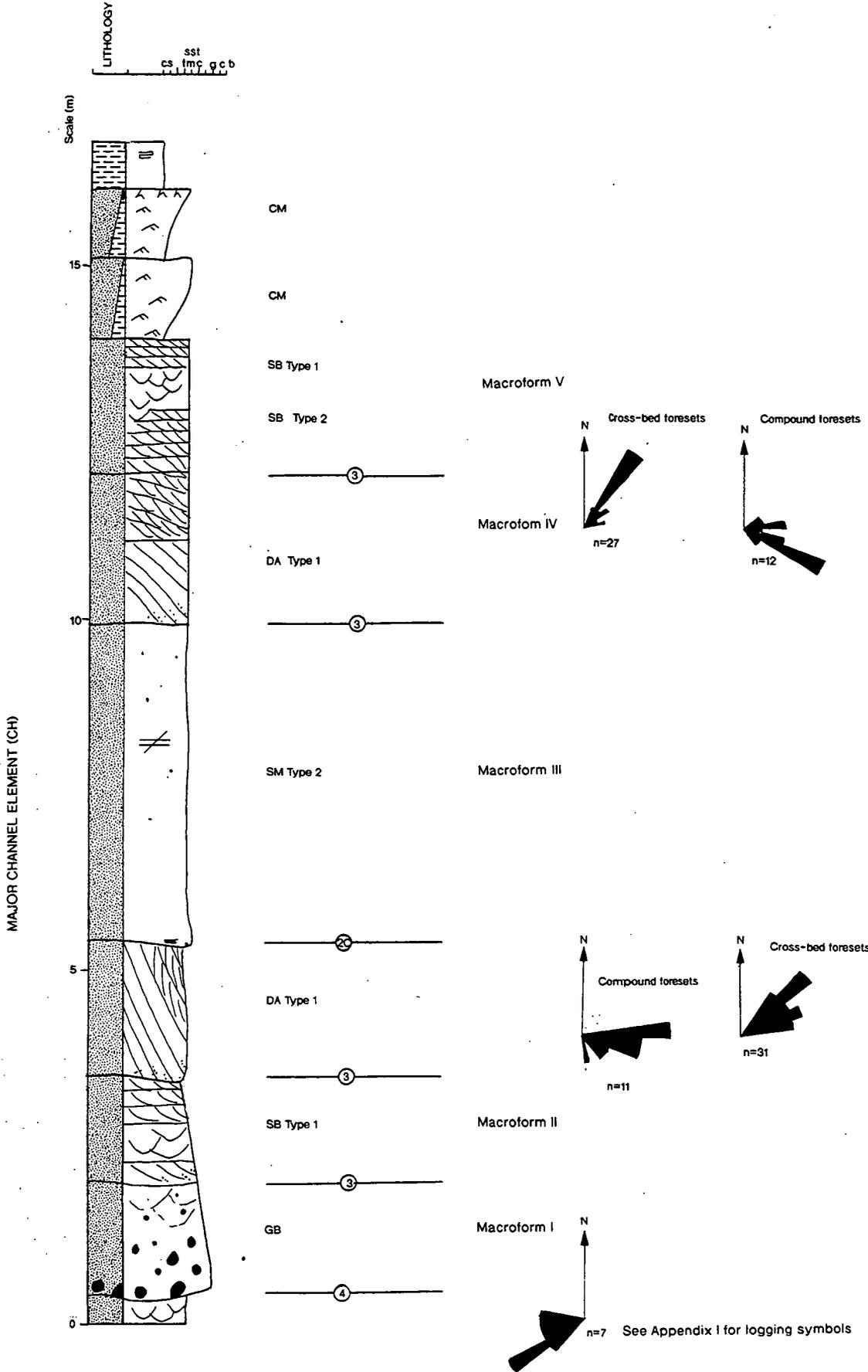
Figure 4.22. A sedimentary log of Corbin Sandstone formation, section 3 (Lat. 36° 58' 20", Long 84° 6' 50").

SSW

ORIENTATION N024/204

Macroform III
Cross-bed foresets
n=31

DA Type 1

SB Type 2

SB Type 2

GB

N

Macroform I
n=8

N

Macroform II
n=12

N

Macroform III
Compound foresets
n=11

N

Macroform IV
Compound foresets
n=12

NNE

N

Macroform V
n=23

N

n=7

N

Macroform IV
Cross-bed foresets
n=27

DA Type 1

SM Type 2

10 m
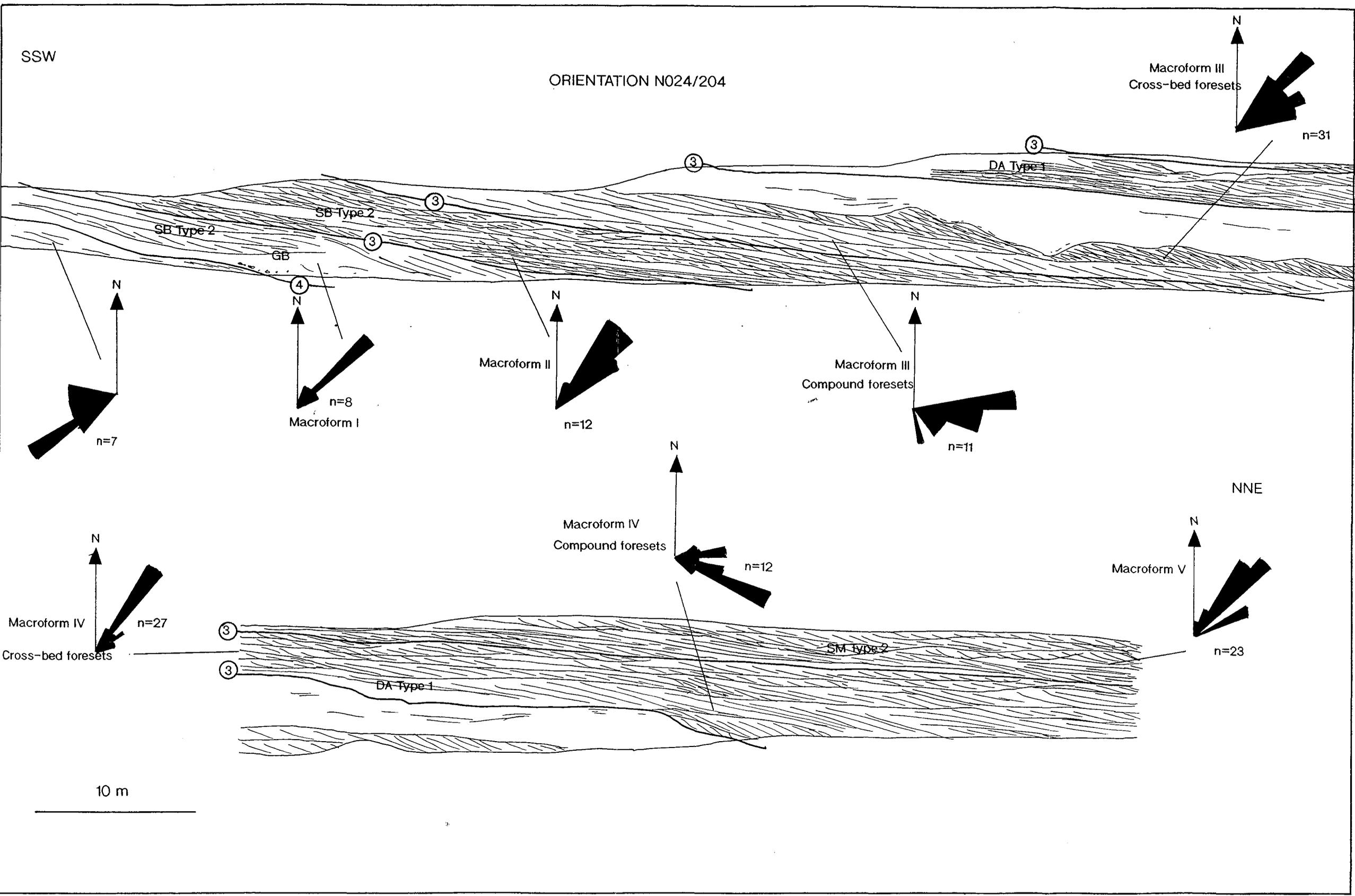
*Figure 4.23. A line drawing of Corbin Sandstone formation, section 3 (Lat. 36° 58' 20",
Long 84° 6' 50").*

palaeoflow was to the northeast (Figure 4.22 & 4.23). This current direction is unusual for the Corbin Sandstone.

The intra-channel architectural elements of the element CH of section 3 are composed of medium grained sandstone arranged in five macroforms separated b y third order bounding surfaces. The base of Macroform I is represented by the fourth order bounding surface, which is overlain by 0.80 m of facies Scg containing quartz pebbles, plant fragments and mudstone clasts. The unit is structured by diffuse trough cross-stratification and is interpreted in terms of a GB architectural element (Figure 4.23). Facies Scg fines upwards into $St_m$ and $Sp_m$ which combine to form SB Type 2 architectural elements (Figures 4.22 & 4.23).

Macroform II is composed of facies $St_m$ and $Sp_m$ combined in SB Type 2 architectural elements separated by second order bounding surfaces (2A). Macroform III is composed of a lower DA Type 1 element which is overlain by an erosively based unit of facies Smc (SM Type 2 architectural element). The DA Type 1 architectural element displays palaeocurrents of low variance to the east and northeast. Figure 4.23. illustrates palaeocurrent measurements taken from compound foresets and simple cross-bed foresets. These show slight variations, with the compound foreset readings more easterly in direction. Facies Smc (SM Type 2 architectural element) is >95 m wide and <4 m deep. The sandbody extends in excess of 30 m perpendicular to the plane of the measured section (i.e. along N 024/204°). The base of the SM Type 2 element has a relief of up to 2.05 m and displays erosional, scour-like structures (Plate 4.19). Within the base of these scours mudclasts (<15 mm in diameter) and organic material are concentrated (Figure 4.23).



*Plate 4.19. Corbin Sandstone formation, Section 3.*
*Scale represents 1 m. Facies Smc displays an erosive, sharply defined base which cuts through cross-stratified facies of a DA Type 1 architectural element. There is no evidence of deformation within the structured sandstones.*

The base of Macroform IV is undulose, and downstream offlaps the channel-like massive sandstone (Figure 4.23) as illustrated in Plate 4.20. Macroform IV is composed of facies St &p$_m$ St$_s$ and Sc of a DA Type 1 architectural element, which interfingers, in the downstream direction, with a SB Type 2 element. Figure 4.23. illustrates palaeocurrent measurements taken from both compound and simple cross-bed foresets. As with readings from Macroform III palaeoflow, as measured from compound foresets, was more easterly in direction than that of the simple cross-bed foresets. Palaeoflow variance with Macroform IV is low.

Macroform V is composed of medium to fine grained sandstone of facies St$_m$, Sp$_m$ and St$_s$ which are arranged in a number of SB Type 2 architectural elements separated by second order bounding surfaces. Palaeoflow variance within these elements is low (Figure 4.23).

The uppermost sediments of section 3 are composed of coarsening-upwards units of mudstone, rippled sandstone and cross-stratified sandstone which are related to levee deposition. These units correspond to CM architectural elements as illustrated in Figure 4.22.



*Plate 4.20. Corbin Sandstone formation, Section 3.*
*Scale represents 1 m. Downstream margin of facies Smc unit. Cross-stratified sandstones offlap the massive sandbody, and form part of a DA Type 1 architectural element.*

*Corbin Sandstone formation, Section 4.*

Section 4 was measured in the Cumberland Falls quadrangle (Figure 4.6a), near Cumberland Falls State Park, and is illustrated in Figure 4.24. The section is located stratigraphically in the upper Corbin Sandstone formation (Chesnut *pers comm*), but the exact position is unknown. The profile extends 40 m parallel to the palaeoflow and encompasses 8 m of vertical section.

Section 4 is composed of two macroforms, as illustrated in Figure 4.24. The palaeoflow, as measured from cross-stratification, was to the west and southwest, and hence mirrors the regional palaeoflow of the Corbin Sandstone formation.

Macroform I is composed of faces $Sp_m$ and Sc arranged in a DA Type 1 architectural element. Palaeflow variance within the macroform is low. The element is capped by a locally preserved unit of facies Fm which is 5-10 cm thick. The overlying SM Type 2 architectural element is composed of facies Smc. It is 28 m wide and reaches a maximum thickness of 3.35 m. The unit is lenticular and displays scours or flute marks along the basal surface, which are oriented towards the northeast (Figure 4.24 & Plate 4.21). A lag of organic material and quartz granules <5 mm in diameter are located within these scours. Internally the element is largely structureless. Laminae 5-50 mm apart are developed parallel to the basal surface and grade into the structureless sandstone fill. Quartz granules (<5 mm ) are found 'floating' within facies Smc.



*Plate 4.21. Corbin Sandstone formation, Section 4.*
*Scale represents 50 cm. Facies Smc displays a scoured base with the development of flute casts oriented in a plane of N109°. The underlying sediments are cross-stratified sandstones combined to form a DA Type 1 architectural element. The element is overlain by a thin mudstone unit (facies fm). Such sediments are normally associated with emergence or abandonment.*
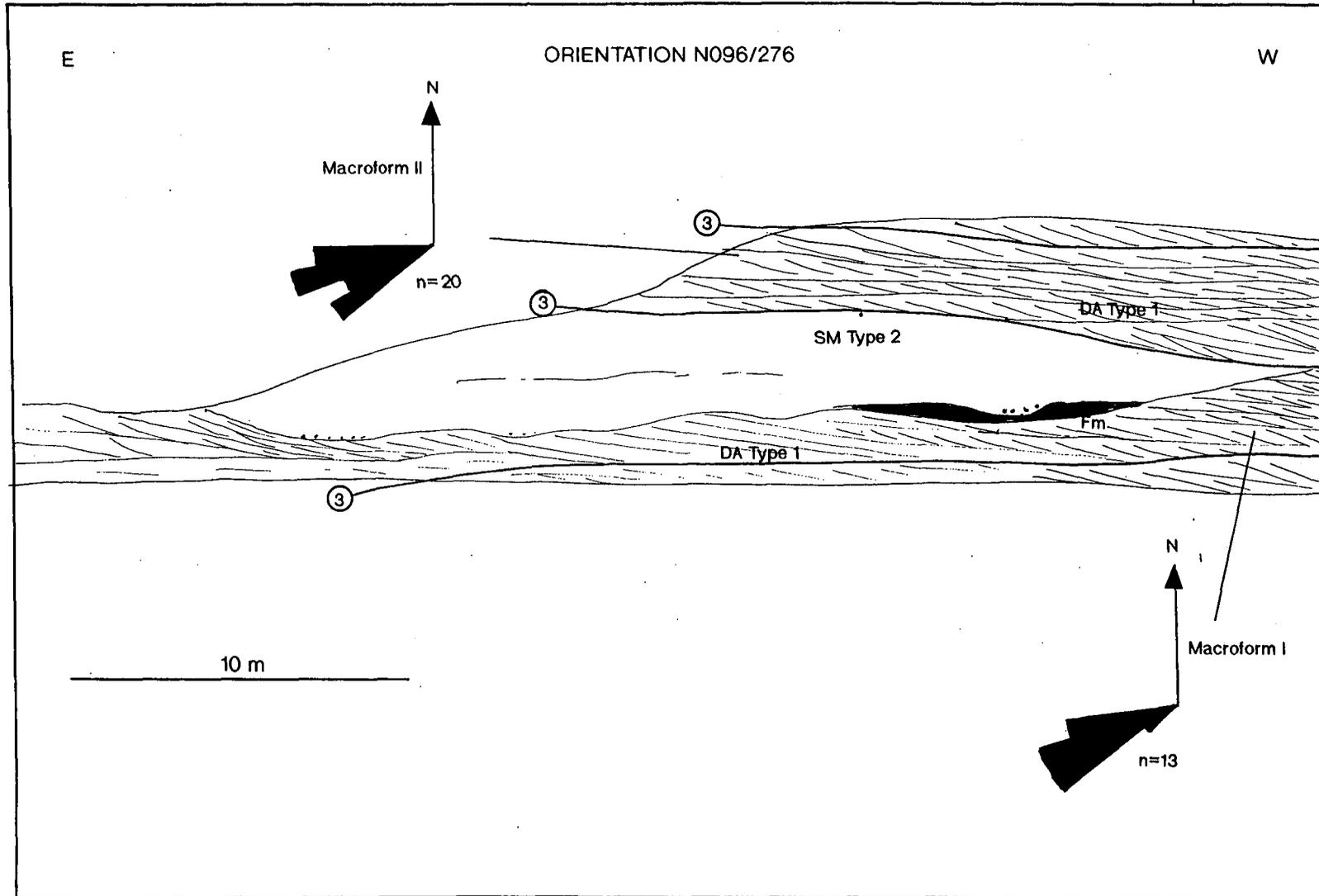
*Figure 4.24. A line drawing of Corbin Sandstone formation, section 4 (Lat. 36° 50' 40", Long 84° 18' 40").*

Macroform II is composed of facies $St_m$, $Sp_m$ and Sc which are arranged to form a DA Type 1 architectural element. Palaeocurrent variance within the macroform is again low (Figure 4.24).

## 4.4.2. Petrology & Textural Characteristics.

Two sections from the Corbin Sandstone formation were studied petrographically. Samples were taken from section 2 and section 3, the lower and uppermost sandstones.

*Textural information and grain size analysis.*

The sands of the basal Corbin Sandstone formation vary in their mean grain size between 2.5-2.7$\phi$, and hence are medium grained sandstones. The sands are moderately well to moderately sorted (Appendix III). The grain size distribution of the basal Corbin sands is illustrated in Figure 4.25a. The sandstones of facies Smc are marginally coarser than the structured facies. The porosity of the sands varies between 11.6-19% with a mean of 15.6% (Appendix III).
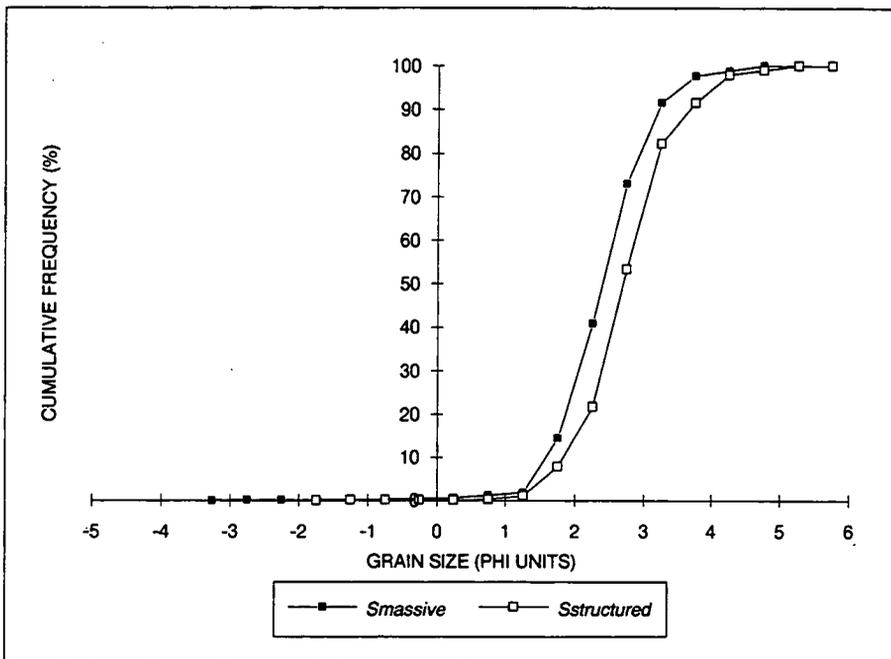


*Figure 4.25a. A cumulative frequency graph of the grain size distribution with in the basal Corbin Sandstone formation (section 1).*
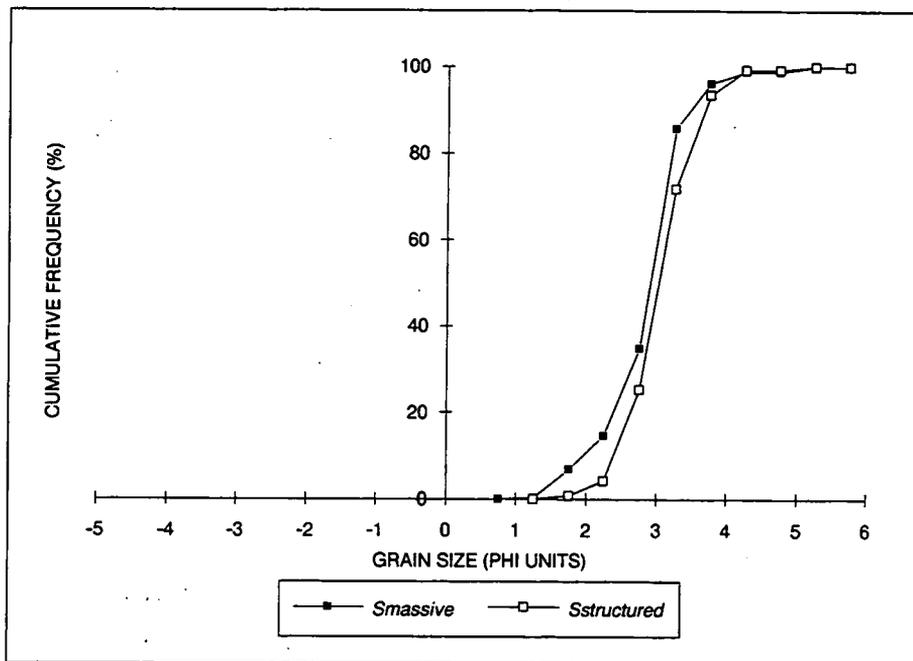
*Figure 4.25b. A cumulative frequency graph of the grain size distribution with in the uppermost Corbin Sandstone formation (section 3).*

The uppermost Corbin Sandstones show a mean grain size which varies between 2.86-3.3 φ, and hence the sands are fine to medium grained. Figure 4.25b illustrates the distribution of grain size. It is clear that the sediments of facies Smc are marginally coarser than the structured sediments. Facies Smc has a mean grain size of 2.9 φ and the cross-stratified sandstones have a mean grain size of 3 φ. Both the structured and massive facies are moderately well sorted (Appendix III). The porosity of the upper Corbin formation sands varies between 4-7.6%, with a mean of 6%. The massive facies tend to have higher porosities with an average of 10.3%, compared with a value of 7.6% for the cross-stratified sandstones (Appendix III).

The packing of the uppermost Corbin Sandstone formation sediments has been assessed through use of the Compaction Index (CI) as detailed in Appendix III. Facies Smc displays an average CI of 4.3 and the cross-stratified sandstones have an average CI of 4.29.

*Composition.*

Figure 4.26a illustrates the composition of the Corbin Sandstone formation samples. The basal Corbin Sandstone samples are quartz arenites and sub-litharenites. The uppermost Corbin Sandstone sediments are also quartz arenites and sub-litharenites. Both sets of samples plot in the recycled orogen province of Dickinson (1985) as illustrated in Figure 4.26b.
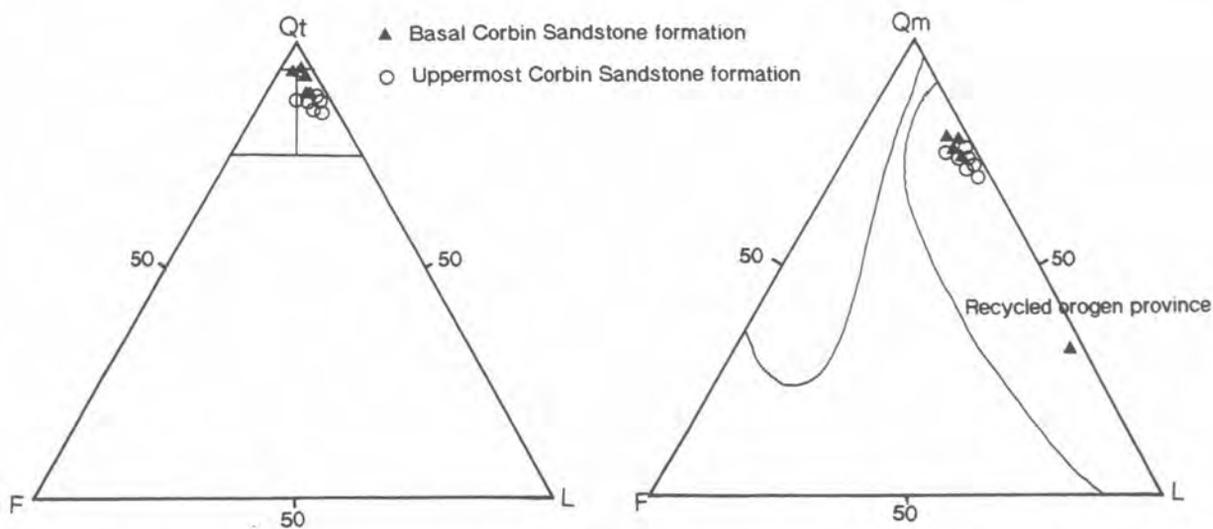
Figure 4.26a. Composition of the
Corbin Sandstone
formation (after Folk 1980).

Figure 4.26b. Provenance of the
Corbin Sandstone
formation (after Dickinson 1985).

The Corbin Sandstone formation samples are composed predominantly of monocrystalline quartz grains (Plate 4.22) which display undulose extinction and trails of fluid inclusions (Plate 4.23). Polycrystalline quartz is generally present in the form of larger quartz grains, particularly in the basal Corbin sediments (Plate 4.22).
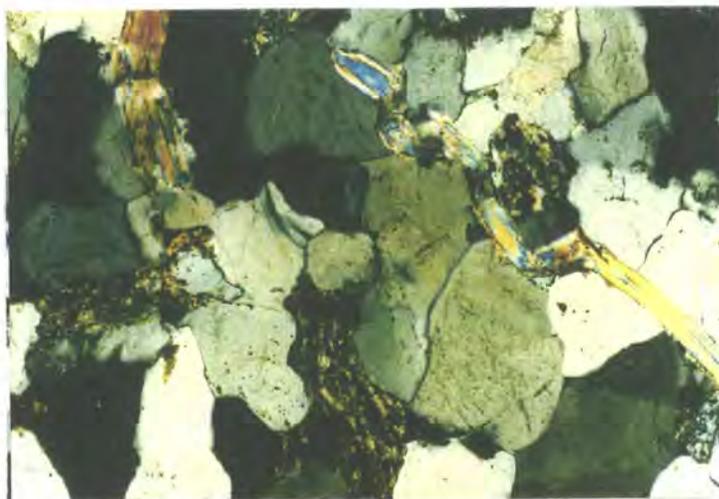


Plate 4.22. Uppermost Corbin Sandstone formation, Facies Smc. Field of view 1.5 mm. Monocrystalline quartz dominates the section. Detrital grains are unclear. Muscovite flakes show evidence of compaction and minor alteration. Lithic fragments are composed of low grade metamorphics and show alteration to clay minerals. Compaction of lithic grains has resulted in the development of a clay rich pseudomatrix.
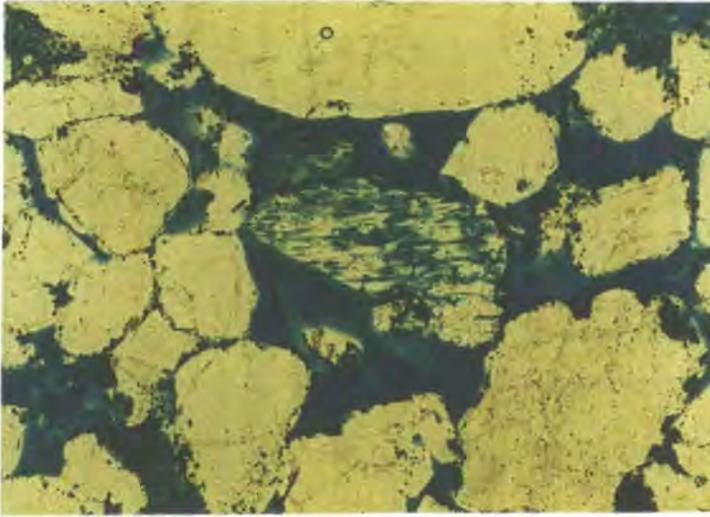
*Plate 4.23. Lower Corbin Sandstone formation, Facies Smc. Field of view 1.5 mm. A bimodal grain size distribution is present. Larger grains tend to be polycrystalline. Detrital quartz grains are sub-angular to sub-rounded and have floating and point contacts. Authigenic quartz overgrowths are developed closely associated with pyrite. A plagioclase feldspar grain displays dissolution and the development of pyrite. Pores are locally filled with kaolinite.*

Rock fragments are represented by metamorphic clasts of shale, phyllite and quartz/mica schist (Plate 4.22), together with locally derived mudstone clasts which form a pseudomatrix in the uppermost sands. Potassium feldspars, in the form of microcline, are the most common feldspar grain type. Where plagioclase feldspar is present it is commonly altered to clay minerals. Mica takes the form of muscovite (Plate 4.22). The heavy mineral fraction is represented by rounded zircon and tourmaline, and intergrowths of magnetite and ilmenite.

*Diagenesis.*

Petrographic and SEM studies reveal no differences in the diagenetic sequence between structured and massive sandstones. The sequence of events is illustrated in Figure 4.27.

The most important diagenetic phase is quartz. In the finer grained upper Corbin samples almost complete cementation by quartz has resulted in the near loss of porosity (Plate 4.22). Planar contacts are the most common, but where detrital grains are clear they are commonly not in contact. In the coarser grained lower Corbin samples quartz cementation is not as advanced (Plate 4.23).

| Diagenetic phase | Early | Late |
|---|---|---|
| Quartz precipitation | —  ——————————— | |
| Pyrite precipitation | —— | |
| Labile grain dissolution | - - - -  ——————————  - - - | |
| Kaolinite precipitation | | ———— |
| Illite precipitation | | —— |

Figure 4.27. The diagenetic sequence displayed by sandstone facies of the Corbin Sandstone formation.
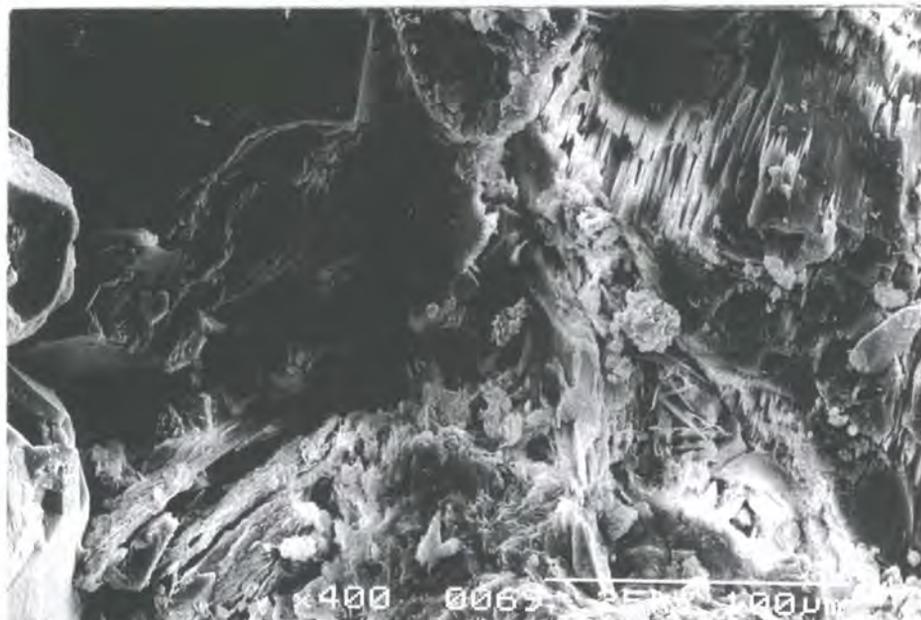


Plate 4.24. Uppermost Corbin Sandstone formation, Facies Smc.
Authigenic quartz overgrowths are well developed, and are coated with vermicular kaolinite & pyrite. Dissolution of feldspars along cleavage planes is clear, and illite is present as a replacive phase.

Kaolinite and illite are both present in the clay fraction (Appendix IV). The kaolinite is a largely pore filling phase (Plates 4.23 & 4.25). Illite is largely replacive. Framework grain dissolution of lithic fragments and feldspar (Plates 4.23 & 4.24) has produced pyrite and illite complexes.
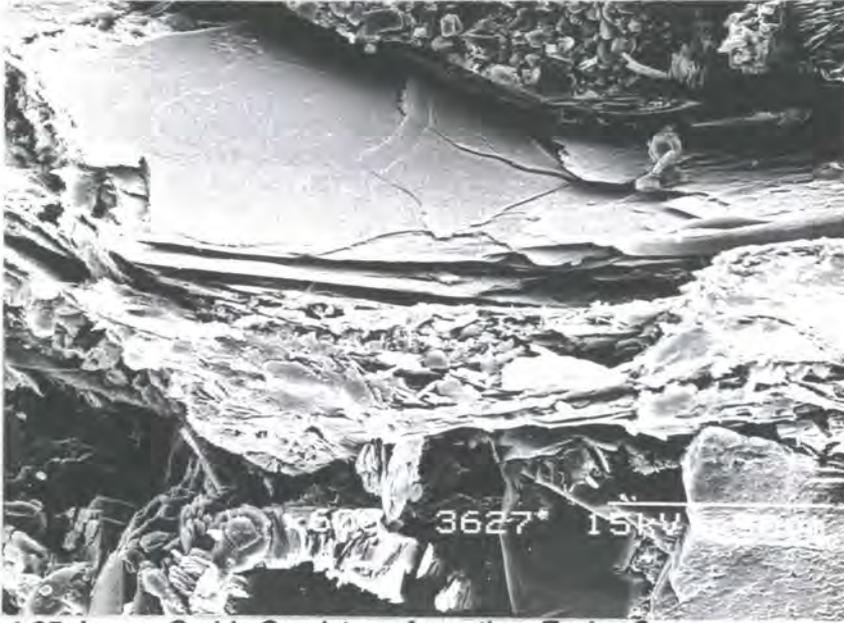
*Plate 4.25. Lower Corbin Sandstone formation. Facies Smc.*
*Authigenic quartz overgrowths are well developed. Kaolinite fills pore spaces. A*
*muscovite flake shows limited alteration to illite.*

*Discussion.*

The composition and texture of the Corbin Sandstone formation is very similar to that of the Bee Rock Sandstone formation. The decrease in grain size to the southwest and reduction in the volume and size of quartz pebbles in this direction indicates a northerly source for these clasts. The rounding of detrital quartz grains also indicates significant reworking prior to deposition. However, the addition of volcanic and low grade metamorphic rock fragments within the upper portion of the Corbin Sandstone indicates a more local source for these grains.

The diagenetic sequence of the Corbin Sandstone formation is also similar to that of the underlying Bee Rock Sandstone formation. The large volume of authigenic quartz cement and the absence of contact between detrital grains indicates input of quartz from an external source which is assumed to be through dewatering of nearby shales.

## 4.5. Fluvial Interpretation Of The Lee-Type Sandstones.

### 4.5.1. The Bee Rock Sandstone formation.

The Bee Rock Sandstone formation is composed of a number of individual sandstones including the Rockcastle/Naese and Pine Creek Sandstones members, which are separated by overbank deposits, thin coals and shales of marine or

brackish affinity (Figure 4.7). These sandstones display differing fluvial characteristics. The interpreted characteristics of the Naese and Pine Creek Sandstones are outline below.


## (i) The Naese Sandstone member.

Twenty bedforms deposited by migrating dunes (i.e. scaled to boundary layer thickness) were measured from the Naese Sandstone member of section 1. The average bedform height is 1.70 m, which when decompacted using a value for $\phi_c$ of 0.11, equates to an original dune thickness of at least 2.60 m. The water depth of the Naese Sandstone river must therefore have been at least 10-20 m (Figure 2.4). The angular range of palaeocurrents measured from the Naese Sandstone member of section 1 is 97°, which gives a stream sinuosity of 1.13 (Schumm 1968b), hence the Naese Sandstone river was of low sinuosity. Using the empirical equations of Schumm (1968b) the width/depth ratio of the Naese Sandstone river was approximately 68. The width of the channel was therefore between 680-1360 m. Such a system is of a similar scale to the modern day Tana River of Norway and Brahmaputra River of Bangladesh (Table 2.5).

The Naese Sandstone river was dominated by downstream accreting bedforms. These are preserved as macroform scale DA Type 1 and 2 and mesoform scale SB Type 1 and 2 architectural elements. DA Type 1 elements relate to deposition from mid-channel bars (Haszeldine 1983a & b) and DA Type 2 elements are interpreted as the migration of solitary dunes, which may be bank attached (Wizevich 1991). The absence of large scale reactivation surfaces and mud drapes within macroforms indicates that bedforms were rarely emergent and hence the river system is interpreted to have been perennial with a low braiding index.

Within section 1 the majority of the outcrop is composed of SB Type 2 architectural elements which are the result of downstream accretion of 2-D and 3-D bedforms. Stacked sets of horizontal and stoss side climbing recumbently overturned cross-stratification are preserved. The deformed unit cannot be traced further than section 1, and hence is interpreted as a localised phenomena. Similar features have been described by Wells *et al* (1993) from Pennsylvanian quartzose sandstones (Sharon Conglomerate) of Ohio.

It is generally accepted that overturning of foresets is achieved through horizontal shear acting on a water saturated sediment layer. If a bed is subjected to horizontal shear, foresets will progressively oversteepen and then stretch out into recumbent folds. Additional shear will destroy primary fabrics and convert the shearing layer into a moving traction carpet (Figure 4.28).

turbidity current

liq. sediment flow
fluidised quicksand

debris flow
dish & pillar

traction carpet

loss of primary fabric

pillars

recumbent foresets

oversteepening

loadcasts

LIQUEFACTION

FLUIDISATION
(INCR WATER/INTENSITY/DURATION)

HORIZONTAL          OBLIQUE              VERTICAL
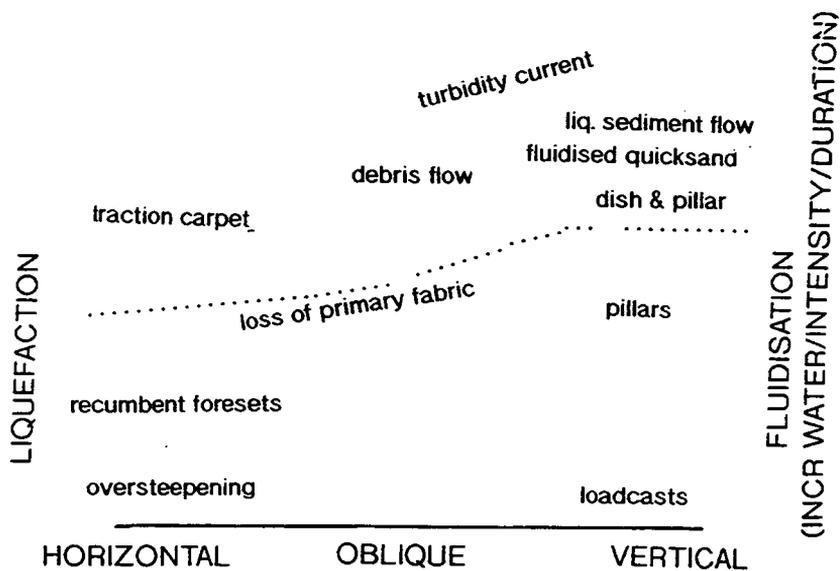
Figure 4.28. Styles of soft sediment deformation. The y axis represents intensity & duration of the deformation and/or the degree of water movement. The x axis represents the angle of the deforming force, from horizontal to vertical (modified from Wells et al 1993).

Owen (1987) divides the soft-sediment deformation process into three distinct phases: 1) driving force which produces the deformation, 2) deformation mechanism which permits the driving force to work, and 3) a trigger that sets off the deformation mechanism. In the past earthquakes have been a popular trigger to produce liquefaction within the sandstone (Allen & Banks 1972). Doe and Dott (1980) suggested that drag under current surges lead to pressure differentials on pore fluids sufficient to induce liquefaction. Røe (1987) indicated that locally high rates of deposition and deformation under normal sediment laden currents should suffice to induce deformation.

The trigger to produce the pervasive overturning of forests in the Naese Sandstone must have been repetitive enough to deform many beds, without being so common that all braided stream deposits show this volume of overturned beds. The fact that the phenomena is only locally developed adds further constraints on any model. The sand grains involved in the overturned beds have lost their internal friction and had their strength reduced close to zero, or they would not be susceptible to such pervasive shearing.

Wells et al (1993) have suggested that deformation of the Sharon Conglomerate may have been initiated by a sudden onslaught flood. However, such

currents are more likely to erode sediment than deposit it. The vertical stacking of the SB Type 2 elements in the Naese Sandstone member indicates a prolonged phenomena acting in association with rapid basin subsidence. The stoss climbing sets of Macroform V indicate rapid sediment accumulation. These deformed sets are interpreted as the deposits of rapidly initiated flood events which occurred on a regular basis. The localised nature of the stacked sets of overturned cross-stratification suggests that they may be related to a river confluence or area of active tectonic movement.

In section 1 a sheet-like massive sandstone unit directly overlies the stacked sets of overturned cross-stratification, and this will be discussed in Chapter 7. The sheet-like massive sandstone unit is overlain by a major bounding surface which is in turn overlain by a DA Type 1 architectural element. The change in sedimentation style across this third order bounding surface is interpreted as a change in fluvial depositional conditions. Deposition over the sheet-like massive sandstone represents deposition from a steady fluvial current in perennial conditions. There is no evidence of flooding and high flow stage.

Sections 2 and 3 of the Naese Sandstone member are composed of SB Type 1 and 2 and DA Type and 2 architectural elements. Channel-like massive sandstone deposits of facies Smc are preserved within the sandstones, and indicate the deposits of sediment laden currents travelling in a direction oblique to the river current. These units will be discussed in detail in Chapter 7.

## (ii) The Pine Creek Sandstone member.

The section through the Pine Creek Sandstone member illustrated in Figure 4.7, illustrates an upward change in fluvial style. Throughout the section sediments remain fine to medium grained quartzose sandstones. The lower unit of the Pine Creek Sandstone member is dominated by LA architectural elements which were deposited within a fluvial system dominated by lateral migration. Such fluvial systems tend to be of low width/depth ratios and sinuous in character, but insufficient palaeocurrent readings could be made to establish the sinuosity of the fluvial system.

The upper unit of the Pine Creek Sandstone member, as exposed in section 1, is dominated by mesoform scale architectural elements deposited by downstream accretion in the form of SB Type 1 elements. These bedforms were deposited by migrating 2-D and 3-D bedforms. The SB Type 1 elements were scaled to depth and have an average height of 0.80 m, which when decompacted using a $\phi_c$ value of 0.08, gives a minimum bedform height of 1.22 m. The water in which these bedforms migrated had to be at least 4.5-6.5 m deep (Figure 2.4). The low palaeocurrent

variance within the sediments of the upper Pine Creek Sandstone member indicates a fluvial channel of low sinuosity.

The absence of large scale reactivation features within the Pine Creek Sandstone member and lack of evidence of low stage reworking, indicate that the river was a perennial system of low braiding index. The abandonment of the Pine Creek Sandstone river channel was rapid with the uppermost troughs infilled with shale (Figure 4.7). Greb & Chesnut (1989) have interpreted the Dave Branch Shale to represent an inundation of brackish water associated with estuarine conditions.

Section 2 of the Pine Creek Sandstone member exposes levee deposits (CM architectural elements) which indicate that the banks of the upper Pine Creek Sandstone river system were relatively stable and subjected to periodic flooding events.

Two units of facies Smc are preserved within the Pine Creek Sandstone member. These are both lenticular in geometry, and display sharp margins which dip at variable angles. The base of facies Smc is coated with a lag of organic debris and quartz granules. Concentric laminae are preserved parallel to the basal margin and these grade into a structureless sandstone fill. The lenticular cross-section of facies Smc suggests that the units were emplaced along a plane oblique to the flow of the Pine Creek river. Facies Smc is discussed further in Chapter 7.

## 4.5.2. The Corbin Sandstone formation.

The northern or upstream sections of the Corbin Sandstone formation are coarser grained than those located at a similar stratigraphic level further downstream which indicates a northern source for the detrital material. The grain size of the formation also decreases upwards through the section.

Complete CH architectural elements have been identified from sections 1, 2 and 3 of the Corbin Sandstone formation, which vary in thickness from 10.5-22.25 m. The base of the CH elements are represented by fourth or fifth order bounding surfaces. Internally the CH elements are composed of a number of macroforms separated by third order bounding surfaces. These macroforms are dominated by elements produced by downstream accretion, with lateral accretion elements less common. CH elements are capped by fine grained sediments of H, and CM architectural elements which relate to either channel abandonment or levee establishment.

All of the Corbin Sandstone formation CH elements, excepting the uppermost element (section 3), display palaeoflow to the southwest. Within the channel elements the dispersion of palaeocurrents is low, and generally does not exceed 50° which indicates fluvial channels of low sinuosity. The uppermost CH element, exposed in section 3, displays a swing in palaeoflow through 180° to an eastwards and northeastwards direction. There is no transition in palaeoflow directions and the swing in palaeocurrent direction corresponds with the inception of a new CH element.

Within the uppermost major channel architectural element of the Corbin Sandstone formation (section 3) palaeohydrological reconstructions have been attempted following the methods outlined in section 2.4.2. The average height of 20 dunes (scaled to the water depth) is 0.80 m, which when decompacted using a $\phi_c$ value of 0.15 relates to an original dune height of at least 1.25 m and a channel depth of between 6-9 m (Figure 2.4). The sinuosity of the channel has been established form the palaeocurrent variance (84°) and gives a sinuosity of 1.07 (low sinuosity), and a width/depth ratio of 80 (Schumm 1968b). The average width of the channel would therefore have been between 480-720 m. Such a system is similar in size to the modern day Tana and Brahmaputra Rivers (Table 2.5).

Within the major channel architectural elements the Corbin Sandstone formation is dominated by the deposits of downstream migrating bedforms which take the form of macroform scale DA Type 1 and 2, and mesoform scale SB Type 1 and 2 architectural elements. These relate to the deposits of migrating mid-channel and bank attached bars and dunes respectively (see Chapter 2.4). Within DA Type 1 architectural elements of section 3 differences in palaeoflow between simple and compound cross-bed foresets were noted (Figure 4.23). These may relate to changes in flow conditions related to the development of a compound bedform (Chapter 2.4).

An absence of reworking associated with large scale fluctuations in water level indicate that the Corbin Sandstone formation was deposited in a perennial system where water level was rarely low. Therefore, the Corbin Sandstone river was a deep system. The bedforms were not emergent for prolonged periods and hence the system would have had a low braiding index.

Stable banks are inferred during deposition of the Corbin Sandstone river, due to the preservation of levee deposits (CM element) within sections 1 and 3. Rapid abandonment of the river channel is indicated at section 3 where form sets of sand are preserved within a mud-dominated unit. The preservation of sandstone form sets implies rapid changes in flow conditions resulting in rapid burial and preservation of dune bedforms.

The channel-like massive sandstone features within the Corbin Sandstone indicate deposition from cross-channel currents. The indicators of the base of the massive sandstone channel preserved in section 3 indicate flow was in a direction perpendicular to the fluvial current flow. These architectural elements will be discussed in more detail in Chapter 7.

### 4.5.3. Synthesis Of The Lee Sandbelts.

### (i) Regional Setting.

During the early Pennsylvanian sedimentation took place in a foreland basin setting in a near equatorial position. Climate was tropical and warm.

The Lee-type sandstones consist of quartz arenites and litharenites which take the form of lenticular sandbelts oriented northeast to southwest (Figure 4.4b). The sediments were deposited by axial rivers. Unimodal cross-stratification indicates flow to the southwest with only small scale deviations, such as in the uppermost Corbin formation. The Lee sandstones interfinger with the lithic-rich Breathitt Group (Figure 4.5).

Breathitt-type lithologies were deposited across a low-lying coastal plain by transverse oriented fluvial systems prograding to the northwest and west from the Appalachian front (Figure 4.4b). Coals were deposited on raised or domed peat swamps (Staub *et al* 1991) formed on a poorly drained coastal plain (Cecil *et al* 1985). The peat swamps required rainfall as the primary source of water (Cecil *et al* 1985) with the rainfall evenly distributed throughout the year. These deposits have been compared with the central Sarawak lowlands of eastern Malaysia (Staub *et al* 1991), where the peat swamp is located anywhere from 4 m above the mean high tide level.

The Breathitt lithologies were sourced from the rising Alleghanian highlands, and the overall coarsening upwards nature of the sediments is attributed to advance and increasing intensity of the front. Cyclothems preserved within the Breathitt relate to deposition of 430 Ka glacio-eustatic driven cycles. Larger cycles of sedimentation of approximately 2.5 Ma years are separated by major marine bands (Figure 4.5) which may be traced over the entire central Appalachian Basin. The marine bands represent periodic inundation of the central Appalachian Basin from the south (Chesnut 1988). Individual sandstone formations of the Lee, such as the Bee Rock Sandstone and Corbin Sandstone, are separated by the marine surfaces (Figure 4.5), and hence were deposited in episodes of sedimentation lasting approximately 2.5 Ma. The

sandstone formations represent the deposits of an entire river system and are comparable with the 1 st order channels of Bristow (1987b).

The Lee/type sandbelts are restricted to the western portion of the central Appalachian Basin (Figure 4.6a & b) and the first order channel sandbelts (i.e. formations) migrated in a stepped fashion westward, away from the approaching Alleghanian thrust front (Figure 4.5). Similar sandbody geometries have been described from the axial Ganges river system by Burbank & Beck (1991). In the Himalayan foredeep the position of the axial Ganges river is a product of progradation or aggradation in the foredeep (Burbank & Beck 1991). Rapid progradation of transverse oriented fluvial sediment from the rising thrust front constrains the axial system beyond the toe of the prograding wedge. In purely aggradational systems the axial system may be unconfined.

It may be assumed that some external control existed on the positioning of the Lee sandbelts. There is no evidence from the detailed work of Rice (1984) or Chesnut (1988) to indicate constraining syn-sedimentary faulting at the western margin of the central Appalachian Basin. The Lee sandbelts may have been confined by the progradation of the Breathitt lithologies, as in the Himalayan foredeep (Burbank & Beck 1991). Alternatively, Rice and Schwietering (1988) described the existence of a north facing cuesta at the western margin of the central Appalachian Basin (Figure 4.4b). It may be possible that this cuesta controlled the location of the Lee sandbelts.

The bases of the Lee-type sandstone formations are marked by erosive fifth order bounding surfaces (Table 2.3). Fifth order bounding surfaces are believed to be controlled by allocyclic mechanisms such as tectonism, eustacy or a combination of the two. The extensive Breathitt lithologies occurring between the Lee sandstone belts represent either westward progradation of Breathitt transverse fluvial systems over the axial Lee sandbodies (tectonic control) or marine transgressions (eustatic control).

Wizevich (1991) cites the westward shift of progressively younger Lee sandbelts as evidence that tectonics was the dominate control on sandbody location. Wizevich (1991, 1993) concluded that the westward shift in Lee sandbody position was related to thrust loading, causing increased lithospheric flexure and progressive migration of the foreland basin to the west. Westward progradation of Breathitt lithologies would have been caused by elevation of the Breathitt highlands, thereby increasing the gradient of the Breathitt rivers and introducing more sediment into the drainage basin. The eastward rotation of the uppermost Corbin fluvial channel, as indicated by a change in palaeocurrent azimuth to the east, may reflect a change in palaeoslope caused by the onset of forebulge uplift (Wizevich 1993).

Lee/type sandstones are commonly overlain by marine or estuarine shales such as illustrated in the Corbin Sandstone formation section 2 (Figure 4.21) and Figure 4.5. The close association between regional marine bands and westwards shift of Lee sandbodies indicates that changes in base level were occurring. Eustatic sea level variations have been documented from the lower Pennsylvanian by Ross & Ross (1988), although these are of smaller intensity than the cycles of the upper Pennsylvanian. Marine transgressions form the Ouachita trough would have raised the base level and halted deposition of the Lee sands (Chesnut 1988).

F also previously

It is proposed here that the position of the Lee sandbelts was controlled by a number of factors including progradation of Breathitt lithologies associated with the advancing Alleghanian thrust front, and eustatic sea level changes. The fifth order bounding surfaces located at the base of Lee-type formations represent avulsion of an entire channel system. The basal scour was initiated during a lowstand in relative sea-level with sediment bypassed into the Black Warrior and Arkoma Basins (Figure 4.4b). The individual formations of the Lee represent deposition during a rise in relative sea level (i.e. transgressive sands). The top of the sandstones may be rooted and covered by a coal before the shale, or may be directly overlain by marine shale in which case the sand is commonly bioturbated. These marine-influenced horizons represent the inland extension of maximum flooding surfaces.

## (ii) Sandbody Architecture.

Members of the Bee Rock Sandstone and Corbin Sandstone formations are composed of major CH architectural elements stacked in a multilateral and multistorey manner. The base of channel elements are represented by fourth order bounding surfaces. Palaeocurrent patterns within CH elements indicate a southwestwards direction of sediment transport with a strongly unimodal character. Dispersion is commonly <90° for individual channel fill successions (Wizevich 1991 & this study).

F

Within the Bee Rock Sandstone formation the Rockcastle and Pine Creek members are preserved. These individual sandbodies are erosively based and capped by coals and/or shales of estuarine affinity. It is suggested that minor changes in base level influenced sedimentation within the Bee Rock Sandstone formation, causing periodic inundation by marine influences. However, such estuarine influences may extend for 100's km's inland from the shoreline. Similar fluctutions is base level are inferred to have occurred during deposition of the Corbin Sandstone formation with coals and fine grained sediments of marine affinity preserved above and below the formation in the Scranton quadrangle (Figure 4.21). Coals are also preserved at the

top of major channel architectural elements in section 2 of the Corbin Sandstone formation (Figure 4.21).

The fourth order bounding surfaces at the base of major CH elements are produced by autocyclic controls. The internal architecture of individual CH elements within the Lee sandbelts consists of more than one macroform separated by third order bounding surfaces. There are two ways of producing such sedimentary patterns (Wizevich 1991):

1) Multiple channels within a larger braided river system. The channels migrate laterally within the river belt and combined with vertical accretion lead to the development of a hierarchical architecture.

2) A single channel with relatively stable banks and mid-channel macroforms. With vertical aggradation the macroforms overlie each other.

In the first model erosively based fourth order bounding surfaces are equated with passage of second order channels (Bristow 1987b). Lateral accretion of mid-channel bars and bank attached macroforms dominate deposits, as the second order channels migrate laterally within the floodplain of the first order channel. Migration produces the sheet like sands which are elongate in the flow direction. Within the Lee sandbodies lateral accretion deposits are virtually absent, hence this model would appear to be non-applicable.

In the second model fourth order bounding surfaces represent instances of avulsion. The sediment preserved between fourth order bounding surfaces represents deposition within the second order channels of Bristow (1987b). Vertical aggradation within the CH element results in the preservation of stacked macroforms. To produce a sheet-like sandbody geometry such as that of the Lee sandbodies a single channel stream must avulse periodically (Bridge & Leeder 1979).

The Bee Rock Sandstone formation is 91 km wide by 150 m thick. The river depositing the sediments is estimated at 1 000 m wide and 15 m deep. The river would therefore have to avulse 2747 times. The Corbin formation is 64 km wide by 60 m thick. The river was 600 m wide and 7 m deep, and would therefore have to avulse 1000 times. 2.5 Ma years is the period estimated for the deposition of these river systems (Ettensohn 1992). Such a rate of avulsion is within modern rates (Bridge 1985).

The macroforms of the Lee sandbelts are separated by third order bounding surfaces. Individual macroforms are dominated by architectural elements which were deposited by downstream accreting bedforms. DA Type 1 and 2 elements, together with Type 1 and 2 SB and GB elements dominate the Lee channels. Strongly uni-

modal palaeocurrents (ie low sinuosity) and paucity of lateral accretion features indicate deposition in a single channel system (ie low braiding index). A lack of facies which suggest low stage reworking indicate that the river system was a perennial one.

The deposits of SM Type 1 and 2 architectural elements represent sedimentation from unusual fluvial currents. The lack of internal structure indicates that the currents responsible for the deposition of these units precluded the establishment of traction currents and hence cross-stratification. These massive sandstone facies will be discussed in detail in Chapter 7.

## (iii) Sediment Source.

Inferred sources for the Lee type sandstones have been to the south and east (Hatcher et al 1989), north (Rice 1984; Rice & Schwietering 1988), and a combination of these (Siever & Potter 1956; Donaldson et al 1985; Chesnut 1988).

Two possibilities exist for the origin of the quartzose sandstones. In the first instance the source for all the clastics entering the fluvial sand belt was from the Appalachian highlands, and included quartz, feldspar and lithic fragments. Tropical weathering (Johnsson et al 1988) and fluvial reworking of the immature clastics preferentially enriched the quartz content of the sandbelt (Chesnut 1988). The modern Rio Negron River of Venezuela and Brazil contains residual quartz deposits which are forming on granite and granodiorite in response to tropical weathering and acid conditions (Cecil et al 1985).

Local westerly palaeocurrents within the Lee Formation (Rice 1984), and the northwest to southeast trend of quartzose and Breathitt type sands, which are the lateral equivalent to the Lee (Ettensohn 1992), support a nearby Appalachian sediment source. However, the lateral equivalent to the Lee sandstones in Virginia rarely contain quartz pebbles (Rice 1984), and hence it is unlikely that the Lee sands were derived entirely from a southeast/easterly source (Wizevich 1991).

In the second model the dominant source for the quartzose clastic material was a previously enriched source to the northeast. The Lee sandstones of the central Appalachian Basin are similar in lithology to those of equivalent age in the Illinois and Michigan Basins (Figure 4.4b). These equivalent strata were all deposited by fluvial systems flowing to the southwest (Potter & Siever 1956). A northeastern source for the Lee type sands must therefore have been volumetrically important. Regional sedimentological studies by BeMent (1976) indicate that the quartz pebbles within the sandbelts increase in size to the northeast, a feature which can be explained by a northeastern source. However, some Lee sands (Naese and upper Corbin) contain

up to 15% labile fragments which would not survive extensive transport (Mack 1981; Cameron & Blatt 1971) indicating a local southeast or southerly source.

The most likely scenario for the source of the northeast/southwest trending Lee-type sandbodies is that of a primarily northern source with a minor influx of sediment from the southeast or east. Chesnut (1988) suggested that the Acadian and Caledonide mountain belts, together with the Canadian Shield areas would have provided sediment during the early Pennsylvanian. Additional recycled Acadian and younger sediment, derived from crystalline rocks of the early Appalachian trend, were added to the Lee sandbelts by transverse tributaries of the Breathitt Group flowing out of the mountains and across low lying alluvial plains.

### (iv) Modern Analogues.

The Orinoco River of Venezuela (Table 2.6) transports quartzose sediment in a deep, low sinuosity (bedload dominated) river system with a low braiding index. Intense tropical weathering has destroyed the labile detrital components derived from the eastern cratonic source (Guyana Shield) and the western orogenic source (Andes Mountains) (Johnsson et al 1988). Tributaries from the Andean highlands have constructed alluvial fans which face the Orinoco River against the exposed craton (Nordin & Perez-Hernandez 1989). The Orinoco is dominated by large scale planar cross-stratification with foresets which dip 24-30°, and minor trough cross-stratification with symmetric and asymmetric fill (McKee 1989). However, the Orinoco River sands are reworked by aeolian processes during periods of low flow. Evidence of such reworking is not apparent in the Lee sands.

### 4.6. Summary.

The Lee-type sandbelts represented by the Bee Rock and Corbin formations were deposited in a northeast/southwest trending belts on the western margin of the Appalachian foreland basin. The formations were deposited during periods of rising relative sea level and were transgressed during periods of marine inundation. Each formation was deposited within a period of approximately 2.5 Ma and represents deposition of a first order channel (Bristow 1987b). Fluctuations in base level during deposition of the Lee-type sandstone formations is indicated by the development of coals and fine grained beds of marine affinity within sandstone formations.

The sediments of the Lee sandbelts were derived from a volumetrically important quartz-rich northeastern source which provided a wide range of grain sizes.

Tropical weathering resulted in the formation of first cycle quartz arenites. The rising Alleghanian front supplied smaller quantities of lithic components to the Lee-type sandbelts via the transverse river systems of the Breathitt Group. Thus, a hybrid sandstone was deposited.

The Lee sandbelts are dominated by multistorey and multilateral major channel element sandbodies which represent deposition within the second order channels of Bristow (1987b). These channels are separated by fourth order bounding surfaces which represent surfaces of channel avulsion. Repeated avulsion across the river floodplain, together with rapid subsidence, resulted in stacking of the sandbodies.

Within major channel elements the Lee-type sandstones are dominated by macroforms separated by third order bounding surfaces. The macroforms are composed of architectural elements indicative of deposition from dominantly downstream accreting bedforms. The lack of large scale reactivation surfaces and evidence of low stage reworking, together with the absence of plane bedding, indicate that deposition was in a perennial system with a low braiding index.

Massive sandstone facies take sheet-like (Sms) and channel-like (Smc) forms, and are preserved as SM Type 1 and 2 architectural elements. These form laterally extensive bodies with definable geometries. Composition of sandstone does not vary between the structured and structureless facies of the Lee-type lithologies. However, textural differences are clear between cross-stratified and massive sandstones. These will be addressed in Chapter 7.

# Chapter 5

# The Illinois Basin

## 5.1. Regional Geological History Of The Illinois Basin.

The Illinois Basin, formerly termed the Eastern Interior Basin, lies to the south of the Canadian Shield (Figure 5.1) The basin is bordered to the west by the Ozark Dome and Mississippi River Arch (Figure 5.2); and to the east by the Nashville Dome and Cincinnati Arch. The Wisconsin and Kankakee Arches form boundaries to the north (Pryor & Sable 1974). The south-west boundary is formed by the Pascola Arch (Figure 5.2).



*Figure 5.1. The position of the Illinois Basin within the central United States, and the surrounding sedimentary basins.*

The Illinois Basin is an intracratonic, symmetrical basin with a sedimentary record spanning the mid Ordovician to early Permian. The origin of the Illinois Basin is

problematic and a number of models have been invoked (see Kolata & Nelson 1990). The generally accepted models of thermal contraction and lithospheric stretching associated with rifting have been challenged by Quinlan & Beaumont (1984) as subsidence in the Illinois Basin is polyphase, and can only be explained by means of multiple heating events.
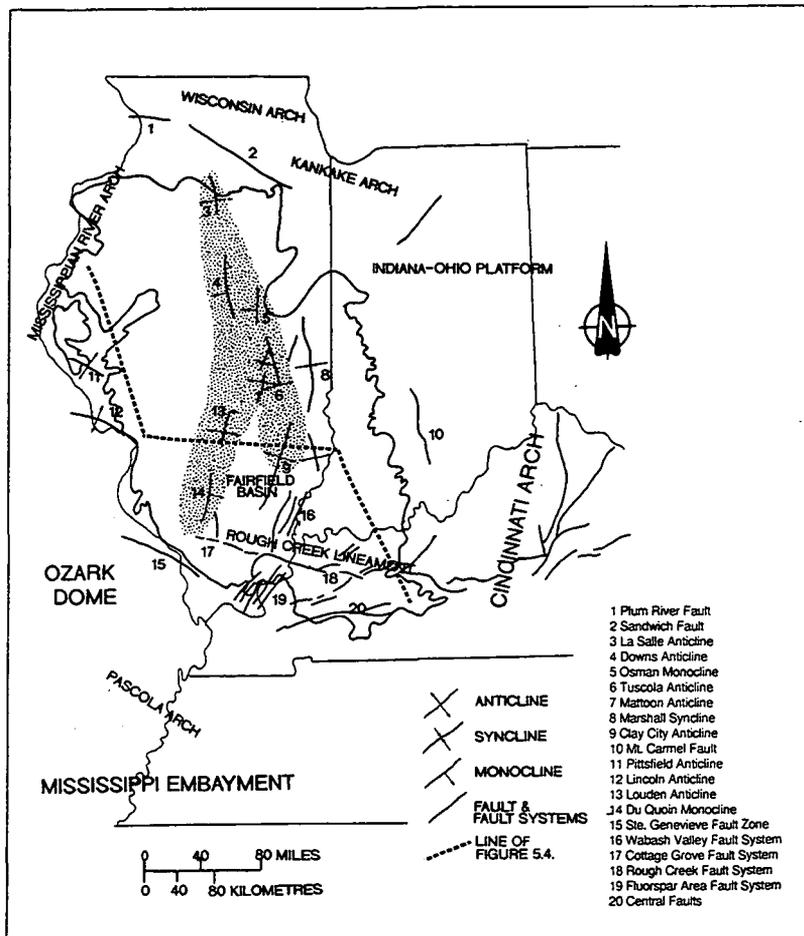


Figure 5.2. The structural elements of the Illinois Basin. Those inferred to be active during the Pennsylvanian are shaded (modified after Trask & Palmer 1986).

Quinlan & Beaumont (1984) postulate that the Illinois Basin, and the related Michigan Basin (Figure 5.1), have subsided as a result of lithospheric flexure in response to crustal loading by successive thrust sheets of the Taconian, Acadian and Alleghanian orogenies centred in the Appalachian fold belt (see Chapter 4). Quinlan & Beaumont (1984) have developed a model which relates lithospheric relaxation to the position of peripheral bulges (Figure 5.3a). If basins are far enough apart there will be no flexural interaction between them. However, where basins are closer together peripheral bulges add constructively to produce an intervening arch which is uplifted

by lithospheric flexure (Figure 5.3b). Figure 5.3c displays a basic pattern similar to the Eastern Interior of the USA with doming occurring where the peripheral bulges of all three basins overlap. Throughout the depositional history of the Illinois Basin it has been periodically yoked with the Appalachian Basin, resulting in regionally persistent sedimentary units. Uplifting of arch systems has resulted in de-coupling of the basins. Tankard (1986a & b) has demonstrated that variations and similarities in the sedimentary fill of the Illinois and Appalachian Basins are related to the migration of peripheral bulge systems in response to lithospheric flexure, as predicted by Quinlan & Beaumont (1984).
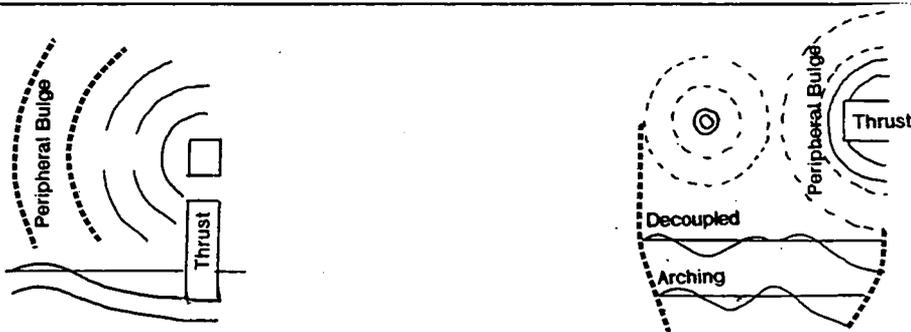


a) Cartoon illustrating initial deformation of lithosphere resulting from loading. Amplitude of the peripheral bulge is exaggerated.

b) Flexural interaction between a foreland basin and an intracratonic basin. Subsequent cross-sections show decreasing distance between basins.



*Figure 5.3. Models of lithospheric interaction (modified after Quinlan & Beaumont 1984)*
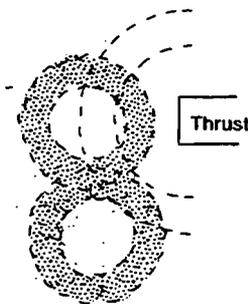
c) Flexural interaction between a foreland and two intracratonic basins.

The major structural elements of the Illinois Basin are illustrated in Figure 5.2, and a generalised history of the Illinois Basin is given in Table 5.1. The basin fill consists of thick, conformable stratigraphic units, separated by regional unconformities. The units of the Illinois Basin fill are the Sauk, Tippecanoe, Kaskaskia and Absaroka

| SYSTEM | SERIES | STAGE | AGE (MA) | CLIMATE | PALAEO LAT | EXTENSION | COMPRESSION | | SEDIMENTATION | TECTONICS |
|---|---|---|---|---|---|---|---|---|---|---|
| PERMIAN | | | 250 | Dry | 5°N | | | ABSAROKA | | |
| CARBONIFEROUS — PENNSYLVANIAN | Virgilian | | | Seasonal Humid | | | Alleghanian | | Missourian/Virgilian deltaic environments. Sediment source: Canadian shield & northern Appalachians. | |
| | Missourian | | 300 | | | | | | | Deformation of basement causing block faulting & folding of sedimentary cover. |
| | Desmoinesian | | | Tropical Humid | | | | | Desmoinesian: major depocentre in southeast. Deltaic environment with cyclic sedimentation & coal development. | |
| | Atokan | | | | | | | | Morrowan/Atokan: Fluvial & marginal marine environments with accumulation of coal in inter-channel areas. | |
| | Morrowan | | | Dry | 5°S | | | | Mid-Carboniferous unconformity. | |
| CARBONIFEROUS — MISSISSIPPIAN | Chesterian | | | | | | | KASKASKIA | Valmeyeran/Chesterian: submarine deltas complex, overlain by transgressive marine carbonates. Marine conditions periodically disturbed by fluvio-deltaic incursions. | |
| | Valmeyran | Meramecian | 350 | | | | Acadian | | Kinderhookian: Albany Shale represents the basinal equivalent of the Catskill delta system of the Appalachian Basin. | Uplift of Acadian landmass. Thrusting dominantly in south |
| | | Osagean | | | | | | | | |
| | Kinderhookian | | | | | | | | | |
| DEVONIAN | Chautauquan | | | | 10-20°S | | | | Influx of clastics associated with orogeny. Progradation of sub-aqueous delta. | Illinois Basin: broad cratonic embayment open to marine influences to the south. Cincinnati & Kankakee Arches subtle features. |
| | Senecan | | | | | | | | | Devonian uplift of dome & arch areas. |
| | Erian | | | | | | | | | |
| | Ulsterian | | 400 | | | | | | Carbonate platform development. | Transgression of epicontinental sea. Marine muds-carbonates. |
| SILURIAN | Cayugan | | | | 20°S | | | | Relative sea level fall & unconformity development | |
| | Niagaran | | | | | | | | | |
| | Alexandrian | | | | | | | | | |
| ORDOVICIAN | Cincinnatian | | | | 20-25°S | | Taconian | TIPPECANOE | Relative sea level rise & transgression | Kankakee & Cincinnati Arches uplifted due to lithospheric flexure. |
| | | | 450 | | | | | | Basinal marine siliciclastics grade upwards into blanket carbonates. | |
| | Champlaninian | | | | | | | | | |
| | Canadian | | | | | | | | Subaerial erosion & hiatus at basin margin. Marine clastic sedimentation in basin centre. | |
| | | | 500 | | | | | | Marine carbonates & supratidal sediments deposited during relative sealevel rise. | |
| CAMBRIAN | St.Croixan | | | | | | | SAUK | | Rifting associated with initiation of Iapetus. |
| | | | 550 | | | | | | | |

Timescale from Shaver et al 1985.

Information derived from: Phillips & Peppers (1984); Quinlan & Beaumont (1984); Kolata & Nelson (1990); Treworthy (1990).

*Table 5.1. A generalised history of the Illinois Basin.*

151

sequences, which were deposited during major transgressive-regressive events. A summary of sedimentation through these sequences is given in Table 5.1.

During Carboniferous times the Illinois Basin formed a major negative element where more than 1,800 m (5,500 ft) of sediment accumulated. The basin took the form of a cratonic embayment open to marine influences to the south. The supply of clastic material was largely influenced by the tectonic uplands east of the Appalachian Basin and the eastern Canadian Shield. Terrigenous detritus originated from these areas, or perhaps further east (Pryor & Sable 1974).

During the early Mississippian (Kinderhookian) the emerging Acadian front supplied large quantities of clastic detritus to the Illinois Basin. The Appalachian and Illinois Basins were yoked together and hence most stratigraphic units are regionally persistent (Tankard 1986a). Fine grained clastics are preserved in the Illinois Basin as the prodelta shales of the New Albany Group (Figure 5.4), the distal deposits of the Acadian clastic wedge. During Valmeyeran times a decrease in tectonic activity was marked by a large accumulation of carbonate sediments (Figure 5.4). Clastic deposits such as those of the Borden Group continued to be deposited by major river systems. Relative positive elements were the Kankakee and Cincinnati Arches, and the Ozark Dome (Kolata & Nelson 1990).

The Illinois Basin continued to subside through the Chesterian, and received sediment from the uplifted Canadian Shield via a major river system termed the Michigan River System (Trask & Palmer 1986; Kolata & Nelson 1990). A compressive regime within the Illinois Basin, related to collision in the Appalachian region, resulted in the uplift of crustal blocks. Areas of deformation include the St. Genevieve fault zone, Du Quoin monocline, Salem and Loudon anticlines and the La Salle anticlinal belt (Figure 5.2). Chesterian sedimentation represents a transition from Valmeyeran marine conditions to the siliciclastic environments of the Pennsylvanian, and is preserved as cyclically alternating limestone-shale and sandstone-shale intervals which have been interpreted as deltaic deposits (Treworgy 1990).

Broad regional uplift marked the end of the Mississippian and the sea withdrew from virtually all the North American Craton. The mid-continent was raised above sea-level and tilted to the south-west (Potter & Siever 1956). Between latest Chesterian and earliest Pennsylvanian the Illinois Basin was eroded by a series of major rivers the largest of which, the Benton-Fairfield Valley (Figure 5.5a), probably represents the through-basin course of the Michigan River system (Droste & Keller 1989). The deeply incised river channels at the basin margins were initiated whilst the retreating sea still occupied the basin centre. The rivers formed a south-west oriented dendritic drainage system entrenched up to 140 m. The larger palaeovalleys tend to have steep sides and broad level floors which reach 30 km in width (Kvale & Barnhill 1994).

| SYSTEM | SERIES | | USA SERIES | AGE (MA) | NORTHERN ARCHES | SW ILLINOIS | SW INDIANA | W KENTUCKY |
|---|---|---|---|---|---|---|---|---|
| PERMIAN | | | | 290 | | | | |
| CARBONIFEROUS | STEPHANIAN | PENNSYLVANIAN | VIRGILIAN | | | | Mattoon Fm | |
| | | | MISSOURIAN | | McLEANSBORO GP: Bond Fm | McLEANSBORO GP: Bond Fm | McLEANSBORO GP: Bond Fm | Sturgis Fm |
| | —?— | | | 310 | Modesto Fm | Modesto Fm | Patoka Fm / Shelburn Fm | |
| | WESTPHALIAN | | DESMOINESIAN | | KEWANEE GP: Carbondale Fm / Springfield Coal / Spoon Fm / Seville Lst | KEWANEE GP: Carbondale Fm / Herrin Coal / Springfield Coal / Spoon Fm | CARBONDALE GP: Dugger Fm / Herrin Coal / Springfield Coal / Linton Fm / Staunton Fm | Herrin Coal / Springfield Coal / Carbondale Fm |
| | | | ATOKAN | 315 | McCORMICK GP: Caseyville & Abbot Fm | McCORMICK GP: Abbot Fm / Pound Sst / Caseyville Fm | RACCOON CREEK GP: Brazil Fmn / Lwr Block Coal / Lead Creek Lst / Mariah Hill Coal / Mansfield Fm / Whetstone Beds | Tradewater Fm / Lead Creek Lst / Caseyville Fm |
| | | | MORROWAN | | | | | |
| | NAMURIAN | MISSISSIPPIAN | CHESTERIAN | 330 | | Menard Lst / Vienna Lst / Tar Springs Sst (OKAW GP) / Cyprus Sst (PAINT CREEK GP) | BUFFALO WALLOW GP: Tobinsport Fm / STEPHENS PORT GP: Vienna Lst / Tar Springs Fm / WEST BADEN GP | Buffalo Wallow Fm / Tar Springs Sst / Golconda Fm / Cyprus Sst / Paint Creek Fm |
| | VISEAN | | VALMEYERAN | 340 | St Louis Lst / Salem Lst / Burlington Lst | Yankeetown Sst / Renault Lst / Aux Vases Sst / St Louis Lst / Salem Lst / Borden Siltst | BLUE RIVER GP: Renault Fm / St Genevieve Lst / St Louis Lst / Salem Lst (SAUNDERS GP) | Renault Fm / St Genevieve Lst / St Louis Lst / Salem Lst |
| | TOURNAISIAN | | KINDER HOOKIAN | | NEW ALBANY / NORTH HILL GP | Chouteau Lst / NEW ALBANY | BORDEN GP: New Providence Shale / Rockford Lst | New Providence Shale / Rockford Lst |

*Figure 5.4. The stratigraphy of the Illinois Basin (after Shaver et al 1985).*

153

The La Salle anticlinal belt (Figure 5.2) was uplifted prior to deposition of the Pennsylvanian strata and was responsible for the deflection of sub-Pennsylvanian river systems. Diversion of major palaeovalleys around the Du Quoin monocline (Figure 5.2) suggest that this structure was also uplifted (Kolata & Nelson 1990). The Cincinnati Arch was incised by streams flowing from the central Appalachian Basin (Figure 5.5a).
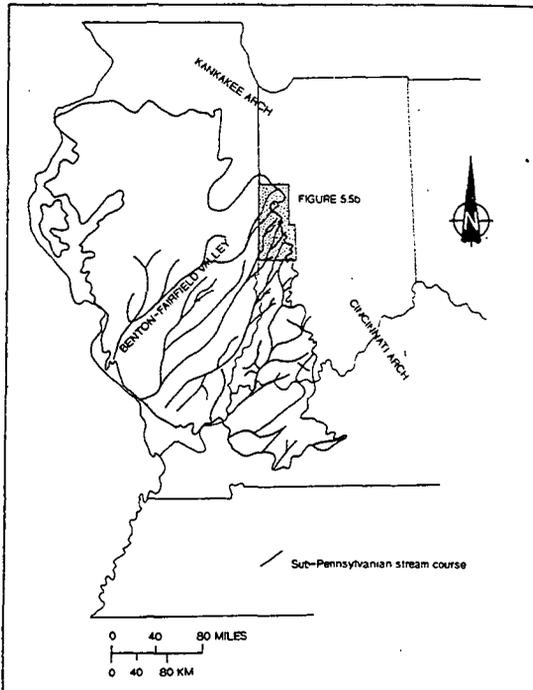


a) The sub-Pennsylvanian palaeovalley system of the Illinois Basin (modified after Pryor & Sable 1974; Droste & Keller 1989).
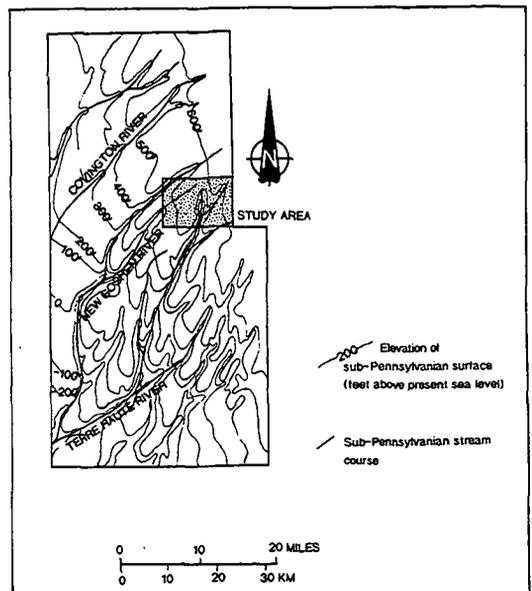


b) The sub-Pennsylvanian palaeovalley system of the study area after Keller (1990), with flow net reconstructed after Alexander (1986).

Figure 5.5. The sub-Pennsylvanian palaeovalley systems of the Illinois Basin.

The mid-Carboniferous unconformity is most pronounced at the margins of the Illinois Basin with magnitude decreasing significantly basinwards (Figure 5.4). Recent work supports the theory that the mid-Carboniferous unconformity is present throughout the entire basin (Treworgy 1990), and is related to the early Pennsylvanian unconformity of the Appalachian Basin (Chapter 4).

Little sediment was deposited in the Illinois Basin during the period of mass wasting. However, within some palaeovalleys slump blocks are preserved. During the Pennsylvanian the sea gradually returned to the Illinois Basin and valleys in the sub-Absaroka surface were back-filled. The shallower streams near the basin centre were the last to begin forming and the first to back fill (Droste & Keller 1989). Strata of the Pennsylvanian system were deposited in a subsiding trough which was open to the south and bordered by the uplifted Cincinnati Arch and Nashville Dome (Figure 5.1). The dominant structures affecting deposition were the Du Quoin Monocline, Louden and Salem anticlines, the La Salle anticlinal belt and the Ozark Dome (Trask & Palmer 1986) which are illustrated in Figure 5.2. The Du Quoin Monocline formed a hinge separating horizontal or gently dipping strata to the west from more steeply dipping strata at the margin of the Fairfield Basin (Figure 5.2).

Deposition of the Pennsylvanian took place on a low lying coastal plain and the adjacent shallow shelf. The deposits are composed largely of terrigenous detritus with small amounts of coal and limestone. Basal Pennsylvanian sediments show evidence for derivation from two sources. The major source was to the east, north-east and north, and carried metamorphic quartz pebbles south-west across the Illinois Basin. Uplifted areas in the location of present-day New England and southeast Canada are believed to be the principle sources of sediment, with Palaeozoic and Proterozoic sandstones, quartzites and conglomerates providing clean quartz sand and gravel (Potter & Siever 1956). A minor sediment source existed to the north-west of the Illinois Basin which provided sediment free of metamorphic quartz clasts (Potter & Siever 1956). The ultimate destination of the sediments was the Ouachita trough of the Arkoma Basin (Figure 5.1). A palaeogeographic reconstruction of this time is illustrated in Figure 5.4b.

Through the McCormick Group and laterally equivalent Raccoon Creek Group (Figure 5.4) sediments become progressively less mature and less sand rich. The changes in sediment type are believed to reflect an unroofing of the source area (Potter & Siever 1956). The pattern of sedimentation within the McCormick & Raccoon Creek Groups is similar to that of equivalent strata in the central Appalachian Basin i.e. the Lee-type and Breathitt-type lithologies (Chapter 4), with cycles of fluvial and marginal marine sediments preserved.

The Kewanee and McLeansboro Groups and lateral equivalents consist of cyclic alternations of thin limestones, shale, sandstone and coal which have been interpreted in terms of the progradation and abandonment of deltas (Pryor & Sable 1974). At least 55 cycles are preserved, and are interpreted as being of eustatic origin (Ross & Ross 1988). The mechanism responsible for the cyclicity remains unclear (Kolata & Nelson 1990).

The most economic coals of the Illinois Basin are preserved within the Desmoinesian and Missourian deposits. Coals may be correlated over wide areas and serve as useful stratigraphic markers. Coals are generally overlain by regionally correlatable shales, for example the Colchester, Springfield and Herrin Coals (Figure 5.4) are overlain by the Francis Creek, Dykersburg and Energy Shales respectively (Archer & Kvale 1993). These sediments are similar to deposits of similar age within the central Appalachian Basin (Chapter 4).

## 5.2. The Mansfield & Brazil Formations (Morrowan-Atokan).

The Mansfield and Brazil Formations of the Raccoon Creek Group drape the mid-Carboniferous unconformity, initially filling valleys carved out of Mississippian strata (Figure 5.5a). Sediments of this age are exposed on the eastern margin of the Illinois Basin.

The Mansfield and Brazil Formations are of Morrowan and Atokan age. The lower Mansfield is Morrowan, with the Morrowan/Atokan boundary generally accepted to lie above the Lead Creek Limestone (Shaver *et al* 1985) as illustrated in Figure 5.4. The upper boundary of the Atokan lies close to the Seville Limestone, encompassing the upper Mansfield and Brazil Formations (Figure 5.4).

The Mansfield Formation varies in thickness across the eastern margin of the Illinois Basin from 15 to 105 m (50-300 ft) due to topography of the sub-Pennsylvanian unconformity. Strata are characterised by quartzose sandstones containing abundant well rounded granules and pebbles of quartz. Silts and mudstones are interbedded with, and laterally interfinger with, the sandstones. Lenticular coals reaching 5 m in thickness are also present and are generally characterised by low sulphur and ash contents. In the study area the Mansfield Formation is defined as those sediments occurring between the mid-Carboniferous unconformity and the Lower Block Coal (Figure 5.4).

The Mansfield Formation, and its lateral equivalents (Figure 5.4), fill sub-Pennsylvanian palaeovalleys. Fluvial sandstones arranged in upward fining units have been extensively documented from the palaeovalleys (Howard & Whitaker

1990; Kvale & Barnhill 1994) and interfluve areas (Fishbaugh *et al* 1989). However, siltstone and mudstone are also volumetrically important. When traced in the downstream direction fluvial sandbodies may be replaced by these fine grained facies, such as in the New Goshen Channel (Figure 5.5b) of western Indiana (Archer & Kvale 1993)

Within the basal Mansfield Formation Kvale *et al* (1989) have identified rhythmically laminated siltstones within the Whetstone beds (Figure 5.4). Laminae occur in paired couplets which range form 0.5 mm to 1 cm thick, separated by thin clay drapes. The laminae within the Whetstones preserve around twenty ichnogenera, the most abundant being *Plangtichnus eraticus, Treptichnus bifurcus* and *Haplotichnus idianesis* (Kvale & Archer 1991). Fin drag marks, arthropod trackways and raindrop imprints are also preserved along the bedding planes of the silt. Plant fossils are principally lycopods, and trunks up to 50 cm in diameter and 5 m in height have been preserved in the upright position (Kvale & Archer 1991). The lycopods are rooted into coal beds underlying the Whetstones. Conodonts have been collected from the intercalated claystones of the Whetstone beds (Kvale & Archer 1991).

Laterally extensive interbedded sandstone and mudstone units have been documented from the Mansfield Formation (Fishbaugh *et al* 1989; Kvale & Barnhill 1994). Locally these beds contain rhythmic alternations of sand and mud which may be grouped into cycles, similar to those of the Whetstone beds.

The Brazil Formation contains volumetrically less sandstone than the Mansfield. The sandstones are less mature and quartz granules are rare. Coal horizons are thicker and more laterally extensive than those preserved within the Mansfield Formation. The Block Coals (Figure 5.4) are pod like bodies which extend 1-2 km in an east-west direction, and 5 km in a north-south direction (Kvale & Archer 1990). The coals are of low ash and sulphur content, and are generally overlain b y rhythmically alternating sandstone and mudstone horizons structured by flasar, wavy and lenticular bedding. The heterogeneous clastic units are laterally extensive, although the underlying coals may not be traced for great distances. The interbedded sandstones and mudstones flank major sandstone filled channels, and may display extensive bioturbation. Palaeosols are preserved within the fine grained sediments in the form of rooted horizons, and roots penetrate up to 2 m below a coal horizon. However, not all palaeosols are capped by coals.

The specific environment of deposition for the Mansfield and Brazil Formations has been controversial. Traditionally the Morrowan and Atokan sediments have been considered to be fluvio-deltaic with most workers placing sediments in the general environment of coastal plain or shallow marine. Sandbodies are structured by uni-directional current indicators and contain no marine fossils, indicating deposition from

fluvial currents. The presence of coals also indicates deposition in a subaerial environment.

Recent work by Kvale *et al* (1989), and Kvale & Archer (1990, 1991) has identified the presence of a marine influence within the Whetstone Beds in the form of tidal bundles of rhythmically interbedded sandstone and mudstone units. A pronounced systematic thickness variation of vertically stacked laminae has been noted (Kvale & Archer 1991) and attributed to neap to spring tidal events in a semi-diurnal tidal system. The tidally influenced units (tidalites of Kvale *et al* 1989) were deposited rapidly, with sedimentation rates estimated at up to I m per year from the tidal cycles preserved (Kvale *pers comm*). The accommodation space required for the preservation of tidalites was provided by compaction of underlying peats, represented by the coal horizons, which are generally preserved under the tidalites. Marine influence is also indicated by the presence of a limited marine fauna of conodonts and brachiopods within discreet shale units within the Mansfield and Brazil Formations (Fishbaugh *et al* 1989; Kvale & Archer 1991; Kvale & Barnhill 1994)

The presence of the tidalites indicates that shallow epicontinental seaways must have existed across the Illinois Basin during the Pennsylvanian. The rhythmically laminated facies are believed to have been deposited in estuarine or distributary channel environments with low tidal flux (Archer & Kvale 1993). The Whetstone laminae are interpreted as flood dominant due to the inland depositional setting, as indicated by the presence of *in situ* lycopod trunks, and landward directed palaeoflow (Kvale & Archer 1991). The low sulphur and ash contents of the basal Pennsylvanian coals are attributed to accumulation in domed (ombrogenous) peat swamps forming in an ever wet climate (Kvale & Archer 1991). Relatively rapid mantling of coals by tidally deposited muds would protect the peats from seawater sulphates.

The fluvial sandstone bodies within palaeovalley fills of the Mansfield and Brazil are believed to represent the fluvial portion of an estuarine system (Howard & Whitaker 1990; Kvale & Barnhill 1994). The intercalation of fluvial and tidally influenced strata with marine bands indicates variations in relative sea level during deposition. Kvale & Barnhill (1994) have interpreted the relative importance of fluvial and estuarine sediments as a function of strength of current and rates of sedimentation related to sea level rise. Periods of relative sea level fall are marked by the presence of coal and palaeosol horizons.

## (I) Sedimentology Of The Study Area.

The sediments of the Mansfield and Brazil Formations were studied in west central Indiana, Parke and Fountain Counties (Figure 5.5b). Sediments were studied from outcrop in Turkey Run State Park and from core material from nearby Indiana Geological Survey boreholes (Figure 5.6).
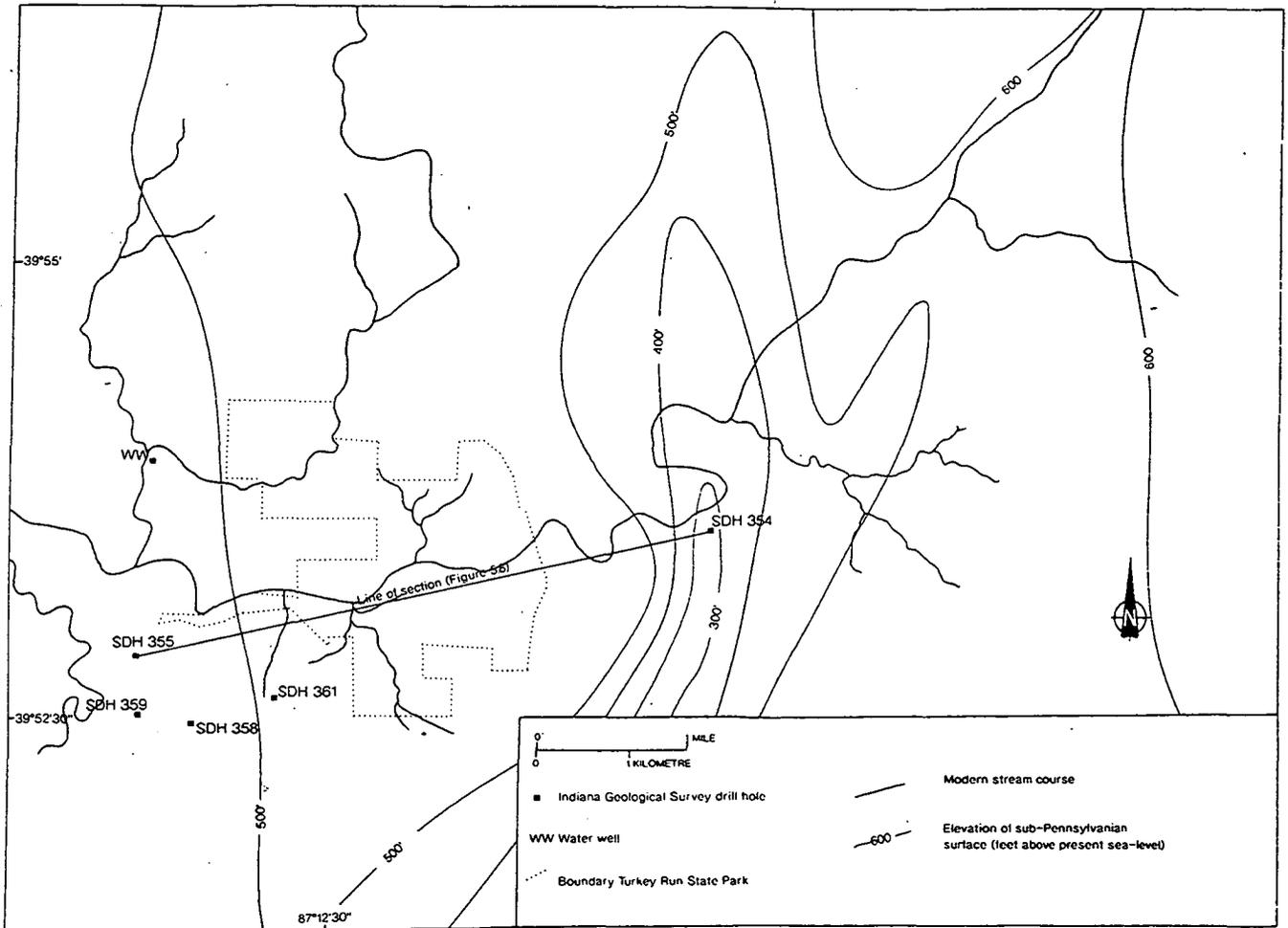


*Figure 5.6. The elevation of the sub-Pennsylvanian surface within the study area (after Keller 1990) and the position of cored sections and outcrop.*

Within the study area the Mississippian is represented by poorly exposed Chesterian sediments of mixed carbonate and clastic character. Palaeovalleys on the sub-Pennsylvanian unconformity are incised into the Borden Group and the intervening ridges are capped by the St. Louis Limestone (Fishbaugh *et al* 1989). The sub-Pennsylvanian topography in this region is well documented (Bristol & Howard 1971; Droste & Keller 1989) and characterised by long straight ridges and valleys

159

(Figure 5.5b). Topography on the Chesterian surface reaches 60 m. Within the study area major sub-Pennsylvanian palaeovalleys are represented by the courses of the New Goshen, Terre Haute and Covington Rivers (Droste & Keller 1989), which are illustrated in Figure 5.5b. These streams formed tributaries of the Benton-Fairfield system (Figure 5.5a).

Using methods outlined by Alexander (1986) it has been possible to reconstruct the flow net of the streams which carved out the palaeovalleys preserved at the mid-Carboniferous unconformity (Figure 5.5b). It is likely that these palaeovalleys remained as important sediment pathways, as the denudated Mississippian surface back-filled at the beginning of the Morrowan.

Within the study area (Figure 5.5b) cored sections from palaeovalley fills were made available by the Indiana Geological Survey. The New Goshen River palaeovalley was penetrated by SDH 362 (Figures 5.5b & 5.6). A sedimentary log of the section is illustrated in Figure 5.7a. Within the cored interval the base of the palaeovalley fill is dominated by conglomerates and coarse sands of the Mansfield Formation, arranged in upward fining packages 3.30 to 42 m (10'-130') thick. The upper Mansfield Formation is represented by finer grained sediments in the form of rippled interbedded sands and organic rich muds which contain unidentified trace fossils, rooted horizons and thin coals (Figure 5.7a). The coarse nature of the basal sediments, and the lack of fines indicates a major fluvial channel deposit. The overlying finer grained deposits indicate that energy within the depositional system waned, probably related to a drop in depositional gradient due to aggradation of sediment within the Illinois Basin.

Within Turkey Run State Park a tributary stream of the Terre Haute system is represented by another palaeovalley penetrated by SDH 354 (Figures 5.6 & 5.7b). The Borden Formation is represented by siltstones and mudstones containing thin shell lags (Figure 5.7b). The mid-Carboniferous unconformity is overlain by the basal palaeovalley fill which consists of 3.30 m (10') of matrix supported conglomerate containing sub-angular limestone, and iron stained sandstone pebbles and cobbles within a coarse grained sandstone matrix. The majority of the Mansfield Formation is represented by interbedded sandstone and mudstone (facies Fx) with rhythmically laminated tidalites (facies Fr) locally developed. The sediments are bioturbated and contain Chondrites and Planolites traces described by Fishbaugh et al (1989). Within the lowest metre of the fine grained sediments Lingula brachiopods indicative of brackish water conditions have been found (Fishbaugh et al 1989).

Sandstones are preserved higher in the SDH 354 section. The units are preserved as erosionally based, fining-upward cycles 0.60 m to 10 m (2-33') thick. Basal scours are lined by rounded mudstone, sandstone and sub-rounded

a) SDH 362                                    b) SDH 354
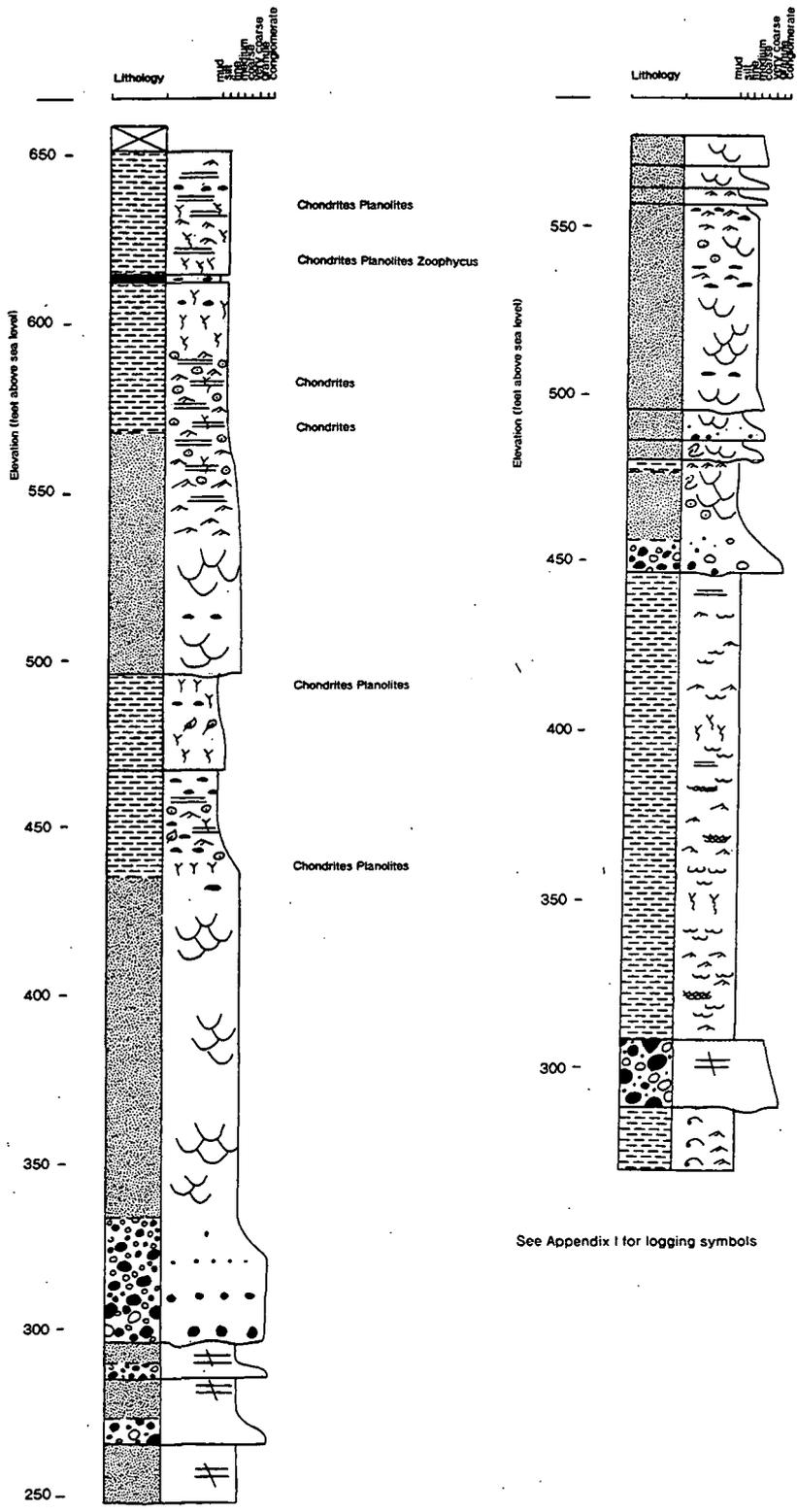


Figure 5.7. Sedimentary logs of cored sections.

See Appendix I for logging symbols

quartz pebbles (<4 cm diameter) within a medium grained sandstone matrix. The conglomerates reach 10 cm in thickness and fine upwards to a medium grained quartzose sandstone which displays uni-directional cross-stratification. The sands are capped by fine grained sandstone of facies Fx. The sands are interpreted as the deposits of fluvial channel systems.

The description of these two palaeovalleys indicates the laterally variable nature of the Mansfield Formation. In the lower Mansfield (early Morrowan) the deeper palaeovalleys such as the New Goshen River channel were utilised to transport coarse detritus to the Illinois Basin depocentre as predicted by the flow net illustrated in Figure 5.5b. Tributary palaeovalleys, such as the one penetrated by SDH 354, were filled by more heterogeneous sediment and were influenced by marine environments, as indicated by the presence of body fossils with brackish water affinity within SDH 354 (Figure 5.7b).

By the Atokan (500' above sea level) palaeotopography was back-filled and sediment spilled out of the palaeovalleys across inter-fluve areas. From this time the palaeotopography appears to have had a limited effect on the distribution of fluvial channels. A schematic cross-section through the study area (Figure 5.8) illustrates the position of fluvial sandstone channels in relation to palaeotopography. Palaeocurrent directions, as measured from cross-stratification within the channels, display wide variations in orientation.
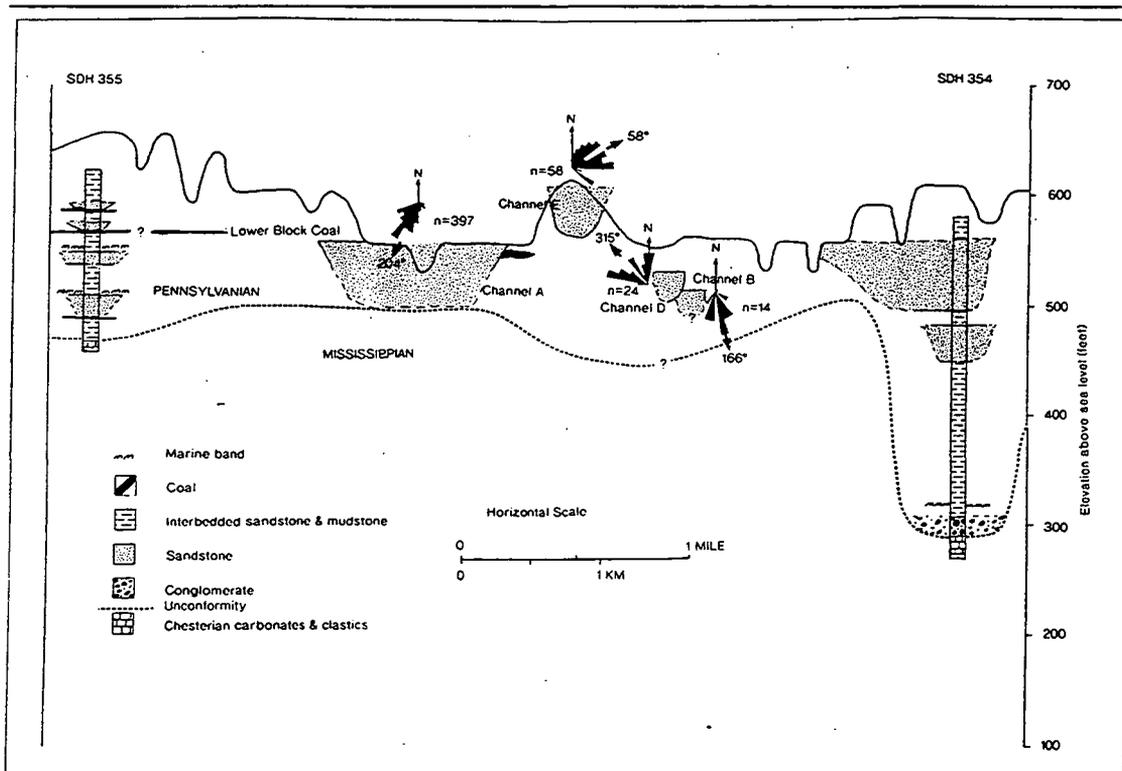


Figure 5.8. A schematic cross-section through the study area.

The fluvial sandstones take the form of shoe-string channel deposits. Channel deposits within the upper Mansfield and Brazil Formations are represented by fine to medium grained sandstone, with subordinate coarse sandstone containing quartz granules. The channels are lenticular in cross-section and reach a maximum thickness of 30 m and a width of 500 m (Martin 1993). The facies preserved within the sandstone bodies are described below.

Fluvial channel sandstones are overlain by, and isolated within interbedded fine sand and mud (Figure 5.8) of facies Fx and Fr. In outcrop the finer grained deposits are largely obscured by vegetation. However, in cored sections the volumetric importance of the heterogenous units is clear. Marine bands have been identified within cored sections of the inter-channel sediments through the presence of *Lingula* brachiopods (SDH 354), conodonts and traces of *Zoophycos* (Figure 5.8). These bands are of limited lateral extent, and cannot be traced between cored sections (Figure 5.8). Palaeosol horizons are locally developed within the intrachannel facies and these may be capped by coal horizons. Thus, the fine grained sediments display characteristics of marine and terrestrial environments.

*Large scale planar cross-stratification (Sp$_l$).*

Planar cross-stratified units are composed of medium grained, moderately well sorted quartzose sandstone. Planar cross-stratification takes the form of stacked sets up to 1.5 m thick which may be traced laterally in excess of 15 m. These large bedforms are only preserved within the channel centre. Foresets are tangential and inclined 28-32°. The foresets show little vertical grading. However, the foresets display 'pin-stripe' grading due to alternations of fine and coarse sandstone laminae. Large scale reactivation surfaces between foresets are absent. Bottomsets are commonly preserved in the thicker sets and consist of ripple laminae produced by counter currents at the toe of the bedform. The bottomset deposits are <25 mm thick and interfinger with the foreset deposits.

*Medium scale planar cross-stratification (Sp$_m$).*

Planar cross-stratification is preserved in sets of 0.40-0.70 m thick and cosets of up to 2 m in thickness. Sets are bounded by tabular surfaces. The sets are composed of medium to fine grained, moderately well sorted quartzose sandstone. Foresets are generally tangential and dip 25-28°. No grading of grain size is apparent through the foresets, and there is little evidence for reactivation of the bedform, with foresets laminae concordant within sets.

*Medium scale trough cross-stratification (St$_m$).*

Trough cross-stratification is developed in sets 0.35-0.90 m thick. The sandstone is medium grained and moderately well sorted. Troughs range between 4-7 m, wide and sediment fills are symmetric. Foresets dip 22-28°, with small scale changes in the angle of dip marking surfaces of discontinuity, and minor foreset reactivation. These discordant surfaces dip <22°. However, the reactivation surfaces are not marked by zones of dune slip face reworking, but appear to represent small scale changes in progradation of the dune. The absence of reworking indicates that water permanently flowed over the dune, but with varying velocity and/or depth. Individual trough cross-stratified sets are separated by first order bounding surfaces which are in places modified by counter current ripples preserved at the toe of the set.

*Compound cross-stratification (Sc).*

Compound bedforms are composed of medium grained, moderately well sorted quartzose sandstone, structured by a combination of medium and small scale planar and trough cross-stratification. Second order bounding surfaces (2B of Figure 2.3) separate cosets of compound cross-stratification which are 1.50-1.80 m thick. The second order bounding surfaces are sub-horizontal, dipping less than 5° in the downstream direction. Within the compound bedform foresets are 35-55 cm thick and are bounded by first order bounding surfaces which dip down-current between 15° and 20°. These foresets are angular or tangential and represent the deposits of smaller bedforms which migrated down the slip-face of larger bedforms. Individual sets may descend as much as 1.30 m.

Internally the compound foresets are structured by intrasets. Planes of discontinuity are common between intrasets indicating changes in palaeoflow, but no re-working of dune slip-faces. Intrasets are commonly overturned downslope, particularly in the upper portion of the compound foreset.

*Small scale trough and planar cross-stratification (St$_s$ & Sp$_s$).*

Small scale cross-stratified sets are composed of fine grained, moderately well sorted quartzose sandstone. Trough cross-stratification occurs in sets 5-30 cm thick (Plate 5.1). Troughs are less than 4 m across, and fill varies between oblique and symmetrical. Scours are commonly preserved at the trough bases (Plate 5.1). Planar cross-stratified sets are also preserved in sets 5-20 cm thick. Foresets are tangentially based and dip 18-20°. Palaeocurrent directions measured from cross-strata are more variable than those of larger scale bedforms. Overturning of foresets is common and takes the form of Type 1 of Allen & Banks (1972). Deformation has locally resulted in

the total loss of structure and thin (<20 cm thick) units of structureless sandstone are preserved (Plate 5.1).



Plate 5.1. Facies $Sp_s$ & $St_s$, Channel A, Mansfield Formation.
Fine grained sandstone is preserved in sets 0.2-0.45 m thick, which are separated by first order bounding surfaces. Cosets are <2 m thick and are bounded by sub-horizontal second order bounding surfaces. Overturning of foresets is common, and takes the form of Type 1 of Allen & Banks (1972). Intense deformation within some horizons has resulted in the total loss of structure, and the preservation of structureless sandstone units 30-50 cm thick.

Cosets of small scale cross-stratification are bounded by second order bounding surfaces (2A) and vary between 0.80 m and 1.20 m in thickness. The cosets laterally interfinger with the deposits of medium and large scale bedforms indicating that they formed contemporaneously.

*Massive sandstone (Smc).*

The massive sandstone channel bodies of facies Smc are lenticular in shape. Within the central portions of fluvial channels the facies reaches 10-45 m wide and 0.6-4 m deep. At the more marginal portions of the fluvial channel, massive sandstone filled channel features are preserved which are 1.75-7 m wide and 1-3 m deep. Units of facies Smc display sharp, erosive bases which contain concentrations of small plant fragments and mudstone clasts <25 mm in diameter. Faint laminations are preserved in the lower portion of the channel which are concentric and parallel to the basal scour surface. The upper surface may be flat to concave and may display undulose, sub-horizontal laminae. De-watering structures are locally developed within facies Smc, and tend to be concentrated in the upper portion of the fill.

*Rippled Fine Sandstone (Fx & Fr).*

This facies is rare in outcrop and where present is poorly exposed. In cored sections rippled horizons are better preserved. The facies is represented by well sorted fine sand to silt, structured by ripple cross-lamination. Ripples are asymmetric and have an amplitude of 2 cm to 5 cm. Mica and disseminated organic matter is commonly concentrated at the base of the ripples. Generally the lee face of individual ripples is preserved, but rare climbing ripples are also developed.

In outcrop the cross-laminated sandstones are preserved in cosets of 1 to 2 m thick at channel margins. In SDH 368 and SDH 354 (Figure 5.7b) rippled sands are preserved at the top of fining-upwards units, with facies Fx reaching 10 m thick. Cross-laminated fine sandstones and siltstones are also preserved as thin (<5 cm thick) beds overlying third order bounding surfaces, and over the upper surface of facies Smc.

Cross-laminated sediments locally display rhythmic lamination (facies Fxr). Flasar to wavy bedded sandstones take a climbing ripple form with each sandstone ripple draped by a laterally extensive mud layer. The height of the sandstone ripples rhythmically increases and decreases in the vertical scale. Symmetrical coarsening and fining-upwards cycles are preserved, and are interpreted as the deposits of tidalites (Fishbaugh *et al* 1989).

*Mudstone (Fm).*

Carbonaceous mudstones, 1 cm to 10 cm thick, are locally interbedded with facies Fx. Mudstones are also locally preserved overlying third order bounding surfaces.

The sediments exposed in western Indiana display a structural dip of 0.5m/km or 0.005 (Kvale *pers comm*). Hence sediments of similar elevations above present sea level are considered to have been deposited contemporaneously (if compaction effects are assumed negligible). Following this assumption, mapping of sedimentary units of similar elevation will allow for the construction of time slices through the study area.

Below 500' sedimentation occurred within the sub-Pennsylvanian palaeovalleys (Figure 5.8). Figures 5.9-5.12 reconstruct the overall geometry of Mansfield and Brazil Formation sands following the filling of palaeovalleys, i.e. between 500' and 650' above sea level. Information from outcrop and core has been used for these reconstructions.

Between 500-549' (Figure 5.9) the study area was dominated by a major fluvial channel, Channel A, with a subordinate Channel B. Flow within these channels was to the southwest (Channel A), and the southeast (Channel B), approximately parallel the regional palaeoslope. The fluvial channels were isolated within interbedded fine grained sandstone and mudstone. The contact between these intra-channel and inter-channel sediments is sharp. Sandstone is also preserved within SDH 354 indicating that a fluvial channel may have flowed down the axis of the palaeovalley.

Internally Channel A is structured by a combination of planar and trough cross-stratification. Within central portions of the channel $Sp_l$ sets are preserved, together with $Sp_m$, $St_m$ and Sc. Facies $St_s$ and $Sp_s$ are preserved in the lower 10 m of the central portion of the channel, and laterally interfinger with the larger scale Sp and St sets. The stratified sediments are in turn cut by lenticular units of facies Smc. At the margin of Channel A facies $Sp_s$ and Fx are preserved, which contain large amounts of organic debris and mica, concentrated in thin bands at the base of sets and along set boundaries.

Channel B is structured only by facies $Sp_m$ and $St_m$ with minor developments of Sc. Channel margins are well exposed and are sharp, cutting through the finer grained inter-channel deposits.

The upper Mansfield Formation is represented by the section 550-574' above sea level (Figure 5.10). The position of Channel A is clear, and displays palaeoflow to the south-west. Internally the structure of Channel A remains identical to that described at 500'. The sandstone channel is flanked to the east by fine grained sediments and a pod-like coal 15 m in lateral extent and 50 cm thick. Two smaller channels (C and D) are also preserved, and are interpreted as tributaries to Channel A, as illustrated in Figure 5.10. Channels C and D are structured by a combination of $Sp_m$ and $St_m$. Herringbone cross-stratification is locally developed in Channel C. The sandstone preserved within SDH 354 suggests that a stream may also occupy this position which marks the palaeovalley axis.

Coals and interbedded fine grained sandstones and mudstones of facies Fx and Fr form inter-channel deposits at this level. At the margin of Channel C tidalites are preserved, again indicating some marine influence on sedimentation. The Mariah Hill Coal is preserved within SDH 359 at 550' and may be traced to a stream section in the north of Turkey Run State Park (Fishbaugh et al 1989). The contact between the Mansfield and Brazil Formations occurs at 560' (Figure 5.8) and is marked by the Lower Block Coal (Figure 5.4). Thus sub-aerial environments of deposition are also indicated.

Figure 5.9. A reconstruction of palaeoenvironments within the study area between 500-549'

ELEVATION
500-549'

Channel B

Channel A

SDH 354

SDH 355

SDH 359

SDH 361

SDH 358

WW

-39°55'

-39°52'30"

87°12'30"

500

600

500

500

N

MILE

KILOMETRE

Indiana Geological Survey drill hole

WW Water well

Boundary Turkey Run State Park

Mean palaeocurrent direction

Channel margin

Elevation sub-Pennsylvanian surface
(ft above sea level)

Coal

Sandstone/mudstone

Sandstone

Chesterian

PENNSYLVANIAN

168

Figure 5.10. A reconstruction of palaeoenvironments within the study area between 550-574'.

ELEVATION
550-574'

Channel C

WW

SDH 354

BEDROCK ABSENT

Channel D

Channel A

SDH 355

SDH 361

SDH 359

SDH 358

-39°55'

-39°52'30"

87°12'30"

550

600

550

600

N

0 _____ MILE
0 _____ KILOMETRE

■ Indiana Geological Survey drill hole

WW Water well

⋯ Boundary Turkey Run State Park

↑ Mean palaeocurrent direction

⋯ Channel margin

╱ Elevation sub-Pennsylvanian surface
(ft above sea level)

▨ Coal

▦ Sandstone/mudstone

▨ Sandstone

▨ Chesterian

PENNSYLVANIAN

In the lower Brazil Formation between 575-599', (Figure 5.11) two sandstone channels are preserved (E and F). Channel E is a large channel internally structured by a combination of facies $Sp_m$ and $St_m$. Channel F is of a smaller scale and is structured by facies $St_m$ and $St_s$. Palaeoflow within the channels was to the east, indicating a shift in depositional slope. Interbedded sandstone and mudstone of facies Fx are preserved within the inter-channel areas together with coals, the lateral extent of which is unknown.

Between 600-624' (Figure 5.12) of the Brazil Formation, Channel E remains active and flowing to the northeast. Smaller channels, <50 m width, are preserved as G and H which display palaeocurrents to the southeast and east. Internally Channels G and H are structured by facies $Sp_m$ and $St_m$ arranged in simple cosets. The presence of other channels is indicated by the sandstones preserved in SDH 359, 355, 358 and 361.

The unimodal palaeoflow of the majority of the sandstone channels preserved within the study area indicates a dominantly fluvial environment. Channel C displays some evidence of tidal influence in the form of herringbone cross-stratification. The channel bases are sharp and erosive, with the fourth order bounding surface lined with thin bands of extra-formational conglomerate. Clast types include rounded quartz pebbles, iron stained sandstone and mudstone <5 cm in diameter. Within the sandstone channels scour surfaces indicative of fourth order bounding surfaces are absent. Each of the channels thus relates to deposition from a single fluvial system, and hence represents the major channel architectural elements of Table 2.6. The finer grained facies of Fx and Fr together with coals represent inter-channel elements.

## (ii) Lateral Profile Analysis.

The stream sections in Turkey Run State Park offer good three dimensional exposure of Channel A. This fluvial channel preserves the widest range of sedimentary structures and is the only channel within which the massive sandstone facies is preserved. Channel A is 30 m thick and 500 m wide in the study area. The base of the channel is marked by a poorly exposed fourth order bounding surface. Internally the channel is structured by a series of vertically stacked macroforms bounded by third order bounding surfaces. The channel is described by the use of a number of lateral sections, derived from photographs and sedimentary logs.

ELEVATION
575-599'

−39°55'

WW ▪

SDH 354

BEDROCK ABSENT

Channel E

SDH 355 ●

Channel F

▪ SDH 361

SDH 359

SDH 358

−39°52'30"

575

600

575

600

N

MILE
0                    1
KILOMETRE
0        1

▪ Indiana Geological Survey drill hole

WW Water well

⋯⋯ Boundary Turkey Run State Park

↟ Mean palaeocurrent direction

⋯ Channel margin

╱ Elevation sub−Pennsylvanian surface
(ft above sea level)

▨ Coal

▦ Sandstone/mudstone

▩ Sandstone

▨ Chesterian

PENNSYLVANIAN

87°12'30"

Figure 5.11. A reconstruction of palaeoenvironments within the study area between 575-599'.

171
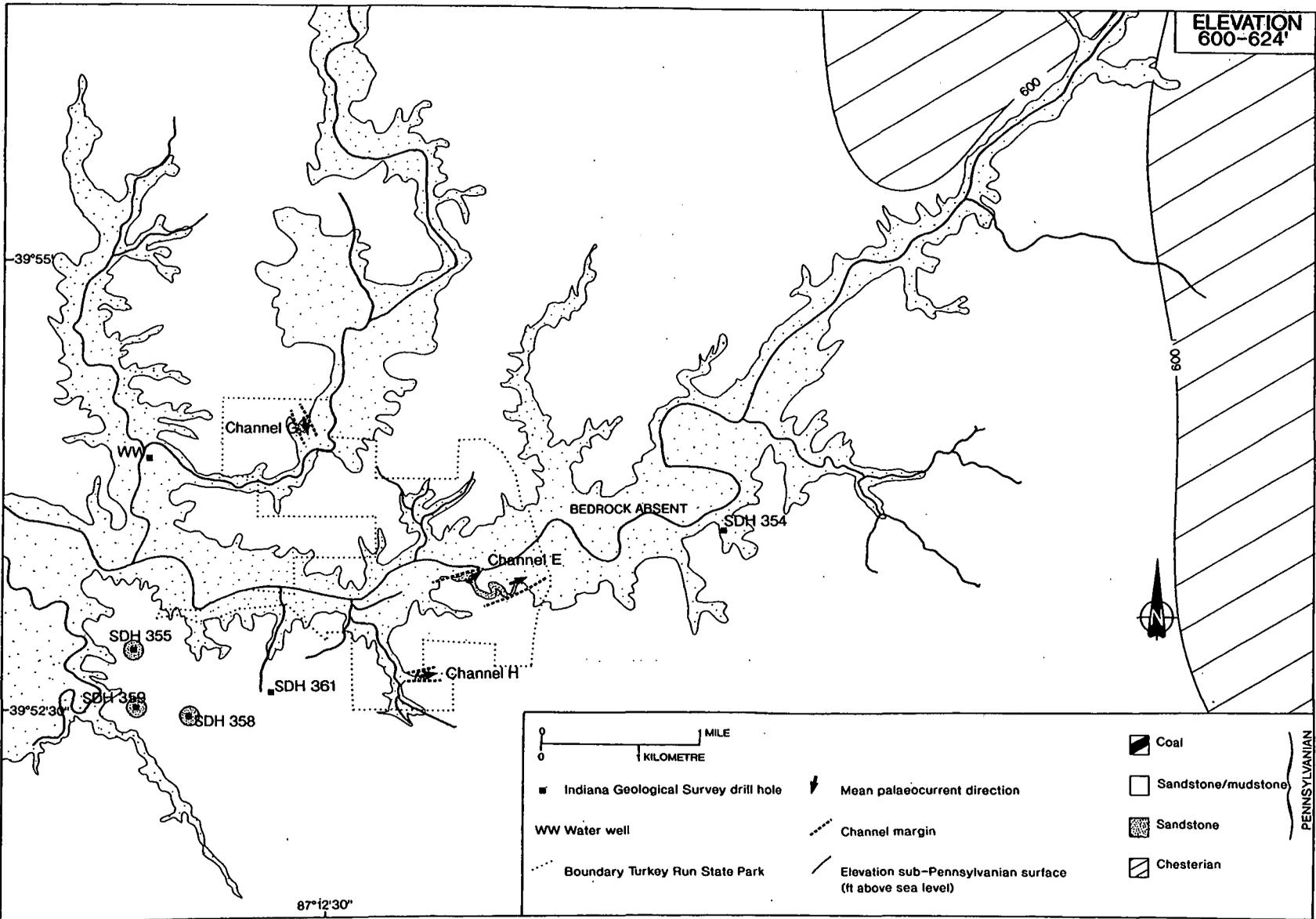
Figure 5.12. A reconstruction of palaeoenvironments within the study area between 600-624'.

Legend:

ELEVATION 600-624'

- ■ Indiana Geological Survey drill hole
- WW Water well
- Boundary Turkey Run State Park
- ↓ Mean palaeocurrent direction
- Channel margin
- / Elevation sub-Pennsylvanian surface (ft above sea level)

PENNSYLVANIAN
- Coal
- Sandstone/mudstone
- Sandstone

- Chesterian

Map labels: Channel G, WW, Channel E, Channel H, BEDROCK ABSENT, SDH 354, SDH 355, SDH 361, SDH 359, SDH 358

Coordinates: 39°55', 39°52'30", 87°12'30", 600

This section is illustrated in Figure 5.13. In the lower portion of the section a third order bounding surface is preserved which dips 3° to the south-west, i.e. downstream. Below this surface a DA Type 2 architectural element is preserved, which consists of facies $Sp_t$. Foresets are dominantly tangential and dip 18-24°, often displaying differentiation of grain size to give a 'pin-stripe' effect. Bottomset deposits are occasionally preserved and take the form of counter-current ripples in the toe of the set. Palaeoflow direction measured from this macroform was to the south. A small unit of facies Smc is preserved below the third order bounding surface (Figure 5.13).

Macroform II (Figure 5.13) is composed of a medium grained, moderately well sorted, quartzose sandstone forming a DA Type 1 element. The sandstone is structured by facies $Sp_t$ with sets varying between 0.4 and 1.20 m in thickness. In the downstream direction sets of facies $Sp_m$ offlap the larger bedform, resulting in the formation of a compound cross-stratified unit (Figure 5.13). Some overturning of sets has developed within facies Sc, particularly in the upper portions of intrasets. The average palaeocurrent azimuth measured from these deposits is 205°

The structured sands of Macroform II are cut by a lenticular unit of facies Smc which is 3.15 m thick and 35 m long (Figure 5.13). There is little deformation of cross-stratification associated with the massive unit. Two stacked, erosionally-based, massive sandstone units are present (Figure 5.13 & Plate 5.2). The lower unit reaches a maximum thickness of 1.90 m and the upper unit is 1.30 m thick. The units may be differentiated by a thin horizon (<5 cm) of sub-round quartz granules and well rounded peat rip-up clasts which are preserved at the base of the individual units (Plate 5.2). The massive sandstone units display laminations at the base which are parallel to the erosive margin and 5-10 mm apart (Figure 5.13 & Plate 5.2). These grade into an otherwise structureless fill. The upper surface of facies Smc is undulose, and covered by a rippled horizon 5-10 cm thick. The ripples have an amplitude of 2 cm and are asymmetric and rounded. Deposition of the ripples was from a uni-directional current flowing to the south.

Facies Smc of section 1 may be traced to a similar massive unit preserved in a canyon wall 30 m to the east thus indicating that the direction of emplacement of the massive units was oriented along a plane N120/300. The plane of transport defines a direction oblique to the palaeocurrent direction measured from the surrounding cross-stratified sandstones (Figure 5.13).

Macroform III is composed of a number of SB Type 2 architectural elements separated by 2A bounding surfaces. Sedimentary structures are dominated by facies

ORIENTATION N028/208°

Macroform III

n=25

SB Type 2

SB Type 2

SM Type 2

SM Type 2

DA Type 1

DA Type 1

N

Macroform II

n=27

SM Type 2

DA Type 2

N

Macroform I

n=7

5 m
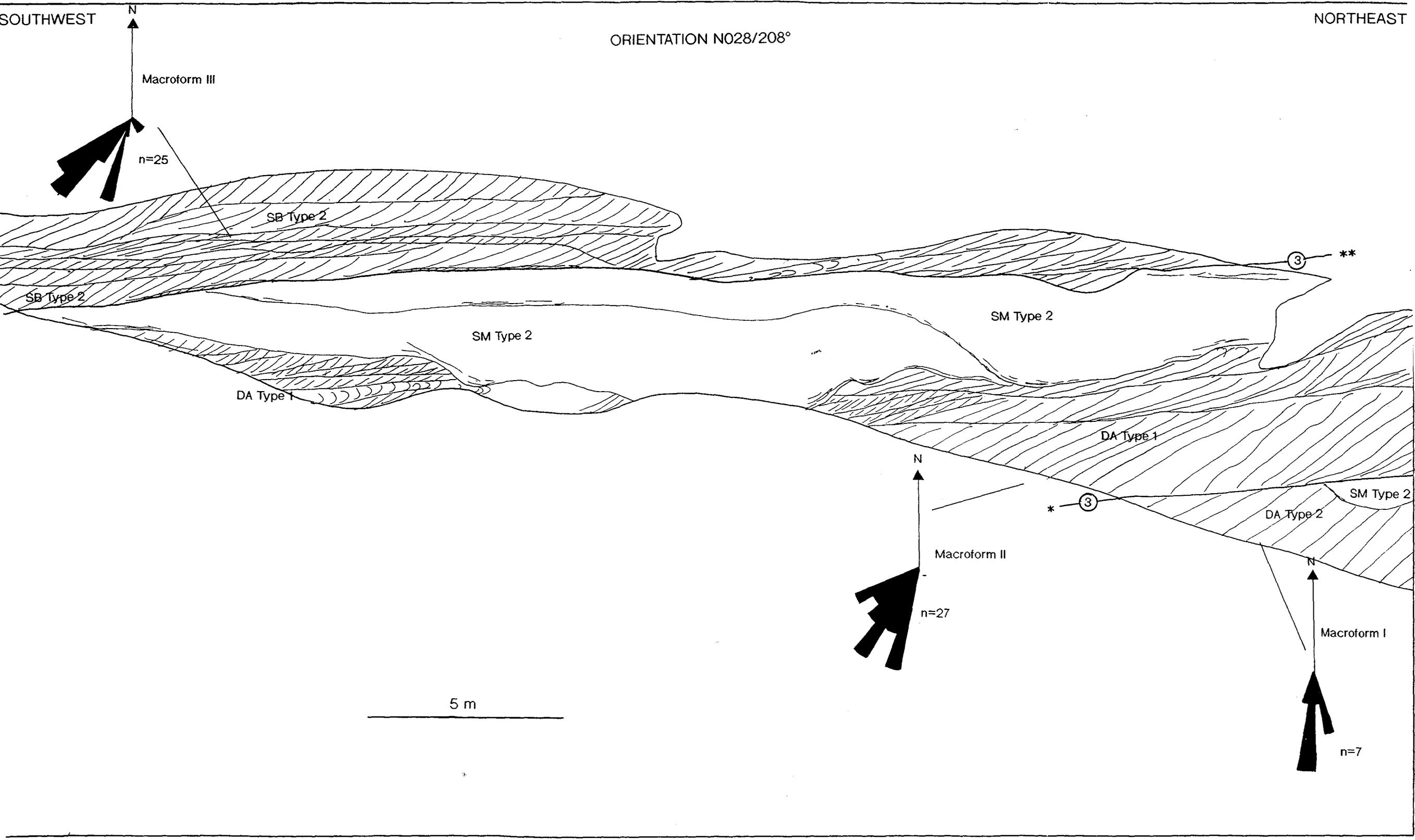
*Figure 5.13. A line drawing of section 1, Mansfield Formation, reproduced from distortion-free photographs.*

Sp$_m$ with minor St$_m$. Sets are 0.2 to 0.6 m thick with tangential foresets dipping 18-24°. Overturning of foresets is locally developed, and takes the form of Type 1 of Allen & Banks (1972). The average palaeocurrent direction taken from these beds is 210° towards the south-west.



*Plate 5.2. Facies Smc, Section 1.*
*Facies Smc displays a sharp base with concentric laminae preserved in the lower 0.2 m of the unit. These laminae grade into a structureless sandstone. The base of facies Smc is marked by a quartz granule-rich unit of <5 cm thick. A second such surface is identified within the sandbody, and indicates that two units of facies Smc are superimposed. Facies Smc is overlain by a rippled horizon (<5 cm thick). Facies Smc is emplaced in a DA Type 1 architectural element of Macroform II (Figure 5.13) and is overlain by a series of SB Type 2 elements.*

The sediments of section 1 may be traced in the downstream direction, where a change in macroform character may be documented. In the downstream direction the DA Type 1 and 2 elements of section 1 (Figure 5.13) interfinger with small scale trough and planar cross-stratified sands of SB Type 2 elements which are sub-divided by 2A bounding surfaces. There is no clear contact between the different facies. Figure 5.14 details a schematic reconstruction of the downstream changes documented in the macroforms of section 1.

ORIENTATION N028/208°

SB Type 2

SB Type 2

SM Type 2

DA Type 1

SM Type 2

DA Type 2

N

N

5 m

10 m

n=27

n=39
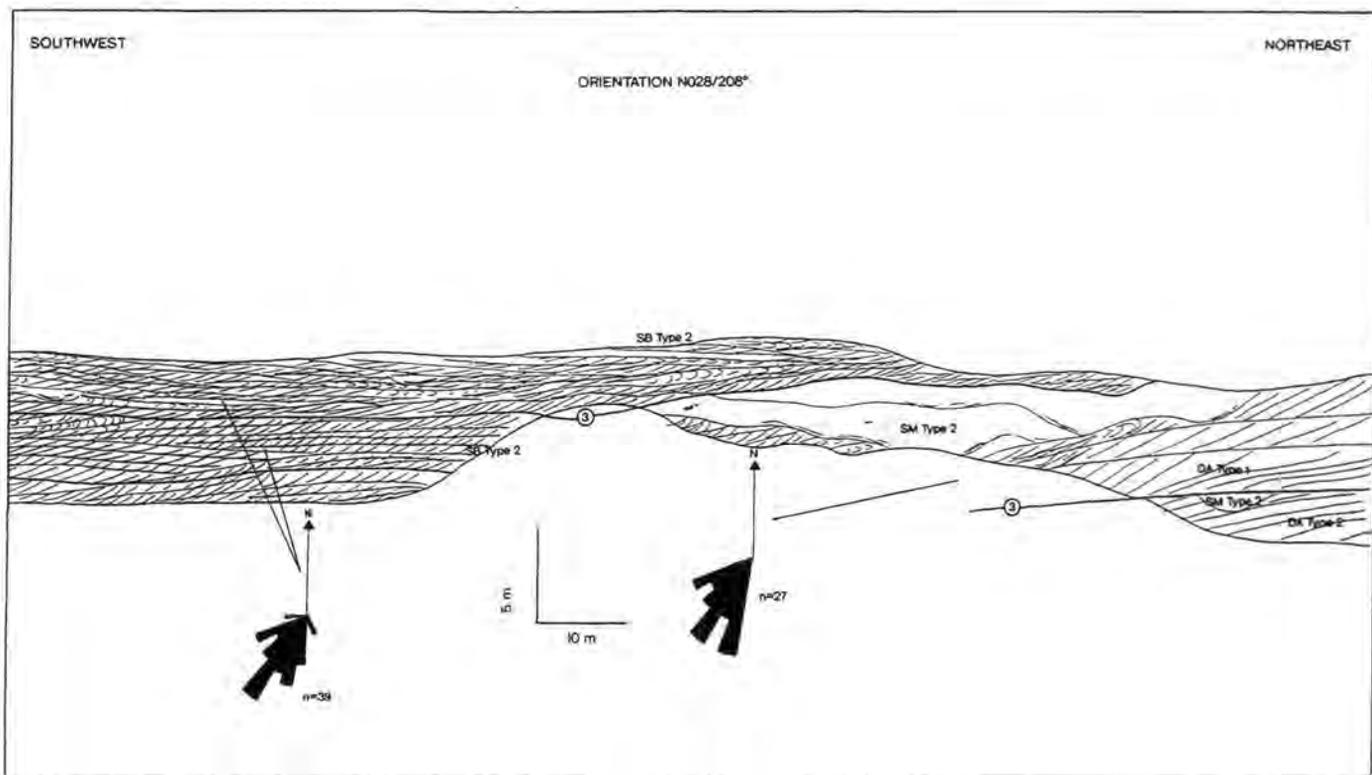
*Figure 5.14. Downstream changes in macroform architecture documented from section 1.*

## Section 2.

This section is illustrated in Figure 5.15 and contains seven macroforms separated by laterally extensive third order bounding surfaces, two of which may be traced from section 1 ("*" & "**" of Figures 5.13 & 5.15). Within individual macroforms palaeocurrent directions display little variability, but there are more pronounced changes in the flow direction between macroforms (Martin 1993). The lithology of these units remains consistent throughout the section. The sandstone is medium to fine grained and moderately well sorted quartz arenite to sub-litharenite.

Macroforms I and II are interpreted as DA Type 1 architectural elements constructed of facies $Sp_m$ which evolves downstream into facies Sc (Figure 5.15). Facies Sc is composed of medium scale planar and trough cross-stratified sets, separated by 2B bounding surfaces dipping 6-10°. Tangential intrasets dip 25-28°. Overlying Macroform I an iron-stained siltstone reaching a thickness of 10 cm is preserved.
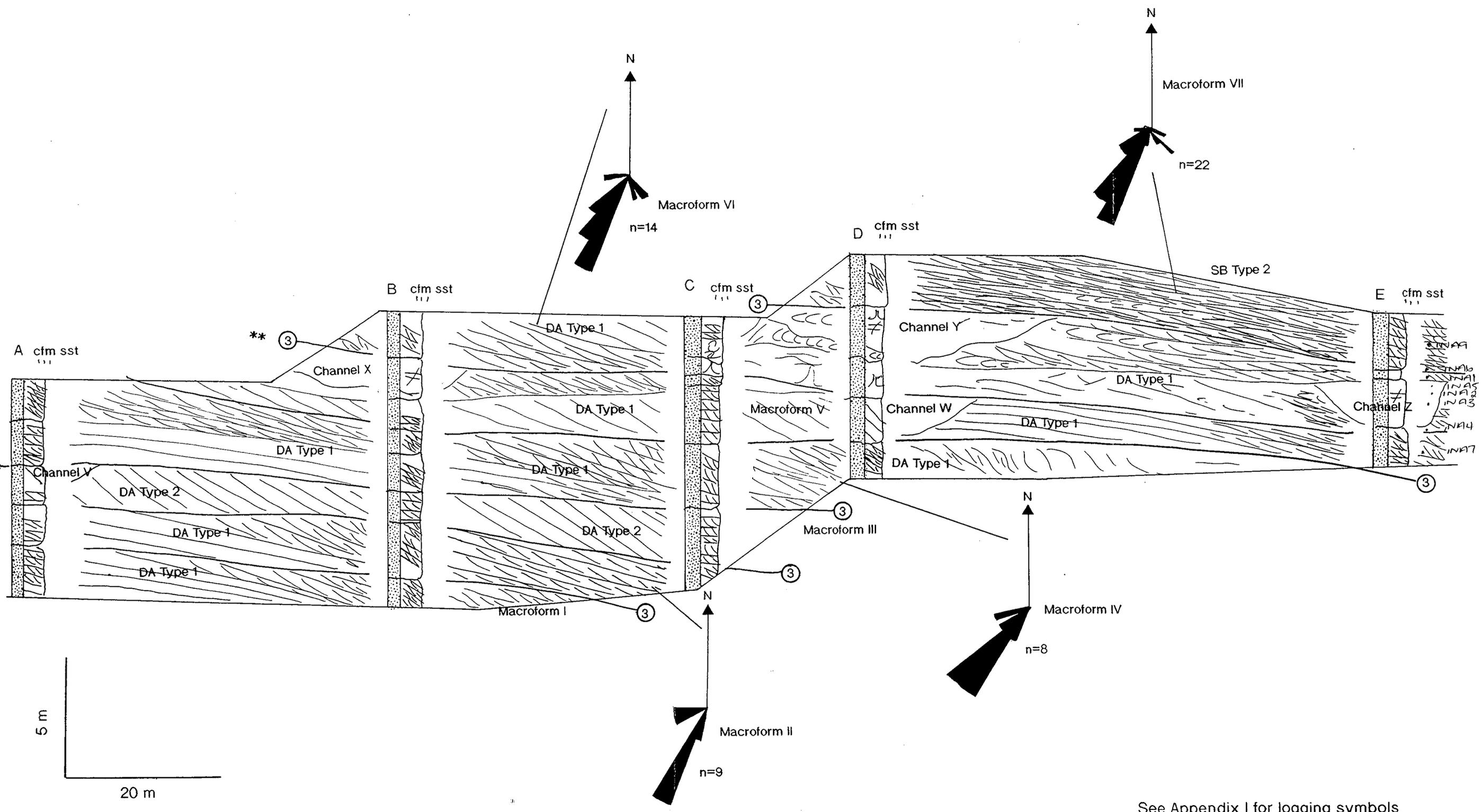
Figure 5.15. A schematic line drawing of section 2, Mansfield Formation.

Macroform III of Figure 5.15 is composed of a single unit of facies Sp, which is equivalent to Macroform I of section 1 (Figure 5.13). Foresets are tangential and dip 18-20°. Counter current re-working of the toesets is common. The simple bedform is cut by a lenticular channel-form of facies Smc (channel V) which is 1 m deep by 3 m wide. Channel V has a sharp base which is not associated with any deformation in the underlying bedform. A third order bounding surface overlies channel-form V, and is marked by a zone of iron staining and weathering. Across the bounding surface a small rippled horizon is locally developed. Ripples have an amplitude of 2 cm with asymmetric, rounded crests.

Macroform IV and V are composed of DA Type 1 architectural elements. The lower portion of the macroforms are simple planar cross-beds, 0.80 m thick, with tangential foresets. Grain size differentiation, with partitioning of medium and fine grained sandstone between foresets, is common. When traced downstream the simple bedforms become compound cosets. Macroforms IV and V preserve two lenticular units of facies Smc (Channels X and W of Figure 5.15) which are overlain by third order bounding surfaces. Channel W (Plate 5.3) is 15 m long and 3 m high. The unit is heavily iron stained and contains abundant organic debris at the base. The upstream margin of the unit dips 12° and the downstream margin dips 20°. Movement occurred along a plane orientated N095/275°. Channel X is 10 m wide and 1.20 m deep. The upstream margin of the unit dips 22° and the downstream margin dips 35°. Channel X is a simple lenticular body which can be traced to a similar lenticular structure 25 m west. The body was deposited by a current moving along a plane orientated N090/270°.

Within Macroform IV a highly deformed coset of facies Sc is preserved (Figure 5.15 & Plate 5.3). The complex relationship between Channel W and the underlying deformed planar compound cross-stratified unit is illustrated in Figure 5.15 and Plate 5.3. The initiation of deformation within the compound bedform is related to facies Smc (Channel W of Figure 5.15). Upstream of channel W the compound bedform displays undeformed tangential foresets which dip 18-25°. Downstream of channel W the foresets within facies Sc steepen to 48° and become progressively more deformed. Failure of the compound bedform resulted in the eventual loss of all structure and flow of the sand downslope. Flow of sand occurred down the slip face of the compound bedform and resulted in the deposition of a lenticular massive sandstone unit. The unit of facies Smc related to bedform collapse is 6 m wide and 1.25 m deep. The margins of the unit are sharp and dip 35°.

Macroform VI (Figure 5.15) is composed of facies $Sp_m$, $St_m$ and Sc arranged in a DA Type 1 element. Downstream the DA Type 1 element grades into a series of SB Type 2 elements. The macroform contains two units of facies Smc (Channels Y and Z
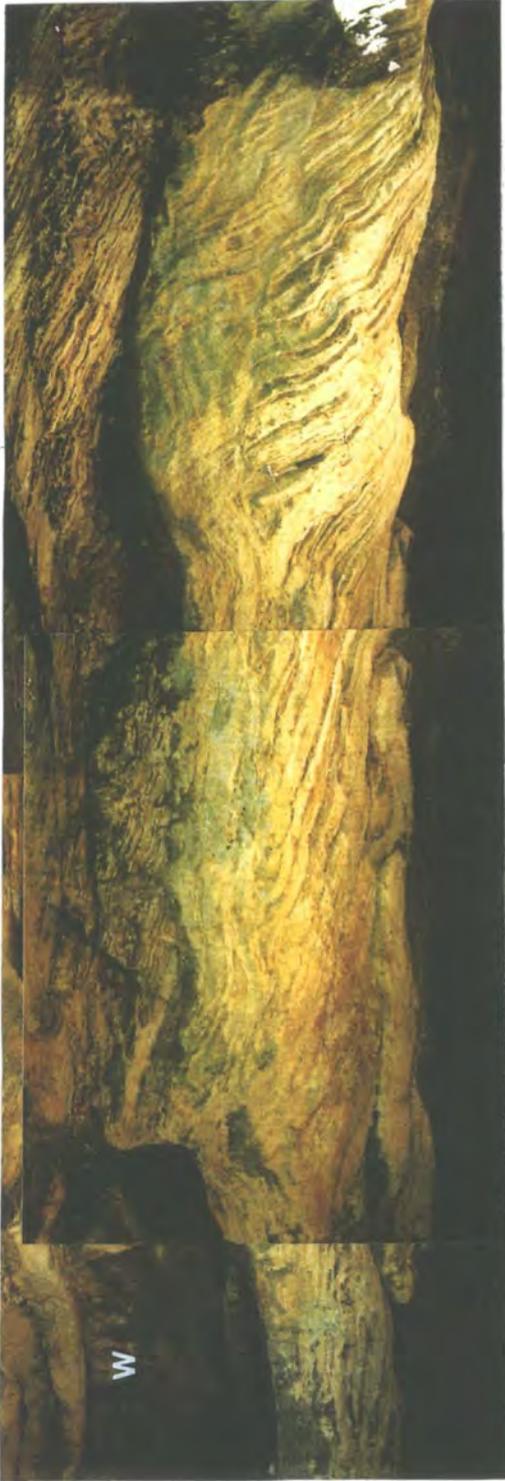
Plate 5.3. Deformed forestes of facies Sc, Section 2.
Channel W of Figure 5.15 is located in the upstream portion of this plate. Downstream of facies Smc deformation becomes apparent in the foresets of the underlying bedform. The foresets become progressively oversteepened and fail when 45° is exceeded.

of Figure 5.15). These units have sharp erosive bases and are lenticular in cross-section.

Channel Y (Figure 5.15 & Plate 5.4) is associated with highly deformed foresets and de-watering structures (Plate 5.4). The channel is 20 m wide and 2.25 m deep, with poorly defined margins which dip 14° in the upstream direction and 18° downstream. The channel fill displays faint laminations parallel to the basal scour surface with elongate peat rip-up clasts oriented parallel to the laminations. These grade into an otherwise structureless fill. The emplacement of Channel Y took place along a plane with orientation N090/270° which is oblique to the palaeoflow direction indicated from cross stratification within the macroform. Channel Z is another lenticular unit of facies Smc which occurs near the margin of Channel A. This area is discussed in more detail in section 3.



*Plate 5.4. Facies Smc, Section 2.*
*Channels W and Y of section 2 are illustrated here. The sandbodies are lenticular in cross-section, and display sharp basal margins. The upstream margin of Channel Y is poorly preserved, and the structureless sandstone of the channel fill grades into a zone of intense deformation and de-watering (Figure 5.15). Channel W shows sharp margins and is heavily iron stained. Both channels are overlain by third order bounding surfaces (Figure 5.15).*

Macroform VII (Figure 5.15) is developed near to the sandstone channel pinch-out and is composed of fine grained sandstone. The macroform is structured by small scale trough and planar cross-stratification combined in SB Type 2 architectural elements. The sediments have a high organic content with disseminated matter present at the base of foresets and along bounding surfaces. The units grades into

rippled fine sands of facies Fx to the southeast. These fine grained units are arranged in upward-fining cycles of 0.25-0.6 m thick related to H architectural elements or channel abandonment.

*Section 3.*

This section presents a more detailed reconstruction of sedimentary log E from section 2 (Figure 5.15). In this area the sandstone is exposed in both sides of the stream thus allowing for a three-dimensional reconstruction of the sedimentary macroform (Figure 5.16).

The lateral profile is dominated by a lenticular shaped channel of facies Smc, (channel Z of section 2). The channel form is 2.50 m thick and 15 m wide (Plate 5.5). Channel margins dip 14-18°. The channel was emplaced with a sense of movement oriented along a plane N050/230, which is oblique to the palaeoflow as measured from cross-stratified sands (Figure 5.16). The massive sandstone filled channel may be traced 17 m in a direction perpendicular to the palaeoflow.



*Plate 5.5. Facies Smc, Section 3.*
*A unit of facies Smc is preserved within sandstones of SB Type 2 elements (Figures 5.15. & 5.16). The sandbody is 15 m wide, 2.50 m thick and can be traced >10 m parallel to the inferred flow direction. Facies Smc has a sharply defined base and an undulose upper bounding surface which is not related to any major bounding surface (Figure 5.15).*

Facies Smc has a sharp base and an undulose upper surface (Plate 5.5) with water escape structures evident within the sandstone body (Figure 5.16). The underlying sediments are structured by small scale planar and trough cross-

NORTH

SOUTH

ORIENTATION N006/186°

N

n=22

③

SB Type 2

H

H

SM Type 2

DA Type 1

H

5 m
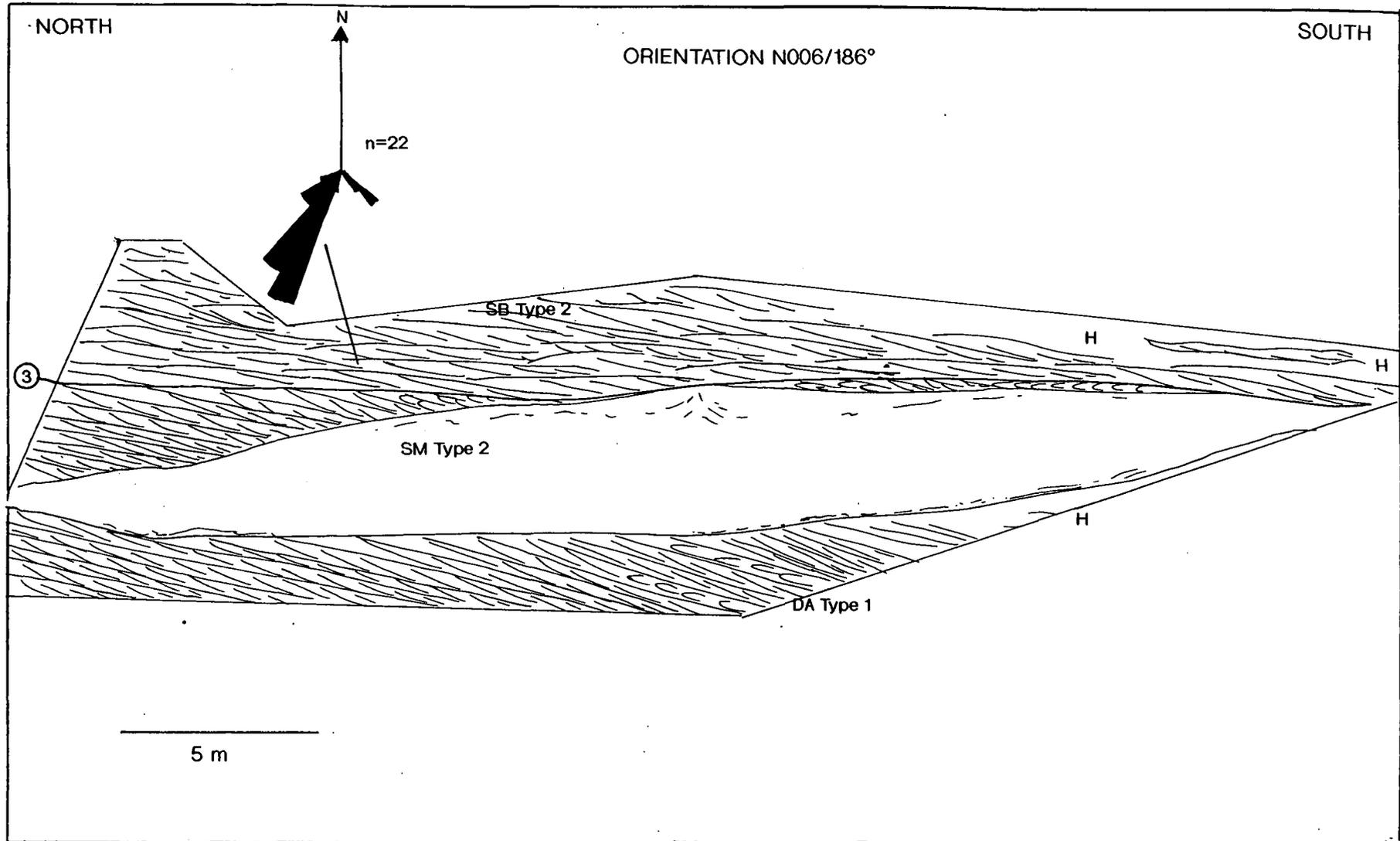
*Figure 5.16. A line drawing of section 3, Mansfield Formation drawn from distortion-free photographs.*

stratification, developed in compound cross-stratified units bounded by 2B bounding surfaces which dip at 5-10°. Cosets are 0.1-0.4 m thick, with many displaying thickening, associated with off-lapping, in the downstream direction. There has been no deformation of the structured sediments related to deposition of the massive unit.

The massive sandstone filled channel is overlain by a third order bounding surface (Figures 5.14 & 5.15) which is in turn overlain by fine grained sandstones structured by small scale trough and planar cross-stratification (Plate 5.5) of SB Type 2 architectural elements (Figure 5.16). The uppermost sediments of the section are composed of facies $Sp_s$ and Fx arranged in upward fining cycles of 0.25-0.5 m thick. These are interpreted as H architectural elements related to deposition under waning flow conditions and channel abandonment.

## Section 4.

The basal sediments of this section (Figure 5.17) are represented by fine grained sandstones of facies Fx with minor interbedded muds. Thin coal horizons (facies C) are developed within these beds, together with siderite nodules (<20 cm diameter) which contain organic fragments. The early development of siderite is indicated by the deformation of bedding around the nodules. The sediments are arranged in upward coarsening units of 0.3-1.20 m thick (Plate 5.6) which are interpreted as CM architectural elements related to levee sedimentation.



*Plate 5.6. CM architectural element, Section 4.*
*A coarsening-upwards unit of facies Fm-Fx-$Sp_s$ is preserved as a CM element. Bed thickness also increases upwards. Coal is present as small layers in the base of the architectural element.*
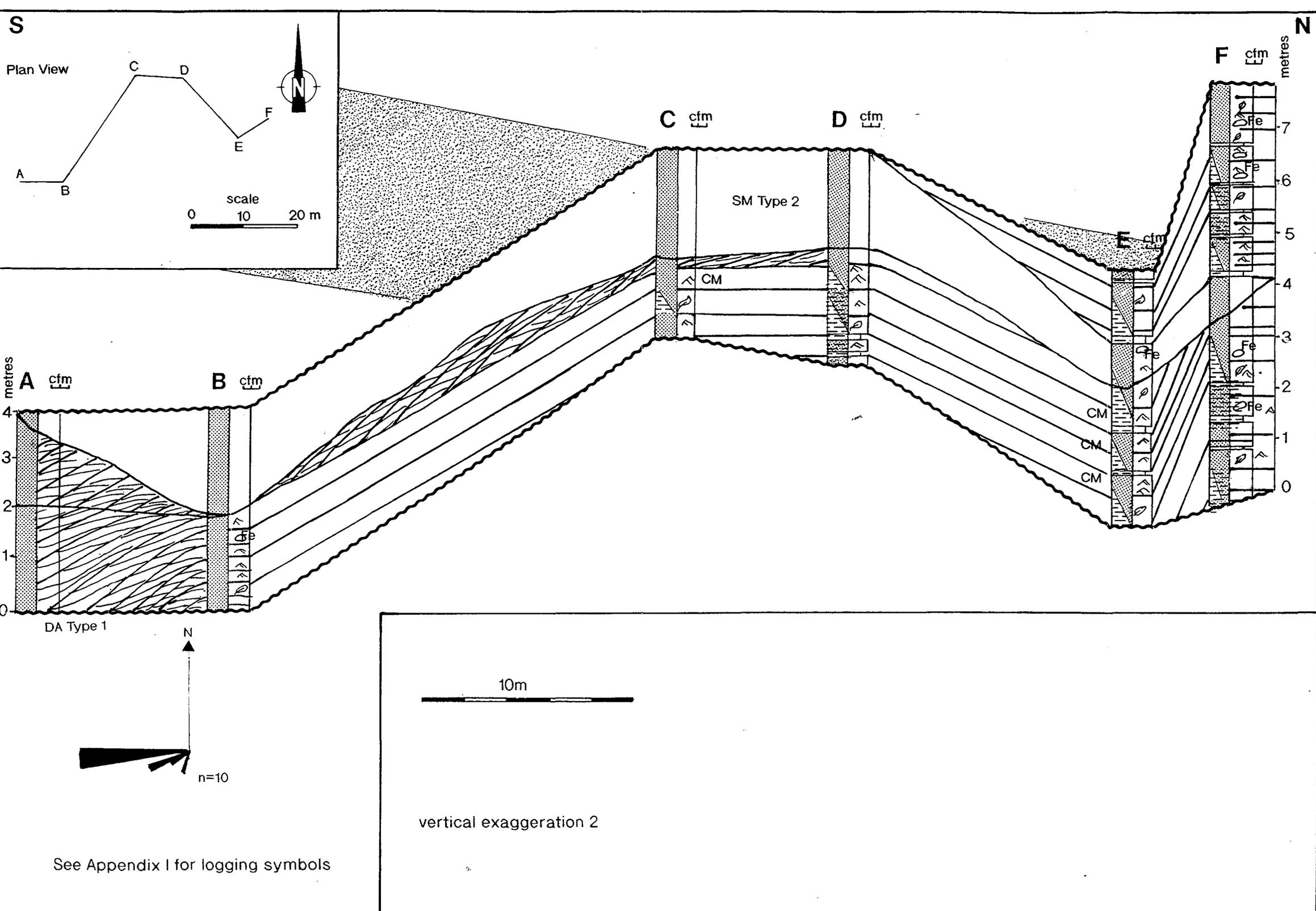
Figure 5.17. A schematic line drawing of section 4, Mansfield Formation.

Plan View

S
N

scale
0    10    20 m

A    cfm
B    cfm
C    cfm
D    cfm
E    cfm
F    cfm

SM Type 2

CM

CM
CM
CM

DA Type 1

N

n=10

10m

vertical exaggeration 2

See Appendix I for logging symbols

Overlying the fine grained deposits the mud and organic content of the sediments reduces, and sand becomes the dominant lithology. The medium grained sands are structured by medium scale planar and trough cross-stratification arranged in cosets of facies Sc (Figure 5.17). Mica and organic matter are locally concentrated at the base of tangential intrasets which dip 20-28°. The foresets of facies Sc display palaeoflow to thewest- southwest (Figure 5.17).

The structured sediments have been cut by a unit of facies Smc (SM Type 2 architectural element) which has a lenticular shape The channel is in excess of 40 m wide and <1.75 m thick. The direction of transport for this feature is impossible to establish. Emplacement of the channel form has caused deformation of the underlying sediments and local overturning of foresets. The base of the channel-form is highly irregular and contains large amounts of organic material and mudstone rip-up clasts <20 mm in diameter, which tend to be concentrated along the erosive scours. Internally the massive channel form contains de-watering structures 10 to 20 cm in height, but no other recognisable structures (Figure 5.17).

## (Iii) Petrology & Textural Characteristics.

*Textural information and grain size analysis.*

A small representative suite of samples was taken from Channel A of Turkey Run State Park. The results of the grain size analysis are shown in Figure 5.18 with more detailed information given in Appendix III. The median grain size of the samples varies between 2.9$\phi$ and 3.6$\phi$, hence the sands are fine to medium grained. The median grain size of the cross-stratified sandstones is 3.1$\phi$, and that of facies Smc is 2.9$\phi$. Figure 5.18 illustrates that the deposits of facies Smc have a marginally coarser grain size distribution than the structured facies. Sorting of the sediments varies between moderate and moderately well sorted. There is no systematic variation in the sorting of structured and structureless sandstones (see Appendix III).

The primary porosity of the Mansfield Formation sandstones varies between 9.6% and 20% with an average of 14%. The development of secondary porosity is limited, and averages 2% across the sample suite (Appendix III). Facies Smc displays an average primary porosity of 15.6% and the cross-stratified facies display an average primary porosity of 15.1%.
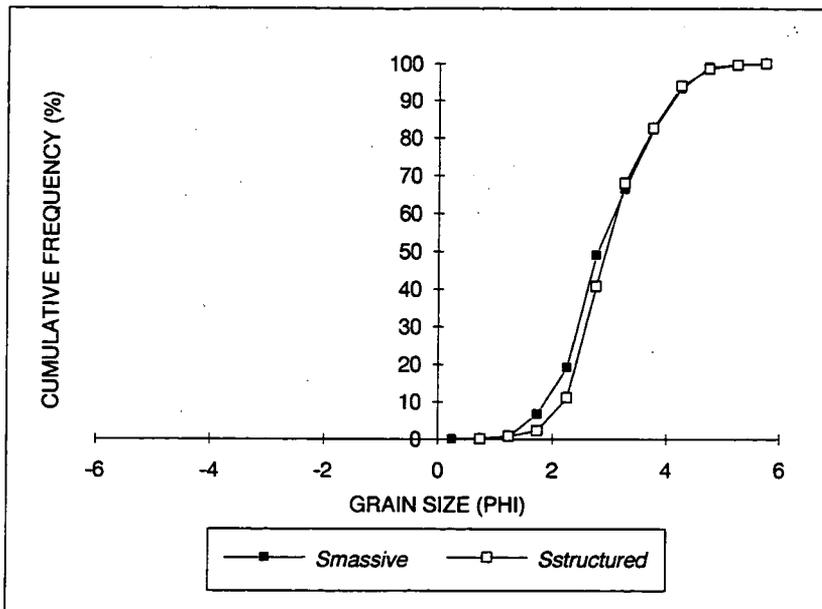
*Figure 5.18. Cumulative frequency curves of grain size distribution within the cross-stratified and massive sandstone facies of the Mansfield Formation.*

A limited study of the permeability of sandstone hand specimens has been undertaken, and the results of permeability versus sorting are illustrated in Figure 5.19. It appears from this small data set that sandstones of facies Smc have a greater range of permeabilities than do structured sediments, for the same degree of sorting, although the study is far from conclusive.
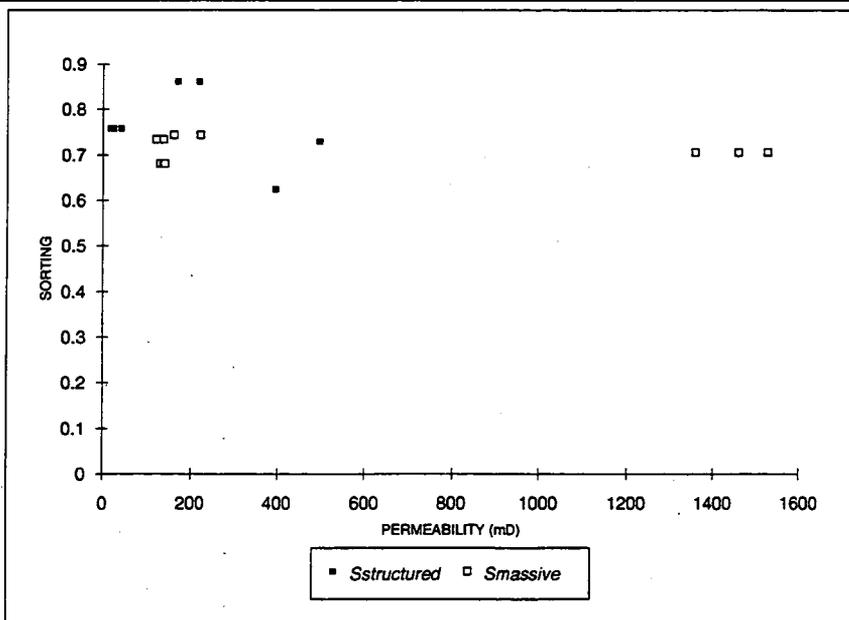


*Figure 5.19. Sorting versus permeability of the cross-stratified and massive sandstone facies of the Mansfield Formation.*

Packing of sandstones has been assessed through use of the compaction index (CI) as outlined in Appendix III. The cross-stratified facies display a CI which varies between 2.68-3.48. Facies Smc sandstones display CI values between 1.84-2.78.

*Composition.*

Figure 5.20a indicates that the sands of Channel A are quartz arenites and sub-litharenites (Folk 1980). The sands lie in the recycled orogen region of Dickinson (1985) as illustrated in Figure 5.20b. There is no recognisable pattern of compositional variation between facies types, or stratigraphical position within the succession (see Appendix III for detail).
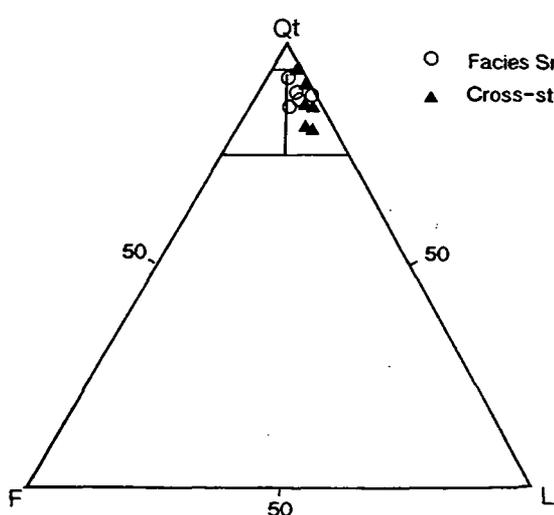


*Figure 5.20a. Composition of the Mansfield Formation (after Folk 1980).*
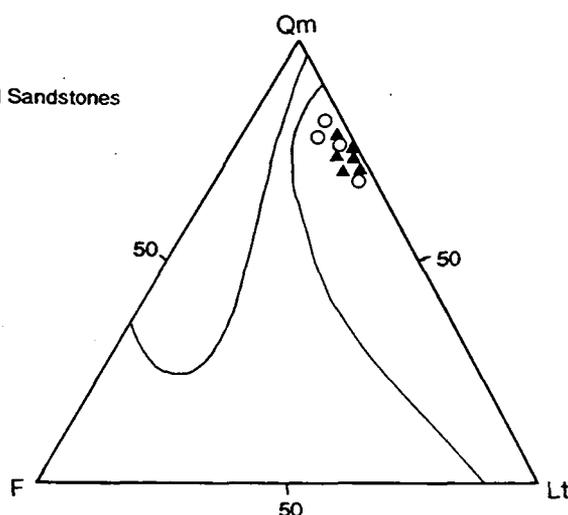
*Figure 5.20b. Provenance of the Mansfield Formation (after Dickinson 1985).*

Quartz grains dominate the Mansfield and Brazil Formations and are both monocrystalline and polycrystalline (Plate 5.7). Monocrystalline varieties dominate, with undulose extinction most common. A number of grains show trails of small inclusions. Detrital quartz grains are sub-angular to sub-rounded and display floating and point grain contacts. The lithic component of the samples includes sub-rounded to rounded sedimentary and metamorphic rock fragments. Metamorphic grains are dominantly mica schist (Plate 5.7) and sedimentary fragments are represented by fine grained sandstone and mudstone particles (Plate 5.7). Lithic grains commonly show alteration to clay minerals (Plates 5.7. & 5.8). Plastic deformation of lithic clasts has resulted in the development of a pseudomatrix (Plate 5.8). The larger lithic fragments are rounded, indicating that they were transported for some distance prior to deposition.
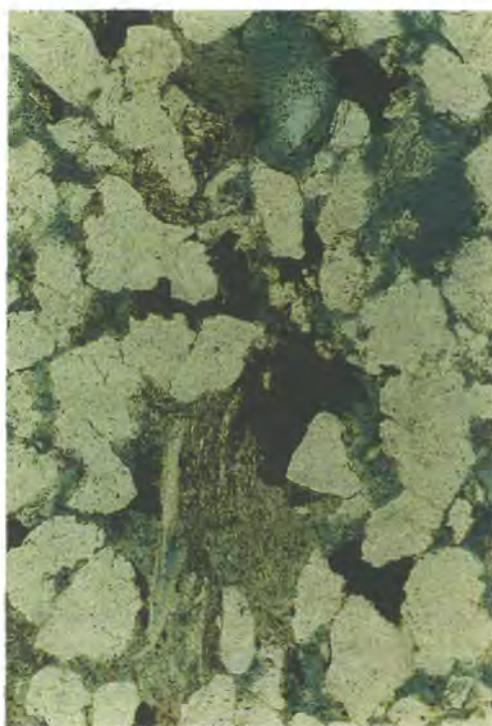
Plate 5.7.                                    Plate 5.8.

*Facies Sp_m, Mansfield Formation. Field of view 1.5 mm.*
*Monocrystalline quartz grains dominate the section, with polycrystalline quartz grains*
*displaying metamorphic textures. Detrital quartz grains are sub-rounded. Authigenic*
*overgrowths have resulted in planar and concavo-convex contacts. Lithic fragments*
*are represented by metamorphic and siltstone clasts which show evidence of*
*alteration to clay minerals and pyrite. Feldspar grains show almost complete*
*dissolution, resulting in the preservation of oversized pores. Muscovite flakes display*
*evidence of compaction and dissolution. Diagenetic siderite displays corrosive margins*
*with detrital quartz grains, and forms a locally important cement.*

Feldspars are not volumetrically important. Potassium feldspars dominate and
are represented by fresh, sub-rounded microcline grains. Plagioclase grains are
generally weathered and altered to clay minerals. Rare feldspar grains have almost
entirely been removed. Mica is present in all sections, and dominated by muscovite
(Plates 5.7 & 5.8). Biotite is also present in small quantities. Mica grains show minor
alteration to clay minerals, and also splitting and deformation due to compaction. The
heavy fraction of the Mansfield Formation consists of zircon, tourmaline, pyroxene,
pyrite and intergrowths of magnetite and illmenite.

*Diagenesis.*

Detailed study of the massive and structured sediment samples reveals no
difference in timing of diagenetic events between facies. The most important diagenetic
phases in the Mansfield Formation are authigenic quartz, pyrite, siderite and authigenic
clays. The inferred succession of events is illustrated in Figure 5.21.

| Diagenetic phase | Early | Late |
|---|---|---|
| Quartz precipitation | ———————————  —— | |
| Pyrite precipitation | — | |
| Siderite precipitation | ———————— | |
| Labile grain dissolution | ———————————— — — — — — — | |
| Kaolinite precipitation | ———— | |
| Illite precipitation | — | —— —— |

Figure 5.21. The diagenetic sequence within the sandstone facies of the Mansfield Formation.

Detrital grains of quartz are coated by an early illitic rim, which is in turn coated by authigenic quartz. Authigenic overgrowths form planar and concavo-convex contacts (Plate 5.8). The authigenic silica is too abundant volumetrically to have been provided simply through pressure solution, and is believed to have been provided by the circulation of silica rich fluids associated with de-watering of local shale horizons. Quartz cementation continued sporadically throughout diagenesis (Figure 5.21).

Dissolution of unstable framework grains followed the development of a stable framework (Plates 5.8 & 5.9). Plagioclase feldspars, lithic fragments and mica all show evidence of dissolution. Pyrite growth occurred mainly in close association with lithic fragments and along mica and feldspar cleavage planes (Plate 5.8 & 5.9). The close association of pyrite with a source of iron suggests that fluid circulation was limited at this time. Siderite growth occurred at times of relatively high porosities as indicated b y the euhedral form of crystals, and deformation of sediment around nodules. Zoning of siderite grains indicates changes in pore water chemistry. Siderite generally forms the last phase of organic decay.

The growth of siderite was followed by a period of compaction, quartz cementation and grain dissolution. Following quartz cementation illite coated many grains (Plate 5.8). Later kaolinite filled many pore spaces and replaced unstable

framework grains. Grain dissolution post dates kaolinite as reflected in the high percentage of over sized pores (Plate 5.8).
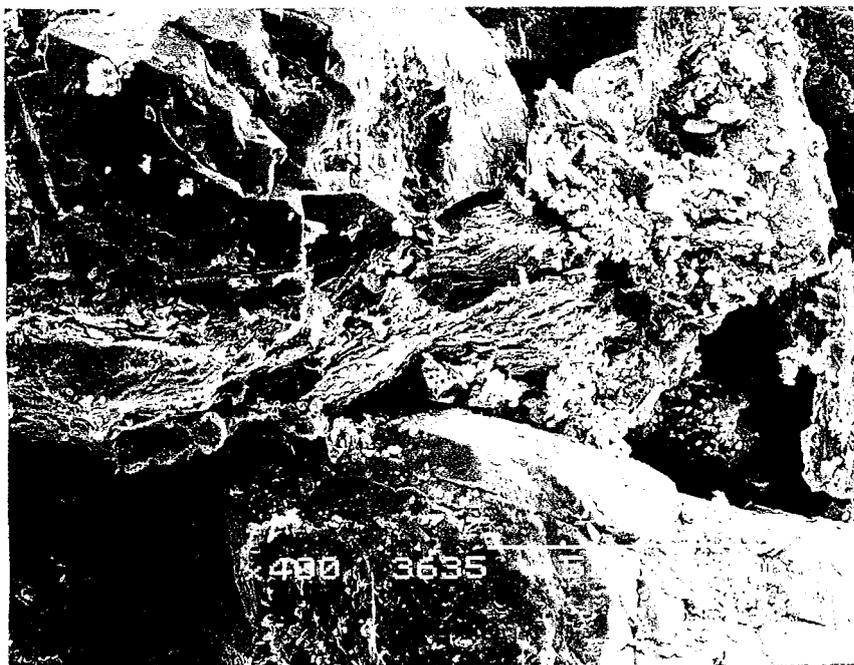


Plate 5.9. Facies $Sp_m$, Mansfield Formation.
Well developed authigenic quartz overgrowths are clear. Framework grain dissolution has resulted in the development of intergranular secondary porosity and replacement by illite and pyrite. Pore spaces remain open.

Diagenesis has subsequently been overprinted by weathering, which is most evident in the oxidation of siderite to form goethite.

*Discussion.*

The similarities in composition between massive and structured facies indicates that they were both derived from the same source. The identical diagenetic sequence in structured and massive sands indicates that the massive sands were formed by a primary depositional process, and they are therefore not an artifact of diagenetic processes.

The texture and composition of sandstones indicates a mature source containing granite and metamorphic rocks. The rounding of grains indicates either a second cycle origin for the grains or a prolonged period of transport. The presence of polycrystalline quartz pebbles is indicative of a first cycle origin. These observations agree with the model of Potter & Siever (1956) which is illustrated as Figure 4.4b. Sediments were sourced from the Canadian Shield area and the northern portion of the Appalachian front. Tropical weathering could then result in first cycle quartz arenites as described in Chapter 4, to explain the composition of the Lee-type sandstone belts.

The presence of pyrite is related to the presence of sulphide and iron. Iron was supplied through the breakdown of feldspars and lithic fragments. Sulphide may be provided through anoxia due to high levels of organic material, or through the presence of marine formation waters. Siderite nodules have been described from other Pennsylvanian strata, particularly the Francis Shale which contains the Mazon Creek fauna and flora, preserved within siderite concretions (Woodland & Stenstrom 1979). Siderite formation was probably related to the presence of saline pore waters and high organic contents associated with peat. The widespread development of a siderite phase indicates that sands may have been deposited in an estuarine environment. The high volumes of diagenetic kaolinite are believed to be related to the presence of meteoric waters within the buried sediments.

## 5.3. Fluvial Interpretation.

### 5.3.1. The Mansfield & Lower Brazil Formations.

A previous study of the Mansfield Formation by Fishbaugh *et al* (1989) interpreted the sands of the Formation as being of braided stream origin. The recognition of tidal influence within the finer grained facies of the Mansfield and Brazil Formations has been used to place sediment deposition in an estuarine or tidally influenced delta model.

The Mansfield and Brazil Formation sandstones of the study area are dominated by uni-directional palaeocurrent indicators and are hence determined to be fluvially (ebb) dominated. This is in contrast with the flood dominated sediments of the Whetstone beds (Kvale & Archer 1991). The fluvial sandstones take the form of lenticular ribbon channel bodies of varying size which lack lateral connectivity (Figure 5.8).

The base of fluvial channels are defined by fourth order bounding surfaces associated with thin, poorly exposed extra-formational conglomerate containing quartz pebbles and locally derived sandstone and mudstone rip-up clasts. Fourth order bounding surfaces relate to avulsion events. The absence of conglomeratic horizons within the channel sandstones indicates that individual sandbodies represent deposition from a single channel. Hence the channels identified within Figures 5.9-5.12 represent deposition from individual major channel architectural elements (CH).

Using methods outlined in Chapter 2.4.2 it is possible to reconstruct some aspects of the palaeohydrology for channel sandbodies exposed within Turkey Run

State Park. These parameters are detailed in Table 5.2. Using methods to estimate sinuosity (Chapter 2.4.2), it may be established that the sands of Turkey Run Sate Park and the surrounding area were deposited within low sinuosity channels, with a sinuosity of <1.5. Using the empirical equations of Schumm (1968b) as outlined in Section 2.4.2 the fluvial channel width/depth, ratios vary between 33 and 61, as detailed in Table 5.2.

| Channel | Palaeo-current variance θ | Sin-uosity | Meas-ured width (m) | Average height of 25 dunes (m) | Decomp-acted dune height (m) φc =0.15 | Water depth (m) | Width/ Depth ratio | Calc-ulated channel width (m) |
|---------|---------|---------|---------|---------|---------|---------|---------|---------|
| A | 152° | 1.36 | 525 | 0.93 | 1.36 | 6-12 | 33.15 | 331 |
| A | 152° | 1.36 | 525 | 1.84 | 2.70 | 11-20 | 33.15 | 513.80 |
| B | 105° | 1.15 | 200 | 0.44 | 0.65 | 2-5.5 | 61.7 | 231 |
| C | 33° | | 110 | | | | | |
| D | 141° | 1.29 | 200 | 0.55 | 0.80 | 2.5-5 | 39.7 | 159 |
| E | 125° | 1.23 | 330 | 0.83 | 1.21 | 5-10 | 48 | 360 |
| F | | | 50 | | | | | |
| G | | | 25 | | | | | |

*Table 5.2. A summary of the palaeohydrological parameters calculated for the channel sandbodies of the Mansfield Formation.*

Within individual channel (CH) elements sandstones take the form of stacked macroforms separated by third order bounding surfaces. Channel A is well exposed and displays sediments related to deposition within a single CH architectural element 30 m thick. The intra-channel sediments of Channel A consist of macroform and mesoform scale cross-stratified sediments related to downstream accretion. There is no evidence of LA architectural elements.

DA Type 1 architectural elements are interpreted as the deposits of mid-channel bars (Haszeldine 1983a & b). The basal facies ($Sp_m$ and $St_m$) represent migrating 2-D and 3-D dunes which were scaled to the channel depth. Compound cross-stratified units represent deposition by migration of medium scale bedforms down the lee face of a larger scale bedform. Palaeocurrent variance within these macroforms is low. Reactivation surfaces associated with low stage reworking are rare and hence these macroforms were rarely emergent.

DA Type 2 elements are interpreted to have been deposited as bank attached bars. Avalanching, grain flow (Lowe 1976a) and counter-current re-working produced the coarse-fine laminations preserved between foresets. The presence of counter-current ripples in these medium and fine grained sandstones implies a relatively forceful, long separation bubble on the lee side of the bedform, and current velocities of at least 0.6 m/sec (Jopling 1961). A significant feature of these bedforms is that most bottomsets are not finer grained than the foresets, and therefore most of the suspension load must have been carried beyond the slip face. The shape of foresets also gives some indication of water velocity. Experiments by Jopling (1965) suggest that angular forests are favoured by lower velocities. At higher velocities foresets reduce in angle and become more tangential. The tangential nature of these foresets therefore agrees with the high velocity of flow indicated by counter current re-working.

The DA Type 2 architectural elements display low palaeocurrent variance. Reactivation surfaces associated with low stage reworking are virtually absent and thus indicate that the bedforms were rarely emergent.

The macroform scale architectural elements grade downstream into mesoform scale SB Type 2 elements structured by small scale planar and trough cross-stratified units as illustrated in Figure 5.14. The mesoform scale elements display palaeocurrents with a greater variation than those of the macroform scale deposits. The interfingering of the coarse and finer grained deposits indicates that they were deposited contemporaneously.

It is suggested that the medium and large scale cross-strata of DA element Types 1 and 2 were deposited in a barhead environment which graded downstream into a bartail environment (SB Type 2 elements) as illustrated in Figures 2.3a & b. The lack of major reactivation surfaces within the deposits indicates that emergence of bedforms was rare, and hence the braiding index would have been low. However, in order to split flow within a fluvial channel bars do not have to be emergent, as shallowing of water over the bar may result in the reduction in flow regime (Bluck

1980). The bar tail contains finer grained sediments due to the sorting of sediments over the bar.

Both the barhead and bartail deposits preserve overturned foresets. In the barhead the overturning of foresets is often associated with the development of 2B bounding surfaces within compound cross-stratified units. Deformation of this type is believed to occur when liquefied sediments are subjected to a shearing flow (Figure 4.28). Deformation of foresets within the bartail may be related to the increased volume of fines. The presence of clays would cause a decrease in permeability and thus an increase in pore pressure which may be responsible for liquefaction of the sediments (Bluck 1980). Alternatively the topography of a large barform may result in internal water level differences within the bar, resulting in sufficient pore pressure differences to cause liquefaction and deformation (Bluck 1980). Deformed cross-stratification grades laterally into dewatered and massive sands (Plate 5.1).

The third order bounding surfaces are locally overlain by thin rippled horizons which indicate partial emergence of bars. However, these rippled sandstones are rare. The paucity of rippled horizons, intra-formational conglomerates and reactivation surfaces indicates limited re-working of the fluvial braidplain. Thus the Mansfield/Brazil Formations fluvial systems was perennial, with little low stage re-working and hence of low braiding index. As detailed in Table 5.1. climate during the Morrowan and Atokan was tropical and consistently wet (Phillips & Peppers 1984). Thus a perennial river system is most likely.

The channel filling massive sands of facies Smc represent deposition under unusual, but not uncommon, fluvial conditions. The channels are erosionally based and cut through pre-existing structured sediments, with a sense of movement oblique to the palaeoflow direction as measured from the cross-stratification of associated sediments. Deformation of underlying sediment may or may not be present. The fill of facies Smc is largely structureless with concentric laminae and organic rip-up clasts locally preserved at the channel margins. The units of facies Smc are often overlain by third order bounding surfaces which are the upper bounding surfaces of bars. This facies is impossible to explain in terms of normal channel processes and is discussed in detail in Chapter 7.

The major channel architectural element (CH) of Channel A is capped by units of fining-upwards sandstone and siltstone. These are interpreted in terms of deposition under waning flow conditions related to channel abandonment, and form H architectural elements. At the margins of Channel A fine grained rippled sandstones and mudstones are preserved. These are arranged in coarsening-upwards cycles

(section 4) and represent deposition under increasing flow velocities. These sedimentary units are interpreted to represent CM architectural elements related to deposition across channel margin levees.

Channel depths of the Mansfield river were estimated using the average thickness of preserved dunes as detailed in Table 5.2. In fluvial Channels B, D and E simple dunes were represented by medium scale trough and planar cross-stratification. The estimated channel widths correspond closely to the preserved width of sediment (Table 5.2).

Channel A contains two scales of cross-strata. The solitary unit bars represented by the DA Type 2 architectural elements give a value of channel depth which corresponds well to the preserved channel width (Table 5.2). The medium scale bedforms give a much smaller value of channel width. It is likely therefore likely that the large scale planar cross-stratified bedforms represent deposition from periods of bankfull discharge, whereas smaller bedforms relate to the average discharge. The width of the channels at the time of deposition may be estimated from outcrop patterns. The close approximation of measured and estimated river widths add credence to this method of determining palaeochannel characteristics. Channel A of the Mansfield Formation is interpreted to have been 500 m wide and 10-15 m deep (Table 5.2) and hence similar in scale to the modern day Platte river of the USA and the Kosi river of India (Table 2.5).

The Mansfield and Brazil Formations examined within this study contain fluvially dominated sandstones deposited in low sinuosity streams. Fluvial channels are represented by individual CH elements separated by fourth order bounding surfaces. These surfaces represent periods of avulsion which are thought to be autocyclically controlled (Wizevich 1991, 1993). Internally the CH elements are composed of stacked macroforms produced through vertical aggradation of mid-channel and bank attached bars. Deposits of lateral accretion are absent within the CH elements indicating that channel sandstones of the Mansfield and Brazil Formations aggraded vertically and avulsed, as opposed to migrating laterally. Abandonment of fluvial courses is interpreted to have been rapid, due to the minor development of architectural element H representing deposition during waning flow.

Palaeoflow variability within individual channel elements (CH) is low (<150°) as illustrated in Table 5.2. However, between channels large changes in mean palaeoflow direction are apparent (Figure 5.8). Below 575', i.e. within the Mansfield Formation (Figure 5.9 & 5.10) palaeoflow was towards the south. Above 575' (Figure 5.11 & 5.12) palaeoflow was to the east. The rotation in the drainage net was sudden,

and hence suggests an allocyclic control such as a change in the tectonic regime, climate or eustacy. Possible allocyclic mechanisms in operation during the Morrowan and Atokan of the Illinois Basin include movements in the Appalachian front causing migration of the forebulge i.e. the Cincinnati Arch, and eustacy. It is impossible to separate the effects of these two controls. Climate is assumed to have been constant through this deposition episode (Phillips & Peppers 1984). Base level changes during this period have been documented in the Lee-type sandstones of the central Appalachian Basin with estuarine shales deposited between Lee-type sandstones (Chapter 4), and hence this may be possible here. In SDH 362 (Figure 5.7a) *Chondrites* trace fossils indicative of marine influences are preserved. The Lower Block Coal is also developed at this horizon, and is underlain and overlain by tidalites (facies Fr). Hence at the time of palaeoflow change inundation by marine or brackish waters occurred.

Inter-channel sediments are locally preserved in outcrop and in more extensively in cored sections (Figure 5.8). The inter-channel sediments are composed of facies Fx, Fm, Fr, P and C. Two architectural elements have been defined (Table 2.6). IC Type elements are composed of facies Fx, P and C which are of terrestrial origin. IC Type 2 elements also contain facies Fr i.e. tidalites which are indicative of marine influences. Inter-channel areas must therefore have been low lying and subjected to periodic inundations of brackish water from marine areas which existed towards the south.

The presence of coal horizons within the Mansfield Formation act as a major control on sedimentary models. These coals are composed of lycopod root material (Phillips & Peppers 1984) and are of low sulphur content indicating deposition in a freshwater environment (Cecil *et al* 1985). Terrestrial conditions are indicated by the presence of coal horizons. However, the close association of the coal beds and IC Type 2 elements (tidalites) indicates deposition across a low lying coastal plain with periodic inundation by tidal currents. Seawater must have been diluted by rainfall and/or river water, in order to maintain low sulphur values (Phillips & Peppers 1984).

Thus, the channel sandbodies of the Mansfield and Lower Brazil Formations are ebb dominated, low sinuosity fluvial channels. The channels were laterally restricted by the presence of levees and aggraded rapidly through vertical accretion punctuated by periodic avulsion. The fluvial systems traversed low lying estuarine influenced mud flats. Palaeosol and coal horizons indicate periodic emergence and vegetation of the mud flats. However, small changes in base level through autocylic and allocyclic mechanisms resulted in the periodic inundation of marine waters. Avulsion events may be related to these changes in base level. The rotation in

palaeoflow is connected with marine horizons indicating a possible eustatic or tectonic control.


### 5.3.2. Modern Analogues.

Archer & Kvale (1993) state that the complete model for basal Pennsylvanian sedimentation must be 1) tidally influenced with a limited tidal range (micro- or mesotidal), 2) have limited marine re-working, 3) be mud dominated, 4) occur in a tropical setting and 5) be laterally associated with extensive peat accumulations. It must also be added that basal Pennsylvanian systems would also have been laterally confined by the bedrock of palaeovalley walls. Above 500' elevation however, the system became unconfined as palaeovalleys filled.

The small estuaries of Sierra Leone have been documented by Tucker (1973). The estuaries face the Atlantic Ocean and experience a semi-diurnal tidal regime, as has been interpreted from the rhythmically laminated sediments of the Mansfield and Brazil Formations. The estuaries along the Sierra Leone coast vary from drowned valleys to complex estuaries and swamps with numerous distributary channels covering many hundreds of square kilometers (Tucker 1973). Rainfall is strongly seasonal and hence in the wet season sedimentary structures are ebb dominated, and in the dry season are modified by flood dominated currents. The estuaries are fringed by mangrove swamps and silty and muddy sands. Semi-permanent channels drain the muddy sand flats. With rising relative sea level channel sediments prograde over earlier inter-tidal flat and mangrove swamp deposits. The lack of flood dominated tidal indicators within the sands of the Pennsylvanian may, however, suggest a more equitable rainfall than is experienced within modern-day West Africa.

Cecil *et al* (1993) use the Sumatra Basin of Indonesia as a modern analogue for the Morrowan and Atokan coals of the Appalachian Basin, which are essentially identical to those of the same age within the Mansfield and Brazil Formations. The Sumatra Basin is located in tropical latitudes and has a consistently wet climate. The Kampur River estuary is tidally influenced for >180 km inland and flood dominated for 100 km. The fluvially dominated section of the estuary contains channels which are laterally restricted by levees and which carry sand. Inter-channel areas are composed of peat swamps and mud flats. The Holocene peats began to accumulate following sea level rise at the end of the last glaciation and now accumulate in domed peat swamps such as those which have been inferred for the Pennsylvanian coals (Cecil *et al* 1985).

Archer & Kvale (1993) have described the estuarine deposits of the Illinois Basin as similar to those deposited in the present day Orinoco delta. The Orinoco maintains tidal conditions for greater than 150 km inland and broad mud flats are commonly developed. Climate is tropical and wet, with little seasonality.

It would appear that the estuaries and tidal inlets of the Indonesia coast or the Orinoco may be a reasonable modern analogue for the sediments of the Mansfield and Brazil Formations. The rise in present relative sea level mirrors conditions of the early Pennsylvanian of the Illinois Basin. The marine bands preserved within the Mansfield and Brazil Formations record times of increased marine influence, which are also recognised within the sediments of modern day estuaries. The large channel sandstones of the Mansfield and Brazil Formations may be interpreted as fluvially (ebb) dominated channels deposited within tidal flats, and swamps, as represented by the inter-channel facies.

## 5.4. Summary.

The Mansfield Formation was deposited in equatorial latitudes in a tropical, consistently wet climate.

Clastic sediments rich in metamorphic quartz pebbles were sourced from the Canadian Shield and the rising Appalachian front. Tropical weathering resulted in the formation of a first cycle quartz arenite. The sediments were carried by low sinuosity streams and deposited in estuarine environments along the eastern margin of the Illinois Basin.

Sediments were deposited in the upper estuarine/fluvial environment at the margin of tidal influence (100-180 km inland).

Channel sandstones of the Mansfield and Lower Brazil Formations represent the deposits of single CH elements. Channels were laterally restricted and had stable banks modified by levees. Fluvial channels aggraded rapidly and avulsed frequently. The avulsion may or may not be associated with changes in base level. Rotation in the drainage net at the Mansfield/Brazil boundary is related to allocyclic controls in the form of tectonics, eustacy or a combination of these factors.

Within CH elements sedimentation was dominated by downstream accreting bars which were composed of well defined barhead and bartail regions. Although

barhead areas were rarely emergent the channel thalweg was split sufficiently to increase flow variability in the lee of the bar.

Channel sedimentation was periodically interpreted by the deposition of facies Smc (SM Type 2 architectural elements) which were deposited by currents moving across the channel as opposed to along it. Facies Smc is commonly overlain by a third order bounding surface. In section 1 sandbodies of facies Smc are stacked.

Inter-channel areas were mud flats with lycopod vegetation and domed peat swamp development. Compaction of the peat allowed for the rapid accumulation of tidalites during periods of increased marine influence.

# Chapter 6
# The Sydney Basin

## 6.1. Regional Geological History Of The Sydney Basin.

The Sydney Basin is a northwest/southeast trending feature, bounded to the northeast by the Hunter Thrust System of the New England Fold Belt (NEFB), and to the southwest by the Lachlan Fold Belt (LFB) (Figure 6.1). The basin forms the southern continuation of the Sydney-Gunnedah-Bowen Basin (Figure 6.1), with the Mount Coricudgy anticline (Figure 6.2) marking the northern boundary (Bembrick *et al* 1980).
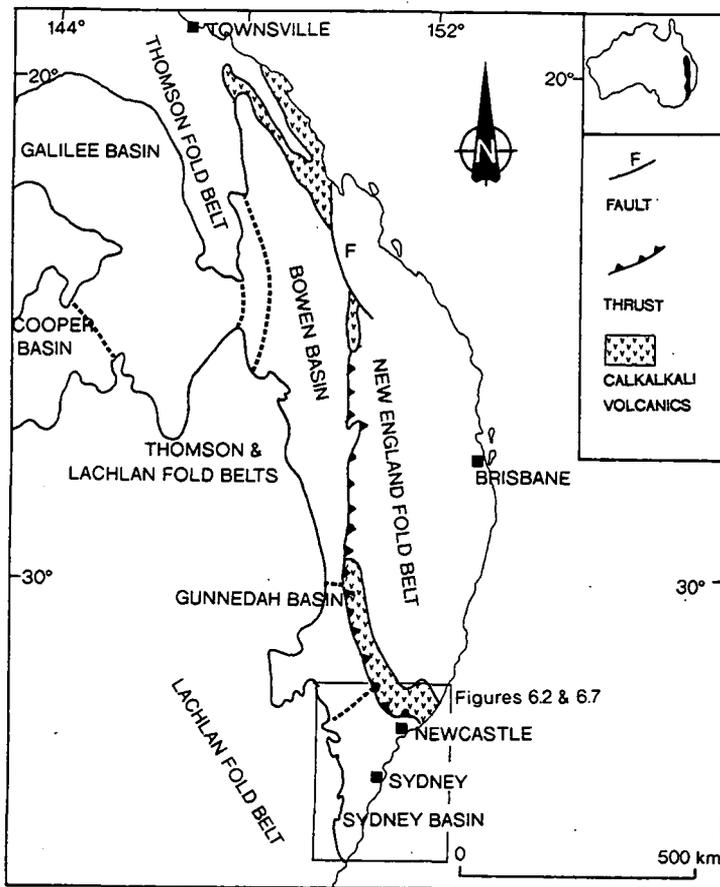


*Figure 6.1. The location of the Sydney Basin in relation to the Bowen-Gunnedah-Sydney Basins.*
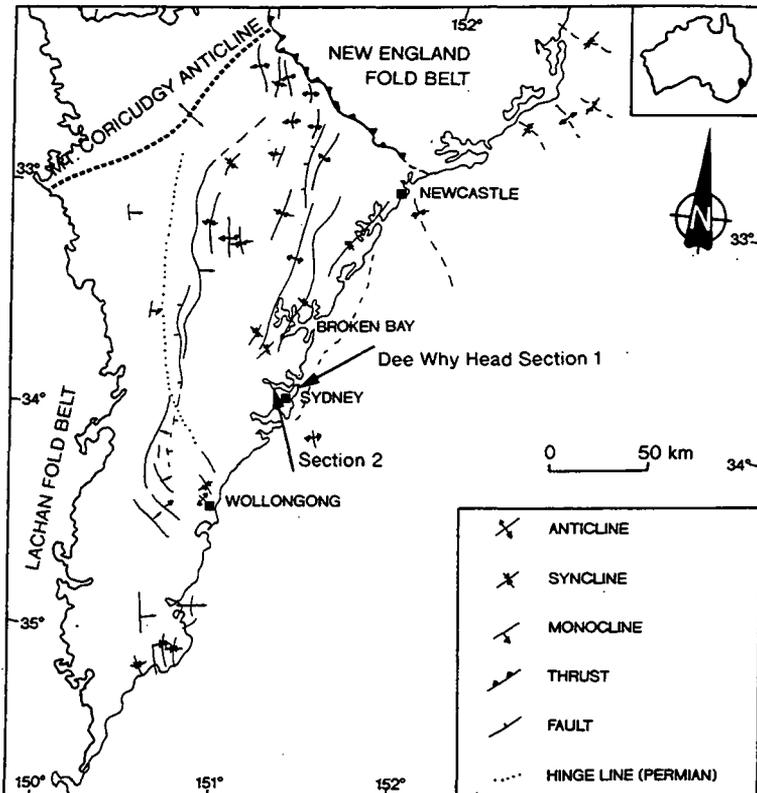
*Figure 6.2. The structural elements of the Sydney Basin (modified after Bembrick et al 1980).*

The Sydney Basin fill is of late Carboniferous to mid Triassic age (Figure 6.3). The structure and stratigraphy of the basin (Table 6.1, Figures 6.2 & 6.3) are highly complex, due to the location of the region on a rapidly evolving continental margin throughout the Permian (Briggs 1993). The area evolved as a back-arc extensional basin during the early Permian (Collins 1991; Ahmad *et al* 1994) before assuming a foreland basin style in the mid-Permian (Table 6.1).

During the late Carboniferous the proto-Sydney basin was situated along the eastern margin of the LFB (Herbert 1980a). The Ayr rift zone (Figure 6.4a) was an area of extensive volcanism with basaltic and rhyolitic lavas reaching 1.5 km thick (Veevers *et al* 1993). Coarse volcanic debris shed from the rift was deposited over the Kullatine shelf (Figure 6.4a). During the late Stephanian and early Sakmarian continental ice sheets covered the majority of eastern Australia (Herbert 1980c) and glaciofluvial deposits of the Seaham Formation and Talaterang Group (Figure 6.3) were deposited in narrow elongate depressions along the eastern margin of the LFB (Dutta & Wheat 1993).

| SYSTEM | SERIES | STAGE | AGE (MA) | CLIMATE | PALAEO LAT | EXTENSION | COMPRESSION | SEDIMENTATION | TECTONICS |
|---|---|---|---|---|---|---|---|---|---|
| TRIASSIC | Rhaetic | | 200 | Warm Temperate | | | | | |
| | Narian | | | | | | | | |
| | Carnian | | | | | | Hunter | Advance of an orogenic wedge in the form of the Wianamatta Group. Cratonic sands (Hawkesbury Sandstone & Narrabeen Group) blanket basin. Onlap NEFB to east. | |
| | Ladinian | | | Warm Temperate | 75°S | | | | 250-260 Ma subsidence in the foreland basin coeval with uplift in the NEFB. Cratonwards transport of sediment slices in thrust sheets. End of volcanic activity. |
| | Anisian | | | | 85°S | | | | |
| | Scythian | | | | | | | Coal measures. Accumulated near to sea-level. Sediment derived from NEFB, and deposited in lagoons and deltas. | |
| PERMIAN | Tatarian | | 250 | | | | | | |
| | Kazanian | | | | | | | Thick sedimentary successions interbedded with tuffs (Wandrawandian & Branxton Formations. | |
| | Kungurian | | | | | | | Sporadic coal formation in fluvio-deltaic and marginal marine alluvial fan environments. | Artinskian: Plate convergence to east of the NEFB causing extensive deformation & metamorphism. |
| | Artinskian | | | Seasonal Ice | | | | | |
| | Sakmarian | | | | | | | Shallow marine environment with mixed carbonates & clastics. Coastal areas face an open ocean. Volcano-clastics provided from rift. | Sakmarian: extension in basin related to back arc extension in Ayr Rift. |
| CARBONIFEROUS | Stephanian | | 300 | | 75°S | | | Limited sedimentation. | Rifting. |
| | Westphalian | | | | | | Currabubula | | |
| | Namurian | | | Glaciated | 72°S | | | No deposition due to presence of continental ice sheets. | |
| | Visean | | | | | | | Emergent area. | Uplifted cratonic areas. Terminal deformation of the Lachlan Fold Belt. |
| DEVONIAN | | | 350 | | | | | | |
| | | | | | | | | | Lachlan Fold Belt amalgamated during series of late Ordovician to Devonian orogens. |
| SILURIAN | | | 400 | | | | | | Timescale from Veevers et al (1993). Information derived from: Herbert 1980a, 1980b); Retallack (1980); Embleton (1984); Quilty (1984); Briggs (1993); Veevers et al (1993); Brakel et al (1993). |

*Table 6.1. A generalised history of the Sydney Basin.*

| SYSTEM | SERIES | AGE (Ma) | NORTH | CENTRAL | SOUTH |
|---|---|---|---|---|---|
| TRIASSIC | CARNIAN | 220 | | | |
| | LANDINIAN | | | WIANAMATTA GP | WIANAMATTA GP |
| | ANISIAN | | | Hawkesbury Sst | Hawkesbury Sst |
| | SCYTHIAN | | | NARRABEEN GP | NARRABEEN GP |
| PERMIAN | TATARIAN | 250 | Wollombi Coal Measures / Newcastle Coal Measures | Illawarra Coal Measures | Illawarra Coal Measures |
| | KAZANIAN | | Mulbring Silt | Berry Silt | Berry Silt |
| | KUNGURIAN | | Muree Sst / Branxton Fmn | Nowra Sst | Nowra Sst |
| | | | | Wandrawandian Silt | Wandrawandian Silt |
| | ARTINSKIAN | | Greta Coal Measures | Snapper Point Fmn | Snapper Point Fmn |
| | | | Farley Fmn / Rutherford Fmn | Pebbly Beach Fmn | Pebbley Beach Fmn / Clyde Coal Measures |
| | SAKMARIAN | | Allandale Fmn | Wasp Head Fmn | Wasp Head Fmn |
| | | 290 | Lochinvar Fmn | | |
| CARBONIFEROUS | STEPHANIAN | | Seaham Fmn | | TALATERANG GP |
| | WESTPHALIAN | 300 | | | |
| | NAMURIAN | | Paterson Volcanics | | |
| | VISEAN | 325 | Mount Johnstone Fmn | | |

*Figure 6.3. The regional stratigraphy of the Sydney Basin (after Herbert 1980a; Veevers et al 1993).*

Active rifting was followed by a period of thermal sag (Briggs 1993), and during the early Permian the NEFB and eastern LFB subsided, to produce the Shoalhaven shelf (Figure 6.4b). Early Permian sediments are represented by the Shoalhaven Group and lateral equivalents (Figure 6.3). During extensive marine transgressions thick successions of marine carbonates and clastics were deposited. Volcanic centres became islands which shed debris into the sea (Allandale & Lochinvar Formations of Figure 6.3). Thinner and less extensive sediments were deposited during two regressions (Herbert 1980a). These are preserved as the lateral equivalents of the Nowra Sandstone, and Greta and Clyde Coal Measures (Figure 6.3).
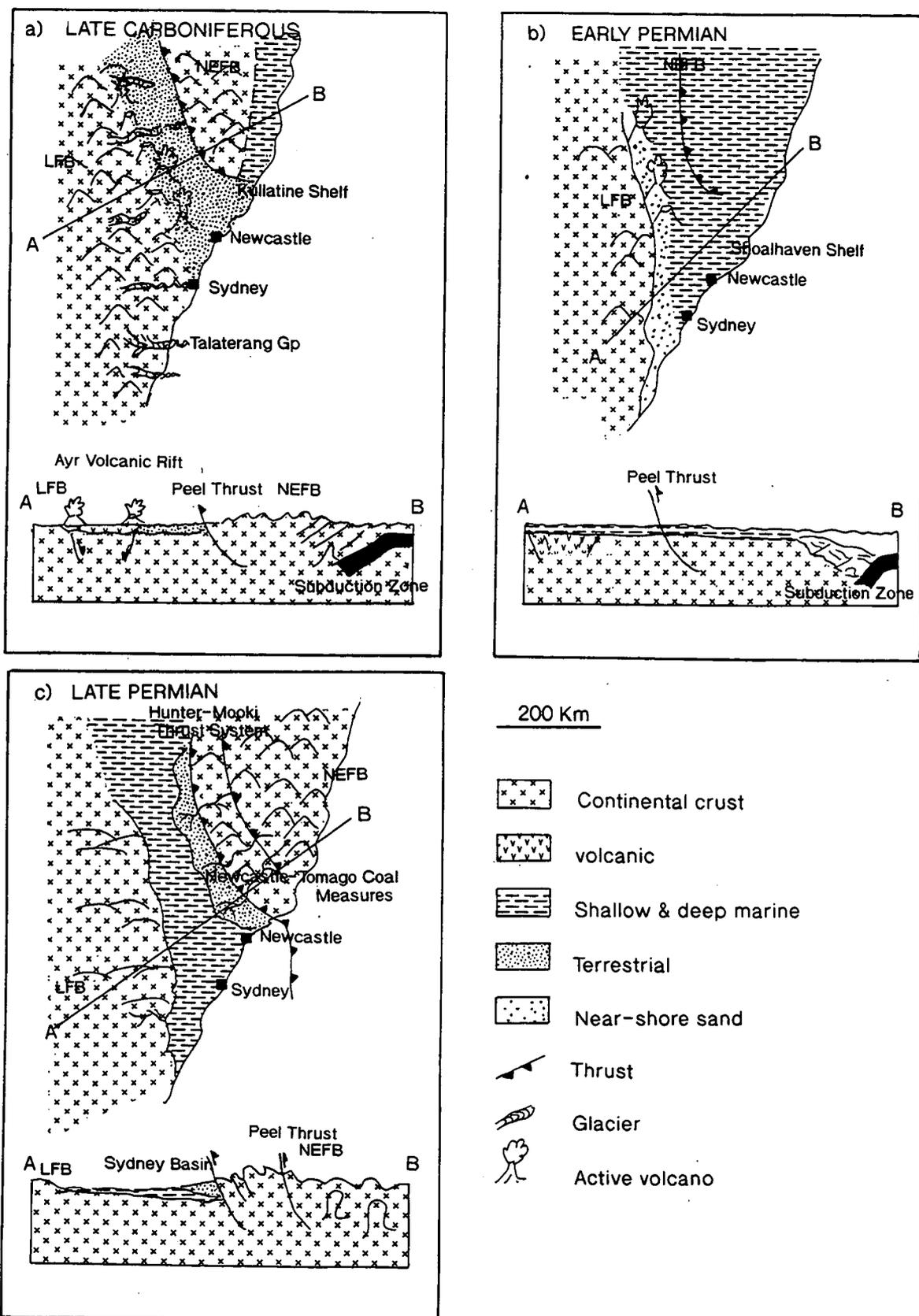
*Figure 6.4. Palaeogeographic reconstructions of the Sydney Basin (modified after Herbet 1980a; Ward 1980; Veevers et al 1993).*

East-west compression and crustal loading associated with the mid-Permian Hunter Orogeny (Collins 1991) initiated subsidence of the Sydney Basin foredeep, and marked the onset of foreland basin style sedimentation (Herbert 1980a). Thrust sheets were carried cratonwards across the NEFB and Sydney Basin (Figure 6.4c).

The foreland basin fill is of mid Permian to mid Triassic age (Table 6.1, Figure 6.5) and was deposited dominantly in fluvial and fluvio-deltaic environments. Permian and Triassic chronostratigraphy is poorly constrained due to sub-aerial environments of deposition, and the most reliable method of dating is by use of palynological schemes such as those outlined by Helby (1973) and Retallack (1977, 1980).

| SYSTEM | SERIES | AGE (Ma) | | SOUTH BROKEN BAY | | | NORTH BROKEN BAY | | SPORE-POLLEN ZONES |
|---|---|---|---|---|---|---|---|---|---|
| TRIASSIC | ANISIAN | | | Hawkesbury Sandstone | | | | | Aratrisporites parvispinosus |
| | | | | | | F | | | Ap |
| | | 240 | | | | E | E | | |
| | | | | Newport Fmn | | D | D | | Aratrisporites tenuispinosus, upper zone |
| | | | | | | C | C | Terrigal Fmn | |
| | | | | Garie Fmn | | B | B | | |
| | | | | Bald Hill Claystone | | | | | At2 |
| | SCYTHIAN | | NARRABEEN GROUP | | | A | A | | lower zone At1 |
| | | | | Bulgo Sandstone | | Patonga Claystone | | | Protohaploxypinus samoilovichii Ps |
| | | | | Stanwell Park Claystone | | Tuggerah Fmn | | | Lunatisporites pellucidus |
| | | | | Scarborough Sandstone | | Munmorah Conglomerate | | | Lp |
| | | | | Wombarra Shale | | | | | Protohaploxypinus reticulatus |
| | | | | Coalcliff Shale | | | | | Pr |
| PERMIAN | TATARIAN | 250 | | Illawarra Coal Measures | | Newcastle Coal Measures | | | Dulhuntyispora D |

Figure 6.5. A detailed stratigraphy of the Sydney foreland Basin fill. Pollen zones after Cowan (1993).

The Permian and Triassic fill of the Sydney Basin involves a complex interplay of sediment supply from two sources. The LFB to the west was composed of Carboniferous calc-alkali volcanics (Cowan 1993), together with plutonic and high grade metamorphic rocks of granitic composition (Dutta & Wheat 1993) which provided quartzose sediment. The NEFB to the east provided lithic sediment from Carboniferous ignimbrites exposed along the southern perimeter of the orogen (Cowan 1993), or from basic to acidic volcanic intrusions and moderately metamorphosed and deformed volcanoclastics and limestone (Dutta & Wheat 1993). Alternative eastern sources of sediment have been postulated by Dutta & Wheat (1993) which are believed to be alkali volcanics of Permo-Trias age located on the present continental shelf.

A model of foreland basin evolution was postulated by Conaghan *et al* (1982) and Jones *et al* (1984) which was later modified by Cowan (1993). The model proposes a complex evolving river network across the Sydney Basin. Longitudinal trunk streams are postulated to have flowed southeast along the basin axis, and these received sediment through tributaries flowing from the southwest (NEFB) and northeast (LFB). Using microfloral zones Conaghan *et al* (1982) examined the time-space relationships of the Sydney Basin fill and interpreted facies boundaries to be diachronous and younging towards the northeast. The time boundaries were correlated to changes in orientation of the drainage net. However, the work of Helby (1973) indicates that unconformities exist within the foreland basin fill, as illustrated in Figure 6.5. Thus, changes in the drainage network were relatively sudden events, and not significantly time transgressive.

Uplift of the NEFB during the late Permian associated with development of a volcanic arc (Dutta & Wheat 1993) supplied massive amounts of detritus south and west into the subsiding Sydney Basin (Figure 6.6a). Sediment wedges were thickest adjacent to the Hunter-Mooki Thrust System, and thinned basinwards (Figure 4.4c) indicating considerable syn-sedimentary subsidence (Jones *et al* 1984). Tuff bands within the coal measures indicate synchronous volcanic activity in the NEFB which has been related to thrust emplacement (Jones *et al* 1984; Briggs 1993).

During the late Permian sub-lithic sediment was deposited during three regressive episodes in marginal marine and lacustrine environments (Jones *et al* 1984). Peat accumulated in extensive swamps close to sea level, and is preserved in the Illawarra/Newcastle and Wollombi/Wittingham Coal Measures (Figures 6.3 & 6.5). The westerly directed palaeocurrent indicators preserved in the north of the basin (Figure 6.6a) have been interpreted to represent tributary streams, which joined a southeast directed longitudinal fluvial system (Cowan 1993). The presence of the southerly directed system indicates the existence of an extension of the NEFB
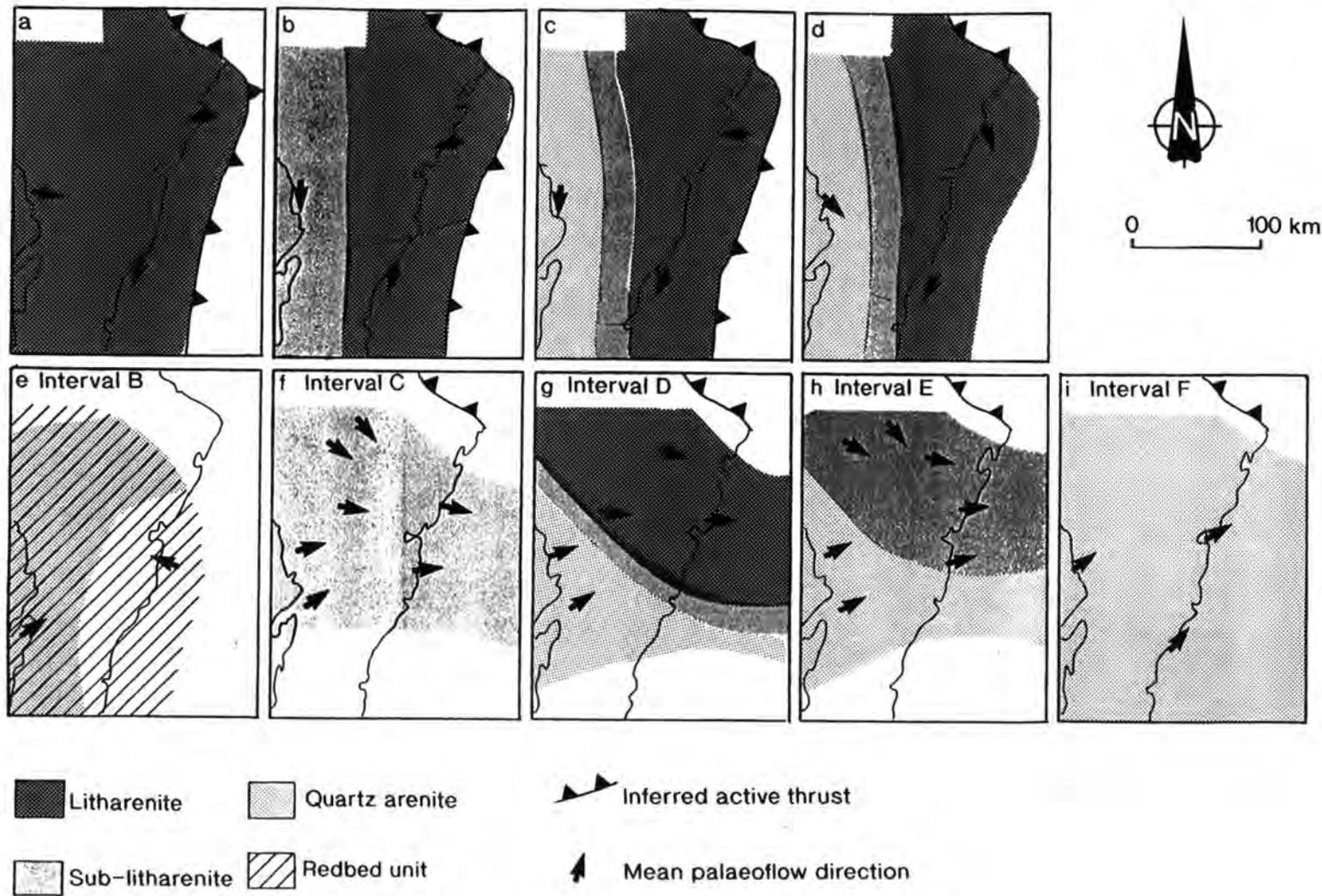
Figure 6.6. Palaeogeography of the Tatarian-Anisian Sydney Basin (modified after Ward 1980; Cowan 1993).

(Cowan 1993; Dutta & Wheat 1993), oriented parallel to the present coastline (Figure 6.6a-c).

At the close of the Permian volcanic activity declined and the NEFB was uplifted resulting in a major depositional break (Figure 6.5). Subsequent sediment deposition occurred within alluvial fan, fluvial and lacustrine environments of the lower Narrabeen Group (Veevers *et al* 1993). The deposition of the lower Narrabeen Group was marked by a retreat of sediments from the NEFB and an advance of quartzose sands from the LFB (Figures 6.6b & c). Lithic sediment provided from the NEFB was deposited in braided fluvial streams which prograded southwest and south across the basin (Conaghan *et al* 1982). Finer grained, sub-lithic sediment was deposited in low gradient, axial meandering rivers with well developed flood plains (Herbert 1980a).

During deposition of the Bulgo Sandstone (Figures 6.5 & 6.6d) sediment dispersal across the Sydney Basin changed from southwesterly to southeasterly dominated (Ward 1980; Conaghan *et al* 1982; Cowan 1993). This time period coincides with the demise of the offshore segment of the NEFB (Cowan 1993). Meandering river systems flowed southeast along the basin axis (Herbert 1980a) and deposited large quantities of moderately mature quartzose channel sands. Differential subsidence across the basin is indicated by the amalgamation of sandbodies to the north (Cowan 1993).

Following rotation of the drainage net, sediment supply from the NEFB virtually ceased (Cowan 1993). Quartzose sediments were sourced from the LFB (Figure 6.6e) and the southern and western portions of the Sydney Basin were blanketed b y the Bald Hill Claystone (Ward 1980). As the topography across the NEFB became subdued (Cowan 1993) a marine incursion occurred which was marked by a kaolinite clay pellet bed (Herbert 1980a), the Garie Formation (Figure 6.5).

The Newport Formation (Figure 6.5) represented a period of rapid drainage pattern evolution within the Sydney Basin. The basin profile at this time was asymmetric (Cowan 1993) due to higher rates of subsidence in the north. A change in the provenance of sediment between Intervals C, D and E (Figure 6.5) is indicated b y jumps in sandstone composition (Cowan 1985, 1993). The NEFB went through numerous eruptive and quiescent phases which resulted in surges in sediment supply (Dutta & Wheat 1993).

The quartzose sandstones of interval C (Figure 6.6f) were deposited by high sinuosity streams sourced from the LFB. Intervals D and E (Figure 6.6g & h) were deposited by low sinuosity streams which carried sub-lithic and lithic sediment from both the NEFB and LFB. The easterly directed palaeodrainage system was oriented

parallel to the onshore segment of the NEFB (Figures 6.6f-h) and has been interpreted in terms of a longitudinal drainage system (Cowan 1993).

In the past workers have interpreted contemporaneous deposition of the upper Narrabeen Group and the Hawkesbury Sandstone (Herbert 1980a; Conaghan *et al* 1982). However, the work of Helby (1973) suggests that a hiatus exists between the units. Prior to, and during deposition of the Hawkesbury Sandstone (Interval F of Figure 6.5), uplift of the LFB tilted the Sydney Basin to the northeast and initiated the erosion of late Permian to mid Triassic sediments. The unconformity increases to the southwest (Herbert 1980a) and may be explained in terms of uplift of the peripheral bulge (Cowan 1993).

Tilting of the basin and quiescence in the NEFB (Dutta & Wheat 1993) resulted in a major palaeocurrent change when sediments of the Hawkesbury Sandstone (Figure 6.5) were transported northeastwards towards the orogen, by braided streams (Figure 6.6i). There is no evidence of a longitudinally oriented trunk stream associated with the transverse Hawkesbury Sandstone river system, and there is no recognisable cross-basin variation in detrital composition of the Hawkesbury sandstones (Cowan 1993).

The advance of the quartzose Hawkesbury Sandstone from the craton marks the last phase of predominantly fluvial deposition in the Sydney Basin. By the early mid Triassic the Hawkesbury Sandstone blanketed the foreland basin. The overlying Mittagong Formation was deposited in swamp and fluvial overbank environments, and contains quartz sands of similar composition to the Hawkesbury Sandstone (Herbert 1980b).

The Wianamatta Group (Figure 6.5) marked the last phase of deposition directly related to the tectonic development of the Sydney Basin. The Group is believed to mark the onset of an orogenically sourced sediment pulse (Conaghan *et al* 1982; Jones *et al* 1984) with lithic sediments deposited in a single regressive episode. The Group contains vertically stacked sedimentary deposits from a succession of environments, from sub-marine to shoreline and alluvial (Herbert 1980b).

## 6.2. The Hawkesbury Sandstone.

The Anisian Hawkesbury Sandstone (Figures 6.3 & 6.5) is an essentially flat lying unit which crops out over the central Sydney Basin. The unit is 30 m thick in the west of the basin, attaining a maximum thickness of 250 m to the north (Standard 1969). The Hawkesbury Sandstone progressively oversteps older units (from the Narrabeen Group to the Illawarra Coal Measures) when traced southwest (Standard

1969). The unit is generally conformable with the overlying Mittagong Formation, although contemporaneous scour surfaces are locally developed across the upper boundary which are filled with black shales of the Mittagong Formation (Standard 1969).

During deposition of the Hawkesbury Sandstone the Sydney Basin was situated at a latitude of approximately 75° south (Embleton 1984 & Table 6.1). The climate is inferred to have been a warm temperate one (Quilty 1984) with a relatively high rainfall (Retallack 1980). The NEFB was a subdued area (Cowan 1993) and no differential subsidence occurred within the basin (Standard 1969). The LFB was uplifted by as much as 2500 m above sea level (Cowan 1993). The Hawkesbury Sandstone sediments were sourced from the uplifted LFB, and flowed north and northeastward towards the NEFB (Figure 6.7).
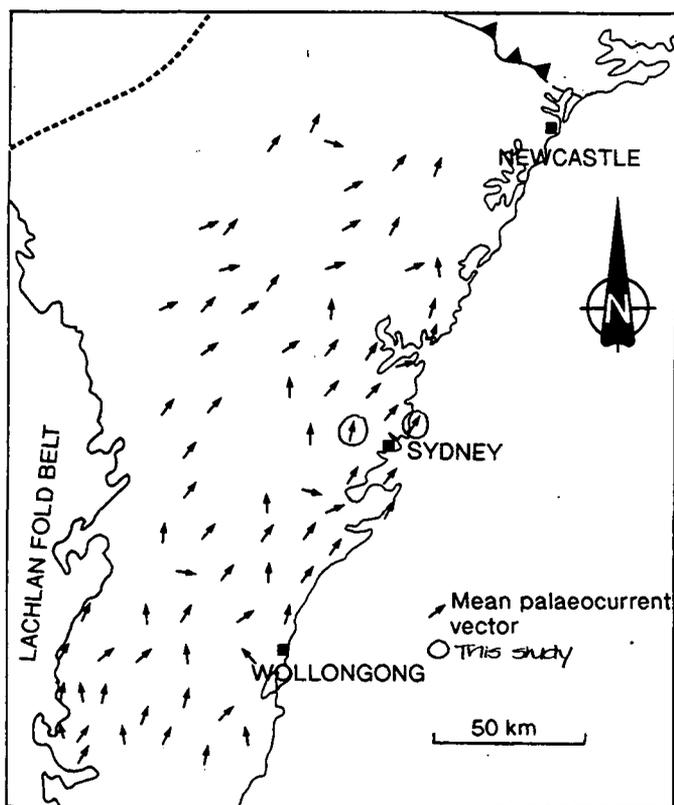


Figure 6.7. Regional palaeoflow vectors from the Hawkesbury Sandstone. Each arrow represents averaged measurements from 12 km² (Standard 1969 & this study).

The Hawkesbury Sandstone is dominated by sandstone with minor intercalations of shale and siltstone. Standard (1969) differentiated two separate source areas for the sands. The main source area lay to the southwest of the basin with a secondary source to the west. The western source area was closer to the

basin and supplied small quantities of conglomerate. The Hawkesbury Sandstone is composed of quartz arenites which are sheet-like in geometry and wedge out to the northeast (Standard 1969). Within the Hawkesbury Sandstone Conaghan & Jones (1975) identified a sheet and massive facies, which were defined on aspect from a distance. Jones & Rust (1983) re-defined this scheme to restrict the massive assemblage to structureless or faintly stratified sands.

The sheet-like cross-stratified sandstones are dominated by stacked sets of trough and planar cross-stratification, with individual set thickness ranging from the centimetre scale to over 5 m. The cross-stratified sandstones form fining-upwards units 6-23 m thick, bounded by planar to erosional surfaces, marked b y extraformational conglomerate (Rust & Jones 1987). Changes in palaeocurrent vectors between vertically adjacent depositional units have caused these depositional units to be interpreted as channel fills (Rust & Jones 1987), equivalent to the major channel (CH) architectural elements of this study.

The massive sandstone facies varies in thickness from 15-20 m and may be traced several kilometres laterally. The facies lacks internal grain size differentiation and is texturally either massive, or displays diffuse lamination. The massive sandbodies have undulose to erosional lower surfaces which display a relief of several metres. Scours or channel-like features are commonly developed along the basal surfaces and have margins which may be inclined by 85° (Conaghan 1980). These scours are generally oriented along a plane which is oblique to the palaeoflow as measured from cross-stratified sediments (Rust & Jones 1987).

The basal scours of the massive sandstone facies are commonly lined with a concentration of quartz pebbles and mudstone clasts. Mudstone clasts of 0.01-10 m diameter are also found floating within the massive sand facies (Conaghan 1980). These mudclasts are lithologically similar to the autochthonous mudstone units (Conaghan 1980) described below.

Mudstone beds account for approximately 3% of the Hawkesbury (Rust & Jones 1987). These occur as interbeds of <0.6 m thick, and as laterally extensive layers of recessive shale up to 12 m thick (Standard 1969). The thicker shales have a lenticular geometry, although Standard (1969) suggests that the units were deposited as laterally extensive layers which were later eroded. Fossils are rare in the Hawkesbury Sandstone, but have been recovered from shale lenses (Standard 1969). Plant fossils and insects, together with bivalves and fish of freshwater origin are preserved.

Conolly and Ferm (1971) initially interpreted the Hawkesbury Sandstone to be the deposit of a marine barrier/tidal delta system. However, the presence of terrestrial

biota (Retallack 1977,1980) and the absence of a marine fauna suggest a terrestrial environment of deposition. Ashley and Duncan (1977) suggested that the Hawkesbury Sandstone was as an aeolian deposit, preserved within a coastal barrier system. However, the presence of mudstone intraclasts is inconsistent with the flow reversals which occur in the shallow marine environment (Rust & Jones 1987).

The work of Standard (1969), Conaghan & Jones (1975) and Conaghan (1980) amongst others has established that the Hawkesbury Sandstone was deposited by a fluvial system. The unimodal flow direction (Figure 6.7) and stacked sets of cross-stratification have been used to infer deposition from braided streams (Standard 1969). The poorly preserved mudstone beds have been interpreted as floodplain deposits (Rust & Jones 1983).

## (i) Sedimentology Of The Study Area.

The coastal sections of the Sydney Basin offer good exposure of the Sydney Basin fill, with the area south of Broken Bay (Figure 6.2) exposing the Hawkesbury Sandstone. During this study the Hawkesbury Sandstone was studied in the area around Sydney. Laterally extensive outcrops were identified, and of these, two are discussed in detail here. Section 1 is located at the base of the Hawkesbury and Section 2 is stratigraphically near the top of the unit. A number of facies have been identified within the Hawkesbury Sandstone which are detailed below.

*Mudstone Breccia (Sb).*

This facies is locally developed and laterally restricted to scour surfaces preserved across the base of facies Sme (see below). The breccia is generally matrix supported, with the matrix being a quartzose granulestone to coarse sandstone. Clasts include angular to sub-angular mudstone and siltstone (<80 cm), sub-angular quartz (<4 mm) and graphite flakes (<5 mm). Other workers (Conaghan 1980; Rust & Jones 1987) have reported larger clasts. The clasts display both normal and inverse grading. Deformation of primary sedimentary structures within fine grained mudstone/siltstone clasts indicate that these sediments were not lithified at the time of breccia deposition.

*Giant scale cross-stratification (Sg).*

Sets take the form of both trough and planar cross-stratification which reach 5 m in thickness. The bedforms may be traced in excess of 200 m parallel to flow and over 30 m transverse to the current direction. Sets are composed of moderately sorted,

quartzose granulestone to coarse sandstone. Normal grading occurs along foresets. Rounded mudclasts, sub-angular quartz pebbles (<40 mm in diameter) and disseminated organic material are commonly concentrated in the base of foresets. Floating quartz pebbles (<10 mm in diameter) are common throughout the sets, and are sub-angular to sub-rounded.

Foresets are concave-up to sigmoidal, and dip 26-28°. Minor reactivation surfaces are preserved as changes in the angle of the foreset. However, there is no evidence of major reworking associated with low water stage, and no mud drapes or ripple modification are preserved across these bounding surfaces. Grain differentiation occurs within foresets, and takes the form of both normal and inverse grading similar to that of aeolian dunes. Intrasets are commonly preserved in the lower portion of the bedforms, and bottomsets are also developed.

*Large scale planar cross-stratification (Sp$_l$).*

Sets are 0.80 to 1.20 m thick, >100 m in length, and may be traced in excess of 30 m transverse to the flow direction. The sets are composed of moderately sorted, quartzose, coarse to very coarse sandstone. Grain differentiation occurs within foresets and may take the form of inverse or normal grading. Normal grading also occurs upwards along the foresets. Mudstone clasts (<6 mm in length) are common in the lower 30 cm of the bedforms. The clasts take the form of elongate flakes which are imbricated along the foreset surface. Quartz pebbles (<30 mm) are also concentrated in the lower portion of the set. Floating, angular to sub-angular equant quartz pebbles (<8 mm in diameter) are present throughout the sets. Graphite flakes are also locally preserved. Mica is concentrated on foreset surfaces and imparts a flaggy appearance.

Foresets are angular to gently tangential, and dip 24-28°. Slight changes in the angle of foresets indicates modification in the direction and/or strength of current flow. There is no evidence of significant reactivation surfaces.

*Large scale trough cross-stratification (St$_l$).*

Sets are developed in medium to coarse grained quartzose sandstone, and are 0.75-1.10 m thick. The trough fill is dominantly asymmetric. Foresets are well defined and normally graded. Sub-angular to sub-rounded quartz pebbles (<15 mm in diameter) and rounded mudclasts (<30 mm in diameter) are preserved in the lower portion of sets. Small changes in the angle of foresets indicate slight modifications in depositional currents. However, there is no evidence of reworking over these surfaces.

*Medium scale planar cross-stratification (Sp$_m$).*

Sets are developed in a moderately sorted quartzose, medium grained sandstone. Sets are 45-60 cm thick with tabular upper and lower contacts (first order bounding surfaces). Foresets are tangential and dip 16-20°. Normal grading is evident within some sets, and disseminated organic matter and quartz pebbles (<10 mm diameter) are commonly preserved in the lower portion of the sets. Deformation of the sets is common and takes the form of recumbently overturned foresets (Types 1 and 2 of Allen & Banks 1972).

*Medium scale trough cross-stratification (St$_m$).*

The facies is developed in medium grained, moderately well sorted, quartzose sandstone. Sets are 40-60 cm thick with scoured bases. Normal grading is common within the sets, and a lag of sub-angular quartz pebbles (<15 mm diameter) and rounded mudclasts (<30 mm diameter) is commonly preserved in the lower third of the set. The trough fill is both symmetric and asymmetric. Overturning of foresets is common, and takes the form of Types 1 and 2 of Allen & Banks (1972).

*Small scale planar & trough cross-stratification (Sp$_s$ & St$_s$).*

Sets 10-40 cm thick are developed in a moderately well sorted, medium grained quartzose sandstone. Planar cross-stratified sets are separated by sub-horizontal first order bounding surfaces and display foresets which dip 18-25°. Normal grading is commonly developed with mudchips and graphite flakes (<15 mm length) concentrated in the lower 2 cm of sets. The trough cross-stratified sets are <2.5 m across and display a symmetrical fill.

*Compound cross-stratified sandstone (Sc).*

These units are composed of moderately well sorted quartzose granulestone to coarse grained sandstone. The compound facies generally forms as the downstream extension of facies Sg or Sp$_i$. Cosets are bounded by planar second order surfaces (2B) and are 2-5 m thick. Along the basal planar surface a lag of coarser grained material is commonly preserved. Clasts are dominantly mudstone (<40 mm in diameter) with minor amounts of sub-angular to sub-rounded quartz pebbles (<15 mm in length).

Internally the compound bedforms are composed of medium and small scale trough and planar cross-stratification separated by first order bounding surfaces. Tangential foresets dip 12-15°. Intrasets are generally angular and dip 28-32°. Small changes in the flow direction and/or strength are indicated by modifications of the intrasets.

*Diffuse cross-stratified sandstone (Sd).*

This facies is developed in medium to coarse grained quartzose sands which are moderately to well sorted. The base of the facies is transitional from the massive sandstone facies (described below) and hence poorly defined. Sets are 10-40 cm thick, and are of trough and planar cross-stratification. Foresets are poorly preserved and take the form of tangential forms which dip 10-20°. Deformation is common, and takes the form of Types 1 and 2 of Allen & Banks (1972).

*Low angle cross-stratification (Sl).*

Rare sets of this facies are developed in very coarse to fine grained, moderately well sorted, quartzose sandstone. Depositional surfaces dip at approximately 5-10°, oblique to the palaeoflow direction established from Sp and St cross-stratification. The foreset surfaces are generally coated with a concentration of mica flakes, and have a flaggy appearance. Normal grading of sediment occurs upwards through the set with mudclasts (<5 mm) and quartz granules preserved in the lower portion.

*Erosively based massive sandstone sheet (Sme).*

The massive sandstone facies is laterally extensive and volumetrically important. Individual units of the massive sandstone facies reach 6 m in thickness. Units of facies Sme are often amalgamated to form thick, laterally extensive sheets which may reach over 20 m in thickness, and which can be traced laterally in excess of 500 m.

Facies Sme is composed of a very coarse to medium grained, predominantly structureless quartzose sandstone. Mudclasts are present throughout massive sandstone units and may reach 80 cm in diameter. These sub-angular to rounded clasts appear to float in a matrix of sandstone. Sub-angular to sub-rounded quartz granules (<5 mm) are also present throughout the massive sandstone beds. Elongate flakes of graphite and mudstone (<5 mm) are present in large volumes.

The basal surface of facies Sme is commonly undulose to erosive. Channel-like features are developed across the lower surface which display a relief of up to 5 m. The channels have sharply defined margins which may lie parallel with the foresets of cross-stratified sediments (i.e. dip <28°) or be steeper and cut through pre-existing cross-stratification (dip <48°). Elongation of channels occurs in orientations both perpendicular to, and near parallel with the palaeoflow, as established from cross-stratification. Within the scoured areas facies Sb (described above) may be preserved. Where facies Sb is absent scour surfaces are marked by slight changes in sandstone texture, or by the presence of a basal lag of quartz granules.

Concentric laminae 5-50 mm apart are commonly developed parallel to the basal scours of facies Sme. These dip <48°, mirroring the scour margins. The laminae are developed due to the presence of mudstone and carbonaceous flakes. The elongate flakes also appear to pick out poorly defined diffuse structures within the massive sandstone units which take the form of sweeping trough-like laminae of <2 m in thickness.

*Fine grained sediments (Fx & Fm).*

The fine grained units of the Hawkesbury Sandstone are dominantly organic rich, micaceous siltstones and mudstones. These beds are laterally restricted to <50 cm and reach 20 cm in thickness. The sediments are most commonly rippled (facies Fx). Where ripples are developed these are approximately 20-30 mm high, and asymmetric with rounded crests.

## (ii) Lateral Profile Analysis.

*Section 1.*

Section 1 consists of coastal exposures at Dee Why Head (Figure 6.2), with laterally extensive sections both perpendicular and parallel to the palaeoflow direction. For ease the section has been split into two separate lateral profiles termed 1a and 1b.

*Section 1a.*

Section 1a is approximately 350 m long and 10 m high. A lateral profile of the section is illustrated in Figure 6.8, and a vertical profile is given in Figure 6.9. At the southeast of section 1a the base of the Hawkesbury Sandstone is marked by a fifth order bounding surface which can be traced for a short distance northwestward before being lost in beach sand (Figure 6.8).

The basal 15 m of the Hawkesbury Sandstone exposed in section 1a consists of amalgamated sheets of facies Sme (Figures 6.8 & 6.9), with minor developments of facies Sb, Sd, Sp$_s$ and St$_s$. These combine to form SM Type 3 architectural elements (Table 2.6).

Individual SM Type 3 elements vary between 50 cm and 11.40 m thick, and are separated by erosional third order bounding surfaces. Thus each SM Type 3 element is a macroform scale deposit. The SM Type 3 elements can be traced laterally

NW

ORIENTATION N128/308°    ORIENTATION N170/350°    ORIENTATION N022/202°

Mesoform II

n=20

Mesoform I

n=16

N

Facies Sme scour axes

n=7

ORIENTATION N146/326°    SE

Plan View

10 m

Figure 6.8. A line drawing of Section 1a, Hawkesbury Sandstone. Reproduced from distortion-free photographs. *Lat. 151° 18′ 15″, Long 33° 48′ 30″*

217
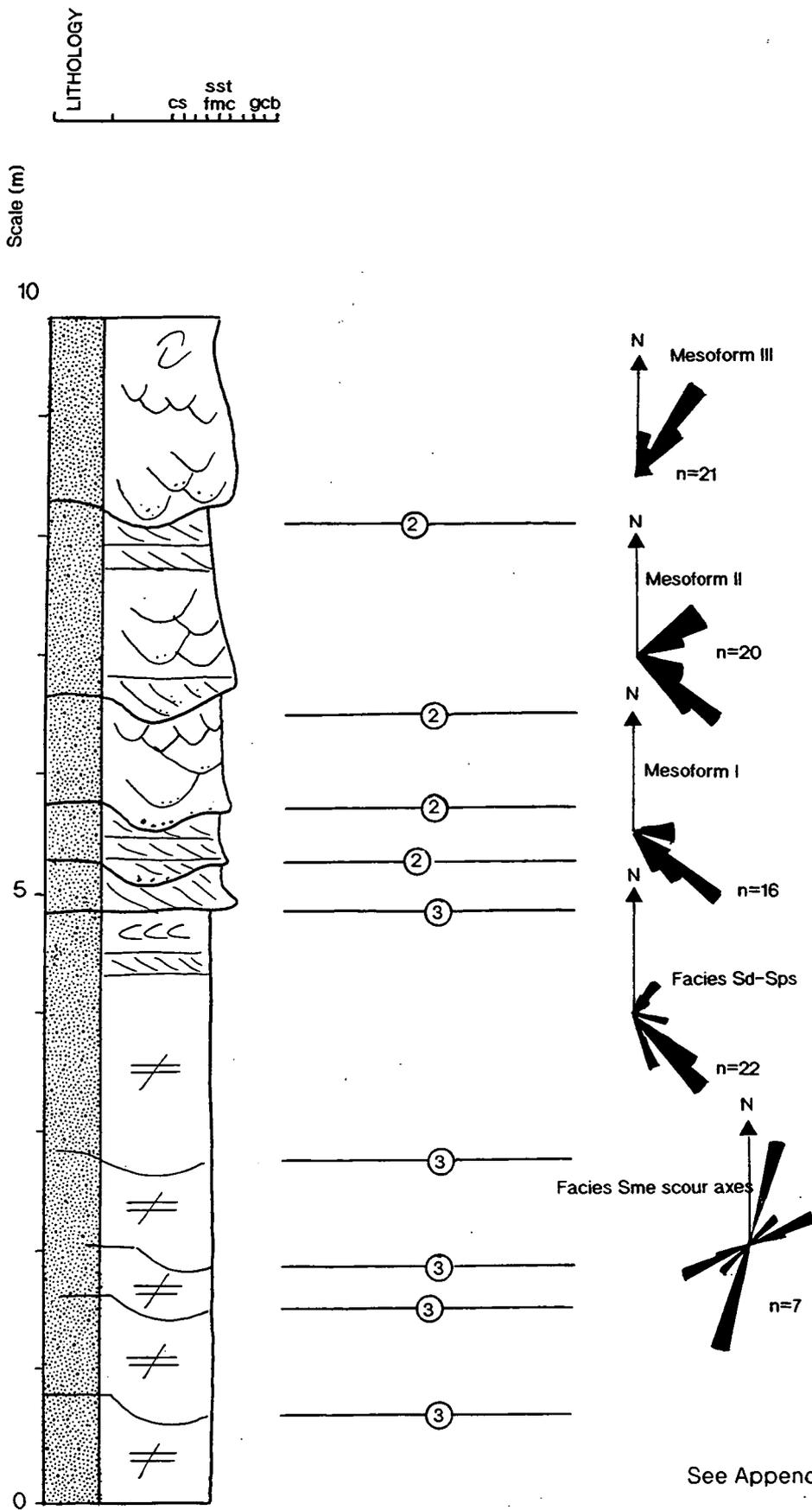
Figure 6.9. A sedimentary log of Section 1a, Hawkesbury Sandstone.

See Appendix I for logging symbols

for up to 50 m, but generally are cut out laterally (<20 m) due to the erosional nature of the lower bounding surfaces.

Channel-like scours are developed on the lower bounding surfaces of the elements (Plates 6.1 & 6.2), which have a relief of up to 7m (Figure 6.8). The margins of the channel-like features dip 30-48° (Figures 6.8 & 6.9). Measurements of scour axes orientation are illustrated in Figures 6.8 and 6.9. The scours are elongated along planes oriented northeast to southeast, i.e. parallel to the regional palaeoslope (Figure 6.7).



*Plate 6.1. Facies Sme. Section 1a, Hawkesbury Sandstone.*
*Scale represents 1 m. A large scour surface is developed in the base of a SM Type 3 architectural element. The scour margins dip 28°. Internally the scour preserves concentric laminae and mudclasts (<5 mm diameter) parallel to the margins. These grade into a massive sandstone fill.*
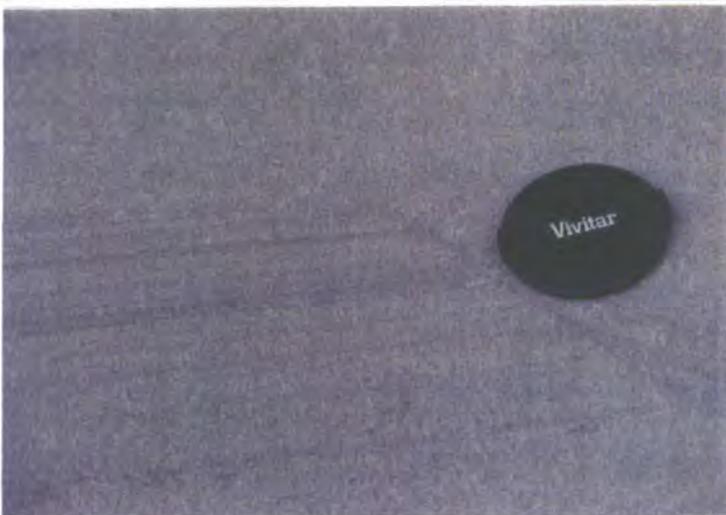


*Plate 6.2. Basal scours of facies Sme. Section 1a, Hawkesbury Sandstone.*
*Facies Sme is represented by a medium to coarse grained sandstone which contains graphite and mudchips <5 mm. The elongate flakes pick out vague structures in facies Sme. The base of facies Sme is represent by a scour surface coated by quartz granules. The erosional contact is defined by truncation of the underlying laminae.*

Facies Sb is locally preserved along the basal scours of SM Type 3 elements, with sub-angular to rounded mudclasts reaching 60 cm in diameter (Plate 6.3). Facies Sb displays both normal and inverse grading. Where facies Sb is not preserved concentric laminae are clearly developed at the margins of scours (Plate 6.2).



*Plate 6.3. Fifth order bounding surface, base of Hawkesbury Sandstone, Section 1a. Facies Sme overlies the finely interbedded sandstones and mudstones of the Narrabeen Group. The basal scour of facies Sme is coated by a unit of facies Sb. Angular to sub-rounded mudclasts < 60 cm diameter are preserved within a matrix supported breccia. Grading is chaotic.*

Facies Sme is composed of medium to coarse grained, quartzose sandstone. Flakes of mudstone and graphite are present in large volumes. The flakes are aligned parallel to basal scour surfaces, and pick out vague banding within the facies (Plates 6.2 & 6.4). However, there are no recognisable changes in sandstone texture associated with the banding developed by the intraclasts.

Within individual SM Type 3 architectural elements facies Sme is overlain by facies Sd and $Sp_S/St_S$ (Plate 6.5). These cross-stratified units display palaeocurrents to the southeast, a direction oblique to the regional palaeoslope (Figure 6.7). Foresets are commonly deformed (Types 1 and 2 of Allen & Banks 1972).

Overlying the SM Type 3 architectural elements are a series of structured sediments (Plate 6.5). These sediments are composed of SB Type 1 architectural elements, showing an upward decrease in sets size associated with deposition during waning flow conditions. Mesoforms are separated by second order bounding surfaces (Figure 6.9). Palaeocurrents measured from the mesoforms display a progressive upward swing in flow direction from the southeast to northeast (Figure 6.9). Thus the palaeoflow rotates towards a direction parallel to the regional palaeoslope (Figure 6.7).

*Plate 6.4. Facies Sme. Section 1a, Hawkesbury Sandstone.*
*Two superimposed units of facies Sme are preserved in this section. Facies Sme is*
*composed of a medium to coarse grained quartzose sandstone which contains small*
*mudchips and graphite flakes. The basal unit contains mudchips which define crude*
*stratification. The contact between the two units is sharply defined with a small*
*development of quartz granules preserved along this surface.*



*Plate 6.5. Amalgamated units of facies Sme overlain by SB Type 1 architectural*
*elements. Scale represents 1 m.*
*The lower portion of the outcrop is composed of a number of superimposed units of*
*facies Sme. These may be distinguished by the development of a thin layer (<5 mm)*
*containing quartz granules and mudchips. The uppermost unit of facies Sme passes*
*upwards into facies Sd. The sheet of facies Sme is overlain by a sharply defined third*
*order bounding surface which is in turn overlain by a number of SB Type 1*
*architectural elements separated by second order bounding surfaces.*

*Section 1b.*

Section 1b is approximately 100 m long and 15 m high (Figure 6.10). Figure
6.11 gives a generalised vertical profile. Within the base of section 1b the fifth order
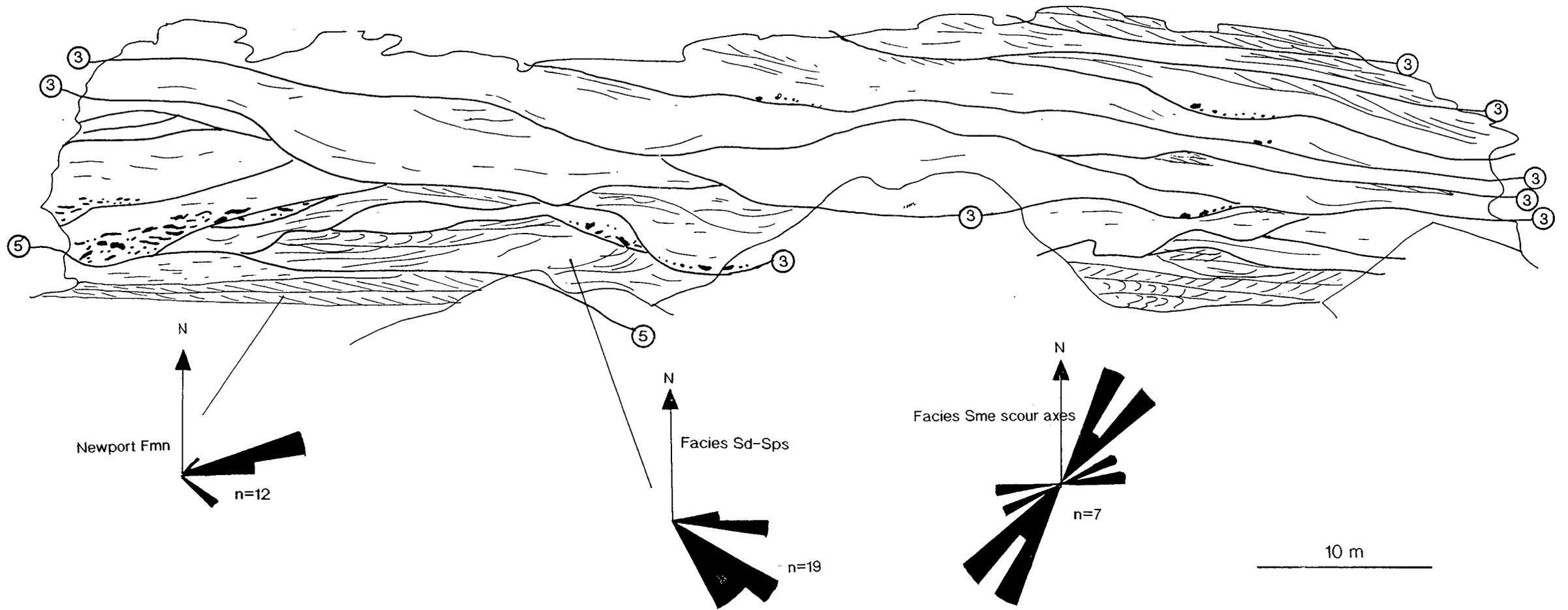
Figure 6.10 A line drawing of Section 1b, Hawkesbury Sandstone. Reproduced from distortion-free photographs. Lat. 151° 18' 15", Long 33° 48' 30".
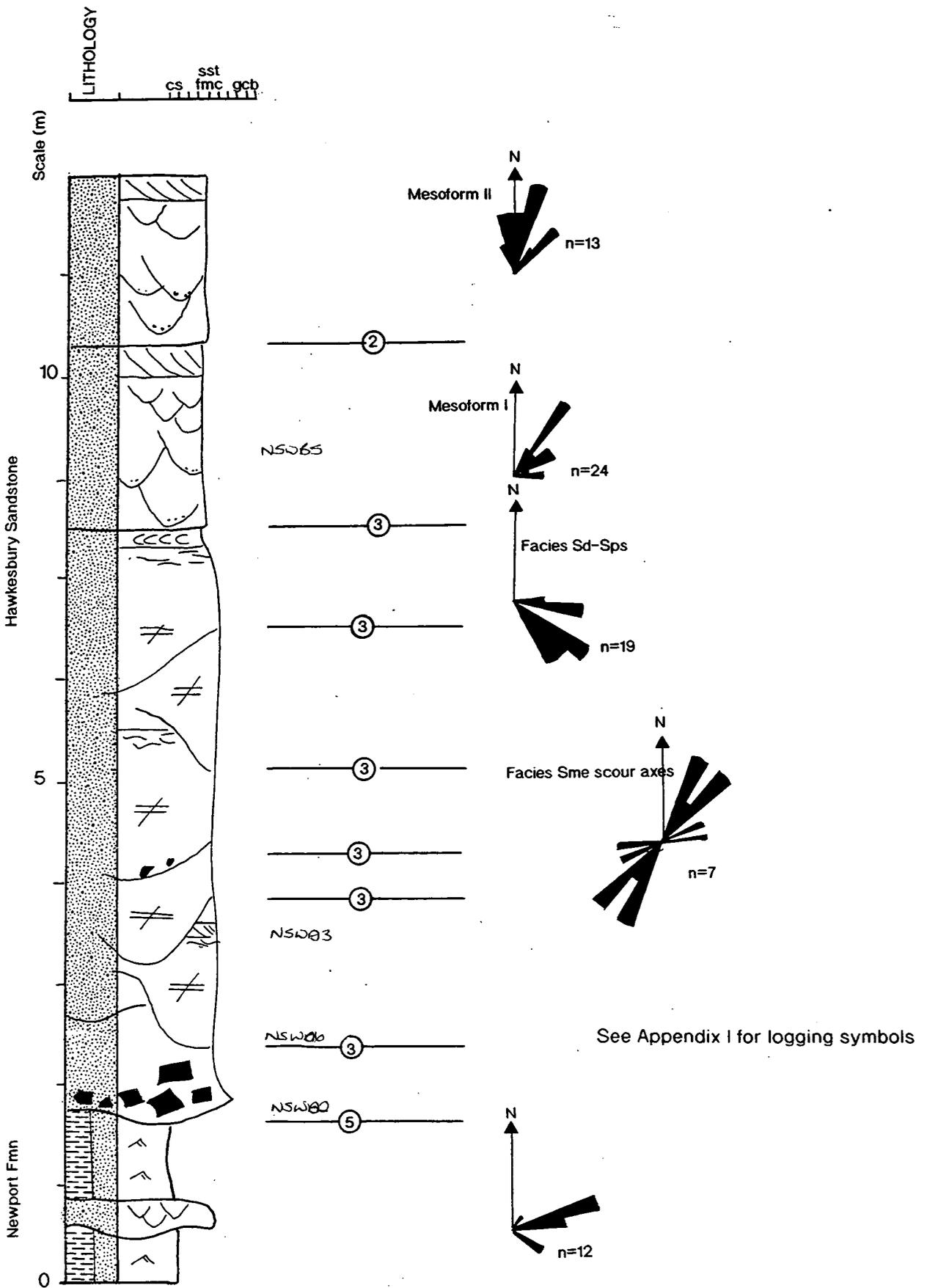
*Figure 6.11. A sedimentary log of Section 1b, Hawkesbury Sandstone.*

bounding surface marking the base of the Hawkesbury Sandstone is preserved (Plate 6.3).

Over the fifth order bounding surface amalgamated SM Type 3 architectural elements are preserved (Figures 6.10 & 6.11). These elements vary between 0.30-5 m in thickness and may be traced laterally between 1 m and 75 m. Individual SM Type 3 elements display scoured bases. The elongation orientation of individual scours is illustrated in Figures 6.10 and 6.11. The scours define a plane oriented northeast to southwest which is parallel to the regional palaeoslope.

Facies Sb is commonly preserved along the scours (Figure 6.11) and contains sub-angular mudclasts up to 50 cm in length. The clasts are generally composed of parallel laminated mudstone and siltstone. Deformation of the primary sedimentary fabric within clasts (Plate 6.6) and smearing of mudchips (Plate 6.6) indicates shearing of the sediment flow. The clasts were therefore not lithified when deposited within the breccia. Deformation of intraclasts indicates flow was to the northeast (Plate 6.6).



Plate 6.6. Facies Sme. Section 1b, Hawkesbury Sandstone.
Facies Sb is preserved within the basal scour of a SM Type 3 architectural element. Facies Sb is composed of a matrix supported breccia. Clasts are < 30 cm in diameter. The interbedded fine sandstone/mudstone clast displays evidence of deformation of the primary depositional fabric. Smaller mudclasts show evidence of smearing. These deformation structures indicate shearing of the flow within which these casts were transported. Flow was towards the northeast.

Where facies Sb is absent scour surfaces are commonly marked by a lag of quartz granules (Figure 6.11, Plate 6.7). Facies Sme is composed of a medium grained quartzose sandstone which contains a high proportion of mud and graphite flakes <5 mm in length. These pick out sweeping trough-like forms within the sandstone.

*Plate 6.7. Contact between facies Sme bodies, Section 1b, Hawkesbury Sandstone. Two units of facies Sme are illustrated which show no visible structure. The facies are separated by a layer of quartz granules and mudclasts.*

Facies Sd, $Sp_s$ and $St_s$ are preserved within the upper portion of the SM Type 3 elements (Figures 6.10 & 6.11; Plate 6.8). The contact between facies Sme and Sd is transitional and poorly defined. The structured sediments of facies $Sp_S$ and $St_S$ display palaeocurrents to the east and southeast. The foresets commonly display Types 1 and 2 deformation of Allen & Banks (1972), as illustrated in Plate 6.8.
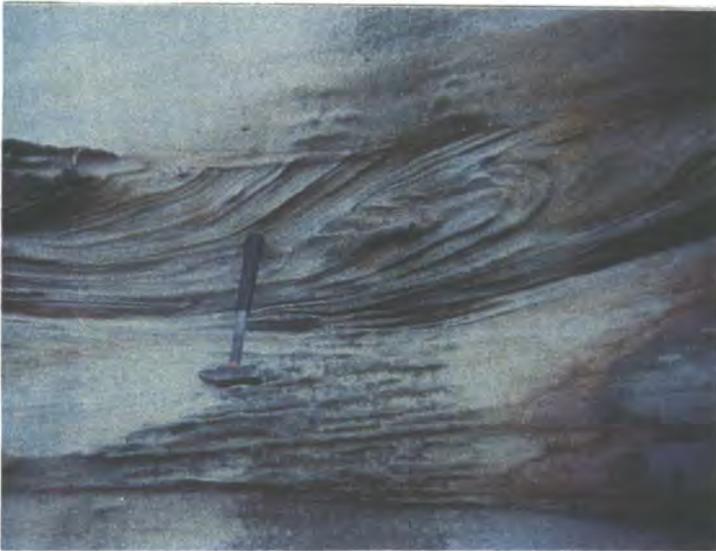


*Plate 6.8. Facies Sme-Sd-Sps-Sme. Section 1b, Hawkesbury Sandstone. A lower unit of facies Sme grades upwards into facies Sd. The overlying sets of facies Sps are deformed (Type 2 of Allen & Banks 1972). The structured sediments are cut out by a successive unit of facies Sme. The base of facies Sme is sharply defined and lined by a lag of quartz granules. Concentric laminae are preserved along the basal surface of facies Sme. These grade into a structureless sandstone.*

Overlying the amalgamated SM Type 3 elements are cross-stratified sandstones of facies $Sp_m$ $St_m$ and $Sp_s$ arranged in SB Type 1 architectural elements separated by second order bounding surfaces. The mesoform scale elements display palaeocurrents towards the northeast and north (Figure 6.11).

The scoured basal surfaces of SM Type 3 elements within section 1 of the Hawkesbury Sandstone describe planes which are oriented northeast/southwest (Figures 6.9 & 6.11). Shear indicators within mudclasts of facies Sb indicate that flow within the elements was to the northeast (Plate 6.6) and hence parallel to the regional palaeoslope as defined by Standard (1969). Facies Sd preserved in the upper portion of SM Type 3 architectural elements display palaeoflow towards the northeast and southeast (Figure 6.9 & 6.11). Cross-stratification of SB Type 1 architectural elements displays flow to the north and northeast which is also parallel to the regional palaeoslope (Figure 6.7).


*Section 2.*

Section 2 is located in the upper Hawkesbury Sandstone along the Parramatta River and Burnsbay Road north of Sydney (Figure 6.2). The vertical profile illustrated in Figure 6.12 has been constructed from two outcrops, of which the upper outcrop, a road cutting, is illustrated as Figure 6.13. The lateral profile of Figure 6.13 is approximately 230 m long and 12 m high. The section is oriented parallel to palaeoflow, with smaller outcrops allowing for inspection of sediments perpendicular to the flow direction.

Within the base of the line drawn section Macroform I is preserved (Plate 6.9) which is composed of a DA Type 1 architectural element (Figures 6.12 & 6.13). Facies $Sp_l$ is developed in a moderately sorted quartz arenite, with quartz granules and mudclasts concentrated on the upper surface of foresets, indicating inverse grading (Plate 6.10). Downstream facies $Sp_l$ evolves into Sc (Figure 6.13). The compound cross-stratified bedform is poorly preserved due to an overlying erosional third order bounding surface. Palaeoflow within the element is to the east and variance is low (Figures 6.12 & 6.13).

Macroform II is composed of a SM Type 3 architectural element (Figures 6.12 & 6.13). The basal third order bounding surface is erosive with a relief of at least 1.85 m (Figure 6.13). Channel-like scours are developed which cut through facies $Sp_l$ and Sc causing little disruption of foresets (Plate 6.9). The angle of the scour margins reaches 45°, although locally margins lie parallel to the foresets of facies $Sp_l$ (Figure 6.13). Scours were emplaced along a plane oriented northwest/southeast (Figure 6.13).
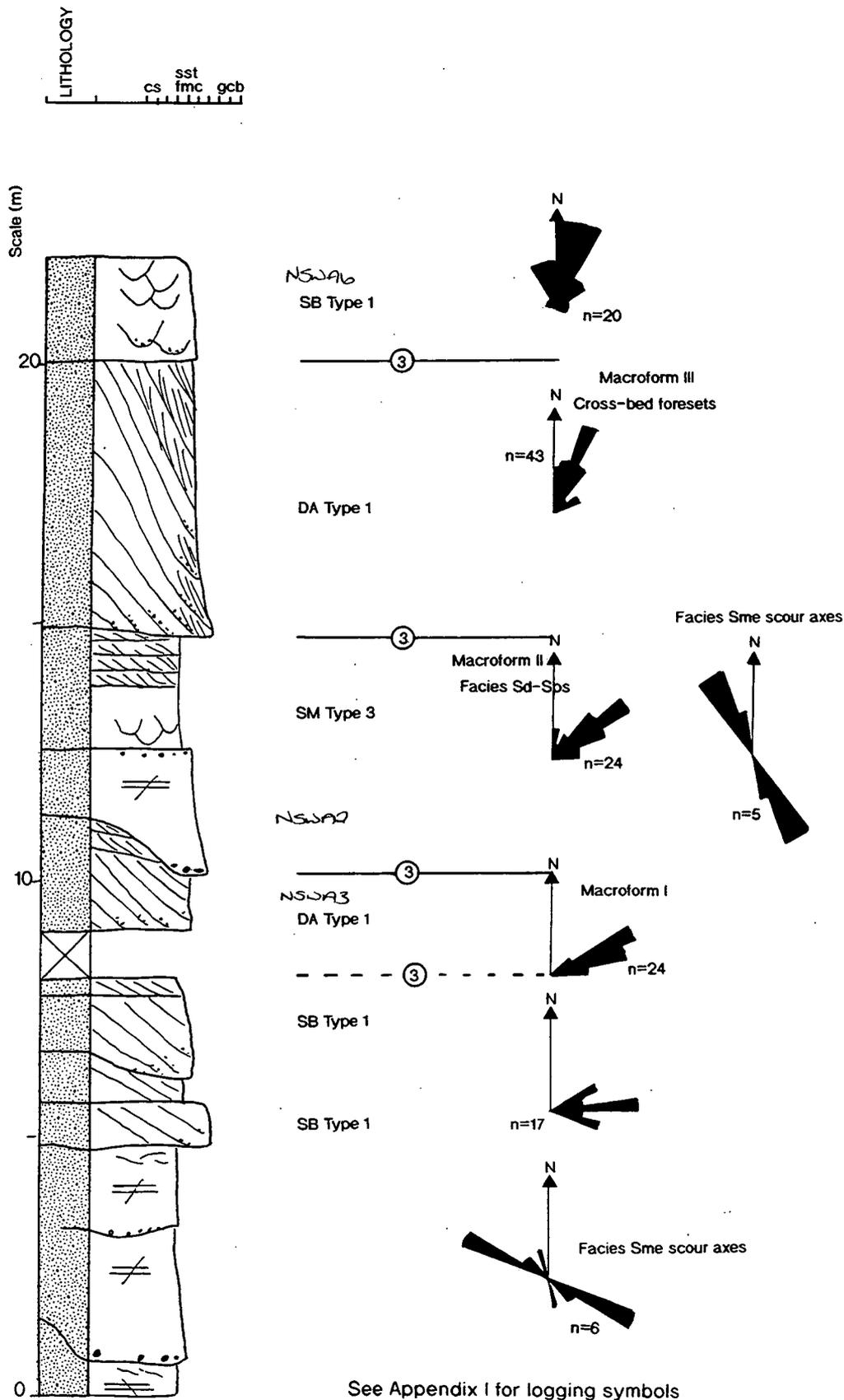
*Figure 6.12. A . A sedimentary log of Section 2, Hawkesbury Sandstone.*

NE

ORIENTATION N042/222°

Macroform III

DA Type 1

N
Cross-bed foresets

n=43

N
Cross-bed intrasets

n=19

20 m
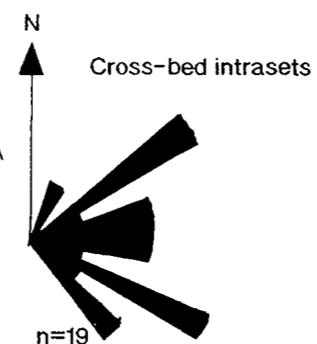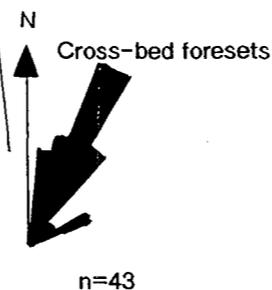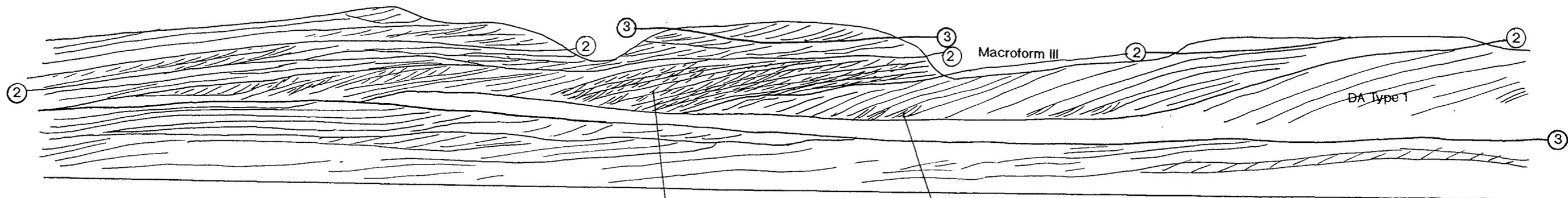
ORIENTATION N042/222°

ORIENTATION N060/210°

SW

Macroform III

Macroform II

DA Type 1

Macroform I

N
Facies Sd-Sps

n=24

N
Facies Sme scour axes

n=5

N

n=24
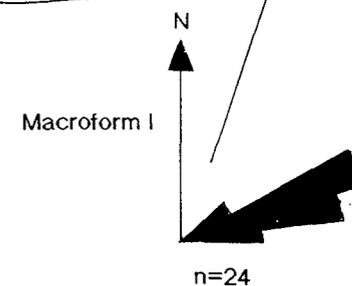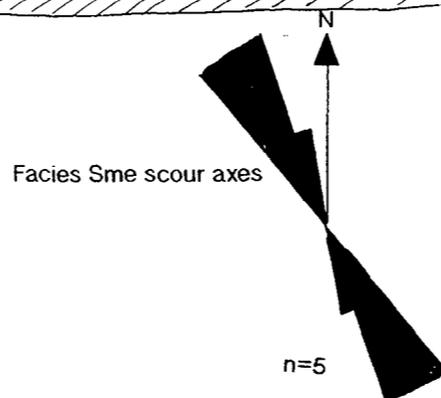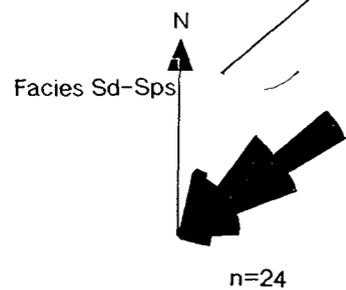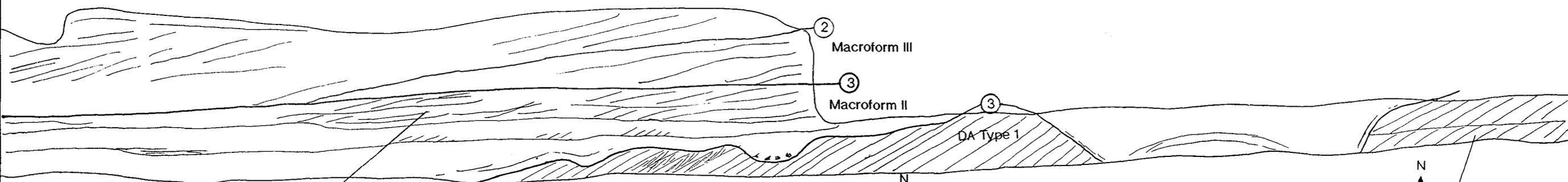
Figure 6.13. A line drawing of Section 2, Hawkesbury Sandstone, reproduced from distortion-free photographs. Lat. 151° 05' 44", Long. 33° 49' 50".

228

Plate 6.9. Facies Spl & Sme. Section 2, Hawkesbury Sandstone. Scale represents 1 m.
Macroform I is represented by a unit of facies Spl. Foresets are difficult to distinguish here. The structured sediments are cut out by a unit of facies Sme. A scour is developed along the lower surface of the facies which is elongate in a plane perpendicular to that of this picture. The margins of the scour dip 45°(upstream) and 38° (downstream).



Plate 6.10. Facies Spl. Section 2, Hawkesbury Sandstone.
Inverse and normal grading are defined here within foresets of facies Spl. Inverse grading is developed due to grain flow (Lowe 1976a) and is generally preserved within aeolian sand dunes.

Facies Sb is locally developed within the base of scours (Figure 6.13). The facies takes the form of a 15 cm thick layer of matrix supported breccia. The matrix is formed of coarse sandstone to granulestone, which contains sub-angular quartz pebbles (<30 mm) and angular to sub-rounded mudclasts (<85 mm).

Facies Sme is a moderately to well sorted coarse sandstone. Within the facies floating sub-angular to sub-rounded quartz granules are common. The sandstone also contains a large quantity of lath shaped mud flakes and graphite chips. Within facies Sme mudchips may indicate surfaces of crude stratification (Figure 6.13). Where facies Sb is not preserved along scoured horizons concentric laminae are developed parallel to the scour surface. These are 19-40 mm apart and defined by elongate flakes. Internal scour surfaces within facies Sme are suggested by thin mudclast-rich horizons (Figure 6.13).

Facies Sme grades upwards into facies Sd which is abruptly overlain by facies Sp$_s$ and St$_s$ (Figure 6.12 & Plate 6.11). The bounding surface between the faintly structured and cross-stratified sediments is undulose to planar, and marked by a mudstone rich layer of 10-15 cm thick. Mudclasts reach 40 mm in diameter. Facies Sp$_s$ and St$_s$ are composed of medium to fine grained sandstone with the grain size decreasing overall up through the section. Palaeocurrents are oriented towards the northeast (Figure 6.12).
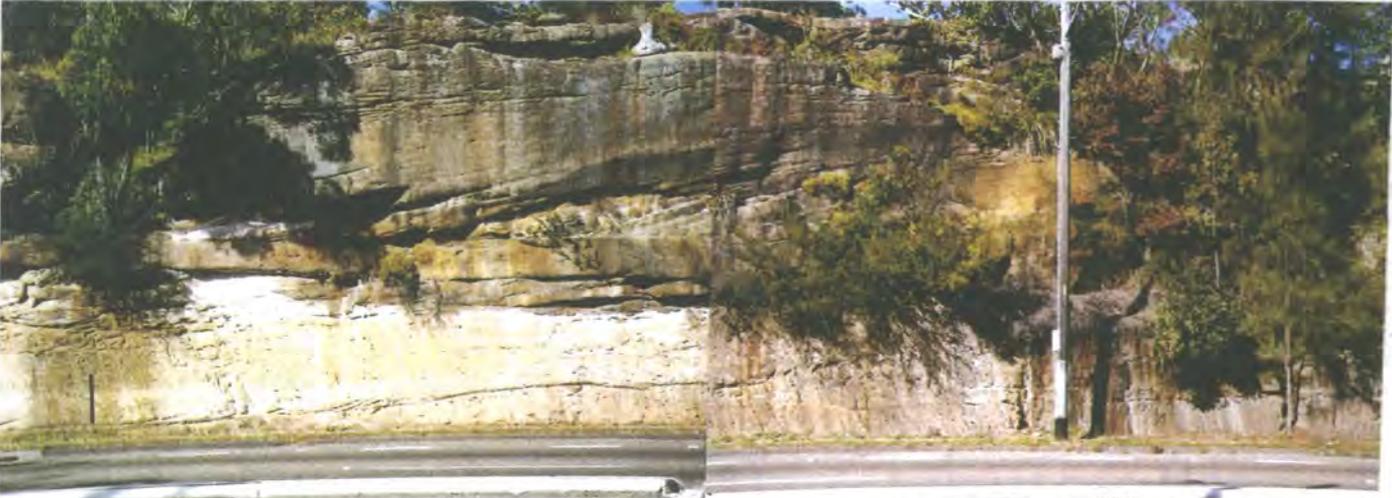


Plate 6.11. SM Type 3 architectural element overlain by a DA Type 1 element. Section 2, Hawkesbury Sandstone. Scale represents 1 m.
The basal macroform of this section is composed of a SM Type 3 element (facies Sme-Sd-Sps/Sts). The unit is bounded by a third order bounding surface which is overlain by Macroform III (Figures 6.12 & 6.13). The DA Type 1 architectural element is complex. In the upstream direction low angle foresets are developed. These steepen downstream and contain intrasets. Bottomsets are well developed. Facies Spl evolves into a unit of facies Sc.

Macroform III (Figures 6.12 & 6.13) consists of a DA Type 1 architectural element composed of coarse to medium grained quartzose sandstone. The DA Type 1 element displays a complex internal organisation of facies (Plate 6.11). Upstream, facies Sg is preserved with poorly developed foresets dipping 8-10° in the downstream direction. Slump structures appear to be developed along the foresets

(Figure 6.13). Progressively downstream the foresets become more clearly defined, and facies Sg is preserved. The Sg set reaches 5 m thick with individual foresets 60 cm thick. The foresets are tangential to concave up, and display both normal and inverse grading. Mica is often concentrated along the foresets resulting in a flaggy appearance. Bottomsets are preserved (Figure 6.13 & Plate 6.11). Palaeocurrent indicators from cross-bed foresets within Macroform III are to the northeast and display low variance. Intrasets are developed around the toes of the foresets, and these display a higher palaeocurrent deviation than that of the foresets (Figure 6.13).

Downstream, facies Sg develops into facies Sc (Figure 6.13 & Plate 6.11). Internally the Sc bedform displays low angle surfaces of reactivation indicating minor changes in hydrodynamic conditions during sedimentation. These are illustrated as second order bounding surfaces in Figure 6.13. There is no evidence of reworking across these second order bounding surfaces.

Overlying the DA Type 1 element a third order bounding surface is developed which is in turn overlain by SB Type 1 architectural elements (Figure 6.12). The elements consists of facies St$_m$ and St$_s$ which are arranged in a coset displaying an upward decrease in set size. Palaeoflow was to the north (Figure 6.12).

In section 2 of the Hawkesbury Sandstone SM Type 3 architectural elements display scoured bases which are elongate in a plane oriented northwest/southeast (Figures 6.12 & 6.13), i.e. oblique to palaeoflow as established from cross-stratification.

Complete major channel (CH) architectural elements have not been identified within the Hawkesbury Sandstone during this study. The low angle dipping erosional surfaces described by Friend (1983) and Allen (1983) as indicative of channel margins, relating to deposition in a low sinuosity fluvial system have also not been identified.

(iii) Petrology & Textural Characteristics.

A small representative suite of samples was taken from the two sections studied. Thirteen samples were used for this study, and these represent all the sandstone facies preserved within the two sections described above.

*Textural information and grain size analysis.*

Sandstone samples used for grain size analysis were divided into cross-stratified facies, facies Sme and Sd. The techniques used to quantify grain size are detailed in Appendix III.

The grain size distribution curves measured from the sandstone samples are illustrated in Figure 6.14. A clear differentiation of grain size distribution between facies is illustrated in Figure 6.14.
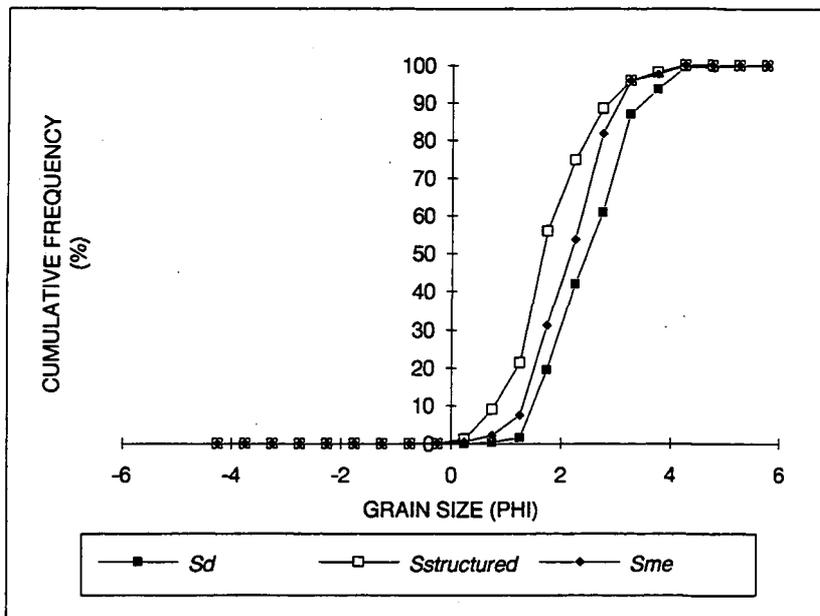


*Figure 6.14. Cumulative frequency curves of grain size distribution within the Hawkesbury Sandstone.*

The median grain size of the cross-stratified facies varies between 1.55-2.55$\phi$ with a mean of 1.9$\phi$. The median grain size of facies Sme is between 2-2.7$\phi$ with a mean of 2.4$\phi$, and the median grain size of facies Sd varies between 2.32-3.32$\phi$ with a mean of 2.6$\phi$ (see Appendix III for detail). Thus the structured facies measured in this study may be termed medium grained, with facies Sme and Sd fine grained. These sediment samples clearly represent the finer grained portions of the Hawkesbury Sandstone, as the field studies described above reveal that the majority of sediments are of a coarser grain size.

The structured sandstones and facies Sme are moderately sorted, and the sandstones of facies Sd are moderately well sorted (see Appendix III). The primary porosity of the sandstone facies has been assessed through point counting. The porosity of the structured sands varies between 4.6-6% with a mean of 5%. The sandstones of facies Sme vary between 0.3-5% porosity with a mean of 2.3%. The sandstones of facies Sd have an average primary porosity of 4.5% (see Appendix III). Thus, there is a clear differentiation in primary porosity between the sandstone facies of the Hawkesbury Sandstone as defined within this study with facies Sme displaying significantly reduced values compared with those of the structured sandstones.

The packing of sandstones within the Hawkesbury has been estimated through use of the compaction index (CI) outlined in Appendix III. The cross-stratified sandstones display average CI values of 3.4. Facies Sd and Sme have CI values of 3.2 and 3.5 respectively.

*Composition.*

Figures 6.15a & b detail the composition of the sandstone samples collected from the Hawkesbury Sandstone. Figure 6.15a details sandstone composition after Folk (1980). The structured sandstones are classified as quartz arenites with facies Sme and Sd classified as quartz arenites and sub-litharenites. Figure 6.15b details sandstone provenance using the Qm-F-Lt plot of Dickinson (1985). The structured sandstone facies clearly plot in the cratonic province with the sandstones of facies Sme plotting in the recycled orogen province. Facies Sd samples are transitionary between these two end members.
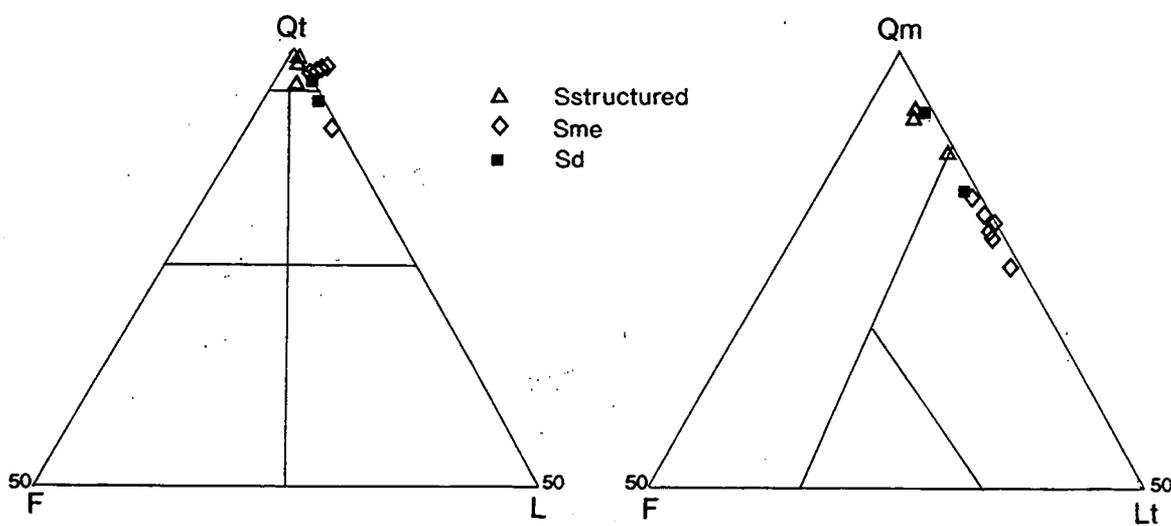


Figure 6.15a. Modal compositional data
from the Hawkesbury Sandstone
(after Folk 1980).

Figure 6.15b. Provenance data
from the Hawkesbury Sandstone
(after Dickinson 1985).

All the sections studied are dominated by monocrystalline quartz which displays dominantly straight extinction (Plate 6.12). Grains with undulose extinction are preserved, and these are more common in facies Sme. The detrital quartz grains are sub-angular to sub-rounded (Plate 6.12). Sub-rounded polycrystalline quartz granules and sand sized grains are largely restricted to the Sme facies. Polycrystalline quartz grains display internally sutured contacts indicating a metamorphic source (Plate 6.12).
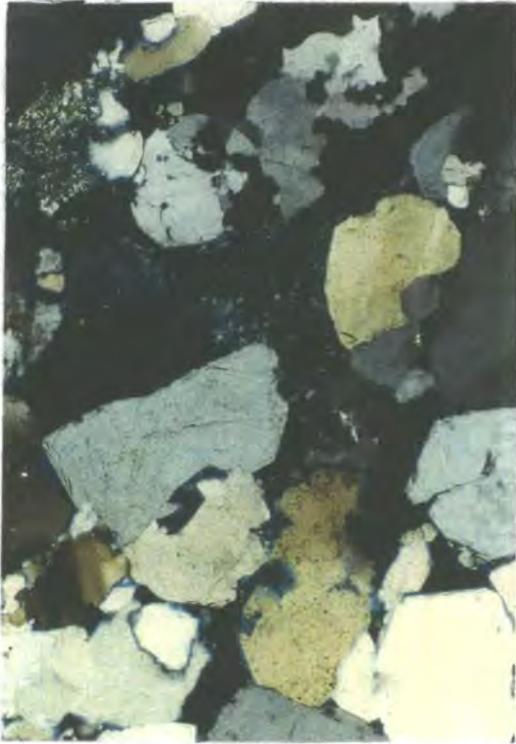


Plate 6.12.                                   Plate 6.13.
*Facies Sp. Hawkesbury Sandstone. Field of view 3.25 mm.*
*Section is dominated by monocrystalline quartz with straight and undulose extinction. A larger granule is polycrystalline. Detrital quartz grains are sub-angular to sub-rounded. Contacts between detrital grains are floating or point. Authigenic quartz overgrowths are extensive, resulting in planar contacts. Kaolinite fills some pore spaces, otherwise the section is largely clean. Dissolution of framework grains has resulted in the development of oversized pores.*

Lithic fragments are uncommon within all samples. A small number of lithic grains of extraformational origin were found within all sandstone facies. Facies Sme and Sd contain a higher percentage of these (Appendix III). The grains are sub-rounded to rounded in shape and generally equant. Recognisable rock fragments include quartz mica schist. Silt and shale clasts of syn-sedimentary origin are preserved within facies Sme and Sd. These clasts have been deformed during compaction and take the form of a pseudomatrix. Feldspar grains are very rare (Appendix III). Highly altered grains of microcline are found in some sections.

Mica is present in large quantities, particularly in facies Sme and Sd (Appendix III). The mica is predominantly muscovite (Plate 6.14), and takes the form of flakes and large laths. Leached biotite is present in some sections. The micas are commonly altered as described below.
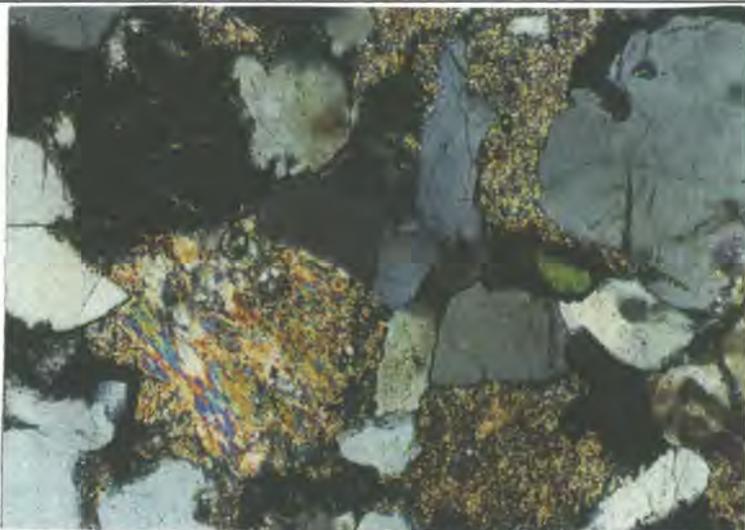


Plate 6.14. Facies Sme, Hawkesbury Sandstone. Field of view 1.5 mm. Sub-angular to sub-rounded mono- and polycrystalline quartz grains display poorly developed authigenic overgrowths. Dissolution of muscovite has resulted in the development of fine grained illitic clays over the section. The presence of clays has inhibited authigenic quartz overgrowths. Continued dissolution of labile grains has resulted in oversize pores.

The heavy mineral fraction of sandstone samples has been analysed to aid provenance studies. The sandstones studied were chosen because of their similar grain size (Appendix IV). Point counting showed that the heavy minerals were found to be more common in facies Sme than in the structured sediments (Appendix III). However study of the separated heavy fraction revealed that there was no apparent difference in heavy mineral species between facies. Rounded zircon together with sub-rounded tourmaline and rutile are ubiquitous within the sandstones. Sub-angular to sub-rounded grains of lazulite, haematite, andradite (garnet), siderite and brookite were also common phases (Appendix IV), particularly in facies Sme. Opaque detrital grains were dominated by intergrowths of magnetite and illmenite.

*Diagenesis.*

The diagenetic sequence of events within the Hawkesbury Sandstone appears to be complex, with the relative timing and importance of mineral phases differing between facies. The major diagenetic phases are authigenic quartz, illite, kaolinite and pyrite. The generalised sequence of events displayed in all facies is illustrated in Figure 6.16.

| Diagenetic phase | Early | Late |
|---|---|---|
| Quartz precipitation | — ——————————————— | |
| Pyrite precipitation | —— | |
| Illite precipitation | ———— | —— |
| Labile grain dissolution | ———————————— – – – – – – | |
| Kaolinite precipitation | ———————— | |

*Figure 6.16. The diagenetic sequence within the sandstone facies of the Hawkesbury Sandstone.*

Authigenic quartz cementation was initiated early during burial, and continued intermittently (Figure 6.16). In the structured facies authigenic quartz forms well developed overgrowths with long contacts between overgrowths (Plates 6.13 & 6.15). However, where detrital grain margins can be discerned, it is apparent that the detrital quartz grains are not in contact. Therefore the source for the quartz cement was not through pressure solution of the detrital grains. In facies Sme and Sd quartz cementation is less well developed (Plate 6.14).
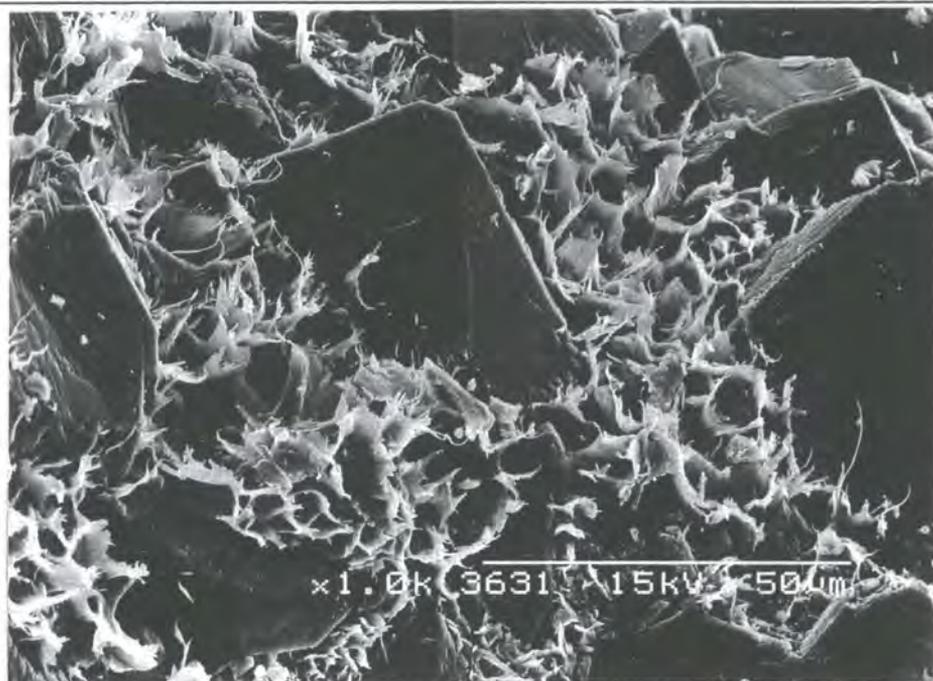


*Plate 6.15. Facies St. Hawkesbury Sandstone.*
*Well developed authigenic quartz overgrowths are developed in open pore spaces. The quartz faces are coated with diagenetic illite.*

The dissolution of unstable framework grains was a continuous process through diagenesis (Figure 6.16). Illite and pyrite are found replacing lithic grains (Plate 6.16). Pyrite forms an early diagenetic phase and developed in an anoxic environment, developed through bacterial decomposition of organic matter. As pyrite is only found within the decomposing detrital grains these are assumed to have been the source for iron, and hence the grains were biotite or iron-rich lithic fragments. Circulation of formation waters must have been reduced at this time.
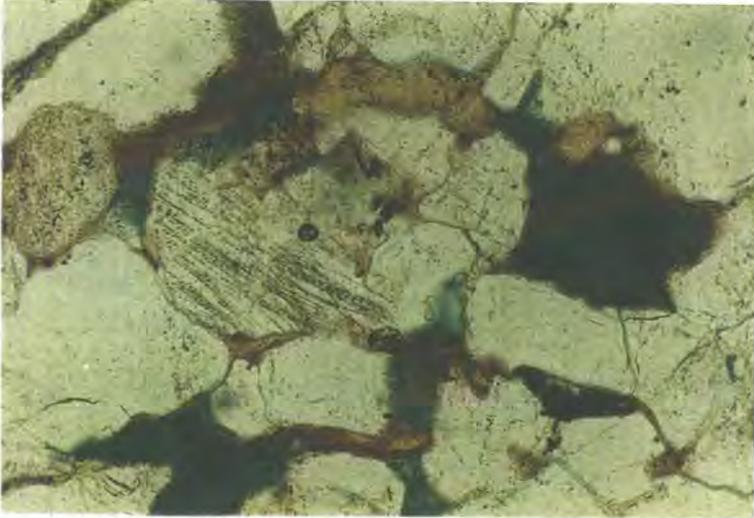


Plate 6.16. Facies Sme, Hawkesbury Sandstone. Field of view 1.5 mm.
Sub-rounded quartz grains are surrounded by fine grained clays formed through the degradation of muscovite mica to illite and pyrite. Pore space is limited. Complete dissolution of labile grains has resulted in the development of oversized pores.

The authigenic clay fraction is composed of kaolinite and illite, which occur in varying proportions (Appendix IV). Clays are more common in facies Sme than in facies Sd, which in turn contains more clay than the cross-stratified sandstones (Appendix III). Within some samples the mixed layer clay montmorillonite has been identified (Appendix IV).

Illite growth occurred during two phases. The early phase is confined to facies Sme and Sd, where illite formed from decomposition of micas (Plates 6.14, 6.16 & 6.17). These clays coat detrital quartz grains and therefore inhibited the growth of quartz cement. Illite requires neutral to alkaline pore fluids, together with sufficient $K^+$, $Si^{4+}$ and $Al^{3+}$. These phases would have been provided from the muscovite mica.
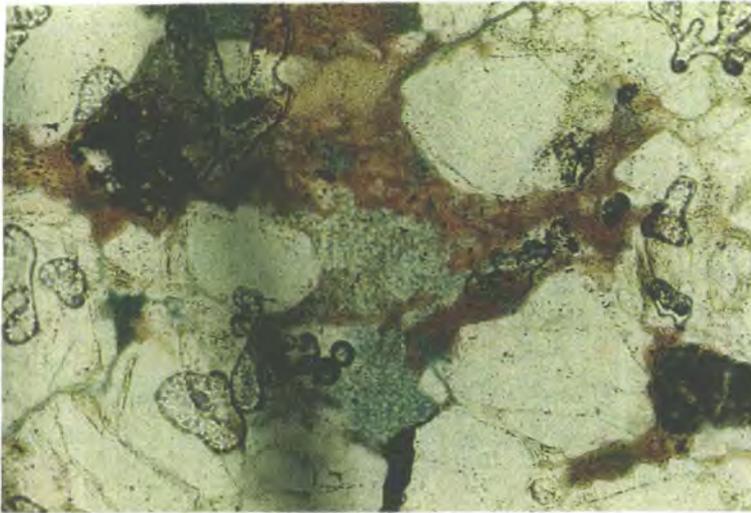
*Plate 6.17. Facies Sme, Hawkesbury Sandstone. Field of view 1.5 mm.*
*Sub-rounded quartz grains are coated with authigenic overgrowths. The grains are*
*surrounded by fine grained clays formed through the degradation of muscovite mica to*
*illite and pyrite. Remaining pore spaces have been partially filled by diagenetic*
*kaolinite.*

Kaolinite formed in all sandstone facies as a pore filling phase, developed within pores created through the dissolution of unstable framework grains including mica, lithic fragments or feldspars (Plates 6.13, 6.17 & 6.18). Large vermicular crystals are common (Plate 6.18). Kaolinite requires acidic pore waters, produced by flushing of the sandstone with fresh water.
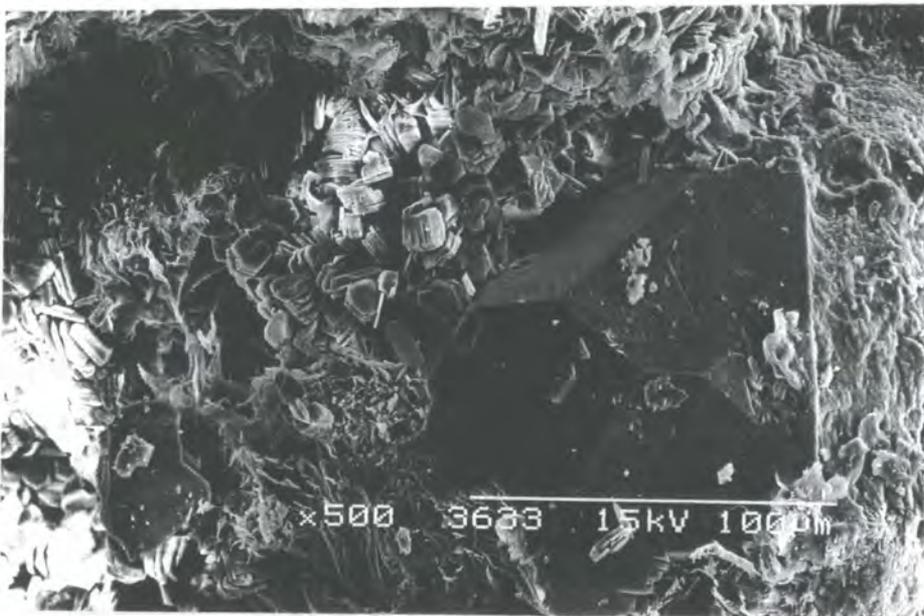


*Plate 6.18. Facies Sme, Hawkesbury Sandstone.*
*Authigenic quartz overgrowths are associated with labile framework grains which have*
*been replaced by illite. Vermicular kaolinite fills the remaining pore spaces.*

A later phase of illite growth is found in all sandstone facies. The clay forms a grain coating phase which blocks pore throats within the sandstone (Plate 6.15). Following the deposition of illite grain dissolution continued, resulting in the development of a number of oversized pores (Plate 6.16).

*Discussion.*

The differences in composition between the sandstone facies of the Hwkesbury Sandstone are not vast, but are significantly different to warrant comment. The structured sediments are quartz arenites, with the sediment source within the cratonic field of Dickinson (1985) as illustrated in Figure 6.15b. The main sources for craton derived quartzose sands are low-lying granitic and gneissic exposures, supplemented by recycling of associated sediments (Dickinson 1985). The higher volume of lithic grains, including polycrystalline quartz, within facies Sme, results in the sandstone plotting in the recycled orogen province of Dickinson (1985). The composition of facies Sd is transitional between facies Sme and the cross-stratified sandstones.

The straight extinction of the detrital quartz grains preserved within the sandstones of all facies suggests a plutonic origin, probably from granite bodies. The presence of quartz grains with undulose extinction also suggests a metamorphic quartz source. The grains are moderately rounded, and thus indicate that they were reworked before deposition within the Hawkesbury Sandstone river system.

Mica flakes, in the form of muscovite and biotite, originated from granite and regionally metamorphosed rocks, particularly schist and gneiss. Illmenite grains containing exsolved laminae, together with ilmenite-haematite, are typical of acid plutonic source terrains. Andradite (garnet) is also common in metamorphic and plutonic igneous rocks (Mange & Maurer 1992), and lazulite is confined to metamorphic rocks (Kerr 1977). Zircon is a widespread phase, particularly common in silicic and intermediate igneous rocks. Rutile is most common in regionally metamorphosed rocks such as schists and gneisses, and tourmaline crystallises in granites, schists and gneisses. The sub-angular grains of rutile, tourmaline, lazulite and andradite are considered to be first cycle. The rounded grains of zircon are believed to be second cycle.

This study therefore suggests that the sands of the Hawkesbury Sandstone were sourced from a cratonic area which contained granite and metamorphic rocks in the form of schist and/or gneiss. Primary petrographic differences between the massive and structured facies are present, with facies Sme and Sd containing a higher proportion of intra- and extra-formational lithic grains, and mica than the structured

facies. The muscovite of facies Sd and Sme degraded to illite during early phases of diagenesis, and hence precluded quartz cementation. The structured facies are well cemented by authigenic quartz. This difference in cementation has previously been noted by Loughnan & Golding (1957) and Conaghan (1980). However, both of these studies have attributed the presence of a higher percentage of clay minerals in the massive sandstone to a primary detrital clay fraction.

Textural differences are also apparent between the facies of the Hawkssbury Sandstone. The structured facies have a higher primary porosity than that of facies Sme and Sd. The structured sandstones and facies Sme are moderately sorted, and the sandstones of facies Sd are moderately well sorted.

All these factors indicate some primary sedimentary control over facies within the Hawkesbury Sandstone.


## 6.3. Fluvial Interpretation.

The pattern of palaeocurrents and cross-basinal variation in facies recorded in the Sydney Basin between Intervals A-E (Figures 6.5 & 6.6d-h) is consistent with the presence of a longitudinal drainage system. Cowan (1993) believes that thrust related loading of the eastern margin of the Sydney Basin may be correlated with changes in fluvial drainage pattern. However, precise correlation of loading events in the NEFB is hindered by a lack of chronological data.

Cowan (1993) comments on the relatively narrow width of the Sydney Basin compared with other foreland basins, and the presence of an uplifted craton represented by the LFB. The narrow width of the basin may have resulted from crustal loading of an extended thermally young lithosphere with low rigidity, or restriction by the presence of the cratonic highland to the west, that initially formed the margin to the extensional basin (Cowan 1993). The uplifted LFB is believed to be inherited from early Permian extension (Cowan 1993).

The basin-wide unconformity which exists between the Hawkesbury Sandstone and the Narrabeen Group (Figure 6.5) indicates a change in tectonic regime. The magnitude of the unconformity increases to the southwest i.e. towards the LFB. Renewed crustal loading and quiescence in the NEFB may explain the orogen directed palaeoflow of the Hawkesbury Sandstone, with the south-west increase in discordance of the basal unconformity (Figure 6.5) resulting from peripheral bulge uplift (Cowan 1993).

The fluvial drainage pattern of the Hawkesbury Sandstone cannot be adequately explained in terms of a foreland basin axial drainage system because of the lack of preserved evidence for either a related trunk stream or cross-basinal variation in composition (Cowan 1993). The Hawkesbury Sandstone was sourced from the cratonic side of a foreland basin which was elevated by up to 2 500 m above sea level (Lambeck & Stephenson 1986). Alpine glaciers are assumed to have been present over the LFB (Cowan 1993).

Individual fluvial systems within foreland basin settings have either axial or transverse orientations. Conaghan & Jones (1975) likened the Hawkesbury Sandstone river to the Brahmaputra, a transverse oriented drainage network. However, although the sedimentary facies exhibited in the craton sourced Hawkesbury Sandstone may resemble those inferred from the Brahmaputra (Conaghan & Jones 1975), its orogen directed palaeoflow is unlike that of the thrust belt sourced Brahmaputra River. Thus the tectonic setting of the Hawkesbury Sandstone river would appear to have no modern analogue.

Rust & Jones (1987) identified erosionally bounded sedimentary successions within the Hawkesbury Sandstone which were interpreted as channel complexes (equivalent to CH elements of this study). A high palaeocurrent variance between these channel successions was attributed to switching of the river channel around in-channel islands. However, this study has not identified such erosionally based stacked sets of cross-strata. The cross-stratified sediments exposed within sections 1 and 2 are believed to form part of channel fills (CH elements) due to the low palaeocurrent variations within measured sections. Channel margins and fourth order surfaces representing channel bases have not been identified.

The absence of low angle erosional channel margins indicates that the Hawkesbury Sandstone river was constantly reworking the floodplain, thus removing evidence of individual channel elements. However, the absence of LA architectural elements indicates that channel migration was not a gradual phenomena, but rather that avulsion was the dominant control on sandbody architecture. Limited subsidence during deposition of the Hawkesbury Sandstone may have resulted in only partial preservation of individual CH elements.

The angular range of the palaeocurrent measurements taken from section 2 is 98°, which equates to a sinuosity of 1.12 (Tables 6.2). Hence the Hawkesbury Sandstone river may be termed a low sinuosity system (Rust 1978a). The structured sediments of the Hawkesbury Sandstone are dominated by sands deposited in downstream accreting bedforms with DA Type 1 and SB Type 1 architectural elements well preserved. Such deposits relate to the migration of mid-channel bars (Haszeldine 1983a & b) and dunes scaled to water depth.

| Section | Average height of 25 dunes (m) | Decomp- acted dune height (m) $\phi c=0.05$ | Water depth (m) | Palaeo- current range. | Sinuosity | Width/ depth ratio | Channel width (m) |
|---------|------|------|------|------|------|------|------|
| 1 | 0.65 | 1.02 | 4-9 | | | | |
| 2 | 4.55 | 7.20 | 40 | 98° | 1.12 | 68 | 2,720 |
| | 1.75 | 2.77 | 10-15 | 98° | 1.12 | 68 | 816 |

Table 6.2. Palaeohydrological parameters of the Hawkesbury Sandstone.

The low palaeocurrent variance of interpolated fluvial channel (CH) elements, combined with the lack of major reactivation surfaces within preserved bedforms, suggests the Hawkesbury Sandstone river was a perennial system. Bars were rarely emergent resulting in a low braiding index. The DA Type 1 architectural elements (mid-channel bars) split the channel flow, and hence increased flow variance in the downstream direction. Intrasets are developed I DA Type 1 architectural elements which are the product of small scale bedforms developed across bar foresets (cf Figure 2.3a).

The fluvial parameters of the Hawkesbury Sandstone river may be estimated from cross-stratification measured in the field, using the methods outlined in Chapter 2.4.2. Hydrogeological parameters are listed in Table 6.2.

Section 2 offers a well developed sandstone succession within which two scales of bedform are preserved. Facies Sg, Sp, and Sc form dunes which have an average thickness of 4.55 m. When decompacted this thickness is equivalent to an original dune thickness of 7.20 m (Table 6.2). Migrating bedforms of this height may only be deposited in water of an estimated 40 m in depth (Figure 2.4). Smaller scale 2-D and 3-D dunes of SB Type 1 architectural elements average 1.75 m (Table 6.2), which relate to an original bedform thickness of 2.77 m. Such bedforms would be produced in water depths of between 10-15 m.

The marked difference in bedform height between facies Sg, $Sp_l$ and Sc and $Sp_m$/$St_m$ indicate that flow depths within the river system varied during deposition of the Hawkesbury Sandstone. The variations in water depth of the Hawkesbury Sandstone river may be interpreted in terms of discharge fluctuations related to flood events, interspersed with normal water levels.

According to the empirical equations of Schumm (1968b) a sinuosity of 1.12 relates to a width/depth ratio of 68. Thus, the Hawkesbury Sandstone river during times of high flow was approximately 2700 m wide, and during periods of lower flow was approximately 800 m wide (Table 6.2). Measurements made from section 1 indicate water depths of 4-9 m. Such a river is similar in scale to the modern day Brahmaputra (Table 2.5).

It is clear that the Hawkesbury Sandstone river was a system of variable flow depth with wide channels of low sinuosity. The periodic increases in flow depth outlined above cannot be identified as cyclical in nature. However, it is reasonable to assume that increases in flow depth relate to a periodic increase in water supply, perhaps associated with glacial melt water provided from the LFB.

In order to produce a sandsheet approximately 100 km wide (Standard 1969) and 250 thick, a river of 15 m depth and 1000 m wide would have to avulse a minimum of 1666 times. The Hawkesbury Sandstone was deposited in approximately 6 Ma (Veevers *et al* 1993), and hence the river would avulse at least once every 3600 years. Such a rate is well within modern rates (Bridge 1985).

The SM Type 3 architectural elements are more difficult to explain in terms of fluvial deposition. The elements are characterised by an upward change in facies of $(Sb)$-Sme-Sd-$Sp_s$/$St_s$. Scours within the base of SM Type 3 elements indicate that depositional currents travelled in a direction oriented parallel (section 1) and oblique (section 2) to the regional palaeoslope. The mudclasts preserved within facies Sb and Sme reach 0.85 m in diameter and are generally sub-angular in shape. Smith (1972) demonstrated that mudstone clasts do not survive for long periods within a fluvial channel, and hence angular mudclasts within fluvial sandstones would imply transport of no more than a few hundreds of meters from the source. The mudclasts preserved within facies Sb and Sme are therefore interpreted as floodplain material.

The petrographic study described above has established that the sandstones deposited within the Hawkesbury Sandstone river were quartz arenites and sub-litharenites, sourced from granitic and low grade metamorphic terrains. Dutta & Wheat (1993) have established that the LFB was composed of plutonic and high grade metamorphic rocks. The roundness of detrital heavy minerals indicates both a first- and multi-cycle origin for the grains.

Generally fluvial transport alone is not sufficient to influence the proportion of quartz in a sand (Dickinson 1985). The work of Johnsson *et al* (1988) has shown that quartzose sand can be produced as a first cycle sediment from deeply weathered bedrock. Dutta & Wheat (1993) have stated that such weathering may also occur in temperate-humid climates. Relief over the source area acts as a further control, as sands derived from drainage basins in tropical highlands with high relief are quartz poor, and with low relief are quartz rich (Johnsson *et al* 1988). This is due to the accumulation of soils within low relief areas, which allow for concentration of quartz.

Pettijohn *et al* (1972) suggested that first cycle sands are likely to be compositionally and texturally less mature than multi-cycle sands. In relation to multi-cycle quartz arenites, first cycle quartz arenites may be more angular, and contain more polycrystalline quartz and quartz showing undulose extinction.

The Hawkesbury Sandstone was deposited in a warm temperate climate with moderate chemical weathering (Dutta & Wheat 1993). The textural and compositional maturity of the structured facies within the Hawkesbury Sandstone indicates a possible first or multi-cycle source for the quartz arenites, with rounded detrital grained of monocrystalline quartz and zircon. The sandstones of facies Sme and Sd, however, are compositionally less mature. The presence of polycrystalline quartz, lithic fragments and high volumes of mica indicate that these sandstones may not have been subjected to the same amount of reworking experienced by the cross-stratified sediments.

The lower textural maturity of facies Sme compared with the structured facies indicates a less mature source for the sands. This suggests that the sands were supplied from a source which allowed for less reworking than that supplying sediment for deposition within the structured facies. The origin of the SM Type 3 architectural elements, and their relation to the cross-stratified sandstones will be explored in Chapter 7.

## 6.4. Summary.

The Hawkesbury Sandstone was sourced from an uplifted cratonic area (LFB) which contained granitic and metamorphic source rocks. These were reworked and temporarily stored prior to deposition within the structured facies of the Hawkesbury Sandstone river. The lower compostional maturity of facies Sme and Sb indicates that reworking of massive sands prior to deposition was limited.

The Hawkesbury Sandstone river flowed from the LFB towards the northeast. The channel was of low sinuosity and over 800 m wide. Depth was variable.

Individual channel (CH) elements cannot be recognised within the Hawkesbury Sandstone, indicating that the river system was continually reworking the floodplain, thus destroying evidence of channel forms.

Within inferred channels the sands of the Hawkesbury are dominated by macroforms separated by third order bounding surfaces. The macroforms are composed of DA Type 1 architectural elements indicative of deposition from mid-channel bars. Mesoform scale bedforms are represented by SB Type 1 architectural elements. The lack of large scale reactivation surfaces, and evidence of low stage reworking, together with the absence of plane bedding, indicate that deposition was in a perennial system with a low braiding index.

The SM Type 3 architectural elements were deposited by currents moving down and across the regional palaeoslope sourced from the LFB. The sandstones contain locally derived mudclasts of floodplain origin and hence indicate deposition during flood events. Superimposition of SM Type 3 architectural elements indicates repeated deposition from sediment laden currents unrelated to the fluvial system.

# Chapter 7
# The Massive Sandstone Facies

## 7.1. Previous Descriptions Of A Massive Sandstone Facies From Fluvial Deposits.

A massive sandstone facies, such as that described in Chapters 3-6, has not been widely recognised in fluvial deposits, and is not included in the comprehensive lithofacies scheme of Miall (1977). However, a number of workers have described the presence of a largely structureless sandstone facies. Table 7.1. details some of these previous descriptions and the interpretations made.

From Table 7.1. it is clear that two broad categories of massive sandstone have been recognised from the rock record: sheet-like and channel-like. The sheet-like massive sandstone facies are limited to the braided fluvial Lee-type sandstones of the central Appalachian Basin and the Fell Sandstone Group of the Northumberland Basin. Channel-like massive sandstone deposits have been described from a number of environments including fluvio-glacial, braided fluvial, marginal marine and fluvio-lacustrine (Table 7.1).

The interpretations made of the massive sandstone facies depositional environments listed in Table 7.1. include deposition under upper flow regime conditions, from high concentration currents, and from sediment gravity flows associated with bank and bar collapse.

Massive sands are more commonly described from the deposits of coarse grained (sandstone-rich) turbidites. The massive sandstones of the Bouma 'A' division have been attributed to upper flow regime antidunes (Harms & Fahnestock 1965), deposition in a wave disturbed quick condition (Middleton 1967), sedimentation from concentrated grain flows maintained either by grain-grain interactions (Stauffer 1967) or by high shear stresses or pore fluid pressures (Lowe 1976a), and to deposition at a sufficiently high rate to suppress grain sorting (Allen 1982). All these processes provide mechanisms for the formation of a massive facies in fluvial deposits.

This study assesses, for the first time, the geometry of massive sandstone facies in detail, and the information gathered has been used to develop a classification scheme for such sandbodies.

| Author(s) | | Description | Interpretation |
|---|---|---|---|
| Collinson (1970) | Kinderscout Grit (Namurian), Pennine Basin, UK. Delta top. | 44 channels developed in delta top. 4-40 m deep. Erosional margins. Cross-section asymmetric with one margin steeper (25-30°, exceptionally 50°). Fill: massive sandstone with mudstone blocks <1.5 m long. Horizontal partings at margins. | Channels cut by traction currents. Massive sandstone fill represents upper flow regime deposits or a frozen traction carpet |
| Turner (1974) | Stubdal Formation, Ringerike Group. Late Silurian, Norway. Low sinuosity fluvial channels | Fine grained sandstone preserved as massive sandstone beds 1-14 m thick . Commonly massive sandstones lie over a scoured surface with a concentration of intra-formational conglomerate at the base. | Deposition from suspended load under high energy conditions. |
| Rust & Romanelli (1978) | Pleistocene, Canada. Fluvio-glacial environment. | Channels 38 m wide by 7 m deep. Symmetrical margins, with relatively steep walls (37°). >100 m long. Channel fill very coarse sandstone - granulestone. Coarser than the surrounding sediments. Marginal laminae preserved. | Channel eroded by powerful spring flow. Massive fill due to rapid deposition from current of high concentration, possibly generated through undercutting of banks. Sediments deposited beneath standing water in a lacustrine environment. |
| Conaghan & Jones (1975) | Hawkesbury Sandstone, Triassic, Sydney Basin, Australia. Low sinuosity fluvial system. | Sandstone sheets with channellised bases and planar tops. Channel walls are inclined <50°. Mudstone breccia is preserved at the channel base. Sediment bodies are internally homogeneous or crudely laminated. Massive sandstones are overlain by structured sandstones | Channels represent plane bed scours. Massive sandstone was deposited by upper flow regime currents in the 'rheological bed' of Moss (1972) during the falling stage of a flood cycle. |
| Hodgson (1978) | Fell Sandstone Group, Lower Carboniferous, Northumberland Basin, UK. Low sinuosity fluvial system. | Sheets of massive sandstone 3 m thick. Apparently structureless appearance with channel boundaries and locally preserved cross-stratification. Water escape structures. Channel boundaries asymmetric, with homogeneous fill | Massive sandstone caused by dissection of braid bars. Channels infilled by re-distributed sandstone from bars. Channels mutually interfering resulting in sandstone sheet. Water escape structures indicate that sandstone was water saturated. |
| Jones (1980) | Roaches Grit, Namurian, Pennine Basin, UK. Delta top. | Channels with very irregular erosional surface. Channel margins dip <70°. Faint laminae are preserved parallel to the erosional surfaces. Massive sandstone beds <10 m. Undulose laminae 5-50 cm high & 2-7 m wide preserved in upper part of beds. Massive sandstones are overlain by giant cross-beds. | Giant cross-beds represent the deposits of alternate bars. Massive sandstone formed quickly as a result of intense turbulence in front of giant bedforms during high discharge. |
| Conaghan (1980) | Hawkesbury Sandstone, Triassic, Sydney Basin, Australia. Low sinuosity fluvial system. | Sheets of massive sandstone with discordant channellised bases and planar tops. Sheets 15-20 m thick and several km lateral extent. Channels have several meters of relief with margins dipping <55°. Channel orientation NE/SW. Massive sandstone fill with faint laminae and low amplitude waves. Mudclasts <5 m diameter floating within the massive sandstone. | Rapid deposition under conditions of concentrated sediment dispersal and upper flow regime. Mudclasts carried in suspension in dense grain flow. |
| Jones & Rust (1983) | Hawkesbury Sandstone, Triassic, Sydney Basin, Australia. Low sinuosity fluvial system. | Massive sandstone sheets containing faint stratification and randomly oriented mudclasts over erosional surfaces. Massive sandstone bodies are elongate structures along planes perpendicular to palaeoflow established from cross-stratification. Channels are erosionally based. | Bank collapse caused loading of bedforms within the fluvial channel and liquefaction of unconsolidated sand. Bank & bar collapse resulted. Mass flows of sand moved across the scours formed in front of large scale bedforms. Falling water level acted as trigger for bank collapse |
| Postma et al (1983) | Drente Formation, The Netherlands Ice marginal lake. | Channels 25 m wide & 7-10 m thick. Semi-circular cross-section. Margins beyond the angle of repose. Fill composed o coarse grained massive sandstone fill. Marginal laminae developed parallel to erosional walls. Water escape structures common | Massive sandstone deposited as rigid plug surrounded by suspended sediment moving through laminar flow. Liquefaction of sediment resulted in the loss of structure. |

*Table 7.1. A summary of the previous descriptions of massive sandstone facies in terrestrial environments.*

| Eschner & Kocurek (1986) | Entrada Formation, Upper Jurassic, Utah, USA. Tide dominated shallow sea. | Massive sandstone channels 0.1-12 m thick & 100's m's lateral extent. Amalgamate to form sheets traceable for several km. Channels concave-up with margins dipping <35°. Channels filled with fine-medium grained structureless sandstone. Dish & pillar structures common. Faint horizontal laminae. | Channels represent mass flows related to storm events. Undercutting of banks resulted in slumping and the formation of liquefied flow which travelled fro several km on gently dipping slopes. Amalgamation of massive sandstone channels due to retrogressive sliding along a retreating scarp. |
|---|---|---|---|
| Rust & Jones (1987) | Hawkesbury Sandstone, Triassic, Sydney Basin, Australia. Low sinuosity fluvial system. | Medium-fine grained sandstone developed in massive sandstone units. Massive sandstones erosionally based, with scour axes oriented perpendicular to the palaeoflow established from cross-stratification. Channel margins dip 40-80°, display marginal laminae parallel to the erosional surfaces. Vertically and horizontally stacked. Massive sandstone sheets contain mudstone blocks <38 m diameter & sand-sized mudstone intraclasts. | Channels formed by large scale re-mobilisation of cross-stratified sandstone in the form of either bank or bar collapse. Liquefaction resulted due to changes in pore pressure during falling stage. Bank failure independent of bedform scour. |
| Fishbaugh et al (1989) | Mansfield Formation, Pennsylvanian, Illinois Basin, USA.. Low sinuosity fluvial/estuarine system. | Massive sandstone (fine - medium grained fills erosionally based channels <30 m wide & 3 m deep. Channel margins sharp to diffuse. Diffuse laminae preserved parallel to the channel walls. Transport direction oblique to palaeoflow as established from cross-stratification. Dish & pillar structured locally preserved. | Massive sandstones are the deposits of sediment gravity flows which developed along the sides of large macroforms. Sediments highly concentrated & deposited rapidly in response to deceleration and frictional freezing. Macroform slumping due to high or falling discharge causing changes in pore water pressure. |
| Turner & Monro (1987) | Fell Sandstone Group, Lower Carboniferous, Northumberland Basin, UK. Low sinuosity fluvial system. | Massive sandstone sheet 3.50-3.75 m thick & >300 m lateral extent. Medium-fine grained and dominantly structureless. Sheet contains channels and undulose laminae together with isolated cross-strata and water escape structures. Massive sandstone filled channels 1.7-2.5 m deep. Steep sided (13-55°). Cross-cutting relationship to palaeoflow established from cross-stratification. | Sheet-like massive sandstones formed through primary depositional mechanisms: traction currents with high sediment concentration to suppress turbulence and the production of cross-stratification

Channels cut & filled near simultaneously. Movement occurred across the channel, associated with channel bank collapse. Sediment-laden currents move across the channel down the transverse scour in front of a bedform. Rapid deceleration & frictional freezing of the flow resulted in the marginal laminae. |
| Boe (1988) | Hitra Group, ORS, Norway. Low sinuosity fluvial. | Basal scour with relief < 2 m overlain by thin intra-formational conglomerate. Channel oriented perpendicular to palaeoflow as established from cross-stratification. Massive sandstone fill < 12 m thick. Containing angular mudclasts. Massive sandstone fill grades in cross-stratified sandstones. | Channels of mass flow origin. Undercutting of banks resulted in slumping and the formation of erosive slurry. Emplacement beneath thalweg of channel resulted in preservation. Collapse triggered by seismic shock, excess loading oversteepened slopes or pore pressure changes. |
| Wizevich (1991) | Lee Formation, Pennsylvanian, Appalachian Basin, USA. | Massive sandstone sheets >100 m wide and < 5 m thick. Lower surface undulatory. Massive sandstone fill with diffuse laminae. Massive sandstone filled channels <10 m wide, 2.5-5 m deep. Near symmetrical, trending at high angle to palaeoflow. Basal concentration of quartz granules and mudclasts. Diffuse laminae within channel fill. | Channel bottom deposits, formed during high flow stage or gravity flow generated by bank failure. Lamination due to dilution of flow. Channels incised into macroforms. Massive sandstone fill deposited during significant reduction in water level in major channels. Rapid deposition. |

*Table 7.1. A summary of the previous descriptions of massive sandstone facies in terrestrial environments continued.*

## 7.2. Classification Of The Massive Sandstone Facies.

### 7.2.1. Characteristics Of Ancient Braided Systems Within Which A Massive Sandstone Facies Is Preserved.

#### (i) Fell Sandstone Group, Northumberland Basin.

The Fell Sandstone Group of the Northumberland Basin was deposited in a humid climate at tropical latitudes (Leeder 1988a) within a braided river with a sinuosity of approximately 1.2 and low braiding index. Discharge is interpreted to have been perennial in character, although fluctuating. The river course was fault controlled (Turner *et al* 1993). The Fell Sandstone river was approximately 350-750 m wide in the study area. Water depth was variable with depth from 6-8 m at periods of low flow and 12-18 m at high flow. The river contained mid-channel and bank attached bars, 2-D and 3-D dunes.

#### (ii) Lee-Type Sandstones, Central Appalachian Basin.

The Lee-type sandstones of the central Appalachian Basin were deposited in a variety of braided river systems in a consistently wet, tropical climate (Cecil 1990; Winston 1990). All the Lee-type river systems described below are interpreted as perennial in character.

*Naese Sandstone member.*

The Naese Sandstone member river had a sinuosity of approximately 1.2 and was 10-20 m deep. The river channel is estimated to have been between 680-1260 m in width. The river was dominated by downstream accreting mid-channel and bank attached bars together with 2-D and 3-D dunes.

*Pine Creek Sandstone member.*

The Pine Creek Sandstone member river was of low sinuosity. The banks were stable and inundated by regular flooding events which resulted in the building of levees. The water depth is estimated at 4.5-6.5 m with the channel dominated by mid-channel bars together with 2-D and 3-D dunes.

*Corbin Sandstone formation.*

The Corbin Sandstone formation river is estimated to have had a sinuosity of approximately 1 with a low braiding index. The channel is interpreted to have been 6-9 m deep and 480-720 m wide, with a width/depth ratio of approximately 80. Stable

banks were established in the later stages of the rivers existence, and these were inundated by floods resulting in the building of levees. The Corbin Sandstone river was dominated by mid-channel and bank attached bars together with 2-D and 3-D dunes.

### (iii) Mansfield & Brazil Formations, Illinois Basin.

The Mansfield and Brazil Formation sandstones of the Illinois Basin were deposited in low sinuosity braided streams which were subjected to some estuarine influence (Chapter 5). The Mansfield Sandstone river was perennial and of variable discharge, with width/depth ratios varying between 30-60. The major channel (Channel A of Chapter 5) had an estimated depth of 11-20 m and width of 500 m at bankfull discharge. During periods of lower flow the river is estimated to have been 6-12 m deep and approximately 330 m wide. The Mansfield Formation river contained mid-channel and bank attached bars, with 2-D and 3-D dunes. Due to the perennial nature of the river it is believed to have had a low braiding index.

### (iv) Hawkesbury Sandstone, Sydney Basin.

The Hawkesbury Sandstone river was deposited in a humid temperate environment (Dutta & Wheat 1993) and was perennial in character. The sinuosity of the river is estimated to have been in the region of 1, with a width/depth ratio of approximately 70. The river is interpreted to have had a low braiding index. The Hawkesbury Sandstone river is believed to have been subject to large discharge variations. The depth of the river during periods of high flow was approximately 40 m and the width 2700 m. During periods of lower flow the river is estimated to have been 10-15 m deep and 800 m wide. The large discharge variations are believed to be due to the additional of seasonal meltwater to the river system provided from highland glaciers to the east. Within the river mid-channel and bank attached bars, 2-D and 3-D dunes were deposited.

All the river systems included within this study are considered perennial in nature with limited emergence of bedforms and bars resulting in a low braiding index. Variable fluctuations in discharge have been documented from the Fell Sandstone, Naese Sandstone, Corbin Sandstone, Mansfield and Hawkesbury Sandstone rivers. The estimates made of channel width and depth enable these ancient braided river systems to be compared with those developed in modern environments (Table 2.5) as detailed in Chapters 3-6.

## 7.2.2. Classification Scheme.

Fieldwork carried out during this study identified three categories of massive sandstone termed Sms, Smc and Sme. These facies are described briefly in Table 2.4 and Chapters 3-6, and will be addressed in more detail below. The three facies have clearly defined geometries (Table 2.4) which may be used to classify the sandbodies.

Facies Sms, Smc and Sme have textural characteristics which differ from those of cross-stratified sandstones within individual Formations and Members. These differences have been documented in Chapters 3-6. Petrographic studies (Chapters 3-6 & Appendix III) indicate that massive and structured sandstone facies within the same strata have similar diagenetic histories, and hence the largely structureless appearance of the massive facies is not related to burial, but rather a primary depositional mechanism.

l.c.

Using architectural characteristics of the massive facies a classification scheme has been developed, and is illustrated in Table 7.2. Facies Smc has been sub-divided into four types using width/depth criteria and characteristics of the basal surface (Table 7.2).

| Carboniferous | Sms | | | | |
|---|---|---|---|---|---|
| | Smc | width/depth <12 | Elongate Perpendicular to flow | Erosive lower contact | *Type 1* |
| | | | | Non-erosive lower contact | *Type 2* |
| | | | Elongate parallel to flow | Non-erosive contact | *Type 3* |
| | | width/depth >20 | Elongate Perpendicular to flow | Erosive lower contact | *Type 4* |
| Triassic | Sme | | | | |

*Table 7.2. A simple classification scheme for the massive sandstone facies identified in this study.*

In the following pages each of the massive sandstone facies will be described in turn. Possible mechanisms for the deposition of the facies are then outlined and discussed.

## 7.3. Facies Sms.

### 7.3.1. Description Of Facies Sms.

### (i) Geometry.

Facies Sms has been described from the Fell Sandstone Group of the Northumberland Basin and the Naese Sandstone member of the Breathitt Group in the central Appalachian Basin. The facies takes the form of laterally extensive sheets up to 8 m in thickness. In the Naese Sandstone member the Sms sheet may be traced >200 m parallel, and approximately 250 m transverse to the palaeoflow direction. In the Fell Sandstone Group facies Sms may be traced for >300 m parallel to the flow direction, but the extent of the facies transverse to flow cannot be quantified due to lack of exposure.

Underlying the Sms unit within the Naese Sandstone member are highly deformed cross-stratified sandstones. Deformation takes the form of stacked sets of recumbently overturned foresets (Figure 4.8). Overturning of cross-stratified foresets is only locally developed underlying facies Sms in the Fell Sandstone Group sections (Figures 3.8 & 3.10).

The massive sandstone sheets display undulose lower bounding surfaces with scour-like structures developed. These have a relief of <1.85 m in the Naese Sandstone member and <0.85 m in the Fell Sandstone Group. The term scour is used to denote isolated, roughly equi-dimensional cut and fill features. The scours are oriented approximately parallel to the flow direction, and cut out the underlying stratified sediments in the downstream direction. The margins of the scours dip <45° and are commonly associated with overturned foresets in the underlying structured sandstones. The upper bounding surface of facies Sms is essentially planar.

Internally, facies Sms is largely structureless. Concentric laminae spaced 5-50 mm apart are preserved parallel to the basal scours. These are defined by small scale changes in sandstone texture. The massive sheets also contain diffuse undulose to trough-like laminae (<1.50 m high) which are also defined by small scale changes in texture. In the sheet-like unit exposed in the Fell Sandstone Group water escape structures <1.20 m in height are preserved in the upper portion of the unit. The water escape features were developed prior to deposition of the overlying cross-stratified sandstones. Also within facies Sms of the Fell Sandstone Group isolated horizons of cross-stratified sandstone are preserved. These occur as solitary sets of 2-D and 3-D dunes < 40 cm high, and form sets of a similar scale (Figures 3.8 & 3.10).

## (ii) Textural characteristics.

The textural characteristics of facies Sms are outlined in Table 7.3. Facies Sms of the Fell Sandstone Group and Naese Sandstone member is composed of a moderately well sorted sandstone with a grain size distribution similar to that of the structured facies (Figures 3.12 & 4.14). The primary porosity of facies Sms is higher than that of the structured facies and the CI is lower (Table III.1).

## 7.3.2. Possible Mechanisms For The Production Of Facies Sms.

The origin of the largely structureless sandstone sheets of faces Sms is difficult to explain in terms of normal fluvial currents. The structureless nature of facies Sms may be the result of primary deposition mechanisms, or the result of post-depositional deformation causing a loss of primary stratification. Both of these possibilities are explored below.

Any mechanism responsible for the production of facies Sms has to take into account the anomalous features of the facies. These include the erosive bases to sheets indicative of turbulent flow conditions and the overlying structureless sandstone sheets which show no evidence of transport and deposition by traction currents. The internal diffuse laminae and locally preserved water escape structures, and isolated 2-D and 3-D dunes must also be included in any model.

Facies Sms has a similar grain size distribution to the cross-stratified sandstones of the braided rivers examined, and hence the sediment within the different facies must have been of the same calibre and type, but deposited in a different manner. The presence of water escape structures and the diffuse laminae indicate liquefaction or deformation of sediments on pore fluid expulsion.

## (i) Syn-Depositional Mechanisms.

The sharp basal contact between the cross-stratified sandstones and facies Sms, together with the presence of undeformed cross-stratification within facies Sms of the Fell Sandstone Group, suggests that facies Sms was formed during primary deposition. However, primary sedimentary structures normally associated with fluvial currents are largely absent, indicating that the flow from which facies Sms was

| Section | Facies | Primary Porosity | Perme-ability (mD) | Sorting | Median grain size ($\phi$) | Packing (CI) |
|---|---|---|---|---|---|---|
| *Northumber-land Basin.* | Sstructured | 14% | 11-5147 mean1100 | Moderate | 2.32-3.18 mean 2.8 | 2.7-3.44 mean 3 |
| | Smc | 15.3% | 87-5947 mean1258 | Moderately well | 2.94-3.06 mean 2.98 | 2.58-2.96 mean 2.8 |
| | Sms | 18.6% | | Moderately well | 2.94-3.18 mean 3 | 2.36-3.64 mean 3.1 |
| *Illinois Basin.* | Sstructured | 15.1% | 18-496 mean 144 | Moderately well-moderate | 2.94-3.64 mean 3.1 | 2.68-3.48 |
| | Smc | 15.6% | 122-1527 mean 508 | Moderately well | 2.56-3.18 | 1.84-2.78 |
| *Appalachian Basin.* Naese Sandstone member | Sstructured | 15.6% | 38-41 mean 39 | Moderate | 3.32 | 5.3 |
| | Smc | 8.6% | 3-49 mean 18.9 | Moderately well-moderate | 2.73-3.32 mean 3 | 4.62-4.78 mean 4.7 |
| | Sms | 9.6% | | Moderately well | 2.55-2.94 mean 2.7 | 4.68-5.14 mean 4.9 |
| Pine Creek Sandstone member | Sstructured | 6.8% | 119-224 mean 156 | Well-Moderately well | 2.84-3.32 mean 3 | 3.62-3.68 mean 3.6 |
| | Smc | 9.3% | 55-310 mean 215 | Well-Moderately well | 2.94-3.32 mean 3.14 | 3.66-4.52 mean 4 |
| Corbin Sandstone formation | Sstructured | 7.6% | | Moderately well | 2.56-3.32 mean 3 | 3.06-4.76 mean 4.29 |
| | Smc | 10.3% | | Moderately well | 2.56-3.32 mean 2.9 | 4.14-4.62 mean 4.3 |
| *Sydney Basin.* | Sstructured | 5% | | Moderate | 1.55-2.55 mean 1.9 | 3.24-3.58 mean 3.4 |
| | Sd | 4.5% | | Moderately well | 2.32-3.32 mean 2.6 | 3.06-3.28 mean 3.3 |
| | Sme | 2.3% | | Moderate | 2-2.7 mean 2.4 | 3-4.44 mean 3.5 |

*Table 7.3. The textural characteristics of the sandstone facies.*

deposited did not maintain traction currents sufficient to develop and preserve bedforms. The scours across the lower bounding surface indicate a turbulent flow and the steep angle of the scours, beyond the angle of repose for sand, indicates that the scours were cut and filled rapidly. However, none of the bedforms normally associated with turbulent flow are preserved within the scours, although concentric laminae are

developed parallel to the scour surface. Such laminae have been described as the deposits of sheared, laminar, high concentration currents (Lowe 1976b; Postma 1986).

Turbulence within a flow may be dampened through a decreasing flow depth and/or velocity, or an increase in flow viscosity (Appendix II). However, the similar grain size distribution in both facies Sms and the structured sediments indicates that depositional current velocities of the two facies were similar. Hence turbulence must have been dampened by increasing of flow viscosity i.e. through an increase in suspended sediment within the flow. This may be achieved by several mechanisms, as outlined below.

*Hyper-concentrated stream flow.*

The term hyperconcentrated stream flow was coined by Beverage & Culbertson (1964) to describe sediment/water mixtures of 40-80% by weight, as the hydraulic properties of such fluids differ from those of clear water and flows with a lower sediment concentration. To maintain sediment concentrations above 20% a minimum clay fraction of approximately 5% is required (Beverage & Culbertson 1964). Above 80% sediment concentration the fluid becomes non-Newtonian in character (see Appendix II).

There is some controversy over the exact nature of hyperconcentrated stream flows. Some workers suggest that turbulence is dampened completely by the high viscosity which develops due to the increase in shear stress force required to move the sediment/water mixture. Other workers consider that the stream flow remains turbulent, with a decrease in the natural life of eddies (Reid & Frostick 1994). Bagnold (1954) demonstrated that dispersive stresses acting between grains are at least partially capable of supporting the suspended load.

Modern-day hyperconcentrated stream flows are generally only observed in areas of high soil erosion. The magnitude of concentration is not, however, directly related to discharge (Beverage & Culbertson 1964). Xu (1993) states that when a modern river has a mean annual suspended concentration greater than 100 kg/m$^3$ the majority of this load is carried in hyperconcentrated flows. A number of modern rivers have been described as being periodically hyperconcentrated including the Colorado River and Rio Grande of the USA (Beverage & Culbertson 1964), and a number of rivers, including the Yellow River, in China (Xu 1993). In modern environments ephemeral rivers tend to have far higher suspended concentrations than perennial streams (Reid & Frostick 1994). However, as Figure 7.1. illustrates, prior to the evolution of grasses i.e. pre-Cretaceous times, the turnover of sediment was higher,

and hence more sediment was available to be transported by streams as either bedload or suspension load.
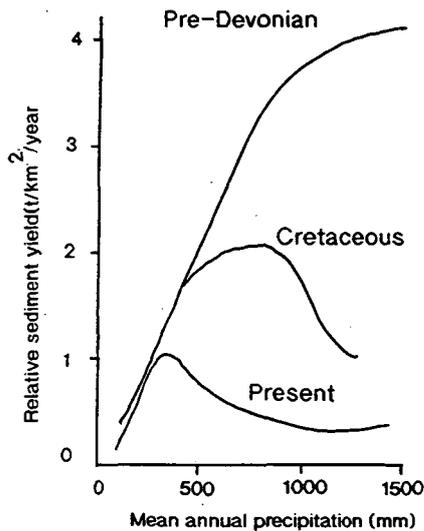


Figure 7.1. Postulated trends in sediment yield as a function of annual precipitation before significant colonisation by plants (pre-Devonian), at inception of angiosperms (Cretaceous) and under present conditions (modified from Schumm 1968b).

Xu (1993) described the majority of modern rivers which carry hyperconcentrations of sediment to be meandering in character. The correlation between channel planform and sediment load illustrated in Figure 7.2 occurs due to the fact that when a river is dominated by hyperconcentrated flow the rate of energy expenditure required for sediment transport declines significantly. The river adjusts to a lower channel gradient by increasing the channel length and hence the sinuosity (Xu 1993). In pre-Cretaceous times river banks would have been highly unstable due to the lack of grasses, and hence a meandering channel planform would be difficult to maintain.
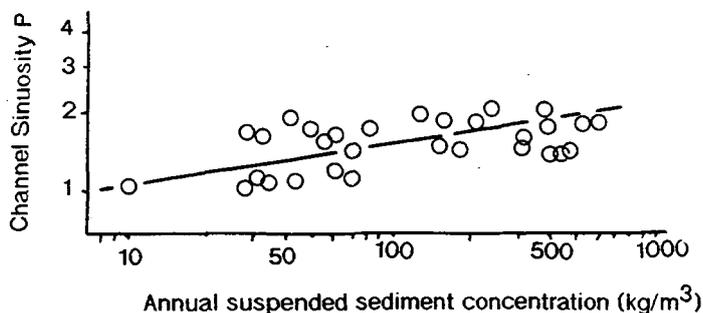


Figure 7.2. Relation of channel sinuosity to mean annual suspended sediment concentration of rivers in China (modified from Xu 1993).

256

Hyperconcentrated stream flows have been documented as the downstream equivalent of lahar deposits by Smith (1986) and Scott (1988) from the Mt. St. Helens eruptions of 1980. Scott (1988) described hyperconcentrated stream deposits as lacking strength and cohesion, but capable of carrying high sediment loads supported by turbulence and particle interaction. The sediments deposited by hyperconcentrated flow associated with the Mt. St. Helens eruption were massive or crudely stratified sands and silts, with locally developed inverse grading and an open sand texture. The massive bedding is interpreted to represent rapid and generally uninterrupted deposition of sediment.

Pierson & Scott (1985) describe hyperconcentrated stream flows as the downstream diluted phase of a debris flow. The deposits of the hyperconcentrated flows were characterised by a coarse sandy texture, poor sorting, faint horizontal stratification and thin layers of gravel suspended in an overall massive bed.

*Ground water charging.*

Traditionally overland flow or surface run-off have been emphasised in drainage network development. However, groundwater may exert a significant influence on modern stream channel form and process. The effects of groundwater flow have been ignored during fluvial studies from the rock record due to the lack of preserved evidence.

Groundwater is classified as that water below the streambed. When discussing the flow of groundwater, positive seepage occurs when groundwater enters the stream, and negative seepage occurs when surface flowing water infiltrates into the stream bed. A groundwater contribution can determine whether a stream is perennial, intermittent or ephemeral (Keller *et al* 1990). Perennial streams are fed continuously by a shallow water table or by discrete point sources of groundwater, whereas ephemeral streams are everywhere above the water table and hence no component of the water is derived from the ground. In this study it has been determined that all the river systems were perennial in character, and hence it is assumed that the channels received a significant contribution of water from the groundwater system.

In natural rivers with sand or gravel beds interaction occurs between the main channel flow and seepage flow (Nakagawa & Tsujimoto 1984). The importance of groundwater seepage is illustrated by the fact that a cohesionless saturated sediment mass will fluidise to a quick condition if it is subjected to an upward seepage force equal in magnitude to the submerged weight of the sediment (Iverson & Major 1986). During seepage, water is forced into a sediment, and hence the process may be

termed a form of fluidisation. The susceptibility of a bed to fluidisation is controlled b y grain size (Figure 7.3). However, positive seepage velocities are generally low resulting in only minor bed expansion (Owen 1987).

Documentation of the physical effects of seepage and experimental studies of the processes are few. One of the most extensive studies of flow in alluvial channels was by Simons & Richardson (1966) who recognised the existence of seepage forces. Quantitatively Simons & Richardson (1966) concluded that negative seepage would tend to increase the effective weight of the bed particles, and therefore result in greater bed stability. Positive seepage would result in a decrease in the effective weight of the particles, and hence an increase in sediment transport, and changes in the predicted bedform. Simons & Richardson (1966) stated that seepage force could change the bedform and therefore the resistance to flow. However, this was not theoretically or analytically documented in their study.
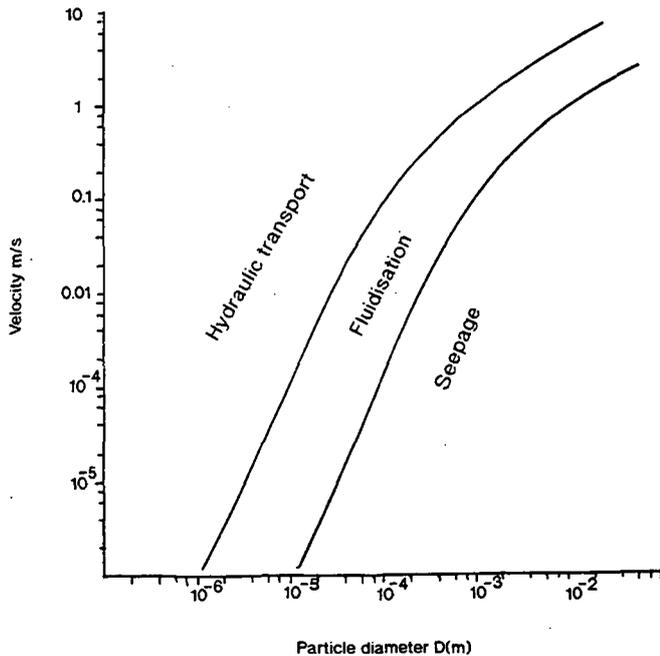


Figure 7.3. The minimum fluidisation velocity of quartz spheres at a temperature of 20°C (modified after Allen 1982).

Harrison (1968) investigated the effects of groundwater seepage on competence, bed roughness and water surface slope of small streams by use of a flume. Harrison (1968) states that theoretically one would expect the effective density of grains to fall with positive seepage and rise with negative seepage, and one would also expect positive seepage to increase stream competence and hence the transport

rate. Other workers, including Watters & Rao (1971) and Richardson & Richardson (1985) agree with these hypotheses.

However, the flume experiments of Harrison (1968) showed that with positive seepage the sediment transport rate decreased, and increased with negative seepage. Negative seepage also increased the flow turbulence and bed roughness.

Field observations by Harrison & Clayton (1970) indicate that seepage of water into or out of a stream may greatly alter stream competence, with reaches subject to positive seepage more competent than those with negative seepage by up to 500 times where stream velocity (U) and slope (S) remained constant. However, laboratory experiments designed to test this observation demonstrated no direct effects of seepage. Harrison & Clayton (1970) credited the differences in competency to a mud seal which infiltrated loosing reaches, thus causing it to be resistant to erosion.

Martin (1970) addressed the influence of seepage on incipient motion of uniform bed materials and concluded that no changes in incipient motion occurred. During their study Watters & Rao (1971) concluded that the particle drag decreased for increasing flow, positive seepage increased the sub-layer thickness, and decreased hydraulic roughness. Turbulence fluctuations were more intense for positive seepage than negative or non-existent seepage.

Richardson & Richardson (1985) also identified the exaggerated boundary layer detailed by Watters & Rao (1971). Richardson & Richardson (1985) determined, through flume studies, that positive seepage caused bedforms such as dunes to become longer and flatter in the channel reach where subsurface water emerged. With positive seepage the unit stream power $(\tau_o.U)$ increased consistently by up to 12 times (Richardson & Richardson 1985). The flume experiments of Richardson & Richardson (1985) also suggested an increase in velocity along the reach where positive seepage occurred, which would be expected due to the increase in discharge within such a reach. Richardson & Richardson (1985) did not detect higher sediment transport rates associated with positive seepage in the lower flow regime, but a possible inhibition of sediment transport in the upper flow regime.

The theoretical expectations and experimental results of seepage effects on competence are conflicting. Positive seepage in the base of fluvial channels is interpreted to increase lift on particles near the bed, and reduce drag forces due to outward discharge (Martin 1970; Watters & Rao 1971). The effects of positive seepage on an individual particle diminish rapidly as it moves away from the bed. In general, studies find that positive seepage enhances entrainment but only negligibly,

even when seepage fluidises the bed to the quick condition (Harrison & Clayton 1970).

The process of seepage leads to uplift and expansion of the sediment bed, thus increasing the sediment concentration near the river bed. This increase in concentration will increase flow viscosity and hence reduce turbulence. Moss (1972) described a layer near the stream bed where particles are maintained by dispersive pressure. However, the existence of such a 'rheological' layer is only theoretically proven.

The lack of structure within facies Sms indicates that some form of fluidisation must have occurred. With increased upward seepage velocity the sediment bed expands until grains are a uniform separation distance. Figure 7.3. illustrates the minimum fluid velocity that would be required to fluidise a bed of medium grained sand. Velocities of between $1.5 \times 10^{-3}$ and $8 \times 10^{-2}$ m/s are required.

*High sediment rain.*

During flume studies investigating the Bouma 'A' division Arnott & Hand (1989) found that when a 0.23 mm diameter (2.13 $\phi$) sand was rained onto an active upper stage plane bed, millimeter scale parallel laminations ceased to form when aggradation of the bed exceeded approximately $6.7 \times 10^{-4}$ m/s. Established dunes persisted in these conditions of high sediment rain. However, it was not possible to ascertain whether dune inception was inhibited by the high sediment rain (Arnott & Hand 1989).

Rapid sediment fallout inhibited tractive transport and reduced lateral segregation of grains to a point where the lamination could not develop. Thus aggradation at a sufficiently high rate was interpreted to form the massive and unlaminated character of the Bouma 'A' division (Arnott & Hand 1989). In the past the Bouma 'A' division has been interpreted in terms of the quick condition (Middleton 1967), grain flows (Stauffer 1967) and modified grain flows (Lowe 1976a; Hiscott & Middleton 1979). During the experiments of Arnott & Hand (1989) the bed was not deposited in the quick condition and was not either subsequently or simultaneously disturbed. The grain flows of Lowe (1976a) were not developed as the volume concentration of the particles did not exceed 1-2%.

Lowe (1982) states that flow unsteadiness will inhibit dune formation and cause an increase in sediment concentration close to the bed similar in character to that observed in the experiments of Arnott & Hand (1989). At high rates of suspended load fall out there is insufficient time for the development of a traction carpet and hence deposition occurs directly from suspension. The deposition of a dense, cohesionless

suspension can be described in terms of a liquefied bed, which is identified through massive or crude graded bedding (Lowe 1982). Such sands may form in units several metres thick, and are prone to secondary water escape due to the loose primary packing of the sediment (Lowe 1982).


## (ii) Post-Depositional Mechanisms.

To produce facies Sms through post-depositional mechanisms requires a method of modelling a total loss of structure through a sediment column up to 8 m thick, except for the local preservation of isolated cross-stratified sets, the production of water escape structures and diffuse laminae. A scoured base must also be established.

Liquefaction and fluidisation are the most likely deformation mechanisms in unconsolidated sands (Owen 1987). These processes are described in Appendix II. Fluidisation is more likely to occupy small discrete zones with the effects irregularly distributed. Lowe (1976b) states that in natural systems fluidisation occurs principally in vertical cylindrical or irregular sheet-like structures. Fluidisation is not recognised as a significant mode of sediment transport (Lowe 1976b) or deformation (Owen 1987). Liquefaction is a more ubiquitous process, and three types of liquefaction are described in the literature. These include static, impulsive and cyclic (Appendix II).


*Liquefaction.*

Flat lying sands and silts may become liquefied over depths of many meters during earthquakes, causing the development of large scale soft-sediment deformation (Allen 1982). Seismic events cause cyclic liquefaction of sediment. According to the work of Obermeier (1988) liquefaction during earthquake shaking can originate in a zone as shallow as 2 m below the ground surface and extend to depths of 20 m. If the water table is close to the ground surface the probability of liquefaction is increased. Seepage forces caused by the upward percolation of water may also continue for many days after an earthquake. Cyclic liquefaction is favoured by earthquakes greater than magnitude 6, and by a small grain size and original grain concentration of approximately 40% (Allen 1982). Sand boils are common features of earthquake induced liquefaction, and take the form of large scale vertical tubes of homogeneous sand created by the expulsion of pore fluid (Allen 1982).

Static or loading liquefaction (Lowe 1975) occurs through an increase in pore pressure due to rapid consolidation associated with rapid deposition. When the water

pressure equals that of the effective stress liquefaction occurs. Such a mechanism is possible in a fluvial system where rates of deposition are high and/or subsidence is continuous.

When the liquefying mechanism is withdrawn the dispersed grains settle out and a new texture is established. Packing is more dense in such re-sedimentated units than it was in the primary sediment (Allen 1982). Lowe (1976a) states that current structures would be absent in beds resedimentation from a liquefied sand. Any structures preserved would be related to resedimentation and water escape. However, Allen (1982) suggest that liquefaction of sediment would not result in the total loss of primary sediment textures.


## 7.3.3. Discussion.

Facies Sms is only preserved in the Fell Sandstone Group of the Northumberland Basin and the Naese Sandstone member of the central Appalachian Basin. Few deposits of facies Sms have been described from the rock record, and therefore it must be assumed that the mechanism responsible for their deposition is either rare, environmentally controlled, or the sediments are of low preservation potential and thus usually removed prior to burial. Within Section 2 (Bowden Doors) of the Fell Sandstone Group two generations of facies Sms are exposed (Figure 3.10). These occur at different stratigraphic intervals, approximately 30 m apart. Such a stacking of facies Sms indicates that deposition was controlled at least in part by an environmental factor.

Water escape structures are clearly preserved in the Fell Sandstone Group and conform to the Type B soft sediment mixing bodies of Lowe (1975) where individual pillars are unrelated to dish structures and occur as vertical or steeply inclined zones of homogeneous sand. Water escape structures such as these form b y a variety of mechanisms including the consolidation of rapidly deposited, under-consolidated or quick beds (Lowe & LoPiccolo 1974; Lowe 1975). The presence of water escape structures are an important consideration when modelling facies Sms deposition. The water escape structures were formed prior to the deposition of the overlying cross-stratified sediment, and hence the sediment had undergone liquefaction and partial fluidisation prior to its burial.

In order to deposit facies Sms through primary deposition mechanisms a large volume of accommodation space is required for the preservation of the sediment. This requires either rapid compaction of the underlying sediment pile which would imply the presence of uncompacted mudstones, or syn-depositional fault movements. The mechanism of deposition must be capable of acting for a prolonged period of time in

order to deposit up to 8 m of sediment over a wide area, presumably across the entire fluvial channel.

Facies Sms displays a grain sorting similar to that of the underlying and overlying cross-stratified sandstones, together with a higher primary porosity and lower CI than these sediments. These textural characteristics must also be explained.

The scoured base to facies Sms indicates a current of turbulent character. However, the overlying sediments lack indicators of such turbulence. Hence any mechanism for the deposition of facies Sms must allow for the development of both turbulent and laminar flows.

The deposits of hyperconcentrated stream flows described by Scott (1988) are similar in character to facies Sms, having scoured bases and a paucity of internal structures. Such sediments are also of a high primary porosity and loose packing, and are likely to be waterlogged and hence susceptible to liquefaction following deposition. Turbulence is at least partially dampened by the high concentration of sediment held in suspension, and may result in laminar flow conditions. Concentric laminae such as those deposited at the margins of the basal scours have been described as the result of shearing of a highly concentrated laminar flow by Lowe (1976a) and Postma (1986). However, turbulence must have developed within the flow at some juncture due to the preservation of solitary 2-D and 3-D dunes within the Fell Sandstone Group.

In pre-Cretaceous times the absence of grasses would mean that during floods large quantities of sediment would be available to be taken into a stream channel and be transported in suspension if of the appropriate grain size. Hence, providing sufficient sediment to a fluvial system to create a hyperconcentrated stream flow is not beyond the realms of possibility. However, in order to deposit a sediment pile 8 m in thickness over a channel >250 m wide requires rapid and prolonged sedimentation and/or rapid subsidence.

The effects of positive seepage on fluvial systems has been poorly documented, and hence any modern or ancient sediment descriptions are lacking. In order to produce sediment lacking any structure the seepage effect would have to be high enough to cause fluidisation, and hence upward velocity would have to be in the region of $1.5 \times 10^{-3}$ to $8 \times 10^{-2}$ m/s for a medium grained sandstone (Figure 7.3) such as that deposited within the Fell Sandstone Group and the Naese Sandstone member. These values of vertical fluid movement would have to be maintained over the entire length of the affected channel base (>300 m long by >250 m wide), and would have to be acting for a long period of time in order to allow for the deposition of >8 m of sediment. The seepage of groundwater may explain the localised nature of such

massive sheets, but prolonged fluid movements necessary to produce such thick sandstone sheets seem unlikely. Lowe (1976b) describes fluidisation to be achieved only with difficulty in natural systems and generally occur in areas of high permeability utilising certain pathways, Hence fluidisation is not likely to cause deformation of a thick, laterally extensive bed.

Groundwater charging does not offer any method to produce the scoured bases to sheets or the internal cross-stratification, unless these features are developed in areas of reduced seepage.

The effects of high sediment rain and flow unsteadiness on a fluvial system have not been documented from natural examples, and are only theoretical considerations. Arnott & Hand (1989) documented a cessation to the deposition of lamination when the rate of sediment aggradation within a flume exceeded $6.7 \times 10^{-4}$ m/s. Such high rates of sediment supply could only be maintained within a fluvial environment with continuous flooding and prolonged high concentrations of suspended sediment. Both of these mechanisms are unlikely, as modern-day floods are generally short-lived. The initial wave of such floods could be responsible for the scouring of the base of facies Sms which was then infilled by rapidly aggrading sediment. Again the concentric laminae observed within the scours of facies Sms would be developed through shear of a highly concentrated flow (cf. Lowe 1976b; Postma 1986).

Liquefaction of unconsolidated sediments deposited from high concentration flows is commonly reported from turbidite deposits (Hiscott & Middleton 1979). Such water escape may have been responsible for the development of the large pillar structures within the Fell Sandstone Group and the sweeping, trough-like laminae.

The development of facies Sms through post-depositional liquefaction requires that the upper surface be unconfined in order to allow for the escape of water prior to burial. Hence loading mechanisms are not possible for the development of facies Sms, and liquefaction must have been triggered by cyclic loading due to earthquakes. However, such large scale loss of structure has not been previously documented from earthquake induced liquefaction.

If post-depositional liquefaction of a sediment pile did occur it would not be expected to produce the erosively based scours which are preserved within the Fell Sandstone Group and the Naese Sandstone member unless liquefaction was associated with flow. Water escape structures would be expected (Lowe 1976b), but the preservation of solitary sets of undeformed 2-D and 3-D dunes within otherwise structureless sandstones seems unlikely. Previous studies of large scale liquefaction and resedimentation (Lowe 1976b; Allen 1982) also suggest that re-sedimentation of a liquefied sediment pile would result in a higher porosity and grain packing than in the

original sediment. In facies Sms Cl and primary porosity are actually higher than those of the cross-stratified sandstones.

From the above discussion it is suggested that facies Sms was produced by a primary depositional mechanism or combination of primary mechanisms acting over a prolonged period of time. The sediment was deposited as a loosely packed sediment with high porosity, which was subjected to liquefaction perhaps because of earthquake shocks or particularly high velocity ground water movements (Owen 1987). The processes responsible for the deposition of facies Sms are of low preservation potential and are therefore rarely observed in the rock record.

### 7.3.4. Interpretation Of Facies Sms.

Facies Sms is interpreted to have been deposited through syn-depositional mechanisms, as illustrated in Figure 7.4. The basal scours of facies Sms were formed by a turbulent flow, possibly related to a flooding event. The remaining portion of the sediment flow was highly concentrated due to high proportions of suspended sediment entrained in the flood waters. The basal scours were rapidly filled by a sediment-laden flow of predominantly laminar character, thus forming marginal concentric laminae.

Traction currents were not maintained in the majority of the flow responsible for the deposition of facies Sms, although locally preserved cross-stratification sets indicate that traction flow was possible in some circumstances. Diffuse laminae were produced due to shearing within the sediment/water flow.

The high concentration sediment/water currents responsible for facies Sms production are believed to have been produced during times of flooding. Sand grade sediment would have been removed from inter-channel areas during high flow, thus forming hyperconcentrated stream flows, and conditions of high sediment rain. Groundwater seepage into the base of the channel may also have acted as a contributory factor in raising sediment concentrations, due to a high water table level associated with flooding.

The higher primary porosity of facies Sms than that of the cross-stratified sandstones of the same sedimentary units (Table 7.3) indicates that sedimentation was rapid, and resulted in a metastable grain packing. This maintained a low Cl and high porosity on burial. The water escape pipes were produced by the expulsion of water from the metastably packed sediment. The trigger for water expulsion could have been cyclic or impulsive loading or the movement of groundwater in the underlying sediments (Owen 1987).

The absence of similar sheet-like massive sandstone units within the sedimentological literature suggests that the facies may be rare, or environmentally controlled. In order to preserve thick successions of facies Sms rapid subsidence during deposition is inferred. In the Northumberland Basin syn-depositional fault movements have been documented within the Fell Sandstone Group (Turner *et al* 1993; this study). Such subsidence cannot be proven in the central Appalachian Basin.

Architectural element SM Type 1 (Table 2.6) is composed of facies Sms. This architectural element may therefore be interpreted in terms of high-concentration sediment/water flows which were deposited rapidly in actively subsiding areas during periods of high flow.
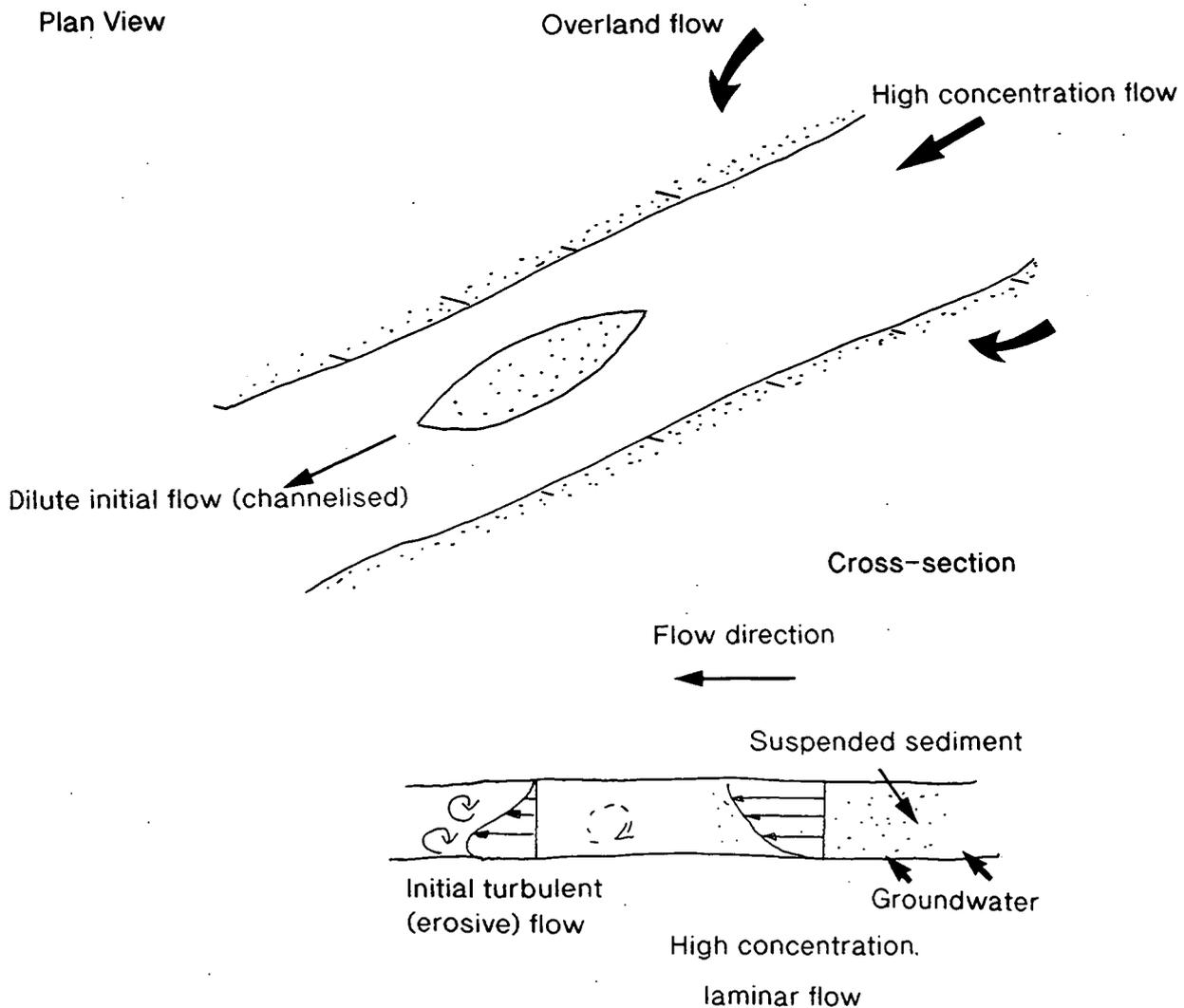


*Figure 7.4. A hypothetical model for the development of facies Sms sandbodies.*

## 7.4. Facies Smc.

### 7.4.1. Description of Facies Smc.

#### (i) Geometry.

Facies Smc is widely recognised from sandstones in the Northumberland, central Appalachian and Illinois Basins (Chapters 3, 4 and 5). The majority of massive sandstone filled channels are exposed in outcrops oriented parallel to the fluvial palaeoflow. In this orientation facies Smc bodies appear near symmetrical and lenticular in cross-section, indicating a high angle trend to the orientation of the major river channel. One channel preserved within the Mansfield Formation is oriented parallel to the palaeoflow.

The margins of facies Smc are generally sharp and well defined. The basal surface of the channel features may be erosive or non-erosive (Table 7.2). Within Section 4 of the Corbin Sandstone (Figure 4.24) scours or flute casts are preserved on the lower bounding surface of a channel. Channel margins vary in inclination with dips reaching 55° as detailed in Table 7.4. In the Fell Sandstone Group the Smc facies cuts through both cross-stratified sandstones and those of facies Sms. Where channels cut through facies Sms they tend to have less well defined margins, and a lower angle of dip.

| Section | Wdth (m) | Depth (m) | Width/ depth ratio | Smc Type | Up-stream margin | Down-stream margin | Smc length (m) | Smc within |
|---------|----------|-----------|--------------------|----------|------------------|--------------------|----------------|------------|
| Fell Sandstone 1 | 5.7 | 3.1 | 1.8 | 1 | 50° | 35° | | DA Type 1 |
| Fell Sandstone 1 | 11.4 | 1.8 | 6.3 | 1 | 25° | 20° | | DA Type 1 |
| Fell Sandstone 2 (1 Fig. 3.10) | 5.3 | 1.3 | 4.1 | 1 | 32° | 34° | | Sms |
| Fell Sandstone 2 (2 Fig. 3.10) | 9.3 | 2.3 | 4 | 1 | 41° | 22° | | Sms |
| Fell Sandstone 2 (3 Fig. 3.10) | 8.6 | 1.6 | 5.4 | 1 | 25° | 38° | | Sms |
| Fell Sandstone 2 (4 Fig. 3.10) | 7 | 2 | 3.5 | 1 | 40° | 32° | | SB Type 2 |
| Naese Sandstone 1 | 10 | 1.75 | 5.7 | 1 | 22° | N/A | | Sms |
| Naese Sandstone 2 | >25 | 1.1 | 22.7 | 4 | N/A | 25° | | DA Type 2 |
| Naese Sandstone 2 | >25 | 3.3 | 7.6 | 1 | N/A | 10° | | DA Type 2 |

| Naese Sandstone 3 | 12 | 1.35 | 8.9 | 2 | 10° | 18° | | DA Type 2 |
|---|---|---|---|---|---|---|---|---|
| Pine Creek Sandstone 1 | 105 | 4.4 | 23.9 | 4 | 55° | 20° | >25 | SB Type 1 |
| Pine Creek Sandstone 2 | 56.6 | 2.08 | 27.2 | 4 | <10° | 20° | | CM |
| Corbin Sandstone 3 | >95 | 4 | 23.8 | 4 | N/A | N/A | >20 | DA Type 1 |
| Corbin Sandstone 4 | 28 | 3.35 | 8.4 | 1 | N/A | N/A | | DA Type 1 |
| Mansfield 1 | 35 | 3.15 | 11.1 | 1 | 14° | 32° | >30 | DA Types 1 & 2 |
| Mansfield 2 (V) | 3 | 1 | 3 | 1 | 20° | 27° | | DA Type 2 |
| Mansfield 2 (W) | 15 | 3 | 5 | 1 | 12° | 20° | | DA Type 1 |
| Mansfield 2 (X) | 10 | 1.2 | 8.3 | 1 | 22° | 35° | >25 | DA Type 1 |
| Mansfield 2 (Y) | 20 | 2.25 | 8.9 | 1 | 10° | 24° | | DA Type 1 |
| Mansfield 2 (Z) | 15 | 2.5 | 6 | 1 | 14° | 18° | >10 | DA Type 1 |
| Mansfield 2 | 6 | 1.5 | 4.8 | 3 | 35° | 35° | <3 | DA Type 1 |
| Mansfield 4 | 40 | 1.75 | 22.9 | 4 | 10° | <10° | | CM |

*Table 7.4. The characteristics of facies Smc sandbodies.*

A simple sub-classification of facies Smc may be made on appearance in cross-section. Table 7.4 & Figure 7.5. detail the width/depth ratio of the measured channels. Figure 7.5 illustrates a clear distinction between channels of facies Smc with a width/depth ratio of <12 and >20. Channels with a width/depth ratio >20 have margins which generally dip 10-20° with the upstream margin tending to be steeper (Table 7.4). Channels with a width/depth ratio <12 display margins which dip 10-50°. Generally facies Smc is seen to erode through underlying cross-stratified sediments of DA Type 1 and 2, SB and CM architectural elements (Table 7.4). In Naese Sandstone Section 2 (Figure 4.9) one of these channel-like units has margins which lie parallel to the foresets of the adjacent cross-stratified sandbody (DA Type 1 architectural element). The upper bounding surface of facies Smc is generally planar and coincident with third order bounding surfaces.
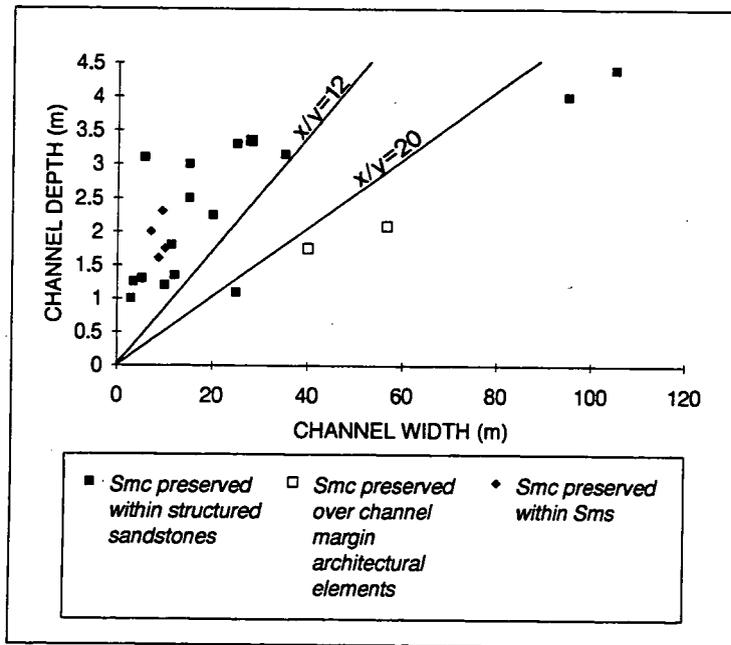
*Figure 7.5. The relationship between width and depth of facies Smc sandbodies.*

Where facies Smc is exposed in three-dimensions it clearly possesses a plane of elongation which is oriented perpendicular to the flow direction established from the fluvial channel through cross-bed foresets (Figure 7.6). However, the length of this plane is difficult to determine. In the Mansfield Formation of the Illinois Basin facies Smc may be traced for >30 m laterally (Table 7.4). Lateral extent of facies Smc is also observed in the Corbin Sandstone formation (Section 3) where a sandstone unit may be traced in excess of 20 m with no observed change in the cross-sectional area of the sediment body (Table 7.4). In Section 2 of the Mansfield Formation a small channel is elongate parallel to the flow direction established from cross-stratification and may be traced for <3 m in this direction (Table 7.4).

Internally facies Smc units are largely structureless. Towards channel margins concentric laminae, 20-40 mm apart, are commonly preserved, and these extend for a maximum of 20 cm into the channels before grading into the homogeneous fill. Diffuse laminae may also be preserved in the upper portion of facies Smc, but these have a more undulose appearance. Ripples have been noted from the upper surfaces of Smc units in the Mansfield Formation (Section 1) and the Pine Creek Sandstone member (Section 1). These ripples are asymmetric and rounded, and display a sense of current movement in a direction parallel to that of the underlying facies Smc.
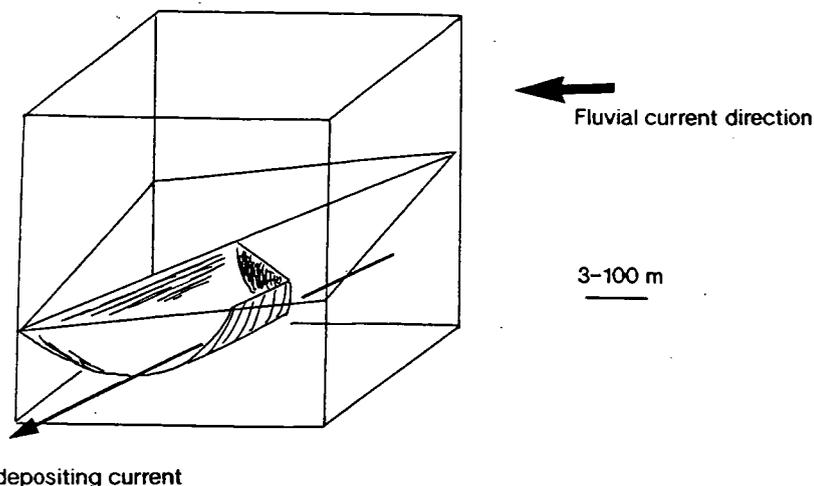
Figure 7.6. A probable three-dimensional reconstruction of facies Smc sandbodies.

Within the Corbin Sandstone formation, the Pine Creek Sandstone member and the Mansfield Formation the base of facies Smc may be defined by a layer of quartz granules and small pebbles, together with iron stained mudclasts and organic debris. These clasts also appear along scour surfaces within facies Smc, such as within the Mansfield Formation Section 1 (Figure 5.13) and Pine Creek Sandstone member Section 2 (Figure 4.12). These internal scour horizons and associated clast lags are interpreted as the basal surface of a successive channel of facies Smc. Dewatering structures in the form of water escape pipes are also locally preserved in the upper portions of channels in the Mansfield Formation.

## (ii) Textural Characteristics.

Facies Smc of the Northumberland, central Appalachian and Illinois Basins tends to be better sorted than the structured facies within which it is preserved (Appendix III), and it is generally coarser grained than the structured facies and sheet-like massive sandstones (Table 7.3). The primary porosity of facies Smc is similar to that of the structured facies and the CI tends to be lower (Appendix III & Table 7.3).

A limited permeability study of Smc sandbodies has been undertaken (Table 7.3) which has shown that the permeability of Smc sandbodies is variable. Smc Types 1 and 4 have been sampled from the Fell Sandstone Group and the Mansfield Formation. These sandbodies have higher permeability than the surrounding cross-stratified sandstones. Type 2 Smc units were sampled from the Naese Sandstone

member and these display a lower permeability than the associated cross-stratified sandstones.


## 7.4.2. Possible Mechanisms For The Production Of Facies Smc.

Previous descriptions of facies Smc have interpreted it to be the result of bank or bar collapse (Turner & Monro 1987; Rust & Jones 1987; Wizevich 1991) or braid channels (Hodgson 1978). In the models of bank or bar collapse the scoured base of facies Smc is developed in front of downstream advancing bedforms. However, the recognition of four types of facies Smc suggests that more than one process of deposition may be responsible for their formation.

The channels of facies Smc are often developed beneath major third order bounding surfaces, are generally lenticular in cross-sectional profile, and elongate parallel to the plane of transport (Figure 7.6). The basal portion of the channels display concentric laminae 5-10 mm apart which grade into the massive sandstone channel fill within approximately 40 cm. Such concentric laminae have been attributed to the deposits of sheared, laminar, high concentration currents in the past (Lowe 1976b; Postma 1986). Water escape structures occur in the upper portions of channels and are interpreted in the literature in terms of liquefaction (Lowe 1976b).

Channels of Types 1,2 and 4 (Tables 7.2, 7.4) display a sense of movement which is oriented in a plane oblique or perpendicular to the fluvial palaeoflow direction, as measured from cross-stratified sandstones within the same channel system. The orientation of facies Smc units indicates that they were formed by sand-laden currents moving across the main fluvial channel. Smc Type 3 is oriented parallel to the flow direction and was produced by currents moving parallel to the local palaeoflow direction.

In order to deposit facies Smc in a fluvial environment a model invoking erosionally based, dense sediment-laden flows is required. Such flows may develop syn-depositionally during initial sedimentation or through re-sedimentation associated with sediment gravity flows.

## (i) Syn-Depositional Mechanisms.

*Dissection of braid bars.*

Dissection of braid channels is a process which has been described from a number of modern braided rivers. Erosively based channels may be created on the upper surfaces of braid bars either at low stage during emergence or during floods.

Cant & Walker (1978) described erosional modification of sand flats (macroforms) during flooding in the South Saskatchewan River. Erosion of macroforms occurred with the development of a channel or number of channels oriented across a macroform surface. These channels were generally <1 m deep and concentrated flow during falling water stage. Cant & Walker (1978) described these channels as being infilled by downstream migrating 2-D and 3-D dunes during falling stage.

In the Donjek River erosional channels created during falling stage shift laterally and form steep, erosional banks on the sides of macroforms (Rust 1972). Such bars are generally located towards the downstream end of bars. With continued water level fall sands accumulate in wedges at the bar margins. The fill of these scours is structured by cross-stratification (Figure 7.7).
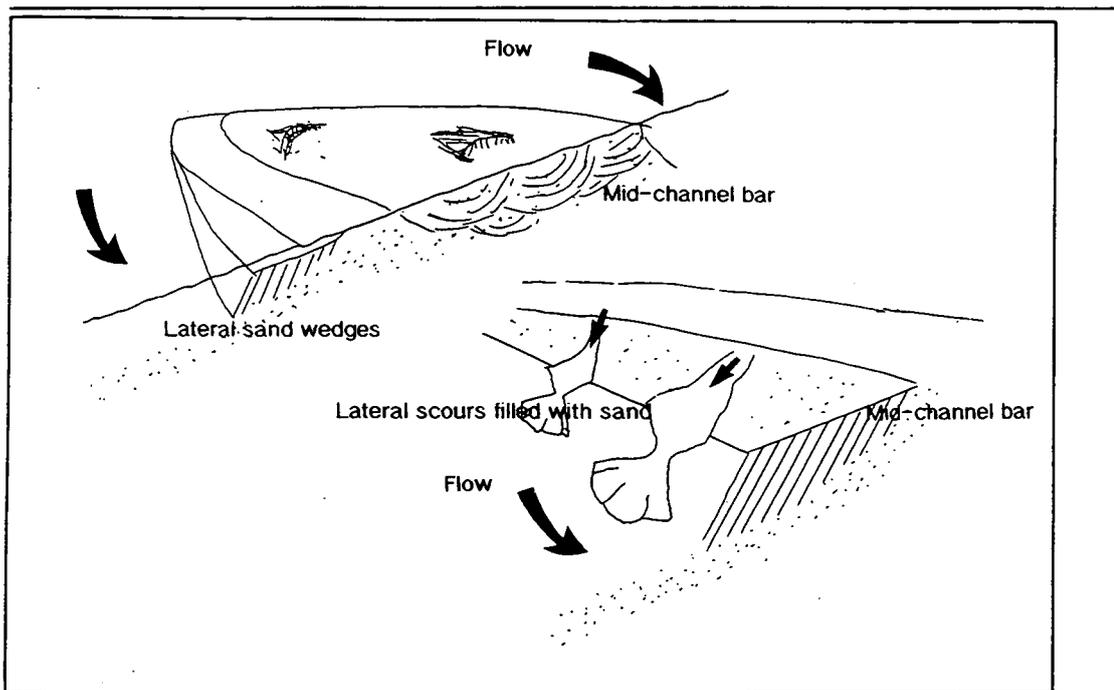


*Figure 7.7. Formation of a sand wedge adjacent to a mid-channel bar. Planar cross-stratification due to outward migration of the slipface. Dissection of sand wedges after further fall in water level (modified after Rust 1972).*

Dissection of a 2-D dune has been documented from the Fell Sandstone (Bowden Doors, Figure 3.10). However, this channel is <0.75 m across and 0.30 m deep. Channels of facies Smc occur on a scale of magnitude greater than this. All the river systems which contain facies Smc are documented to have been perennial in character, with little evidence of emergence and foreset reworking of macroforms. Hence, channel or scour development during a period of significant falling stage is unlikely.

Dissection of bedforms during floods provides a possible mechanism for producing facies Smc (Types 1,2 & 4). However, comparable channels documented from modern examples such as those within the South Saskatchewan River are filled with cross-stratified sandstone, not a structureless sandbody. Thus turbulence must have played a major role in their formation. In order to create a massive sandstone flow turbulence must be dampened somehow. This can be achieved by raising flow viscosity and promoting the development of laminar flow conditions. Such conditions could be created during floods, but would have to be maintained for a prolonged period of time, including the falling stage, in order to allow for the deposition of structureless sandstone. The concentric laminae could be explained as a result of shearing of the highly concentrated flow (cf. Postma 1986). Rapid deposition of a highly concentrated sediment dispersion would result in an underconsolidated unit which could de-water to produce the fluid expulsion structures documented in the field. The ripples which have been observed to overlie some units of facies Smc represent re-working of the top of the abandoned channel fill.

*Scour in front of a downstream migrating bedform.*

Scouring at channel confluences and braid bar confluences has been described by Best (1988) and Bristow *et al* (1993) respectively. The two processes are believed to be similar in character. Confluence areas are highly complex, with sediment dispersal in the junction controlled by a complex interplay of hydrodynamic flow parameters relating to the joining segments of a channel.

Best (1988) and Bristow *et al* (1993) describe the major controls on channel morphology in the confluence area as the junction angle and the ratio of discharge between the two confluent channels (Figure 7.8a). Mutual deflection of flow and sediment by each of the confluent streams results in a large separation zone (Figure 7.8a). This causes segregation of sediment loads from each channel at the centre of the junction, and together with high velocities and levels of turbulence results in an avalanche face at the mouth of each confluent channel (Figure 7.8a). The avalanche faces dip into a pronounced scar or confluence scour (Figure 7.8a). A larger junction

angle result in larger scours and larger bars to form in the separation zone (Bristow *et al* 1993).

In both symmetric and asymmetric planform junctions the confluence scour originates near the upstream junction. The orientation of the scour varies with the discharge ratio (Best 1988). As the contribution of flow from one tributary channel increases, so the scour aligns with this (Bristow *et al* 1993). The amount of scour generally exceeds that generated in the lee of bedforms, and therefore such scours are likely to be areas of maximum erosion (Figure 7.8b). In large rivers such as the Brahmaputra, scours reach 30 m in depth (Bristow *et al* 1993). The most likely mechanism of scour fill is through the downstream migration of tributary bars.

Asymmetric Confluence       Symmetric Confluence

Tributary mouth bar

Confluence scour

Separation zone bar

Tributary mouth bar

Confluence scour

Separation zone bar

Mid-channel bar
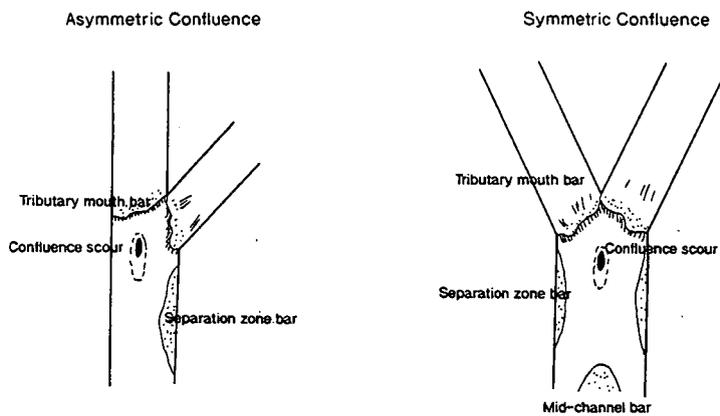
*a) Plan view*
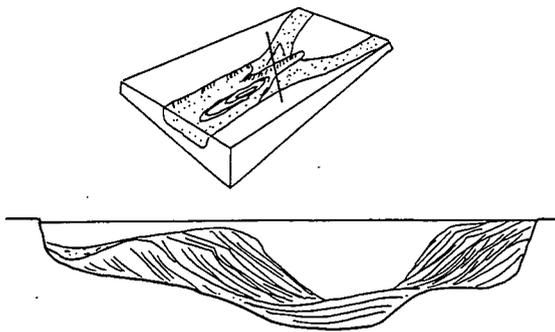
*b) Hypothetical cross-section of symmetrical confluence zone.*

*Figure 7.8. Bed morphology at confluence scours (modified after Bristow et al 1993).*

As described above the most usual method of filling confluence scours is through the migration of bedforms, thus producing cross-stratified sediments. In order

to fill the scours with facies Smc Types 1,2 & 4 sediment-laden currents must move across the channel. These current must be of high sediment concentration and hence flow by laminar means. The confluence scour may then be filled with a structureless sandstone. Marginal laminae would result from freezing of the flow margins. Alternatively, collapse of an avalanche face may occur, causing sediment to be re-deposited in the scour. Such flows would be liquefied (Lowe 1976b) and result in the deposition of a highly concentrated sediment/fluid mixture capable of flowing under laminar conditions.

*Flooding & Crevasse Splay Deposition.*

Deposition following high water flood stages in a river channel may result in the rapid dumping of sediment, thus temporarily precluding sorting of sediment and the formation of traction related structures. High sediment concentrations will also dampen turbulence and thus prevent the development of traction bedforms. These processes have been described above and in Appendix II.

Crevasse splay sandstones are described from many ancient meandering river systems including the Ravenscar Group (Mjøs *et al* 1993). A number of these crevasse splay deposits have been documented to be massive in character with a sharp or erosive lower surface (Mjøs *et al* 1993). Crevasse splay sandstones are oriented in a plane oblique to the fluvial palaeoflow, and are lobe-shaped, decreasing in size away from the fluvial channel.

Within Pine Creek Sandstone Section 2 (Figure 4.12) a unit of Smc is preserved overlying CM architectural elements of levee origin. Thus the Pine Creek Sandstone river had stable banks inundated by periodic flood events. Breaching of the levees may have resulted in the deposition of a sandstone unit which flowed away from the fluvial channel i.e. in a direction oblique to the fluvial current.

The massive nature of the Pine Creek sandbody would suggest it was deposited rapidly from a highly concentrated stream flow, related to high flow stage within the fluvial channel. In order for flood waters to be of sufficiently high concentration to deposit a massive sandstone unit, the sediment concentration of the river water must have been high, and the suspended sediment must have been evenly dispersed throughout the entire water column. Such uniform vertical sediment concentration distribution has been documented from modern day rivers in China (Figure 7.9).
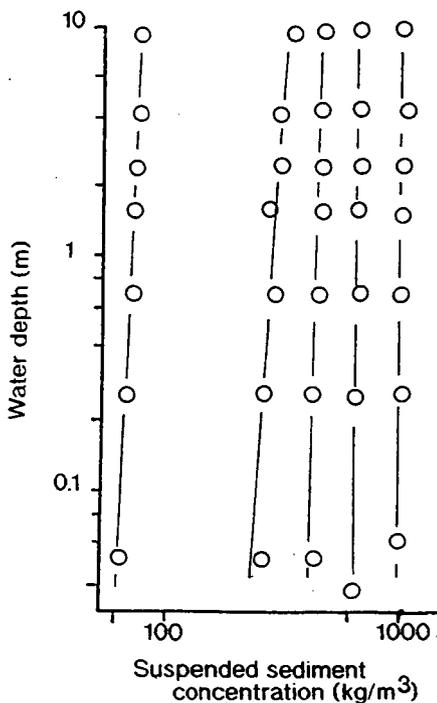
*Figure 7.9. Vertical distribution of suspended sediment concentration in the Wudibghe River, China (modified after Xu 1993).*

## (ii) Post-Depositional Mechanisms.

In order to produce facies Smc through post-depositional mechanisms it is necessary to produce sediment laden currents moving across, and less commonly along, the fluvial channel. These currents must either erode a channel or utilise already existing channels, within which a unit of facies Smc is deposited. The currents which deposit the massive sandstone fill of facies Smc is assumed to be highly concentrated and predominantly laminar in nature.

*Bank collapse.*

Collapse of a fluvial channel bank is capable of producing a sediment-laden current moving across the channel, in the manner indicated from the deposits of facies Smc Types 1,2 and 4. Channel bank collapse has been documented from many modern rivers. Coleman (1969) and Thorpe *et al* (1993) have described large bank collapse features from the Brahmaputra which reach 330 m in length. Laury (1971) described collapse features from the Mississippi, and similar features have been documented from the Ohio River by Hagerty *et al* (1981). Three dominant types of

276

bank failure have been recognised: 1) shearing, 2) liquefaction and sediment flow and 3) rotational sliding (Laury 1971; Hooke 1979).

Shearing failures occur in the upper bank, generally as the result of channel undermining. Slumps of bank material are typically on the metre scale. Upon failure slumps may remain coherent or become flows entrained by the flow (Bridge 1993a). In rotational failures large blocks of bank sediment fail along an axis and slump into the channel. Flow failure due to liquefaction results from a sudden loss of shear resistance (Sasitharan *et al* 1993). If the pore pressure rises or the total stress falls to a point where the value is zero then the sand looses all shear strength and becomes liquid-like or quick. Even where the shear strength does not reach zero, a drop in strength can cause slumping or landslip (Kramer 1988). Sediment flow failures occur beneath the water level or in the zone between high and low water and are usually associated with some form of undrained loading to trigger the collapse.

The type of bank failure is controlled by the textural characteristics of the bank material. Factors such as bank sediment type, thickness, cohesiveness, effective porosity and depth of thalweg scours are all important in determining the nature of bank failure, together with magnitude and frequency of floods (Laury 1971). The cohesive strength of banks is increased by the presence of clay minerals and vegetation. The presence of roots can impart a shear strength to banks, and as roots are hydraulically rough they tend to reduce flow velocities at the bank (Keller *et al* 1990). Thus vegetation reduces bank erodability.

Rotational failures are most likely in cohesive soils (Figure 7.10). Such rotational failures have been documented from the rock record and include deposits from the Desmoinesian of Iowa, USA (Laury 1971). However, the deposits of facies Smc examined in the field are composed of medium to fine grained sand, with little matrix fines (<10%), and hence it is assumed that they would not have remained cohesive blocks during rotational failures. Clean sand has no cohesive strength; all the shear strength is derived from friction between the grains. Fine to medium grained sands are most susceptible to liquefaction (Lowe 1976b), and it would therefore appear that the sediments were deposited at least in part by liquefaction of bank material.

Bank erosion is determined by a number of factors. Where a river is eroding near banks a deep pool is eroded in the thalweg of a channel (Figure 7.10) which leads to oversteepening, and thus failure (Turnbull *et al* 1966). In meandering rivers erosion takes place on only one bank. However, in braided channels both banks may experience deposition or erosion simultaneously. Coleman (1969) defines several factors responsible for bank changes in braided rivers which include rate and rise of water level, number and position of active channels, angle at which the thalweg

approaches the bankline, formation and movement of large bedforms, and the relationship of abandoned river courses to present channels. These factors are impossible to quantify from ancient deposits, however, it may be assumed that bank erosion within braided systems would have been an active process in the past.



COHESIVE TOPSTRATUM

POROUS SUBSTRATUM
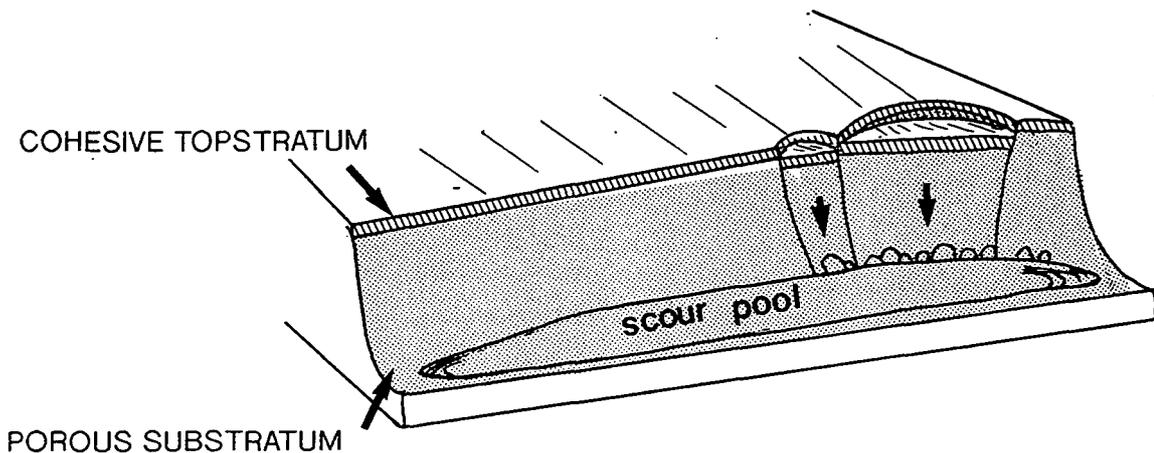
*Figure 7.10. The effect of topstratum on bank failure. For thin topstratum failures are numerous. Failures are initiated in the subaqueous zone, with liquefaction of sediment followed by bank failure (modified after Turnbull et al 1966).*

The effects of seepage on bank erosion were investigated by Burgi & Karaki (1971) whose experiments suggested that both positive seepage and velocity of channel flow are important considerations for bank erosion. At channel flow velocities of <0.3 m/s bank erosion was found to be sensitive to positive seepage, and to vary directly with the local hydraulic gradient. Above this velocity the dominant cause of bank erosion was the velocity of flow, producing shear stress exceeding that of the bank material. Iverson & Major (1986) and Howard & McLane (1988) have also addressed the role of seepage in inducing bank failure. From these studies it becomes clear that seepage undermines slopes, with the seepage path most conducive to failure occurring when flow paths make an acute angle outward from the surface of the slope. Seepage induced failure has been documented by Carter (1975a) from a dam site. Escaping groundwater was seen to produce fluidised flows of fine to medium grained sand 1-3 cm wide and <1 cm deep.

Cyclic liquefaction of soils due to the effects of earthquakes has also been described as a major factor in the development of landslips. Seed (1968) has documented liquefaction of sandy soils related to earthquakes of 5.5-8.5 magnitude. The landslides were in excess of 400 m across in a number of areas including Alaska (1964) and Chile (1960). Jibson & Keefer (1993) have documented large rotational and flow slides from the Mississippi valley, USA, related to the earthquakes of 1811-1812.

The frequency of landslides in the tropical environment of South Africa have been examined by Garland & Olivier (1993) who documented a valid statistical relationship between landslides and wet seasonal rainfall. During periods of flooding, water is forced into the bank sediment, raising the pore pressure. As the water level in the river falls the pore pressure in the bank sediments drops and the water moves back into the river. This will cause the movement of sand and silt into the channel, and induce flow failure. Kramer (1988) states that liquefaction can be triggered on gentle slopes by rapid, moderately sustained drawdowns of relatively small magnitude.

Andresen & Bjerrum (1967) have documented flow slides from modern marine environments. These flows generally start in the lower part of a slope as the result of local oversteepening due to erosion or seepage pressures. Following the initial slip the flow develops slice by slice due to the liquefaction of sands. The flow then moves away leaving an unsupported face of sand behind (Andresen & Bjerrum 1967). Flows such as these develop retrogressively, and in many cases increase in width (Andresen & Bjerrum 1967). The slides may be long, tongue-like or circular depressions with bottle-neck openings (Andresen & Bjerrum 1967). The liability of a slope to flow depends on excess pore pressure with sands of 40% porosity failing at very small strains (Andresen & Bjerrum 1967).

Due to the migration and avulsion of channels in braided fluvial systems the river banks are intersected by a number of abandoned channels which contain porous, well sorted sands and silts (Coleman 1969). The presence of sediments highly susceptible to liquefaction will cause the failure of banks to occur in specific places. Repeated failure of bank sediments due to retrogressive slumping will cause stacking of flow deposits such as those described by Andresen & Bjerrum (1967).

Flow of a sediment/fluid mass may only occur when the strength of the mass produced by cohesion and internal friction is overcome. In cohesionless sands frictional and inertial forces dominate. Obermeier (1988) has documented liquefaction and flow slides on slopes of over 5°. On such shallow slopes soil masses can move as blocks of intact materials riding on liquefied flows (Obermeier 1988), or waterlogged unconsolidated sand can be transformed to a viscous liquid by liquefaction or fluidisation (Allen 1982).

During flow and deposition the laminar or turbulent character of a flow is governed by a combination of flow velocity, density, cohesive strength, flow thickness and viscosity (Postma 1986). The Smc deposits studied are composed of sandstone with less than 10% mud matrix (Appendix III), thus the sediment gravity flows produced from these deposits would have lacked cohesion. The sandstones preserved are massive in character, indicating that the flows which deposited them must have been, at least in part, laminar. High concentration dispersions tend to be laminar in nature (Fisher 1971; Allen 1982) and clean sandstones, such as those preserved within facies Smc, are likely to maintain Newtonian behaviour i.e. a linear relationship between shear stress and shear rate (Appendix II) with sediment concentration of up to 40% (Pierson & Scott 1985). However, initial liquefaction or incorporation of sediment during the life of the flow may raise the sediment concentration beyond this point.

Laminar, high concentration, cohesionless gravity flows take the form of liquefied flows or grain flows (Appendix II), with deposits generally termed cohesionless debris flows (Postma 1986). Two cases of laminar high concentration flow are possible: 1) flows that were transformed from a fully sheared either laminar, or more likely turbulent flow, and 2) flows that were never fully sheared and hence were deposited as relict plug flows (Postma 1986).

Liquefied flows have been described extensively (Lowe 1976b; Hiscott & Middleton 1979; Postma 1986). Such flows tend to have flat, unscoured bases. Middleton & Southard (1978) state that liquefied flows could not move down a substantial slope without becoming turbulent. However, evidence from modern (Andresen & Bjerrum 1967) and ancient deposits (Postma et al 1983) suggest that liquefied, fully homogenised sands and sand-rich gravels can move as laminated flows over relatively long distances on steep to gentle underwater slopes without becoming turbulent.

Nemec (1990) describes two possibilities for movement of a liquefied flow. Following mobilisation and slight dilation due to liquefaction a sediment/water mixture may either rapidly accelerate to become a turbidity current (Figure 7.11) or collapse and continue to move as a cohesionless debris flow or liquefied slide (Figure 7.11) in the form of a non-Newtonian flow. Lowe (1976b) ascribes massive sandstones to settling out of flows transitional between liquefied flows and turbidity currents. As transport in the bedload layer becomes dominated by grain collisions a traction carpet develops which is maintained by dispersive pressure (Lowe 1982). Such flows are estimated to be of a maximum of 5 cm in thickness and create crude laminae. At higher suspended loads deposition occurs direct from suspension. Such deposits are of a grain supported fine sand which may be massive or show evidence of water escape structures (Lowe 1982).

SLIDE

Coherent mass

SLUMP

Coherent mass with
internal deformation

FLOW WITH PLASTIC BEHAVIOUR
Non-turbulent

Possibly with entrained turbidity flow

FLOW WITH FLUIDAL BEHAVIOUR
Fully turbulent
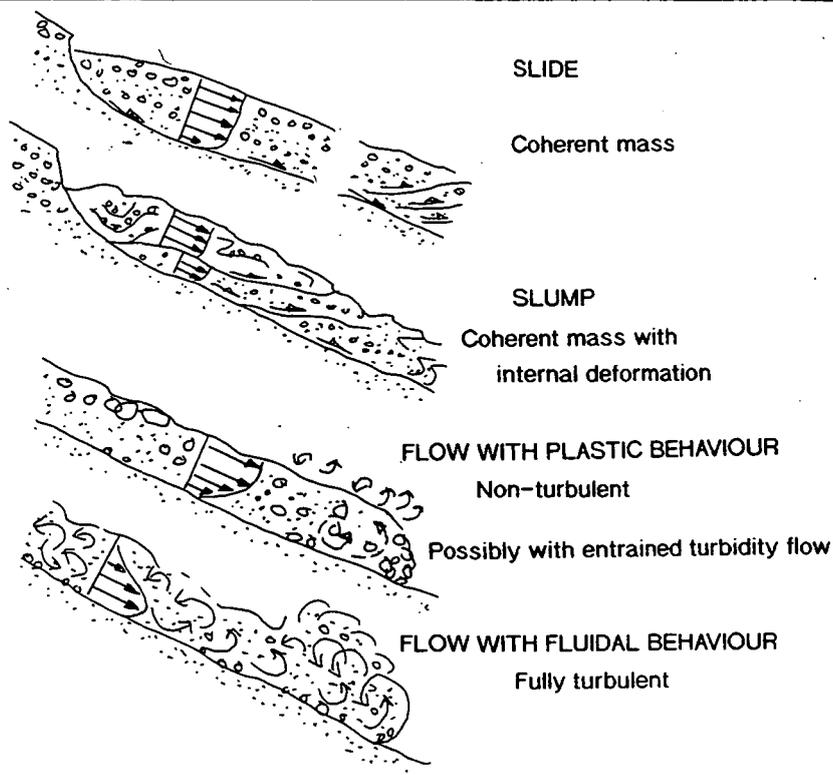
*Figure 7.11. Range of gravity driven processes operative on steep slopes (modified after Nemec 1990).*

Dense non-Newtonian slurries flowing in open channels may exhibit a tendency for shear to be concentrated at flow boundaries and for rigid plugs to form towards the centre of the flow (Johnson 1970; Pierson & Scott 1985) i.e. the relict plug flows of Postma (1986). Shearing of highly concentrated suspensions must involve dilation along a shear surface (Postma 1986) and may result in crude centimetre laminations such as those described by Hiscott & Middleton (1979) and Lowe (1976a). Such laminae have been noted at the margins of facies Smc. Deposition of flows is interpreted to be characterised by freezing caused by outward growth of a plug as a result of 'frictional strength'(Carter 1975b; Lowe 1976a). Such plug-flow deposits have been described by Postma *et al* (1983) and, as documented in Table 7.1, these flows are characterised by a U-shaped trough with diffuse bedding at the scour margins. However, plug flows tend to display random orientations of clasts within them. These are not seen in facies Smc.

*Bar collapse.*

It may be assumed that the processes described above for mass flow related to bank collapse may also hold true for mass flow due to bar collapse. However, the amount of sediment available for remobilisation is more limited due to the size of the macroform or mesoform involved. Bar collapse may occur either parallel or transverse to the fluvial flow direction. Currents moving transverse to the flow direction would be capable of producing Smc of Types 1,2 and 4, with collapse parallel to flow capable of producing Smc Type 3.

Bar collapse is expected to occur through liquefaction in the manner described above. Liquefaction may be cyclic or impulsive. Cyclic liquefaction, in the form of wave induced failure, has been documented from the Bay of Fundy by Dalrymple (1979). The study documented isolated slump-like bodies located on the crest and stoss side of steep dunes. A rapid increase in applied stress such as would accompany sudden increases in wave height, or rapid water level fall during ebb tide or declining river flood are favourable for production of deformation (Dalrymple 1979).

Impulsive liquefaction occurs due to a single large shock which destroys the metastable grain packing of an unconsolidated sand (Owen 1987). Such instantaneous events may be due to impact or loading related to a landslide event. Oversteepening of the bedform or a sudden loss of shear strength may result. Plate 5.3. illustrates deformation of a DA Type 1 macroform element due to the emplacement of a sandbody of facies Smc.

A bedform with low relief would not be expect to produce an erosively based sedimentary gravity flow due to the lack of potential for acceleration. Such flows would be expected to move away from the point of failure slowly, perhaps in the form of a modified grain or liquefied flow (Lowe 1976b). As described above such flows are typically non-erosive. Freezing of the flow may result in the production of marginal laminae (Lowe 1976b).

## 7.4.3. Discussion.

The channels of facies Smc display margins which dip at a steep angle, many of them beyond the angle of repose for wet sand (Table 7.4). Thus the channel-like features must have been cut and filled rapidly. The four types of facies Smc share characteristics which include the steep channel margins, a massive sandstone fill with concentric marginal laminae, and the presence of diffuse near horizontal laminae in the upper portion of the channels.

The turbulent nature of the initial currents forming facies Smc scours is illustrated by the presence of flute clasts preserved across the base of Corbin Section 4 (Table 7.4 & Figure 4.24). Plate 5.3 illustrates an example of a Type 1 Smc unit causing deformation within a pre-existing bedform thus indicating a dynamic mode of deposition. However, the massive sandstone fill of facies Smc, and preservation of concentric marginal laminae are features which have been related by previous workers to the deposits of high concentration laminar sediment gravity flows (Carter 1975b; Lowe 1976b; Postma 1986), or to freezing of the outside of a debris or plug flow as the inside was still moving (Postma et al 1983). Random clast orientations will occur within a rigid plug where the plug was developed at the onset of flow (Carter 1975b). Such random clast orientations are not preserved within facies Smc and hence deposition is believed to have been through laminar flow. The undulose laminae in the upper portion of facies Smc may be produced by reverse shear formed at the sediment/water interface (Carter 1975b). The ripples which are preserved over some Smc deposits (Mansfield Section 1, Pine Creek Section 1) may be due to late dilution of the flow and the return to turbulent current conditions, or they could be produced b y re-working of the top of the channel fill following abandonment.

The positioning of the area of preservation of facies Smc scours within fluvial channel macroforms is of importance in the interpretation of these features. In the past, the scoured portion of facies Smc has been interpreted to have been created initially in front of an advancing bedform or macroform (Turner & Monro 1987). However, many units of facies Smc are seen to cut out previously deposited structures from within macroforms (Figures 4.11, 4.23, 5.13, 5.15), and hence at least some Smc sandbodies were deposited on the top of fluvial channel macroforms, as opposed to in the advancing scour.

A number of possible mechanisms capable of creating a scoured channel, filled by massive sandstone have been described above. A possible syn-depositional process is braid bar dissection. Post-depositional mechanisms include mass flow related to bank and bar collapse.

Dissection of braid bars has been documented from modern deposits during flood and low stage reworking (Rust 1972; Cant & Walker 1978). However, the perennial nature of the river systems studied, together with lack of evidence of low stage reworking indicates that any dissection must have occurred at high stages. The scale of flood created scours documented by Cant & Walker (1978) is small when compared to the size of Smc deposits. Scours associated with flooding also have no preferred axis of orientation, and may develop either parallel or oblique to the channel flow direction. All Smc sandbodies, with the exception of one, are oriented perpendicular to the flow direction.

Deep scours of up to 30 m have been documented from confluence zones in front of braid bars in the Brahmaputra river (Bristow *et al* 1993). Such scours provide a syn-sedimentary mechanism to produce the basal scour of facies Smc. It has been established from palaeohydrological reconstructions detailed in this study, that the Corbin and Naese Sandstone rivers were of a similar scale to the Brahmaputra. In the lee of macroforms (DA Type 1 architectural elements)· of the Naese and Corbin Sandstone rivers confluence scours of a similar size to those of the modern day Brahmaputra could be expected. However, the dominant mechanism of filling such scours is through downstream accretion of bedforms.

The massive sandstone fill of facies Smc displays better sorting characteristics, and higher primary porosity than the structured sediments within which the facies is preserved (Table 7.3). Types 1 and 4 Smc sandbodies also display higher permeability values than the surrounding cross-stratified sandstones. Such textural differences indicate that the sediments of facies Smc were reworked prior to deposition, and hence suggest that the sandbodies represent deposition from remobilised sediment.

Re-sedimentation of bank or bar deposits to produce facies Smc has been used as a possible model of sandbody deposition in the past (Turner & Monro 1987; Wizevich 1991). Gravity flows are capable of producing sediment-laden currents which move across the fluvial channel i.e. in the same orientation as the sandbodies of Smc Types 1, 2 and 4 (Table 7.2). Remobilisation of sediment to fill confluence scours through collapse and flow of an advancing bedform avalanche face may produce a deposit of non-erosional nature, lying parallel to the foresets of the advancing bedform slipface. The massive sandstone would then be buried by the advancing braid bar. Such characteristics are displayed by Smc facies Type 2 (Table 7.4).

Some sediment bodies of facies Smc are exposed in three dimensions, and hence a volume estimate may be made of the sediment involved in such flows (Table 7.5). Channels are irregularly shaped, and may be approximated to either a semi-cylindrical pipe or a rectangular body. These two volume estimates give highest and lowest possible values.

The sediment volumes of Smc Types 1 and 4 deposited within the deposits of major channel elements are considerable (Table 7.5) and are interpreted to be much larger in volume than the channel macroforms through which they cut. Therefore bar collapse could not have produced the large volumes of sediment deposited within Smc Types 1 and 4, and bank collapse must have provided the sediment.

| Smc Type | Formation | Sediment volume |
|---|---|---|
| Type 1 Smc | Mansfield Formation.<br>Section 1 (Figure 5.13)<br>Section 2 (Channel X, Figure 5.14)<br>Section 2 (Channel Z, Figure 5.14) | 467.50-3307 m$^3$<br>113.10-300 m$^3$<br><br>196-375 m$^3$ |
| Type 3 Smc | Mansfield Formation.<br>Section 2 (Figure 5.14) | 7.30-13.50 m$^3$ |
| Type 4 Smc | Corbin Sandstone formation.<br>Section 3 (Figure 4.23) | 500-6000 m$^3$ |

Table 7.5. Volume estimates for sediment preserved in facies Smc sandbodies.

Large scale bank collapse features have been documented from modem environments. However, as illustrated in Figure 7.1, during pre-Cretaceous times a lack of grasses resulted in a lack of bank cohesion and hence banks would have been far more susceptible to collapse. The sediments of facies Smc are composed of fine to medium grained sandstone which is highly susceptible to liquefaction (Lowe 1976b). It may be assumed that during the deposition of the formations studied bank erosion was an active process.

Methods of bank failure are described above. Flooding and related drawdown, earthquakes and groundwater seepage are all documented as causing liquefaction and flow of banks. These may also act in combination. In the Mansfield Formation facies Smc is concentrated in specific areas of the outcrop and may take the form of stacked units (Section 1, Figure 5.13). This indicates that there was some environmental control on the location of bank collapse. Coleman (1969) described the intersection of ancient river courses with the active channel of the Brahmaputra. If such abandoned river courses were present at the margins of the Mansfield Formation river they may have been responsible for the localisation of collapse features. The stacked bodies of facies Smc may have been deposited through retrogressive slumping of bank material in the manner described by Andresen & Bjerrum (1967).

From the evidence presented above it is suggested that the sediments of facies Smc Types 1 and 4 were most likely deposited from a non-Newtonian, cohesionless debris flow. Thus it is possible to estimate the velocity at which the

transition from laminar to turbulent flow would occur (see Appendix II). Table 7.6. details the flow and physical parameters of cohesionless debris flows. The symbols used are detailed in Appendix I.

$\tau_c$ (Table 7.6) represents the critical shear stress for turbulent flow character (Appendix I). Hence for subaerial flows the turbulent/laminar flow transition will occur for velocities in excess of 70 m/s, in channels at 17 m/s, and in subaqueous environments at 5 m/s (Table 7.6). The slope required for a debris flow to move may also be estimated. A flow will not move if $\tau_c > \tau_o = \gamma\,d\,S$ (Appendix II). Where d is the thickness of the flow, $\gamma$ is the specific submerged weight, S is the slope and tan S is $\lambda$, the angle of slope (Appendix I & II). To produce a cohesionless debris flow 2 m thick therefore, a channellised debris flow requires a slope in excess of 0.05 (2.8°) for movement, and a subaqueous flow demands a slope in excess of $4.16 \times 10^{-3}$ (0.23°). Hence even a shallow angle of channel bank slope may fail in the right conditions to form a cohesionless debris flow.

| | Critical Velocity for Turbulent/Laminar flow transition (m/s) $U \ge \sqrt{1000\,\tau_c / \rho}$ | Angle of slope required to deposits 2 m sediment. |
|---|---|---|
| **Dry Debris Flow** $\tau_c = 103\ Ns/m^2$ $\rho = 2000\ kg/m^3$ $\gamma = 1 \times 10^4\ kg/m^2/sec^2$ | $U \ge 70$ m/s | |
| **Open Channel** $\tau_c = 600\ Ns/m^2$ $\rho = 2000\ kg/m^3$ $\gamma = 1 \times 10^4\ kg/m^2/sec^2$ | $U \ge 17.3$ m/s | 0.05 (2.8°) |
| **Sub-Aqueous** $\tau_c = 50\ Ns/m^2$ $\rho = 2000\ kg/m^3$ $\gamma = 1 \times 10^4\ kg/m^2/sec^2$ | $U \ge 5$ m/s | $4.16 \times 10^{-3}$ (0.23°) |

Table 7.6. Physical parameters of cohesionless debris flow (see Appendix I for symbols). Values for $\tau_c$ from Johnson (1970) & Hiscott & Middleton (1979); Values of $\rho$ from Pierson (1981). Value of $\gamma$ from Johnson (1970).

### 7.4.4. Interpretation Of Facies Smc.

Four types of facies Smc have been recognised from within this study. These are described within the text and summarised in Tables 7.2 & 7.4 and Figure 7.5.

### (i) Smc Types 1 and 4 (within channel).

Types 1 and 4 of the Smc facies are preserved within fluvial channel (CH) element sediments, and are interpreted to have been deposited in the form of sediment gravity flows originating from failure of high, unstable river banks. Bank failure was laterally restricted to certain areas due to the existence of intersecting abandoned channels containing porous fine and medium grained sandstones. Collapse was probably triggered by a combination of falling water levels, groundwater seepage and earthquake shocks.

Failure caused the mobilisation of sediment in the form of gravity flows which accelerated rapidly, and had sufficient energy to drive across the fluvial channel to deposit lenticular channel features (Figure 7.12). Erosive channel bases were developed due to the turbulent nature of the initial flow. Sediment concentration was increased due to the addition of suspended load, and rapid deposition resulted. The depositing flows were transitional between liquefied flow and a high density turbidity current or hyperconcentrated flow. Marginal concentric laminae developed due to freezing of the sediment flow in the late stages of transport.

Type 1 Smc channels cut through both cross-stratified sandstones and facies Sms in the Fell Sandstone (Figure 3.10). Where facies Smc is preserved in facies Sms the margins of the channels dip at a lower angle. This change in the channel margin angle of repose may be due to the more open grain framework of facies Sms, which would have therefore been able to support only lower angles of loose sand.

The differences in the width/depth ratio of Types 1 (<12) and 4 (>20) channels deposited within cross-stratified sandstones (Figure 7.5, Table 7.4) indicate different conditions of sedimentation. If Smc Types 1 and 4 were deposited by mass flow processes as the evidence suggests, then the differences in width/depth ratio and channel margin angle may relate to confined and unconfined flows across the channel floor. In flows with higher width/depth ratios the sediment gravity flow may have been less confined and thus able to spread out more laterally (Figure 7.12), as in the debris flows of Rodine & Johnson (1976).

Transerse scour

Mid-channel bar

Retrogressive flow

Slump scour

Confined flow

B

B'

Uncontined flow

Bank Collapse

Turbulent flow

laminar flow

Groundwater movements

freezing

Mid-channel bar

A ___ Smc Type 1 ___ A'

B ___ B'
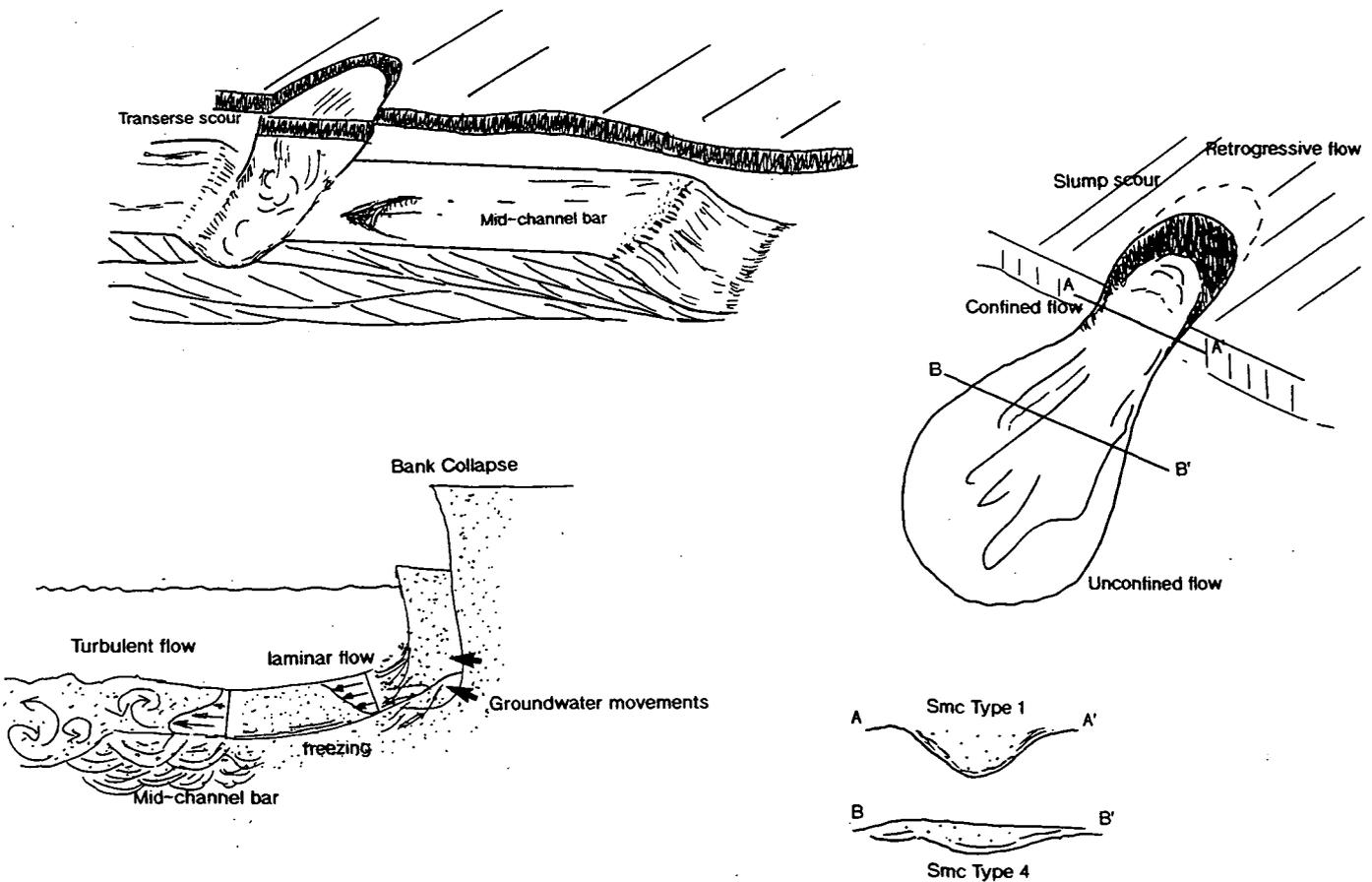
Smc Type 4

*Figure 7.12. A schematic model for the deposition of Smc Types 1 & 4 sandbodies.*

## (ii) Smc Type 4 (channel margin).

The deposition of these sediment bodies over recognised levees or channel margin architectural elements (Table 7.4) indicates that they were deposited outside of the fluvial channel by currents flowing away from the channel. Such sandstones must have been deposited during periods of flooding when levees were breached. Sediment must have been deposited from a highly concentrated sediment/water mixture in the manner of liquefied flows described above (Figure 7.9). These sandbodies are termed crevasse splays.

## (iii) Smc Type 2.

These flows display non-erosive lower boundaries and are oriented perpendicular to the flow direction as established from cross-stratification. Naese

Sandstone Section 3 preserves the only recorded example of this type of deposit (Table 7.4). The Smc feature is preserved with margins lying parallel to the foresets of the adjacent bedform. The sandbody is interpreted to have been formed through separate scour and fill process. The scour is believed to have formed in from of a downstream migrating braid bar (cf Best 1988, Figure 7.8a & b). This scour was then at least partially filled by a highly concentrated sediment flow, possibly triggered by the collapse of an adjacent bedform or sand-rich bank. The resultant flow was non-erosive and deposited structureless sand. The lack of marginal laminae in Naese Sandstone indicate that the flow was not deposited through shear or grain flow but rather through a liquefied flow (cf Lowe 1976b).

### (iv) Smc Type 3.

Type 3 Smc deposits are non-erosive in character, and are oriented parallel to the palaeoflow as established from cross-stratification. Only one deposit of this type is preserved, in Section 2 of the Mansfield Formation (Table 7.4, Plate 5.3). This feature is interpreted in terms of a bar collapse feature. The amount of sediment involved is small (Table 7.5). The non-erosive nature of the facies boundary and absence of marginal laminae suggest that the sediment flow was similar to the liquefied flow of Lowe (1976b).

### (v) SM Type 2 architectural element.

The SM type 2 architectural element of Table 2.6 is therefore interpreted as the deposit of a sediment gravity flow/highly concentrated sediment-laden current. Initially the flow was dilute and erosive. Rapid deceleration of the flow margins resulted in concentric laminae and a massive sandstone fill.

Smc Type 1 is the most common massive sandstone unit preserved within the rock record (Table 7.1 & this study). These sediment bodies represent bank collapse features. Bank collapse is widely documented in modern environments, and the lack of bank stability during the pre-Cretaceous would suggest that bank collapse features would have been more common.

## 7.5.1. Description of facies Sme.

### (i) Geometry.

Facies Sme is only preserved within the Hawkesbury Sandstone of the Sydney Basin (Chapter 6). The facies is highly complex and difficult to delineate. It takes the form of sheets which may be traced in excess of 200 m parallel, and >20 m perpendicular to the flow direction established from cross-stratification. Individual facies Sme units may reach 6 m in thickness, with generally linear upper bounding surfaces, and lower bounding surfaces marked by a series of channel-like depressions which attain a relief of 5 m. These channels or scours are elongate depressions, which have been traced for <20 m in the field. The depressions are oriented parallel and oblique to the palaeoflow as measured from the associated cross-stratification. Scour margins dip between 22-48° although Rust & Jones (1987) have documented dips of 80°.

Individual units of facies Sme amalgamate to form sheets which may be traced for over 300 m transverse and parallel to flow, and which reach 20 m in thickness. Commonly only the channellised portion of facies Sme is preserved, with the basal scours defined due to erosional relationships with the underlying strata. The scours are commonly lined with facies Sb which consists of angular to sub-rounded mudclasts <80 cm in diameter. The clasts are both normally and inversely graded.

Internally facies Sme is either massive or displays faint laminae picked out b y the alignment of platy mudstone and graphite clasts (<5 mm diameter). At the base of scours the layering is inclined by up to 55°, and is generally concordant with the erosional basal margin, becoming progressively more horizontal upwards. The laminae describe undulose to trough-like structures within the facies. Mudclasts of <10 m in diameter have been described 'floating' within the sandstone matrix (Rust & Jones 1987).

### (ii) Textural Characteristics.

Facies Sme of the Sydney Basin is less well sorted than the stratigraphically equivalent structured facies and the transitional facies (Sd), discussed in Chapter 6. Facies Sme also has a lower primary porosity and finer grain size than the cross-stratified sandstones. The values measured for CI are similar to those of the structured facies (Appendix III & Table 7.3).

## 7.4.2. Possible Mechanisms For The Production Of Facies Sme.

Previous descriptions and interpretations of the massive sandstone facies preserved within the fluviatile Hawkesbury Sandstone are listed in Table 7.1. The facies has been interpreted as a peak flood event of upper flow regime conditions (Conaghan & Jones 1975; Conaghan 1980), as the result of sediment gravity flows (Jones & Rust 1983) or plug flow deposits of scours eroded by liquefied sediment gravity flows (Rust & Jones 1987).

The massive sandstone facies of the Hawkesbury Sandstone forms individual sheets <6 m thick, which extend laterally >200 m in the direction of flow. The volume of sediment involved in a single Sme unit (Hawkesbury Sandstone Section 2) is estimated to be in excess of 184,000 m$^3$. These sandbodies may then amalgamate to cover wide areas.

Features are present within the Hawkesbury Sandstone which are not related to normal fluvial processes of sedimentation. These include the presence of angular to sub-rounded mudclasts up to 10 m in diameter (Rust & Jones 1987) which float within a massive sandstone matrix, and the presence of undulose and diffuse lamination. These laminae describe sweeping trough-like structures with an angle of repose of up to 50°.

The base of Sme units are commonly marked by scours which are elongate in a direction varying between oblique and parallel to the overall palaeoflow direction established from cross-stratification. Hence, the flow responsible for the deposition of the massive sandstone did not utilise the existing channel network but cut across it. Within scours facies Sb (Table 2.4) is preserved. The mudclasts within the breccia are identical in texture to those preserved floating within the sandstone, and those preserved as floodplain deposits (Rust & Jones 1987). The clasts display folds and delicate shear fabrics (Plate 6.6). Clasts are commonly inversely graded and may be either randomly aligned or show evidence of imbrication.

Facies Sme contains a high percentage of matrix mud (approximately 10%, see Appendix III) composed predominately of illite which was formed during diagenesis from the degradation of muscovite. The primary sediment was therefore highly micaceous, more so than the surrounding cross-stratified sediments (Chapter 6 & Appendix III).

Features such as inverse grading of brecciated deposits are generally seen in deposits of mass flow origin and highly concentrated sediment gravity flows (Lowe 1976b; Enos 1977). Inverse grading is generally accepted to be the result of dispersive pressure produced by cohesionless grain interaction (Carter 1975b). Lowe (1976a) suggested that with a small amount of clay matrix (>5%) viscous modified

grain flows would aid clast support, together with dipersive pressure, and form thick inversely graded sedimentary units. The inverse grading of facies Sme is therefore likely to be the result of a combination of grain interaction and the cohesive nature of the sediment/fluid mixture.

As with facies Sms and Smc the lack of structure within facies Sme is attributed to a lack of turbulence within the depositing flow.


## (i) Syn-Depositional Mechanisms.

*Highly concentrated sediment flows/ Glacial Outwash or Jökulhlaup.*

Catastrophic flood events relating to glacial environments are termed jökulhlaups and are derived from the sudden draining of ice dammed or sub-glacial geothermal lakes (Maizels 1993). Jökulhlaups have been documented from modern Icelandic environments, with the flow volumes generated in excess of $10^4$-$10^5$m/s (Maizels 1989). Few data are available which document the amount of sediment transported by jökulhlaups. However, the deposits of outburst floods have been described from the Pleistocene by Baker (1973) to cover 100's of square km's, and deposits of a similar scale have been described from the Holocene of Iceland (Maizels 1989).

Maizels (1989) has described the deposits of recent jökulhlaups from the sandur plains of Iceland. Typically the sand and gravel sediments are massive in character and display diffuse laminae along the upper and lower surfaces. Inverse grading of clasts is common. Massive beds reach 3 m in thickness and may be channelled into the underlying stratified sediments, with the channels up to 11.5 m wide and 1.4 m deep. The jökulhlaup deposits are interbedded with sandur or braidplain sediments which display structures characteristic of gravel bed braided streams including trough and planar cross-stratification.

The massive units are interpreted by Maizels (1993) as flood-surge deposits. Inversely graded cycles are interpreted to be the result of hyperconcentrated grain flow surges. Basal laminae indicate discrete shear zones at the base of a concentrated sediment/water mixture, with indistinct bedding in the upper portions of the flows indicating deposition from less concentrated, more dilute flows. The jökulhlaup flows are inferred to have been sediment/water mixtures with a concentration of 40-80% i.e. the hyperconcentrated flows of Beverage & Culbertson (1964). Maizels (1993) interpreted the massive jökulhlaup sands to have been deposited following rapid freezing of the material during fluid expulsion. The overlying structured deposits are regarded as post-surge traction flows.

The mudclasts of facies Sme were not transported any great distance prior to deposition (Smith 1972). Buoyancy may support plastic, semi-lithified mudclasts with a low specific gravity, provided that the sediment/fluid density and viscosity are sufficiently high due to sediment concentration (Lowe 1979). Mudclasts with a specific gravity between 1.5-2 x $10^3$ kg/m$^3$ could be entirely supported in a sediment/fluid mixture of 20-40% quartz (Lowe 1979). Facies Sme is assumed to have been deposited under hyperconcentrated flow conditions. The sheared fabrics displayed by mudclasts provide additional evidence for a laminar mode of flow.

Clast orientations may also be expected to be affected by shearing within a flow moving in a laminar fashion. In sediment gravity flows the long axis of a clast is commonly oriented approximately parallel to the bedding of a deposit. It has been theoretically demonstrated that elongate particles within an inhomogeneous material deformed by shear within a laminar flow will exhibit a preferred grain orientation with the longest axis oriented parallel to the plane of shear (Fisher 1971). Such clast orientations have been documented from facies Sme of the Hawkesbury Sandstone.

The uplands of the Lachlan Fold Belt are known to have been glaciated during the deposition of the Hawkesbury Sandstone (Chapter 6), and it is possible that highly concentrated jökulhlaup-type flows could have been generated in the uplands, which deposited sediment across the braidplain. The heat required to melt ice to form glacial outbursts may have been created through annual melting of highland glaciers or possibly through volcanic or geothermal activity.

## (ii) Post- Depositional Mechanisms.

### Bank Collapse

Jones & Rust (1983) documented a transverse to palaeoflow orientation for the scours of facies Sme and interpreted a post-depositional mode of origin for these structures. The scours were interpreted to have formed due to scour in front of advancing bedforms and augmented through erosion during bank collapse. Rust & Jones (1987) identified semi-cylindrical erosion surfaces beneath the massive sandstone facies of the Hawkesbury Sandstone which were interpreted in terms of planes of retrogressive flow sliding along the channel bank. The banks of the Hawkesbury Sandstone river were estimated to be at least 11 m high by Rust & Jones (1987). Thus to produce the quantity of sediment described above through bank collapse an 11 m high bank would have to liquefy over an area of at least 129 m$^2$.

Concave-up scours identified from the channels of ancient and modern turbidites by Mutti & Normark (1987) bear a striking resemblance to those developed across the base of facies Sme. The scours described by Mutti & Normark (1987) are commonly found in the base of sandstone beds as deeply incised features commonly located along amalgamation surfaces. Scours 2-3 m deep and 10-60 m wide have been identified downslope of a delta front in British Columbia (Mutti & Normark 1987). In modern fans, scour depressions are found in areas where turbidity currents undergo an hydraulic jump as the slope decreases and currents spread laterally. When a sandy turbidity current undergoes a hydraulic jump the rapid dilution resulting from increased turbulence reduces the competence of the flow and leads to rapid deposition of coarse material together with the formation of large scale scour features (Mutti & Normark 1987).

All the mechanisms for initiating bank failure described in section 7.4.2 above are possible processes leading to the collapse of the Hawkesbury Sandstone river banks. The banks are believed to have been high (Rust & Jones 1987) and were probably poorly consolidated due to the lack of binding vegetation in the form of grasses. Trees and shrubs were, however, present on the flood plain (Retallack 1980).

### 7.5.3. Discussion.

The scoured bases of facies Sme indicate that the flow must have been turbulent. However, the internal characteristics of facies Sme indicate laminar flow. Thus a flow transformation must have occurred sometime in the life of the flow responsible for deposition of facies Sme.

The orientation of the scours within facies Sme is critical to the development of any depositional model. Rust & Jones (1987) described the scours to be oriented perpendicular to the flow direction, whereas Conaghan (1980) inferred a parallel orientation. This study has shown an oblique to near parallel relationship in the scours (Figures 6.8 & 6.12). A perpendicular orientation of scours would fit a post-depositional bank collapse model for deposition for facies Sme. However, the scours are variable in their orientation, and hence more consistent with deposition by a primary depositional mechanism.

The textural characteristics of facies Sme are also not consistent with a sedimentary gravity flow origin. The sandstones of facies Sme are poorly sorted and contain large amounts of mica (Chapter 6 & Appendix III), features inconsistent with storage in channel banks where one would expect better sorting and the removal of mica due to weathering. The presence of well developed and amalgamated units of

facies Sme at the base of the Hawkesbury Sandstone (Figure 6.8) also supports a primary mode of deposition especially as there is no evidence of fluvial deposition prior to the deposition of facies Sme which infers that no river banks would have been present, or too poorly developed to provide sediment.

A primary mode of deposition from highly concentrated stream flows is postulated here as the mechanism of deposition of facies Sme. The highly concentrated currents were probably initiated by glacial outburst in the Lachlan Highlands to the west (Figure 6.2 ). It is suggested that the initial flow was turbulent and of relatively low concentration and this current scoured out the hollows along the base of the facies. Following this initial low concentration flow was a higher concentration laminar flow which deposited material in the eroded-out hollows. Concentration was increased due to the addition of suspended sediment provided through erosion in source areas. The amalgamated nature of facies Sme suggests multiple events, with each flow successively emplaced after the previous flow had time to develop internal lamination.

The steeply dipping concentric laminae preserved at the margins of scours are due to the shear developed at the base of the flow. The orientation of mudchips and mica supports the suggestion of a laminar, sheared sediment/water flow. The angular mudclasts preserved within facies Sb were derived from nearby floodplain, and deposited near the source. Dispersive pressure and buoyancy resulted in inverse grading. Clasts show evidence of deposition under the influence of shear (Plate 6.6).

The upward transition from massive sandstone to diffusely cross-stratified sandstones with better sorting characteristics indicates a dilution of the sediment/water mixture and the beginning of turbulent flow characteristics.


### 7.5.4. Interpretation Of Facies Sme.

As discussed in Chapter 6 the Hawkesbury Sandstone river was a perennial system which flowed towards the northeast. The river carried quartzose sandstone, deposited as a quartz arenite. Reworking of the sand prior to deposition is therefore interpreted.

Facies Sme is interpreted as a primary depositional unit. The poor sorting and high mica content of the facies are interpreted in terms of derivation from an immature (first cycle) source. The basal scours developed from dilute, turbulent flows produced through a sudden flooding event, probably related to glacial outburst such as that described by Maizels (1989, 1993). Scours are oriented both parallel and oblique to the regional palaeoflow of the Hawkesbury Sandstone river indicating overbank

flooding. The initially turbulent flow evolved into a hyperconcentrated stream flow with laminar flow characteristics. Floodplain material in the form of mudclasts was rafted within the laminar currents (cf. Postma *et al* 1988). Shear fabrics preserved within the clasts support evidence of laminar flow conditions.

Shearing occurred at the flow margins resulting in concentric marginal laminae. The structures within the main body of facies Sme are similar in character to those of facies Sms, in that there is a virtual absence of structure relating to deposition from traction currents. These sediments were deposited from the highly concentrated flow. Facies Sd (Table 2,4) indicates dilution of the flow and a return to traction deposition due to turbulence. The increase in maturity of facies Sd (Chapter 6) indicates that it was transitional with normal fluvial currents.

Architectural element SM Type 3 (Table 2.6) is therefore interpreted as a flood/glacial outburst related deposit. Basal scours and diffuse cross-stratification represent turbulent flow. Facies Sme represents deposition from laminar, high concentration currents. The flood events may have been related to annual spring thawing in the glaciated Lachlan highlands. However, the paucity of such sediments within the rock record, and the documentation of modern glacial outburst floods (Maizels 1989) suggests a less periodic occurrence.

## 7.6. Implications Of The Presence Of A Massive Sandstone Facies Within Braided Alluvium.

The massive sandstone facies identified and described within this study are all the deposits of highly concentrated sediment/water mixtures which were deposited in a variety of environments and under differing climatic regimes. The sediment flow types may however, be generalised and incorporated into a simple model which is illustrated in Figure 7.13.

Due to the higher sediment yield, and hence larger amounts of material available for fluvial transport during pre-Cretaceous times, massive sandstones would be expected to be deposited more often and preserved within these sediments. The deposits of facies Sms and Smc would be expected in tropical environments where perennial conditions and tropical weathering may result in rapid sedimentation and continuous erosion. Facies Sme would be expected in proglacial or warm temperate climates associated with highland glaciers.

Facies Sms is a largely homogenous sediment body containing no lateral discontinuities. The sediment has a higher primary porosity than the surrounding structured sediments and a lower Cl, indicating that it would be a better reservoir

sandstone than the associated cross-stratified sandstones. Facies Smc bodies are moderately well sorted and lack matrix fines (<10%). These bodies can be laterally extensive and would form good reservoirs due to the re-sedimented character of the sediments. Facies Sme has low porosity values, is poorly sorted and has a high matrix clay percentage, which would probably reduce permeability. These sandstones would make poor reservoirs, and although the associated cross-stratified sandstones have good poroperm characteristics, facies Sme would prevent lateral and vertical flow of formation fluids. These sandstones are of lateral and vertical extent and would therefore act as important barriers to flow.
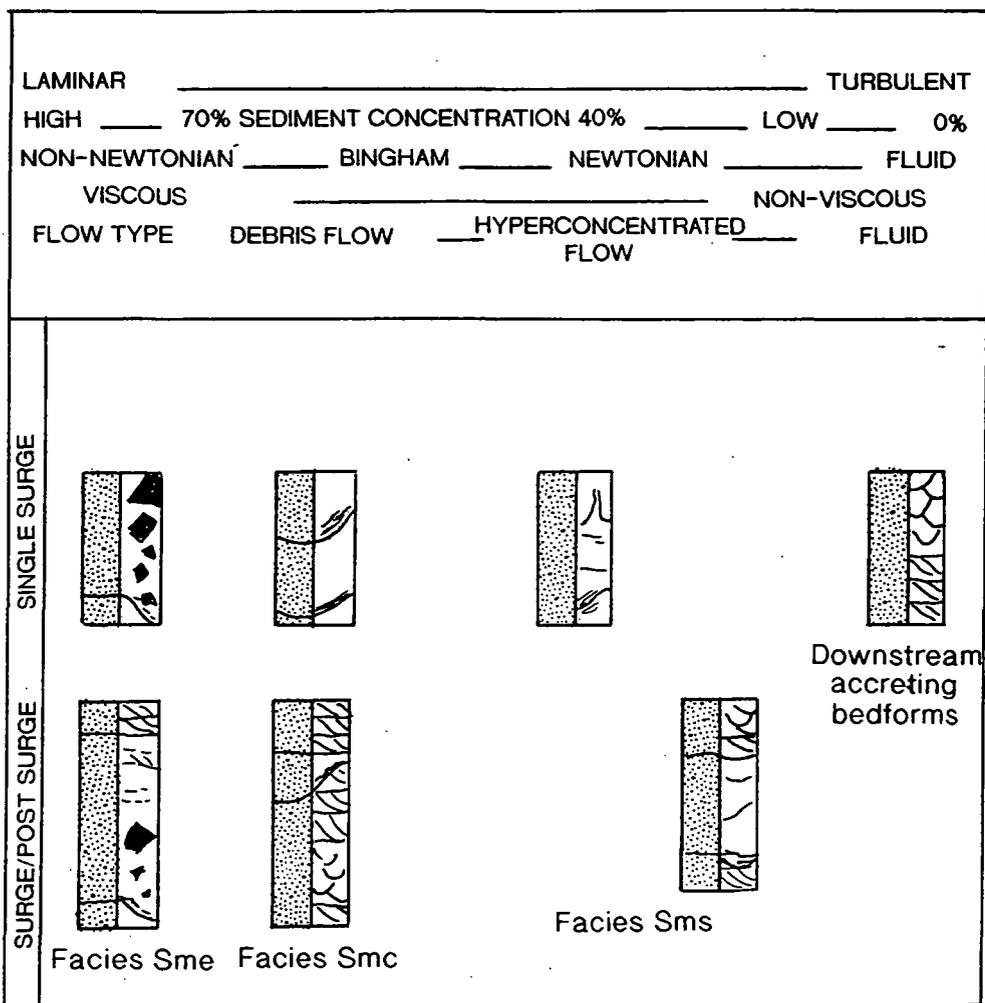


Figure 7.13. A unifying model for the sediments of facies Sms, Smc and Sme.

# Chapter 8
# Conclusions

## 8.1. General Conclusions.

A number of architectural elements have been identified within this study. These relate to deposition within the fluvial channel, at channel margins and in inter-channel areas.

Major channel elements are composed of a number of macroform and mesoform scale elements divided by a hierarchy of bounding surfaces (first to fifth order). DA Type 1 and 2 elements represent the deposits of downstream accreting macroforms and are interpreted as mid-channel and bank attached bars. Mesoform scale elements are represented by SB Type 1 and 2 elements which were deposited through downstream and vertical accretion during periods of changing conditions in flow. Lateral accretion surfaces are rare within the channel elements identified.

Low palaeocurrent variance within major channel elements, and a lack of evidence of reworking associated with low stage emergence of bedforms, indicate that the river systems studied herein were perennial in character, and of low braiding index.

Using measurements made from the height of preserved bedforms it has been possible to estimate the depth of water present within fluvial channels. Palaeocurrent variance has been used to assess channel sinuosity, and hence width/depth ratio. These calculations are prone to error, but offer information concerning the order of magnitude of river systems responsible for deposition of the channel sandstones.

## 8.1.2. The Fell Sandstone Group, Northumberland Basin, UK.

The Fell Sandstone was deposited by a low sinuosity river system across a laterally restricted braidplain controlled by syn-depositional faults. Movements across these faults resulted in the development of accommodation space and funnelling of fluvial channels.

The source of the Fell Sandstone river system lay to the northeast, and was composed of metasedimentary, volcanic and plutonic bodies. Sediment was

transported for considerable distances prior to deposition in the study area. The resultant sediments were quartz arenites and sub-litharenites.

The migration of the Fell Sandstone river system was dominated by avulsion. Lateral migration was limited. Channel elements are therefore isolated within lenticular inter-channel fines.

The Fell Sandstone Group contains massive sandstones in the form of facies Sms and Smc which are interbedded with the structured sandstones.

### 8.1.3. The Lee-Type Sandstones, central Appalachian Basin, USA.

The Lee-type sandbelts are represented by the Bee Rock Sandstone and Corbin Sandstone formations which were deposited in a northeast/southwest trending belt, on the western margin of the Appalachian foreland basin. The formations were deposited during periods of rising relative sea level and were transgressed during periods of marine inundation.

The sediments of the Lee sandbelts were derived from a volumetrically important quartz-rich northeastern source, with the rising Alleghanian front supplying smaller quantities of lithic components via the transverse river systems of the Breathitt Group. Sediments deposited within the fluvial channels were quartz arenites and sub-litharenites.

The Lee sandbelts are dominated by stacked multi-storey and multi-lateral major channel element sandbodies. The channels are separated by fourth order bounding surfaces which represent surfaces of channel avulsion. Repeated avulsion across the river floodplain, together with rapid subsidence, resulted in stacking of the sandbodies. Lateral channel migration was limited.

Massive sandstones of facies Smc and Sms are preserved within the Lee-type sandstones.

### 8.1.4. The Mansfield & Brazil Formations, Illinois Basin, USA.

The sediments deposited within the Mansfield and Brazil Formations were sourced from a predominately metamorphic and plutonic area the north and east. This is believed to be the same area as that providing quartzose sediment to the Lee-type sandbelts. Sediment transport and tropical weathering resulted in the deposition of first cycle quartz arenites.

Channel sandstones of the Mansfield and Brazil Formations are isolated within fine grained sediments which were deposited across estuarine mudflats. Fluvial channel margins were stable, and flanked by levees. Channels avulsed frequently, possibly in response to base level change. The resultant sandbody architecture is ribbon-like.

The Mansfield and Brazil Formations contain massive sandstones in the form of facies Smc units.

## 8.1.5. The Hawkesbury Sandstone, Sydney Basin, Australia.

The Hawkesbury Sandstone was sourced from an uplifted cratonic area (the Lachlan Fold Belt), which contained granitic and metamorphic source rocks. These sediments were reworked and temporarily stored prior to deposition within the structured facies of the Hawkesbury Sandstone river, resulting in a quartz arenite sandstone composition.

The Hawkesbury Sandstone river contains thick successions of facies Sme, particularly in the basal portion of the unit.

## 8.2. The Massive Sandstone Facies.

The massive sandstone facies share many characteristics. These include deposition within predominantly perennial braided systems of pre-Cretaceous age; well defined geometry; basal scour surfaces with marginal concentric laminae; and internally structureless sandbodies containing undulose laminae and soft-sediment deformation structures.

The absence of well developed bedforms related to deposition from traction currents, and the presence of concentric laminae at flow margins indicate deposition from predominately laminar flows. These flows are believed to have formed due to dampening of turbulence associated with the addition of high suspended sediment concentrations.

## 8.2.1. Facies Sms.

Facies Sms takes the form of laterally extensive sheets up to 8 m in thickness which may be traced >200 m parallel, and approximately 250 m transverse to the

palaeoflow direction. Facies Sms sandbodies display undulose lower bounding surfaces with relief of <1.85 m. Scours are oriented approximately parallel to the flow direction. Internally facies Sms is largely structureless containing only diffuse undulose to trough-like laminae and water escape structures. Facies Sms is formed of a moderately well sorted sandstone with a porosity higher than that of the associated structured sandstone facies and a lower CI.

Facies Sms is interpreted to have been deposited by a hyperconcentrated stream flow produced through flooding. The basal scours were formed by an initially turbulent, dilute flow. An increase in sediment concentration of the flow resulted in the dampening of turbulence. The sandstone maturity and texture indicate rapid deposition of a previously reworked sediment. The concentric laminae preserved in basal scours indicate shearing at the margins of a highly concentrated flow. Locally preserved cross-stratification sets indicate that traction flow was possible in some circumstances. The sweeping trough-like laminae and water escape pipes were produced by the expulsion of water from metastabley packed sediment.

Facies Sms is only locally developed in ancient braided stream deposits due to the poor preservation potential of the facies. It is believed that the two sandbodies of facies Sms studied were located in actively subsiding areas, which provided accommodation space necessary to preserve the sandstone.

### 8.2.2. Facies Smc.

Facies Smc sandbodies are oriented perpendicular, and less commonly parallel to the fluvial palaeoflow. The margins of facies Smc are generally sharp and dip <55°. Internally facies Smc units are largely structureless. Diffuse laminae may also be preserved in the upper portion of facies Smc, and these have an undulose appearance. Facies Smc sandbodies have better sorting characteristics than the sediments within which they are preserved, together with higher permeabilities. This indicates previous re-working of the sediment.

Four types of facies Smc have been recognised from within this study. Smc Types 1 and 4 are preserved within major channel elements. The sandbodies were deposited from sediment gravity flows originated from failure of high, unstable river banks. Failure was restricted to certain bank areas due to the existence of intersecting abandoned channels containing re-worked porous fine and medium grained sandstones. Retrogressive flow sliding was common. Bank collapse was probably triggered by a combination of falling of water levels, groundwater seepage and earthquake shocks.

Bank failure caused the initiation of sediment gravity flows. The highly concentrated sediment-laden currents were initially turbulent and hence capable of eroding channels. The concentration of the flow increased with the addition of suspended sediment. The depositing flows were transitional between liquefied flow and a high density turbidity current or hyperconcentrated flow. Rapid deposition resulted in the filling of scours with structureless sandstone. Marginal concentric laminae developed due to freezing of the sediment flow in the late stages of transport. Laminae across the upper surface of sandbodies resulted due to shearing across the upper surfaces of the sediment flow.

Smc Type 4 are preserved overlying levees and hence are interpreted as the deposits of crevasse splays. Such sandstones must have been deposited during periods of flooding when levees were breached. Sediment must have been deposited from a highly concentrated sediment/water mixture as a liquefied flow.

Smc Type 2 units display non-erosive bases and are oriented perpendicular to the flow direction established from cross-stratification. The initial scour is believed to have formed in the lee of a downstream migrating braid bar. This scour was then at least partially filled by a non-erosive liquefied flow triggered by the collapse of an adjacent bedform.

Smc Type 3 sandbodies are non-erosive in character, and are oriented parallel to the palaeoflow. These sandbodies are interpreted in terms of a bar collapse. Impulsive liquefaction of the bedform was initiated due to a sudden deformation event.

### 8.2.3. Facies Sme.

Facies Sme takes the form of sheets, which may be traced in excess of 200 m parallel, and >20 m perpendicular to the flow direction. The sheets may reach 6 m in thickness. The base of the sandstone sheets are marked by a series of channel-like depressions which attain a relief of 5 m. The depressions are oriented parallel to oblique to the palaeoflow as measured from the associated cross-stratification. Scour margins dip between 22-48°.

Internally facies Sme is either massive, or displays faint laminae picked out by the alignment of platy mudstone and graphite clasts. At the base of scours the layering is inclined by up to 55°, and is generally concordant with the erosional basal margin, becoming progressively more horizontal upwards. The laminae describe undulose to trough-like structures within the facies. Angular mudclasts 'float' within the sandstone matrix.

Facies Sme is poorly sorted and is compositionaly different to the cross-stratified sandstones through which it cuts. These factors indicate rapid deposition with little or no re-working.

The basal scours of facies Sme are interpreted to have been created by a dilute, turbulent flow produced through a sudden flooding event, probably related to a glacial outburst within the Lachlan Fold Belt. With addition of sediment the flow became a laminar hyperconcentrated stream flow. Shearing at the flow margins resulting in concentric marginal laminae and the different orientations of mudclasts. Rapid deposition precluded sediment sorting. The overlying deposits of facies Sd indicate dilution of the flow and a return to traction deposition.

## 8.3. Possible Future Research.

This study has described the occurrence of geometrically defined sandbodies of three massive sandstone facies. The textural and compositional characteristics of these facies have been assessed through petrographic study. However, only a limited study of sandstone porosity and permeability characteristics has been achieved. Further insight into the implications of the preservation of a massive sandstone facies would be possible with a greater understanding of the properties of the facies regarding fluid flow.

With the documented examples of the massive sandstone outlined in this thesis it will now be possible to describe and interpret such sandbodies within ancient fluvial systems. Until recently these sandbodies have been largely ignored. It is now possible for these strata to be adequately explained, and hence the presence of 'massive sandstones' may contribute to the overall sedimentological model, rather than be ignored and omitted from it.

# References

ADAMS, J. 1977. Sieve size statistics from grain size measurements. *Journal of Geology*, **85**. 209-227.

AHMAD, R., TIPPER, J. C. & EGGLETON, R. A. 1994. Compositional trends in the Permian sandstones from the Denison Trough, Bowen Basin, Queensland reflect changing provenance and tectonics. *Sedimentary Geology*, **89**. 197-217.

ALEXANDER, J. 1986. Idealised flow models to predict alluvial sandstone body distribution in the middle Jurassic Yorkshire Basin. *Marine and Petroleum Geology*, **3**. 298-306.

ALLEN, J. R. L. 1968. *Current Ripples: Their Relation To Patterns Of Water And Sediment Motion.* North Holland Publishing Company.

ALLEN, J. R. L. 1982. *Sedimentary Structures: Their Character And Physical Basis.* Developments in Sedimentology, 2 Volumes. **30A**. 593p **30B**. 663p

ALLEN, J. R. L. 1983a. River bedforms: progress and problems. *In* J. D. COLLINSON & J. LEWIN (eds). *Modern and Ancient Fluvial Systems.* International Association of Sedimentologists Special Publication **6**. 19-33.

ALLEN, J. R. L. 1983b. Studies in fluviatile sedimentation: bars, bar complexes and sand sheets (low sinuosity braided streams) in the Brownstones (L. Devonian), Welsh Borders. *Sedimentary Geology*, **33**. 237-293.

ALLEN, J. R. L. 1994. Fundamental properties of fluids and their relation to sediment transport processes. *In* K. PYE (ed). *Sediment Transport and Depositional Processes.* Blackwell. 25-60.

ALLEN, J. R. L. & BANKS, N. L. 1972. An interpretation and analysis of recumbent-folded deformed cross bedding. *Sedimentology*, **19**. 257-283.

ALLEN, J. R. L. & COLLINSON, J. D. 1974. The superimposition and classification of dunes formed by unidirectional aqueous flows. *Sedimentary Geology*, **12**. 169-178.

ANDRESEN, A & BJERRUM, L. 1967. Slides on subaqeous slopes in loose sand and silt. *In* A. F. RICHARDS (ed). *Marine Geotechnique.* 221-239.

ARCHER, A. W. & KVALE, E. P. 1993. Origin of gray-shale lithofacies ("clastic wedges") in U.S. mid-continental coal measures (Pennsylvanian): an alternative

explanation. *In* J. C. COBB & C. B. CECIL (eds*). Modern and Ancient Coal-Forming Environments*. Geological Society of America Special Paper, **286**. 181-192.

ARMSTRONG, H. A. & PURNELL, M. A. 1987. Dinantian conodont biostratigraphy of the Northumberland Trough. *Journal of Micropalaeontology*, **6**. 97-112.

ARNOTT, R. W. C. & HAND, B. M. 1989. Bedforms, primary structures and grain fabric in the presence of suspended sediment rain. *Journal of Sedimentary Petrology*, **59**. 1062-1069.

ASHLEY, G. M. (Chairperson & others) 1990. Classification of large-scale subaqueous bedforms: a new look at an old problem. *Journal of Sedimentary Petrology*, **60**. 160-172.

ASHLEY, G. M. & DUNCAN, I. J. 1977. The Hawkesbury Sandstone: a critical review of proposed environmental models. *Journal of the Geological Society of Australia*, **24**. 117-119.

BAGNOLD, R. A. 1954. Experiments on a gravity-free dispersion of large solid spheres in a Newtonian fluid under shear. *Proceedings of the Royal Society, London*, **A249**. 235-297.

BAKER, V. R. 1973. Palaeohydrology and sedimentology of Lake Missoula flooding in eastern Washington. *Geological Society of America Special Paper*, **144**. 79pp

BEMBRICK, C., HERBERT, C., SCHEIBNER, E. & STUNTZ, J. 1980 Structural subdivision of the Sydney Basin *In* C. HERBERT & R. HELBY (eds). *A Guide to the Sydney Basin*. Geological Survey of New South Wales Bulletin, **26**. 2-9.

BeMENT, W. O. 1976. *Sedimentological aspects of middle Carboniferous sandstones on the Cumberland overthrust sheet*. PhD thesis (unpublished) University of Cincinnati, Ohio, USA.

BEST, J. L. 1987. Flow dynamics at river channel confluences: implications for sediment transport and bed morphology. *In* F. G. ETHERIDGE, R. M. FLORES & M. D. HARVEY (eds). *Recent Developments in Fluvial Sedimentology*. Society of Economic Palaeontologists and Mineralogists Special Publication, **39**. 27-35.

BEST, J. L. 1988. Sediment transport and bed morphology at river channel confluences. *Sedimentology*, **35**. 481-498.

BEVERAGE, J. P. & CULBERTSON, M. 1964. Hyperconcentrations of suspended sediment. *American Society of Civil Engineers, Journal of the Hydraulics Division*, **90**. 117-128.

BLATT, H., MIDDLETON, G. V. & MURAY, R. C. 1980. *Origin Of Sedimentary Rocks*. Prentice-Hall Inc 782p.

BLOGETT, R. H. & STANLEY, K. O. 1980. Stratification, bedforms and discharge relationships of the Platte braided river system, Nebraska. *Journal of Sedimentary Petrology*, **50**. 139-148.

BLUCK, B. J. 1980. Structure, generation and preservation of upward fining, braided stream cycles in the Lower Old Red Sandstone of Scotland. *Transactions of the Royal Society of Edinburgh, Earth Sciences*, **71**. 29-46.

BOE, R. 1988. Alluvial channel bank-collapse phenomena in the Old Red Sandstone Hitra Group, Western Central Norway. *Geological Magazine*, **125**. 51-56.

BOOTHROTD, J. C. & ASHLEY, G. M. 1975. Process, bar morphology and sedimentary structures on braided outwash fans, northeastern gulf of Alaska. *In* A. V. JOPLING & B. C. McDONALD (eds). *Glaciofluvial and Glaciolacustrine Sedimentation*. Society of Economic Palaeontologists and Mineralogists Special Publication, **23**. 193-222.

BRAKEL, A. T. & TOTTERDELL, J. M. 1993. The Sakmarian-Kungurian palaeogeography of Australia. *In* R. H. FINDLAY, R. UNRUG, M. R. BANKS & J. J. VEEVERS (eds). *Gondwana Eight: Assembly, Evolution And Dispersal*. Proceedings of the 8th Gondwana Synposium. 385-396.

BRIDGE, J. S. 1985. Palaeochannel patterns inferred from alluvial deposits: a critical evaluation. *Journal of Sedimentary Petrology*, **55**. 579-589.

BRIDGE, J. S. 1993a. The interaction between channel geometry, water flow, sediment transport and deposition in braided rivers. *In* J. L. BEST & C. S. BRISOW (eds). *Braided Rivers*. Geological Society, London Special Publication **75**. 13-72.

BRIDGE, J. S. 1993b. Description and interpretation of fluvial deposits: a critical perspective. *Sedimentology*, **40**. 801-810.

BRIDGE, J. S. & LEEDER, M. R. 1979. A simulation model of alluvial stratigraphy. *Sedimentology*, **26**. 617-644.

BRIDGE, J. S., SMITH, N. D., TRENT, F., GABEL, S. L. & BERNSTEIN, P. 1986. Sedimentology and morphology of a low sinuosity river: Calmus River, Nebraska sand hills. *Sedimetology*, **33**. 851-870.

BRIGGS, D. J. C. 1993. Time control in the Permian of the Sydney-Bowen Basin and the New England Orogen. *In* R. H. FINDLAY, R. UNRUG, M. R. BANKS & J. J.

VEEVERS (eds). *Gondwana Eight: Assembly, Evolution And Dispersal.* Proceedings of the 8th Gondwana Synposium. 371-384.

BRISTOL, H. M. & HOWARD, R. H. 1971. Palaeogeologic map of the sub-Pennsylvanian Chesterian (Upper Mississippian) surface in the Illinois Basin. *Illinois State Geological Survey Circular,* **458**. 14p

BRISTOW, C. S. 1987a. *Sedimentology of large braided rivers : Ancient and Modern.* Ph D thesis (unpublished) University of Leeds, UK.

BRISTOW, C. S. 1987b. Brahmaputra River: Channel migration and deposition. *In* F. G. ETHRIDGE, R. M. FLORES & M. D. HARVEY (eds). *Recent Developments in Fluvial Sedimentology.* Society of Economic Palaeontologists and Mineralogists Special Publication **39**. 63-74.

BRISTOW, C. S. & BEST, J. L. 1993. Braided rivers: perspectives and problems. *In* J. L. BEST & C. S. BRISTOW (eds). *Braided Rivers.* Geological Society, London Special Publication **75**. 1-12.

BRISTOW, C. S., BEST, J. L. & ROY, A. G. 1993. Morphology and facies models of channel confluences. *In* M. MARZO & C. PUIDEFABREGAS (eds). *Alluvial Sedimentation.* International Association of Sedimentologists Special Publication, **17**. 91-100.

BURBANK, D. W. & BECK, R. A. 1991. Models of aggradation versus progradation in the Himalayan foreland. *Geologische Rundschau,* **80**. 623-638.

BURGI, P. H. & KARAKI, S. 1971. Seepage effects on channel bank stability. *Proceedings of the American Society of Civil Engineers. Journal of the Irrigation and Drainage Division,* **7968**. 59-72.

CAMERON, K. L. & BLATT, H. 1971. Durabilities of sands size schist and 'volcanic' rock fragments during fluvial transport, Elk Creek, Black Hills, South Dakota. *Journal of Sedimentary Petrology,* **41**. 505-576.

CANT, D. J. 1978. Development of a facies model for sandy braided river sedimentation: comparison of the South Saskatchewan River and the Battery Point Formation. *In* A. D. MIALL (ed). *Fluvial Sedimentology.* Canadian Society of Petroleum Geologists Memoirs, **5**. 627-641.

CANT, D. J. & WALKER, R. G. 1978. Development of a braided-fluvial facies model for the Devonian Battery Point Sandstone, Quebec. *Canadian Journal of Earth Science,* **13**. 102-119.

CARTER, R. M. 1975a. Mass-emplaced sand fingers at Mararoa construction site, southern New Zealand. *Sedimentology*, **22**. 275-288.

CARTER, R. M. 1975b. A discussion and classification of sub-aqueous mass-transport with particular application to grain-flow, slurry-flow and fluxoturbidites. *Earth Science Review*, **11**. 145-177.

CECIL, C. B. 1990. Palaeoclimate controls on stratigraphic repetition of chemical and siliciclastic rocks. *Geology*, **18**. 533-536.

CECIL, C. B., DULONG, F. T., COBB, J. C. & SUPARDI 1993. Allogenic and autogenic controls on sedimentation in the Central Sumatra Basin as an analogue for Pennsylvanian coal-bearing strata in the Appalachian Basin. *In* J. C. COBB & C. B. CECIL (eds). *Modern and Ancient Coal-Forming Environments*. Geological Society of America Special Paper, **286**. 3-22.

CECIL, C. B., STANTON, R. W., NEUZIL, S. G., DULONG, F. T., RUPPERT, L. E. & PIERCE, B. S. 1985. Palaeoclimate controls on late Palaeozoic sedimentation and peat formation in the central Appalachian Basin (USA). *International Journal of Coal Geology*, **5**. 195-230.

CHADWICK, R. A. & HOLLIDAY, D. W. 1991. Deep crustal structure and Carboniferous basin development within the Iapetus convergence zone, northern England. *Journal of the Geological Society, London*, **148**. 41-54.

CHADWICK, R. A., HOLLIDAY, D. W., HOLLOWAY, S. & HULBERT, A. G. 1993. The evolution and hydrocarbon potential of the Northumberland-Solway Basin. *In* J. R. PARKER (ed). *Petroleum Geology of Northwest Europe: Proceedings of the 4th Conference*. 717-726.

CHESNUT, D. R. Jr. 1988. *Stratigraphic Analysis Of The Carboniferous Rocks Of The Central Appalachian Basin*. PhD thesis (unpublished) University of Kentucky, USA.

CHESNUT, D. R. Jr. 1989. Pennsylvanian rocks of the eastern Kentucky coalfield. *In* CECIL, C. B. & EBLE, C (eds). *Carboniferous Geology of the eastern United States*. 28 th. International Congress Fieldtrip T143.

CLIFF, R. A., DREWERY, S. E. & LEEDER, M. R. 1991. Sourcelands for the Carboniferous Pennine river system: constraints from sedimentary evidence and U-Pb geochronology using zircon and monazite. *In* A. C. MORTON, S. P. TODD & P. D. W. HAUGHTON (eds). *Developments in Sedimentary Provenance Studies*. Geological Society London, Special Publication, **57**. 137-159.

COLEMAN, J. M. 1969. Brahmaputra River: channel processes and sedimentation. *Sedimentary Geology*, **3**. 129-239.

COLLIER, R. E. LL. 1989. Tectonic evolution of the Northumberland Basin; the effects of renewed extension upon an inverted extensional basin. *Journal of the Geological Society, London*, **146**. 981-990.

COLLINS, W. J. 1991. A reassessment of the 'Hunter-Bowen Orogeny': tectonic implications for the southern New England Fold Belt. *Australia Journal of Earth Science*, **38**. 409-423.

COLLINSON, J. D. 1970. Bedforms of the Tana River, Norway. *Geografiska Annaler*, **52A**. 31-56.

COLLINSON, J. D. 1978. Vertical sequence and sandbody shape in alluvial sequences. *In* MIALL, A. D. (ed) *Fluvial Sedimentology*. Canadian Society of Petroleum Geologists Memoirs, **5**. 577-586.

CONAGHAN, P. J. 1980. The Hawkesbury Sandstone: gross charcteristics and depositional environment. *In* C. HERBERT & R. HELBY (eds). *A Guide to the Sydney Basin*. Geological Survey of New South Wales Bulletin, **26**. 188-253.

CONAGHAN, P. J. & JONES. J. G. 1975. The Hawkesbury Sandstone and the Brahmaputra: a depositional model for a continental sheet sandstone. *Journal of the Geological Society of Australia*, **22**. 275-283.

CONAGHAN, P. J., JONES, J. G., McDONNELL, K. L. & ROYCE, K. 1982. A dynamic fluvial model for the Sydney Basin. *Journal of the Geological Society of Australia*, **29**. 55-70.

CONOLLY, J. R. & FERM, J. C. 1971. Permo-Triassic sedimentation patterns, Sydney Basin, Australia. *American Assocaition of Petroleum Geologists, Bulletin*, **55**. 2018-2032.

COTTER, E. 1971. Palaeoflow characteristics of a late Cretaceous river in Utah from analysis of sedimentary structures in the Ferroan Sandstone. *Journal of Sedimentary Petrology*, **41**. 129-138.

COWAN, E. J. 1985. *A Basin Analysis Of The Triassic Systems, Central Coastal Sydney Basin*. BSc (Hons) thesis, Macquarie University, Australia.

COWAN, E. J. 1993. Longitudinal fluvial drainage patterns within a foreland basin-fill: Permo-Triassic Sydney Basin, Australia. *Sedimentary Geology*, **85**. 555-557.

DALRYMPLE, R. W. 1979. Wave induced liquefaction: A modern example from the Bay of Fundy. *Sedimentology*, **26**. 835-844.

DICKINSON, W. R. 1985. Interpreting provenance relations from detrital modes of sandstones. *In* G. G. ZUFFA (ed). *Provenance of Arenites*. NATO ASI Series C: Mathematical and Physical Sciences, **148**. 333-362.

DOE, T. W. & DOTT, R. H. 1980. Genetic significance of deformed cross-bedding with examples from the Navajo and Weber Sandstones of Utah. *Journal of Sedimentary Petrology*, **50**. 793-812.

DONALDSON, A. C., RENTON, J. J. & PRESLEY, M. W. 1985. Pennsylvanian deposystems and palaeoclimates of the Appalachians. *International Journal of Coal Geology*, **5**. 167-193.

DONALDSON, A. C. & SCHUMAKER, R. L. 1981. Late Palaeozoic molasse of central Appalachians. *In* MIALL, A. D. (ed). *Sedimentation and Tectonics in Alluvial Basins*. Geological Association of Canada, Special Paper, **23**. 99-124.

DROSTE, J. B. & KELLER, S. J. 1989. Development of the Mississippian-Pennsylvanian unconformity in Indiana. *Indiana Geological Survey Occasional Paper*, **55**. 11p.

DUTTA, P. K. & WHEAT, R. W. 1993. Climatic and tectonic control on sandstone composition in the Permo-Triassic Sydney foreland Basin, earstern Austalia. In M. J. JOHNSSON & A. BASU (eds). *Processes Conrolling The Composition Of Clastic Sediments*. Geological Society of America Special Papaer, **284**. 187-202.

EMBLETON, B. J. J. 1984. Past Global settings. *In* J. J. VEEVERS (ed). *Phanerozoic Earth History of Australia*. Oxford. 11-16.

ENGLUND, K. J. 1968. Geology and coal resources of the Elk valley area, Tennessee and Kentucky. *United States Geological Survey Professional Paper*, **572**. 59p.

ENGLUND, K. J. & THOMAS, R. E. 1990. Late Palaeozoic depositional trends in the central Appalachian basin. *United States Geological Survey Bulletin*, **1839-F**. 19p.

ENOS, P. 1977. Flow regimes in debris flow. *Sedimentology*, **24**.133-142.

ESCHNER, T. B. & KOCUREK, G. 1986. Marine destruction of eolian sand seas: origin of mass flows. *Journal of Sedimentary Petrology*, **56**. 401-411

ETTENSOHN, F. R. (ed). 1992 Changing Interpretations of Kentucky Geology-Layer-cake, Facies, Flexure and Eustacy. Geological Society of America Fieldtrip. 184p.

FIALL, R. T. 1985. The Acadian orogeny and the Carskill delta. *In* D. L. WOODROW & W. D. SEVON (eds). *The Catskill Delta.* Geological Society of America Special Paper, **201**. 15-37.

FISHBAUGH, D. A., KVALE, E. P. & ARCHER, A. W. 1989. *Association Of Tidal And Fluvial Sediments Within Lower Pennsylvanian Rocks, Turkey Run State Park, Parke County, Indiana.* Indiana Geological Survey Guidebook.

FISHER, R. V. 1971. Features of coasre grained, high concentration fuilds and their deposits. *Journal of Sedimentary Petrology,* **41**. 916-927.

FISHER, R. V. 1983. Flow transformations in sediment gravity flows. *Geology,* **11**. 273-274.

FOLK, R. L. 1980. *Petrology of Sedimentary Rocks.* Texas, Hemphill. 159pp.

FORDHAM, C. E. 1989. *The Influence Of Sedimentary Structures And Facies On Fluid Flow (Permeability) In The Fell Sandstone, Northumberland.* M Phil thesis (unpublished) University of Newcastle upon Tyne, UK.

FRASER, A. J. & GAWTHORPE, R. L. 1990. Tectono-stratigraphic development and hyrodcarbon habitat of the Carboniferous in northern England. *In* R. F. P. HARDMAN & J. BROOKS (eds). *Tectonic Events Responsible for Britain's Oil and Gas Reserves.* Geological Society London, Special Publication, **55**. 49-86.

FRIEDMAN, G. M. 1958. Determination of sieve-size distribution from thin-section data for sedimentary petrological studies. *Journal of Geology,* **66**. 394-416.

FRIEDMAN, G. M. 1962. Comparison of moment measures for sieving and thin section data for sedimentary petrological studies. *Journal of Geology,* **32**. 15-25.

FRIEND, P. F. 1983. Towards the field classification of alluvial architecture or sequence. *In* J. D. COLLINSON & J. LEWIN (eds) *Modern and Ancient Fluvial Systems.* International Association of Sedimentologists Special Publication **6**, 345-354.

GARLAND, G. G. & OLIVIER, M. J. 1993. Predicting landslides from rainfall in a humid, sub-tropical region. *Geomorphology,* **8**. 165-173.

GAWTHORPE, R. L., GUTTERIDGE, P. & LEEDER, M. R. 1989. Late Devonian and Dinantian basin evolution in northern England and north Wales. *In* R. S. ARTHURTON, P. GUTTERIDGE & S. C. NOLAN (eds). *The Role of Tectonics in Devonian and Carboniferous Sedimentation in the British Isles.* Yorkshire Geological Society Occasional Publication, **6**. 1-24.

GRAHAM, S. A., INGERSOLL, R. V. & DICKINSON, W. R. 1976. Common provenance for lthic grains in Carboniferous sandstones from Ouachita mountains and Arkoma basin. *Journal of Sedimentary Petrology,* **46**. 620-632.

GREB, S. F. & CHESNUT, D. R. Jr. 1989. Geology of lower Pennsylvanian strata along the western outcrop belt of the eastern Kentucky coalfield. *In* COBB, J (ed). *Geology of the Lower Pennslyvanian in Kentucky, Indiana and Illinois.* Illinois Basin Consortium, No. 1. Kentucky Geological Survey, Lexington. 29-44.

GREB, S. F. & CHESNUT, D. R. Jr. 1992a. Transgressive channel-filling in the Breathitt Formation (Upper Carboniferous), eastern Kentucky coal field, USA. *Sedimentary Geology,* **75**. 209-221.

GREB, S. F. & CHESNUT, D. R. Jr. 1992b. Coastal and terrestrial environments of the lower Breathitt and Lee Formations (lower middle Pennsylvanian), near Frenchburg, Kentucky. *In* C. B. CECIL. (ed). *Palaeoclimate Controls on Carboniferous Sedimentation and Cyclic Stratigraphy in the Appalachian Basin.* United States Geological Survey Open File Report **92-546**. 90-101.

HAGERTY, D. J., ULLRICH, C. R. & SPOOR, M. F. 1981. Bank failure and erosion on the Ohio River. *Engineering Geology,* **19**. 119-132.

HAMILTON-SMITH, T. 1993. Startigraphic effects of the Acadian orogeny in the autochthonous Appalachian Basin. *In* D. C. ROY & J. W. SKEHAN (eds). *The Acadian Orogeny: Recent Studies In New England, Maritime Canada And The Autochthonous Foreland.* Geological Society of America Special Paper, **275**. 153-164.

HARDY, R. & TUCKER, M. E. 1987. X-ray powder diffraction of sediments. *In* M. E. TUCKER (ed) *Techniques In Sedimentology.* 191-228.

HARMS, J. C. & FAHNESTOCK, R. K. 1965. Stratification, bedforms and flow phenomena (with an example from the Rio Grande). *In* G. V. MIDDLETON (ed). *Primary Sedimentation Structures and Their Hydrodynamic Interpretation.* Society for Economic Palaeontologists and Mineralogists Special Publication, **12**. 84-115.

HARMS, J. C., SOUTHARD, J. B. & WALKER, R. G. 1982. *Structures and Sequences in Clastic Rocks.* Society for Economic Palaeontologists and Mineralogists Short Course Notes **9**.

HARRELL, J. A. & ERIKSSON, K. A. 1979. Empirical conversion equations for thin-section and sieve derived size parameters. *Journal of Sedimentary Petrology*, **49**. 273-280.

HARRISON, S. S. 1968. *The effects of Groundwater Seepage on Stream Regimen - A Laboratory Study*. PhD thesis (unpublished) University of North Dakota, USA.

HARRISON, S. S. & CLATYON, L. 1970. Effects of groundwater seepage on fluvial processes. *Geological Society of America Bulletin*, **81**. 1217-1226.

HASZELDINE, R. S. 1983a. Descending tabular cross-bed sets and bounding surfaces from a fluvial channel in the Upper Carboniferous coalfield of northeast England. *In* J. D. COLLINSON & J. LEWIN (eds) *Modern and Ancient Fluvial Systems*. International Association of Sedimentologists Special Publication **6**, 449-456.

HASZELDINE, R. S. 1983b. Fluvial bars reconstructed from a deep straight channel, Upper Carboniferous coal field of northeast England. *Journal of Sedimentary Petrology*, **53**. 1233-1248.

HATCHER, R. D. & ODOM, A. L. 1980. Timing of thrusting in the southern Appalachians, USA: model for orogeny? *Journal of the Geological Society, London*, **137**. 321-328.

HATCHER, R. D., THOMAS, W. A., GEISER, P. A., SNOKE, A. W., MOSHER, S. & WILTSCHKO, D. V. 1989. Alleghanian Orogeny. *In* R. D. HATCHER, W. A. THOMAS & G. W. VIELE (eds). *The Appalachian-Ouachits Orogen In The United States*. The Geology of North America F-2. Geological Society of America. 233-318.

HELBY, R. J. 1973. Review of Late Permian and Triassic palynology of New South Wales. *Special Publication of the Geological Society of Australia*, **4**. 141-155.

HERBERT, C. 1980a. Depositional development of the Sydney Basin. *In* C. HERBERT & R. HELBY (eds). *A Guide to the Sydney Basin*. Geological Survey of New South Wales Bulletin, **26**. 10-52.

HERBERT, C. 1980b. Wianamatta Group and Mittagong Formation. *In* C. HERBERT & R. HELBY (eds). *A Guide to the Sydney Basin*. Geological Survey of New South Wales Bulletin, **26**. 254-273.

HERBERT, C. 1980c. Southwestern Sydney Basin. *In* C. HERBERT & R. HELBY (eds). *A Guide to the Sydney Basin*. Geological Survey of New South Wales Bulletin, **26**. 82-99.

HEWARD, A. P. 1981. Lower Carboniferous fluvial facies in Northumberland and Borders. In T. ELLIOTT (ed). *Field Guides To Modern And Ancient Fluvial Systems In Britain And Spain.* Proceedings of the 2nd International Conference on Fluvial Sediments.

HIGGINS, M. W., ATKINS, R. L., CRAWFORD, T. J., CRAWFORD, R. F., BROOKS, R & COOK, R. B. 1988. The structure, stratigraphy, tectonostratigraphy and evolution of the southern-most part of the Appalachian orogen. *United States Geological Survey Professional Paper,* **1475.**

HISCOTT, R.N. & MIDDLETON, G. V. 1979. Depositional mechanics of thick bedded sandstones at the base of a submarine slope, Tourelle Formation (Lower Ordovician), Quebec, Canada In L. J. DOYLE & D. R. DILKEY (eds). *Geology of Contienetal Slopes.* Society for Economic Palaeontologists and Mineralogists Special Publication **27.** 307-326.

HODGSON, A. V. 1978. Braided river bedforms and related sedimentary structures in the Fell Sandstone Group (Lower Carboniferous) of north Northumberland. *Proceedings of the Yorkshire Geological Society,* **41.** 509-532.

HOOKE, J. M. 1979. An anaysis of the processes of riverbank erosion. *Journal of Hydrology,* **42.** 39-62.

HORNE, J. C., FERM, J. C. & SWINCHATT, J. P. 1974. Depositional model for the Mississippian-Pennsylvanian boundary in northeastern Kentucky. *In* G. BRIGGS (ed). *Carboniferous of the Southeastern United States.* Geological Society of America Special Paper, **148.** 97-114.

HOWARD, A. D. & McLANE III, C. F. 1988. Erosion of cohesionless sediment b y groundwater seepage. *Water Resources Research,* **24.** 1659-1674.

HOWARD, R. H. & WHITAKER, S. T. 1990. Fluvial-estuarine valley fill at the Mississippian-Pennsylvanian unconformity, Main Consolidated Field, Illinois, *In* J. H. BARWIS, J. G. McPHERSON, & J. R. J. STUDLICK (eds). *Sandstone Petroleum Reservoirs.* 319-341.

IVERSON, R. M. & MAJOR, J. J. 1986. Groundwater seepage vectors and the potential fro hillslope failure and debris mobisation. *Water Resources Research,* **22.** 1543-1546.

JACKSON, R. G. II 1975. Hierarchical attributes and a unifying model of bed forms composed of cohesionless material and produced by shearing flow. *Geological Society of America Bulletin,* **86.** 1523-1533.

JACKSON, R. G. II 1976. Sedimentological and fluid dynamic implications of the turbulent bursting phenomena in gephysical flows. *Journal of Fluid Mechanics, 77.* 531-560.

JIBSON, R. W. & KEEFER, D. K. 1993. Analysis of the seismic origin of landslides: Examples from the New Madrid seismic zone. *Geological Society of America Bulletin,* **105**. 521-536.

JOHNSON, A. M. 1970. *Physical Processes in Geology.* Freeman, Cooper & Co. 577pp

JOHNSON, G. A. L. 1984. Subsidence and sedimentation in the Northumberland Trough. *Proceedings of the Yorkshire Geological Society,* **45**. 71-83.

JOHNSON, M. R. 1994. Thin section grain size analysis revisted. *Sedimentology,* **41**. 985-999.

JOHNSSON, M. J., STALLARD, R. F. & MEADE, R. H. 1988. First-cycle quartz arenites in the Orinoco River basin, Venezuela and Columbia. *Journal of Geology,* **96**. 263-277.

JONES, B. G. & RUST, B. R. 1983. Massive sandstone facies in the Hawkesbury Sandstone, a Triassic fluvial deposit near Sydney, Australia. *Journal of Sedimentary Petrology,* **53**. 1249-1261.

JONES, C. M. 1980. Deltaic sedimentation in the Roaches Grit and associated sediments (Namurian R2b) in the southwest Pennines. *Proceedings of the Yorkshire Geological Society,* **43**. 39-67.

JONES, J. G. CONAGHAN, P. J. McDONNEL, K. L. FLOOD, R. H. & SHAW, S. E. 1984. Papuan Basin analogue and a foreland basin model for the Bowen-Sydney Basin. *In* J. J. VEEVERS (ed). *Phanerozoic Earth History of Australia.* Oxford. 243-262.

JOPLING, A. V. 1961. Origin of regressive ripples explained in terms of fluid-mechanic processes. *United States Geological Survey Professional Paper,* **424D**. 15-17.

JOPLING, A. V. 1965. Hydraulic factors controlling the shape of laminae in laboratory deltas. *Journal of Sedimentary Petrology,* **35**. 777-791.

JOPLING, A. V. 1966. Some applications of theory and experiment to the study of bedding genesis. *Sedimentology,* **7**. 71-102.

KAHN, J. S. 1956. The analysis and distribution of the properties of packing in sand size sediments. *Journal of Geology,* **64**. 385-395.

KELLER, E. A., KONDOLF, G. M. & HAGERTY, D. J. 1990. Groundwater and fluvial processes; selected observations. *In* C. G. HIGGINS & D. R. COATES (eds). *Groundwater Geomorphology.* Geological Society of America Special Paper, **252**. 319-340.

KELLER, S. J. 1990. Maps of southwestern Indiana showing geology and elevation of the sub-Pennsylvanian surface. Indiana Geological Survey.

KELLING, G. 1968. Patterns of sedimentation in Rhondda beds of South Wales. *American Association of Petroleum Geologists Bulletin,* **52**. 2369-2386.

KERR, P. F. 1977. *Optical Mineralogy.* McGraw-Hill. 492p.

KIMBELL, G. S., CHADWICK, R. A., HOLLIDAY, D. W. & WERNGREN, O. C. 1989. The structure and evolution of the Northumberland Trough from new seismic reflection data and its bearing on modes of continental extension. *Journal of the Geological Society, London,* **146**. 775-787.

KLEIN, G. deV. & WILLARD, D. A. 1989. Origin of the Pennsylvanian coal-bearing cyclothems of North America. *Geology,* **17**. 152-155.

KOLATA, D. R. & NELSON, W. J. 1990. Tectonic history of the Illinois Basin. *In* M. W. LEIGHTON, D. R. KOLATA, D. F. OLTZ & J. J. EIDEL (eds). *Interior Cratonic Basins.* American Association of Petroleum Geologists Memoir, **51**. 236-286.

KRAMER, S. L. 1988. Triggering of liquefaction flow slides in coastal soil depostis. *Engineering Geology,* **26**. 17-31.

KVALE, E. P., ARCHER, A. W. 1990. Tidal deposits associated with low-sulphur coals, Brazil Formation (Lower Pennsylvanian), Indiana. *Journal of Sedimentary Petrology,* **60**. 563-574,

KVALE, E. P., ARCHER, A. W. 1991. Characteristics of two, Pennsylvanian-age, semidiurnal tidal deposits in the Illinois Basin, USA. *In* D. G. SMITH, G. E. REINSON, B. A. ZAITLIN & R. A. RAHMANI (eds). *Clastic Tidal Sedimentology.* Canadian Society of Petroleum Geologists Memoir **16**. 179-188.

KVALE, E. P., ARCHER, A. W. & JOHNSON, H. R. 1989. Daily, monthly and yearly tidal cycles within laminated siltstones of the Mansfield Formation of Indiana. *Geology,* **17**. 365-368.

KVALE, E. P. & BARNHILL, M. L. 1994. Evolution of lower Pennsylvanina estuarine facies within two adjacent palaeovalleys, Illinois Basin, Indiana. *In Incised-Valley Systems: Origin and Sedimentary Sequences.* Society of Economic Palaeontologists and Mineralogists Special Publication, **51**. 191-207.

LAMBECK, K & STEPHENSON, R. 1986. The post-Palaeozoic uplift history of southeatsern Australia. *Australian Journal of Earth Science*, **33**. 253-270.

LAURY, R. L. 1971. Stream bank failure and rotational slumping: preservation and significance in the geologic record. *Geological Society of America Bulletin*, **82**. 1251-1266.

LEEDER, M. R. 1973. Fluviatile fining-upwards cycles and the magnitude of palaeochannels. *Geological Magazine*, **110**. 265-276.

LEEDER, M. R. 1974. Lower Border Group (Tournaisian) fluviodeltaic sedimentation and palaeogeography of the Northumberland Basin. *Proceedings of the Yorkshire Geological Society*, **40**. 129-180.

LEEDER, M. R. 1987. Sediment deformation structures and the palaeotectonic analysis of sedimentary basins, with a case study from the Carboniferous of northern England. *In* M. E. JONES & R. M. F. PRESTON (eds). *Deformation of Sediments and Sedimentary Rocks.* Geological Society, London Special Publication, **29**. 137-146.

LEEDER, M. R. 1988a. Recent developments in Carboniferous geology: a critical review with implications for the British Isles and N. W. Europe. *Proceedings of the Geological Association*, **99**. 73-100.

LEEDER, M. R. 1988b. Devono-Carboniferous river systems and sediment dispersal from the orogenic belts and cratons of NW Europe. *In* A. L. HARRIS & D. J. FETTES (eds). *The Caledonian-Appalachian Orogen.* Geological Society, London Special Publication, **38**. 549-558.

LEEDER, M. R., FAIRHEAD, D., LEE, A., STUART, G., CLEMMEY, H.,EL-HADDAHEH, B. & GREEN, C. 1989. Sedimentary and tectonic evolution of the Northumberland Basin. *In* R. S. ARTHURTON, P. GUTTERIDGE & S. C. NOLAN (eds). *The Role of Tectonics In Devonian and Carboniferous Sedimentation In The British Isles.* Yorkshire Geological Society Occasional Publication, **6**. 207-223.

LEEDER, M. R. & GAWTHORPE, R. L. 1987. Sedimentary models for extensional half grabens. *In* M. P. COWARD, J. F. DEWEY & P. L. HANCOCK (eds). *Continental Extensional Tectonics.* Geological Society, London Special Publication, **28**. 139-152.

LEOPOLD, L. B. & WOLMAN, M. G. 1957. River channel patterns: braided, meandering and straight. *United States Geological Survey Professional Paper*, **262B**. 39-85.

LE ROUX, J. P. 1992. Determining the channel sinuosity of ancient fluvial systems from palaeocurrent data. *Journal of Sedimentary Petrology*, **62**. 283-291.

LE ROUX, J. P. 1993. Determining the channel sinuosity of ancient fluvial systems from palaeocurrent data - reply. *Journal of Sedimentary Petrology*, **63**. 308-310.

LE ROUX, J. P. 1994. The angular deviation of palaeocurrent directions as applied to the calculation of channel sinuosities. *Journal of Sedimentary Research*, **A64**. 86-87.

LOUGHNAN, F. C. & GOLDING, H. G. 1957. Clay minerals in some Hawkesbury Sandstones. *Journal of the Proceedings of the Royal Society of New South Wales*, **90**. 147-150.

LOWE, D. R. 1975. Water escape structures in coarse-grained sediments. *Sedimentology*, **22**. 157-204.

LOWE, D. R. 1976a. Grain flow and grain fall deposits. *Journal of Sedimentary Petrology*, **46**. 188-199.

LOWE, D. R. 1976b. Subaqueous liquefied and fluidised sediment flows and their deposits. *Sedimentology*, **23**. 285-308.

LOWE, D. R. 1979. Sediment gravity flows: their classification and some problems of its application to natural flows and deposits. *In* L. J. DOYTE & O. H. PILKEY (eds). *Geology of the Continental Slopes*. Society of Economic Palaeontologists and Mineralogists Special Publication, **27**. 75-84.

LOWE, D. R. 1982. Sediment gravity flows: II Depositional models with special reference to deposits of high-density turbididty currents. *Journal of Sedimentary Petrology*, **52**. 279-297.

LOWE, D. R. & LoPICCOLO, R. D. 1974. The chacrateristics and origins of dish and pillar structures. *Journal of Sedimentary Petrology*, **44**. 484-501.

MACK, G, H, 1981. Composition of modern stream sand in a humid climate derived from a low-grade metamorphic and sedimentary foreland fold-thrust belt of North Georgia. *Journal of Sedimentary Petrology*, **51**. 1247-1258.

MAIZELS, J. K. 1983. Palaeovelocity and palaeodischarge determination for coarse gravel deposits. *In* K. J. GREGORY (ed). *Background to Palaeohydrology*. Wiley.

MAIZELS, J. K. 1989. Sedimentology and palaeohydrology of Holocene flood deposits in front of a Jokulhlaup glacier, South Iceland. *In* K. BEVEN & P. CARLING (eds). *Floods: Hydrological Sedimentological and Geomorphic Implications.* 239-251.

MAIZELS, J. K. 1993. Lithofacies variations within sandur deposits: the role of runoff regime, flow dynamics and sediment supply charcteristics. *Sedimentary Geology,* **85**. 299-325.

MANGE, M. A. & MAURER, F. W. 1992. *Heavy Minerals in Colour.* 147p. Chapman & Hall, London.

MARTIN. C. A. L. 1993. The occurrence of a massive sandstone facies in ancient braided stream deposits; Turkey Run State Park, Parke County, Indiana. *Report for the Department of Natural Resourses, Indiana, USA.* 43p.

MARTIN. C. S. 1970. Effect of a porous sand bed on incipient sediment motion. *Water Resources Research,* **6**. 1162-1174.

MARTINO, R. L. & SANDERSON, D. D. 1993. Fourier and autocorrelation analysis of estuarine tidal rhythmites, lower Breathitt Formation (Pennsylvanian), eastern Kentucky, USA. *Journal of Sedimentary Petrology,* **63**. 105-119.

McCABE, P. J. 1977. Deep distributary channels and giant bedforms in the Upper Carboniferous of the Central Pennines, Northern England. *Sedimentology,* **24**. 271-291.

McCABE, P. J. & JONES, C. M. 1977. Formation of re-activation surfaces within super-imposed deltas and bedforms. *Journal of Sedimentary Petrology,* **47**. 707-715.

McKEE, E. D. 1989. Sedimentary structures and textures of Rio Orinoco channel sands, Venezuela and Columbia. *United States Geological Survey Water Supply Paper,* **2326-B**. 23p.

McKEE, E. D., CROSBY, E. J. & BERRYHILL, H.L. 1967. Flood deposits, Bijou Creek, Colorado, June 1965. *Journal of Sedimentary Petrology,* **37**. 829-851.

McKEE, E. D. & WEIR, G. W. 1953. Terminology of stratification and cross-stratification in sedimentary rocks. *Geological Society of America Bulletin,* **64**. 381-390.

McMANUS, J. 1989. Grain size determination and interpretation. *In* M. E. TUCKER (ed) *Techniques in Sedimentology.* 63-86.

MIALL, A. D. 1976. Palaeocurrent and palaeohydrological analyses of some vertical profiles through a Cretaceous braided stream deposit, Banks Island, Arctic Canada. *Sedimentology*, **23**. 459-483.

MIALL, A. D. 1977. A review of the braided-river depositional environment. *Earth Science Reviews*, **13**. 1-62.

MIALL, A. D. 1978. Lithofacies types and vertical profile models in braided rivers. *In* MIALL, A. D. (ed) *Fluvial Sedimentology*. Canadian Society of Petroleum Geologists Memoirs, **5**. 597-604.

MIALL, A. D. 1985. Architectural element analysis: a new method of facies analysis applied to fluvial deposits. *Earth Science Reviews*, **22**. 261-308.

MIALL, A. D. 1988. Facies architecture in clastic sedimentary basins. *In* K. KEINSPEHN & C. PAOLA (eds) *New Perspectives In Basin Analysis*. 67-81.

MIDDLETON, G. V. 1967. Experiments on density and turbidity currents III. Deposition of Sediment. *Canadian Jouranal of Earth Science*, **4**. 475-505.

MIDDLETON, G. V. & SOUTHARD, J. B. 1978. *Mechanics of sediment movement*. Society of Economic Palaeontologists and Mineralogists Short Course, **3**.

MJO, R., WALDERHAUG, O. & PRESTHOLM, E. 1993. Crevasse splay sandstone geometries in the Middle Jurassic Ravenscar Group of Yorkshire, UK. *In* M. MARZO & C. PUIDEFABREGAS (eds). *Alluvial Sedimentation*. International Association of Sedimentologists Special Publication, **17**. 167-184.

MONRO, M. 1986. *Sedimentology of the Carboniferous Fell Sandstone Group Of Nothumberland*. PhD thesis (unpublished) University of Newcastle-Upon-Tyne, UK.

MORRIS, R. C. 1974. Sedimentary and tectonic history of the Ouachita mountains. *In* W. R. DICKINSON (ed). *Tectonics and Sedimentation*. Society of Economic Palaeontologists and Mineralogists Special Publication, **22**. 120-142.

MOSS, A. J. 1972. Bedload sediments. *Sedimentology*, **18**. 159-219.

MURRAY, A. B. & PAOLA, C. 1994. A cellular model of braided rivers. *Nature*, **371**. 54-57.

MUTTI, E. & NORMARK, W. R. 1987. Comparing examples of modern and ancient turbidite systems: problems and concepts. *In* J. K. LEGGETT & G. G. ZUFFA (eds). *Marine Clastic Sedimentology*. Graham & Trotman. 1-38.

NAKAGAWA, H. & TSUJMOTO, T. 1984. Interaction between flow over a granular permeable bed and seepage flow; a theoretical analysis. *Journal of Hydroscience and Hydraulic Engineering*, **2**. 1-10.

NANSON, G. C., RUST, B. R. & TAYLOR, G. 1986. Coexsistent mud braids and anastomosing channels in an arid-zone river: Cooper Creek, central Australia. *Geology*, **14**. 175-178.

NEMEC, W. 1990. Aspects of sediment movements on steep delta slopes. *In* A. COLELLA & D. B. PRIOR (eds). *Coarse Grained Deltas.* International Association of Sedimentologists Special Publication **10**. 29-73.

NORDIN, C. F. & PEREZ-HERNANDEZ, D. 1989. Sand waves, bars, and wind-blown sands of the Rio Orinoco, Venezuela and Columbia. *United States Geological Survey Water Supply Paper*, **2326-A**. 74p.

OBERMEIER, S. F. 1988. Liquefaction potential in the Central Mississippi Valley. *United Sates Geological Survey Bulletin*, **1832**. 21p.

OLSEN, T. 1993. Determining the channel sinuosity of ancient fluvial systems from palaeocurrent data - discussion. *Journal of Sedimentary Petrology*, **63**. 306-307.

OWEN, G. 1987. Deformation processes in unconsolidated sands. *In* M. E. JONES & R. M. F. PRESTON (eds) *Deformation of Sediments and Sedimentary Rocks.* Geological Society, London, Special Publication, **29**. 11-24.

PETTIJOHN, F. J., POTTER, P. E. & SIEVER, R. 1972. *Sand and Sandstone.* New York, Springer-Verlag. 618p.

PHILLIPS, T. L. & PEPPERS, R. A. 1984. Changing patterns of Pennsylvanian coal-swamp vegetation and implications of climatic control on coal occurrence. *International Journal of Coal Geology*, **3**. 205-255.

PICKERING, K. T., HISCOTT, R. N. & HEIN, F. J. 1989. *Deep marine environments; clastic sedimentation and tectonics.* 416p. Unwin-Hyman, London.

PIERSON, T. C. 1981. Dominant particle support mechanisms in debris flows at Mount Thomas, New Zealand, and implications for flow mobility. *Sedimentology*, **28**. 49-60.

PIERSON, T. C. & SCOTT, K M. 1985. Downsteam dilution of a lahar:transition from debris flow to hyperconcentrated stream flow. *Water Resources Research*, **21**. 1511-1524.

POSTMA, G. 1986. Classification for sediment gravity flow deposits based on flow conditions during sedimentation. *Geology*, **14**. 291-294.

POSTMA, G., NEMEC, W. & KLEINSPEHN, K. L. 1988. Large floating clasts in turbidites: a mechnaism for their emplacement. *Sedimentary Geology*, **58**. 47-62.

POSTMA, G., ROEP, T. B. & RUEGG, G. H. J. 1983. Sandy-gravelly mass flow deposits in an ice-marginal lake (Saalian, Leuvenumsche Beek Valley, Veluwe, The Netherlands), with emphasis on plug-flow deposits. *Sedimentary Geology*, **34**. 59-82.

POTTER, P. E. & SIEVER, R. 1956. Source of basal Pennsylvanian sediments in the Eastern Interior Basin. *Journal of Geology*, **64**. 225-244.

PRYOR, W. A. 1973. Permeability-porosity patterns and variations in some Holocene sandbodies. *American Association of Petroleum Geologists Bulletin*, **57**. 162-189.

PRYOR, W. A. & SABLE, E. G. 1974. Carboniferous of the Eastern Interior Basin. *In* G. BRIGGS (ed). *Carboniferous of the Southeastern United States*. Geological Society of America Special Paper, **148**. 281-313.

QUILTY, P. G. 1984. Phanerozoic climates and environments of Australia. *In* J. J. VEEVERS (ed). *Phanerozoic Earth History of Australia*. Oxford. 48-57.

QUINLAN, G. M. & BEAUMONT, C. 1984. Appalachian thrusting, lithospheric flexure, and the Palaeozoic stratigraphy of the eastern interior of North America. *Canadian Journal of Earth Sciences*, **21**. 973-996.

RAST, N. 1988. Tectonic implications of the timing of the Variscan orogeny. *In* A. L. HARRIS & D. J. FETTES (eds). *The Caledonian-Appalachian Orogeny*. Geological Society, London, Special Publication, **38**. 585-595.

RAST, N & SKEHAN, J. W. 1993. Mid-Palaeozoic orogenesis in the north Atlantic: the Acadian orogeny. *In* D. C. ROX & J. W. SKEHAN (eds). *Recent Studies In New England, Maritime Canada And The Autochthonous Foreland*. Geological Society of America Special Paper, **275**. 1-25.

RAYMOND, A. 1985. Floral diversity, phytogeography, and climatic amelioration during the Early Carboniferous (Dinantian). *Paleobiology*, **11**. 273-293.

REID, I. & FROSTICK, L. E. 1994. Fluvial transport and deposition. *In* K. PYE (ed). *Sediment Transport and Depositional Processes*. Blackwell. 89-155.

RETALLACK, G. 1977. Reconstructing Triassic vegetation of eastern Australia: a new approach to the biostratigraphy of Gondwanaland. *Alcheringa*, **1**. 247-277.

RETALLACK, G. 1980. Late Carboniferous to middle Triassic megafossil floras from the Sydney Basin. *In* C. HERBERT & R. HELBY (eds). *A Guide to the Sydney Basin*. Geological Survey of New South Wales Bulletin, **26**. 384-430.

RICE, C. L. 1984. Sandstone units of the Lee Formation and related strata in eastern Kentucky. *United States Geological Survey Professional Paper*, **1151-G**. 52p.

RICE, C. L. & NEWELL, W. L. 1990. Geologic map of part of the Jellico East quadrangle, Campbell and Claiborne counties, Tennessee (GQ-1674).

RICE, C. L. & SCHWIETERING, J. F. 1988. Fluvial deposition in the central Appalachians during the early Pennsylvanian. *United States Geological Survey Bulletin*, **1839-B**. 1-10.

RICHARDSON, J. R. & RICHARDSON, E. V. 1985. Inflow seepage influence on straight alluvial channels. *Journal of Hydraulic Engineering*, **111**. 1133-1147.

ROBSON, D. A. 1956. A sedimentary study of the Fell Sandstone of the Coquet Valley, Northumberland. *Quarterly Journal of the Geological Society, London*, **112**. 241-262.

ROBSON, D. A. 1980. *The Geology of North East England*. Special Publication of the Natural History Society of Northumbria.

ROE, S. L. 1987. Cross-strata and bedforms of probable transitional dune to upper stage plane bed origin from a Late Precambrian fluvial sandstone, northern Norway. *Sedimentology*, **34**. 80-101.

RONDINE, J. D. & JOHNSON, A. M. 1976. The ability of debris, heavily freighted with coarse clastic materials, to flow on gentle slopes. *Sedimentology*, **23**. 213-234.

ROSS, C. A. & ROSS, J. R. P. 1988. Late Palaeozoic transgressive-regressive deposition. *In* C. R. WILGUS, B. S. HASTINGS, C. G. KENDALL, H. W. POSAMENTIER, C. A. ROSS & J. C. WAGONER (eds). *Sea-level Changes: An Integrated Approach*. Society of Economic Palaeontologists and Mineralogists Special Publication, **42**. 227-247.

RUDLOFF, W. 1981. *World-Climates*. 632p. Wissenschaftliche Verlagsgesellschaft

RUST, B. R. 1972. Structure and process in a braided river. *Sedimentology*, **18**. 221-245.

RUST, B. R. 1978a A classification of alluvial channel systems. *In* MIALL, A. D. (ed) *Fluvial Sedimentology*. Canadian Society of Petroleum Geologists Memoir, **5**. 187-198.

RUST, B. R. 1978b. Depositional models for braided alluvium. *In* MIALL, A. D. (ed) *Fluvial Sedimentology.* Canadian Society of Petroleum Geologists Memoir, **5**. 605-626.

RUST, B. R. & JONES, G. G. 1987. The Hawkesbury Sandstone south of Sydney, Australia, Triassic analogue for the deposit of a large braided river. *Journal of Sedimentary Petrology*, **57**. 222-233.

RUST, B. R. & ROMANELLI, R. 1975. Late Quaternary subaqueous outwash deposits near Ottowa, Canada. *In* A. V. JOPLING & B. C. McDONANLD (eds). *Glaciofluvial And Glaciolacustrine Sedimentation.* Society of Economic Palaeontologists and Mineralogists Special Publication, **23**. 177-192.

SASITHARAN, S., ROBERTSON, P. K. SEGO, D. C. & MORGENSTERN, N. R. 1993. Collapse behaviour of sand. *Canadian Geotechnical Journal*, **30**. 569-577.

SAUNDERS, W. B. & RAMSBOTTOM, W. H. C. 1986. The mid Carboniferous eustatic event. *Geology*, **14**. 208-212.

SCHUMM, S. A. 1960. The effect of sediment type on the shape and stratification of some modern fluvial deposits. *American Journal of Science*, **258**. 177-184.

SCHUMM, S. A. 1968a. River adjustment to altered hydrologic regiment - Murrabridge River and palaeochannels, Australia. *United States Geological Survey Professional Paper*, **598**. 65p.

SCHUMM, S. A. 1968b. Speculation concerning palaeohydraulic controls of terrestrial sedimentation. *Geological Society of America Bulletin*, **79**. 1573-1588.

SCHUMM, S. A. 1972. Fluvial palaeochannels. *In* J. K. RIGBY & W. K. HAMBLIN (eds). *Recognition of Ancient Sedimentary Environments*, Society of Economic Palaeontologists and Mineralogists Special Publication, **16**. 98-107.

SCHUMM, S. A. 1977. *The Fluvial System.* Wiley.

SCHUMM, S. A., MOSLEY, M. P. & WEAVER, W. E. (eds) 1987. *Experimental Fluvial Geomorphology.*

SCOTESE, C. R. 1990. *Atlas of Phanerozoic Plate Tectonic Recontructions.*

SCOTT, K. M. 1988. Origins, behaviour and sedimentology of lahars and lahar-runout flows in the Toutle-Cowlitz River System. *United States Geological Survey Proffesional Paper*, **1447A** 74p

SECOR, D.T., SNOKE, A. W. & DALLMEYER, R. D. 1986. Character of the Alleghanian orogeny in the southern Appalachians. Part III: Regional tectonic relations. *Geological Society of America Bulletin*, **97**. 1345-1353.

SEED, H. B. 1968. Landslides during earthquakes due to soil liquefaction. *Proceedings of the American Society of Civil Engineers. Soil Mechanics Foundation Division*, **94**. 1053-1122.

SHAVER, R. H. (regional coordinator) 1985. Midwestern basins and arches region. *In* F. A. LINDBERG (ed). *Correlation of Stratigraphic Units of North America* American Association of Petroleum Geologists COSUNA chart series.

SHU, L. & FINLAYSON, B. 1993. Flood management on the lower Yellow River: hydrological and geomorphological perspectives. *Sedimentary Geology*, **85**. 285-296.

SIEVER, R & POTTER, P. E. 1956. Sources of basal Pennsylvanian sediments in the Eastern Interior basin: 2 sedimentary petrology. *Journal of Geology*, **64**. 317-335.

SIMONS, D. B. & RICHARDSON, E. V. 1966. Resistence to flow in alluvial channels. *United Sates Geological Survey Professional Paper*, **422J**. 61pp

SINGH, B & KUMAR, S. 1974. Mega- and giant ripples in the Ganga, Yamuna, and Son Rivers, Utter Pradesh, India. *Sedimentary Geology*, **12**. 53-66.

SINGH, H., PARKASH, B. & GOHAIN, K. 1993. Facies analysis of the Kosi megafan deposits. *Sedimentary Geology*, **85**. 87-113.

SINHA, A. K., HUND, E. A. & HOGAN, J. P. 1989. Palaeozoic accretionary history of the North American plate margin (central and southern Appalachians): constraints from the age, origin and distribution of granitic rocks. *In* J. W. HILLHOUSE (ed). *Deep Structure and Past Kinematics of Accreted Terranes*. 219-238.

SINHA, R. & FRIEND, P. F. 1994. River systems and their sediment flux, Indo-Gangetic plains, Northern Bihar, India. *Sedimentology*, **41**. 825-845.

SLINGERLAND, R., FURLONG, K. P., MANSPEIZER, W., HUNTOON, J., LUCAS, M., BEAUMONT, C. & DIEMER, J. 1989. Sedimentology and thermal-mechanical history of basins in the central Appalachian orogen. Fieldtrip T152 28th International Geological Congress.

SMITH, G. A. 1986. Coarse grained non-marine volcanoclatic sediment: terminology and depositional process. *Geological Society of America Bulletin*, **97**. 1-10.

SMITH, N. D. 1970. The braided stream depositional environment: comparison of the Platte River with some Silurian clastic rocks, north-central Appalachians. *Geological Society of America Bulletin*, **81**. 2993-3014.

SMITH, N. D. 1971. Transverse bars and braiding in the Lower Platte River, Nebraska. *Geological Society of America Bulletin*, **82**. 3407-3420.

SMITH, N. D. 1972. Flume experiments on the durability of mud clasts. *Journal of Sedimentary Petrology*, **42**. 378-383.

SMITH, N. D. 1978. Some comments on terminology for bars in shallow rivers. *In* A. D. MIALL (ed) *Fluvial Sedimentology*. Canadian Society of Petroleum Geologists Memoir, **5**. 85-88.

SMITH, S. A. & HOLLIDAY, D. W. 1991. The sedimentology of the Middle and Upper Border Groups (Visean) in the Stonehaugh borehole, Northumberland. *Proceedings of the Yorkshire Geological Society*, **48**. 435-446.

SOUTHARD, J. B. & BOGUCHWAL, L. A. 1990. Bed configurations in steady uni-directional water flow, Part II: synthesis of flume data. *Journal of Sedimentary Petrology*, **60**. 658-679.

STANDARD, J. C. 1969. Hawkesbury Sandstone. *Journal of the Geological Society of Australia*, **16**. 407-417.

STAUB, J. R., ESTERLE, J. S. & RAYMOND, A. L. 1991. Comparative analysis of central Appalachian coal beds and Malaysian peat deposits. *Bulletin de la Societe Geologique de France*, **162**. 339-351.

STAUFFER, P. H. 1967. Grain flow deposits and their implications, Santa Ynez Mountains, California. *Journal of Sedimentary Petrology*, **37**. 487-508.

TANKARD, A. J. 1986a. Depositional response to foreland deformation in the Carboniferous of eastern Kentucky. *American Association of Petroleum Geologists Bulletin*, **70**. 853-868.

TANKARD, A. J. 1986b. On the depositional response to thrusting and lithospheric flexure: examples from the Appalachian and Rocky Mountain basins. *In* P. A. ALLEN & P. HOMEWOOD (eds). *Foreland Basins*. International Association of Sedimentologists Special Publication, **8**. 369-392.

TAYLOR, J. M. 1950. Pore space reduction in sandstones. *American Association of Petroleum Geologists Bulletin*, **34**. 710-716.

THORNE, C. R., RUSSELL, A. P. G. & ALAM, M. K. 1993. Planform pattern and channel evolution of the Brahmaputra River, Bangladesh. *In* J. L. BEST & C. S. BRISTOW (eds). *Braided Rivers*. Geological Society, London Special Publication **75**. 257-276.

TRASK & PALMER 1986. *Structural and depositional history of the Pennsylvanian System in Illinois*. Geological Society of America Special Paper, **210**. 63-77.

TREWORGY, J. D. 1990. Kaskaskia Sequence: Mississippian Valmeyeran and Chesterian Series. *In* M. W. LEIGHTON, D. R. KOLATA, D. F. OLTZ & J. J. EIDEL (eds). *Interior Cratonic Basins*. American Association of Petroleum Gelogists Memoir, **51**. 125-142.

TUCKER, M. E. 1973. The sedimentary environments of tropical African estuaries: Freetown Peninsula, Sierra Leone. *Geologie en Mijnbouw*, **52**. 203-215.

TURNBULL, W. J., KINNITSKY, E. L. & WEAVER, F. S. 1966. Bank erosion in the soils of the lower Mississippi valley. *Proceedings of the American Society of Civil Engineers Soil Mechanic Foundation*, **93**. 121-136.

TURNER, B. R. 1980. Palaeohydraulics of an upper Triassic braided river system in the main Karoo Basin, South Africa. *Transactions of the Geological Society of South Africa*, **83**. 425-431.

TURNER, B. R. 1989. *The Geology and Hydrocarbon Potential of the Northumberland Basin*.

TURNER, B. R. & MONRO, M. 1987. Channel formation and migration by mass-flow processes in the Lower Carboniferous fluviatile Fell Sandstone Group, north-east England. *Sedimentology*, **34**. 1107-1122.

TURNER, B. R. & O'MARA, P. T. in press Tectonic controls on fluvial depositional style, base level change and hydrocarbon prospectivity in the Westphalian B Coal Measures: northeast England and southern North Sea.

TURNER, B. R., YOUNGER, P. L. & FORDHAM, C. E. 1993. Fell Sandstone Group lithostratigraphy south-west of Berwick-upon-Tweed: implications for the regional development of the Fell Sandstone. *Proceedings of the Yorkshire Geological Society*, **49**. 269-281.

TURNER, P. 1974. Lithostratigraphy and facies analysis of the Ringerike Group of the Öslo region. *Norges Geol. Undersokelse*, **314**. 101-132.

VEEVERS, J. J., CONAGHAN, P. J. & SHAW, S. E. 1993. Permian and Triassic New England Orogen/ Bowen-Gunnedah-Sydney Basin in the context of Gondwana and Pangea. *In* P. G. FLOOD & J. C. AICHISON (eds). *New England Orogen:. Eastern Australia.* Depsrtment of Geology & Geophysics, University of New England, Armidale. 31-51.

VISHER, G. S. 1969. Grain size distribution and depositional processes. *Journal of Sedimentary Petrology,* **39**. 1074-1106.

WALKER, R. G. 1990. Facies modelling and sequence stratigraphy. *Journal of Sedimentary Petrology,* **60**. 777-780.

WANLESS, H. R. 1975. Appalachian region *In* E. D. McKEE & E. J. CROSBY (eds). *Introduction and regional analysis of the Pennsylvanian System in the United States.* United States Professional Paper, **853** Part 1. 17-62.

WARBURTON, J., DAVIES, T. R. H. & MANDL, M. G. 1993. A meso-scale field investigation of channel change and floodplain characteristics in an upland braided gravel-bed river, New Zealand. *In* J. L. BEST & C. S. BRISTOW (eds). *Braided Rivers.* Geological Society, London Special Publication **75**. 241-255.

WARD, C. R. 1980. Notes on the Bulgo Sandstone and the Baldhill Claystone. *In* C. HERBERT & R. HELBY (eds). *A Guide to the Sydney Basin.* Geological Survey of New South Wales Bulletin, **26**. 178-186.

WATTERS, G. Z. & RAO, V. P. 1971. Hydrodynamic effect of seepage on bed particles. *American Society of Civil Engineers Journal of Hydraulic Division,* **97**. 421-439.

WELLS, N. A., RICHARDS, S. S., PENG, S, KEATTCH, S. E., HUDSON, J. A. & COPSEY, C. J. 1993. Fluvial processes and recumbently folded crossbeds in the Pennsylvanian Sharon Conglomerate in Summit County, Ohio, USA. *Sedimentary Geology,* **85**. 63-83.

WILLIAMS, G. E. 1971. Flood deposits of the sand bed ephemeral streams of central Australia. *Sedimentology,* **17**. 1-40.

WILLIAMS, P. F. & RUST, B. R. 1969. The sedimentology of a braided river. *Journal of Sedimentary Petrology,* **39**. 649-679.

WILSON, J. C. & MCBRIDE, E. F. 1988. Compaction and porosity evolution of Pliocene sandstones, Ventura Basin, California. *American Association of Petroleum Geologists Bulletin,* **72**. 664-661.

WINSTON, R. B. 1990. Implications of palaeobotany of Pennsylvanian age coal of the central Appalachian Basin for climate and coal bed development. *Geological Society of America Bulletin*, **102**. 1720-1726.

WIZEVICH, M. C. 1991. *Sedimentology and Regional Implications Of Fluvial Quartzose Sandstone Of The Lee Formation, Central Appalachian Basin.* PhD thesis (unpublished) Virginia Polytechnic and State Institute, USA.

WIZEVICH, M. C. 1992. Sedimentology of Pennsylvanian quartzose sandstones of the Lee Formation, Central Appalachian Basin: fluvial interpretation based on lateral profile analysis. *Sedimentary Geology*, **78**. 1-47.

WIZEVICH, M. C. 1993. Depositional control in a bedload-dominated fluvial system:internal architecture of the Lee Formation, Kentucky. *Sedimentary Geology*, **85**. 537-556.

WOODLAND, B. G. & STENSTROM, R. C. 1979. The occurrence and origin of siderite concretions in the Francis Creek Shale (Pennsylvanian) of northeastern Illinois. *In* M. H. NITECKI (ed) *Mazon Creek Fossils*. 69-104.

XU, JIONGXIN. 1993. Meanders caused by hyperconcentrated water flow: an example from the loess plataeu, China. *Earth Surface Processes and Landforms*, **18**. 687-702.

# Appendix I:
# Glossary Of Symbols.

## I.1. Symbols Used Within The Text.

| | |
|---|---|
| Q | Discharge ($m^3$/sec) |

Qm — Mean annual discharge ($m^3$/sec)

Qma — Mean annual flood discharge ($m^3$/sec)

Qmax — maximum recorded discharge ($m^3$/sec)

D — Particle size (m)

$D_{50}$ — Median particle size (m)

D — Mean particle size (m)

P — Sinuosity

S — Valley slope or gradient (m/m), $\lambda$ represents dip (tan S)

$\theta$ — Angular range of palaeocurrent measurements

F — Width/depth ratio

d — mean channel depth (m)

db — Bankfull channel depth (m)

W — Channel width (m)

Ad — Area of drainage($km^2$)

v — average velocity (m/sec)

U — Mean flow velocity averaged across channel cross-sectional area (m/sec)

h — Mean dune height (m)

$X_o$ — original dune thickness (m)

$Y_c$ — compacted dune thickness (m)

$\phi$ — Porosity (%)

$\phi_o$ — Depositional porosity (0.40)

$\phi_c$ — Porosity of compacted sediment (estimated through point counting)

$\rho_l$ — Liquid density

$\rho_s$ — Sediment density

$\mu_l$ — liquid viscosity

$\gamma'$ — Submerged weight per unit volume of sediment

k — Permeability (mD or D)

$\tau$ — Shear stress

$\tau_o$ — Boundary shear stress

$\tau_c$ — Critical shear stress

## I.2. Sedimentary Logging Symbols.

### Lithology.

Conglomerate

Breccia
o o   Intra-formational clasts
●●●   Extra-formational clasts

Sandstone

Mudstone

Limestone

Coal

### Interbedded Lithologies.

Relative proportions shown
by subdivision of blocks.

50% mudstone & sandstone

### Sedimentary Structures

Massive

Graded bedding

Slump/contorted bedding

Load casts

Water escape structures

Trough cross-stratification

Planar cross-stratification

Ripple lamination

Rhythmically bedded

Diffuse cross-stratification

Low angle cross-stratification

Compound cross-stratification

### Fossils

| | |
|---|---|
| Brachiopoda | |
| Plant remains | |
| Ostrocods | |
| Bioturbation | |
| Shell debris | |
| Rooting | |

# Appendix II:
# Sediment And Fluid Transport Processes.

The subject of sediment and fluid transport processes has been reviewed by a several workers, most noteably Middleton & Southard (1978) and Allen (1982, 1994). A general review of these processes relevant to this study are outlined here.

Fluids may be defined by viscosity, designated by $m$, and measured in Newton seconds per square metre ($Ns/m^2$). The dynamic or molecular viscosity is constant at constant temperature. Fluids follow Newton's Law of viscosity which is defined by a simple experiment where a thin film of fluid is held between two plates, one of which is free to move steadily under the action of a tangential force. In Newtonian fluids the relationship between shear stress and shear rate is linear.

$$\tau = \mu_i. \, dU/dy \qquad (1)$$

where $\tau$ is the shear stress (measured in $N/m^2$), U the fluid velocity (measured in m/s) and y the distance from a stationary plate (measured in m).

The ratio of dynamic viscosity to density ($\mu/\rho$) is termed the kinematic viscosity or $\upsilon$ and varies with temperature in a similar fashion to dynamic viscosity (Allen 1994).

$$\tau = (\mu/\rho). \, d \, (\rho U)/dy \qquad (2)$$

where $d \, (\rho U)/dy$ is the momentum gradient and ($\mu/\rho$) is equivalent to $\upsilon$.

When water becomes mixed with a substantial concentration of sediment, viscosity increases and the relationship between shear stress and shear rate is no longer linear. Such substances are described as non-Newtonian. One important sub-class of non-Newtonian fluids is the Bingham plastic, which behaves as an elastic solid up to a characteristic yield strength, but at greater shear stresses is a Newtonian fluid with a constant apparent viscosity. Many sediment-water mixtures approximate to Bingham plastics (Allen 1994).

Fluid flow generally involves a solid boundary, typically of loose, potentially mobile sediment. Where flow is partially bounded by a solid boundary it is termed open channel flow (Middleton & Southard 1978). The rate of fluid flow is defined by discharge Q ($m^3/sec$ or cumecs), and velocity U (m/sec). A steady flow does not

change with time whereas a uniform flow is the same at all cross-sections down the flow (Middleton & Southard 1978). However, natural currents vary in space and time.

Steady and uniform flow of a liquid down an inclined plane is a simplified model of natural flow in open channels with a large ratio of width to depth. By using equation (1) Middleton & Southard (1978) illustrate the variation in velocity and shear strength with depth in such a flow. A layer of liquid with depth d flows down an infinitely wide plane with a slope angle $\lambda$ such that

$$\tau_o = \gamma' \, d \tag{3}$$

Where $\tau_o$ is the shear stress acting at the bottom boundary and $\gamma' = \rho \, g \sin \lambda$, the downslope component of the weight of the fluid (Middleton & Southard 1978). Away from the boundary:

$$\tau = \gamma' \, (d-y) \tag{4}$$

For given values of $\gamma'$ $\mu_i$ and d the velocity U, varies parabolically from zero at the boundary to a maximum at the surface, thus defining laminar flow (Middleton & Southard 1978). This condition holds for a certain range of conditions involving shallow depths, low velocities and high viscosities. However, flow becomes turbulent with an increase in depth or velocity or a decrease in viscosity.

Flow transformation is defined by Fisher (1983) as changes in flow behaviour between laminar and turbulent stages. For Newtonian fluids the criteria for turbulence is given by the dimensionless Reynolds number Re, expressed as

$$Re = \rho \, U \, L \, / \, \mu_i = UL \, / \, \upsilon \tag{5}$$

where L is a characteristic length (Allen 1994). In open channel flow turbulence begins at Re >500, with completely turbulent flow at Re >2000 (Middleton & Southard 1978; Allen 1994). The laminar to turbulent transformation is influenced by particle concentration, i.e. viscosity, and the flow velocity U (Fisher 1983). In the past turbulent flow has been thought of as essentially chaotic. However, more recently it has been recognised that turbulent flow is partially deterministic, involving coherent flow structures (Allen 1994).

In open channel flow of given discharge, with a water depth d, the total energy of the system may exist in two states, each of which is specified by a particular value of the dimensionless Froude number defined by:

$$F = U / \sqrt{(g. \, d)} \tag{6}$$

Where F <1 flow is described as sub-critical, and F >1 flow is described as super-critical (Blatt *et al* 1980). Thus in open channel flow there are four possible states of flow defined by the dimensionless Froude and Reynolds numbers. The transition form lower to upper flow regime conditions occurs at values of F~0.75.

Sediment movement occurs when the lift force produced by the fluid exceeds the downward force of the particle. Thus sediment lying on the bed of a stream will not begin to move unless the stream achieves a certain intensity of flow. Alternatively there will be a maximum size of sediment that a flow can move which defines the competence of the flow (Blatt *et al* 1980). Grain, fluid and flow properties combine to determine the entrainment threshold, and the modes and rate of sediment transport. Forces acting on a particle include the fluid drag, fluid lift, and the particles immersed weight, and interparticle cohesion. These forces vary in their importance(Allen 1994). The threshold of entrainment is difficult to defined due to the various methods of sediment transport.

Grains entrained from a bed travel in various ways within a current depending on size, shape, excess density and the viscosity and speed of the transporting fluid (Allen 1994). Four modes of transport are recognised. Sliding, rolling and saltation are defined as bedload or bed contact load, with the sediment carried fully in suspension defined as suspended load. There are no sharp divisions between these types of transport (Allen 1994).

*There are only 3 mentio~ here*

Once sediment starts to move on a bed a complex natural feedback system evolves. As transport begins the flow moulds the cohesionless bed into bedforms which migrate and change in form in response to changes in flow. In turn the rate of bed material movement depends on the nature of bedforms (Blatt *et al* 1980).

The boundary layer is the zone of the flow immediately adjacent to the solid surface and it defines the area in which the fluid is affected by the frictional resistance exerted by the boundary. Boundary layers may be defined as either hyraulically smooth with a viscous sub-layer or hydraulically rough where the boundary particles protrude into the turbulent portion of the flow (Allen 1994).

Jackson (1976) established the relationship between the boundary layer structure, sediment transport and bedforms in rivers. The near bed fluid in a laminar or turbulent boundary layer has little momentum, and where it travels into a regime of adverse pressure gradient may become halted (Allen 1994). The faster fluid then breaks away or separates from the bed, isolating the lower momentum fluid within a closed region in which there is sluggish recirculation. This region is termed the

separation bubble and is separated from the faster external stream by a zone of rapid velocity change termed the free shear zone (Allen 1994). Such structures are termed burst-sweep cycles. Separation bubbles form downstream of sharp changes in attitude, such as dune slip faces. The pattern and dynamic properties of the turbulent separated flows associated with structures have a significant part to play in determining the shape and motion of mobile bed features. Burst-sweep cycles are largely responsible for sediment transport.

Secondary flows are also of sedimentary importance. The term secondary flow describes a mean channel flow or boundary layer with superimposed one or more streamwise corkscrew vorticies, which are counter-rotating if more than one is present (Allen 1994). Secondary flows occur in curved rivers and tidal channels (Allen 1994).

When a fluid is mixed with sediment to a high concentration that sediment/water mixture may act as a non-Newtonian fluid as described above. Moss (1972) has suggested that "as bedload motion becomes more intense in sand-sized particles, a stage is reached wherein collisions between particles become inevitable and thereafter the load proceeds as a dense mass of colliding particles, buoyed up b y dispersive pressure". Moss (1972) termed these layers 'rheological', and described them in terms of laminar flow. The existence of such zones of high sediment concentration close to the solid boundary have been established, but there is no indication that flow in this layer is not turbulent (Middleton & Southard 1978).

An *in situ* bed of silt or sand may be changed into a fluid-like state of high concentration by liquefaction or fluidisation (Allen 1994). Liquefaction occurs in a closed system, whereas fluidisation requires the input of an external body of fluid. Fluidisation is the term applied to the vertical movement of sediment upwards through a sediment bed. Each particle experiences an upward fluid drag which counteracts its downward weight. On slowly increasing fluid discharge, there will come a stage where these two forces balance, where the sediment will loose contact between grains and the bed fluidises. The fluidised state may only be maintained as long as the upward flow of fluid is maintained. A reduction or cessation of flow will cause settling of the bed.

The process of changing the state of a granular bed from solid-like to fluid-like by the application of stress is termed liquefaction (Allen 1982). The fluid-like state is short-lived, and is followed by resettling of grains. Liquefaction is of three types. *Static liquefaction* is induced by an increase in pore fluid pressure relating to ground water movements. *Impulsive liquefaction* is induced by a single large pulse, destroying loose, metastable packing. *Cyclic liquefaction* is induced by a gradual build-up of pore

pressure to a value equivalent to the overburden in response to a repeated stress whose magnitude is less than the shear strength of the sand (Owen 1987).

A sedimentary gravity flow is defined as a flow where the force of gravity acting on the sediment particles moves the fluid (Middleton & Southard 1978). Sediment gravity flows are classified according to their rheology and dominant particle-support mechanism during steady flow (Postma 1986). Sedimentary gravity flows occur in both sub-aerial and sub-aqueous environments and are generally rapid, short-lived events.

The rheology of a sediment gravity flow in its depositional phase is determined by three parameters: 1) flow character (turbulent or laminar), 2) concentration of flow; and 3) flow behaviour (either cohesionless or plastic/cohesive) (Postma 1986). These conditions describe eight types of gravity flow (Postma 1986) which are summarised in Table II.1.

| Flow Character During Deposition | Flow Type During Steady State. |
|---|---|
| Turbulent, low concentration, cohesionless | Turbidity current |
| Turbulent, low concentration, cohesive | Turbidity current |
| Turbulent, high concentration, cohesionless | Pyroclastic turbidity current |
| Turbulent, high concentration, cohesive | Cohesive turbulent flow |
| Laminar, low concentration, cohesionless | None existent |
| Laminar, low concentration, cohesive | None existent |
| Laminar, high concentration, cohesionless | Liquefied flow<br>Fluidised flow<br>Grain flow/traction carpet |
| Laminar, high concentration, cohesive | Cohesive debris flow |

Table II.1. A summary of gravity flow types as defined by Postma (1986).

Four types of sediment support mechanisms are recognised within gravity flows: turbulence, upward intergranular flow, grain dispersive pressure and matrix strength (Middleton & Southard 1978). More than one of these mechanisms may operate within the life of a flow.

Five parameters determine whether a sediment gravity flow is laminar or turbulent: 1) velocity; 2) density; 3) cohesive strength; 4) flow thickness; and 5) fluid viscosity (Postma 1986). For non-Newtonian fluids or Bingham plastics with yield

strength the criteria for turbulence, additional to the Re number, is given by the dimensionless Bingham number

$$B = \tau_c \, d \, / \, \mu_l \, U \qquad\qquad (7)$$

Middleton & Southard (1978) approximate the boundary between laminar and turbulent flow as

$$Re >= 1000 \, B \qquad\qquad (8)$$

and hence

$$\tau_c \, / \, \rho \, U^2 < 0.001 \qquad\qquad (9)$$

# Appendix III:
# Textural & Compositional Data.

## III. 1. Grain Size Analysis.

Texture is a fundamental property of sediments. Grain size normally reflects the energy level of a sedimentary system, with grain sorting related to the type and duration of current action (Johnson 1994). Thus an understanding of textural characteristics gives information on the sedimentary processes responsible for the deposition of a sediment body.

The grain size of the sediments studied within this volume varies from conglomerate to mudstone. The Wentworth scheme for grain size was applied in the field, but for detailed analysis of sediments a more sophisticated approach was required.

Direct measurement of pebbles and larger sized clasts was achieved in the field using callipers to measure representative grain axes. In this syudy the measured value of the intermediate axis has been used to quantify the mean diameter of coarse particles. For grains of sands size and smaller another method of size determination was necessary.

The easiest method of measuring true grain size is by the use of sieving and sedimentation methods, with results displayed as weight percent (Blatt *et al* 1980; McManus 1989). However, as the sediments studied were lithified, measurement of grain size had to be made directly from thin sections. There are certain disadvantages to this method of grain size determination as a thin section cut across a population of randomly oriented spheres known to be uniform in size, will not yield a uniform size distribution. Only the maximum size observed will correspond to the true size of the parent population (Blatt *et al* 1980). In practice the shape of sedimentary particles is irregular and unknown and hence the original size distribution must be inferred from the observed section-size distribution. There is no unique solution to the problem of inferring the parent (three-dimensional) size distribution from the observed (two-dimensional) distribution, and the problem is therefore theoretically unsolvable (Blatt *et al* 1980).

It is necessary, however, to be able to estimate the grain size population from thin sections. The probability that a grain will be cut by a random section is proportional to the size of the grain, and hence the size distributions observed in thin sections are weighted by the size of grains (Blatt *et al* 1980). The selection of grains

on a traverse adds another weighting by size, so that the frequencies obtained are weighted by cross-sectional area. If grains are selected at grid points then the frequencies will be weighted by volume, similar to distributions obtained in sieve and sedimentation.

A standardised technique for the measurement of grain size through thin section work is not established, and hence one had to be developed for this study. Two options exist for the development of grain size statistics:

a) Adopt a standardised method of size measurement in thin section. Such measurements may then be compared with other measurements made using the same technique but not with size determined by sieving.

b) Correct from thin section to sieve sizes by using empirical correction factors developed by measuring a set of "average" sands by both methods (Friedman 1958, 1962; Adams 1977; Harrell & Eriksson 1979).

A preferred grain orientation exists in most sediments, with the long and intermediate axis of the grain lying parallel to the depositional surface. Therefore, thin sections for use within this study were cut parallel to the depositional surface (bedding or cross-bedding). Traverses across the thin section were made using a mechanical stage, with 300 detrital quartz grains measured from each section. Quartz grains were counted, as they are the most volumetrically important in all samples. The length of the shortest axis encountered at the grid intersections (i.e. the intermediate axis of the grain) was recorded. The results were then grouped into 1/2 phi intervals.

Errors introduced into grain size measurement in this manner are unquantifiable. Error exists due to sampling techniques, the cutting of thin sections within a sample and the error introduced by measurement of the grain size. The process of converting raw data to sieve data using equations such as those of Friedman (1958) and Harrell & Eriksson (1979) introduces a greater error into the grain size analysis. It was therefore decided to use only raw data in this study.

From the raw frequency data the parameters of sorting (standard deviation), mean and median grain size of the sediments were assessed (Table III.1). In Chapters 3 to 7 the sediment sorting characteristics, mean and median grain size of samples have been used to aid the description of sedimentary facies present within formations. The parameters of skewness and kurtosis have not been included within this study as the errors introduced in data collection make the results of such statistical analysis highly questionable.

| SAMPLE | FACIES | MEAN (PHI) | MEDIAN (PHI) | SORTING | COMPACTION INDEX |
|---|---|---|---|---|---|
| *FELL SANDSTONE GP* | | | | | |
| BD2 | Sms | 3.02 | 2.94 | 0.6 | 3.64 |
| BD3 | Sms | 3.08 | 2.94 | 0.63 | 3.26 |
| BD4 | St | 2.98 | 2.94 | 0.53 | 2.9 |
| BD5 | Sc | 3.11 | 2.94 | 0.52 | 3.44 |
| BD6 | Smc | 3.18 | 3.06 | 0.57 | 2.58 |
| BD7A | Spt | 3.07 | 2.94 | 0.58 | 3.06 |
| BD7B | Spt | 3.17 | 3.18 | 0.57 | 3.16 |
| BD8 | Sms | 3.18 | 3.18 | 0.65 | 3.12 |
| BD9 | St | 2.94 | 2.94 | 0.49 | 2.88 |
| BDX10 | Smc | 2.94 | 2.94 | 0.51 | 2.96 |
| BD11 | St | 2.89 | 2.94 | 0.46 | |
| CH1 | Sc | 2.78 | 2.73 | 0.64 | 2.98 |
| CH2 | St | 3.02 | 3.06 | 0.81 | 2.7 |
| CH3 | Sms | 2.92 | 2.94 | 0.49 | 2.36 |
| CH4 | Spa | 3.18 | 3.32 | 0.56 | 3.06 |
| CH5 | Smc | 2.98 | 2.94 | 0.46 | 2.82 |
| CH6 | Spt | 2.47 | 2.32 | 0.6 | 3.02 |
| CH7 | Sc | 2.44 | 2.47 | 0.49 | 3.06 |
| *LEE TYPE SANDS* | | | | | |
| *ROCKCASTLE MB.* | | | | | |
| KYB1 | Sm | 2.04 | 2.32 | 0.96 | 3.14 |
| KYB2 | Spa | 2.29 | 2.32 | 0.86 | 3.26 |
| KYNB1 | Sg | 2.03 | 2.12 | 0.77 | 1.98 |
| KYNC1 | Sm | 3.27 | 3.18 | 0.56 | |
| KYNC2 | Sm | 3 | 2.94 | 0.43 | |
| KYNC3 | Scg | 2.9 | 2.94 | 0.46 | |
| *NAESE SST. MB.* | | | | | |
| TNA1 | Sms | 2.68 | 2.55 | 0.71 | 4.68 |
| TNA2 | Sms | 3.02 | 2.94 | 0.55 | 5.14 |
| TNB1 | Spt | 3.24 | 3.32 | 0.7 | 5.3 |
| TNB2 | Smc | 2.98 | 3.06 | 0.82 | 4.7 |
| TNB3 | Smc | 3.05 | 3.06 | 0.7 | 4.78 |
| TNB4 | Smc | 2.69 | 2.73 | 0.62 | 4.62 |
| TNC1 | Smc | 3.44 | 3.32 | 0.53 | 4.72 |
| *PINE CREEK SST. MB.* | | | | | |
| KYA1 | Fx | 3.57 | 3.32 | 0.43 | |
| KYA2 | Smc | 3.48 | 3.32 | 0.61 | 4.5 |
| KYA3 | Smc | 3.49 | 3.32 | 0.64 | 4.52 |
| KYC1 | Spt | 2.89 | 2.84 | 0.39 | 3.68 |
| KYC2 | Smc | 2.88 | 2.94 | 0.42 | 3.76 |
| KYC3 | Smc | 2.93 | 2.94 | 0.48 | 3.68 |
| KYC4 | Smc | 3.14 | 3.18 | 0.52 | 3.66 |
| KYC5 | Spt | 3.05 | 2.94 | 0.6 | 3.62 |
| *CORBIN SST. FM.* | | | | | |
| KYE2 | Spt | 3.23 | 3.32 | 0.54 | 4.76 |
| KYE3 | Spt | 3.34 | 3.32 | 0.56 | 4.7 |
| KYEX4 | Smc | 3.03 | 3.06 | 0.62 | 4.26 |
| KYE5 | Smc | 3.23 | 3.32 | 0.58 | 4.62 |
| KYE6 | Sc | 3.23 | 3.06 | 0.57 | 4.64 |
| KYE7 | Smc | 2.86 | 3.06 | 0.54 | 4.44 |
| KYH2 | St | 2.57 | 2.56 | 0.67 | 3.06 |
| KYH4 | Sm | 2.56 | 2.56 | 0.72 | 2.96 |
| KYH5 | Sm | 2.72 | 2.73 | 0.68 | 3.16 |
| KYH6 | Fx | 3.4 | 3.32 | 0.52 | |
| *MANSFIELD FM.* | | | | | |
| INA1 | Spt | 3.31 | 3.18 | 0.86 | 2.68 |
| INA2 | Smc | 3.33 | 3.18 | 0.74 | 1.84 |
| INA3 | Smc | 3.43 | 3.18 | 0.73 | 2.78 |
| INA4 | Spt | 3.6 | 3.64 | 0.62 | 2.96 |
| INA5 | Smc | 2.66 | 2.56 | 0.7 | 2.86 |
| INA6 | Spt | 3.24 | 3.18 | 0.72 | 3.14 |
| INA7 | Spt | 3.05 | 3.06 | 0.75 | 3.34 |
| INA8 | Smc | 3.09 | 2.94 | 0.68 | 2.02 |
| INA9 | Spt | 3.19 | 3.18 | 0.56 | 3.32 |
| INB2 | Spt | 3.17 | 2.94 | 0.53 | 3.48 |
| *HAWKESBURY SST.* | | | | | |
| NSWA1 | Sme | 2.32 | 2.32 | 0.73 | 3.88 |
| NSWA2 | Sme | 2.39 | 2.32 | 0.78 | 4.44 |
| NSWA3 | St | 1.73 | 1.55 | 0.76 | 3.24 |
| NSWA4 | Sme | 2.16 | 2 | 0.69 | 4.24 |
| NSWA5 | Sd | 3.36 | 3.32 | 0.63 | 3.28 |
| NSWA6 | St | 1.83 | 2 | 0.56 | 3.58 |
| NSWA7 | Sd | 2.57 | 2.32 | 0.66 | 3.26 |
| NSWB1 | Sd | 1.9 | 1.88 | 0.55 | 3.06 |
| NSWB2 | Sme | 2.41 | 2.32 | 0.72 | 2.64 |
| NSWB3 | Sme | 2.58 | 2.73 | 0.72 | 3.16 |
| NSWB4 | Sme | 2.67 | 2.73 | 0.57 | 3.1 |
| NSWB5 | St | 2.64 | 2.55 | 0.63 | 3.28 |
| NSWB6 | Sme | 2.49 | 2.55 | 0.5 | 3 |

*Table III.1. A summary of the textural parameters measured from sandstone samples.*

Many sediments are composed of a combination of grain size sub-populations, rather than a single population. In log normal plots it is considered possible to sub-divide the cumulative frequency curve into a series of segments which correspond to a set of depositional conditions (McManus 1989). Visher (1969) proposed that each cumulative frequency curve comprised a number of straight-line segments of different slope, separated by sharp breaks. The straight line segments were interpreted as truncated log-Gaussian sub-populations associated with bedload, saltation and suspension deposition. Visher (1969) interpreted sediments with a well developed suspension population and an absence of traction population as being deposited in a fluvial environment.

Middleton & Southard (1978) assumed that grain size distributions comprised two or more overlapping log-Gaussian sub-populations. Each of these sub-populations was interpreted as the deposit of a distinct mode of transport: traction, intermittent suspension and suspension. Fluvial sands were interpreted as those composed predominantly of an intermittent suspension population.

It seems unlikely that a universal technique of abstracting depositional environment from grain size and grain size distribution data exists. In nature the interpretation of textural gradients or populations in terms of hydraulic sorting is complicated by two important factors: the inheritance of textural characteristics produced by the provenance of sediment, and the wide range of variability in both the type and intensity of hydraulic mechanisms operating on the sediment (Middleton & Southard 1978).

The grain size distribution curves obtained from this study have not been used to aid environmental analysis. The interpretation of a fluvial depositional environment has been made largely on the basis of preserved sedimentary structures. The grain size distribution curves have been produced for their use as a descriptive tool. Using the curves illustrated in Figures III.1 to III.8 it is possible to compare the grain size distribution between structured and massive sediments within the same formation. The graphs may also be used to assess the change in grain size distribution through a formation, such as between the basal and upper Corbin Formation (Figures III.5 & III.6).
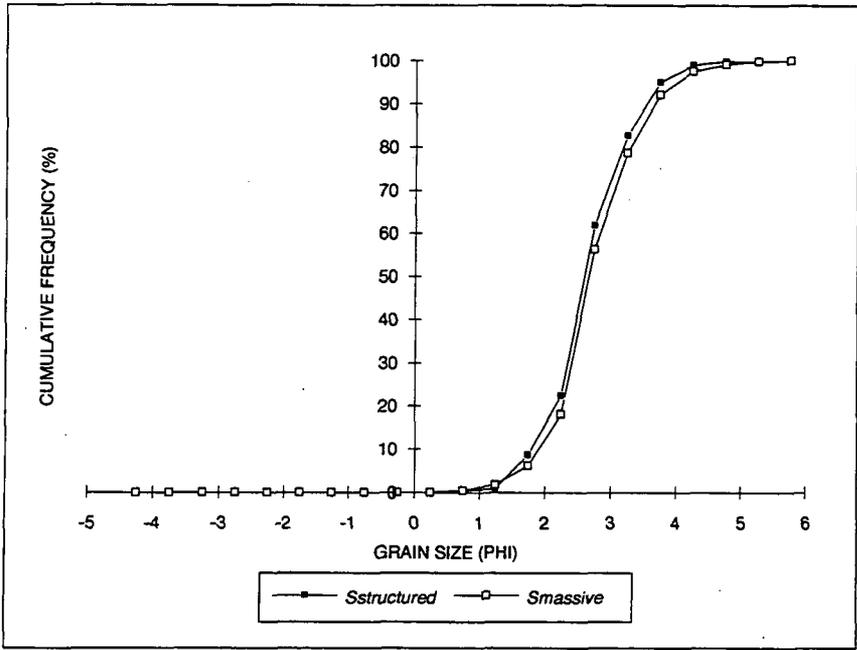
*Figure III.1. Grain size distribution of the Fell Sandstone Group, Northumberland Basin, UK.*
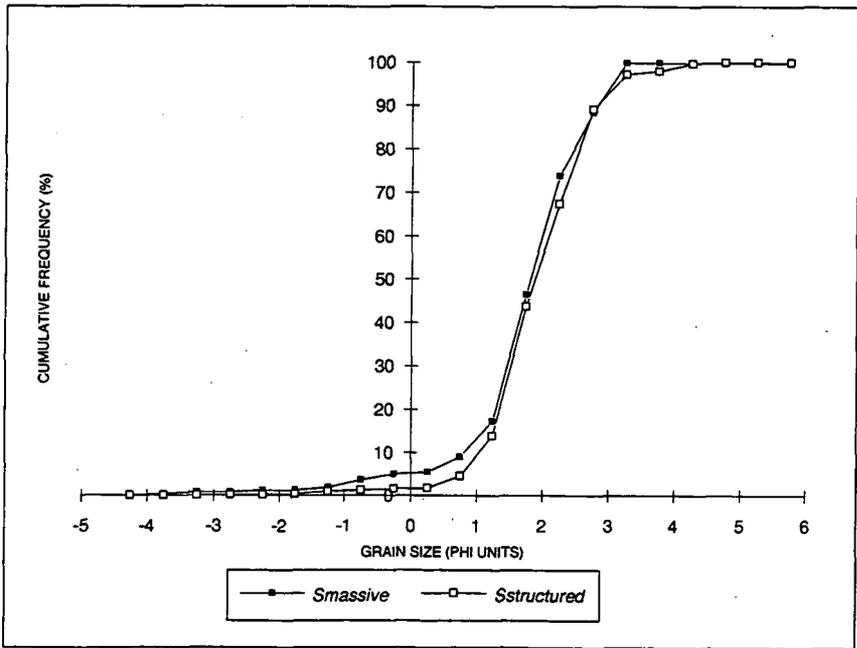


*Figure III.2. Grain size distribution of the Rockcastle Sandstone member of the central Appalachian Basin, USA.*
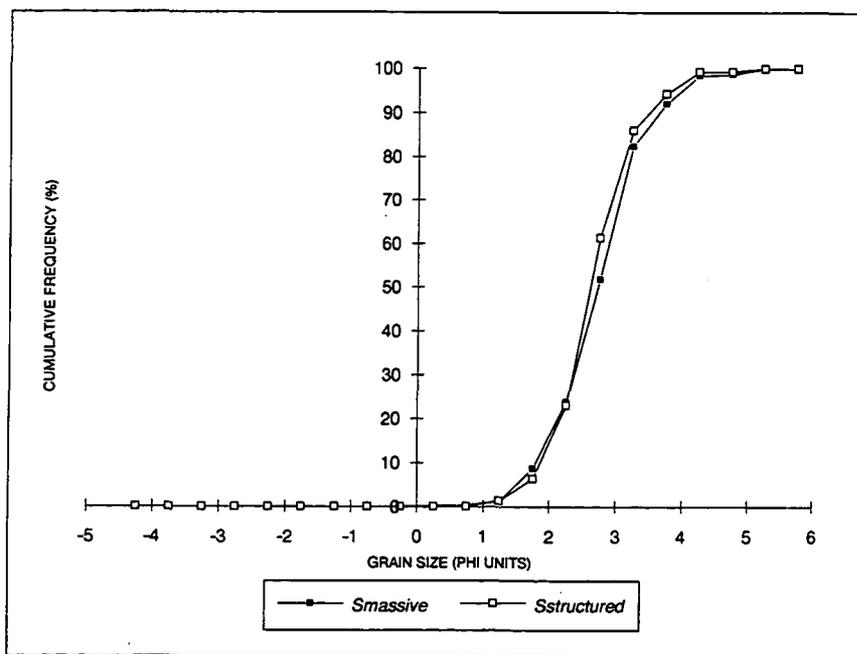
*Figure III.3. Grain size distribution of the Naese Sandstone member of the central Appalachian Basin, USA.*
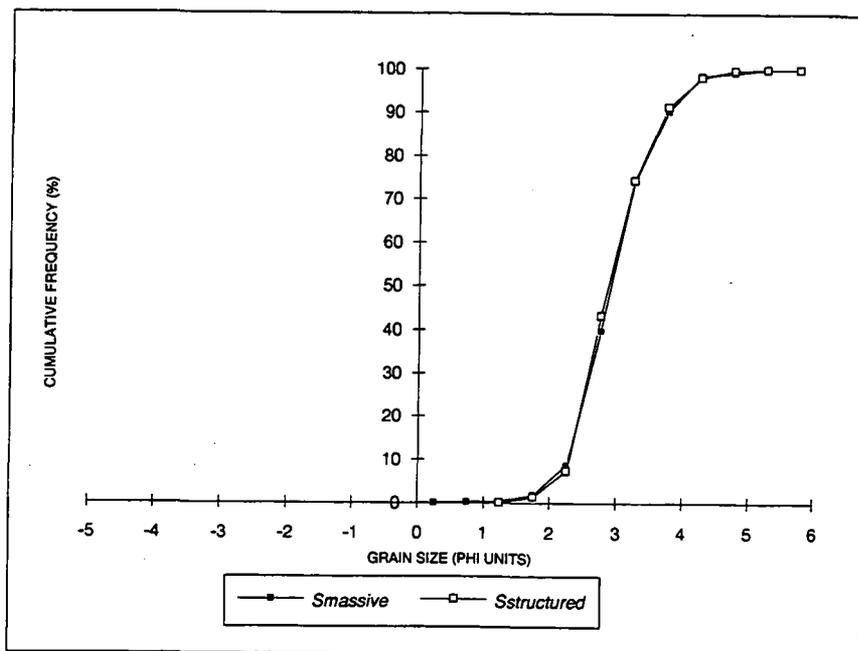


*Figure III.4. Grain size distribution of the Pine Creek Sandstone member of the central Appalachian Basin, USA.*

A14

BASAL CORBIN SANDSTONE FORMATION, CENTRAL APPALACHIAN BASIN, USA.



UPPERMOST CORBIN SANDSTONE FORMATION, CENTRAL APPALACHIAN BASIN, USA.
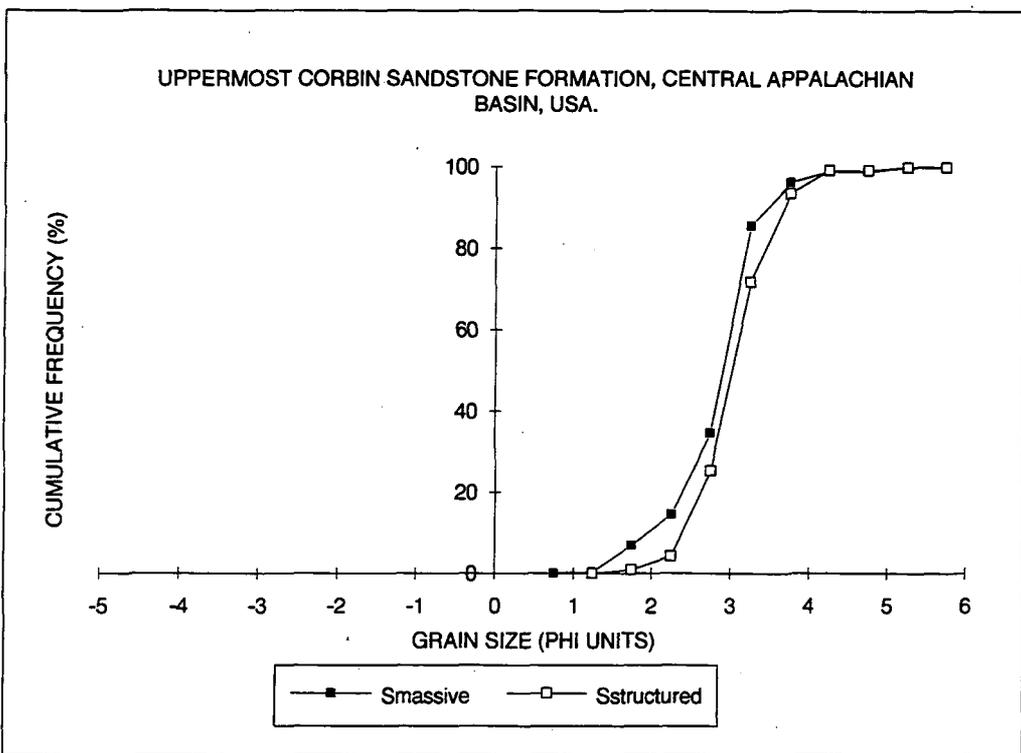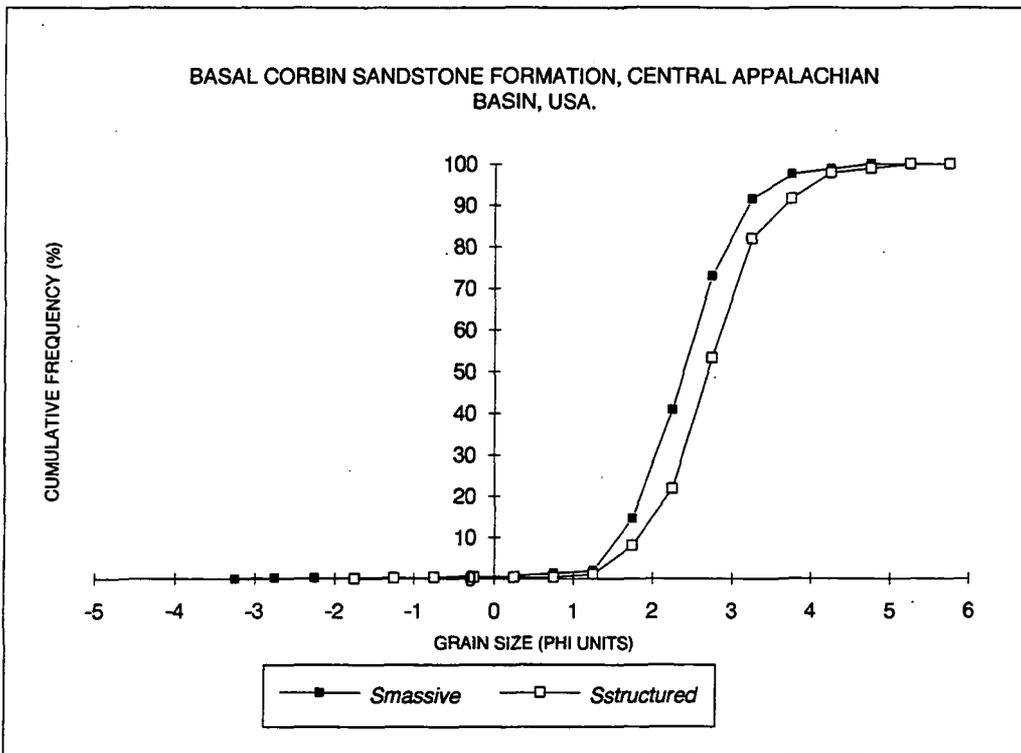
*Figure III.5 & III.6. Grain size distribution of the Corbin Sandstone formation of the central Appalachian Basin, USA.*
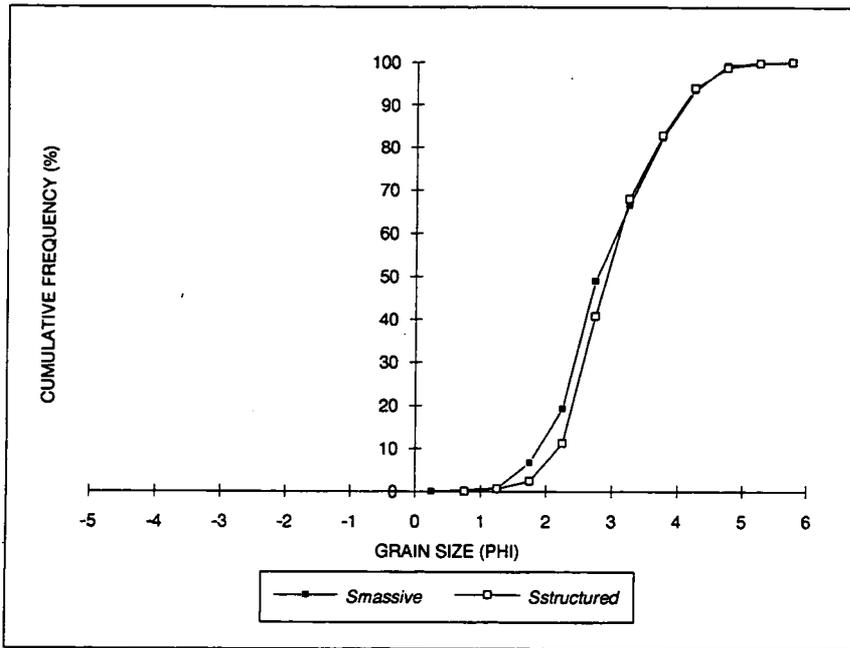
*Figure III.7 Grain size distribution of the Mansfield Formation of the Illinois Basin, USA.*
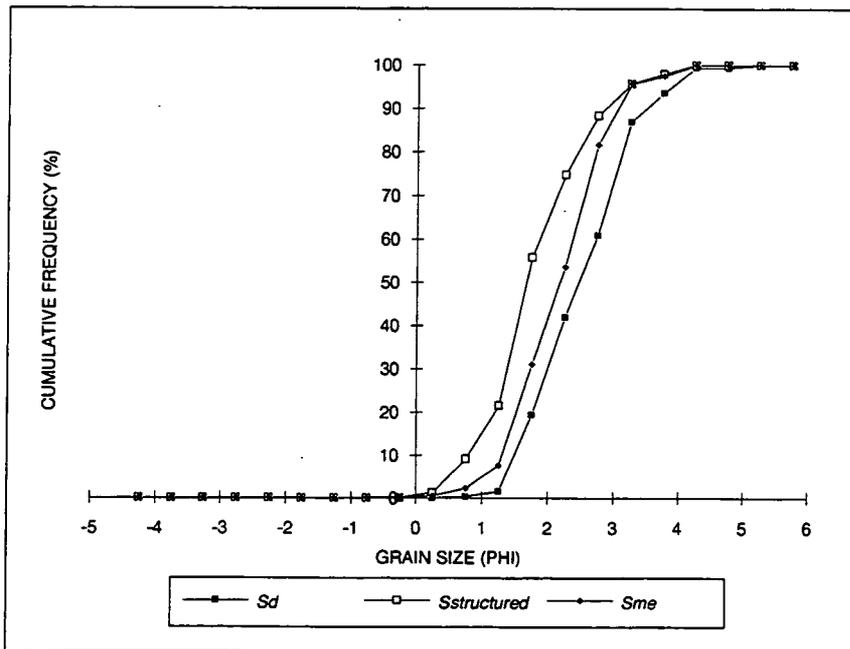


*Figure III.8. Grain size distribution of the Hawkesbury Sandstone of the Sydney Basin, Australia.*

## III. 2. Grain Packing Analysis.

The packing of a sedimentary rock is dependant on the compaction of that sediment resulting from burial. Within closely spaced outcrops of the same unit, it may be assumed that the sediments have undergone similar amounts of burial. Thus any differences in packing between facies may be interpreted as the result of primary depositional fabrics.

Compaction has been addressed by a number of workers. Taylor (1950) described grain contacts as floating (no contacts), tangential (or point), long, concavo-convex (embayed) and sutured. The presence of floating and tangential contacts were interpreted to indicate primary packing of the sediment, with long contacts due to either primary packing characteristics or pressure solution and precipitation of cement. Concavo-convex contacts were interpreted in terms of pressure solution. The Compaction Index (CI) was developed by Taylor (1950) and describes the average number of contacts per grain within a sediment.

Kahn (1956) developed the packing density parameter, which defines the intercept size of grains along a traverse as the percentage of the total length of the traverse. This measurement is essentially a way of expressing grain volume. The Tight Packing Index (TPI) was developed by Wilson & McBride (1988), and details the average number of long, sutured or embayed contacts per grain.

For the purposes of this study the compaction index (CI) was established. The number of grain contacts of 100 randomly selected grains were measured. The CI is dependant on sorting, and to a lesser extent grain size (Wilson & McBride 1988) and hence only sandstones of moderately well sorted or better were used for this study. The results of the CI study are listed in Table III.1, and are discussed in detail within Chapters 3-7.

## III. 3. Composition.

Sandstone composition has been established through the point counting of resin impregnated sections, cut parallel to depositional fabric. Framework grains, matrix and cement were all assessed. Porosity was established through point counting, and this is described as either primary or secondary. The results of the compositional analysis are detailed below (Tables III.2-III.7). Ternary diagrams were produced from these results which are detailed in Chapters 3-6.

| | BD2 | BD3 | BD4 | BD5 | BD6 | BD7A | BD7B | BD8 | BD9 | BDX1O | BD11 | CH1 | CH2 | CH3 | CH5 | CH6 | CH7 |
|---|---|---|---|---|---|---|---|---|---|---|---|---|---|---|---|---|---|
| MONO QTZ | 133 | 144 | 143 | 165 | 159 | 132 | 155 | 144 | 135 | 168 | 154 | 148 | 180 | 143 | 159 | 150 | 162 |
| POLY QTZ | 29 | 24 | 40 | 23 | 19 | 34 | 33 | 25 | 23 | 15 | 15 | 22 | 17 | 19 | 20 | 28 | 21 |
| CHERT | 0 | 0 | 1 | 0 | 0 | 1 | 2 | 1 | 1 | 1 | 1 | 3 | 0 | 4 | 2 | 1 | 1 |
| 1 POROSITY | 62 | 56 | 38 | 35 | 39 | 38 | 34 | 43 | 43 | 45 | 49 | 56 | 43 | 63 | 55 | 53 | 55 |
| 2 POROSITY | 1 | 5 | 3 | 5 | 2 | 18 | 4 | 4 | 8 | 8 | 6 | 2 | 2 | 1 | 3 | 5 | 1 |
| ACCESSORY | 0 | 0 | 0 | 0 | 0 | 1 | 0 | 0 | 1 | 0 | 0 | 0 | 1 | 0 | 0 | 0 | 0 |
| CLAYS | 13 | 9 | 6 | 7 | 4 | 19 | 6 | 6 | 8 | 27 | 1 | 11 | 11 | 6 | 11 | 14 | 4 |
| AUTH. QTZ | 52 | 41 | 51 | 57 | 68 | 39 | 45 | 55 | 59 | 19 | 50 | 39 | 32 | 49 | 42 | 26 | 41 |
| SYN-SED. LITHIC | 0 | 0 | 0 | 0 | 0 | 0 | 0 | 0 | 0 | 0 | 0 | 0 | 0 | 0 | 0 | 0 | 0 |
| SED. LITHICS | 1 | 3 | 4 | 3 | 4 | 4 | 4 | 3 | 4 | 3 | 7 | 2 | 2 | 3 | 1 | 2 | 3 |
| VOLC. LITHICS | 0 | 6 | 2 | 2 | 1 | 4 | 5 | 6 | 3 | 1 | 2 | 2 | 1 | 0 | 0 | 1 | 1 |
| FELDSPAR | 7 | 5 | 10 | 3 | 3 | 10 | 8 | 11 | 10 | 10 | 9 | 15 | 6 | 10 | 5 | 19 | 8 |
| K FELDSPAR | 4 | 3 | 5 | 1 | 2 | 7 | 6 | 8 | 6 | 5 | 6 | 9 | 4 | 6 | 3 | 11 | 6 |
| PLAGIOCLASE | 3 | 2 | 5 | 2 | 1 | 3 | 2 | 3 | 4 | 5 | 3 | 6 | 2 | 4 | 2 | 8 | 2 |
| OPAQUES | 2 | 4 | 1 | 0 | 0 | 0 | 3 | 2 | 1 | 1 | 6 | 0 | 4 | 1 | 0 | 0 | 3 |
| MICA | 0 | 3 | 1 | 0 | 1 | 0 | 1 | 0 | 4 | 2 | 0 | 0 | 0 | 1 | 2 | 1 | 0 |
| IRON OXIDE | 0 | 0 | 0 | 0 | 0 | 0 | 0 | 0 | 0 | 0 | 0 | 0 | 1 | 0 | 0 | 0 | 0 |
| DOLOMITE | 0 | 0 | 0 | 0 | 0 | 0 | 0 | 0 | 0 | 0 | 0 | 0 | 0 | 0 | 0 | 0 | 0 |
| CALCITE | 0 | 0 | 0 | 0 | 0 | 0 | 0 | 0 | 0 | 0 | 0 | 0 | 0 | 0 | 0 | 0 | 0 |
| ORGANICS | 0 | 0 | 0 | 0 | 0 | 0 | 0 | 0 | 0 | 0 | 0 | 0 | 0 | 0 | 0 | 0 | 0 |
| TOTAL | 300 | 300 | 300 | 300 | 300 | 300 | 300 | 300 | 300 | 300 | 300 | 300 | 300 | 300 | 300 | 300 | 300 |

*Table III.2. Fell Sandstone Group, Northumberland Basin.*

| | KYB1 | KYB2 | KYNB1 | KYNC1 | KYNC2 | KYNC3 | TNA1 | TNA2 | TNB1 | TNB2 | TNB3 | TNB4 | TNC1 |
|---|---|---|---|---|---|---|---|---|---|---|---|---|---|
| MONO QTZ | 153 | 161 | 150 | 121 | 138 | 145 | 150 | 177 | 180 | 170 | 178 | 171 | 134 |
| POLY QTZ | 50 | 44 | 52 | 54 | 38 | 41 | 33 | 42 | 25 | 22 | 29 | 30 | 47 |
| CHERT | 2 | 0 | 1 | 0 | 0 | 2 | 1 | 1 | 2 | 2 | 1 | 1 | 0 |
| 1 POROSITY | 37 | 27 | 41 | 18 | 25 | 15 | 44 | 14 | 17 | 26 | 20 | 33 | 25 |
| 2 POROSITY | 0 | 0 | 0 | 0 | 2 | 2 | 1 | 1 | 1 | 0 | 0 | 0 | 0 |
| ACCESSORY | 0 | 0 | 0 | 0 | 0 | 0 | 0 | 1 | 0 | 0 | 0 | 0 | 0 |
| CLAYS | 5 | 20 | 10 | 37 | 22 | 21 | 16 | 15 | 20 | 23 | 15 | 13 | 26 |
| AUTH. QTZ | 34 | 26 | 38 | 46 | 50 | 41 | 44 | 32 | 37 | 41 | 39 | 37 | 38 |
| SYN-SED. LITHIC | 0 | 0 | 0 | 0 | 2 | 0 | 0 | 0 | 0 | 0 | 0 | 0 | 0 |
| SED. LITHICS | 4 | 3 | 2 | 4 | 2 | 4 | 1 | 2 | 0 | 3 | 1 | 0 | 10 |
| VOLC. LITHICS | 5 | 6 | 2 | 5 | 10 | 13 | 7 | 10 | 4 | 6 | 11 | 7 | 12 |
| FELDSPAR | 8 | 10 | 3 | 3 | 3 | 9 | 2 | 3 | 3 | 4 | 3 | 4 | 3 |
| K FELDSPAR | 6 | 8 | 2 | 2 | 2 | 6 | 1 | 2 | 2 | 2 | 2 | 3 | 2 |
| PLAGIOCLASE | 2 | 2 | 1 | 1 | 1 | 3 | 1 | 1 | 1 | 2 | 1 | 1 | 1 |
| OPAQUES | 1 | 2 | 1 | 10 | 7 | 5 | 1 | 0 | 0 | 3 | 1 | 2 | 3 |
| MICA | 1 | 1 | 0 | 2 | 1 | 2 | 0 | 2 | 2 | 0 | 2 | 2 | 2 |
| IRON OXIDE | 0 | 0 | 0 | 0 | 0 | 0 | 0 | 0 | 0 | 0 | 0 | 0 | 0 |
| DOLOMITE | 0 | 0 | 0 | 0 | 0 | 0 | 0 | 0 | 9 | 0 | 0 | 0 | 0 |
| CALCITE | 0 | 0 | 0 | 0 | 0 | 0 | 0 | 0 | 0 | 0 | 0 | 0 | 0 |
| ORGANICS | 0 | 0 | 0 | 0 | 0 | 0 | 0 | 0 | 0 | 0 | 0 | 0 | 0 |
| TOTAL | 300 | 300 | 300 | 300 | 300 | 300 | 300 | 300 | 300 | 300 | 300 | 300 | 300 |

*Table III.3. Rockcastle & Naese Sandstone members (Bee Rock Sandstone formation), Central Appalachian Basin.*

| | KYA1 | KYA2 | KYA3 | KYC1 | KYC2 | KYC3 | KYC4 | KYC5 |
|---|---|---|---|---|---|---|---|---|
| MONO QTZ | 158 | 142 | 143 | 156 | 151 | 170 | 166 | 157 |
| POLY QTZ | 29 | 35 | 41 | 33 | 19 | 22 | 20 | 29 |
| CHERT | 0 | 2 | 1 | 0 | 1 | 0 | 0 | 1 |
| 1 POROSITY | 12 | 29 | 27 | 17 | 34 | 26 | 25 | 24 |
| 2 POROSITY | 0 | 1 | 0 | 2 | 1 | 2 | 3 | 1 |
| ACCESSORY | 0 | 0 | 1 | 0 | 0 | 0 | 1 | 0 |
| CLAYS | 21 | 9 | 24 | 10 | 22 | 6 | 14 | 16 |
| AUTH. QTZ | 53 | 42 | 41 | 65 | 50 | 58 | 48 | 53 |
| SYN-SED. LITHIC | 2 | 2 | 2 | 0 | 0 | 0 | 0 | 0 |
| SED. LITHICS | 3 | 4 | 2 | 4 | 7 | 2 | 4 | 8 |
| VOLC. LITHICS | 9 | 12 | 8 | 7 | 6 | 3 | 5 | 4 |
| FELDSPAR | 10 | 15 | 8 | 4 | 8 | 10 | 9 | 4 |
| K FELDSPAR | 7 | 10 | 5 | 3 | 6 | 7 | 6 | 2 |
| PLAGIOCLASE | 3 | 5 | 3 | 1 | 2 | 3 | 3 | 2 |
| OPAQUES | 3 | 6 | 1 | 1 | 0 | 0 | 3 | 1 |
| MICA | 0 | 1 | 1 | 0 | 1 | 1 | 2 | 2 |
| IRON OXIDE | 0 | 0 | 0 | 1 | 0 | 0 | 0 | 0 |
| DOLOMITE | 0 | 0 | 0 | 0 | 0 | 0 | 0 | 0 |
| CALCITE | 0 | 0 | 0 | 0 | 0 | 0 | 0 | 0 |
| ORGANICS | 0 | 0 | 0 | 0 | 0 | 0 | 0 | 0 |
| TOTAL | 300 | 300 | 300 | 300 | 300 | 300 | 300 | 300 |

*Table III.4 Pine Creek Sandstone member (Bee Rock Sandstone formation). Central Appalachian Basin.*

| | KYE1 | KYE2 | KYE3 | KYEX4 | KYE5 | KYE6 | KYE7 | KYH2 | KYH3 | KYH4 | KYH5 | KYH6 |
|---|---|---|---|---|---|---|---|---|---|---|---|---|
| MONO QTZ | 158 | 143 | 150 | 157 | 151 | 143 | 166 | 151 | 72 | 151 | 147 | 149 |
| POLY QTZ | 28 | 27 | 31 | 20 | 23 | 33 | 27 | 29 | 135 | 27 | 31 | 29 |
| CHERT | 1 | 0 | 0 | 1 | 1 | 0 | 1 | 1 | 0 | 3 | 2 | 0 |
| 1 POROSITY | 23 | 19 | 16 | 21 | 18 | 12 | 19 | 45 | 35 | 51 | 57 | 47 |
| 2 POROSITY | 2 | 0 | 0 | 0 | 1 | 0 | 2 | 1 | 0 | 2 | 1 | 0 |
| ACCESSORY | 2 | 0 | 0 | 1 | 0 | 0 | 0 | 0 | 0 | 1 | 0 | 2 |
| CLAYS | 15 | 13 | 17 | 10 | 15 | 21 | 10 | 15 | 9 | 8 | 8 | 16 |
| AUTH. QTZ | 40 | 63 | 56 | 53 | 62 | 54 | 43 | 33 | 27 | 39 | 36 | 38 |
| SYN-SED. LITHIC | 0 | 0 | 0 | 0 | 0 | 0 | 0 | 0 | 0 | 0 | 0 | 0 |
| SED. LITHICS | 6 | 7 | 4 | 4 | 9 | 8 | 4 | 4 | 1 | 3 | 2 | 1 |
| VOLC. LITHICS | 13 | 17 | 18 | 21 | 12 | 19 | 11 | 13 | 12 | 8 | 6 | 4 |
| FELDSPAR | 8 | 7 | 5 | 8 | 5 | 5 | 14 | 7 | 5 | 5 | 4 | 9 |
| K FELDSPAR | 6 | 5 | 3 | 6 | 3 | 3 | 8 | 6 | 3 | 3 | 3 | 6 |
| PLAGIOCLASE | 2 | 2 | 2 | 2 | 2 | 2 | 6 | 1 | 2 | 2 | 1 | 3 |
| OPAQUES | 0 | 2 | 0 | 1 | 0 | 0 | 0 | 0 | 1 | 1 | 6 | 3 |
| MICA | 4 | 2 | 3 | 3 | 3 | 5 | 3 | 1 | 2 | 1 | 0 | 2 |
| IRON OXIDE | 0 | 0 | 0 | 0 | 0 | 0 | 0 | 0 | 1 | 0 | 0 | 0 |
| DOLOMITE | 0 | 0 | 0 | 0 | 0 | 0 | 0 | 0 | 0 | 0 | 0 | 0 |
| CALCITE | 0 | 0 | 0 | 0 | 0 | 0 | 0 | 0 | 0 | 0 | 0 | 0 |
| ORGANICS | 0 | 0 | 0 | 0 | 0 | 0 | 0 | 0 | 0 | 0 | 0 | 0 |
| TOTAL | 300 | 300 | 300 | 300 | 300 | 300 | 300 | 300 | 300 | 300 | 300 | 300 |

*Table III.5. Corbin Sandstone formation, Central Appalachian Basin.*

| | INA1 | INA2 | INA3 | INA4 | INA5 | INA6 | INA7 | INA8 | INA9 | INB2 |
|---|---|---|---|---|---|---|---|---|---|---|
| MONO QTZ | 139 | 133 | 149 | 131 | 119 | 153 | 133 | 129 | 130 | 131 |
| POLY QTZ | 31 | 11 | 13 | 19 | 41 | 15 | 10 | 18 | 16 | 34 |
| CHERT | 1 | 2 | 1 | 2 | 2 | 1 | 2 | 2 | 2 | 2 |
| 1 POROSITY | 32 | 49 | 19 | 50 | 63 | 43 | 23 | 57 | 60 | 64 |
| 2 POROSITY | 2 | 3 | 6 | 0 | 2 | 4 | 2 | 5 | 0 | 0 |
| ACCESSORY | 0 | 0 | 0 | 0 | 0 | 0 | 0 | 0 | 0 | 0 |
| CLAYS | 14 | 17 | 18 | 8 | 5 | 5 | 1 | 15 | 7 | 16 |
| AUTH QTZ | 43 | 32 | 24 | 53 | 52 | 36 | 9 | 24 | 40 | 40 |
| SYN-SED. LITHIC | 0 | 0 | 0 | 0 | 0 | 0 | 0 | 0 | 0 | 0 |
| SED. LITHICS | 5 | 1 | 4 | 7 | 2 | 9 | 14 | 8 | 13 | 5 |
| VOLC. LITHICS | 14 | 11 | 8 | 13 | 3 | 13 | 12 | 6 | 13 | 3 |
| FELDSPAR | 4 | 12 | 8 | 3 | 8 | 6 | 10 | 7 | 11 | 3 |
| K FELDSPAR | 3 | 9 | 6 | 2 | 6 | 5 | 7 | 4 | 7 | 2 |
| PLAGIOCLASE | 1 | 3 | 2 | 1 | 2 | 1 | 3 | 3 | 4 | 1 |
| OPAQUES | 2 | 12 | 14 | 4 | 0 | 0 | 0 | 0 | 1 | 0 |
| MICA | 1 | 2 | 2 | 2 | 0 | 0 | 1 | 0 | 2 | 0 |
| IRON OXIDE | 12 | 15 | 34 | 8 | 3 | 15 | 83 | 29 | 5 | 2 |
| DOLOMITE | 0 | 0 | 0 | 0 | 0 | 0 | 0 | 0 | 0 | 0 |
| CALCITE | 0 | 0 | 0 | 0 | 0 | 0 | 0 | 0 | 0 | 0 |
| ORGANICS | 0 | 0 | 0 | 0 | 0 | 0 | 0 | 0 | 0 | 0 |
| TOTAL | 300 | 300 | 300 | 300 | 300 | 300 | 300 | 300 | 300 | 300 |

Table III.6. Mansfield Formation, Illinois Basin.

| | NSWA1 | NSWA2 | NSWA3 | NSWA4 | NSWA5 | NSWA6 | NSWA7 | NSWB2 | NSWB3 | NSWB4 | NSWB5 | NSWB6 |
|---|---|---|---|---|---|---|---|---|---|---|---|---|
| MONO QTZ | 133 | 135 | 183 | 123 | 139 | 164 | 141 | 146 | 119 | 131 | 158 | 125 |
| POLY QTZ | 37 | 21 | 8 | 25 | 15 | 8 | 16 | 19 | 19 | 24 | 4 | 15 |
| CHERT | 1 | 0 | 0 | 0 | 0 | 0 | 0 | 1 | 0 | 0 | 0 | 1 |
| 1 POROSITY | 5 | 1 | 18 | 5 | 13 | 15 | 14 | 7 | 6 | 15 | 14 | 11 |
| 2 POROSITY | 6 | 19 | 15 | 15 | 1 | 20 | 9 | 23 | 33 | 31 | 17 | 30 |
| ACCESSORY | 7 | 6 | 5 | 3 | 2 | 1 | 6 | 5 | 5 | 9 | 5 | 10 |
| CLAYS | 52 | 39 | 19 | 57 | 94 | 30 | 39 | 32 | 59 | 47 | 52 | 38 |
| AUTH QTZ | 37 | 47 | 48 | 42 | 9 | 51 | 63 | 36 | 31 | 18 | 36 | 41 |
| SYN-SED. LITHIC | 5 | 5 | 0 | 10 | 0 | 0 | 0 | 7 | 2 | 5 | 0 | 7 |
| SED. LITHICS | 4 | 4 | 2 | 5 | 7 | 1 | 1 | 5 | 4 | 3 | 2 | 3 |
| VOLC. LITHICS | 1 | 1 | 1 | 0 | 2 | 1 | 2 | 2 | 2 | 4 | 3 | 10 |
| FELDSPAR | 0 | 2 | 0 | 0 | 1 | 0 | 0 | 0 | 0 | 1 | 1 | 0 |
| K FELDSPAR | 0 | 2 | 0 | 0 | 1 | 0 | 0 | 0 | 0 | 1 | 1 | 0 |
| PLAGIOCLASE | 0 | 0 | 0 | 0 | 0 | 0 | 0 | 0 | 0 | 0 | 0 | 0 |
| OPAQUES | 8 | 7 | 0 | 5 | 5 | 4 | 2 | 4 | 4 | 4 | 3 | 1 |
| MICA | 3 | 13 | 1 | 9 | 11 | 4 | 6 | 13 | 13 | 6 | 3 | 7 |
| IRON OXIDE | 1 | 0 | 0 | 0 | 0 | 0 | 0 | 0 | 0 | 0 | 1 | 0 |
| DOLOMITE | 0 | 0 | 0 | 0 | 0 | 0 | 0 | 0 | 0 | 0 | 0 | 0 |
| CALCITE | 0 | 0 | 0 | 0 | 0 | 0 | 0 | 0 | 0 | 0 | 0 | 0 |
| ORGANICS | 0 | 0 | 0 | 1 | 1 | 1 | 1 | 0 | 3 | 2 | 1 | 1 |
| TOTAL | 300 | 300 | 300 | 300 | 300 | 300 | 300 | 300 | 300 | 300 | 300 | 300 |

Table III.7. Hawkesbury Sandstone, Sydney Basin.

# Appendix IV:
# XRD Analysis.

XRD analysis has been used to aid the identification of the clay and heavy mineral fractions of a representative suite of samples. Only qualitative analysis has been attempted for this study. Using the data gathered it has been possible to comment on the provenance and diagenesis of the samples, and make comparisons between the different facies within a formation. The methods used for this study are outlined in Hardy & Tucker (1989) and are detailed here.

## IV.1 Sample Preparation.

Samples were broken by use of a jaw crusher, and then ground with a pestle and mortar to completely disaggregate grains. 15g of each sample was then placed in 300 ml of distilled water. To ensure complete disaggregation, each sample was placed in an ultrasonic bath for a period of one hour. Following this, the clay mineral and heavy mineral fractions were removed from the sample, using the methods outlined below.

## IV.2. Clay Fraction Analysis.

After one hour's immersion in an ultrasonic bath, each sample was agitated, and then allowed to stand for 10 minutes. After this period the suspended clay faction (<2mm diameter), was transferred to a settling column. A glass slide was placed in the base of the column. The samples were then placed into an oven at 60°C and the distilled water was allowed to evaporate. In this way an oriented smear mount was produced. Un-oriented mounts were produced through agitation of the clay minerals in a small amount of acetone on a glass slide.

Each smear sample was run from 2°-32° 2θ using iron filtered copper radiation in a Philips PW1130 2 Kilowatt generator/diffractometer assembly. Clay mineral phases were identified from the traces, and the relative proportions of kaolinite and illite were qualitatively established (Table IV.1).

| Sample | Kaolinte | Illite | Kaolinite: Illite | Mixed Layer Clays | Type | Dissem- inated Iron | Heavy Minerals |
|---|---|---|---|---|---|---|---|
| BD1 | Y | Y | 95:5 | | | | |
| BD6 | Y | | | | | | |
| CH5 | Y | | | | | | |
| CH6 | Y | Y | 99:1 | | | | |
| KYC4 | Y | Y | 90:10 | | | | |
| KYC5 | Y | Y | 90:10 | | | | |
| KYH1 | Y | Y | 33:66 | | | | |
| KYH2 | Y | Y | 90:10 | | | | |
| KYH4 | Y | Y | 80:20 | | | | Y |
| TNB4 | Y | Y | 90:10 | Y | Vermicu- lite | | Y |
| KYNB1 | Y | Y | 15:85 | | | | Y |
| INA1 | Y | Y | 33:66 | Y | Montmor- illinite | Y | |
| INA5 | Y | Y | 25:75 | Y | Vermicu- lite | Y | Y |
| NSWA2 | Y | Y | 10:90 | | | | Y |
| NSWA3 | Y | Y | 50:50 | | | | Y |
| NSWA6 | Y | Y | 25:75 | | | | Y |
| NSWB5 | | Y | | | | | Y |
| NSWB6 | Y | Y | 40:60 | Y | Montmor- illinite | | Y |
| NSWB6/2 | | Y | | | | | |

*Table IV.1 XRD analysis results.*

Following the first run, samples were then treated with ethylene glycol. The samples were introduced into a desiccator containing ethylene glycol for a period of 24 hours, and then dried for 4 hours in an oven at 60°C. The samples were run again between 2°-20°2θ to aid the identification of any mixed layer clays (see Hardy & Tucker 1989). Samples with unidentified mixed layer clays were then heated to 500°C for 30 minutes to identify vermiculite and confirm the other clay mineral phases (Table IV.1).

The results of the clay mineral analysis are listed in Table IV.1. These results are detailed in the text (Chapters 3-6), where samples are related to the relevant formations.

## IV.3. Heavy Mineral Analysis.

During petrographic work a small number of samples were found to contain high volumes of heavy minerals (see Appendix III). It was therefore felt that a limited study of the heavy mineral fraction might help to identify these grains. Only a small number of samples were examined, which are listed in Table IV.2. This limited study was only required to identify the heavy mineral species present to enable some comparisons to be made within formations.

| Sample | Heavy mineral phase identified through thin section. | Heavy mineral phase indentified through XRD. |
|---|---|---|
| KYH4 | Rutile, Opaques | |
| TNB4 | Rutile, Opaques, Zircon | |
| KYNB1 | Rutile, Opaques | |
| INA5 | Opaques | |
| NWSA2 | Rutile, Zircon, Tourmaline | Pseudorutile, Muscovite |
| NSWA3 | Rutile, Zircon, Tourmaline | Lazulite, Andradite |
| NSWA6 | Rutile, Zircon, Tourmaline | Rutile, Zircon, Tourmaline. Haematite, Spinel |
| NSWB5 | Rutile, Zircon, Tourmaline | Brookite, Ritile, Spinel |
| NSWB6 | Rutile, Zircon, Tourmaline, Monozite | Brookite, Siderite, Muscovite |

Table IV.2. Heavy mineral phases.

Preparation of samples for heavy mineral analysis is fraught with complications, particularly with regards to the problem of hydraulic equivalence (Blatt *et al* 1980, Mange & Maurer 1992). Hydraulic equivalence is the process whereby grains of different sizes and densities, but of the same settling velocity, will be deposited under the same conditions. Consequently the 'hydraulic equivalent size' is defined as the difference in size between a given heavy mineral species and the size of a quartz sphere with the same settling velocity in water (Mange & Maurer 1992). However, studies have illustrated that in most sediments the heavy and light mineral fractions are not in hydraulic equilibrium (Mange & Maurer 1992). Results of recent studies which investigated the mechanisms of fluvial placer evolution, have facilitated a better appreciation of processes operating in the entrainment, concentration and hydraulic equivalence relationships of light and heavy minerals (Mange & Maurer 1992). A number of heavy mineral species have an affinity to certain grain sizes. This reflects their initial size in the source rocks, a factor controlled primarily by crystallisation. Grain size of the host rock may also influence heavy mineral suite compositions. Sorting of heavy minerals by shape is as important as sorting by size (Mange & Maurer 1992).

Fine to medium grained sandstones yield the optimum mineral assemblages (Mange & Maurer 1992), and hence only samples of this grain size have been used within this study. As both the size of the individual heavy minerals and the mean grain size of sediments are controlled by factors operating in the depositional environment, a uniform grain size range suitable for all heavy mineral studies cannot be established (Mange & Maurer 1992). One can either restrict the heavy minerals to a specific size range, or examine the whole size range (Mange & Maurer 1992). The first method has the disadvantage of neglecting some diagnostic species, and is not advised especially in coarse sediments. Using the whole size range provides a good characterisation of the entire heavy mineral spectrum.

For the purposes of this study the entire heavy mineral suite has been used, regardless of grain size. The heavy mineral fraction was extracted from a 10 g sample of clay free, fine to medium grained sandstone following the procedures laid out by Mange & Maurer (1992). The sample had been previously disaggregated as outlined above. Concentration of the heavy minerals (those with a specific gravity greater than 2.89 g/cm$^3$) was achieved by the use of bromoform. The washed sample was placed in a settling funnel of bromoform and agitated vigorously. The sediments were then allowed to settle for a period of 30 minutes before the heavy fraction was poured off. Samples were washed with acetone and allowed to dry.

Grain mounts were made, using Canada balsam as the mounting medium. Where possible grains were identified using the petrographic microscope, and the relative abundances of the heavy minerals were ascertained by point counting. The

identification of heavy minerals with the petrographic microscope is, however, prone to error.

XRD analysis was used to improve the identification of the heavy mineral suite. Grains obtained through the use of heavy liquids were ground to a powder using a pestle and mortar, and then used to produce smear mounts. Samples were run from 2°-70°2θ using iron filtered copper radiation to establish the mineral phases present. The traces collected were highly complex, due to the number of phases present. It has been possible to identify some of the heavy minerals and thus improve the understanding of sample composition and provenance. Results are listed in Table IV.2, and are detailed in the individual chapters (Chapters 3-6).